PROPOSAL FOR A Φ–FACTORY

Laboratori Nazionali di Frascati - INFN

LNF-90/031(R)
30 Aprile 1990

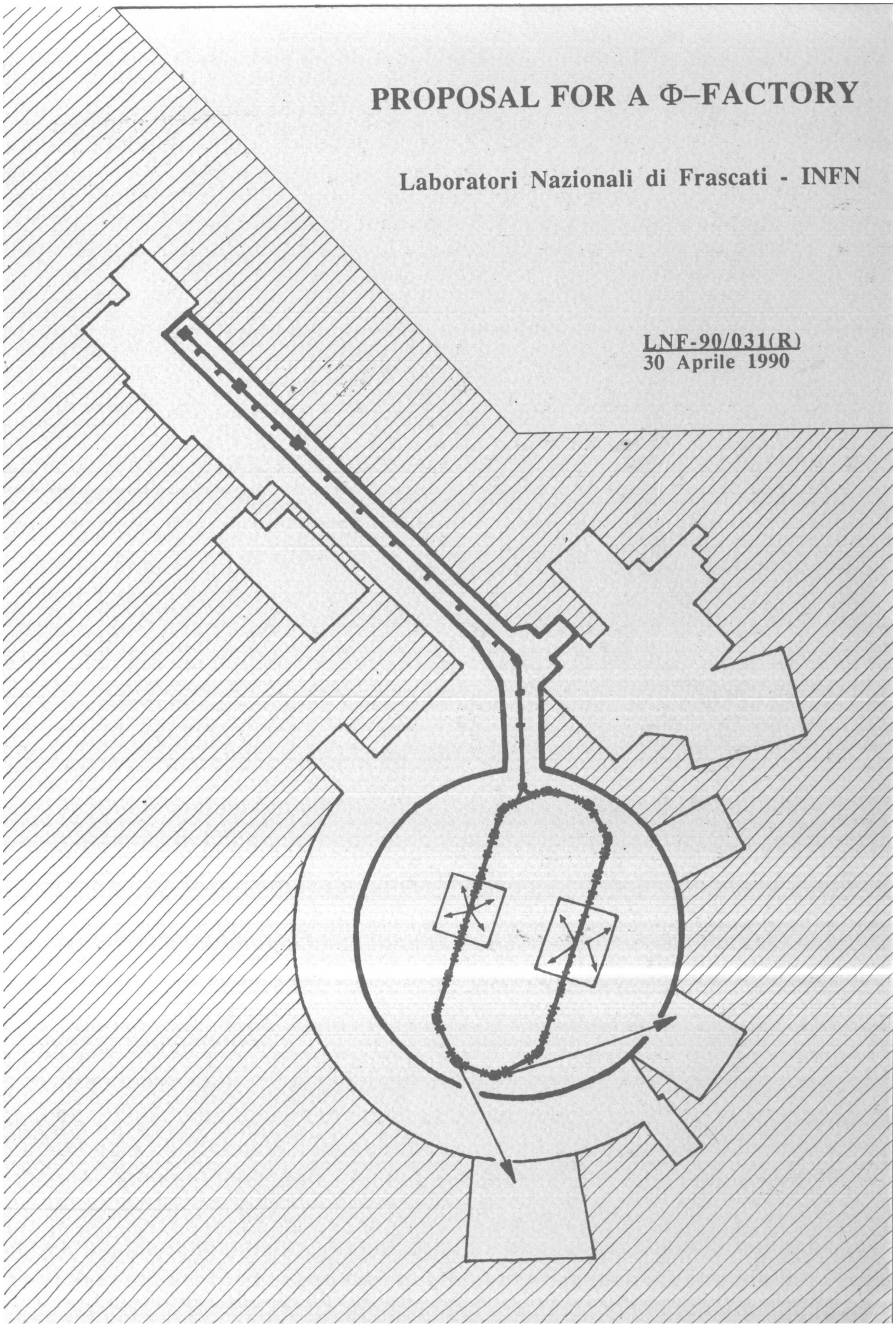

INFN - Laboratori Nazionali di Frascati

LNF-90/031(R)
30 Aprile 1990

PROPOSAL FOR A Φ–FACTORY

Printed and Published by
Servizio Documentazione dei
Laboratori Nazionali di Frascati

TABLE OF CONTENTS

PART I: THE PHYSICS

PART II: THE MACHINE

PART I: THE PHYSICS

Conveners: M. Giorgi[4,6] M. Greco[1] M. Piccolo[1]

The Φ-Factory Study Group

R. Baldini-Celio[1], G. Barbiellini[5], G. Batignani[4], R. Battiston[11], M.E. Biagini[1], S. Bianco[1], D. Bisello[8], F. Bossi[1], F. Buccella[6], M.P. Bussa[7], A. Calcaterra[1], M. Calvetti[11], G. Carboni[4], D. Cocolicchio[10], G. D'Ambrosio[6], R. De Sangro[1], A. Del Guerra[6], P. De Simone[1], E. Drago[6], S. Dubnicka[1], M. Ferrario[12], G.L. Fogli[9], F. Forti[4], P. Franzini[13], J. Lee-Franzini[14], A. Ghigo[1], P.F. Loverre[2], M. Lusignoli[3], P. Michelato[12], M. Miragliuolo[6], M. Napolitano[6], A. Nappi[4], W.R. Nelson[6], M. Nigro[8], C. Pagani[12], N. Paver[5], A. Peretti[12], I. Peruzzi[1], A. Pugliese[3], C. Rizzo[6], P. Russo[6], G. Salvini[3], C. Sanelli[1], C. Santoni[10], L. Serafini[12], P. Sartori[8], M. Spinetti[1], G. Triggiani[4], A. Zallo[1]

1) INFN - Laboratori Nazionali di Frascati P.O. Box 13, 00044 Frascati (Italy)
2) Universita' della Basilicata e Sezione INFN di Roma
3) Universita' di Roma "La Sapienza" e Sezione di Roma
4) Universita' di Pisa e Sezione INFN di Pisa
5) Universita' di Trieste e Sezione INFN di Trieste
6) Universita' di Napoli e Sezione INFN di Napoli
7) Universita' di Genova e Sezione INFN di Genova
8) Universita' di Padova e Sezione INFN di Padova
9) Universita' di Bari, Sezione INFN di Bari e CERN
10) CERN
11) Universita' di Perugia e Sezione INFN di Perugia
12) Universita' di Milano e Sezione INFN di Milano
13) Columbia University
14) Stony-Brook University

PHYSICS PROGRAMME AT A Φ-FACTORY

PHYSICS AND DETECTOR SUMMARY

1. Introduction

Basic progress in the understanding of the properties of the fundamental interactions has been typically achieved both by *pioneering* observations at the highest available energies and by high accuracy measurements at *much lower* energy. Higher order corrections to the values of physical parameters are typically sensitive to very large energy scales. Precision measurements of such parameters can therefore reflect the appearance of new physics at those scales. Well known examples are the electron anomaly which led to QED and later the muon anomaly which, when measured to accuracies of one half part per million, can reflect the existence of new interactions and particles up to 1–10 TeV.

Another example is provided by the study of K–meson decays, especially the neutral one, which has played a fundamental role in the development of the Standard Model, from the initial hint that parity is not conserved in weak interactions,[1] to Cabibbo mixing[2] and the absence of flavor changing neutral currents which led to the GIM mechanism suggestion.[3]

K decays have thus far given us the only proof of the existence of CP violation. More than two decades of study of these decays have not quite yet completely elucidated the origin of CP violation. In particular it's not yet clear whether CP violation is only present in the mass terms ($\Delta S = 2$) or in the decay amplitude ($\Delta S = 1$) as well. In other words we do not really know whether the ratio ϵ'/ϵ vanishes or not. Studies of the well prepared quantum state $K_L^0 K_S^0$ as produced in the decay $\phi \to K_L^0 K_S^0$, where the ϕ meson is produced at rest in the laboratory frame, in e^+e^- annihilations, promise the possibility of new precise measurements of the CP violation parameters. Such studies require a high luminosity e^+e^- collider, the so called "ϕ–factory".

In the following we discuss the physics capabilities of a high luminosity e^+e^- facility with $\sqrt{s} = 2E \sim 1$ GeV, where E is the energy of the colliding beams, and the minimal requirements for a suitable detector after first briefly reviewing physics issues and experimental implications. An e^+e^- collider operated at $\sqrt{s} =$

$M(\phi)$ allows measurements of ϵ'/ϵ of better statistical accuracy than achieved so far, using high energy neutral kaon beams, if the luminosity of the machine is $\gtrsim 1 \times 10^{32}$. Moreover, systematic errors can be controlled much better than in present experiments, thanks to the clean initial state and the over–constrained kinematics. It's quite unlikely that the present experiments will ever be able to push their systematic uncertainties below $\sim 3\times10^{-4}$ while the approach discussed in this report gives good promise of a definitive measurement of ϵ'/ϵ or, at least, an upper limit considerably smaller than the present one.

We also note that if the e^+e^- facility were to provide luminosities in the range $\mathcal{L} = 1 - 2 \times 10^{33}$ cm^{-2} sec^{-1} a completely new field of opportunities would open up regarding the study of CP violation in K^0_S decays, hardly feasible with K^0_S beams.

At $\mathcal{L} = 1 - 2 \times 10^{32}$ cm^{-2} sec^{-1}, many other interesting physics topics can be investigated at a ϕ–factory. While CP violation effects remain the major physics aims, in this report we will also discuss:

1. Measurements of the e^+e^- total cross section up to energies of 1 GeV to obtain the hadronic contribution to the photon propagator spectral function, of interest in the evaluations of the muon anomaly.
2. Search for rare K decays, another field of great interest where observations of very small decay rates reflect on new physics at large energy scales.
3. Improved limits on the ν_μ mass, of great interest especially in view of the new recent limits on neutrino species.
4. High statistics study of the η and/or η' mesons, in particular better determination of their mixing.
5. High statistic study of low lying narrow states, in particular a better understanding of the nature of the S^*.

Each of these measurements will require particular abilities from the experimental apparatus. The optimization of the detector for the ϕ–factory must

however be performed in such a way that most of the experiments can be carried out with the same detector, since the design of the high luminosity collider is based on a single interaction region. Ultimately the most demanding task is that of the measurement of ϵ'/ϵ.

2. Physics Goals

2.1 CP Violation in the Kaon System

CP violation is one of the most interesting phenomena in the entire field of particle physics. The existence of CP invariance violation was first established experimentally in kaon decays in 1964[4] but its origin is not completely clear. The "Standard Model" with three generations of quarks, allows for a free phase in the quark mixing matrix.[5] This offers an automatic, *built in*, possibility for the existence of CP violation, without however the power of predicting its actual existence nor the magnitude of the effect. It is very important to establish whether CP violation is fully explained in the framework of the standard model or whether physics beyond the standard model is involved. Even the question of whether the *superweak* hypothesis[6] is ruled out or not, by the latest experimental findings of NA-31[7] and E-731[8] is still open.

The general formalism describing the decay $\phi \rightarrow K_L^0 K_S^0$ has been widely discussed in the literature.[9] We recall in the following some results, necessary to our presentation. In e^+e^- annihilation the ϕ mesons, pure $J^{PC} = 1^{--}$ states, are produced with a cross section of $\sim 4.8\mu$b and decay to $K_L^0 K_S^0$ with a branching fraction of 34.3%.

The decay amplitude corresponding to the appearance of a final state f_1 at

the time t_1 and f_2 at time t_2 is given by (assuming CPT invariance):

$$\begin{aligned} A\big(f_1(t_1), f_2(t_2)\big) =& \frac{1+|\alpha|^2}{2\sqrt{2}\alpha}\langle f_1|K_S^0\rangle\langle f_2|K_L^0\rangle e^{-i(\lambda_S+\lambda_L)t/2} \\ &\times\Big((\eta_1-\eta_2)\cos\big(\frac{\Delta\lambda\Delta t}{2}\big)+i(\eta_1+\eta_2)\sin\big(\frac{\Delta\lambda\Delta t}{2}\big)\Big) \\ &\text{where}\quad \Delta t\equiv t_2-t_1,\quad t\equiv t_1+t_2. \end{aligned} \tag{2.1}$$

In the above $\alpha=(1+\epsilon)/(1-\epsilon)$, $\lambda_{S,L}\equiv m_{S,L}-i\Gamma_{S,L}/2$ are the "complex" $K_{S,L}$ masses and $\eta_i\equiv\langle f_i|K_L^0\rangle/\langle f_i|K_S^0\rangle$.

If $\Delta t=0$, the decay amplitude vanishes for $K_{S,L}$ decays to identical final states. At equal times and $f_1=\pi^+\pi^-$, $f_2=\pi^0\pi^0$, the amplitude is proportional to $\eta_{+-}-\eta_{00}=3\times\epsilon'$, where $\eta_{+-}=\epsilon+\epsilon'$ and $\eta_{00}=\epsilon-2\epsilon'$.

Measurements of $\mathrm{Re}(\epsilon'/\epsilon)$ can be obtained by detecting events where one K meson decays into charged pions and the other into neutral ones and observing the difference of the two decay times. Integrating the decay amplitude over all times for fixed time difference and defining the intensity asymmetry:

$$A(\Delta t)=\frac{I(\Delta t)-I(-\Delta t)}{I(\Delta t)+I(-\Delta t)} \tag{2.2}$$

where

$$I(\Delta t)=\frac{1}{2}\int_{|\Delta t|}^{\infty}\Big|A\big(\pi^+\pi^-(t_1),\pi^0\pi^0(t_2)\big)\Big|^2dt \tag{2.3}$$

with $t=t_1+t_2$ and $\Delta t=t_1-t_2$ fixed, for $\Delta t\gg\tau_s$, one finds $A(\Delta t)\sim-3\mathrm{Re}(\epsilon'/\epsilon)$.

Alternatively, instead of comparing rates at fixed time differences, one can measure fully integrated rates corresponding to different decay channels as suggested by Bernabeu et al.[10] One finds:

$$\begin{aligned} N(f_1,f_2)=&\int_{\tau_1}^{\tau_2}dt_1\int_{\tau_1}^{\tau_2}dt_2\Big|A\big(f_1(t_1),f_2(t_2)\big)\Big|^2= \\ &=\frac{(1+|\alpha|^2)^2}{8|\alpha|^2}\times\frac{1}{\Gamma_s\Gamma_l}\times\big|\langle f_1|K_S^0\rangle\big|^2\big|\langle f_2|K_L^0\rangle\big|^2 \\ &\times\big(C_1|\eta_1|^2+|\eta_2|^2-2C_2\times Re(\eta_1\eta_2^*)\big) \end{aligned} \tag{2.4}$$

where C_1 and C_2 are known functions of τ_1 and τ_2.

From equation (2.4) one finds the following relation between branching ratios (BR):

$$\frac{BR(\pi^+\pi^-\pi^+\pi^-)}{BR(\pi^0\pi^0\pi^0\pi^0)} = \frac{BR(K_s \to \pi^+\pi^-)^2}{BR(K_s \to \pi^0\pi^0)^2} \times \left(1 + 6 \times \mathrm{Re}(\frac{\epsilon'}{\epsilon})\right) \qquad (2.5)$$

and similarly for other ratios.

So far the we have assumed that the $K\overline{K}$ system produced in e^+e^- annihilations is odd under charge conjugation or a pure $K_L^0 K_S^0$ state. The decay chain:

$$\phi \to S^* + \gamma \to (K^0\overline{K}^0)_{C=+1} + \gamma \to \gamma + \frac{1}{\sqrt{2}}(K_S^0 K_S^0 - K_L^0 K_L^0) \qquad (2.6)$$

leads to an admixture of $K_S^0 K_S^0$ and $K_L^0 K_L^0$ states with a branching ratio estimated in the range $10^{-4} - 10^{-7}$. Since the photon energy is ~ 10 MeV it will often escape detection.

This C–even background has been carefully analyzed by Cocolicchio *et al.*[11] who have shown that suitable cuts on the K_0 path length allow an almost complete suppression of the unwanted positive C–even events, retaining practically the entire sample of the C–odd events. Conversely, the decay $\phi \to S^*\gamma$ can be of interest on its own[12] in order to clarify the nature of the S^* state, in terms of its quark and gluon content. In this case the $K_S^0 K_S^0$ state (cfr. eq. (2.6)) dominates the short path length region.

2.2 Other CP Violation Studies and Rare K Decays.

The study of the K meson has been very rewarding and has greatly helped to extend our understanding of the physical world. This understanding culminated in the construction of the Standard Model, but then we got stuck. Beautiful as the SM model might be, it can only be phenomenological and approximate. Therefore, we expect some new phenomena to emerge at energy scales in the few

TeV range in order to explain a host of conceptual problems and perhaps begin to understand the reason for the existence of so many free parameters in the SM and to predict their values. Direct attacks on these problems require very high energies and complicated detectors and might not become reality for several years. We know however that most guesses about what the new physics is, at the several TeV scale, subtly reflect on kaon physics and we have reasons to believe that the study of K mesons, at a new level of accuracy will open new horizons.

At first thought it might seem bizarre to propose to study K meson decays at a facility where the "K beam" flux could range from 350 to 7000 neutral K's and 500 to 10000 charged K's per second, for $\mathcal{L} = 1 - 20 \times 10^{32}$ cm^2 s^{-1}. Present experiments are performed at beams of much higher intensities and indeed even higher intensities, 10^9 K_L^0 sec^{-1}, are planned at Brookhaven.[13] Still higher intensities are mentioned in K factory plans.[14]

There are however very clear benefits at a ϕ–factory, such as:[15]

1. The unique possibility of tagging the presence of a K_S^0 or K_L^0. One can therefore effectively have a beam of K_S^0, with no background and delivering $5 - 100 \times 10^9$ kaons per year.

2. While for the study of very rare decays, the incident flux might be inferior to other approaches, the very large acceptance of a general purpose detector to all decay modes, the effective absence of background and the unique possibility of choosing, by tagging, the parent state of interest make possible the study of several interesting channels.

3. Typical CP violation experiments detect decays of 1-2% of the K_L^0 beam, in the presence of very large neutron backgrounds. Searches for rare decays in hadroproduced kaon beams, require complex detectors to reject background, must be able to handle very high trigger rates and large amount of data in order to extract minute signals. The large acceptance at a ϕ–factory and the low background open up the possibility of studying CP violation in charged K decays and, for the case of neutral K's, to study CP in channels

other then the pions.

A general discussion of the status and perspectives of the K-decay physics can be found in reference 15. Table 1 , taken from there shows a summary of the present situation.

For some of the quoted reactions limits are already in the 10^{-8} to 10^{-10} range and are expected to reach the $10^{-11} - 10^{-12}$ level, although it is not really clear when nor how realistic those expectations are. Moreover a systematic study with different techniques is always highly valuable.

The role of a ϕ–factory is complementary to that of high intensity K beams, the former being more suited for a study of a broader set of CP violating $K_{S,L}$ and $K^{\pm}$ decays and rare K_S^0 decays, while search for specific, very rare K_S^0 and K^+ decays are probably better done with high intensity beams.

At a ϕ–factory CP violating asymmetries can be studied for the decays: $K^{\pm} \to \pi^{\pm}\pi^{\pm}\pi^{\mp}$, $K^{\pm} \to \pi^0\pi^0\pi^{\pm}$, $K^{\pm} \to \pi^{\pm}\pi^0\gamma$ and $K_{S,L} \to \pi^+\pi^-\gamma$, $K_L^0 \to \pi^{\pm}l^{\mp}\nu$, $K_L^0 \to \pi^+\pi^-\pi^0$. A search for direct CP violation in $K^{\pm}$ decays looks particularly interesting, because of possible enhancements effects.[16] Similarly CP violation effects can be found in the decays of neutral kaons into two photons.[17]

The situation is particularly favorable concerning K_S^0 decays at a ϕ–factory. With very few exception, all the studies performed at high intensity K beams use K_L or $K^{\pm}$ since clean, intense K_S^0 beams are very difficult to obtain. The pure K_S^0 at a ϕ–factory will dramatically improve knowledge of K_s branching ratios (most are not measured yet) for $K_S^0 \to \pi^0\nu\bar{\nu}$, $e^+e^-\gamma$, $\mu^+\mu^-\gamma$, $\pi^0e^+e^-$, $\pi^0\mu^+\mu^-$ etc., down to the 10^{-8} or better, range. It will also be possible to improve the existing limits on the CP-violating reaction $K_S^0 \to 3\pi^0$, by looking for 6 low energy photons in the detector. A search for $K_S^0 \to \pi^0\gamma\gamma$ might yield a few detected events. Tens to hundreds of decays $K^{\pm} \to \pi^{\pm}\gamma\gamma$ or $K^{\pm} \to \pi^{\pm}\mu^+\mu^-$, can also be detected. Existing limits on $K^{\pm} \to \pi^0\mu^{\pm}\nu\gamma$, $\pi^{\pm}\pi^{\pm}\mu^{\mp}\nu$, $\pi^{\pm}\gamma\gamma\gamma$ and $l^{\pm}\nu\nu\nu$, may be substantially improved.

As discussed in detail in the previous sections the most challenging and stimulating goal of an experiment at a ϕ–factory is the measurement of ϵ'/ϵ. The apparatus needed to perform this measurement has to be a rather sophisticated one. Such a general purpose detector will be able to accurately measure all kinds of $K_{S,L}$, $K^{\pm}$, η and ρ decays.

2.3 e^+e^- Annihilations into Hadrons from Threshold to 1 GeV

A precise measurement of $\sigma(e^+e^- \rightarrow \text{hadrons})$ at low energy, mostly at the ρ meson peak is of particular relevance for the theoretical prediction of the muon anomalous gyromagnetic ratio $g_\mu - 2$.[18] The muon $g-2$ value or the anomaly $a_\mu = (g-2)/2$, a basic property of the muon, can provide sensitive tests of the theory and indeed much effort has been devoted to improve the theoretical and experimental accuracy of its value. The experimental value for $g-2$ has been determined by three progressively more precise measurements at CERN, the last one[19] reporting:

$$\begin{aligned} a_{\mu^-} &= 11659370\,(120) \times 10^{-10} \\ a_{\mu^+} &= 11659110\,(110) \times 10^{-10} \\ a_\mu &= 11659240\,(85) \times 10^{-10} \end{aligned} \tag{2.7}$$

where the numbers enclosed in parentheses represent the experimental uncertainties (both systematic and statistical) of the measured values. The theoretical value for a_μ is obtained as the sum of three contributions:[20]

$$a_\mu^{theor} = a_\mu^{QED} + a_\mu^{hadr} + a_\mu^{weak} \tag{2.8}$$

The hadronic contributions to a_μ are due to vacuum polarization and light by light scattering. These can be estimated using measurements of the total hadronic e^+e^- annihilation cross section, while the weak part involves contribution from $W^{\pm}, Z$ and Higgs particles. While the electron anomaly is dominated by QED contributions, the muon anomaly is $\sim 4 \times 10^4$ times more sensitive to small

distance physics because of the larger muon mass. The QED contribution to a_μ has been evaluated to $\mathcal{O}(\alpha^4)$ to be:[20]

$$a_\mu^{QED} = 11658480(3) \times 10^{-10} \tag{2.9}$$

The hadronic contribution to a_μ is the cause of the largest theoretical uncertainty. The estimate is based on the poorly known cross section for hadronic e^+e^- annihilation from the 2π threshold up to $\sim$ 1 GeV. The latest estimate gives:[20]

$$a_\mu^{hadr} = 702\,(19) \times 10^{-10} \tag{2.10}$$

Finally the weak interaction contribution, to one loop, gives:[21]

$$a_\mu^{weak} = 19.5\,(0.1) \times 10^{-10} \tag{2.11}$$

The present best estimate for the muon anomaly is therefore:

$$a_\mu^{theor} = 11659202(20) \times 10^{-10} \tag{2.12}$$

in good agreement with the experimental value. A new experiment[22] under construction at Brookhaven aims to measure a_μ to 0.35 ppm in order to observe the weak contribution and possible additional contributions of *physics beyond the standard model.* A theoretically clear interpretation of the new data will not be possible if the hadronic contributions to $g-2$ are not reliably evaluated. To this aim more accurate measurements of $\sigma(e^+e^- \rightarrow \text{hadrons})$ at low energy and in particular in the ρ region are needed.

The required accuracy for the measurements,[23] $\sim 0.5\%$, is readily accessible at machines like the one under design. The σ's to be measured are of the order of $10^{-31} - 10^{-30}$ cm^2 so that luminosities of the order of 10^{30} cm^{-2} sec^{-1} would be ample.

As a last item under this physics topic we recall that an accurate determination of the K form factor at the ϕ mass will allow measurements of the interference of the ϕ meson with the δ, ω mesons and possibly with higher $s\bar{s}$ excitations.[24]

2.4 $\eta - \eta'$ Mixing and Radiative ϕ Decays

The determination of the $\eta - \eta'$ mixing angle has been a long-standing problem, which is still matter of discussions. This parameter plays a central role in the description of flavor SU(3) symmetry breaking, and is a crucial input in a large number of theoretical predictions for transitions involving the nonet of pseudoscalar mesons. One example relevant to the present context of a ϕ factory is represented by the long-distance contributions to the rare, GIM suppressed radiative kaon decays, which are reviewed elsewhere in this volume. In addition to that, the $\eta - \eta'$ mixing has important bearing on quark models and QCD, in particular on the question whether there is a gluonium component in the η and in the η'.

In this regard measurements of the radiative ϕ decays to η and to η', which are presumably feasible with great sensitivity at a ϕ factory, can lead to a really decisive test, when combined with the information coming from other sources such as e.g. the analogous J/Ψ decays and the two-photon decays of η and η'.

In the quark-basis it is convenient to define the η and η' wave functions as:[25]

$$\begin{aligned} |\eta\rangle &= X_\eta \frac{1}{\sqrt{2}}|\bar{u}u + \bar{d}d\rangle + Y_\eta|\bar{s}s\rangle + Z_\eta|G\rangle \\ |\eta'\rangle &= X_{\eta'}\frac{1}{\sqrt{2}}|\bar{u}u + \bar{d}d\rangle + Y_{\eta'}|\bar{s}s\rangle + Z_{\eta'}|G\rangle, \end{aligned} \tag{2.13}$$

where in general

$$X_\eta^2 + Y_\eta^2 + Z_\eta^2 = X_{\eta'}^2 + Y_{\eta'}^2 + Z_{\eta'}^2 = 1. \tag{2.14}$$

In (2.13) Z measures the gluonic content of the η and of the η' states. In the familiar SU(3) octet-singlet basis, and with no gluonium admixture i.e. $Z = 0$

and $X^2 + Y^2 = 1$:

$$\begin{aligned} |\eta\rangle &= \cos\theta_p|\eta_8\rangle - \sin\theta_p|\eta_0\rangle \\ |\eta'\rangle &= \sin\theta_p|\eta_8\rangle + \cos\theta_p|\eta_0\rangle, \end{aligned} \tag{2.15}$$

where θ_p is the $\eta - \eta'$ mixing angle, and

$$\begin{aligned} |\eta_8\rangle &= \frac{1}{\sqrt{6}}|\bar{u}u + \bar{d}d - 2\bar{s}s\rangle \\ |\eta_0\rangle &= \frac{1}{\sqrt{3}}|\bar{u}u + \bar{d}d + \bar{s}s\rangle. \end{aligned} \tag{2.16}$$

The value of θ_p has been revised over the years since SU(3) was proposed: while $\theta_p = -10°$ was historically suggested by the Gell-Mann-Okubo quadratic mass formula for pseudoscalar mesons, the value $\theta_p \sim -20°$ now seems to be favoured by the present experimental data on radiative meson decays.[26,27] Such a value would be consistent with a linear mass formula, derived under the same assumptions, or with a quadratic one including chiral symmetry breaking corrections.[28] The advantage of radiative meson decays, in order to extract the values of X, Y and Z in equation (2.13), is clearly due to the sensitivity of the photon to the quark components of the wave function via the couplings to the quark electric charges. Thus precision measurements of these decays give the values of X and Y, and then the value of Z can be indirectly obtained through the normalization condition in equation (2.14).

The decays which are relevant to the parameters of the η are the transitions $\rho \to \eta\gamma$ and $\phi \to \eta\gamma$. One finds[29-31] with $\frac{m_u}{m_s} = 0.7$:

$$|X_\eta| = 0.76 \pm 0.06, \tag{2.17}$$

and

$$|Y_\eta| = 0.62 \pm 0.03 \tag{2.18}$$

Correspondingly $|X_\eta|^2 + |Y_\eta|^2 = 0.96 \pm 0.09$, compatible with unity, and thus with no admixture at all of the η with a hypothetical gluonium state.

Coming to the η', the non-strange quark component is determined from the $\eta' \to \rho\gamma$ transition which leads to :

$$|X_{\eta'}| = 0.57 \pm 0.05. \tag{2.19}$$

On the other hand from the decay $\eta' \to \gamma\gamma$ on gets :

$$|X_{\eta'} + \frac{\sqrt{2}}{5} Y_{\eta'}| = 0.75 \pm 0.03. \tag{2.20}$$

To complete the determination of the η' parameters one then needs a direct information on the rare transition $\phi \to \eta'\gamma$, which is proportional to $Y_{\eta'}$:

$$\frac{\Gamma(\phi \to \eta'\gamma)}{\Gamma(\phi \to \eta\gamma)} = \left(\frac{Y_{\eta'}}{Y_\eta}\right)^2 \left(\frac{k_{\eta'}}{k_\eta}\right)^3 \sim 4.6 \times 10^{-3} \left(\frac{Y_{\eta'}}{Y_\eta}\right)^2. \tag{2.21}$$

This decay is as yet unobserved, and the presently available experimental upper limit is $BR(\phi \to \eta'\gamma) \leq 4.1 \times 10^{-4}$.[30]

The values in equations (2.19) and (2.20) still leave some room for a non vanishing $Z_{\eta'}$ in equation (2.13), and thus for a small gluonium admixture of the η', so that the observation of this decay would represent an important piece of information in this regard. To give an idea of the expected order of magnitude of the branching ratio, for $Z_{\eta'} = 0$ and $\theta_p = -20°$ we would have $BR(\phi \to \eta'\gamma) \sim 1.2 \times 10^{-4}$.

In conclusion, it will be very useful to improve the experimental determination of $\phi \to \eta\gamma$ and to measure $\phi \to \eta'\gamma$, as these decays are particularly sensitive to the $\bar{s}s$ components of η and η', and thus have a special role in the context of quark models and QCD.

In addition, at a ϕ factory the decay $\phi \to \eta\gamma$ would provide a quite large η sample, well tagged by the monochromatic photon, which might enable to

study η decays with very good statistics. The present sensitivity to η decays is of the order of $10^{-4} - 10^{-6}$ in branching ratio, depending on the particular modes. Therefore it might be worthwhile to explore also this possibility from the experimental point of view.

3. Experimental considerations

3.1 The experimental situation

Until now, the CP violation effects have been measured only with K_L^0 beams at hadron machines; the present experimental situation is the subject of two excellent reviews[32,33] in this report.

Both the CERN and Fermilab ϵ'/ϵ experiments are planning upgrades of their detectors and expect a significant increase in statistics in the coming years. The data samples now available for the rarest decay ($K_L^0 \to \pi^0\pi^0$) amount to $\sim 200\,000$ events, even if the published results refer only to part of the available statistics. It seems reasonable to expect that the statistical errors on the value of ϵ'/ϵ will reach the 5×10^{-4} level in the next couple of years; it's not completely clear, however, how much the systematic errors will be reduced.

If we assume, as a working hypothesis, that the planned improvements on the existing detectors will allow a reduction of 50% of the systematic uncertainties, then a few years from now, the overall error in the measurement of ϵ'/ϵ will be of the order of $6 - 7 \times 10^{-4}$. A measurement at a ϕ–factory with luminosity $\gtrsim 10^{32}\mathrm{cm}^{-2}\mathrm{sec}^{-1}$ would yield a statistical accuracy at least as good as the one foreseeable in the near future from K_L^0 beams while the systematic effects could be substantially reduced thanks to the kinematics, which is well defined, and to the signal to background ratio which is extremely favorable.

3.2 Experimental procedures and counting rates

The value of ϵ'/ϵ can be extracted from the data collected at an e^+e^- collider operating at the ϕ mass using several different techniques. In the following we will describe four *different* methods; the first three require the final state to be a well defined decay channel of *both* K_L^0 and K_S^0; the fourth one is the well known method of the double ratio, widely used at hadronic machines: it does not require the final state to be a specific decay channel of the $K_L^0 K_S^0$ pair.

The first of these methods, specific to e^+e^- measurements, proposed by Dunietz et al.,[34] consists of measuring the path length asymmetry for the charged and the neutral pion pair in the final state $\pi^+\pi^-\pi^0\pi^0$. It has be shown (section 2.1, reference 34) that this quantity is proportional to $-3 \times \mathrm{Re}(\epsilon'/\epsilon)$, if evaluated over decay paths very long compared to the K_S^0 lifetime; the same asymmetry, if measured in the $K_L^0 K_S^0$ interference region, allows in principle the evaluation of the imaginary part of ϵ'/ϵ. (The $\mathrm{Im}(\epsilon'/\epsilon)$ measurement is however severely hampered by the C–even background resulting from the radiative decays of the ϕ mentioned in section 2.1.)

The statistical significance of the asymmetry measurement which can be carried out at a ϕ–factory with $\sim 10^{32}$ cm^{-2} sec^{-1} average luminosity, has been discussed by Barbiellini and Santoni[35] and by contributors[24] [36] to this study group for measuring both the real and the imaginary part of ϵ'/ϵ.

In the following we will assume that the machine, based on the design described in the first part of this report,[37] will deliver, shortly after turn-on, a luminosity of $1 - 2 \times 10^{32}$ cm^{-2} sec^{-1} . The present statistical error on ϵ'/ϵ could be reduced by roughly a factor 1.5 by an experiment using the path length asymmetry technique.

A method suggested by Bernabeu et al.[10] is based on the measurement of the ratio between different final states involving at least one CP violating decay; ϵ'/ϵ can be extracted from:

$$\frac{\Gamma(\phi \to +-+-)}{BR(K_S^0 \to +-) \times BR(K_S^0 \to +-)} \times \frac{BR(K_S^0 \to +-) \times BR(K_S^0 \to 00)}{\Gamma(\phi \to +-00)} = 1 + 3 \times Re(\frac{\epsilon'}{\epsilon}) \tag{3.1}$$

The analogous expression if one of the final states is completely neutral yields:

$$\frac{\Gamma(\phi \to +-+-)}{BR(K_S^0 \to +-) \times BR(K_S^0 \to +-} \times \frac{BR(K_S^0 \to 00) \times BR(K_S^0 \to 00)}{\Gamma(\phi \to 0000)}$$
$$= 1 + 6 \times Re(\frac{\epsilon'}{\epsilon}) \tag{3.2}$$

The last method, already mentioned, is the double ratio; it has the best statistical sensitivity of the four , since the measurement itself is proportional to $1 - 6 \times Re(\frac{\epsilon'}{\epsilon})$ and the rate is higher than the one obtained in the measurement of the ϕ width in the totally neutral final state.

These measurements hold the promise of a significant step forward in statistical significance, when performed at an e^+e^- collider with a luminosity of 10^{32} cm^{-2} sec^{-1}.

It's worth noting that while the four measurements are not statistically independent they do however have different sensitivity to systematic uncertainties. The possibility of extracting ϵ'/ϵ simultaneously in four different ways is unique to a ϕ–factory and will lend additional confidence to the ability of controlling systematic uncertainties to the necessary level.

In the following we consider the sources of possible systematic uncertainties and evaluate their effects. This analysis ultimately leads to the strictest constraints on the design of the detector.

If we use as a bench-mark the double ratio technique, we can calculate the statistical error on the double ratio as following:

$$\frac{\delta r}{r} \sim \sqrt{\frac{3}{2} \times \frac{1}{N(K_L^0 \to \pi^0\pi^0)}} \tag{3.3}$$

At an average luminosity of 10^{32} cm^{-2} sec^{-1} and assuming a spherical fiducial volume 1.5 m in radius, $\sim 500\,000$ $K_L^0 \to \pi^0\pi^0$ decays could be detected in one year of running (with the usual *physics year* defined as 10^7 seconds); assuming

for ϵ'/ϵ the NA-31 value, this rate would translate into a relative error on ϵ'/ϵ roughly at the 10% level.

3.3 Systematic uncertainties

The only non vanishing measurement of ϵ'/ϵ is quoted with a systematic error roughly equivalent to the statistical one:[7] the next generation experiments using K_L^0 beams could in principle reduce the systematic uncertainties; the systematic effects will however constitute the limiting factor for this technique.

The goal of the ϕ–factory approach to the ϵ'/ϵ measurement is to reduce the systematic uncertainties to a level $\lesssim 5\%$, *i.e.* a factor 2 less than the statistical error obtainable in a one year run. This is by no means a trivial task, since the K_S^0 and K_L^0 decay products populate different regions of the fiducial volume, and no *cancellation trick* can be used to make the K_L^0 and the K_S^0 acceptance equal to first order, as it is done in experiments performed at K_L^0 beams. In order to succeed, both the acceptance and the background subtraction contribution to the systematic error on the double ratio have to be kept to the $\sim 9 \times 10^{-4}$ level. This requirement will also define the amount of background one might tolerate in the selected signal.

In the case of the path length asymmetry, for instance, following the analysis originally developed by Barbiellini and Santoni,[35] we consider the background from the semileptonic decay of the K_L^0. The asymmetry in the decay path is defined as:

$$A = \frac{N(l_{\pi^+\pi^-} > l_{\pi^0\pi^0}) - N(l_{\pi^+\pi^-} < l_{\pi^0\pi^0})}{N(l_{\pi^+\pi^-} > l_{\pi^0\pi^0}) + N(l_{\pi^+\pi^-} < l_{\pi^0\pi^0})} = -3 \times \mathrm{Re}\left(\frac{\epsilon'}{\epsilon}\right) \qquad (3.4)$$

If βN_{back} is the contamination from the semimuonic decay of the K_L^0 (where β indicates the rejection factor against the unwanted decay), $N(l_{\pi^+\pi^-} > l_{\pi^0\pi^0})$ will be increased by $\Delta N = \beta N_{back}$. In our case, taking into account all the branching ratios involved, the relative rate would be $N_{back}/N_{signal} \sim 70$. The added error

on the asymmetry due to this background subtraction, is $\alpha \times \beta \times N_{back}/N_{tot}$, where α is the relative accuracy with which the background is known.

If we require a rejection ratio of 1×10^{-5} for this decay, we would allow an uncertainty on βN_{back} up to 100%: a lower rejection rate would demand a better knowledge of this contamination, the scaling law being linear. Also in this respect, the double ratio method is favoured, for the greater analyzing power.

The detector acceptance is another important item to discuss since a detailed knowledge of this parameter is needed, for both the K_L^0 and the K_S^0 decays. The decay *fiducial* volume for the K_L^0 has to be known very precisely in order to meet the requirements previously stated for the systematic error: the boundaries must be defined to 1 mm (inner) and 2 mm (outer).

When designing the apparatus, as noted before, further important factors are the uniformity of response and the resolutions: the average decay path is very different for K_L^0 and K_S^0 (0.6 and 342 cm respectively), and for *each* decay channel the acceptance must be controlled at the few 10^{-4} level. Keeping under control the acceptance and all the efficiencies and resolutions will represent a major challenge for the experimenters. On the other hand, a measurement at the top of a resonance has the advantage of a very high signal to background ratio and the kinematics of the chain of two–body decays is well overconstrained. These will be in the end the winning factors for reaching the goal we have set forth.

4. The Detector

A conceptual design of a detector able to fulfill the requirements we have indicated in the previous chapter, should be matched to the characteristics of the events to reconstruct. The decay modes we are interested in are:

$K_S^0 \to \pi^0\pi^0$ $\quad K_S^0 \to \pi^+\pi^-$ $\quad K_L^0 \to \pi^0\pi^0$ $\quad K_L^0 \to \pi^+\pi^-$

$K_L^0 \to \pi^+\pi^-\pi^0$ $\quad K_L^0 \to \pi^0\pi^0\pi^0$ $\quad K_L^0 \to \pi^-\mu + \nu$ $\quad K_L^0 \to \pi^- e + \nu$

The relevant spectra are shown in fig. 1

The experimental apparatus must be able to track π's of momenta between 50 and 250 MeV/c; detect with very high efficiency γ's with energy as low as 20 MeV and measure the energy of electromagnetic (e.m.) showers with a resolution $\delta E_\gamma / E_\gamma \sim 0.15$ at 100 MeV.

We shall see later in more detail how much could be gained if the detector had the ability of determining the showers' conversion point. Particle identification is also needed since muon and electron rejection of at least 50 to 1 must be provided in order to reduce to an acceptable level the background to the $\pi^+\pi^-$ channel, due to the semileptonic decay of the K_L^0.

Most important is the choice of the size of the detector decay volume. The value of $\beta\gamma c\tau$ for K_L^0 from ϕ's decaying at rest is $\sim 342cm$. The fiducial volume of the detector (visualized here as a sphere) cannot have a radius smaller than 1 m in order not to loose too much counting rate while a radius over 2 m would push the size (and the cost) of the apparatus to unreasonably big values. We will therefore tentatively define our decay volume as a sphere of 1.5 m radius. This implies that close to 35% of the K_L^0 decays can be detected.

The general features of the detector are the same as for the *standard* general purpose collider apparatus: a cylindrical structure surrounding the beam pipe and consisting of a tracking device, a particle identifier, an electromagnetic calorimeter, a solenoidal magnet and a muon identifier, more or less in order of increasing radius. The overall dimensions are quite respectable: 5 m radius, and

10 m length.

4.1 THE TRACKING SYSTEM

Given the low momenta of the K^0 decay products and the large decay volume needed, momentum measurement in the tracking chamber will not be limited by spatial resolution but will be affected by multiple scattering.

There are two only two ways for reducing multiple scattering effects:

1. Very high magnetic field (multiple scattering scales as $1/B$).
2. Very *transparent* detector.

The first solution cannot be pursued in our case, since too many tracks will curl up in a high field and will not reach the particle identification device.

The tracking chamber's size must be chosen with these criteria: the outer radius should be considerably larger than the external boundary of the fiducial decay volume, to allow a comparable resolution for all the tracks we need to measure; the inner radius should be small enough to provide a good resolution in measuring the K^0_S decay vertex.

A magnetic field of at least 1 kG is needed in order to obtain an adequate momentum resolution; with a chamber covering radially from 15 to 200 cm., the cut-off for curling tracks would be $\sim$ 60 MeV/c for tracks originating near the collider luminous region (I.P.) and $\sim$ 15 MeV/c for tracks starting at the outer boundary of the decay volume.

In order to keep the momentum resolution for tracks of different lengths as uniform as possible, it might be necessary to have radially increasing cell density in the tracking chamber. Given the high repetition rate of the machine, we propose an axial drift chamber with a helium-based gas mixture as the appropriate choice.

Fig. 2 shows a possible, but not yet optimized scenario for a drift chamber operating in a 1 KG axial field and with a 0.15 mm point resolution. A reduction

of the fiducial volume improves the uniformity of the detector at the cost of rate. An optimization is possible only after the final assessment of both the machine and detector parameters.

Finally we consider the resolution in the determination of the K_S^0 vertex. If tracking begins at a radius of ~ 10 cm, the impact parameter resolution is ~ 0.15 mm (including the multiple scattering contribution of a 0.5 mm thick Be beam pipe), and the K_S^0 decay path could be adequately measured. The use of a gas tracking device would also minimize the amount of material along the K_L^0 path, thus reducing the amount of regeneration which would be a more serious problem if solid state silicon based vertex detectors were used.

4.2 CALORIMETRY

Calorimetry is the most demanding item for this detector: the reconstruction of the $\pi^0\pi^0$ decay mode of a 110 MeV/c momentum K_L^0, and the determination of its decay point are indeed a formidable challenge: the requirements for the vertex spatial resolution and for the background suppression against the $\pi^0\pi^0\pi^0$, to be achieved at the $\sim 1 \times 10^{-5}$ level, require a state of the art detector.

The problem of the background rejection can be solved by a really complete solid angle coverage and by using a device able to detect γ's down to 20 MeV energy. The design of the machine interaction region is such that the calorimeter can cover all of the solid angle but a 150 mrad cone around the beam direction. If all the available area will be covered by the calorimeter's active device, a rejection ratio $\sim 5 \times 10^{-5}$ against the $K_L^0 \to \pi^0\pi^0\pi^0$ decay can be obtained counting the number of detected γ's. The total measured energy could then be used to dispose of any remaining background.

The hardest experimental problem to be solved is the determination of the K_L^0 decay point. The ordinary technique used to reconstruct π^0 and K^0 decay vertices is to use the π^0 and/or K^0 mass constraint. This technique however, as can be seen in fig. 3 , loses some of its power at low energy, where wide

opening angles imply a more important role for spatial measurements, compared to energy measurements. It is worth to stress that the mass constraint technique yields vertex resolutions linearly dependent on both energy resolution and flight paths.

The importance of spatial measurements is furthermore enhanced if a complete kinematic fit of the event is performed: a very interesting feature one obtains after kinematic fitting[38] is that the vertex resolutions is not only improved, but becomes quite independent of both the energy resolution of the calorimeter and the decay path length itself. In fig. 4 one can see how insensitive to the decay length the actual vertex resolution is for the $\pi^0\pi^0$decay of the K_L^0. Fig. 5 shows the vertex resolution for the two body neutral decay of the K_L^0 plotted versus the shower's conversion point resolution, with different energy resolutions: here too we notice a remarkable *robustness* of the vertex resolution.

Fig. 6 shows the performance of an *extremely good* calorimeter ($\delta E/E = 0.01/\sqrt{E}$) for the $\pi^0\pi^0$ decays (each event contributes four entries to the plot). Fig. 7 shows the reconstructed γ energy after fitting; the calorimeter resolution in this case is five times worse than in the previous case.

The requirements on the energy resolution for the e.m. calorimeter are set by the need of correctly pairing the γ's from the neutral decay of the K_S^0 and of achieving an efficiency as close to one as possible in the kinematic fitting of the events: our preliminary analyses shows some dependence of the fitting efficiency on the calorimeter resolution.

Realistic, although sophisticated imaging calorimeters, could give the needed resolutions (15% at 100 MeV and 0.5 cm in the conversion point). Techniques to be used are based either on liquid homogeneous calorimeters[39] or on very fine sampling gas calorimeters.[40]

In the section devoted to systematics we will address the minimum vertex resolution needed to reach the level of systematics insensitivity mentioned in section 3.3.

An interesting solution is also the one envisaged by Batignani *et al.*,[41] who propose to build a calorimeter with good timing resolution, to take advantage of the *slow* speed of the K_L^0 ($\beta \sim 0.25$), and measure the time of flight between the e^+e^- interaction and the γ's energy deposition. A resolution of 500 psec in the time measurement would correspond to $\sim$ 4 cm in the decay distance. The device should, however, be able to measure the conversion point, in order to avoid the uncertainty in the photons path length (33 psec for each cm).

Since the e.m. calorimeter is the crucial element of the detector, we believe that a robust research and development program should be started as soon as possible, so that a well optimized solution can be adopted in the final design. As a last remark on this subject, we would like to point out that the accurate reconstruction of low energy π^0's is a common problem for all the e^+e^- *factory* projects now being considered at various laboratories: a b-factory, for example, requires performances only marginally different from those of a ϕ–factory.

4.3 Particle identification

In order to reduce the background to the $K_L^0 \to \pi^+\pi^-$ channel to a level compatible with the precision required, the rejection factor against the *unwanted* semileptonic decays must be of the order of 1.5×10^{-5} (1.0×10^{-5} for $\pi e \bar{\nu}$).[35] Topological and kinematical cuts are in this case far from being adequate (by a substantial factor) and should be complemented by some form of particle identification.

In the previous section we have discussed how demanding are the requirements on the electromagnetic calorimeter: given the low energy of the photons to be measured, the addition of a particle identifier in front of the calorimeter doesn't appear as a viable possibility. It appears therefore that the e.m. calorimeter itself must be used to provide $\pi - \mu e$ discrimination.

This appears quite feasible. We assume for example, a homogeneous liquid argon calorimeter. Such device can measure with good resolution the total kinetic

energy of charged particles and their range. For a 200 MeV/c momentum track, the difference in kinetic energy for a π or a μ is $\sim$ 14%, and the range difference is roughly 30%. Since straggling is $\sim$ 3%, we conclude that the needed additional rejection factor can be achieved. The results of preliminary simulations obtained with the GEANT program are shown in fig. 8 . The kinetic energy difference between a pion and an electron is large enough, for the momentum range of interest, that the electron identification should not pose real problems.

In conclusion, particle identification can be achieved at the desired level of accuracy if we use a calorimeter having a high longitudinal segmentation and a reasonably good energy resolution.

5. Acceptance, resolutions and systematics

A review of the physics program at a ϕ–factory would not be a comprehensive one if the problems related to the detector acceptance, the efficiencies, and the experimental resolutions were not addressed. We wish to emphasize, once again, the uniqueness of the ϕ–factory approach to the ϵ'/ϵ measurement, in contrast to the measurements with K_L^0 beams: the kinematically simple and precisely prepared initial $K_S^0 K_L^0$ state and the very large signal to background ratio, allow the determination the detector acceptance, and all relevant efficiencies and resolutions, from the data themselves, using measured quantities.

5.1 Determination of efficiencies and resolutions

In the following, we will discuss how these parameters can be determined with the accuracy discussed in section 2.3.

As an example, we describe the procedure that allows the determination of charged particles tracking and vertex finding efficiencies as a function of the K_L^0 decay path. For the single track reconstruction we can proceed as follows: $K_L^0 K_S^0$ events can be *tagged* from the observation of $K_S^0 \to \pi^+\pi^-$ decays; with a luminosity of 10^{32} cm^{-2} sec^{-1}, 1.5×10^9 such events will be collected in one year of running, providing a large data base for evaluation of efficiencies.

In this sample there will be $\sim 1.2 \times 10^9$ K_L^0 decays into two charged prongs; if we divide our spherical decay volume into *shells* 15 cm thick, we expect to have $\sim 50 \times 10^6$ decays originating in each shell.

Using the well known K_L^0 lifetime value, it's possible to evaluate the expected number of decays in each shell and compare with the number of measured tracks; given our sample's size, the statistical error on the tracking efficiency for each 15 cm interval, will be $\sim 1.5 \times 10^{-4}$. The error resulting from the less than perfect knowledge of the K_L^0 lifetime is of the same order of magnitude as the statistical error quoted above, given the small size of the extrapolation distance in moving

from one shell to the next with respect to the K_L^0 decay distance. With the same data it's also possible to measure the K_L^0 vertexing efficiency, as a function of the K_L^0 decay path, by counting the reconstructed vertices in each shell, and comparing to the expected number.

We need, of course, to use these efficiencies to extract the branching ratio BR($K_L^0 \to \pi^+\pi^-$) from the relatively small number of observed events in this channel. The tracks from this decay will have a slightly harder momentum distribution than the ones from the 3-body modes, but the difference is small enough to make us confident that neither the single track or the vertex efficiency can be significantly affected.

A similar method can be used to evaluate the π^0 acceptance and reconstruction efficiency; in this case we can start by *tagging* a sample of K^+ K^- events where one of the two kaons decays in the detector, leading to a final state $K^\pm$ $\pi^\mp$ π^0. The two charged prongs completely determine the π^0 energy, momentum vector and point of origin. Again the sample of events of this type is large enough to allow the efficiency determination with the necessary accuracy. At a distance of 1 m. from the I.P., there would be $\sim 10^7$ tagged π^0 available in a 15 cm thick shell, for calibration and acceptance measurements for a one year run at the initial luminosity.

The two method described above do have the statistical potential to determine the efficiency and resolution of the various components of the apparatus at the needed level of precision. It is worth to stress that because experimental data collected during the actual run would be used to evaluate efficiency, eventual upgrades of the machine will automatically provide better determination of such parameters if and when an improved estimate of them would be needed to reduce the systematic errors.

As a last point concerning the determination of efficiencies, we would like to stress that the neutral decay products of K_L^0 and K_S^0 will be detected in the same calorimeter and the different decay length of the two kaons will not affect

at all the basic detection of the resulting γ's. The situation is somehow different in the case of the charged channels. K_L^0 decays will tend to populate the outer part of the tracking chamber, it is however difficult to imagine how a common gas volume would show significant inhomogeneity as a function of radius in its performances. Should such a mechanism develop, the tools to detect it, at the needed level of sensitivity, are automatically built–in.

5.2 Geometric Acceptance

Two basic effects lead to experimental correction to the exponential behavior of the decay curve for the K_L^0 and K_S^0:

1. Finite beam dimensions.

2. Vertexing resolution.

The effect of the first item is extremely small, at least in the plane perpendicular to the beam direction: as a matter of fact the expected beam dimension would be ~ 1 mm (radial) and ~ 20 μm (vertical) so that no effect is foreseen on the decay distribution. The longitudinal dimension of the luminous region is expected to be ~ 2 cm, and could in principle smear the decay distribution and alter the total counting rate (especially of the K_S^0decay).The actual distribution of the longitudinal coordinate, however, can be measured to an extremely high degree of accuracy from Bhabha scattering for instance, and folded in the experimental decay distribution.

With respect to the second point we must address separately charged and neutral decays. In the charged decays case, the drift chamber spatial resolution and the opening angles of the decay products are such that the expected 2-tracks vertex resolution is well below the 1 mm level, low enough that smearing effects would be completely negligible even in the K_S^0 case ($l_S \sim 6$ mm).

The totally neutral decays pose the hardest challenge in the determination of the decay vertex. In the calorimeter section we have seen that the vertexing

resolution for the $\pi^0\pi^0$ decays of K_S^0 and K_L^0 is at the level of $\sim 1-2$ cm using a very sophisticated calorimeter and the kinematics of ϕ decay. The loss in total rate resulting from the finite vertex resolution in the case of the K_S^0 decay is shown in fig. 9 : a cut in decay volume at 6 cm would result in a loss of $\sim 1 \times 10^{-3}$, but the actual decay distribution can be measured with a relative accuracy of 1×10^{-3} so that the resulting systematic error is of the order of 1×10^{-6}.

Concerning the fiducial volume definition for $K_L^0 \to \pi^0\pi^0$, as can be seen from fig. 10 the losses can be kept at the level of few $\times 10^{-4}$, allowing also for some non-gaussian tails, provided that the vertex resolution is of the order of 1 cm. In this case the eventual correction is more difficult to evaluate as the reconstruction of vertices has to be done with γ's originating near the face of the calorimeter, which might therefore enter at grazing incidence. The vertex resolution needed, for totally neutral decays of the $K_L^0 K_S^0$ is in conclusion of the order of 1 cm: with this value geometric acceptance will be known at an accuracy level which will imply a systematic error on the double ratio of the order of 5×10^{-4} which in turn will reflect in a systematic error on ϵ'/ϵ of 1×10^{-4}.

5.3 The systematics in a K_L^0 beam experiment

To conclude this chapter we would like to quickly review the systematic uncertainties typical of a fixed target experiment, and compare them with what can be anticipated for a ϕ–factory experiment. To do that we will use the published analysis of NA–31.[7] The biggest contribution to the systematic error of the double ratio for these type of experiments (neglecting background subtraction $\sim$0.2%), is due to the relative energy scale, $\sim$0.3%. The K_L^0 and K_S^0 momentum spectra must be determined from the observed decays and reflect uncertainties in the knowledge of the energy scales for charged and neutral decay products. This systematic uncertainty is of course absent in the ϕ–factory approach, where produced kaons are monochromatic. The next biggest systematic uncertainty is due to subtraction of accidentals, $\sim$0.2%. This error is also absent in an experiment at a ϕ–factory. Next generation apparata at FNAL and CERN will

reduce detector-related uncertainties; the use of more intense beams, however, will lead to an increase of the subtraction due to accidentals. Other contribution at the level on 1×10^{-3} in the double ratio listed in reference 7 will not be present in a ϕ–factory experiment with the exception of calorimeter instability and acceptance evaluation.

In the ϕ–factory approach the acceptance has to be known at the 5×10^{-4} level, while in the K_L^0 beam experiments acceptance differences cancel to first order. To achieve the ultimate accuracy, corrections have ultimately to be *computed.* At a ϕ–factory the data themselves are used to *measure* the acceptance with little or no need of calculations.

6. Conclusions

In this summary we have outlined the more important features of the physics program which could be carried out at a ϕ–factory able to deliver an average luminosity of $\sim 10^{32}$ cm^{-2} sec^{-1} and we have proved that the physics output from such a facility will be extremely interesting. The measurement of ϵ'/ϵ that can be performed at a ϕ–factory is very important in its own right, since is obtained in completely different conditions with respect to the measurements achievable at K_L^0 beams. Furthermore, such a facility holds the promise of reducing by a factor two the overall error on ϵ'/ϵ, in one year of running.

In many respects the ϕ–factory approach to K physics is similar to the one proposed at LEAR. In the ϕ–factory case, however, the signal to background ratio for all sorts of K physics is 100 to 1, compared to 1 to 1000 typical of antiproton annihilations at rest.

Several interesting K physics topics will also be addressed at a ϕ–factory. Depending on luminosity there is a long list of rare K_S^0 decays which can be studied in an unique environment, this line of research nicely complementing the one which is being pursued at kaon factories, where *ultra–rare* decays are searched for with specialized detectors.

Moreover all the e^+e^- physics in the energy range up to $\sim$ 1 GeV will be studied in such detail from the statistical point of view that very interesting results (*i.e.* hadronic correction to the muon gyromagnetic ratio, low lying narrow states *etc.*) could be extracted from the data.

Limits on the ν_μ mass could be improved substantially, with luminosities on the high side of what is anticipated for the project.[42]

The experimental apparatus presents many interesting challenges, especially the electromagnetic calorimeter does require performances quite impressive. The electronics and data acquisition for this detector will be a very interesting testing ground for the next generation of high energy colliders as the inter–bunch timing

is roughly the same as LHC/SSC and the data acquisition should be able to *digest* $1Khz$ of good data.

CP violation measurements are the ones which set the requirements on the experimental apparatus: measurements other than CP violation can be carried out by the same apparatus optimized for CP violation: performances will be exuberant for the task.

We would like to emphasize that, in addition to the very interesting physics opportunities that a ϕ–factory would offer, the training potential for young physicists of such a machine is enormous and must be considered an added bonus to the entire program.

ACKNOWLEDGEMENTS

We would like to acknowledge Prof. Nello Paver's work on the $\eta - \eta'$ mixing section.

The help and encouragement of Prof. Paolo Franzini throughout the entire study group and his critical and constructive reviewing of the manuscript are also gratefully acknowledged.

REFERENCES

1. T.D.Lee C.N.Yang Phys. Rev. **50**, 263, (1956)
2. N. Cabibbo, Phys. Rev. Lett.**10**, 531, (1963); N. Cabibbo Phys.Rev. Lett. **12**, 62, (1964)
3. S.L.Glashow,J. Iliopulos,L. Maiani Phys. Rev **D2** , 1285, (1970)
4. J. Christenson, J. Cronin, V. Fitch, R. Turlay, Phys. Rev. Let. **138**, (1964)
5. M. Kobayashi, K. Maskawa Prog. Theor. Phys. **49**, 652, (1973); L. Maiani Hamburg 1977, see also the pioneer work of Cabibbo, 1963
6. L. Wolfenstein Phys..Rev.Lett.**13** 562,(1964)
7. Burkhardt et al. P.L. **B209**, 169, (1988)
8. B. Winstein 14th International Symposium on Lepton and Photon Interactions, Stanford 1989.
9. see for instance H. Lipkin Phys. Rev.**176** 1715 (1968),
   I. Dunietz, J. Hauser, J.L.Rosner , Phys. Rev. **D35** 2166, (1987).
10. J.Bernabeu,F.J. Botella and J.Roldan Phys. Lett. **B 211**,266, (1988)
11. D. Cocolicchio , G.L. Fogli, M. Lusignoli, A. Pugliese, "CP violation measurements at the ϕ resonance." Contribution to this Report and CERN-TH 5610/89
12. D. Cocolicchio," A ϕ–factory to understand light and narrow mesons." Contribution to this Report.
13. A.J. Malensek, Fermilab Report FN-341
14. M. K. Craddock Proceedings of the International Conference on High Energy Accelerators, (Tsukuba 1989)
15. R. Battiston ,D. Cocolicchio, G. L. Fogli, N. Paver, "Status and perspectives of K decay physics." Contribution to this Report.
16. A.A. Bel'kov, G. Bhom, D. Ebert and A.V. Lanjov, Phys. Lett. 232B (1989) 118; A.A. Bel'kov, G. Bhom, D. Ebert and A.V. Lanjov, Serpukhov preprint 89-11 (1989).
17. F. Buccella, G. D'Ambrosio and M. Miragliuolo , " CP violation in the decays of neutral kaons into two photons". Contribution to this Report.
18. M. Greco, Nuovo Cimento **100A** 597, (1988)
19. J. Bailey *et al.*Nucl. Phys. **B150** 1 , (1979)

20. T. Kinoshita, B. Nižićand Y. Okamoto, Phys. Rev. D **31**, 2108 (1985), and reference therein, see in particular their reference 28.

21. R. Jackiw and S. Weinberg, Phys. Rev D **5**, 2396 (1972); G Altarelli, N. Cabibbo and L. Maiani, Phys. Lett. **40B**, 415 (1972), I. Bars and M. Yoshimura, Phys. Rev. D, **6**, 373 (1972); W. A. Bardeen, R. Gastmans and B. E. Lartrup, Nucl. Phys. **B46**, 319 (1972).

22. Brookhaven experiment E821, Boston, BNL, CCNY, Columbia, Cornell, Heidelberg, LANL, Michigan, Sheffield, Tokio, KEK, Riken, Yale collaboration, V. Hughes et al.

23. P. Franzini, '89 Electroweak Interactions and Unified Theories, XXIV Rencontre de Moriond, J. Tran Than Van Ed., Edition Frontière, Gif-sur-Yvette, 1989

24. R. Baldini-Celio, M.E. Biagini,S. Bianco, M. Spinetti, A. Zallo, S. Dubnička, "Kaon physics at a ϕ factory." Contribution to this Report.

25. J. L. Rosner, Phys. Rev. **D27** (1983) 1101; H. J. Lipkin, Phys. Lett. **B67** (1977) 65.

26. F. J. Gilman and R. Kauffman, Phys. Rev. **D36** (1987) 2761; **D37** (1988) 3348; and references therein.

27. J. Donoghue, B. R. Holstein and Y.-C. Lin, Phys. Rev. Lett. **55** (1985) 276.

28. P. Langacker and H. Pagels, Phys. Rev. **D10** (1974) 2904; J. Gasser and H. Leutwyler, Nucl. Phys. **B250** (1985) 465.

29. D. Andrews et al., Phys. Rev. Lett. **38** (1977) 198.

30. Particle Data Group, Phys. Lett. **B204** (1988) 1.

31. Y. M. Aulchencko, Phys. Lett. **B186** (1987) 432.

32. M. Calvetti,"Relazione sulla situazione sperimentale della violazione di CP nei decadimenti dei mesoni K neutri." Contribution to this Report.

33. A. Nappi,"ϵ'/ϵ measurements at hadron machines.", Contribution to this Report.

34. I. Dunietz, J. Hauser and J. L. Rosner Phys. Rev. D **35** 2166 ,(1987).

35. G. Barbiellini and C. Santoni"A measurement of ϵ'/ϵ at a ϕ–factory." Contribution to this Report and CERN-EP/89-88.

36. M. P. Bussa and G. Carboni, "Statistical accuracy on the measurement of ϵ'/ϵ at a ϕ–factory." Contribution to this Report.

37. S. Tazzari *et al.* "The Ares design study"

38. A. Calcaterra ,R. de Sangro , P. De Simone, "Measurement of K_L^0 decay point and mass via kinematic fit" , Contribution to this Report.

39. A.Calcaterra, R. de Sangro, P. De Simone, M. Piccolo, "Low energy γ calorimetry: Monte-carlo simulations" L.N.F. Nota Interna (in preparation)

40. A. Del Guerra, W. R. Nelson, C. Rizzo, P. Russo, "Monte Carlo study of the development of a low energy electromagnetic showers: preliminary results." Contribution to this Report.

41. G. Batignani, F. Forti, M. A. Giorgi, and G. Triggiani, "A modern apparatus for the study of the K^0 $\bar{K}^0$ system from the $\phi(1020)$ production in e^+e^-." Contribution to this Report.

42. P.F. Loverre,"Measurement of the ν_μ mass at a ϕ–factory" Contribution to this Report.

TABLE I Branching ratios of some rare kaon decays.

mode	theory	experiment
$K_S \to \gamma\gamma$	2×10^{-6} [1.4×10^{-6}]	$(2.4 \pm 1.2) \times 10^{-6}$
$K_S \to \pi^0\gamma\gamma$	3.3×10^{-8} [$10^{-8} - 10^{-9}$]	———
$K_S \to e^+e^-\gamma$	3.2×10^{-8}	———
$K_S \to \mu^+\mu^-\gamma$	7.5×10^{-10}	———
$K_S \to \pi^0e^+e^-$	$5 \times 10^{-9} - 5 \times 10^{-10}$ [10^{-8}]	$< 4.5 \times 10^{-5}$
$K_S \to \pi^0\mu^+\mu^-$	$1 \times 10^{-9} - 1 \times 10^{-10}$	———
$K_L \to \gamma\gamma$	[10^{-4}]	$(4.9 \pm 0.4) \times 10^{-4}$
$K_L \to \pi^0\gamma\gamma$	6.8×10^{-7} [$< 10^{-7}$]	$< 2.7 \times 10^{-6}$
$K_L \to e^+e^-\gamma$	9.1×10^{-6}	$(1.7 \pm 0.9) \times 10^{-5}$
$K_L \to \mu^+\mu^-\gamma$	2.3×10^{-7}	$(2.8 \pm 2.8) \times 10^{-7}$
$K_L \to \pi^0e^+e^-$	$10^{-11} - 10^{-12}$	$< 4.2 \times 10^{-8}$
$K_L \to \pi^0\mu^+\mu^-$	$10^{-11} - 10^{-12}$	$< 1.2 \times 10^{-6}$
$K^\pm \to \pi^\pm e^+e^-$	input [10^{-6}]	$(2.7 \pm 0.5) \times 10^{-7}$
$K^\pm \to \pi^\pm\mu^+\mu^-$	6.1×10^{-8}	$< 2.3 \times 10^{-7}$
$K^+ \to \pi^+\gamma\gamma$	$\geq 4 \times 10^{-7}$ [$10^{-6} - 10^{-7}$]	$< 1 \times 10^{-6}$

FIGURE CAPTIONS

1. Relevant momentum spectra for K_L^0 decays
2. Momentum resolution for the proposed central tracker
3. Relative flight path resolution for π^0 as a function of energy from the mass constraint (symmetric decay in the π^0 rest frame)
4. Difference between actual and reconstructed path length vs path length after kinematic fitting
5. Vertex resolution for the $K_L^0 \rightarrow \pi^0\pi^0$ decay as a function of the shower's apex resolution for different energy resolution of the calorimeter
6. δE_γ vs E_γ for the measured γ energy from $\pi^0\pi^0$decays ($\frac{\delta E}{E} = 0.01\frac{1}{\sqrt{E}}$).
7. $\delta\ E_\gamma$ vs E_γ for the fitted γ energy from $\pi^0\pi^0$ decays ($\frac{\delta E}{E} = 0.05\ \frac{1}{\sqrt{E}}$).
8. Range distribution for π's and μ's in a Liq. Ar homogenous calorimeter .
9. Smearing losses in total K_S^0 rate as a function of the fiducial volume for different vertex resolutions
10. Smearing losses in total K_L^0 rate as a function of the vertex resolution

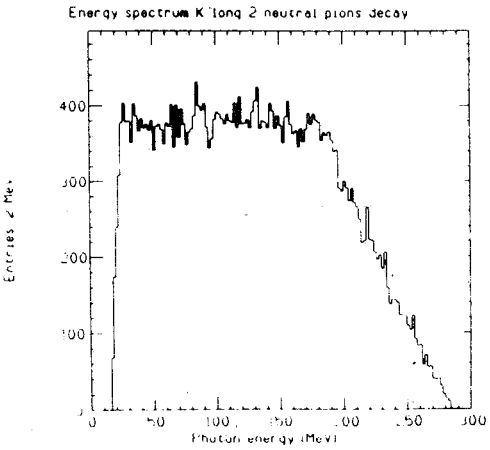
Energy spectrum K long 2 neutral pions decay
Photon energy (MeV)

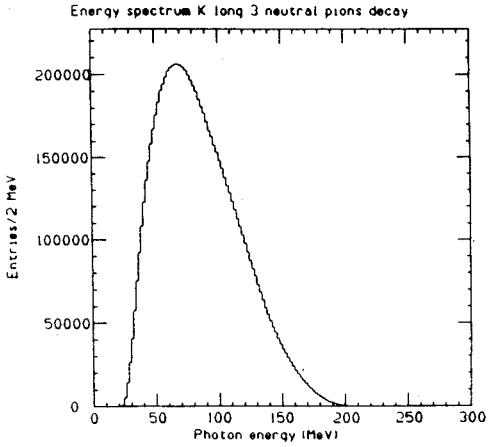
Energy spectrum K long 3 neutral pions decay
Entries/2 MeV
Photon energy (MeV)

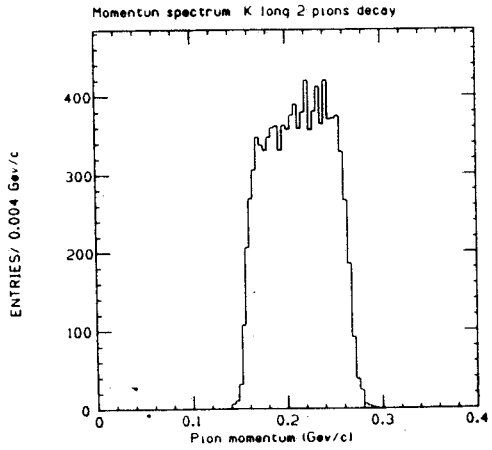
Momentum spectrum K long 2 pions decay
ENTRIES/ 0.004 GeV/c
Pion momentum (GeV/c)

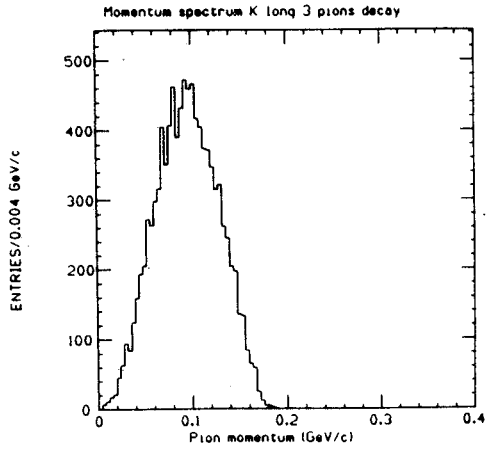
Momentum spectrum K long 3 pions decay
ENTRIES/0.004 GeV/c
Pion momentum (GeV/c)

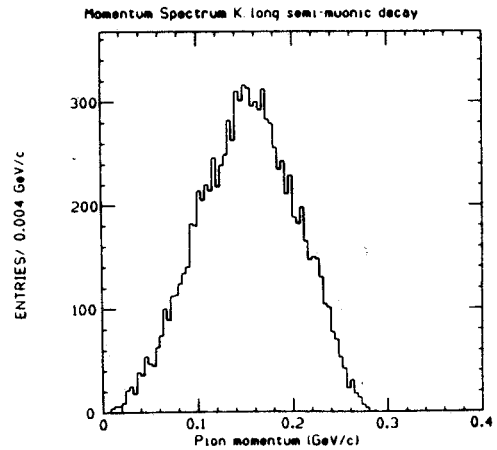
Momentum Spectrum K long semi-muonic decay
ENTRIES/ 0.004 GeV/c
Pion momentum (GeV/c)

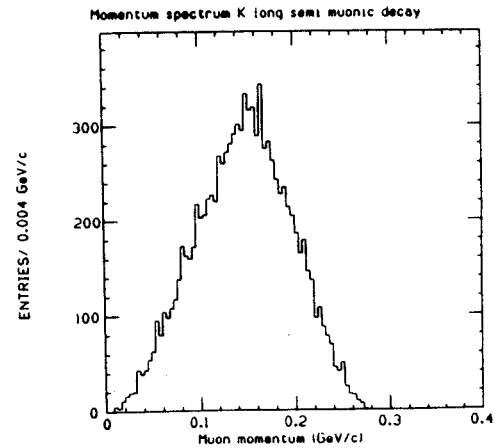
Momentum spectrum K long semi muonic decay
ENTRIES/ 0.004 GeV/c
Muon momentum (GeV/c)

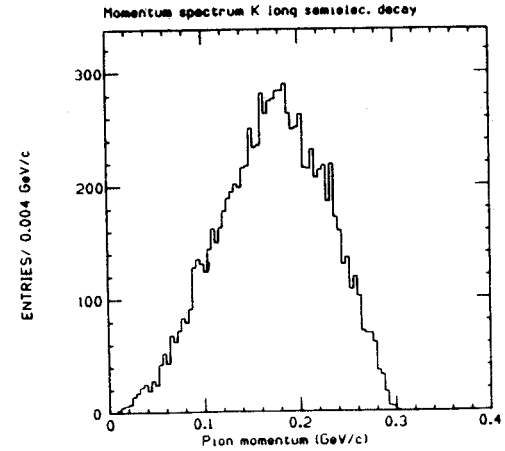
Momentum spectrum K long semielec. decay
ENTRIES/ 0.004 GeV/c
Pion momentum (GeV/c)

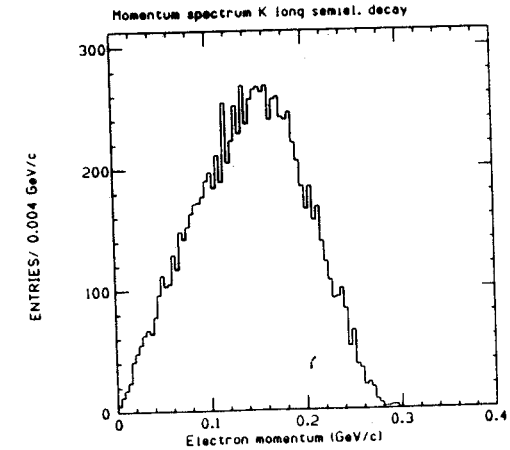
Momentum spectrum K long semiel. decay
ENTRIES/ 0.004 GeV/c
Electron momentum (GeV/c)

FIG. 1

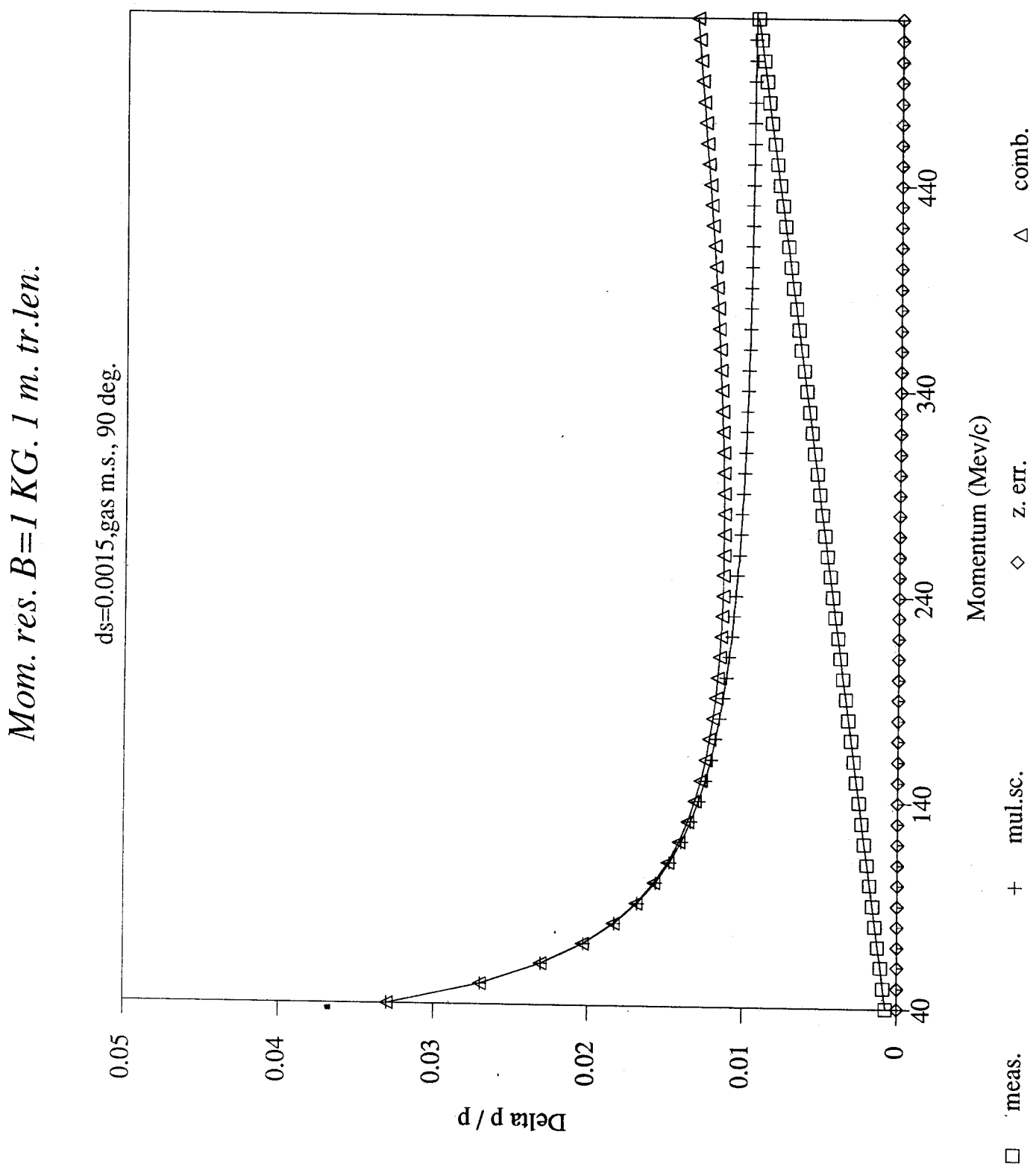
Mom. res. B=1 KG. 1 m. tr.len.
ds=0.0015,gas m.s., 90 deg.
Delta p / p
0.05
0.04
0.03
0.02
0.01
0
40
140
240
340
440
Momentum (Mev/c)
□ meas.
+ mul.sc.
◇ z. err.
△ comb.

FIG. 2

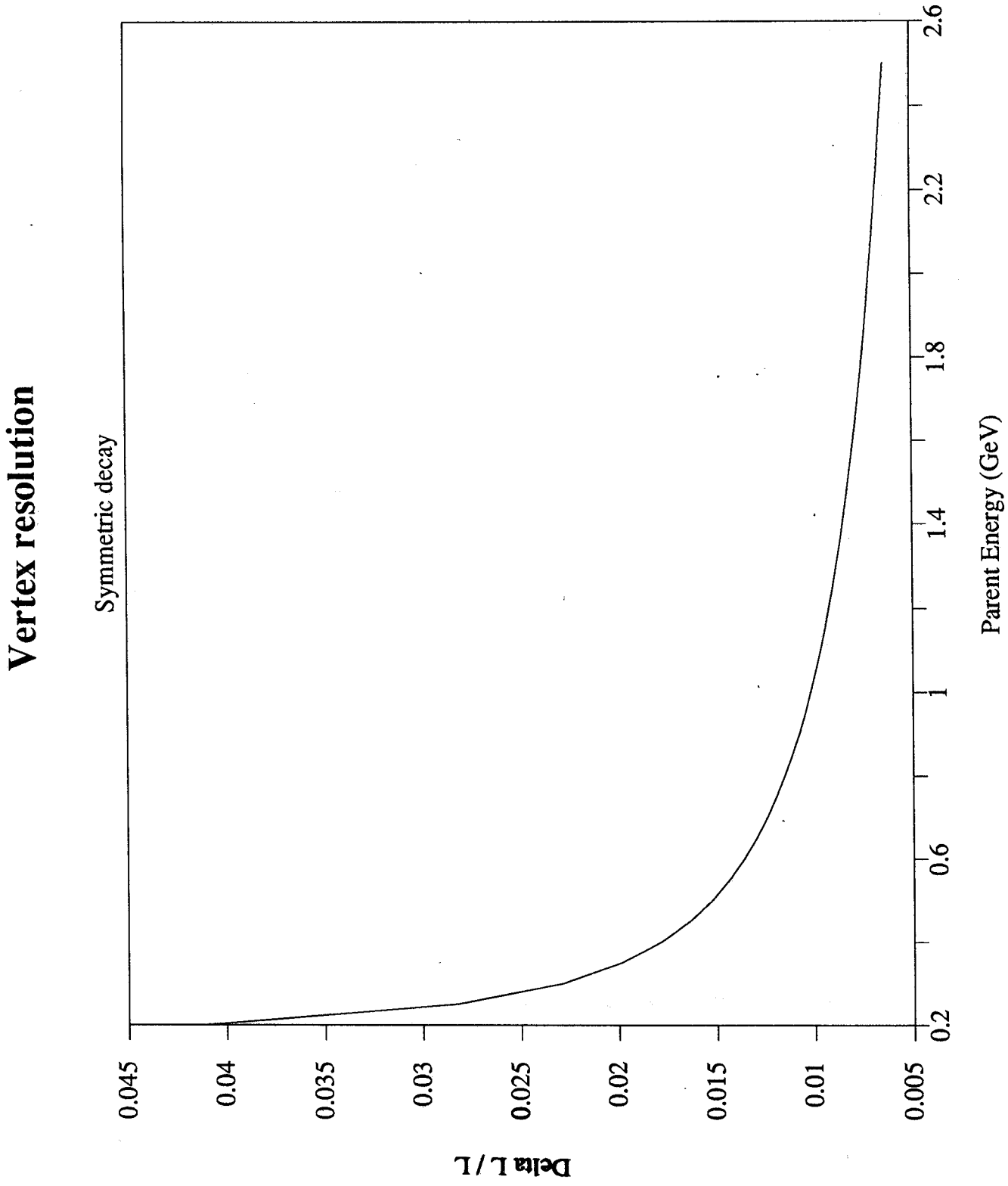
Vertex resolution
Symmetric decay
Delta L / L
0.045
0.04
0.035
0.03
0.025
0.02
0.015
0.01
0.005
0.2
0.6
1
1.4
1.8
2.2
2.6
Parent Energy (GeV)

FIG. 3

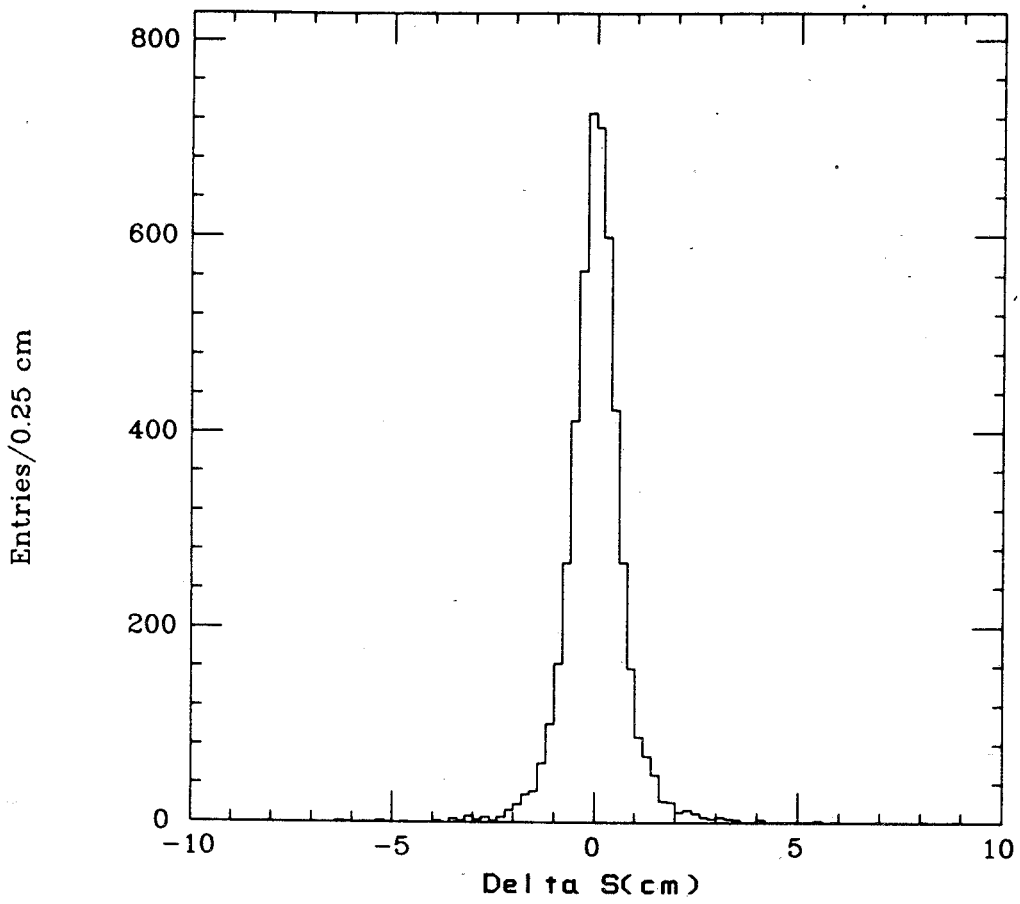
800
600
400
200
0
Entries/0.25 cm
-10
-5
0
5
10
Delta S(cm)

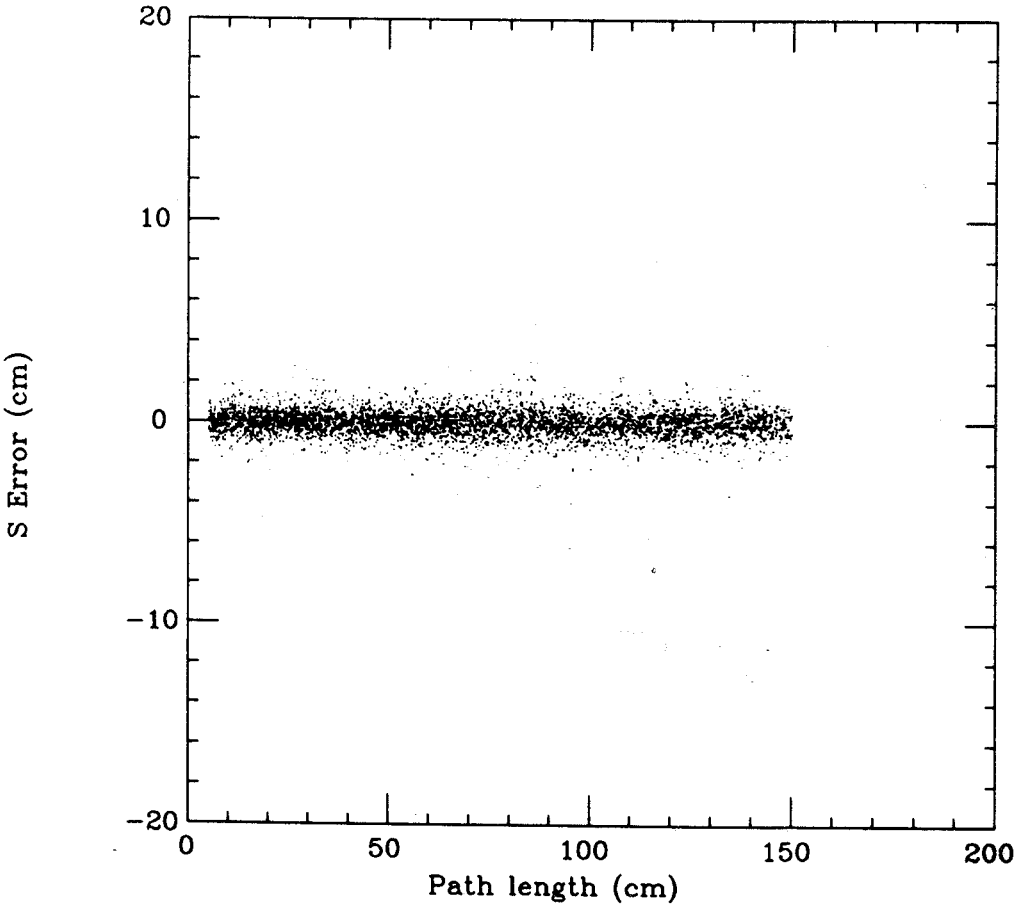
20
10
0
-10
-20
S Error (cm)
0
50
100
150
200
Path length (cm)

FIG. 4

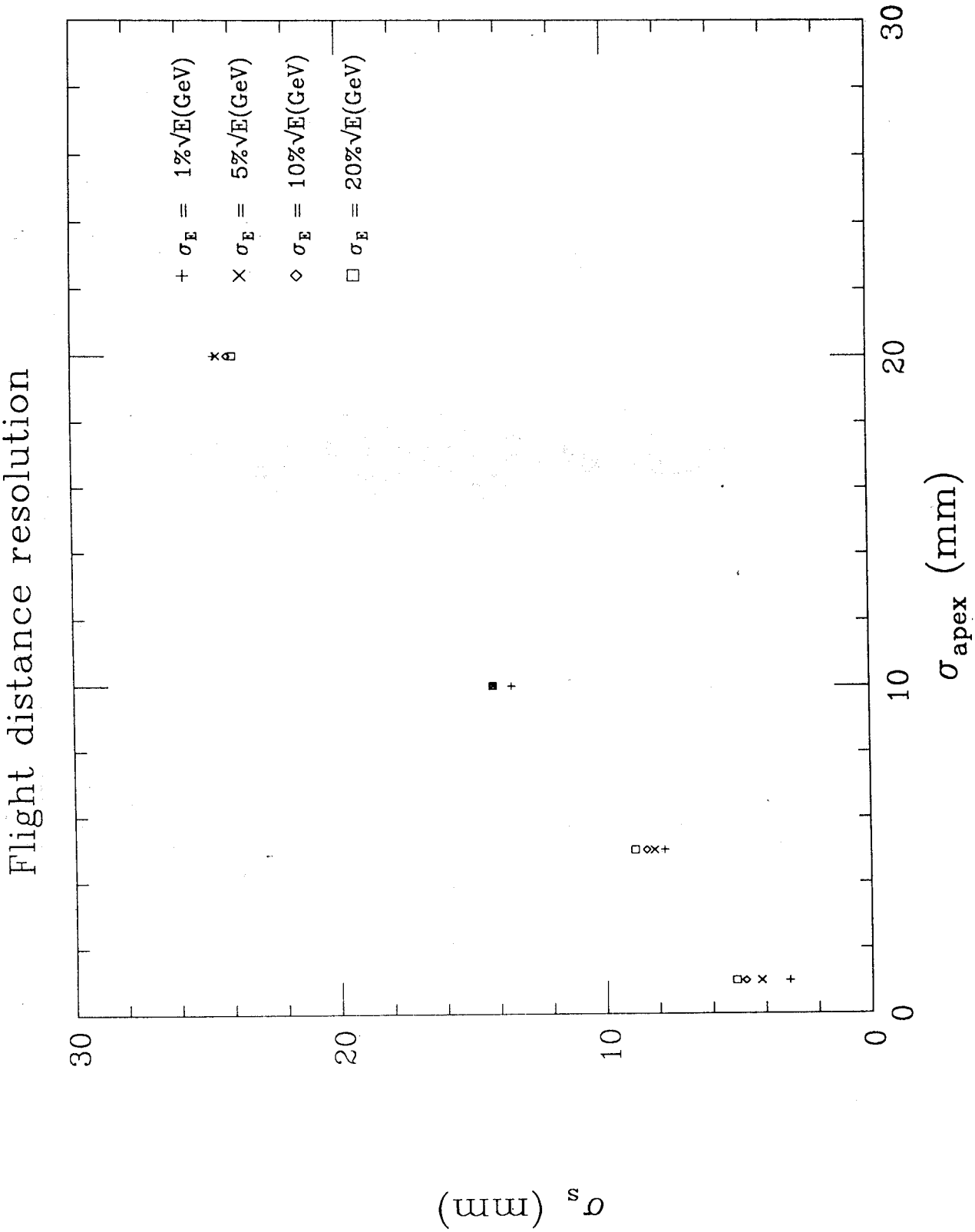
Flight distance resolution
+ σ_E = 1%√E(GeV)
× σ_E = 5%√E(GeV)
◇ σ_E = 10%√E(GeV)
□ σ_E = 20%√E(GeV)
σ_{apex} (mm)
σ_s (mm)
0
10
20
30

FIG. 5

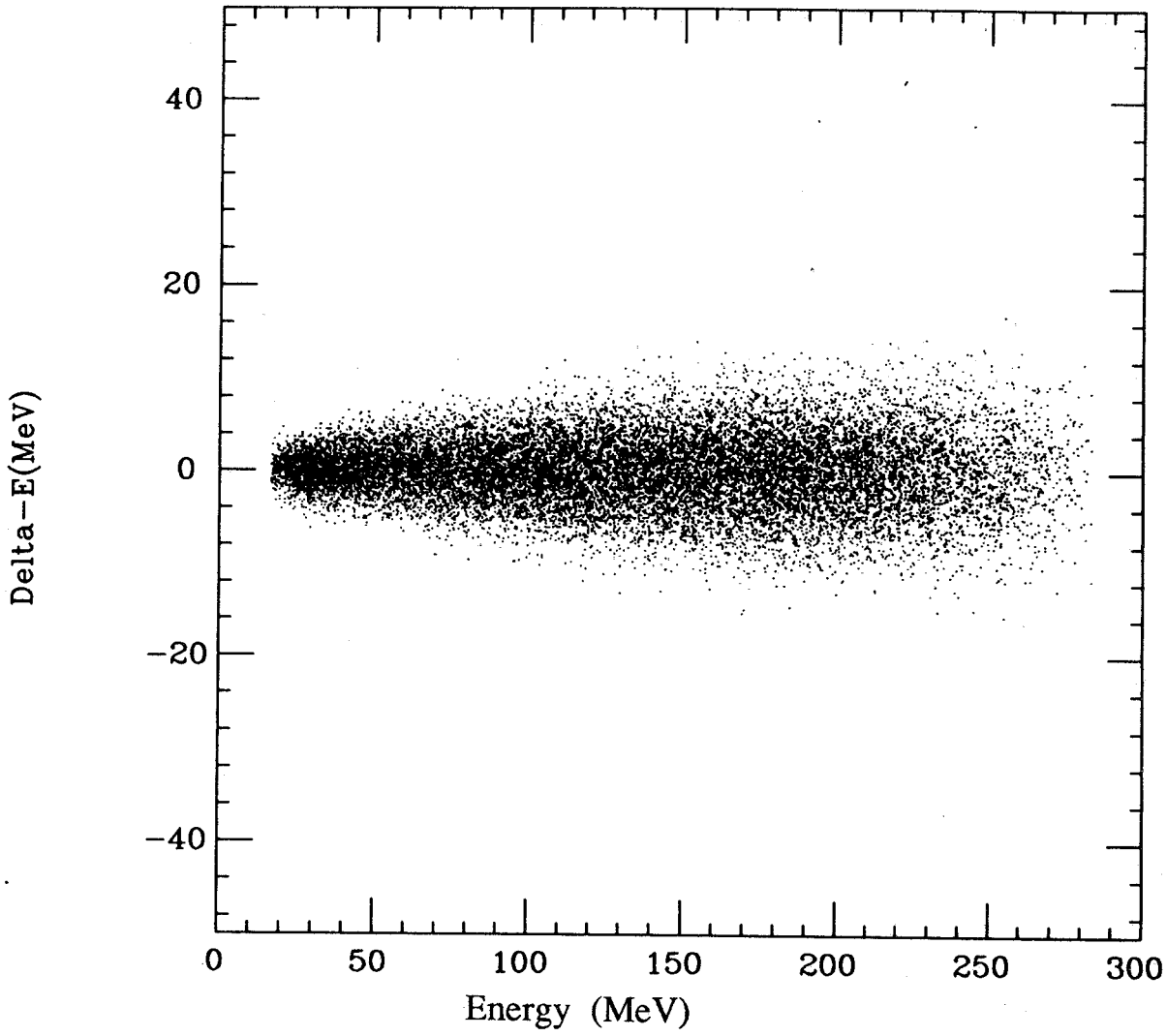

FIG. 6

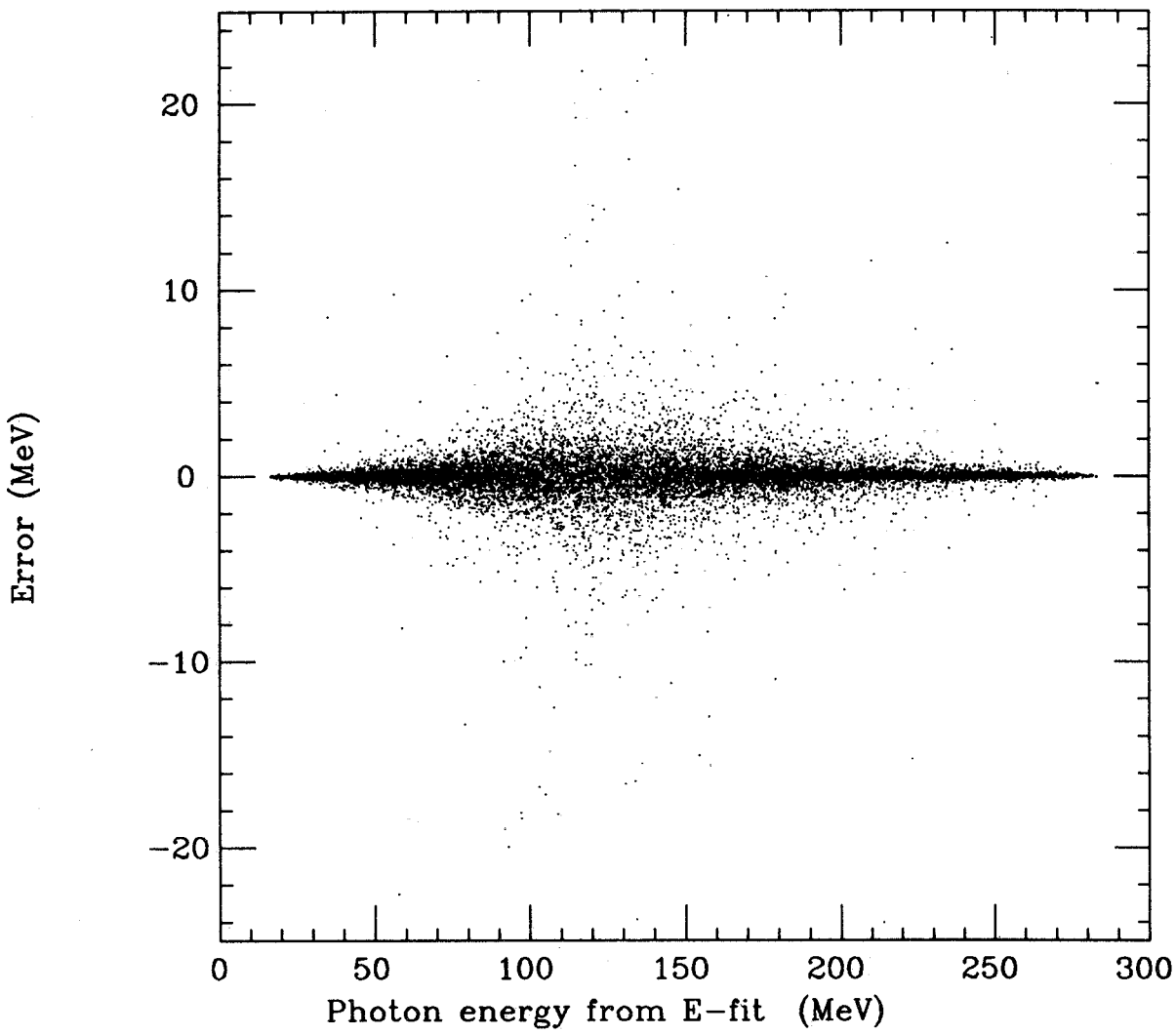
20
10
0
−10
−20
Error (MeV)
0
50
100
150
200
250
300
Photon energy from E−fit (MeV)

FIG. 7

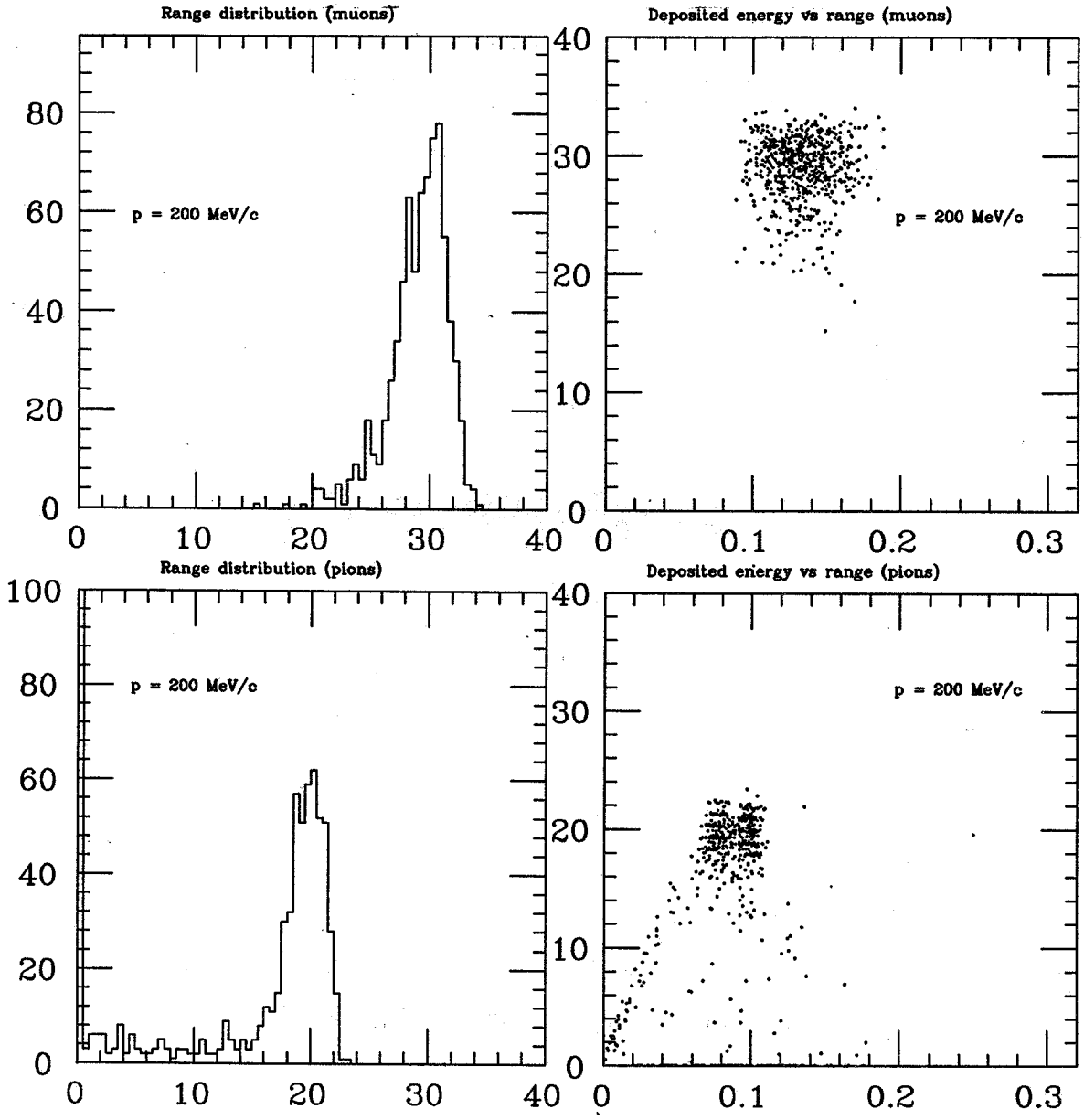
Range distribution (muons)
p = 200 MeV/c
Deposited energy vs range (muons)
p = 200 MeV/c
Range distribution (pions)
p = 200 MeV/c
Deposited energy vs range (pions)
p = 200 MeV/c

FIG. 8

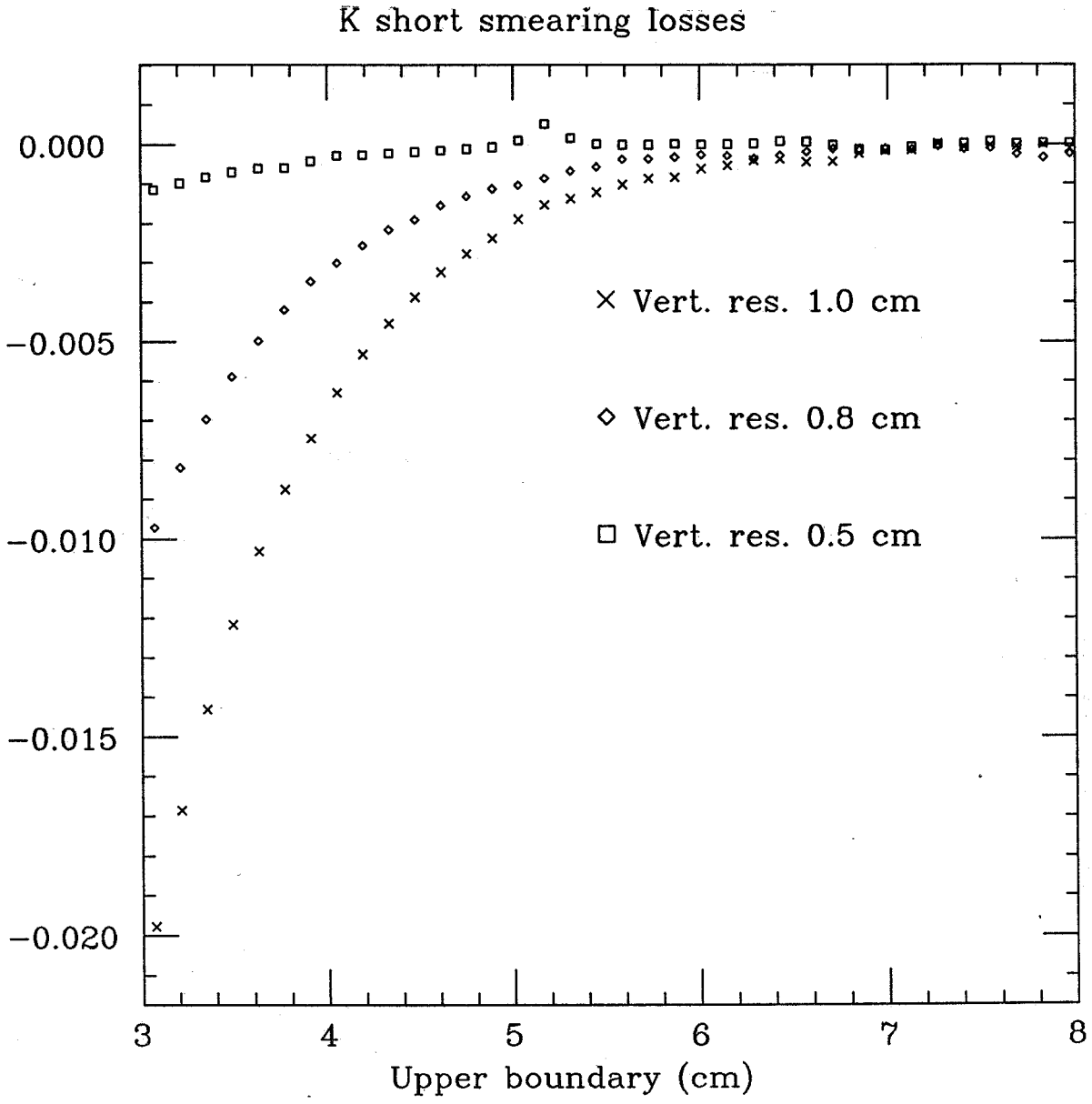
K short smearing losses
0.000
−0.005
−0.010
−0.015
−0.020
× Vert. res. 1.0 cm
◇ Vert. res. 0.8 cm
□ Vert. res. 0.5 cm
3
4
5
6
7
8
Upper boundary (cm)

FIG. 9

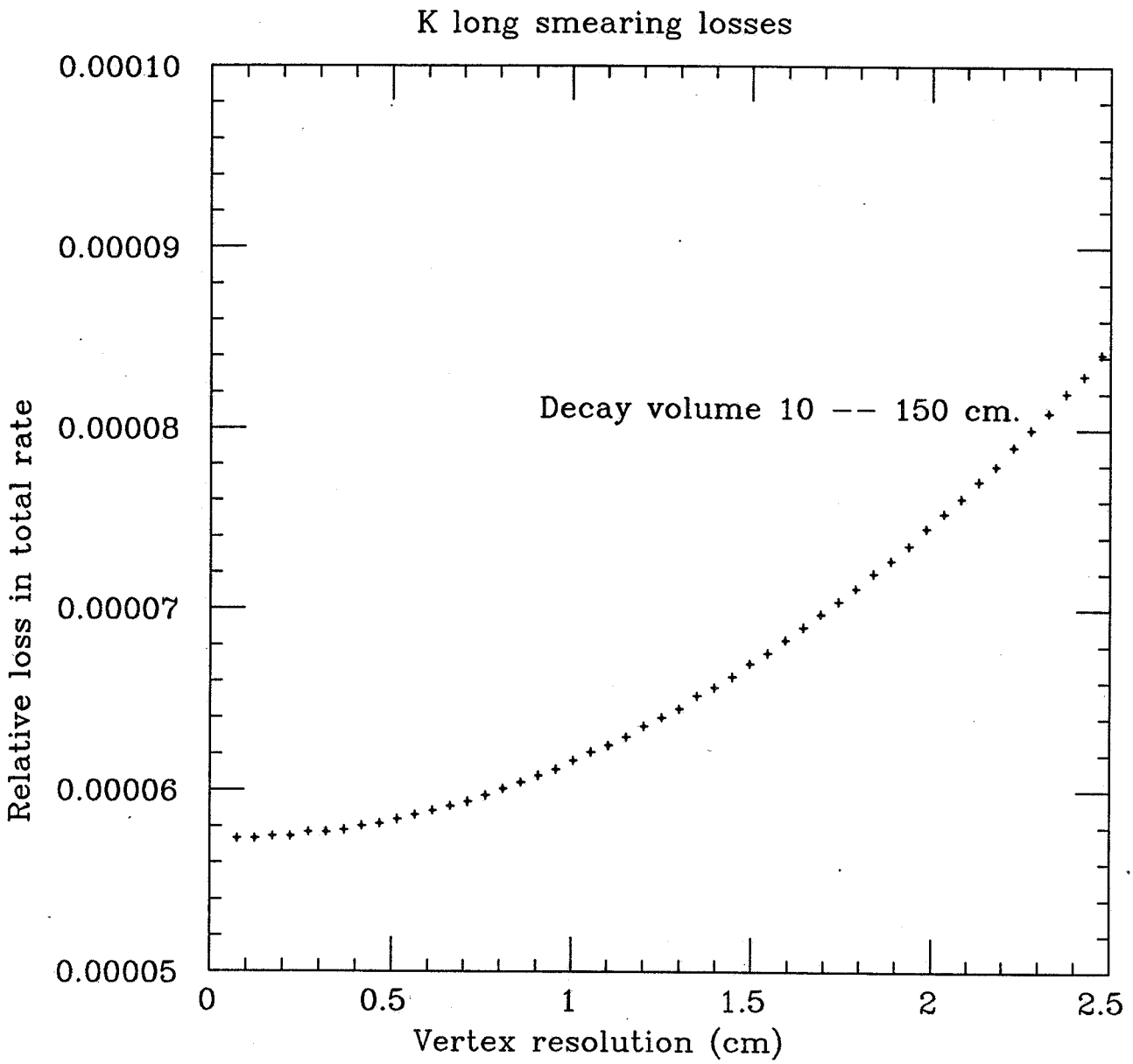
K long smearing losses
Decay volume 10 -- 150 cm.
Relative loss in total rate
0.00010
0.00009
0.00008
0.00007
0.00006
0.00005
0
0.5
1
1.5
2
2.5
Vertex resolution (cm)

CP violation measurements at the ϕ resonance

D. Cocolicchio, G. L. Fogli†
CERN, CH-1211 Geneva 23, Switzerland

M. Lusignoli and A. Pugliese
Dipartimento di Fisica, Università di Roma, Roma, Italy
Istituto Nazionale di Fisica Nucleare, Sezione di Roma I

ABSTRACT

We discuss how to determine the parameter ϵ'/ϵ from ϕ factory data, with special attention taming the background coming from decays of $(K^\circ\overline{K^\circ}$,C=+) pairs produced in association with a low-energy photon.

†On leave of absence from *Dipartimento di Fisica, Università di Bari, Bari, Italy*
Istituto Nazionale di Fisica Nucleare, Sezione di Bari, Italy

The measurement of CP violating parameters in the coherent decay in $K^\circ\overline{K^\circ}$ of the ($J^{PC} = 1^{--}$) ϕ resonance has recently excited much interest [1], [2], [3], the ϕ mesons being copiously produced in high-luminosity e^+e^- annihilation machines (ϕ factories). As stressed by many people [4] the ϕ meson decays in an antisymmetric K_SK_L state, and from the study of the 4π final states (time asymmetry in $\pi^+\pi^-$, $\pi^0\pi^0$ [5] or different branching ratios in different charge configurations [6]) one can hope to get a clean determination of the ratio ϵ'/ϵ.

Very recently Nussinov and Truong [7] remarked the presence of a dangerous background coming from the following chain of decays:

$$\phi \to \gamma + S^*/f_0(976) \to \gamma + (K^\circ\overline{K^\circ})_{C=+} \to \gamma + \frac{1}{\sqrt{2}}(K_SK_S - K_LK_L) \qquad (1)$$

Due to the small value of ϵ, a contamination at 10^{-3} level will induce a number of 4π events nearly equal to that coming from the ($K^\circ\overline{K^\circ}$, $C = -$) state. Since the maximum photon energy is

$$E_\gamma = \frac{m_\phi^2 - 4m_K^2}{2m_\phi} \simeq 24 \text{ MeV} \quad , \qquad (2)$$

it will be very difficult to distinguish the direct ϕ decay from that mediated by the S^*/f_0 intermediate state, by reconstructing the $K^\circ\overline{K^\circ}$ mass spectrum. The partial width of this process is strongly model dependent. The value obtained by Nussinov and Truong is $\Gamma(\phi \to \gamma + K^\circ\overline{K^\circ}) = 1.5 \cdot 10^{-7}$ MeV, which corresponds to $\Gamma(\phi \to \gamma + S^*/f_0) = 6 \cdot 10^{-6}$ MeV. One could also estimate the partial width for the dipole transition $\phi \to \gamma + S^*/f_0$ using a non relativistic potential model as done for radiative decays of charmonium and bottomonium. One has for a confining linear potential [8]

$$\frac{\Gamma(\phi \to \gamma + S^*/f_0)}{\Gamma(\psi' \to \gamma + \chi_{c0})} = \frac{1}{4}\left(\frac{q_s}{q_c}\right)^3 \left(\frac{m_c}{m_s}\right)^{\frac{2}{3}} \tag{3}$$

where q_s and q_c are the photon energy for a ϕ or a ψ' state decaying at rest, and m_c and m_s are the constituent masses of the charm and strange quarks (m_c/m_s=3). In this way one obtains $\Gamma(\phi \to \gamma + S^*/f_0) = 6 \cdot 10^{-5}$ MeV, ten times more than in Nussinov and Truong. If the confining potential is quadratic, the decay width reaches nearly 10^{-4} MeV.

None of these models is very compelling, therefore one should not trust too much the smallness of the values obtained; we think that it would be helpful to obtain a determination of ϵ'/ϵ free from the uncertainty due to this contribution.

In this letter we show that with a suitable geometrical cut one can suppress almost completely the bad C-even events, while still retaining a very large fraction of good events.

Let us consider the $(\pi^+\pi^-,\pi^0\pi^0)$ final state and denote by $d_1(d_2)$ the path length of a neutral kaon decaying into $\pi^+\pi^-(\pi^0\pi^0)$. Let N_A be the number of events falling in the rectangle of the (d_1, d_2) plane defined by

$$d_0 < d_1 < d < d_2 < D \quad , \tag{4}$$

and N_B the number of those having

$$d_0 < d_2 < d < d_1 < D \quad , \tag{5}$$

d_0 and D being the minimun and the maximum paths inside the detector, respectively. As will be discussed presently, it is possible to choose the distance d in such a way that

i) N_A (N_B) represents almost the total number of events with $d_0 < d_1 < d_2 < D$ ($d_0 < d_2 < d_1 < D$) coming from a C-odd $K^\circ\overline{K^\circ}$ state;

ii) very few events coming from a C-even $K^\circ\overline{K^\circ}$ state satisfy the constraints of equations 4 and 5;

it follows that the value of ϵ'/ϵ can be derived from the asymmetry $A = (N_A - N_B)/(N_A + N_B)$ without problems coming from the C-even contamination.

In terms of the usual CP violating amplitudes

$$\eta_{+-} = \frac{A(K_L \to \pi^+\pi^-)}{A(K_S \to \pi^+\pi^-)} = \epsilon + \epsilon' \qquad (6)$$

$$\eta_{00} = \frac{A(K_L \to \pi^0\pi^0)}{A(K_S \to \pi^0\pi^0)} = \epsilon - 2\epsilon'$$

and for each initial $(K^\circ\overline{K^\circ}, C = -)$ state, with a straightforward calculation one obtains

$$N_A^- = \frac{\Gamma_S^{+-}\Gamma_S^{00}}{\Gamma_S\Gamma_L}\{|\eta_{+-}|^2 S_1 + |\eta_{00}|^2 S_2 + \mathrm{Re}(\eta_{+-}\eta_{00}^*)S_3 + \mathrm{Im}(\eta_{+-}\eta_{00}^*)S_4\} \quad . \qquad (7)$$

In eq. (7) $\Gamma_S(\Gamma_L)$ is the $K_S(K_L)$ width, whereas Γ_S^{+-} and Γ_S^{00} are the partial widths for K_S decaying into $\pi^+\pi^-$ and $\pi^0\pi^0$, respectively. The coefficients S_i are given by

$$S_1 = (e^{-\frac{d}{d_S}} - e^{-\frac{D}{d_S}})(e^{-\frac{d_0}{d_L}} - e^{-\frac{d}{d_L}}) \quad ,$$

$$S_2 = (e^{-\frac{d_0}{d_S}} - e^{-\frac{d}{d_S}})(e^{-\frac{d}{d_L}} - e^{-\frac{D}{d_L}}) \quad , \qquad (8)$$

$$S_3 = t(d, D) + t(d_0, d) - t(d_0, D) - t(d, d) \quad ,$$

where

$$t(d_\alpha, d_\beta) = -\frac{2\Gamma_S\Gamma_L}{\Gamma^2 + (\Delta m)^2}\cos\left[\frac{\Delta m}{\Gamma_S}\left(\frac{d_\alpha - d_\beta}{d_S}\right)\right] e^{-\frac{\Gamma}{\Gamma_S}\frac{d_\alpha + d_\beta}{d_S}} \quad , \qquad (9)$$

S_4 being obtained from S_3 with the replacement (cos $\rightarrow$ sin). In eqs. (8) and (9) $d_S \simeq 0.6$ cm and $d_L \simeq 342$ cm are the mean decay paths of K_S and K_L from a ϕ meson at rest, $\Gamma = (\Gamma_S + \Gamma_L)/2$ and $\Delta m = m_L - m_S$.

N_B^- can be obtained from N_A^- (eq. (7)) by interchanging η_{00} and η_{+-}, namely

$$N_B^- = \frac{\Gamma_S^{+-}\Gamma_S^{00}}{\Gamma_S\Gamma_L}\{|\eta_{00}|^2 S_1 + |\eta_{+-}|^2 S_2 + \mathrm{Re}(\eta_{+-}\eta_{00}^*)S_3 - \mathrm{Im}(\eta_{+-}\eta_{00}^*)S_4\} \quad . \tag{10}$$

The two quantities, N_A^- and N_B^-, differ because of the different dependence of η_{+-} and η_{00} on ϵ'/ϵ. The two most recent experiments, however, both say that ϵ'/ϵ is small (and probably real): we have in fact ϵ'/ϵ ranging from the value published by the CERN NA31 Collaboration [9]

$$\frac{\epsilon'}{\epsilon} = (3.3 \pm 1.1) \cdot 10^{-3} \quad , \tag{11}$$

to the recent preliminary result of the Chicago-Fermilab Collaboration [10]

$$\frac{\epsilon'}{\epsilon} = (-0.5 \pm 1.5) \cdot 10^{-3} \tag{12}$$

It follows that apart from small terms $O(\epsilon'/\epsilon)$ we have the same number of events in the two regions, i.e.

$$N_A^- \simeq N_B^- \simeq \frac{\Gamma_S^{+-}\Gamma_S^{00}}{\Gamma_S\Gamma_L}|\epsilon|^2 S \quad , \tag{13}$$

with the "signal" S given by

$$S = S_1 + S_2 + S_3 \simeq S_2 \quad , \tag{14}$$

as can be seen from Table I, where the four coefficients S_i are given for several choices of d_0, d and D.

In Fig. 1 we report the normalized distribution of the events C-odd *vs.* the distance from the vertex of the "second" K-decay (in d_S units). By taking a given value d, all the events characterized by a smaller distance represent all that we lose by applying the cut of eq. (4): i.e. the events having $d_0 < d_1 < d_2 < d$ coming from a C-odd state, defined in the following as

$$N_C^- \simeq \frac{\Gamma_S^{+-}\Gamma_S^{00}}{\Gamma_S\Gamma_L}|\epsilon|^2 C^- \quad . \tag{15}$$

If the cut is chosen to be appreciably larger than d_S, then the remaining distribution is "practically" that of the events N_A^- (or N_B^-) (the number of events with $d < d_1 < d_2$ is quite negligible), to be further cut in correspondence with D, the maximum path inside the detector (in the figure a small vertical arrow indicates the position of $D = \frac{1}{2}d_L$).

In the case of a $(K^\circ\overline{K^\circ}, C = +)$ pair, for symmetry reasons there is no difference between the two regions A and B. The corresponding quantities, N_A^+ and N_B^+, are equal and can be written in the form

$$N_A^+ = N_B^+ = \frac{\Gamma_S^{+-}\Gamma_S^{00}}{\Gamma_S\Gamma_L}|\epsilon|^2 B \quad , \tag{16}$$

where we have explicitly extracted the $|\epsilon|^2$ dependence, typical of N_A^- and N_B^-, in order to make the comparison easier. We give also the explicit expression for the "background" making the approximations $\epsilon' \simeq 0$ (and therefore $\arg(\eta_{+-}) \simeq \arg(\eta_{00}) \simeq \arg(\Gamma + i\Delta m)$) and $e^{-\frac{D}{d_S}} \simeq 0$,

$$\begin{aligned} B = {} & \frac{\Gamma_L}{\Gamma_S|\epsilon|^2}\left(e^{-\frac{d_0}{d_S}} - e^{-\frac{d}{d_S}}\right)e^{-\frac{d}{d_S}} + \frac{\Gamma_S|\epsilon|^2}{\Gamma_L}\left(e^{-\frac{d_0}{d_L}} - e^{-\frac{d}{d_L}}\right)\left(e^{-\frac{d}{d_L}} - e^{-\frac{D}{d_L}}\right) - \\ & - \frac{2\Gamma_S\Gamma_L}{\Gamma^2 + \Delta m^2}\{e^{-\frac{\Gamma}{\Gamma_S}\frac{d+d_0}{d_S}}\cos\left[\frac{\Delta m}{\Gamma_S}\left(\frac{d_0+d}{d_S}\right)\right] - e^{-\frac{\Gamma}{\Gamma_S}\frac{2d}{d_S}}\cos\left[\frac{\Delta m}{\Gamma_S}\left(\frac{2d}{d_S}\right)\right]\} \end{aligned} \tag{17}$$

It is easy to verify from eqs. (8) and (17) that B can be very much suppressed if d is chosen to be much larger than d_S but still much smaller than D, in order to retain a large fraction of the signal. This is shown in Fig. 2, where the signal S, the background B and the number C^- of "good" (C-odd) events that we lose by applying the cut in eq. (4) are plotted as functions of d for $d_0 = 0$ and $D = \frac{1}{2}d_L = 171$ cm: it can be seen that for $10\ d_S < d < 20\ d_S$ one has at the same time a strong suppression of the C-even background B and a large fraction of good events retained ($C^- \ll S$).

In Table II we give the values of the signal S, the background B and the lost events C^- for several values of d_0, d and D. In the same Table the values of C^+ are listed too, C^+ being related, analogously to C^- in eq. (15), to the fraction of "bad" (C=+) events N_C^+ falling in the excluded region $d_0 < d_1 < d_2 < d$.

We come now to the determination of ϵ'/ϵ from the asymmetry between N_A and N_B induced by the different dependence on ϵ' of η_{+-} and η_{00}. If the initial state contains a fraction α of $(K^\circ\overline{K^\circ}, C = +)$ pairs one has

$$A = \frac{N_B^- + \alpha N_B^+ - (N_A^- + \alpha N_A^+)}{N_B^- + \alpha N_B^+ + (N_A^- + \alpha N_A^+)} \simeq 3\mathrm{Re}\left(\frac{\epsilon'}{\epsilon}\right) \cdot \frac{1}{(1+\alpha\rho)} \tag{18}$$

where $\rho = N_A^+/N_A^- \simeq B/S$. In deriving eq. (18) we take into account that the background is symmetric (see eq.(16)) and make use of the S_i of Table I. It is easily seen that the coefficient of $\mathrm{Re}(\epsilon'/\epsilon)$ is 3 to a very high precision and independent of the cut we choose. Conversely, that of $\mathrm{Im}(\epsilon'/\epsilon)$ is cut-dependent and negligible ($\sim 10^{-3}$ or several orders of magnitude smaller) for all the cases of interest here. Expected to be zero from CPT invariance, as confirmed by the new experimental result [11] on the phases ϕ_{+-} and ϕ_{00}, also if not zero, $\mathrm{Im}(\epsilon'/\epsilon)$ cannot be appreciated in the present approach.

The C-even background would induce a systematic error $\Delta(\epsilon'/\epsilon)/(\epsilon'/\epsilon) \simeq \alpha\rho$. For the cuts given in Table I, this is less than $4 \cdot 10^{-2}$, and therefore quite tolerable even if α were to be near to 1. In any case, for not too negligible values of α, we can attempt to determine it by measuring the $K^\circ\overline{K^\circ}$ decays with both decay paths larger than d. Let $D^+(X_1, X_2)$ and $D^-(X_1, X_2)$ be the fraction of events falling in this region and coming

from the decay in the $|X_1, X_2>$ final state of a $(K^\circ\overline{K^\circ}, C = +)$ or $(K^\circ\overline{K^\circ}, C = -)$ pair, respectively. The values of D^+ and D^- for different final states and for $d = 10\, d_S$ or $d = 20\, d_S$ are reported in Table III. If $d = 20\, d_S$, essentially all the events in the most external regions of the detector come from the C-even component of the initial state and their number is

$$N_D(X_1, X_2) \simeq N^+ D^+(X_1, X_2) = \alpha N^- D^+(X_1, X_2) \quad , \tag{19}$$

where N^- is the total number of $(K^\circ\overline{K^\circ}, C = -)$ pairs produced. Clearly the K_L allowed decay channels are the most suitable for the determination of α.

We come now to discuss the minimum number of ϕ (N_ϕ) to be produced in order to observe ϵ'/ϵ to n standard deviations accuracy when we consider only the events selected in the regions A and B. For a small asymmetry ($A \ll 1$),

$$N_\phi = \frac{1}{\mathrm{BR}[\phi \to (K^\circ\overline{K^\circ})] \cdot \mathrm{BR}[(K^\circ\overline{K^\circ}) \to \pi^+\pi^- + \pi^0\pi^0]} \cdot \frac{2}{S} \cdot \left(\frac{n^2}{2A^2}\right) \quad , \tag{20}$$

where $S/2$ represents the fraction that we observe of the produced events,

$$\begin{aligned} \mathrm{BR}[(K^\circ\overline{K^\circ})_{C=-} \to \pi^+\pi^- + \pi^0\pi^0] =& \mathrm{BR}(K_S \to \pi^+\pi^-)\mathrm{BR}(K_L \to \pi^0\pi^0) \\ &+ \mathrm{BR}(K_S \to \pi^0\pi^0)\mathrm{BR}(K_L \to \pi^+\pi^-) \quad , \end{aligned} \tag{21}$$

and $\mathrm{BR}(\phi \to K^\circ\overline{K^\circ}) = (34.4 \pm 0.9)\%$ [12]. In Table II one can find N_ϕ for different choices of d_0, d and D and for $\mathrm{Re}(\epsilon'/\epsilon) = 10^{-3}$, when a sensitivity to the asymmetry of three standard deviations is required. It is seen that N_ϕ grows strongly for $d_0 \neq 0$ so that the maximum effort must be made to reduce d_0. We note that one does not need the precise position of the vertex but only to know if it is inside or outside a circle of radius d: for this reason we think that $d_0 \sim 0$ is not an irrealistic hope.

Acknowledgements. We gratefully acknowledge helpful discussions with M. Greco. One of us (D. C.) would like to thank the Theory Division of CERN for hospitality and the Istituto Nazionale di Fisica Nucleare for a postdoctoral fellowship.

References

[1] U. Amaldi and G. Coignet, *Proceedings of the Workshop on Heavy Quark Factory and Nuclear Physics Facility with Superconducting Linacs*, E. De Sanctis, M. Greco, M. Piccolo and S. Tazzari eds. (Courmayeur, 1987) p. 59.

[2] C. Rubbia, "*A $\phi \rightarrow K_L K_S$ factory using the Trieste synchroton light source*", CERN UA1 Internal Note (1988).

[3] G. Barbiellini and C. Santoni, CERN preprint CERN-EP/89-88 (1989).

[4] T. Kamae, T. Kifune and T. Tsumemoto, Prog. Theor. Phys. **41** (1967) 1267; H. J. Lipkin, Phys. Rev. **176** (1968) 1715.

[5] I. Dunietz, J. Hauser and J. L. Rosner, Phys. Rev. **D35** (1987) 2166.

[6] J. Bernabeu, F. J. Botella and J. Roldan, Phys. Lett. **B211** (1988) 226; University of Valencia preprint, FTUV/89-35 (1989).

[7] S. Nussinov and T. N. Truong, Phys. Rev. Lett. **63** (1989) 2003.

[8] See for example E. Eichten et al., Phys. Rev. **D17** (1978) 3090, Phys. Rev. **D21** (1980) 203.

[9] NA31 Collab., H. Burkhardt et al., Phys. Lett. **B206** (1988) 169.

[10] B. Winstein, *Proceedings of the XIV International Symposium on Lepton and Photon Interactions* (Stanford, 1989), University of Chicago preprint EFI 89-60 (1989).

[11] NA31 Collab., presented by D. Fournier, talk given at the "*14th International Symposium on Lepton and Photon Interactions*" (Stanford, 1989), CERN preprint CERN-EP/90-01 (1990).

[12] Particle Data Book, Review of Particle Properties,Phys. Lett. **B204** (1988) 1.

Table I. The time-flight integrated factors which parametrize the coherent decay rate of a (C^-) $K_L K_S$ pair into a $\pi^+\pi^-$, $\pi^0\pi^0$ state (see eq. (8)), for different values of the cut d and of the minimum (d_0) and the maximum (D) path inside the detector. As units the mean decay paths of K_S ($d_s \simeq 0.6$ cm) and K_L ($d_L \simeq 342$ cm) are used.

d_0/d_S	d/d_S	D/d_L	S_1	S_2	S_3	S_4
0	10	$\frac{1}{2}$	$7.76 \cdot 10^{-7}$	0.38	$-2.60 \cdot 10^{-6}$	$-4.80 \cdot 10^{-5}$
0	10	1	$7.76 \cdot 10^{-7}$	0.62	$-2.60 \cdot 10^{-6}$	$-4.80 \cdot 10^{-5}$
0	20	$\frac{1}{2}$	$6.99 \cdot 10^{-11}$	0.36	$3.19 \cdot 10^{-7}$	$-3.90 \cdot 10^{-8}$
0	20	1	$6.99 \cdot 10^{-11}$	0.60	$3.19 \cdot 10^{-7}$	$-3.90 \cdot 10^{-8}$
2	10	$\frac{1}{2}$	$6.20 \cdot 10^{-7}$	$5.09 \cdot 10^{-2}$	$1.41 \cdot 10^{-5}$	$-1.11 \cdot 10^{-5}$
2	10	1	$6.20 \cdot 10^{-7}$	$8.32 \cdot 10^{-2}$	$1.41 \cdot 10^{-5}$	$-1.11 \cdot 10^{-5}$
2	20	$\frac{1}{2}$	$6.28 \cdot 10^{-11}$	$4.87 \cdot 10^{-2}$	$7.94 \cdot 10^{-8}$	$8.74 \cdot 10^{-8}$
2	20	1	$6.28 \cdot 10^{-11}$	$8.10 \cdot 10^{-2}$	$7.94 \cdot 10^{-8}$	$8.74 \cdot 10^{-8}$

Table II. In terms of the same distances used in Table I, we report here the signal S, the background B, the C-odd and C-even events falling in the cut region and finally the number of ϕ (N_ϕ) required to observe an asymmetry A with a sensitivity of 3 standard deviations. N_ϕ is estimated assuming $\mathrm{Re}(\epsilon'/\epsilon) = 10^{-3}$: for different values one has to divide by the square of $\mathrm{Re}(\epsilon'/\epsilon)$ in units of 10^{-3}.

d_0/d_S	d/d_S	D/d_L	S	B	C^-	C^+	N_ϕ
0	10	$\frac{1}{2}$	0.38	$1.51 \cdot 10^{-2}$	$1.35 \cdot 10^{-2}$	$1.66 \cdot 10^{2}$	$5.88 \cdot 10^{9}$
0	10	1	0.62	$1.51 \cdot 10^{-2}$	$1.35 \cdot 10^{-2}$	$1.66 \cdot 10^{2}$	$3.60 \cdot 10^{9}$
0	20	$\frac{1}{2}$	0.36	$3.74 \cdot 10^{-5}$	$3.03 \cdot 10^{-2}$	$1.66 \cdot 10^{2}$	$6.15 \cdot 10^{9}$
0	20	1	0.60	$6.18 \cdot 10^{-5}$	$3.03 \cdot 10^{-2}$	$1.66 \cdot 10^{2}$	$3.70 \cdot 10^{9}$
2	10	$\frac{1}{2}$	$5.09 \cdot 10^{-2}$	$2.05 \cdot 10^{-3}$	$1.35 \cdot 10^{-3}$	3.04	$4.35 \cdot 10^{10}$
2	10	1	$8.32 \cdot 10^{-2}$	$2.06 \cdot 10^{-3}$	$1.35 \cdot 10^{-3}$	3.04	$2.66 \cdot 10^{10}$
2	20	$\frac{1}{2}$	$4.87 \cdot 10^{-2}$	$3.31 \cdot 10^{-5}$	$3.64 \cdot 10^{-3}$	3.04	$4.55 \cdot 10^{10}$
2	20	1	$8.10 \cdot 10^{-2}$	$5.50 \cdot 10^{-5}$	$3.64 \cdot 10^{-3}$	3.04	$2.73 \cdot 10^{10}$

Table III. Number of events D^- and D^+ coming from a $(C = -1)$ and a $(C = +1)$ state respectively, and falling in the most external region of the detector $(d < d_1 < d_2 < D)$, reported for the different final states and two values of the cut d in units of the mean decay path of K_S. The limits for the three π's decays are obtained by using the upper values of the $K_S \to 3\pi$ branching ratios given in ref. [12].

final states	D^-		D^+	
	$d = 10\, d_S$	$d = 20\, d_S$	$d = 10\, d_S$	$d = 20\, d_S$
$\pi^+\pi^-$ $\pi^0\pi^0$	$2.1 \cdot 10^{-8}$	$9.2 \cdot 10^{-13}$	$2.3 \cdot 10^{-7}$	$2.1 \cdot 10^{-7}$
$\pi^+\pi^-$ $\pi^+\pi^-$	$4.7 \cdot 10^{-8}$	$2.1 \cdot 10^{-12}$	$5.2 \cdot 10^{-7}$	$4.7 \cdot 10^{-7}$
$\pi^+\pi^-\pi^0$ $\pi^+\pi^-$	$2.4 \cdot 10^{-8}$	$1.0 \cdot 10^{-12}$	$3.1 \cdot 10^{-5}$	$2.9 \cdot 10^{-5}$
$\pi^+\pi^-\pi^0$ $\pi^+\pi^-\pi^0$	$2.1 \cdot 10^{-12}$	$9.1 \cdot 10^{-17}$	$1.9 \cdot 10^{-3}$	$1.7 \cdot 10^{-3}$

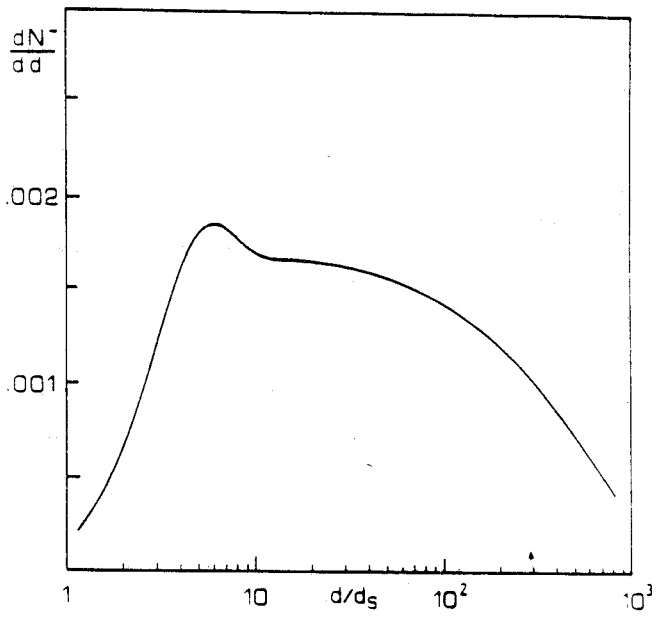

Fig. 1 - Normalized distribution of the events C-odd as a function of the decay distance d of the "second" K. The distance d is expressed in units of the mean decay path d_S of K_S. The small arrow indicates $\frac{1}{2}$ of the mean decay path d_L of K_L.

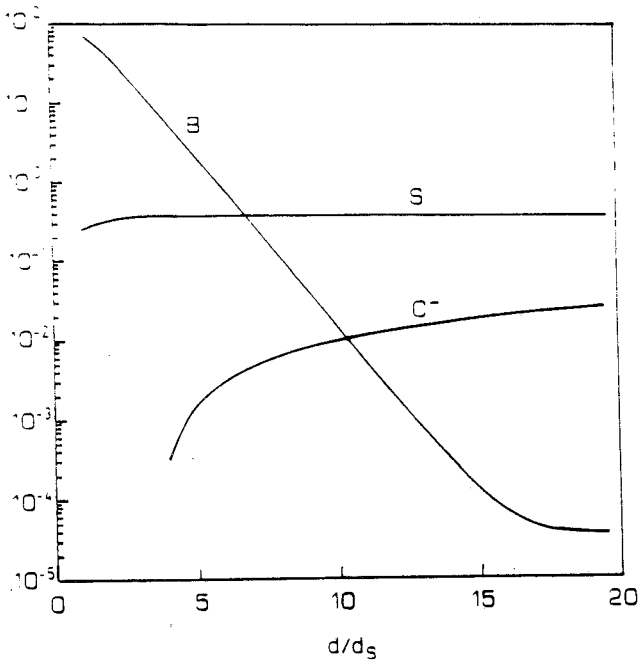

Fig. 2 - Signal S, lost events C^- and background B in arbitrary units (see eqs. (12), (14) and (15), respectively) *vs.* the distance of the cut d in units of the mean decay path d_S of K_S.

STATUS AND PERSPECTIVES OF THE K DECAY PHYSICS

R. Battiston

Dipartimento di Fisica, Università di Perugia, Perugia, Italy
Istituto Nazionale di Fisica Nucleare, Sezione di Perugia, Italy

D. Cocolicchio, G. L. Fogli†

CERN, CH-1211 Geneva 23, Switzerland

and

N. Paver

Dipartimento di Fisica Teorica, Università di Trieste, Trieste, Italy
Istituto Nazionale di Fisica Nucleare, Sezione di Trieste, Italy

ABSTRACT

The current status of K-decay physics is reviewed. Together with an analysis of the different decay modes, emphasizing their significance as tests of the standard model and as probes for new physics, a discussion of the experimental capabilities of the various existing facilities is presented. Also surveyed are the perspectives offered to such studies by future plans of high intensity machines.

†On leave of absence from *Dipartimento di Fisica, Università di Bari, Bari, Italy*
Istituto Nazionale di Fisica Nucleare, Sezione di Bari, Italy

I. Introduction

The study of K decays marks some of the most relevant steps in the understanding of particle physics. Related to the K physics are, in fact:

i) The parity violation [1], of which the $K \to 2\pi, 3\pi$ puzzle has represented one of the first indications [2].

ii) The CP violation [3], discovered in the analysis of the $K\overline{K}$ system twenty-five years ago [4]. At present the $K\overline{K}$ system still remains the only known manifestation of CP violation and a laboratory to study it. From this point of view, also the introduction of the third generation of quarks and leptons [5] finds its primary motivation in the K physics, being related to the attempt of justifying the CP violation in the standard model in a natural way.

iii) The GIM mechanism [6], which implies that neutral currents naturally conserve flavour at the tree level and that flavour-changing neutral currents are naturally suppressed at one-loop level. Based on the postulated existence of the charm quark, it finds in the $K_L \to \mu^+\mu^-$ one of its cleanest motivations.

Even though the present interest of particle physics seems now to be shifted to a large extent towards the physics which can be performed at the energies recently reached with the new colliders (typically the Z^0 physics studied presently at LEP/SLC) and towards the studies of heavy flavours, there are, however, good reasons to assert that K physics still maintains unaltered its interest and should well be the source of important results. Indeed, fundamental features such as e.g. the $\Delta I = 1/2$ rule are still difficult to account for, from the theoretical point of view, and the origin of P and CP violations is not well identified as yet. Moreover the so–called "new physics", i.e. those manifestations which can be interpreted as clear indications of new effects beyond the standard model, could manifest itself also in low energy processes such as K-decays (of course, through experiments with improved systematics and high statistics).

We can thus make in the following a list of the aspects on which K decays provide particularly important and detailed information:

a) A better understanding of the nature of CP violation. K decays offer a unique way to study old and/or new sources of CP violation, a point which is of crucial importance.

b) Clean and specific tests of the standard model. Specifically

   - sensitivity to the still unknown mass of the top quark;
   - precision measurements (number of generations, universality, radiative corrections);
   - specific models (vector and axial form factors, short and long distance effects, chiral perturbation theory).

c) Possible existence of light neutral particles such as Higgs, hyperphotons, familons, axions, etc., even though the recent LEP experiments [7] appreciably reduce the margins of this kind of searches, in particular as far as light Higgs bosons are concerned.

d) Possible glimpses on the so–called "new physics". Here many possibilities and alternatives are open. Among the most interesting ones:

   - New alternative or complementary sources of CP violation, besides that related, in the standard model, to the phase in the Cabibbo-Kobayashi-Maskawa matrix, which is easily accommodated within the standard model. An example is the spontaneous CP violation induced by multi–Higgs systems [8].
   - Indications of a fourth generation: essentially ruled out at the level of a light fourth neutrino by the recent results of the LEP/SLC experiments [9], there still remains the – admittedly less appealing – possibility of a fourth generation characterized by a heavy neutrino.
   - New kinds of interactions, mediated by quanta not "envisaged" in the

standard model, such as leptoquarks, superheavy Higgs, etc. Here the point is that there exist specific processes that, being forbidden in the standard model, are a clear evidence of "new physics" once observed. This is the case of all the processes related to a lepton flavour violation, typically for example $K_L^0 \to \mu e$.

The aim of this paper is to present in a synthetic way a scheme of the present status of K decays, and to describe the perspectives potentially offered by a future analysis of some of them. A particular emphasis will be given to those processes which could be studied at a ϕ factory.

The paper is organized as follows. In Sect. II we consider the problems posed by K physics from the experimental point of view: the different experimental facilities proposed to study K decays are compared in terms of their characteristics, as available statistics, detector performances, background conditions, etc.: the present situation is briefly discussed, together with the perspectives offered in a rather near future. In the following sections the different processes are analysed, by grouping them into different categories, distinguished on the basis of their "rareness". We are aware that this introduces an element of arbitrariness. Nevertheless this facilitates the approach to the large number of processes to be discussed. Accordingly, in Sect. III the "common decays", $K \to 2\pi$, $K \to 3\pi$, $K_{\ell 3}$, $K_{\ell 2}$, $K_{\mu 3}$, $K_{\ell 4}$ are reviewed, while in Sect. IV we consider under the name "not so rare decays" the radiative leptonic and non-leptonic transitions $K \to (\ell\nu)\gamma$, $K \to (\ell\nu)(\ell\bar{\ell})$, $K_{2\gamma}$, $K \to (\ell\bar{\ell})\gamma$, $K \to \pi\pi\gamma$, $K^\pm \to \pi^\pm\gamma\gamma$. In Sect. V we consider the "rare decays" $K^\pm \to \pi^\pm(\ell^+\ell^-)$, $K^\pm \to \pi^\pm(\nu\bar{\nu})$, $K \to \mu^+\mu^-$, $K \to e^+e^-$. These are still accessible at the existing high intensity K beams and, of course, at the future K factories. In Sect. VI the "very rare" decays $K^0 \to \pi^0(\ell^+\ell^-)$ and $K^0 \to \pi^0(\nu\bar{\nu})$ are described, very rare because both GIM suppressed and proceeding, as far as the K_L is concerned, through CP violating amplitudes. Finally, in Sect. VII we consider the "not expected or forbidden decays" $K \to \mu e$, $K \to \pi\mu e$, whose observation would be an unambiguous signal of "new physics".

We have no hope to be exhaustive, because the material to be covered is huge. Certainly, some topics reviewed in the present report would require a more accurate and

specific analysis. For example, we consider only marginally the well–known problem of CP violation in the $K\overline{K}$ system and in $K \to 2\pi$, whose phenomenological and theoretical properties need a detailed description. Concerning the weak decays $K \to 3\pi$ we will give only a brief account of the perspectives offered by them as a possible test of the CP violation.

A further point is worth noting before closing this Introduction. Two relevant topics, typical of kaon decay physics, are essentially missing here, with only a brief mention when required. They are the search of a light Higgs and the search of a light fourth generation neutrino. Both would have been in principle well studied through K decays, but they have lost their significance after the recent results of the LEP experiments [7], [9].

II. Experimental considerations on K physics

Kaons are normally hadroproduced from high intensity proton beams colliding on fixed targets (CERN, FNAL, KEK, BNL, future Kaon factories) or in low energy $p\overline{p}$ collisions (CERN/LEAR). With the advent of ϕ factories other clean and intense K sources will become available.

In the case of high energy hadroproduction, the K's energy may range from as low as (few) GeV (used in high rate $K^+ \to \pi^+(\nu\overline{\nu})$ or $K_L \to \mu e$ experiments and muon polarization measurement in $K_{\mu 3}$ decay) to 100 GeV or more (suitable for experiments measuring $\mathrm{Re}(\epsilon'/\epsilon)$, $K_L \to \pi^0 e^+ e^-$ and $K_S \to 3\pi$). The beam intensity may be extremely high, reaching few 10^9 K_L s^{-1} as in the case of the upgrade proposed at the Tevatron [10], or even more as it is foreseen at the future Kaon factories [11]. These fluxes are much larger than what is expected at a ϕ factory or at LEAR (10^3 to $10^4 K$ s^{-1}); however what matters is the rate of K decaying in the detector fiducial volume, for example in the case of high energy K_L (and $K^{\pm}$) beams, the experimental acceptance is normally very low (few %) due to their long decay path. Moreover, pure

TABLE I. Recent progress in rare kaon decay. Some results are preliminary, while others are published.

decay mode	experiment	result	sensitivity	comments
$K^+ \to \pi^+ +$nothing	BNL E787	$< 3 \times 10^{-8}$	10^{-10}	detector works well
$K^+ \to \pi^+ \mu^+ e^-$	BNL E777	$< 1.1 \times 10^{-9}$	1.5×10^{-10}	limited by beam halo
$K_L \to \mu^\pm e^\mp$	BNL E780	$< 1.9 \times 10^{-9}$		limited by beam halo
$K_L \to e^+ e^-$		$< 1.2 \times 10^{-9}$		
$K_L \to \pi^0 e^+ e^-$		$< 3.2 \times 10^{-7}$		will pursue ($\sim 10^{-10}$) in E845
$K_L \to \mu^\pm e^\mp$	BNL E791	$< 3.0 \times 10^{-10}$	$\sim 2 \times 10^{-11}$	limited by accidental from K_L decays
$K_L \to \mu^\pm e^\mp$	KEK E137	$< 4 \times 10^{-10}$	$\sim 2 \times 10^{-11}$	will pursue in E162
$K_L \to e^+ e^-$				$K_L \to \pi^0 e^+ e^- (\sim 10^{-10})$
$K_S \to \pi^+ \pi^- \pi^0$	FNAL E621	$< 1.5 \times 10^{-7}$	$\sim 3 \times 10^{-9}$	expected rate $\sim 1.2 \times 10^{-9}$
$K_L \to \pi^0 e^+ e^-$	FNAL E731	$< 4.2 \times 10^{-8}$	$\sim 1 \times 10^{-8}$	
	CERN NA31	$< 4 \times 10^{-8}$		
$K_L \to \pi^0 e^+ e^-$	KEK-162		10^{-10}	
$K_L \to \pi^0 e^+ e^-$	FNAL P799		$10^{-10} - 10^{-11}$	

K_S beams are difficult to produce at fixed target sources. Conversely, at low energy a large fraction of the produced K's decay in the detector fiducial volume.

where In addition, experiments performed at intense K beams have to face severe backgrounds (muons, pions, neutrons, photons) accompanying the K's, and to tolerate ex-

TABLE II. Characteristics of the various kaon facilities.

experiment	status	physics	statistics	notes
CP-LEAR	ready soon	* $\not{CP}$ in K decays * CPT test	* expected $\sigma(\epsilon'/\epsilon)$=few 10^{-3}	* $p\bar{p}$ interaction at rest * statistics to small for $\sigma(\epsilon'/\epsilon) < 10^{-3}$ * other particles in the final states
ϕ factory	1993-94 (?) (to be approved and built)	* ϵ'/ϵ and other $\not{CP}$ in K decays * rare K_S decays * CPT test	* 10^{10} ϕ/year at $2.5 \times 10^{32}\text{cm}^{-2}\text{s}^{-1}$ * few 10^9 expected $K^{\pm}$ decays * 10^8–10^9 expected $K_{L,S}$ decays	* e^+e^- * very clean exp. environment * tagged ultrapure $K_{S,L}$, $K^{\pm}$ beams * $\sigma(\epsilon'/\epsilon) = 3 \cdot 10^{-4}$ with $\geq 10^{10}\phi$
NA31/E731	analysing '88-'89 data	* ϵ'/ϵ * CPT test	* few 10^6 observed $K_S \rightarrow 2\pi$ decays * few 10^5 observed $K_L \rightarrow 2\pi$ decays * $\sigma(\epsilon'/\epsilon) \simeq 10^{-3}$	* disagreement (2σ) on ϵ'/ϵ * new planned measurements
high intensity kaon beams	running + upgrades	* K_L, K^+ decays very rare or forbidden * $K_S \rightarrow \pi^+\pi^-\pi^0$	* 10^8–10^{11} observed decays	* dedicated exps. * some exps. are background limited
kaon factories	> 1995 planned	* K_L, K^+ decays very rare or forbidden	* 10^{11}–10^{13} expected decays	* dedicated exps. * background

tremely high trigger rates. For this reason, in addition to experiments optimized for the study of direct CP violation in $K \to 2\pi$ decays, each experiment normally concentrates on only one (few) rare or forbidden reaction(s) like: $K^+ \to \pi^+ +$ nothing, $\pi^+\mu^+e^-$, $K_L \not\to \mu e, e^+e^-, \pi^0e^+e^-$ and $K_S \to \pi^+\pi^-\pi^0$. As summarized in Table I (taken from ref. [12]), the limits obtained on the above reactions are already in the 10^{-8} to 10^{-10} range and will reach in the next years the 10^{-11} to 10^{-13} level with the upgrade of the existing facilities and the construction of the proposed K factories.

On the other side, low energy $K\overline{K}$ pairs produced in $p\overline{p}$ (K^-K^0, $K^+\overline{K}^0$) and e^+e^- (K^+K^-, K_LK_S) annihilations are more suited to study a broader set of CP violating $K_{L,S}$ and $K^\pm$ decays, and rare K_S decays, because of their unrivalled background conditions, K tagging capabilities and redundance of kinematical constraints. The two experimental approaches seem then complementary, with the exception of few issues like the challenging measurement of $\mathrm{Re}(\epsilon'/\epsilon)$ where they are likely to be in direct competition. Table II summarizes the characteristics of the various K sources.

Whichever is the topic studied (better understanding of CP and T violation, test of the standard model, search for "new physics"), the precision reached in a K experiment is always determined by the interplay of i) available statistics; ii) detector performances (acceptance, particle identification, calorimetry, tracking, systematics, etc.); iii) background conditions. In the following, on the basis of these items, we present some general considerations concerning the expected impact on various open K issues during the next few years and at the various facilities.

i) *Available statistics*

The number of K_L and K^+ decays already detected at high intensity K beams by experiments looking for rare decays is roughly of the same order of magnitude (few times 10^9) of what is expected in a year at a ϕ factory running at a luminosity of 2.5×10^{32} cm^{-2}s^{-1}. The expected upgrades of both experiments and beam lines should allow an increase of the beam intensities by one order of magnitude. In addition the ad-

vent of K factories around mid '90 should allow a gain of two more orders of magnitude, bringing the limits on selected K_L and K^+ decays, such as $K_L \to \mu e$ or $K^+ \to \pi^+ \mu^\pm e^\mp$, to the 10^{-13} level. For what concerns K_S, it is more difficult to obtain pure and intense K_S beams, because their short lifetime limits the separation from the accompanying background. However $K_S \to \pi^+\pi^-\pi^0$ is actively pursued by experiment E621 at Fermilab, where it is expected to improve the existing limit (BR $< 1.5 \times 10^{-7}$) by about two orders of magnitude before the advent of Kaon factories (see Table I).

TABLE III. Expected kaon fluxes at a ϕ factory for two different luminosities L.

	$L = 1 \times 10^{32}$ cm^{-2} s^{-1}	$L = 2.5 \times 10^{32}$ cm^{-2} s^{-1}
ϕ/year	4.1×10^9	1.0×10^{10}
$\phi \to K_L^0 K_S^0$	1.4×10^9	3.5×10^9
$\phi \to K^+ K^-$	2.0×10^9	5.0×10^9
tagged K_S^0	2.1×10^8	5.2×10^8
tagged K_L^0	9.6×10^8	2.4×10^9

On the other side, to be competitive on the measurement of $\mathrm{Re}(\epsilon'/\epsilon)$, a ϕ factory should be able to produce at least $\sim 10^{10}$ ϕ/year (see Table III). Thanks to their very low energy, a large kaon fraction (100% of K_S, $\sim 25\%$ of K_L and $\sim 70\%$ of K^+) decays in the detector fiducial volume (assumed 1 m of radius). In addition, at a ϕ factory both charged and neutral K's are produced democratically (C-odd K^+K^- and K_LK_S pairs), allowing for instance the study of CP violating effects in $K^\pm$ decays. Concerning other experiments studying direct CP violation in $K \to 2\pi$ decays, this sample should allow a better statistical precision ($\simeq 3 \times 10^{-4}$ [13]) than at CP-LEAR (expected $\simeq 2 \times 10^{-3}$

[14]) and it would be comparable in size with the samples collected by the two most precise experiments, NA31 at CERN [15] and E731 at Fermilab [16].

Using this statistics, at a ϕ factory it would be possible to study other very interesting CP violating decays, by looking for the appropriate asymmetries in channels like $K^{\pm} \to \pi^{\pm}\pi^{\pm}\pi^{\mp}$, $K^{\pm} \to \pi^0\pi^0\pi^{\pm}$, $K^{\pm} \to \pi^{\pm}\pi^0\gamma$, $K_{L,S} \to \pi^+\pi^-\gamma$, $K_L \to \pi^{\pm}l^{\mp}\nu$ and $K_L \to \pi^+\pi^-\pi^0$. In particular, the study of direct CP violation in $K^{\pm}$ decays, because of possible enhancement effects [17], looks promising: at a ϕ factory it should be possible to improve by one order of magnitude the accuracy of the measurement on charge and Dalitz plot asymmetries, reaching the level of some theoretical predictions.

The situation seems also particularly favorable here for what concerns K_S decays. In fact, for the first time it would be possible to produce extremely pure (tagged) K_S beams, dramatically improving the knowledge of K_S branching ratios (most of them not measured, like $K_S \to \pi^0\nu\overline{\nu}$, $e^+e^-\gamma$, $\mu^+\mu^-\gamma$, $\pi^0e^+e^-$, $\pi^0\mu^+\mu^-$, $\pi^{\pm}\mu^{\mp}\nu_{\mu}(\overline{\nu}_{\mu})$, $\pi^{\pm}\, e^{\mp}\nu_e(\overline{\nu}_e)$, etc.) down to the 10^{-8} level (if the contamination coming from $\phi \to K\overline{K}\gamma$ is not unexpectedly large). As an example, by selecting events where the K_L decays into $\pi^{\pm}l^{\mp}\nu$ it should be possible to substantially improve the existing limit on the CP violating reaction $K_S \to 3\pi^0$, by looking for 6 low energy photons in the detector (the experiment discussed in ref. [13] should be capable of efficiently detecting photons down to energies of (few) ten(s) MeV). Another difficult search that could be performed concerns the decay $K_S \to \pi^0\gamma\gamma$, where it may be possible to detect a few events.

At CP-LEAR, the goal is to collect in the next few years $\sim 10^{13}$ $p\overline{p}$ annihilations at rest to study the (C-even) $K^+\pi^-K^0$ and $K^-\pi^+\overline{K}^0$ decays (the fraction $p\overline{p} \to K^{\pm}\pi^{\mp}K^0(\overline{K}^0)$ being of the order $\simeq 4 \times 10^{-3}$). Concerning direct CP violation in $K \to 2\pi$ decays, although the statistical error corresponding to this sample ($\sigma(\epsilon'/\epsilon) \simeq 2 \times 10^{-3}$) will be larger than for NA31 and E731, the systematic errors are expected to be completely different, motivating this experimental approach. In addition, this sample should allow a measurement of CP violation in the $K_{L,S} \to 3\pi$ channel (through the parameters η_{+-0} and η_{000}, discussed in the next Section). Finally, as a source of pure K^0 and $\overline{K}^0$ final states, LEAR represents a unique chance to study order ϵ CP-violations in $K^0(\overline{K}^0) \to \gamma\gamma$ decays.

ii) *Detector performances*

To accurately measure the different K decays one needs detectors capable to identify $\pi^{\pm}, e^{\pm}, \mu^{\pm}$ and γ and to measure their energy.

At very low energy (ϕ factories, LEAR, stopped K^+ beams) good π/μ separation and efficient γ detection become difficult. For instance, in $K^+ \to \pi^+\nu\overline{\nu}$ experiments, K^+ are stopped in the target and then the detectable reaction signature consists of a single pion of non discrete energy occurring at a very low rate ($\sim 10^{-10}$) in the presence of a large background of muons (from $K^+ \to \mu^+\nu$ and $K^+ \to \mu^+\nu\gamma$). In this case the π/μ rejection factor ($\sim 10^{-6}$) given by energy and momentum-range measurement is definitely not sufficient [18] (see Fig. 1, taken from ref. [19]), and it is necessary to follow the decay chain $\pi^+ \to \mu^+ \to e^+$. This method allows an additional few 10^{-5} rejection power but requires a continuous reading of the detector by means of high frequency (500 MHz) transient digitizers [20].

At higher energy ($p_K \sim O(10$ GeV/c)), like in experiments searching for $K_L \to \mu^{\pm}e^{\mp}$ or $K^+ \to \pi^+\mu^{\pm}e^{\mp}$, the leading potential background arises from the decay $K_L \to \pi^{\pm}e^{\mp}\nu_e$ followed by $\pi^{\pm} \to \mu^{\pm}\nu_\mu$ in flight. In order to suppress this background, high precision tracking of the charged decay products in a magnetic field is performed, to determine their momenta and trajectories and to reconstruct the K_L mass. To detect momentum change in flight a redundant muon energy determination is performed, measuring the momentum twice. Additional μ/π rejection is obtained also in this case by means of a range measurement, as it is shown schematically in Fig. 2 in the case of the experiment E777 at Brookhaven [21].

As far as γ detection is concerned, at low energy it is rather difficult to reliably detect them. In fact, in addition to the probability of not converting in the calorimeter, assuming $L/L_{rad} \simeq 15$

$$I_\gamma = e^{-\frac{7}{9}L/L_{rad}} \simeq 10^{-5} \quad , \tag{1}$$

shower fluctuations may cause additional inefficiencies. As an example, with a typical

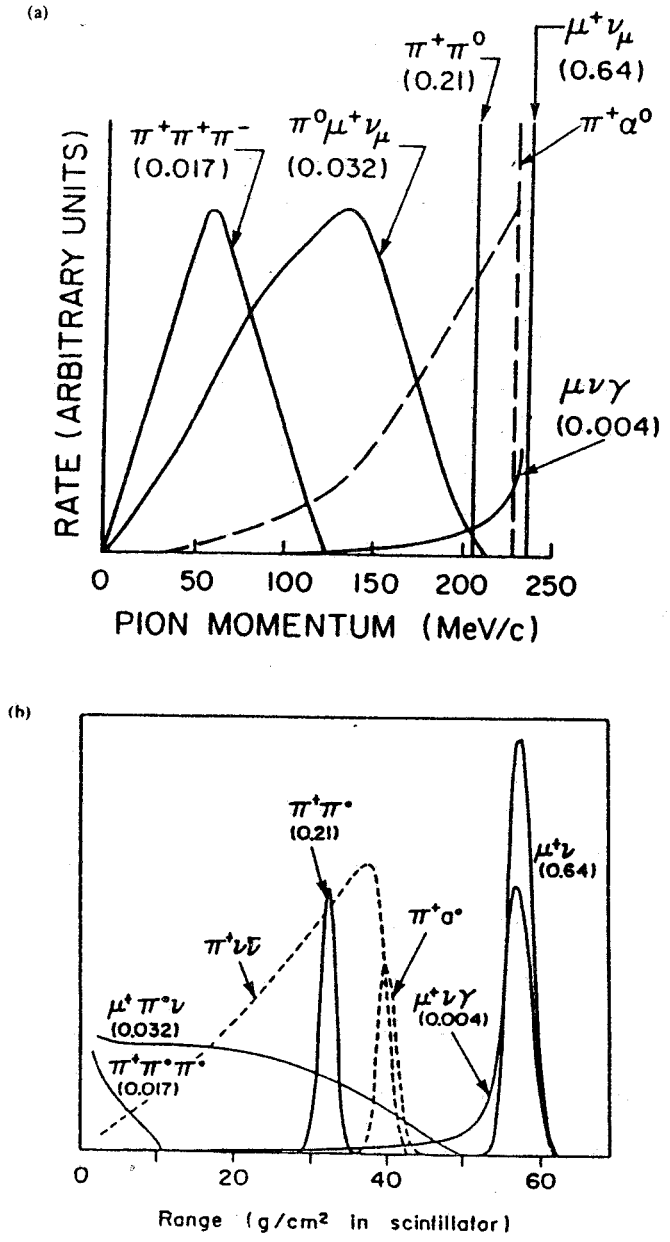

Fig. 1 - Spectra of K^+ decay modes. Dashed lines: $K^+ \to \pi^+\nu\bar{\nu}$ and $K^+ \to \pi x$. Solid lines: other modes. Branching ratios are shown in parentheses. The vertical scales are arbitrary and different for each decay. (a) Momentum spectra, and (b) range spectra in scintillator with finite resolution (taken from Ref. [19]).

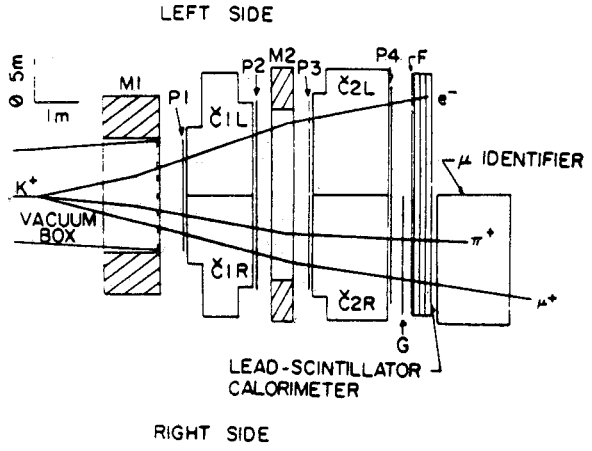

Fig. 2 - Schematic of the apparatus of BNL E777, used in the search for $K^+ \to \pi^+\mu e$ (from ref. [21]).

calorimeter (15 L_{rad} long, 1mm Pb/5mm scintillator sandwich) at $E_\gamma = 20$ MeV the visible energy results

$$E_{vis} = 0.44E_\gamma \pm 0.03\sqrt{E_\gamma} \simeq 8.8 \pm 4.2 \text{ MeV} \quad , \tag{2}$$

which implies, for $E_{\text{thres}} = 4$ MeV, a probability of $\simeq 15\%$ of not detecting the converted photon. Finally, a small γ fraction interacts directly with the nuclei instead of undergoing an electromagnetic shower, so much of the energy goes in neutral reaction products and the photon is lost. Fig. 3 (taken from ref. [22]) shows the behaviour of the probability for a γ of not being detected as a function of its energy, in the range $20 - 220$ MeV relevant for ϕ factories, LEAR and stopped K^+ beams. More sophisticated detectors using liquid Xenon or Krypton discussed in [13] are expected to improve substantially the e.m. calorimetry at low energy.

The ability of detecting all photons in the event is essential to tag or veto various decays. For instance, when searching for $K^+ \to \pi^+\nu\bar{\nu}$ decays one has to reject $K^+ \to \mu^+\nu\gamma$ or $K^+ \to \pi^+\pi^0$ decays by detecting all low energy photon(s) present in the events.

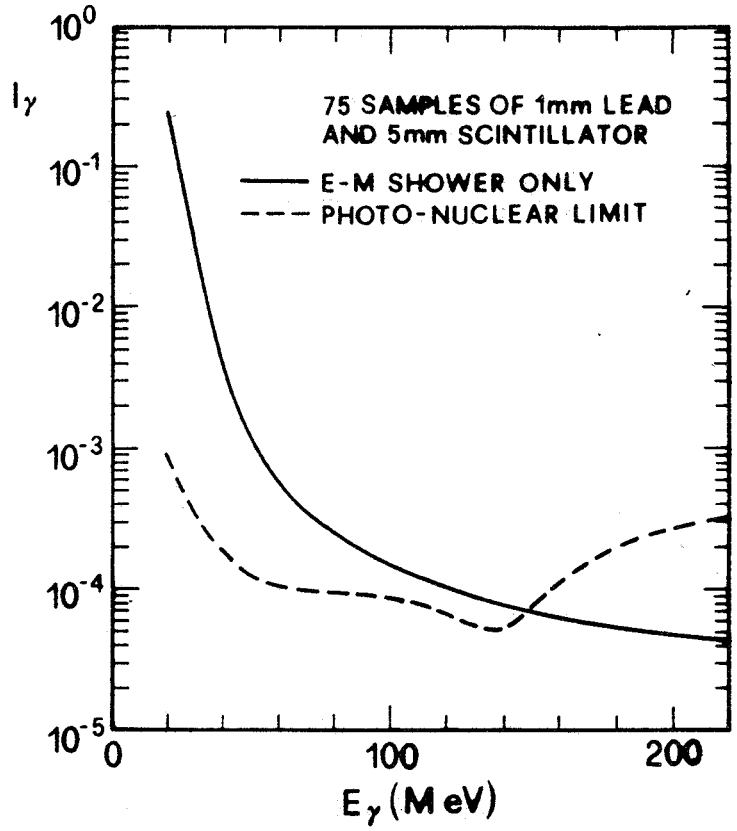

Fig. 3 - Photon detection inefficiency with lead scintillator calorimeter in the 20-220 MeV range (from ref. [22]).

Similarly, to search for the $K_S \to 3\pi^0$ decays at the ϕ resonance one needs a very good acceptance on rather low energy photons.

At higher energies, the photon detection is easier because of the boost. Also the electromagnetic energy resolution, improving as $E^{-\frac{1}{2}}$, tends to favour the use of high energy K beams. On the other hand, high energy π^0's decay into photon pairs that often overlap, requiring good calorimetric resolution to be separated. Conversely, at low energy facilities, where the γ detection is more difficult, opening angles are large.

One should also recall that at higher energy, additional techniques of particles identification become available, like Čerenkov radiation detection and transition radiation detection (both useful for instance in π/e separation). However, as we will see in discussing the next point, although high energy experiments clearly have a better set of

experimental techniques for particle identification, it is also true that their background conditions are much worse than at LEAR or at the future ϕ factories, because of the contamination of K^+ and K_L beams with pions, muons, photons and neutrons.

At a ϕ factory one expect that a sophisticated 4π detector designed to measure $\mathrm{Re}(\epsilon'/\epsilon)$ [13], characterized by an excellent electromagnetic calorimetry, good momentum measurement, vertex reconstruction and $\pi/\mu/e$ separation, should be able to accurately measure all kinds of $K_{L,S}$, $K^\pm$ decays with rather good statistics, as it has been discussed above. From this point of view it would be superior to single purpose experiments looking for one or few rare decays at high intensity K beams. One could expect for instance to improve the existing limits on $K^\pm \to \pi^\pm\gamma\gamma$ or $K^\pm \to \pi^\pm\mu^+\mu^-$, detecting tens or hundreds of events. Also the existing limits on $K^\pm \to \pi^0\mu^\pm\nu\gamma, \pi^\pm\pi^\pm\mu^\mp\nu, \pi^\pm\gamma\gamma\gamma$ and $l^\pm\nu\nu\nu$ could be substantially improved.

It is also useful to recall that, in order to reach branching ratios of the order of 10^{-10} or less, which is the goal of most experiments at high intensity K beams, great care is needed to handle the large amount of data coming from the detector: trigger and data acquisition are clearly a key element in this kind of experiments.

When performing high precision measurements as in the case of CP violating effects, systematic errors play a very important rôle. This matter is clearly rather complicated, but, without entering into details, it seems reasonable to expect that experiments performed at high intensity K beams will suffer from different kinds of systematics, more than experiments performed at $p\bar{p}$ or e^+e^- machines. Given similar statistical errors, this fact may help in the comparison of the various results.

iii) *Background conditions*

One of the strongest points in favor of a ϕ factory is the cleanliness of the final K state in comparison to the more complex final state in $p\bar{p}$ interactions or to the background induced by neutrons, muons, pions and photons accompanying high energy, high intensity K beams. Even if in high luminosity e^+e^- interactions we may expect a considerable flux of low energy photons (keV region), it should be possible to min-

imize this background by making use of the existing kinematical constraints. About 74% of ϕ's decay in fact into pure $K\overline{K}$ pairs (with a very small radiative $K\overline{K}\gamma$ contribution well under control [23]). By making use of $K_{L,S}$ different decay lengths and selecting properly $K_L(K_S)$ decays containing two charged particles and no photons (i.e. $K_L \rightarrow \pi^{\pm} l^{\mp} \nu$, BR = 65.6%, and $K_S \rightarrow \pi^+\pi^-$, BR = 68.6%) it would be possible, for instance, to "tag" $K_S(K_L)$ decays containing many photons with negligible background contributions, as mentioned in the previous point.

The situation is clearly more critical at hadroproduced K beams, where one routinely has to tolerate neutron fluxes one order of magnitude larger than the number of K decaying in the apparatus [10] . This fact is one of the basic elements to take into account when designing experiments at these machines, and in some case limits the sensitivity of the existing detectors.

We then tentatively conclude that, for what concerns the study of some K issues, like for instance the neutral K (in particular K_S) decays containing many particles in the final states, a ϕ factory equipped with a good 4π detector would be superior both to LEAR and to high intensity K beams.

In the following sections, various K physics issues still open (except $\mathrm{Re}(\epsilon'/\epsilon)$) are reviewed, keeping in mind the kind of experimental constraints discussed above. It turns out that some issues will be better studied at high energy K beams (very rare and forbidden K decays), others at LEAR (CP violation in $K^0(\overline{K}^0)$ decays) and others at a ϕ factory.

The advent of this last facility, with a production of $10^9 - 10^{10}$ ϕ/year, would give a dramatic boost to our understanding of the K's system, allowing a detailed study of many aspects of CP violation better than elsewhere. Ultrapure and remarkably intense $K_{L,S}$ and $K^{\pm}$ beams will be available, allowing the study of all possible K decays down to the $10^{-8} - 10^{-9}$ level, with an accuracy that, at least in the case of K_S decays, will basically be without comparison. Finally, regarding the challenging measurement of $\mathrm{Re}(\epsilon'/\epsilon)$, all experimental approaches seem worth pursuing, because, while the statistical significance of the samples collected at the various machine seems comparable, the systematics are expected to be different.

III. Common decays: $K \to 2\pi$, $K \to 3\pi$, $K_{\ell 2}$, $K_{\ell 3}$, $K_{\ell 4}$

We consider here the purely hadronic decays

$$K \to 2\pi \quad , \qquad K \to 3\pi \quad , \tag{3}$$

together with the relatively common semileptonic decays

$$K_{\ell 2}(K \to \ell \nu_\ell) \quad , \qquad K_{\ell 3}(K \to \pi \ell \nu_\ell) \quad , \qquad K_{\ell 4}(K \to \pi\pi \ell \nu_\ell) \quad . \tag{4}$$

All these decays represent important sources of information either because of the appearance of violation effects related to their asymmetry properties (typically the CP violation in the $K \to 2\pi$ decays), or for the possibility of performing precision tests.

The purely hadronic decays $K \to 2\pi$ play a very important rôle in K decay physics. The decay $K_L \to 2\pi$, with typical branching ratio of the order of 10^{-3}, is until now the unique manifestation of "indirect" CP violation, measured by the parameter ϵ and induced by the state mixing. Furthermore, the comparative analysis of the two processes $K_L \to 2\pi$ and $K_S \to 2\pi$, through the simultaneous estimate of the two familiar amplitude ratios

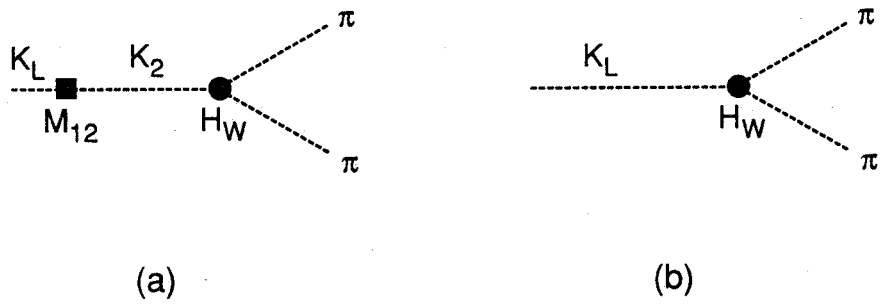

Fig. 4 - The decay $K_L \to 2\pi$ can manifest: (a) mass mixing and (b) direct $\Delta S = 1$ CP violation effects.

$$\eta_{+-} = \frac{< \pi^+\pi^- | H_w | K_L >}{< \pi^+\pi^- | H_w | K_S >} = \epsilon + \epsilon' \quad , \quad \eta_{00} = \frac{< \pi^0\pi^0 | H_w | K_L >}{< \pi^0\pi^0 | H_w | K_S >} = \epsilon - 2\epsilon' \qquad (5)$$

allows a measure of the ratio ϵ'/ϵ, i.e. a test of the direct CP violation (see Fig. 4). A substantial effort has been recently performed from the experimental side, but with a rather controversial result, because of a certain disagreement between the the two most recent and precise determinations, those of the NA31 collaboration at CERN [15] and of the E731 experiment of the Chicago–Fermilab collaboration [16]:

$$\mathrm{Re}\left(\frac{\epsilon'}{\epsilon}\right) = \begin{cases} (3.3 \pm 1.1) \times 10^{-3} & [\,15\,] \\ -(0.5 \pm 1.5) \times 10^{-3} & [\,16\,] \end{cases} \qquad (6)$$

We do not discuss here the $K \to 2\pi$ problem and its connection with the CP violation in the $K\overline{K}$ system, since the general formalism and its parametrization are considered in an exhaustive way in several reviews (for instance in [24] and more recently in [25]). We only give in Fig. 5 an account of the graphs that in the standard model are supposed to contribute to the kaon CP violation. A brief comment of their relevance is reported in the figure caption.

In particular the problem of determining $\mathrm{Re}(\epsilon'/\epsilon)$ at a ϕ factory from an analysis of the decay $\phi \to (K\overline{K})_{C=-1}$ has been faced in [26], [13], [27] and [23]: in the latter reference the possibility of performing the measurement also in presence of a possible contamination coming from the alternative decay $\phi \to \gamma S^*$ with $S^* \to (K\overline{K})_{C=+1}$ [28] has been considered too.

While the analysis of the $K \to 2\pi$ decays has to be considered of central interest in the K decay physics, a potentially important rôle is covered also by the $K \to 3\pi$ processes. The possibility of finding an evidence of CP nonconservation in $K \to 3\pi$ transitions could enable us to obtain further information, useful to distinguish between the various models of CP violation. The cleanest way to observe CP violation would be the search for the CP-forbidden decay $K_S \to 3\pi^0$, as $\mathrm{CP}(3\pi^0) = -1$. This search appears unpracticable at high energy K_S beams mainly because of background problems. It would become much easier at a ϕ factory, provided one had an efficient detection sys-

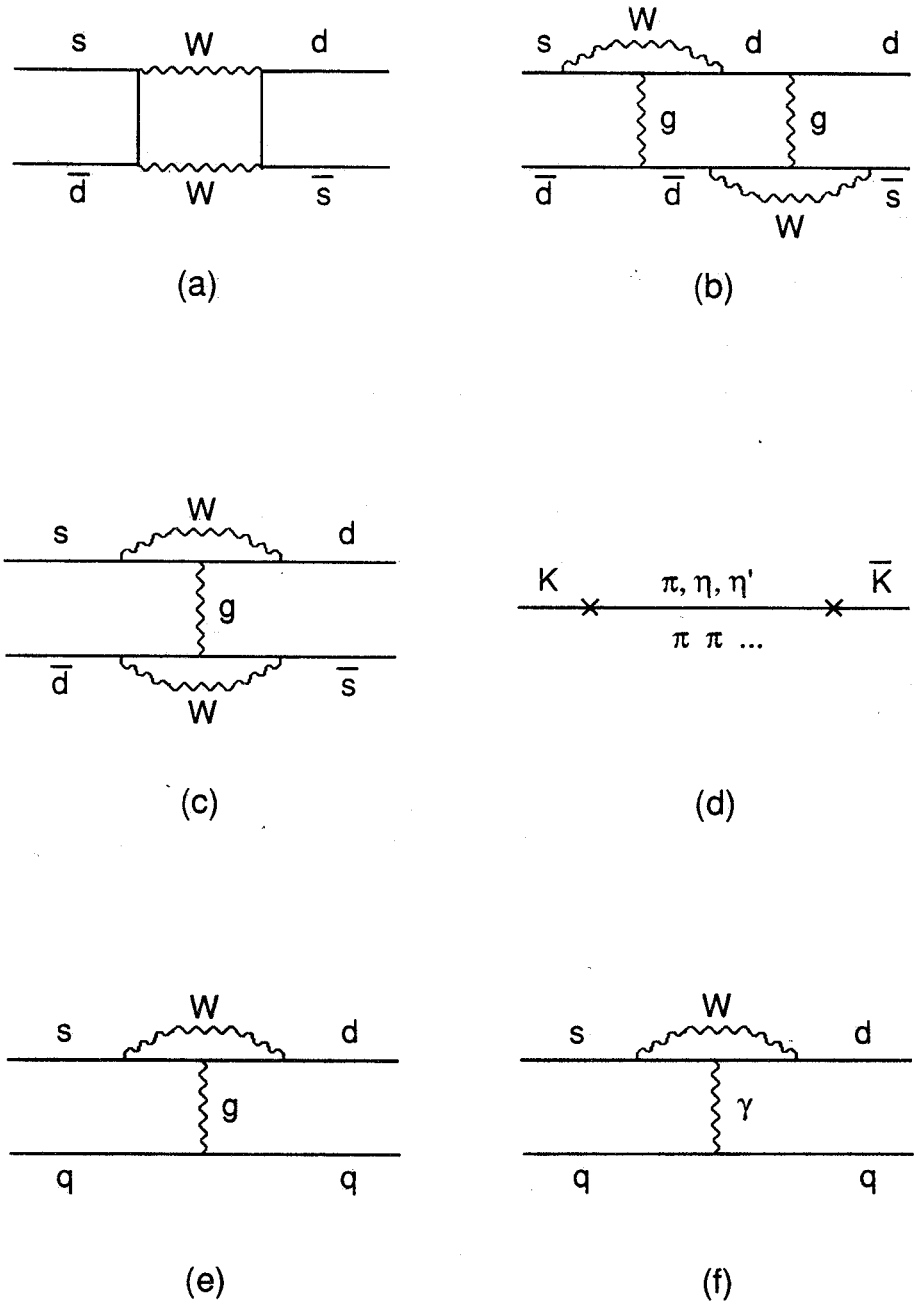

Fig. 5 - Diagrams contributing to CP violation in the $K\overline{K}$ system. Diagrams (a), (b), (c) and (d) are indirect (mass mixing) effects, while (e) and (f) are direct transitions. The so-called double penguin (b) and siamese penguin (c) give contributions smaller than the box diagram (a) because of the lack of heavy quark loops.

detection system to detect low energy photons. In fact, tagging the K_S, by selecting $K_L \to \pi\mu\nu_\mu, \pi e\nu_e$ decays, one should search for events having 6 photons in the detector; it should not be too difficult to significantly improve the existing limit $\mathrm{BR}(K_S \to 3\pi^0) < 4 \times 10^{-5}$ [29].

From just mass mixing one would naively expect the branching ratio of $K_S \to 3\pi^0$ to be of the order of 10^{-9}, so that an improvement by several orders of magnitude is required to be sensitive to this process. Actually it could be interesting to analyze theoretically the possibility of some dynamical enhancement of the amplitude. Besides the well–known phenomenological analysis of Devlin and Dickey [30], there is a considerable amount of theoretical work on the $K \to 3\pi$ processes [31]. From the paper of Li and Wolfenstein [32] to the most recent papers as [33], [34], the problem has been faced of connecting the new parameters characteristic of the $K \to 3\pi$ decay to the CP–violating parameters of the $K \to 2\pi$ decay. In particular the amplitude ratio for $K_S \to 3\pi$ has been studied:

$$\eta_{+-0} = \frac{< \pi^+\pi^-\pi^0 | H_w^{(-)} | K_S >}{< \pi^+\pi^-\pi^0 | H_w^{(+)} | K_L >} = \epsilon + \epsilon'_{+-0} \tag{7}$$

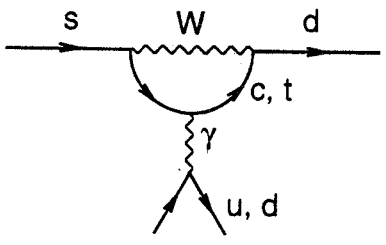

Fig. 6 - Electromagnetic penguin diagram, contributing to CP violation.

where $H_w^{(\pm)}$ are the CP–even and the CP–odd parts of the weak non–leptonic Hamiltonian. Within the standard model and using current algebra and the simplest linear parametrization of the $K \to 3\pi$ amplitudes Li and Wolfenstein [32] derive $\epsilon'_{+-0} = -2\epsilon'$. From this one could expect a situation where there is a dominant CP–conserving, $\Delta I = \frac{3}{2}$ amplitude, giving [35] $\mathrm{BR}(K_S \to \pi^+\pi^-\pi^0) \simeq (1-3) \times 10^{-7}$ (to be compared with the experimental upper limit of 1.5×10^{-7}), while the CP–violating transition would be an effect of order ϵ and then $\sim 10^{-9}$. But one should expect a considerable modification of this result, coming from the electromagnetic penguin diagram (see Fig. 6) and isospin mixing contributions, together with possible effects of terms of higher order in the pion momenta in the $K \to 3\pi$ amplitudes [33], and/or meson rescattering effects [17]. It follows that an enhancement of the Li-Wolfenstein prediction cannot be excluded, with values for ϵ'_{+-0} about one order of magnitude larger, so reaching $\epsilon'_{+-0} \simeq \epsilon/10$ [33]. This conclusion does not seem to be unanimous, however, see e.g. [36]. Of course deviations of η_{+-0} from ϵ are hard to be seen, but also a measurement of η_{+-0} to order ϵ is significant: a theory of CP violation purely parity–conserving could generate ϵ in the $K\overline{K}$ system and could have $\tilde{\eta}_{+-0}$ different from zero (and also as large as several times ϵ, at least in principle) while ϵ' could be strictly zero being related to a parity–violating process [33].

The existing limit on $K_S \to \pi^+\pi^-\pi^0$ should soon be substantially improved by experiment FNAL E621; the expected sensitivity is in fact $\simeq 3 \times 10^{-9}$, close to the predicted rate $\simeq 1.2 \times 10^{-9}$ [12], but a proposed upgrade of the same experiment should allow a test of this theoretical prediction. This measurement would also be possible at a ϕ factory, following the same tagging strategy discussed above: with 10^{10} ϕ produced it should be possible to reach the 10^{-8} region.

Also the charged $K^\pm \to 3\pi$ are of interest, because the enhancement effects of direct CP violation mentioned above might lead to charge asymmetries (both in the rates Γ's and in the linear slopes g's), in the perspective of a high statistics experiment [17]:

	theory	experiment
$\|\Delta\Gamma(K^\pm \to \pi^\pm\pi^\pm\pi^\mp)\|$	$\sim 0.39 \times 10^{-4}$	$\Delta\Gamma = (0.35 \pm 0.6) \times 10^{-3}$
$\|\Delta\Gamma(K^\pm \to \pi^0\pi^0\pi^\pm)\|$	$\sim 0.11 \times 10^{-3}$	$\Delta\Gamma = -(0.15 \pm 2.7) \times 10^{-3}$
$\|\Delta g(K^\pm \to \pi^\pm\pi^\pm\pi^\mp)\|$	$\simeq 0.14 \times 10^{-2}$	$\Delta g = -(0.75 \pm 0.5) \times 10^{-2}$
$\|\Delta g(K^\pm \to \pi^0\pi^0\pi^\pm)\|$	$\simeq 0.14 \times 10^{-2}$	not available

(8)

This kind of measurements seems well suited for an experiment running at a ϕ factory, where K^+'s and K^-'s are produced in pairs and populate in the same way the detector fiducial region. This seems to allow for keeping the experimental systematics under control: with 10^{10} ϕ one expects to easily improve the existing experimental limits on the asymmetries by an order of magnitude, reaching the level of the theoretical predictions in eq. (8).

We consider now the most common semileptonic decays. From $K_{\ell 2}$ ($K \to \mu\nu_\mu$, $K \to e\nu_e$) decay rates several precision measurements are possible. Let us mention:

- test of e–μ universality and V–A charged currents, inclusive of radiative correction effects, by improving the measurement of the ratio

$$R_K = \frac{\Gamma(K \to e\nu_e)}{\Gamma(K \to \mu\nu_\mu)} = (2.42 \pm 0.11) \times 10^{-5} \quad ; \tag{9}$$

- constraints on non-(V–A) couplings in the strange sector.

As a byproduct of the analysis of these decays it was possible to include the search for effects of heavy neutrinos (ν_H), whose mixing was expected to influence the experimental ratio $(K \to e\nu)/(K \to \mu\nu)$, and whose presence was expected [37] to induce low energy peaks in the μ momentum distribution in the reaction $K \to \mu\nu_H$. At present the possibility of relatively light neutrinos is, however, excluded by the recent results of LEP experiments [9].

$K_{\ell 3}$ decays ($K \to \pi\mu\nu_\mu$, $K \to \pi e\nu_e$), are relevant in testing the CKM matrix element $|V_{us}|$: the best determination of $|V_{us}|$ comes in fact from an analysis of $K_{\ell 3}$

decays performed in [38], which find

$$|V_{us}| = 0.2196 \pm 0.0014 \pm 0.0023 \quad , \tag{10}$$

The uncentainty combines the experimental errors and the uncertainties induced by SU(3) breaking and by the isospin violation between the $K^+_{\ell 3}$ and the $K^0_{\ell 3}$ modes. On the other hand V_{us} enters, together with V_{ud} and V_{ub}, in the fundamental test of the unitarity of the CKM matrix in the usual scheme of three generations. At present [39]

$$|V_{ud}|^2 + |V_{us}|^2 + |V_{ub}|^2 = 0.9979 \pm 0.0021 \quad . \tag{11}$$

Since V_{ud} is expected to be improved, an improvement in the estimate of V_{us} through $K_{\ell 3}$ decays seems of relevance.

Another important aspect is the measurement of form factors, which can severely test the models used to realize the non–perturbative, long–distance QCD.

Very importantly, the charge asymmetry in $K_L \to \pi \ell \nu$ decay provides an alternative measurement of the indirect CP violation parameter ϵ. The experimental result, averaged over $\ell = e, \mu$ is $\mathrm{Re}\,\epsilon = (3.30 \pm 0.12) \times 10^{-3}$ [31].

An interesting search involving $K_{\mu 3}$ decays is the measurement of the muon transverse polarization $\sigma_\mu \cdot (p_\pi \times p_\mu)$, where a finite value would indicate a violation of the time–reversal invariance [31], [40], up to higher order Coulomb corrections. The existing experimental limit on the T-violating component of the μ polarization $P_N = (-1.85 \pm 3.60) \times 10^{-3}$, derived [41] from both $K^+_{\mu 3}$ and $K^0_{\mu 3}$ decays, has been obtained with a rather small number of events ($\simeq 2 \times 10^7$), and the uncertainties are almost wholly statistical. The standard model would predict zero muon polarization apart from electromagnetic corrections which are negligible for the $K^+_{\mu 3}$. Therefore this kind of measurement could be helpful to constrain alternative ideas on CP violation [42]. From a statistical point of view, with the available and future K sources, there is clearly the possibility to improve the accuracy by at least one order of magnitude.

However, such an experiment would require a highly segmented polarimeter to measure the μ polarization through its $e\nu_e$ decays. While the feasibility of this kind of detector has already been demonstrated at (low energy) K beams, the possibility to operate a 4π detector with μ polarimetry at a ϕ factory has not been analysed yet. In the affirmative case, this would be an important tool to study T-violating processes in K decays involving μ's, and in any case an interesting experiment *per se*.

Again in $K_{\mu 3}$ decays, only an extremely high statistics analysis of the three–body decays [43] seems it could allow an improvement of the existing limit of the ν_μ mass ($m_{\nu_\mu} < 250$ keV).

We close by stressing the interest of the $K_{\ell 4}$ decays $K \to \pi\pi e\nu_e$ and $K \to \pi\pi\mu\nu_\mu$, which occur at the level of $(2-6) \times 10^{-5}$, depending on the specific mode. They give important information on the $\pi\pi$ low–energy phase shifts [44], and in general the measurement of the vector and axial–vector form factors represents a test of the prediction of the various theoretical approaches, in particular those based on effective chiral lagrangians [45], [46]. Also in this case T–odd correlations can be searched for [40], [42].

IV. Not so rare decays: $K \to (\ell\nu)\gamma$, $K \to (\ell\nu)(\ell\bar{\ell})$, $K_{2\gamma}$, $K \to (\ell\bar{\ell})\gamma$, $K \to \pi\pi\gamma$, $K^\pm \to \pi^\pm\gamma\gamma$

This sector involves a conspicuous number of radiative leptonic and non-leptonic decays, whose branching ratios make still possible precision meassurements. On the other hand, a theoretical understanding of these decays requires an accurate description of the hadronic structure and an estimate of the strong interaction effects.

A measurement of vector and axial–vector structure dependent form factors is possible from the analysis of the spectrum of the high energy γ's in the decay $K \to (\ell\nu)\gamma$ [47]. This information is needed as it represents a portion of the $O(\alpha)$ corrections to

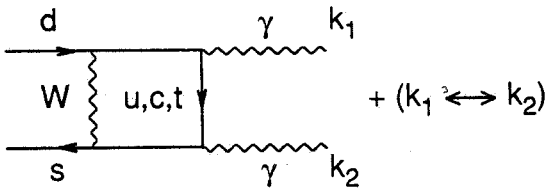

Fig. 7 - The short distance contribution to the $K_L \to \gamma\gamma$ decay.

the ratio R_K of eq. (9).

The processes $K^0 \to \gamma\gamma$, $K^0 \to \gamma\ell^+\ell^-$ ($\ell = e, \mu$), $K \to \pi\pi\gamma$ and $K^\pm \to \pi^\pm\gamma\gamma$ introduce the class of flavour–changing neutral current transitions with photons in the final state, suppressed in the standard model by the GIM mechanism, and with branching ratios in the range below 10^{-4}. They are described by an electroweak transition hamiltonian H_{eff} in terms of quark (and gluon) fields, where the dominance of short–distance physics is assumed. The example relevant to the decay $K_L \to \gamma\gamma$ is shown in Fig. 7. It is then necessary to estimate the hadronic matrix elements of such a H_{eff}. In addition long–distance effects are also expected, arising from non–perturbative strong interaction corrections to the quark diagrams at a low mass scale, which are determined by the confinement physics. An example of this kind of effect is represented, for $K_L \to \gamma\gamma$, by the polar diagrams of Fig. 8.

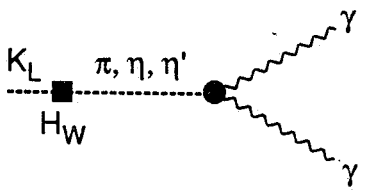

Fig. 8 - The pole diagrams for the $K_L \to \gamma\gamma$ decay.

Besides probing the standard model, these decays can thus be very useful in order to test the various dynamical approaches followed in estimating the hadronic matrix elements. In ref. [48], where these decays were first considered in the context of the standard model, simple quark model estimates were used. The framework which recently has become most popular is represented by the so-called "chiral perturbation theory", where effective chiral lagrangians are used as computational tools. The basic idea is represented by an assumed $SU(3)_L \times SU(3)_R$ chiral symmetry of strong interactions, valid in the zero mass limit of the lightest quarks (u, d and s). A spontaneous symmetry breaking to $SU(3)_V$ is supposed to occur in that limit, giving rise to an octet of massless Goldstone bosons, which are associated to the usual pseudoscalar octet of the lowest lying mesons, i.e. pions, kaons and eta. It is possible to implement this idea in the framework of QCD, and to integrate out the gluon and quark degrees of freedom of the basic QCD lagrangian to obtain an effective (non linear) interaction lagrangian in terms of pseudoscalar meson fields, the photon and the lepton fields, with the desired symmetry properties mentioned above [49]. In particular such a lagrangian contains the soft pion results of current algebra and PCAC. Finite pseudoscalar meson masses and momenta are accounted for by respectively expanding in the quark masses and by considering meson loops and the addition of higher derivative interactions, whose form is fixed by the chiral symmetry. The advantage of this scheme, which is supposed to realize QCD at low energy (i.e. at long distances), is that one can predict by means of the effective lagrangian a multitude of transition amplitudes involving pions and kaons (and the eta) in terms of a reduced number of constants. For this reason it has been extensively applied to kaon semileptonic and non-leptonic decays.

Indeed specific treatments of the different decays within the chiral lagrangian approach with refinements of the computational schemes can be found in the literature. Examples are the analysis of the non–leptonic radiative K decays with at most one pion in the final state ($K \to \gamma\gamma$, $K \to (\ell\bar{\ell})\gamma$, $K \to \pi\gamma\gamma$, $K \to \pi\ell^+\ell^-$), performed by Ecker, Pich and de Rafael [50], that of the semi–leptonic processes ($K_{\ell 3}$, $K_{\ell 3\gamma}$, $K_{\ell 4}$) of Donoghue and Holstein [46], or the estimate of the branching ratio of the decay $K \to \gamma\gamma$ [51], recently reexamined in [52], [53]. In Table IV, taken from ref. [54], the predictions derived within the chiral perturbation theory [50] for the branching ratios of

TABLE IV. Branching ratios of some rare kaon decays.

mode	theory	experiment
$K_S \to \gamma\gamma$	2×10^{-6} [1.4×10^{-6}]	$(2.4 \pm 1.2) \times 10^{-6}$
$K_S \to \pi^0\gamma\gamma$	3.3×10^{-8} [$10^{-8} - 10^{-9}$]	———
$K_S \to e^+e^-\gamma$	3.2×10^{-8}	———
$K_S \to \mu^+\mu^-\gamma$	7.5×10^{-10}	———
$K_S \to \pi^0e^+e^-$	$5 \times 10^{-9} - 5 \times 10^{-10}$ [10^{-8}]	$< 4.5 \times 10^{-5}$
$K_S \to \pi^0\mu^+\mu^-$	$1 \times 10^{-9} - 1 \times 10^{-10}$	———
$K_L \to \gamma\gamma$	[10^{-4}]	$(4.9 \pm 0.4) \times 10^{-4}$
$K_L \to \pi^0\gamma\gamma$	6.8×10^{-7} [$< 10^{-7}$]	$< 2.7 \times 10^{-6}$
$K_L \to e^+e^-\gamma$	9.1×10^{-6}	$(1.7 \pm 0.9) \times 10^{-5}$
$K_L \to \mu^+\mu^-\gamma$	2.3×10^{-7}	$(2.8 \pm 2.8) \times 10^{-7}$
$K_L \to \pi^0e^+e^-$	$10^{-11} - 10^{-12}$	$< 4.2 \times 10^{-8}$
$K_L \to \pi^0\mu^+\mu^-$	$10^{-11} - 10^{-12}$	$< 1.2 \times 10^{-6}$
$K^\pm \to \pi^\pm e^+e^-$	input.[10^{-6}]	$(2.7 \pm 0.5) \times 10^{-7}$
$K^\pm \to \pi^\pm\mu^+\mu^-$	6.1×10^{-8}	$< 2.3 \times 10^{-7}$
$K^+ \to \pi^+\gamma\gamma$	$\geq 4 \times 10^{-7}$ [$10^{-6} - 10^{-7}$]	$< 1 \times 10^{-6}$

the radiative decays considered above are reported together with those obtained for more rare decays which will be considered in the following. To fit the coefficients of higher order terms in the chiral lagrangian, the measured rate of the decay $K^+ \to \pi^+ e^+ e^-$ has been used as an input. In the same Table we report, for comparison, the values originally obtained in [48]. The considerable agreement between theory and experiment [55] in the estimate of the decay $K_S \to \gamma\gamma$ is considered an important success of the approach.

Briefly commenting the most important aspects, $K_S \to \gamma\gamma$ has only long–distance contributions, so it is determined by meson loops, an example of which is reported in Fig. 9. The same is true for $K_S \to \gamma\ell^+\ell^-$, where one photon becomes virtual. Conversely, $K_L \to \gamma\gamma$ (and $K_L \to \gamma\ell^+\ell^-$) has both short– and long–distance contributions. Indeed the latter, represented in Fig. 8, should be the dominant one, and is quite sensitive to the details of $SU(3)$ symmetry breaking and $\eta - \eta'$ mixing [53].

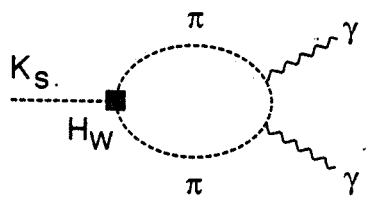

Fig. 9 - Chiral loop mechanism for $K_S \to \gamma\gamma$.

Also of interest, in the context of CP violation and of the high statistics measurements of the kaon decays, should be the asymmetry (τ being the proper time)

$$A(\tau) = \frac{\Gamma(K^0 \to \gamma\gamma) - \Gamma(\overline{K}^0 \to \gamma\gamma)}{\Gamma(K^0 \to \gamma\gamma) + \Gamma(\overline{K}^0 \to \gamma\gamma)} \quad , \tag{12}$$

for which various estimates exist [56]. The two photons can be in two different CP states corresponding to the two states of polarization. Therefore both $K_S \to \gamma\gamma$ and

$K_L \to \gamma\gamma$ are allowed. Anyway in presence of CP violation, interference between K_S and K_L amplitudes in an originally pure $K^0(\overline{K}^0)$ beam should occur and it could be detected in the measurement of the decay rate asymmetry.

This measurement seems ideal for LEAR, where pure (tagged) $K^0(\overline{K}^0)$ beams are available by selecting $K^\pm\pi^\mp K^0(\overline{K}^0)$ events where the $K^\pm$ decays semileptonically. With a sample of $\simeq 10^{13}$ $p\bar{p}$ interactions at rest (expected for CP-LEAR during the next few years) an attempt to measure this asymmetry seems feasible, at least from a statistical point of view. In fact, from the branching ratios for $K_S \to \gamma\gamma$ and $K_L \to \gamma\gamma$ measured by NA31 [55] and using 50% as detection efficiency, the expected statistical error is $\leq 10^{-3}$, i.e. of the same order of the ϵ effect.

The decays $K \to \pi\pi\gamma$ could give in principle additional information on direct CP violation, via charge asymmetries in Dalitz plots or through interference between $K_S \to \pi^+\pi^-\gamma$ and $K_L \to \pi^+\pi^-\gamma$ similarly to $K_{L,S} \to 3\pi$. They bear on the question whether the $\Delta I = \frac{1}{2}$ enhancement in $K^\pm \to \pi^\pm\pi^0$ persists in $K^\pm \to \pi^\pm\pi^0\gamma$. Moreover, they have a rôle in the determination of ϵ' from $K_L \to 2\pi$ as they are a radiative correction there [57]. The $K \to \pi\pi\gamma$ amplitudes have two components which can be measured separately: the inner bremsstrahlung (IB), reliably computed in terms of $K \to 2\pi$, and the direct emission (DE) (in turn split into short–distance plus long–distance polar amplitudes), which suffers from theoretical uncertainties coming from the incomplete knowledge of the confining physics. Recent attempts to estimate the DE amplitudes have appeared [58], [59]. In Table V we have reported the results obtained in [58], as well as the available experimental data [60], [61], [62], [63]. The comparison seems to indicate that more theoretical effort should be needed in this case.

Finally, the possibility of observing CP violation in the $K \to \pi\pi\gamma$ decays has been examined in [64]. The perspectives do not seem very good, even with high statistics.

Regarding the $K^\pm \to \pi^\pm\gamma\gamma$ decays, chiral perturbation theory is not able to predict the absolute rate, which depends on an unknown parameter. However it predicts in general the lower bound reported in Table IV, as well as a characteristic form of the $\gamma\gamma$ invariant mass spectrum. The latter closely reflects the dynamics underlying such a calculation, so it should be interesting to try to measure it. A CP–violating asymmetry

TABLE V. Branching ratios of $K \to \pi\pi\gamma$ decays. The theoretical predictions of the two components of inner bremsstrahlung (IB) and direct emission (DE) come from ref. [58]. The experimental references are also given.

mode	theory	experiment	reference
$K^+ \to \pi^+\pi^0\gamma\|_{IB}$	2.9×10^{-4}	$(2.75 \pm 0.16) \times 10^{-4}$	[60, 61]
$K^+ \to \pi^+\pi^0\gamma\|_{DE}$	0.5×10^{-5}	$(1.56 \pm 0.35) \times 10^{-5}$	[60]
		$(2.05 \pm 0.46) \times 10^{-5}$	[62]
		$(2.3 \pm 3.2) \times 10^{-5}$	[61]
$K_L \to \pi^+\pi^-\gamma\|_{IB}$	1.4×10^{-5}	$(1.52 \pm 0.16) \times 10^{-5}$	[63]
$K_L \to \pi^+\pi^-\gamma\|_{DE}$	1.58×10^{-5}	$(2.89 \pm 0.28) \times 10^{-5}$	[63]
$K_S \to \pi^+\pi^-\gamma\|_{IB}$	2.4×10^{-3}	$(1.82 \pm 0.10) \times 10^{-3}$	[60]
$K_S \to \pi^+\pi^-\gamma\|_{DE}$	2.05×10^{-8}	$< 6 \times 10^{-5}$	[60]

can be defined also in this case, and we obtain qualitatively [50]

$$\frac{\Gamma(K^+ \to \pi^+\gamma\gamma) - \Gamma(K^- \to \pi^-\gamma\gamma)}{\Gamma(K^+ \to \pi^+\gamma\gamma) + \Gamma(K^- \to \pi^-\gamma\gamma)} \leq 10^{-3} \quad , \tag{13}$$

corresponding to the lower bound on the rate mentioned above. While the measurement of the CP-violating asymmetry seems out of reach, this decay has not yet been observed: it should be possible to detect a few events with the statistics required for CP-LEAR or with $\simeq 10^{10}$ ϕ.

The decays $K_{S,L} \to \pi^0\gamma\gamma$ are nice tests of the chiral lagrangian realization of the standard model, as they can be predicted with no free parameters in chiral pertubation

theory [50]. In particular, the $K_S \to \pi^0\gamma\gamma$ is dominated by $K_S \to \pi^0\pi^0(\eta) \to \pi^0\gamma\gamma$, and there is no cancellation between the π^0 and η contributions (actually the η seems to be suppressed), contrary e. g. to the $K_L \to \mu^+\mu^-$ case discussed later on. The predicted branching ratio in Table IV is 3.8×10^{-8}, while there is no experimental upper limit at the present. The decay $K_L \to \pi^0\gamma\gamma$ is also unambiguously calculable, with $\mathrm{BR}(K_L \to \pi^0\gamma\gamma) \simeq 6.8 \times 10^{-7}$, while a new experimental limit has been recently obtained: 2.7×10^{-6} [65]. Also, analogously to the $K^\pm \to \pi^\pm\gamma\gamma$, there is a characteristic two-photon mass distribution. An alternative description of the $K_L \to \pi^0\gamma\gamma$ including also vector mesons is given in [66], still compatible with the previous experimental limit. The other important point is that $K_L \to \pi^0\gamma\gamma$ is needed to estimate the CP-conserving, two-photon exchange contribution to $K_L \to e^+e^-$, and thus to decide whether the CP-violating one photon amplitude can dominate the latter processes. Thus the measurement of $K_L \to \pi^0\gamma\gamma$ would have important bearing on CP-violation studies. On the other hand, from an experimental point of view, this decay is a good example of how a good e.m. calorimetry together with the tagging capabilities and the unrivalled background conditions expected at a ϕ factory should allow a dramatic improvement of the knowledge of some K_L and K_S decays.

Finally it might be interesting to mention that amplitudes of non-leptonic radiative K decays with at most one final pion are necessarily of higher order in chiral perturbation theory (the lowest order vanishes). This implies in general a characteristic suppression of order $m_K^2/(16\pi^2 f_\pi^2) \ll 1$, which can overcome the $\Delta I = \frac{1}{2}$ enhancement of the basic non-leptonic $\Delta S = 1$ weak hamiltonian. Indeed such a suppression effect is observed in the $K^\pm \to \pi^\pm(e^+e^-)$ decay discussed later on.

V. Rare decays: $K^\pm \to \pi^\pm(\ell^+\ell^-)$, $K^\pm \to \pi^\pm(\nu\bar{\nu})$, $K \to \mu^+\mu^-$, $K \to e^+e^-$

All of these decays are extremely important, and, at the same time, accessible through the present experimental techniques: most of them belong to the category that

can be studied only at the existing high intensity K beams and at the future K factories.

They are all allowed within the standard model, but only through one–loop graphs, in this way testing more intimately the standard model. At the same time, they may become sensitive to specific extensions of the standard model, so representing probes of "new physics". Let us consider their main properties.

$K^{\pm} \to \pi^{\pm}(\ell^{+}\ell^{-})$

This decay is a typical process in which effects due to (virtual) heavy quarks may play an important rôle. It is expected to be dominated by the so-called "electromagnetic penguin diagram", which involves the replacement of a gluon by a virtual photon in the usual penguin: the short–distance contribution comes then from the quark diagrams depicted in Fig. 10. The largest contribution is seen to come from the transition charge radius term in the effective $sd\gamma$ vertex of the first graph in Fig. 10, which was estimated within the four-quark model by Gaillard and Lee [48]. The loop is only logarithmically GIM suppressed, so that the c–quark contribution is expected to dominate. With $|V_{cs}^{*}V_{cd}| \simeq 0.21$ and $m_c = 1.5$ GeV the c–quark contribution gives

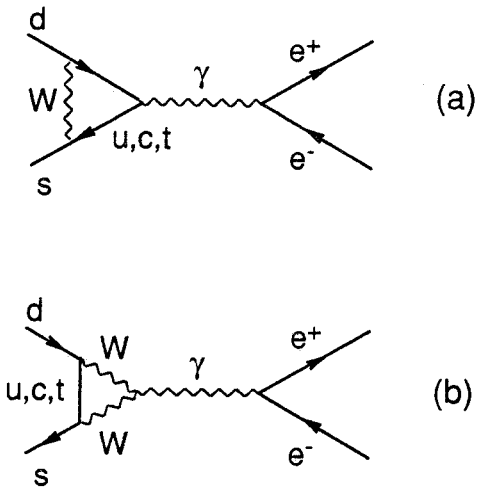

Fig. 10 - The short distance contribution to the $K^{\pm} \to \pi^{\pm}e^{+}e^{-}$.

$$\mathrm{BR}[K^{\pm} \to \pi^{\pm}(e^{+}e^{-})]_{\mathrm{th}} \simeq 2.6 \times 10^{-7} \quad , \tag{14}$$

in good agreement with the observed rate [67]

$$\mathrm{BR}[K^{\pm} \to \pi^{\pm}(e^{+}e^{-})]_{\mathrm{exp}} = (2.7 \pm 0.5) \times 10^{-7} \quad , \tag{15}$$

whereas the present upper limit at the 90% of C.L. for the μ case is [68]

$$\mathrm{BR}[K^{\pm} \to \pi^{\pm}(\mu^{+}\mu^{-})]_{\mathrm{exp}} < 2.3 \times 10^{-7} \quad . \tag{16}$$

Note that also with a t–quark mass rather large, as expected on the basis of the most recent analyses [69], the c-quark contribution remains the dominant one. The above agreement is regarded as a success of the theory. However, QCD effects are presumably present, and may alter in a substantial way the free-quark result, with further contributions coming from the action of the effective hamiltonian for $\Delta S = 1$ non–leptonic weak decays, represented in a pictorial way in Fig. 11 [70]. It follows that the decay $K^{\pm} \to \pi^{\pm}(\ell^{+}\ell^{-})$ is regarded with considerable interest within the approach of the chiral perturbation theory. Indeed this represents a relatively simple context in which the penguin contributions and more generally long–distance effects can be studied [50] and in fact in Table IV the decay $K^{\pm} \to \pi^{\pm}(e^{+}e^{-})$ is used to fix one free parameter in the chiral lagrangian.

It is worth mentioning that the transition $K^{\pm} \to \pi^{\pm}(\ell^{+}\ell^{-})$ has been one of the most promising ones in the search of a light Higgs ($K^{\pm} \to \pi^{\pm}H$) with H decaying into ($\ell^{+}\ell^{-}$) or other light scalar or pseudoscalar particles, as familons, axions, etc., a subject which has been intensively pursued until recently (a very recent approach to the decays $K \to \pi H$ and $K \to \eta H$ is given in [71]). One of the most interesting results of the first phase of LEP is, however, the very strong limit posed on the H mass: 32 MeV $< m_H <$ 24 GeV at 95% C.L. [7], which discourages further light Higgs searches.

$K^{\pm} \to \pi^{\pm}(\nu\bar{\nu})$

The experimental limit on the branching ratio of this decay has been recently improved: at present we have [72]

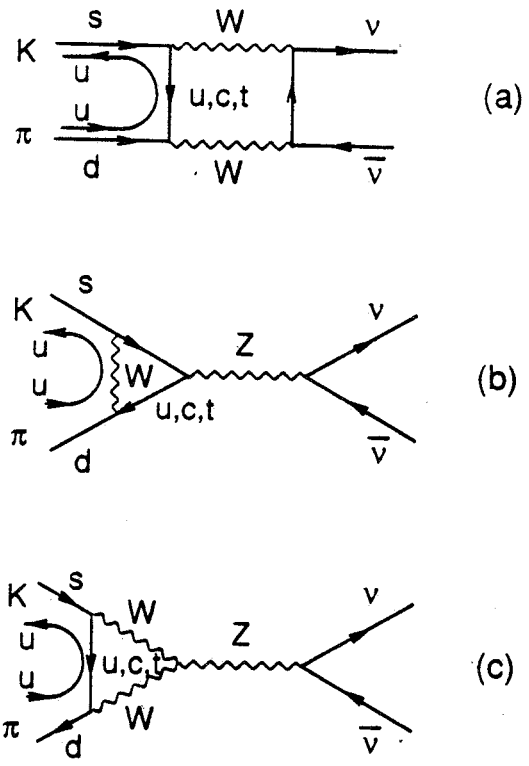

Fig. 12 - Second-order weak diagrams for $K^{\pm} \to \pi^{\pm}\nu\bar{\nu}$.

$$\mathrm{BR}[K^{\pm} \to \pi^{\pm}(\nu\bar{\nu})]_{\mathrm{exp}} < 3.4 \times 10^{-8} \quad , \tag{18}$$

to be compared with the previous limit 1.4×10^{-7}. This is one of the decays better studied within the standard model, and it proceeds through the second order weak diagrams of Fig. 12. Within the standard model with three generations (in particular with three light neutrinos) one can distinguish [73], [74] two main contributions to the total amplitude, coming from the charm and the top quark loops (including the

interference, which is generally constructive). The recent prediction about the t–quark mass [69] leads to expect that the top contribution dominates: taking $|V_{ts}^* V_{td}/V_{cs}^* V_{cd}| \simeq 4 \times 10^{-3}$ and m_t in the interval $100 - 170$ GeV [69], one derives

$$\mathrm{BR}[K^{\pm} \to \pi^{\pm}(\nu\bar{\nu})]_{\mathrm{th}} \simeq (1 - 7) \times 10^{-10} \tag{19}$$

A detailed account of the dependence of the above branching ratio on the t-quark mass and on other parameters of the standard model can be found in [75], from which Fig. 13 has been taken.

The important feature of this process is that the short–distance contributions to the branching ratio (19), estimated from the diagrams in Fig. 12, are numerically much larger than the long–distance corrections, which have been recently estimated in [76]. Consequently these long–distance effects should not obscure the short–distance H_{eff} one is interested in, so that the decay $K^{\pm} \to \pi^{\pm}(\nu\bar{\nu})$ offers a unique possibility to directly test the electroweak short–distance dynamics at quark level, and thus to significantly constrain the parameters of the heavy quarks which mediate the transition.

A branching ratio larger than that reported in eq. (19) can be an indication of some effect difficult to be controlled within the standard model: one would expect either a very large top mass, but this would be in contradiction with the prediction coming from the compatibility of the radiative correction effects in the neutral current sector when compared with the present estimates of the vector boson masses [69], or a large value of $|V_{ts}^* V_{td}|$, which, however, tends to violate the three generation unitarity constraint analogous to eq. (11). Moreover, one has to take into account the bound on both $|V_{ts}^* V_{td}|$ and t-quark mass coming from the estimate of the short–distance amplitudes of the $K_L \to \mu^+\mu^-$ decay, which is discussed later on.

It follows that a branching ratio larger than expected would be a signal of a "new physics", such as the existence of a fourth generation heavy quark dominating the quark loop (but with a heavy neutrino and requiring a rather large mixing between third and fourth generation), or of some exotic quark mixing [77], [75]. Indeed, a fourth generation with standard couplings and light neutrinos is practically excluded by LEP

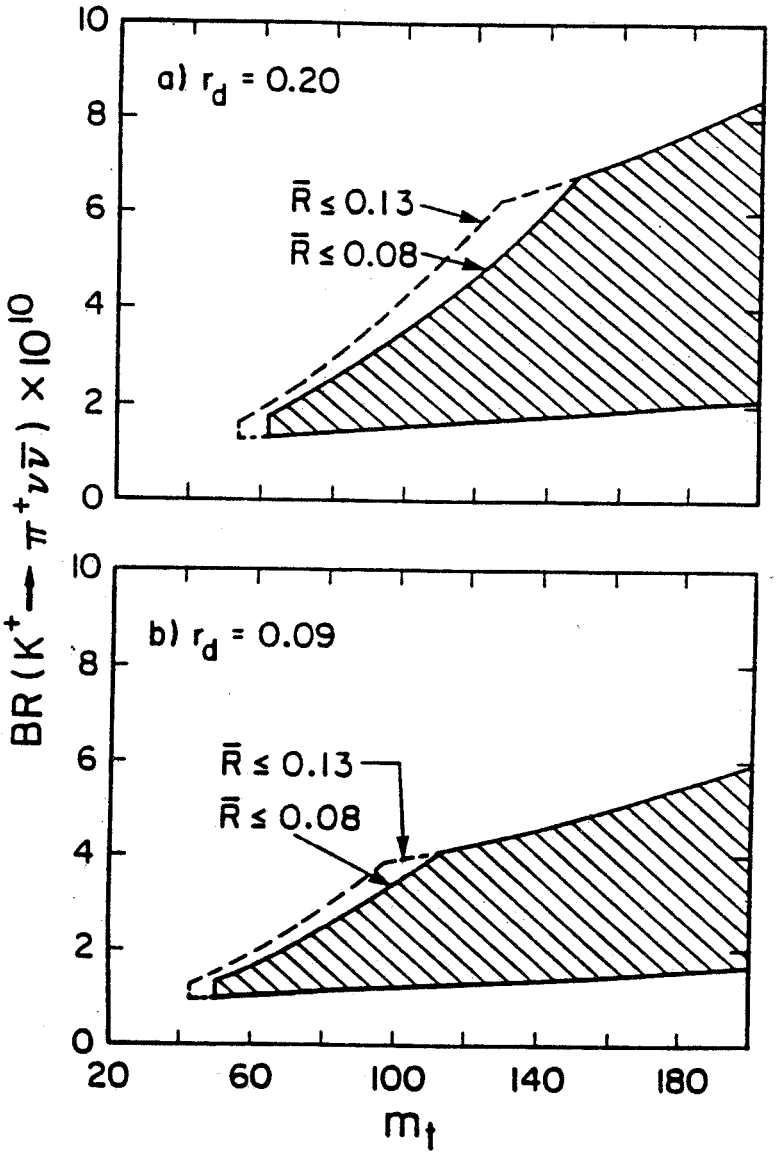

Fig. 13 - Allowed branching ratio for $K^+ \rightarrow \pi^+ \nu\bar{\nu}$ under the $B - \bar{B}$ mixing versus the top-quark mass m_t (GeV) from Ref. [75]. In this figure $\bar{R} = \Gamma(b \rightarrow u)/\Gamma(b \rightarrow c)$ whereas $r_d = \Gamma(B_d^0 \rightarrow \ell^+ X)/\Gamma(B_d^0 \rightarrow \ell^- X)$.

experiments [9]. There remains, however, the possibility of a fourth fermion family characterized by a heavy neutral lepton, which cannot be excluded experimentally and still has some room from the theoretical point of view.

Other effects of "new physics" can also be the source of an enhancement of the branching ratio of $K^{\pm} \to \pi^{\pm}(\nu\overline{\nu})$, in principle related to comparable or higher contributions of other decays simulating the $K^{\pm} \to \pi^{\pm}(\nu\overline{\nu})$ decay. For example, $K^{+} \to \pi^{+}xx'$, $K^{+} \to \pi^{+}x$, with x, x' representing neutral scalar or pseudoscalar particles which only weakly interact with the apparatus and thus escape detection.

Other competitive decays, which actually belong to the category of "forbidden" decays but which from the experimental point of view are more similar to $K^{\pm} \to \pi^{\pm}(\nu\overline{\nu})$, could imply lepton flavour violation. The general process $K^{\pm} \to \pi^{\pm}(\nu\overline{\nu}')$ can be mediated by hypothetical horizontal gauge bosons, by leptoquarks, and also by specific Higgs particles. Although severely constrained by the measured $K_S - K_L$ mass difference [78], nevertheless the process $K^{\pm} \to \pi^{\pm}(\nu\overline{\nu}')$ could be enhanced by specific choices of the masses and mixing, and cannot be ruled out [79].

The two–body decay $K^{+} \to \pi^{+}x$, where x can be an axion [80], or a hyper-photon [81], or a familon [82], i. e. a light or massless particle arising either from a spontaneously broken global symmetry or mediating new fundamental interactions, is characterized by the recent experimental limit [72]

$$\mathrm{BR}(K^{+} \to \pi^{+}x)_{\mathrm{exp}} < 6.4 \times 10^{-9} \quad . \tag{20}$$

This kind of decay is easily distinguished from the three-body decay $K^{\pm} \to \pi^{\pm}(\nu\overline{\nu})$ and, if observed, would be unambiguously an evidence of "new physics".

The limit (20) would exclude that x is a conventional axion [83], since such an axion should already been observed in this decay. In the case in which x would be a familon, one could expect a branching ratio of the order of 10^{-10}, which means that the familon will be observed or ruled out in the coming generation of experiments.

$K_L \to \mu^+\mu^- , e^+e^-$

It is well known that the decay $K_L \to \mu^+\mu^-$ has played an important rôle in the study of the electroweak theory. The branching ratio is of the order 10^{-9}, the two recent experimental determinations coming from KEK [84] and Irvine [85] give in fact

$$\mathrm{BR}(K_L \to \mu^+\mu^-) = \begin{cases} (8.4 \pm 1.1) \times 10^{-9} & [84] \\ (5.8 \pm 0.6\,\mathrm{stat} \pm 0.4\,\mathrm{syst}) \times 10^{-9} & [85] \end{cases} \tag{21}$$

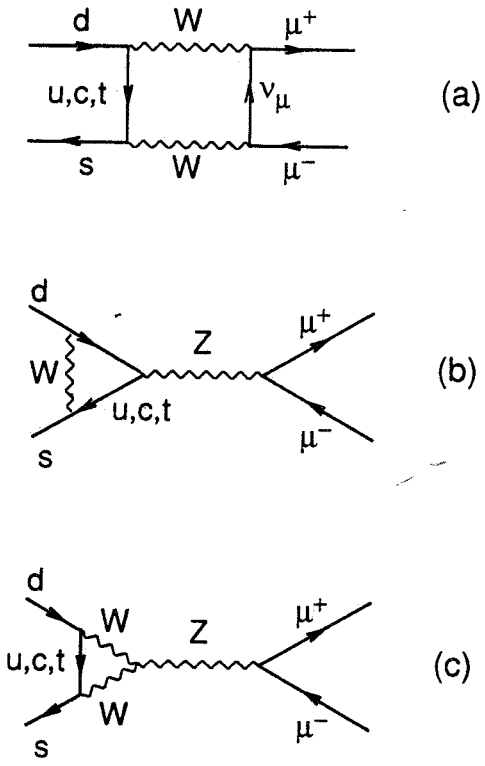

Fig. 14 - Short distance diagrams for $K_L^0 \to \mu^+\mu^-$.

These improve the old result $(9.1 \pm 1.9) \times 10^{-9}$. This small branching ratio indicates the suppression of weak processes induced by strangeness changing neutral currents and actually motivated the introduction of the c-quark and of the GIM mechanism [6]. In addition there is a suppression from helicity selection rules. The second order electroweak short–distance contributions to these process is represented by the $s\bar{d} \to$

$s\bar{d} \to \mu^+\mu^-$ annihilation of Fig. 14. These short–distance contributions have been estimated in several refs. [86], and are clearly dominated by the t-quark contribution for large enough m_t and $|V_{ts}^* V_{td}|$. Indeed, more recently, additional calculations including the case of large m_t and QCD effects have been performed [75], with the conclusion that for m_t large but constrained by the flavour-conserving neutral current data and including the QCD effects the short distance contribution is not able to account for the branching ratio (21). In fact the latter turns out to be almost completely saturated by the long-distance non-perturbative diagram where the transition proceeds via a two-photon intermediate exchange, i.e. $K_L \to \gamma\gamma \to \mu^+\mu^-$ (Fig. 15). The imaginary (absorptive) part of the amplitude of the process $K_L \to \gamma\gamma \to \mu^+\mu^-$ can be reliably estimated, since the two photons are on the mass-shell there, in terms of the measured $K_L \to \gamma\gamma$ amplitude and of the pure QED amplitude for the process $\gamma\gamma \to \mu^+\mu^-$. In terms of the rate of the process $K_L \to \gamma\gamma$ it is possible to derive [87]

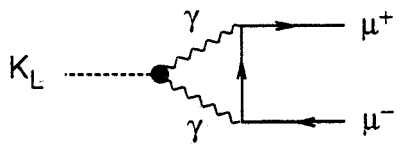

Fig. 15 - Long-distance contribution to the $K_L \to \mu^+\mu^-$ decay with two photon intermediate state.

$$\Gamma(K_L \to \mu^+\mu^-)_{\rm abs} = 1.2 \times 10^{-5} \cdot \Gamma(K_L \to \gamma\gamma) \quad , \tag{22}$$

so that, using the recent estimate of the experimental rate of $K_L \to \gamma\gamma$ [15], one finds

$$\frac{\Gamma(K_L \to \mu^+\mu^-)_{\rm abs}}{\Gamma(K_L \to {\rm all})} = (7.6 \pm 0.1) \times 10^{-9} \quad , \tag{23}$$

quite close to the experimental values in (21).

This leaves very little room to the dispersive contribution, consisting of the short–distance amplitude, which is reliably estimated as discussed above, and of the long–distance part, which involves the integration over the photon momenta and thus is sensitive to the confinement non-perturbative physics. It follows that the final result could be somewhat model–dependent [51], [88], and the experimental measurement of $BR(K_L \to \mu^+\mu^-)$ can be utilized only to constrain the value of the short–distance amplitude (assuming that it does not interfere with the long–distance one). This can be turned into a constraint (for large m_t) on the quantity $|\mathrm{Re}V_{ts}^* V_{td}|$ as a function of m_t. Such a constraint could be very useful and indeed it has been already introduced in the previous discussion on $K^\pm \to \pi^\pm(\nu\overline{\nu})$.

All of the above properties can be extended to the process $K_L \to e^+e^-$. This decay has not been seen yet: preliminary limits has been recently reported by KEK [84] and Irvine [89] experiments:

$$BR(K_L \to e^+e^-) < \begin{cases} 5.4 \times 10^{-10} & [84] \\ 3.1 \times 10^{-10} & [89] \end{cases} . \qquad (24)$$

From the theoretical point of view, the helicity suppression is much larger than for $K_L \to \mu^+\mu^-$ due to $m_e/m_\mu \ll 1$, and the long–distance amplitude should similarly dominate the transition. To have an idea of the order of magnitude expected in the standard model, we can take the unitarity limit, namely just the absorptive part of the long–distance amplitude [87]. Using again the rate of the process $K_L \to \gamma\gamma$ of [15] one finds:

$$BR(K_L \to e^+e^-) \geq 2.5 \times 10^{-11} \quad , \qquad (25)$$

almost two orders of magnitude far from the experimental limit (24).

As far as the $K_S \to \mu^+\mu^-$ is concerned, the partial width from $K_S \to \gamma\gamma \to \mu^+\mu^-$ is comparable to the K_L case, but there is a suppression of two orders of magnitude in the branching ratio due to $\Gamma_L \ll \Gamma_S$.

The decay $K_L \to \mu^+\mu^-$ can provide information on the CP violation through an estimate of the muon longitudinal polarization [90] defined as

$$P_L = \frac{N_R - N_L}{N_R + N_L} \quad , \tag{26}$$

where N_R (N_L) is the number of μ^- with positive (negative) helicity. It is possible to see that in the standard model the longitudinal polarization for $K_L \to \mu^+\mu^-$ essentially comes from the CP impurity in the K_L state, and can be related to the absorptive part of the (dominant) process $K_L \to \gamma\gamma \to \mu^+\mu^-$: this contribution is rather small and has been estimated as

$$|P_L^{(K)}| \simeq 7.1 \times 10^{-4} \tag{27}$$

A potentially important source of enhancement could arise from the Higgs exchange diagram reported in Fig. 16 and estimated in [91]. However the recent results of LEP concerning the limits on the Higgs mass [7] makes such a contribution too small to be observed. Thus a muon polarization larger than that of eq. (27) would suggest the existence of a non–standard CP–violating quark–lepton interaction. Some possibilities, related to flavour–violating Higgs boson exchanges or to leptoquark exchanges, are discussed in [92].

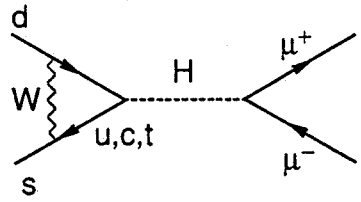

Fig. 16 - The Higgs exchange diagram which contributes to the longitudinal polarization of $K_L \to \mu^+\mu^-$ decay.

Although some hundreds of events have already been observed, and many more are expected in the coming years, the μ polarization is not being measured in the existing experiments (even if it was foreseen in the proposal of the Brookhaven E791 experiment). If this study is continued at higher statistics, the μ polarimetry would be one important tool in distinguishing between the various sources of CP-violation.

VI. "Very rare" decays: $K^0 \to \pi^0(\ell^+\ell^-)$, $K^0 \to \pi^0(\nu\overline{\nu})$

Although still in the class of the GIM suppressed decays considered so far, these transitions are expected to be extremely rare in the standard model, at the branching ratio level of 10^{-11} or less. On the other hand they are particularly interesting as they can offer an alternative opportunity (to the $K^\circ - \overline{K^\circ}$ system) to study CP violation [93], and for this reason they have received much attention recently [94].

The point which makes the decay $K_L \to \pi^0(\ell^+\ell^-)$ extremely rare is that, differently from the corresponding charged one (and from the decay $K_S \to \pi^0(\ell^+\ell^-)$), it cannot proceed through a one-photon exchange diagram without violation of CP [95]. The CP-conserving part of the decay $K_L \to \pi^0(\ell^+\ell^-)$ comes from the diagram involving two photons ($K_L \to \pi^0\gamma^*\gamma^* \to \pi^0(\ell^+\ell^-)$), suppressed by a factor (α/π) (see Fig. 17, where both diagrams are reported). Calculations in the framework of chiral perturbation theory [50], [96] indicate indeed a clear dominance of the one-photon exchange amplitude, and thus confirm the nice perspective to directly measure CP violation from this process. Instead, the opposite situation, namely a one-photon amplitudes smaller or (at most) equal to the two photon one, has been found in [97] using a vector dominance model. Results midway between [96] and [97] have been obtained in [98]: Thus more theoretical work is needed, and probably a clarification will be possible by the inclusion of vector mesons in the chiral effective lagrangians [99]. Anyway, to give an idea of the orders of magnitude, we can say that the various references agree in predicting $\mathrm{BR}(K_L \to \pi^0 e^+ e^-) \simeq 10^{-11} - 10^{-12}$, so that this is the sensitivity required to make

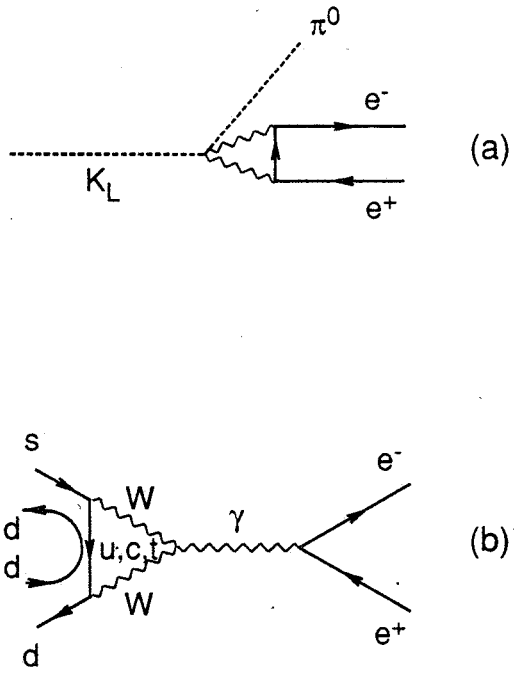

Fig. 17 - Diagrams for $K_L^0 \to \pi^0 e^+ e^-$: (a) CP conserving two photon process; (b) CP violating penguin diagram.

this interesting measurement of CP. From the experimental point of view, the current limits

$$\mathrm{BR}(K_L \to \pi^0 e^+ e^-) < \begin{cases} 3.2 \times 10^{-7} & [100] \\ 4.2 \times 10^{-8} & [101] \\ 4 \times 10^{-8} & [102] \end{cases} \tag{28}$$

lie more than two orders of magnitude above the standard model prediction, affording a large window for new physics. For example, in the Weinberg model, where CP violation is generated by extra Higgs doublets [8], the CP violating amplitude is estimated of the order of 4×10^{-10} [103].

We may also mention that other interesting CP-odd observables have been proposed, such as the asymmetry between the energy spectra of the electron and of the positron [97], or the muon polarization in the $K_L \to \pi^0\mu^+\mu^-$ mode [50]. This asymmetry depends on interference between the 1γ and 2γ amplitudes.

The decay $K_L \to \pi^0\nu\bar{\nu}$ should represent an even cleaner test of CP violation effects because there is no photon contributions to the amplitude. In addition, and very interestingly, the largest contribution should come from direct CP violation [104]. Unfortunately, the expected branching ratio is tiny, of the order of 10^{-12}, while a possible experimental upper limit is $\mathrm{BR}(K_L \to \pi^0\nu\bar{\nu}) < 1 - 4 \times 10^{-3}$. We note here that the study of this decay looks extremely difficult, if not impossible, at high intensity K beams because of background and lack of experimental constraints. A significant improvement on the BR limit both for K_S and K_L would be expected at a ϕ factory (and at LEAR) thanks to low background and $K_S(K_L)$ tagging capability; however the expected statistics at these facilities will not allow to reach the theoretical value.

VII. "Not expected or forbidden" decays: $K \to \mu e$, $K \to \pi\mu e$

The decays $K \to \mu e$ and $K \to \pi\mu e$ are strictly forbidden in the standard model with massless neutrinos by the separate conservation of muon and of electron leptonic numbers. Actually in an extension of the standard model implying massive neutrinos these transitions could proceed via the neutrino mixing. The rates would be, however, unmeasurably small, as being proportional to the small neutrino mass. Therefore, the observation of these decays would represent the unambiguous experimental evidence for new physics, outside the standard model, and indeed in this regard they probably are the most interesting ones. The most stringent experimental upper limits available at present are:

$$\begin{aligned} &\mathrm{BR}(K_L \to \mu e) < 3 \times 10^{-10} \qquad [105] \ , \\ &\mathrm{BR}(K \to \pi\mu e) < 2.6 \times 10^{-10} \qquad [106] \ . \end{aligned} \tag{29}$$

These limits are susceptible of further improvements in a not too distant future.

Various theoretical schemes for extending the standard model have been proposed, in the attempt to find an answer to some challenging conceptual difficulties of the model, such as the excessive number of parameters, the existence of fermion generations with their observed masses and mixing angles, and some disappointing features of the Higgs particle. Clearly such questions can only find a solution in an extended framework, containing new physics beyond the standard model one. Examples of these schemes are grand unification [107], left-right symmetry [108], supersymmetry [109], technicolor [110], "horizontal" gauge symmetry [111], compositeness of quarks leptons and/or gauge bosons W, Z [112], and combinations thereof. More recently a well defined class of grand-unified supersymmetric models have been inspired by superstring theory [113], [114].

TABLE VI. Some theoretical extensions to the standard model.

Model	Flavour violator
Additional generations	Heavy neutral leptons
L-R Symmetric models	Majorana Particles
Extended Higgs sector	Horizontal gauge models
Extended technicolor	Gauge bosons, leptoquarks
Supersymmetry	Scalar partners of fermions
Substructure models	Leptoquarks, gauge bosons
Family symmetry	Familon
Superstrings	Leptoquarks

The important common feature of these schemes is that in general they predict the existence of new fundamental fields, some of which mediate new, flavour violating interactions among quarks and leptons. A list of model extensions and of the corresponding quantum exchanges leading to flavour violation is presented in Table VI. In Fig. 18 we schematically show the various mechanisms for $\bar{s} + d \rightarrow \mu e$, relevant to $K \rightarrow \mu e$ (and to $K \rightarrow \pi \mu e$). The other interesting aspect is that these new interactions are supposed to be effective at extremely large mass scales $\Lambda \gg M_W$, such as the mass of the exchanged heavy objects in Fig. 18 or the compositeness scale Λ_c. The masses determine in fact the big suppression of these (otherwise totally forbidden) flavour violating transitions, and thus are new constants of nature. Consequently these "forbidden" K-decays have the role of being a testing ground for the standard model extensions and of providing in addition glimpses on the above-mentioned large mass scales. We may also notice that $K \rightarrow \pi \mu e$ tests vectorial couplings, while $K \rightarrow \mu e$ only proceeds via axial-like couplings, so that these two processes are logically independent.

To give an idea of the experimental sensitivities which are expected to be significant, we should notice that the "horizontal" exchange of Fig. 18a can also directly mediate the $\Delta S = 2$ $K^\circ \overline{K^\circ}$ mixing, and thus this mechanism is constrained by the measured $\Delta m_K = m_{K_L} - m_{K_S} = 3.5 \times 10^{-15}$ GeV. As a rule, the corresponding branching ratios should be not larger than $10^{-12} - 10^{-13}$ [78], [115]. The same should be true for the Higgs exchange mechanism of Fig. 18b, although examples of models have been proposed where the Δm_K constraint can be evaded [116].

The leptoquark exchange of Fig 18c is not constrained by Δm_K, because it cannot induce direct $K^\circ \overline{K^\circ}$ transitions, and therefore leptoquark masses are directly probed by the decays discussed here. From the limits (29), and by making the (model) assumption of gauge couplings in Fig. 18a equal to the standard W couplings, one can derive for the typical mass scale of these new interactions, represented by the mass of the exchanged heavy object:

$$M > 39 \text{ TeV}/c^2 \tag{30}$$

It is a little unfortunate that the bound on M only grows like the 1/4 power of the experimental sensitivity on the branching ratio. Nevertheless M in eq. (30) is quite a large mass, which can be already considered as significant in order to test models. For

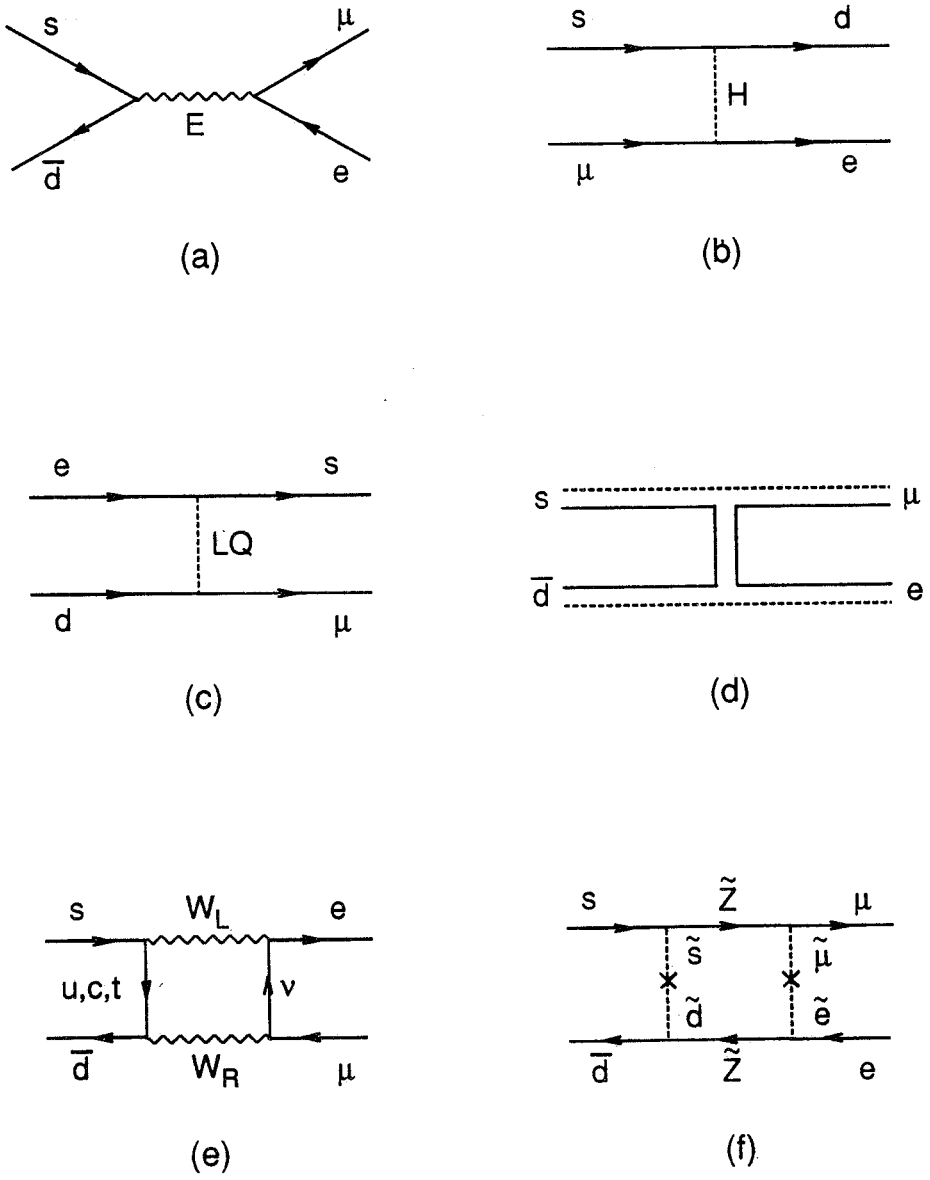

Fig. 18 - Contribution to $K_L \to \mu e$ from (a) horizontal boson exchange, (b) Higgs exchange, (c) leptoquark exchange, (d) composite model mechanisms, (e) left-right models, and (f) supersymmetric particles.

example, in extended technicolor models the typical heavy boson masses are constrained to be in the range 10-100 TeV.

The composite model mechanism of Fig. 18d represents the exchange of a heavy bound state made of quark and lepton "subconstituents", with a mass of the order of the compositeness scale Λ_c. Then the bound in eq. (30) applies to Λ_c. The constraint from Δm_K also works for composite models, and limits the predicted branching ratios for $K \to \mu e$ and $K \to \pi \mu e$. The transition amplitude estimates are very model dependent, but roughly speaking branching ratios can be expected in the range $10^{-12} - 10^{-13}$ or less. Also in this case there are possibilities for larger branching ratios, such as e.g. the model in ref. [117], which interestingly predicts $\sim 10^{-10}$, and thus is at the point of being tested by experiment.

Finally, in closing this section, we mention that left-right symmetric models, with heavy neutrino masses, induce contributions like that of Fig. 18e with branching ratios of the same order [118]. Also, useful constraints on supersymmetric parameters can be obtained from the decays considered here, because in the minimal version of supersymmetry there are no lepton number violations at the tree level as effect of direct exchange of new superparticles [119]. Nevertheless, for some relevant supersymmetric GUT inspired models, like flipped $SU(5) \times U(1)$, off-generational mass terms can be induced and can give rise to off-generational mass insertions in slepton propagators resulting in lepton number violating processes such as $K_L \to \mu e$, as seen in Fig. 18f, taken from the last of refs. [119]. From the experimental values of eq. (29) we find a rather strong constraint on the slepton mass split that exceeds the estimates ever for the most optimistic supersymmetric scenario. We conclude that $K_L \to \mu e$ is not a viable place to look for flavour changing neutral currents in supersymmetric flipped $SU(5) \times U(1)$ or in any other simple extension of the minimal supersymmetric model, like SU(5) or SO(10), in which the branching ratio for the process becomes a million times smaller. In a similar way, the same conclusion applies to $K \to \pi \mu e$ also for a further phase space suppression.

References

[1] T. D. Lee and C. N. Yang, Phys. Rev. **104** (1956) 254;
C. S. Wu et al., Phys. Rev. **105** (1957) 1413.

[2] R. H. Dalitz, Repts. Progr. in Phys. **20** (1957) 163.

[3] For an update review, see *"CP Violation"*, C. Jarlskog ed. (World Scientific, 1989).

[4] J. H. Christenson, J. W. Cronin, V. L. Fitch and R. Turlay, Phys. Rev. Lett. **13** (1964) 138.

[5] M. Kobayashi and K. Maskawa, Prog. Theor. Phys. **49** (1973) 652.

[6] S. L. Glashow, J. Iliopoulos and L. Maiani, Phys. Rev. **D2** (1970) 1285.

[7] OPAL Collaboration, M. Z. Akrawy et al., Phys. Lett. **236B** (1990) 224;
Aleph Collaboration, D. Decamp et al., Phys. Lett. **236B** (1990) 233, CERN preprint CERN-EP/90-16 (1990).

[8] S. Weinberg, Phys. Rev. Lett. **37** (1976) 657;
T. D. Lee, Phys. Rep. **9C** (1974) 144;
S. Weinberg, Phys. Rev. Lett. **63** (1989) 2333.

[9] L3 Collaboration, M. Aguilar-Benitez et al., Phys. Lett. **231B** (1989) 509;
Aleph Collaboration, J.-P. Lees et al., Phys. Lett. **231B** (1989) 519, D. Decamp et al., preprint CERN-EP/89-169;
OPAL Collaboration, J. Allison et al., Phys. Lett. **231B** (1989) 530;
Delphi Collaboration, W. Adam et al., Phys. Lett. **231B** (1989) 539.

[10] A. J. Malensek, Fermilab Report FN-341 (1981), unpublished.

[11] See for instance: M. K. Craddock, in *Proceedings of the International Conference on High-Energy Accelerators* (Tsukuba, 1989), to appear.

[12] B. Winstein, talk at the *Workshop on Physics at the Main Injector* (Fermilab, 1989), University of Chicago preprint EFI 89-59 (1989).

[13] G. Barbiellini and C. Santoni, CERN preprint CERN-EP/89-88 (1989).

[14] R.Landua, talk at *Fermilab Low-Energy Antiproton Facility Workshop* (Batavia, 1986), preprint CERN-EP/86-136 (1986), unpublished.

[15] NA31 Collaboration, H. Burkhardt et al., Phys. Lett. **206B** (1988) 169.

[16] E731 Collaboration, J. P. Patterson et al., University of Chicago preprint EFI 90-05 (1990).

[17] A. A. Bel'kov, G. Bohm, D. Ebert and A. V. Lanjov, Phys. Lett. **232B** (1989) 118;
A. A. Bel'kov, D. Ebert and A. V. Lanjov, Serpukhov preprint 89-11 (1989).

[18] D. A. Bryman, Int. Jour. Mod. Phys. **A4** (1989) 79.

[19] Y. Asano, Phys. Lett. **113B** (1987) 195.

[20] I. H. Chiang et al., Experiment BNL E787.

[21] C. Campagnari et al., AGS Experiment 777, Phys. Rev. Lett. **61** (1988) 2062.

[22] S. Smith, talk given at the SLAC Summer Institute, 1988.

[23] D. Cocolicchio, G. L. Fogli, M. Lusignoli and A. Pugliese, CERN preprint CERN-TH. 5610/89 (1989).

[24] K. Kleinknecht, Ann. Rev. Nucl. Sci. **16** (1976) 1;
J. W. Cronin, Rev. Mod. Phys. **53** (1981) 373.

[25] J.Donoghue, B. R. Holstein and G. Valencia, Int. J. Mod. Phys. **2** (1987) 319;
E. Paschos and U. Turke, Phys. Rep. **178** (1989) 145;
A. J. Buras, *Proceedings of the Rare Decay Symposium*, D. Bryman, J. Ng, T. Numao and J.-M. Poutissou eds. (Vancouver, 1988) p. 249.

[26] I. Dunietz, J. Hauser and J. L. Rosner, Phys. Rev. **D35** (1987) 2166;
J. Bernabeu, F. J. Botella and J. Roldan, Phys. Lett. **211B** (1988) 226.

[27] Y. Fukushima et al., KEK preprint 89-159 (1989).

[28] S. Nussinov and T. N. Truong, Phys. Rev. Lett. **63** (1989) 2003.

[29] Particle Data Book, Review of Particle Properties, Phys. Lett. **204B** (1988) 1.

[30] T. J. Devlin and J. O. Dickey, Rev. of Mod. Phys. **51** (1979) 237.

[31] For a review of the subject see L. Wolfenstein, Ann. Rev. Nucl. Part. Sci. **36** (1986) 137.

[32] L.-F. Li and L. Wolfenstein, Phys. Rev. **D21** (1980) 178.

[33] J. F. Donoghue, B. R. Holstein and G. Valencia, Phys. Rev. **D36** (1987) 798;
J. M. Gérard, Zeit. Phys. – Particles and Fields**C42** (1989) 425.

[34] H.-Y. Cheng, C. Y. Cheung and W. B. Yeung, Mod. Phys. Lett. **A4** (1989) 869.

[35] R. S. Chivukula and A. V. Manohar, Harvard preprint HUTP–86/A050 (1986), unpublished;
H.-C. Cheng, "$K \to \pi\pi\pi$ Decays in Large N_C Chiral Pertubation Theory", BNL preprint (1989).

[36] S. Fajfer and J. M. Gérard, Zeit. Phys. – Particles and Fields **42** (1989) 425.

[37] R. Shrock, Phys. Lett. **96B** (1970) 159.

[38] H. Leutwyler and M. Roos, Zeit. Phys. – Particles and Fields **C25** (1984) 91.

[39] W. J. Marciano, *Proceedings of the Rare Decay Symposium*, D. Bryman, J. Ng, T. Numao and J.-M. Poutissou eds. (Vancouver, 1988) p. 1.

[40] N. Cabibbo and A. Maksymowicz, Phys. Lett. **9** (1964) 352;
G. Kane et al., *Proceedings of the Workshop on CP Violation at a Kaon Factory*, J. N. Ng ed. (1988), to appear;
W. M. Morse et al., ibid..

[41] W. M. Morse et al., Phys. Rev. **21** (1980) 1750;
S. R. Blatt et al., Phys. Rev. **D27** (1983) 1056.

[42] M. Leurer, Phys. Rev. Lett. **62** (1989) 1697;

P. Castoldi, J. M. Frère and G. L. Kane, Phys. Rev. **D39** (1989) 2633.

[43] P. F. Loverre, University of Rome preprint "*Measurement of the ν_μ mass at a ϕ factory*" (1990).

[44] L. Rosselet et al., Phys. Rev. **D15** (1977) 574.

[45] See e.g. E.P. Shabalin, Sov. J. Nucl. Phys. **49** (1989) 365, and reference therein.

[46] J. F. Donoghue and B. R. Holstein, Phys. Rev. **D40** (1989) 3700.

[47] K. S. Heard et al., Phys. Lett. **55B** (1975) 324;
J. Heintze et al., Nucl. Phys. **B149** (1979) 365.

[48] M. K. Gaillard and B. W. Lee, Phys. Rev. **D10** (1974) 897.

[49] J. Gasser and H. Leutwyler, Ann. Phys. (N.Y.) **158** (1984) 142; Nucl. Phys. **B250** (1985) 465, 517.

[50] G. Ecker, A. Pich and E. de Rafael, Nucl. Phys. **B291** (1987) 692; **B303** (1988) 665; Phys. Lett. **189B** (1987) 363.

[51] L. L. Chau and H. Y. Cheng, Phys. Rev. Lett. **54** (1985) 1768;
G. D'Ambrosio and D. Espriu, Phys. Lett. **175B** (1986) 237;
J. L. Goity, Zeit. Phys. – Particles and Fields **C34** (1987) 341.

[52] A. A. Bel'kov, Yu. L. Kalinowski, V. N. Pervushin and N. A. Sarikov, Sov. J. of Nucl. Phys. **44** (1986) 448;
J. O. Eeg, Nucl. Phys. **289** (1987) 613.

[53] J. F. Donoghue, B. R. Holstein and Y.-C. Lin, Nucl. Phys. **B277** (1986) 651.

[54] A. Pich, talk at the *Workshop on Rare K-Decays and CP Violation* (Upton, NY, 1988).

[55] NA31 Collaboration, H. Burkhardt et al., Phys. Lett. **199B** (1987) 139.

[56] R. Decker, P. Pavlopoulos and G. Zoupanos, Zeit. Phys. – Particles and Fields **C28** (1985) 117;

L. L. Chau and H. Y. Cheng, Phys. Lett. **195B** (1987) 275;
F. Buccella, G. D'Ambrosio and M. Miragliuolo, University of Napoli preprint "*CP violation in the decays of neutral kaons into two photons*" (1989).

[57] P. K. Kabir and A. Sirlin, presented by P. K. Kabir, *Proceedings of the XXIV Int. Conference on High Energy Physics* R. Kotthaus and J. Kühn eds. (Münich, 1988) p. 541.

[58] S. Fajfer, Zeit. Phys. – Particles and Fields **C45** (1989) 293.

[59] H. Y. Cheng, S. C. Lee, H. -L. Yu, Zeit. Phys. – Particles and Fields **C41** (1988) 223.

[60] R. J. Abrams et al., Phys. Rev. Lett. **29** (1972) 1118.

[61] K. M. Smith et al., Nucl. Phys. **B109** (1976) 173.

[62] V. N. Bolotov et al., in *Proceedings of the XXIII Int. Conference on High Energy Physics*, S. C. Loken ed. (Berkeley, 1986) p. 887.

[63] A. S. Carroll et al., Phys. Rev. Lett. **44** (1980) 529.

[64] M. McGuigan and A. I. Sanda, Phys. Rev. **D36** (1987) 1415;
Y. C. Lin and G. Valencia, Phys. Rev. **D37** (1988) 143.

[65] V. Papadimitriou et al., Phys. Rev. Lett. **63** (1989) 28.

[66] L. M. Sehgal, Phys. Rev. **D41** (1990) 161.

[67] A. M. Diamant-Berger et al., Phys. Lett. **62B** (1976) 897.

[68] BNL-E787 Collaboration, M.S. Atiya et al., Phys. Rev. Lett. **63** (1989) 2177.

[69] J. Ellis and G. L. Fogli, Phys. Lett. **232B** (1989) 139.

[70] F. J. Gilman and M. B. Wise, Phys. Rev. **D21** (1980) 3150.

[71] H. Leutwyler and M. A. Shifman, University of Bern preprint BUTP-89/29 (1989).

[72] BNL-E787 Collaboration, M. S. Atiya et al., Phys. Rev. Lett. **64** (1990) 21.

[73] J. Ellis and J. S. Hagelin, Nucl. Phys. **B217** (1983) 189.

[74] J. Ellis, S. Hagelin, S. Rudaz and D.D. Wu, Nucl. Phys. **B304** (1988) 205.

[75] J. Ellis, S. Hagelin and S. Rudaz, Phys. Lett. **192B** (1987) 201.

[76] D. Rein and L. M. Sehgal, Phys. Rev. **D39** (1989) 3325;
C. Dib, I. Dunietz and F. J. Gilman, Stanford preprint SLAC PUB 4840 (1989).

[77] U. Turke, Phys. Lett. **168B** (1986) 296;
G. Eilam, J. L. Hewitt and T. Rizzo, Phys. Lett. **193B** (1987) 533;
W. Marciano and Z. Parsa, Ann. Rev. Nucl. Part. Sci. **36** (1986) 171.

[78] P. Herczeg, *Proceedings of the Kaon Factory Workshop*, M. K. Craddock ed. (Vancouver, 1979) p. 20;
G. L. Kane and R. Thun, Phys. Lett. **94B** (1980) 513.

[79] R. N. Cahn and H. Harari, Nucl. Phys. **176** (1980) 135.

[80] R. D. Peccei and H. R. Quinn, Phys. Rev. Lett. **40** (1978) 233;
F. D. Wilczek, Phys. Rev. Lett. **40** (1978) 279.

[81] S. Aronson, E. Fishbach, D. Sudarsky and C. Talmadge, BNL report BNL–41475 (1988), unpublished.

[82] F. Wilczek, Phys. Rev. Lett. **49** (1982) 1549.

[83] J. M. Frère, M. B. Gavela and J. Vermaseren, Phys. Lett. **103B** (1981) 129.

[84] E137 Collaboration, T. Inagaki et al., *Proceedings of the Rare Decay Symposium*, D. Bryman, J. Ng, T. Numao and J.-M. Poutissou eds. (Vancouver, 1988) p. 125; Phys. Rev. **D40** (1989) 1712.

[85] C. Mathiazhagan et al., Phys. Rev. Lett. **63** (1989) 2185.

[86] M. K. Gaillard, B.W. Lee and R. E. Shrock, Phys. Rev. **D13** (1976) 2674;
R. E. Schrock and M. B. Voloshin, Phys. Lett. **87B** (1979) 375;

T. Inami and C. S. Lim, Prog. Theor. Phys. **65** (1981) 297, 1772(E).

[87] L. M. Sehgal, Phys. Rev. **183** (1969) 1511;
B. R. Martin, E. de Rafael and J. Smith, Phys. Rev. **D2** (1970) 179.

[88] V. Barger, W. F. Long, E. Ma and A. Pramudita, Phys. Rev. **D25** (1982) 1860.

[89] C. Mathiazhagan et al., Phys. Rev. Lett. **63** (1989) 2181.

[90] A. Pais and S. B. Treiman, Phys. Rev. **176** (1968) 1974;
L. M. Sehgal, Phys. Rev. **181** (1969) 2151.

[91] F. J. Botella and C. S. Lim, Phys. Rev. Lett. **56** (1986) 1651.

[92] P. Herczeg, Phys. Rev. **D27** (1983) 1512.

[93] L. M. Sehgal, Phys. Rev. **D6** (1972) 367.

[94] A. Pich, "$K_L \to \pi^0 e^+ e^-$ and CP violation", *Proccedings of the 1989 Europhysics Conference on HEP* (Madrid, 1989), to appear.

[95] M. Baker and S. L. Glashow, Nuovo Cimento **25** (1962) 857;
A. Pais and S. B. Treiman, Phys. Rev. **176** (1968) 1974.

[96] J. F. Donoghue, B. R. Holstein and G. Valencia, Phys. Rev. **D35** (1987) 2769.

[97] L. M. Sehgal, Phys. Rev. **D38** (1989) 808.

[98] T. Morozumi and H. Iwasaki, KEK preprint KEK-TH-206 (1988), unpublished;
J.M. Flynn and L. Randall, Phys. Lett. **216B** (1989) 221; Nucl. Phys. **B326** (1989) 31;
C. Dib, I. Dunietz and F. J. Gilman, Phys. Lett. **218B** (1989) 487; Phys. Rev. **D39** (1989) 2639.

[99] G. Ecker, J. Gasser, A. Pich and E. de Rafael, Nucl. Phys. **321B** (1989) 311.

[100] E780 Collaboration, E. Jastrzembski et al., Phys. Rev. Lett. **61** (1988) 2300.

[101] E731 Collaboration, L. K. Gibbons et al., Phys. Rev. Lett. **61** (1988) 2661.

[102] NA31 Collaboration, G. D. Barr et al., Phys. Lett. **214B** (1988) 303; CERN preprint CERN-EP/89-156 (1989).

[103] X.-G. He and B. H. J. McKellar, Univ. of Melbourne preprint UMP 88-40 (1988), unpublished.

[104] L. S. Littenberg, Phys. Rev. **D39** (1989) 3322.

[105] E791 Collaboration, W. R. Molzon et al., BNL report KL-164 (1989).

[106] A. M. Lee et al., Phys. Rev. Lett. **64** (1990) 165.

[107] For a review see e. g. D. V. Nanopoulos, *Proceedings of the XXII International Conference on High Energy Physics*, eds. A. Meyer and E. Wieczorek (Leipzig, 1984) p. 36.

[108] For a general survey of the left-right symmetric models, see R. Mohapatra, *Unification and Supersymmetry* (Springer Verlag, 1986).

[109] For a review see H. Haber and G. L. Kane, Phys. Rep. **117** (1985) 75.

[110] E. Farhi and L. Susskind, Phys. Rep. **74** (1981) 277.

[111] See e.g. A. Davidson and K. C. Wali, Phys. Rev. Lett. **26** (1981) 691.

[112] For a review see R. Peccei, *Proceedings of the XXIII International Conference on HEP*, S. Loken ed. (World Scientific, Singapore, 1986) p. 3.

[113] For a review on phenomenological implications see B. A. Campbell, J. Ellis, K. Enqvist, M. K. Gaillard and D. V. Nanopoulos, Int. J. Mod. Phys. **A2** (1987) 831.

[114] G. G. Ross, *Proceedings of the 1987 International Symposium on Lepton and Photon Interactions at High Energies*, W. Bartel and P. Rückl eds. (Hamburg, 1987) p. 743; this paper also contains a comprehensive survey on recent developments in standard model extensions.

[115] R. Cahn and H. Harari, Nucl. Phys. **B185** (1981) 382;
E. J. Eichten and D. Lane, Phys. Lett. **90B** (1980) 125.

[116] O. Shanker, Nucl. Phys. **B206** (1982) 253;
D. Cocolicchio and G. L. Fogli, Phys. Rev. **D30** (1984) 2391.

[117] J. C. Pati and H. Stremnitzer, Phys. Lett. **172B** (1986) 441.

[118] A. Barroso, G. C. Branco and M. C. Bento, Phys. Lett. **134B** (1984) 123.

[119] B. A. Campbell, Phys. Rev. **D28** (1983) 209;
S. Bertolini and A. Masiero, Phys. Lett. **174B** (1986) 343;
J. Ellis, J. S. Hagelin, S. Kelley and D. V. Nanopoulos, Nucl. Phys. **B311** (1988) 1.

CP VIOLATION IN THE DECAYS OF NEUTRAL KAONS INTO TWO PHOTONS

F. Buccella

Istituto di Fisica Teorica, Università di Napoli

G. D'Ambrosio

Istituto Nazionale di Fisica Nucleare, Sez. di Napoli

M. Miragliuolo

Istituto di Fisica Teorica, Università di Napoli

SUMMARY

We compute the amplitudes for the decay into two photons of neutral kaons in the framework of the chiral effective lagrangians. In particular we relate the ratios $\eta_{||} = \frac{A(K_L \to 2\gamma_{||})}{A(K_S \to 2\gamma_{||})}$ and $\eta_{\perp} = \frac{A(K_S \to 2\gamma_{\perp})}{A(K_L \to 2\gamma_{\perp})}$; which would vanish according to CP symmetry, to the parameters ϵ and ϵ', appearing in the 2π decays of K_L. We find for $\eta_{||}$ the value $\epsilon + i|\epsilon'|$. For the amplitudes into $2\gamma_{\perp}$, the CP conserving amplitude $A(K_2 \to 2\gamma_{\perp})$ depends very strongly on the parameter f, which gives the percentage of the amplitude $A(K_1 \to 2\pi^0)$ arising from the "penguin" contributions. We predict two possible values for $\eta_{\perp}$:one is $\simeq \epsilon$. For the other $= \epsilon + i70|\epsilon'|$, which appears to us as more likely, the difference with respect to the superweak theory is larger than in the 2π decays. A distinction between the two theories requires a more precise measurement of $\Gamma(K_S \to \gamma\gamma)$.

1. INTRODUCTION

In this paper we study the decays of neutral kaons in two photons with the main purpose of predicting the asymmetry in strangeness for this process, which

is a CP violating effect to be measured in future experiments[1].

The photons produced in the decay of neutral kaons have parallel ($F_{\mu\nu}F^{\mu\nu}$) or perpendicular ($\epsilon_{\lambda\rho\sigma\tau}F^{\lambda\rho}F^{\sigma\tau}$) polarization. If CP would be conserved, the two final states would be produced by K_S or K_L respectively. As a consequence of CP violation one expects non-vanishing amplitudes for $K_S \to 2\gamma_\perp$ and $K_L \to 2\gamma_{||}$. The amplitude $A(K_1 \to 2\gamma_{||})$ has been evaluated [2] and found in agreement with the experimental value[3] for the rate $\Gamma(K_S \to 2\gamma)$. The amplitude $A(K_L \to 2\gamma_\perp)$ is dominated by the contributions of the intermediate pseudoscalar mesons[4,5] and depends critically on SU(3) violation and on corrections to the Gell-Mann Okubo formula [6] which are proportional to the parameter $\xi = (4/3)(f_K/f_\pi - 1)$ in chiral perturbation theory.

Here we will evaluate $A(K_2 \to 2\gamma_\perp)$, $A(K_2 \to 2\gamma_{||})$ and $A(K_1 \to 2\gamma_\perp)$ in the framework of effective lagrangians. In particular we shall write the amplitudes in $2\gamma_\perp$ in terms of the parameter ξ.

$A(K_1 \to 2\gamma_\perp)$ will result a smooth function of ξ, while $A(K_2 \to 2\gamma_\perp)$ changes sign in the allowed range of ξ and reaches the values consistent with the experimental rate $\Gamma(K_L \to 2\gamma)$[3] at the boundaries of that range. For one of the possible choices for the sign, which is the one giving rise to a more consistent picture, there is substantial deviation from the prediction of the superweak theory. In the second section we shall give a general expression for the asymmetry in strangeness. In the third and fifth sections we shall compute the decay amplitudes of neutral kaons into a pair of photons with parallel and perpendicular polarizations respectively, while in the fourth section we study the decay of S=0 pseudoscalar mesons into two photons. Finally we shall give our conclusions.

2. ASYMMETRY IN STRANGENESS FOR THE DECAYS OF NEUTRAL KAONS IN THE TWO PHOTONS.

The interference between the amplitudes $A(K_S \to 2\gamma)$ and $A(K_L \to 2\gamma)$ is a CP violating effect giving rise to the asymmetry, which doesn't require the measurements of the polarizations of the produced photons[1,7,8]:

$$\Delta(t) = \frac{\Gamma[K^0 \to \gamma\gamma(t)] - \Gamma[\bar{K}^0 \to \gamma\gamma(t)]}{\Gamma[K^0 \to \gamma\gamma(t)] + \Gamma[\bar{K}^0 \to \gamma\gamma(t)]} \tag{2.1}$$

where $\Gamma[K^0(\bar{K}^0) \to \gamma\gamma(t)]$ is the rate for the production of two photons as a function of time from a neutral kaon with positive (negative) strangeness at t=0. $\Delta(t)$ depends on the four amplitudes $A[K^0(\bar{K}^0) \to 2\gamma_\perp$ or $2\gamma_{||}]$ and on the parameter $\tilde{\epsilon}$ appearing in the expression of the mass eigenstates

$$K_{S,L} = \frac{K_{1,2} + \tilde{\epsilon}K_{2,1}}{\sqrt{1 + |\tilde{\epsilon}|^2}} \tag{2.2}$$

where

$$K_{1,2} = \frac{K^0 \mp \bar{K}^0}{\sqrt{2}}$$

From (2.2) one finds:

$$\Gamma[K^0(\bar{K}^0) \to \gamma\gamma(t)] = \frac{1+|\tilde{\epsilon}|^2}{2[1+|\tilde{\epsilon}|^2 \pm 2Re(\tilde{\epsilon})]}\{\Gamma(K_S \to \gamma\gamma)e^{-\Gamma_S t} +$$

$$+\Gamma(K_L \to \gamma\gamma)e^{-\Gamma_L t} \pm 2Fe^{\frac{-(\Gamma_S+\Gamma_L)t}{2}} Re[A(K_S \to 2\gamma_{\|})A^*(K_L \to 2\gamma_{\|})e^{i(M_L-M_S)t} +$$

$$+A(K_S \to 2\gamma_{\perp})A^*(K_L \to 2\gamma_{\perp})e^{i(M_L-M_S)t}]\} \qquad (2.3)$$

where

$$F \equiv \frac{\Gamma(K^0 \to \gamma\gamma)}{|A(K_0 \to 2\gamma)|^2} = \frac{1}{32\pi m_K}$$

By considering only terms at first order in CP violation for the difference of the two Γ in (2.3) and at zero order in the sum one gets:

$$A_+(t) \equiv \Gamma[K^0 \to \gamma\gamma(t)] + \Gamma[\bar{K}^0 \to \gamma\gamma(t)] =$$

$$= \Gamma(K_S \to \gamma\gamma)e^{-\Gamma_S t} + \Gamma(K_L \to \gamma\gamma)e^{-\Gamma_L t}$$

$$A_-(t) \equiv \Gamma[K^0 \to \gamma\gamma(t)] - \Gamma[\bar{K}^0 \to \gamma\gamma(t)] =$$

$$= -2Re(\tilde{\epsilon})A_+(t) + 2\Gamma(K_L \to \gamma\gamma)e^{\frac{-(\Gamma_S+\Gamma_L)t}{2}} Re[(R\eta_{\|}^* + \eta_{\perp})e^{i(M_L-M_S)t}]$$

$$\Delta(t) = \frac{A_-(t)}{A_+(t)} = -2Re(\tilde{\epsilon}) + \frac{2e^{\frac{-(\Gamma_S+\Gamma_L)t}{2}} Re[(R\eta_{\|}^* + \eta_{\perp})e^{i(M_L-M_S)t}]}{R \quad e^{-\Gamma_S t} + e^{-\Gamma_L t}} \qquad (2.4)$$

where we have introduced the CP violating quantities:

$$\eta_{\|} = \frac{A(K_L \to 2\gamma_{\|})}{A(K_S \to 2\gamma_{\|})}$$

$$\eta_{\perp} = \frac{A(K_S \to 2\gamma_{\perp})}{A(K_L \to 2\gamma_{\perp})} \qquad (2.5)$$

and

$$R = \frac{\Gamma(K_S \to \gamma\gamma)}{\Gamma(K_L \to \gamma\gamma)}$$

For values of t$\gg \frac{2}{\Gamma_S}$, $\Delta(t) \to -2Re\tilde{\epsilon}$, since K^0 has a smaller component in the direction of K_L than $\overline{K}^0$ and consequentely a slightly shorter "effective lifetime".

The time depending term in the r.h.s. of (2.4) depends on the complex number $R\eta_{||}^* + \eta_\perp$, which in the superweak theory would be given by $R\tilde{\epsilon}^* + \tilde{\epsilon}$. From (2.4) one derives the following expression for the integrated asymmetry:

$$\Delta_{int}(T) = \frac{\int_0^T A_-(t)dt}{\int_0^T A_+(t)dt} =$$

$$= -2Re(\tilde{\epsilon}) + \frac{2\Gamma_S Re\{e^{i\frac{\pi}{4}}(R\eta_{||}^* + \eta_\perp)[e^{i(M_L - M_S)T - \frac{(\Gamma_S+\Gamma_L)T}{2}} - 1]\}}{R \quad (e^{-\Gamma_S T} - 1) + (e^{-\Gamma_L T} - 1)\frac{\Gamma_S}{\Gamma_L}} \tag{2.6}$$

The quantities in (2.5) appear also in the expression of the rate to produce a pair of photons from a neutral kaon beam, which at t=0, is in the state $K_S + zK_L^\dagger$:

$$\Gamma[K_S + zK_L \to \gamma\gamma(t)] = \Gamma(K_L \to \gamma\gamma_\perp)\{e^{-\Gamma_S t}(R + |\eta_\perp|^2) +$$

$$+|z|^2 e^{-\Gamma_L t}(1 + R|\eta_{||}|^2) + 2e^{\frac{-(\Gamma_S+\Gamma_L)t}{2}} Re[(R\eta_{||}^* + \eta_\perp)z^* e^{i(M_L - M_S)t}]\} \tag{2.7}$$

to be compared with the corresponding expression for the two pions final states:

$$\Gamma[K_S + zK_L \to \pi_0^+\pi_0^-(t)] = \Gamma(K_S \to \pi_0^+\pi_0^-)\{e^{-\Gamma_S t} +$$

$$+|z|^2 e^{-\Gamma_L t}|\eta_{00}^{+-}|^2 + 2e^{\frac{-(\Gamma_S+\Gamma_L)t}{2}} Re[\eta_{00}^{*+-} z^* e^{i(M_L - M_S)t}]\} \tag{2.8}$$

where

$$\eta_{+-} = \frac{A(K_L \to \pi^+\pi^-)}{A(K_S \to \pi^+\pi^-)} = \epsilon + \epsilon'$$

$$\eta_{00} = \frac{A(K_S \to \pi^0\pi^0)}{A(K_L \to \pi^0\pi^0)} = \epsilon - 2\epsilon' \tag{2.9}$$

The superweak theory predicts:

$$\eta_{+-} = \eta_{00} = \eta_{||} = \eta_\perp = \tilde{\epsilon}$$

The result found by the NA31 collaboration [9]:

$$Re(\frac{\epsilon'}{\epsilon}) = (3.1 \pm 1.1)10^{-3} \tag{2.10}$$

indicates a deviation from the superweak theory (which predicts $\epsilon' = 0$). The determination of the complex number $R\eta_{||}^* + \eta_\perp$, which might be obtained by a measurement of $\Delta(t)$ defined in (2.1) or by a careful analysis of the decay into two photons as a function of time according to (2.7), will give further information on CP violation. We are going to evaluate $\eta_{||}$ and $\eta_\perp$ in the standard model, where

the CP violation arises from the phase in the Kobayashi-Maskawa matrix and one expects for ϵ' the order of magnitude found by NA31[9].

3. EVALUATION OF A($K^0 \to 2\gamma_{||}$).

The short range direct contributions to $A(K^0 \to 2\gamma)$ come from the diagram in Fig. 1. The photons are in a CP= -1 state according to Furry theorem and therefore there is no contribution for the case with the photons with parallel polarization[4]. As long as for the long range contributions, they are described in the chiral lagrangian approach by the diagrams in Fig. 2. The CP conserving amplitude has been computed[2] from the chiral effective lagrangian:

$$\mathcal{L} = \frac{f^2}{4} tr D_\mu \Sigma D^\mu \Sigma^\dagger + \mu tr M(\Sigma + \Sigma^\dagger) + \frac{f^2}{4} h_8 tr \lambda_6 D_\mu \Sigma D^\mu \Sigma^\dagger \qquad (3.1)$$

where

$$\Sigma = e^{\frac{2i\pi_a T_a}{f}} \quad (a = 1..8), \quad T_a = \frac{\lambda_a}{2} \quad D_\mu \Sigma = \partial_\mu \Sigma + ie[Q, \Sigma]$$

$$Q = \begin{pmatrix} \frac{2}{3} & 0 & 0 \\ 0 & -\frac{1}{3} & 0 \\ 0 & 0 & -\frac{1}{3} \end{pmatrix}, \quad M = \begin{pmatrix} m_u & 0 & 0 \\ 0 & m_d & 0 \\ 0 & 0 & m_s \end{pmatrix},$$

λ_a are the Gell-Mann matrices, f at tree level is equal to F_π=92 MeV, μ is the appropriate scale factor to reproduce the meson masses in the lagrangian and h_8 and h_{27}, which we will introduce in the next formula, are determined from K$\to \pi\pi$ decays.

To take into account also the contribution of the 27 one has to add to the Lagrangian defined in (3.1) the term:

$$\mathcal{L}_{27} = \frac{h_{27} f^2}{4} T^{kl}_{ij} (\Sigma D_\mu \Sigma^\dagger)^i_k (\Sigma D^\mu \Sigma^\dagger)^j_l + h.c. \qquad (3.2)$$

where the tensor T is the U=1,ΔS=1,ΔQ=0 element of the 27 with components:

$$T^{12}_{13} = T^{21}_{13} = T^{21}_{31} = T^{12}_{31} = \frac{3}{5} \quad T^{22}_{23} = T^{22}_{32} = T^{23}_{33} = T^{32}_{33} = -\frac{3}{10} \qquad (3.3)$$

By adding $\mathcal{L}_{27}$ to the $\mathcal{L}$ the result in ref. [2] is modified into:

$$A(K_1 \to 2\gamma_{||}) = \frac{\alpha}{\pi m_K^2} A(K_1 \to \pi^+\pi^-) \frac{1 + \frac{\omega}{\sqrt{2}}}{e^{i\delta_0} + \frac{e^{i\delta_2}\omega}{\sqrt{2}}}$$

$$(k_1 \cdot \epsilon_2 k_2 \cdot \epsilon_1 - \epsilon_1 \cdot \epsilon_2 k_1 \cdot k_2)[1 + \frac{m_\pi^2}{m_K^2} ln^2 \frac{\beta - 1}{\beta + 1}] \qquad (3.4)$$

where

$$\omega \equiv \frac{Re < (\pi\pi)_{(I=2)}|H_W|K^0 >}{Re < (\pi\pi)_{(I=0)}|H_W|K^0 >} = .045 \qquad (3.5)$$

δ_I is the phase shift for S-wave $\pi - \pi$ scattering with isospin I at the mass of K^0, k_i and ϵ_i are the impulses and polarizations of the final photons and $\beta = \sqrt{1 - \frac{4m_\pi^2}{m_K^2}}$; the negative sign of $\frac{\beta-1}{\beta+1}$ gives the imaginary part required by unitarity. From (3.4) and (3.5) we get $\Gamma(K_S \to \gamma\gamma)$=1.52·10^{-11} eV (slightly larger than the value 1.49·10^{-11} eV found with only the octet contribution) in agreement with the experimental value $(1.8\pm.8) \cdot 10^{-11}$eV [3].

The amplitude in (3.4) is finite as a consequence of gauge invariance and of the proportionality of $A(K_1 \to \pi^+\pi^-)$ to $(m_K^2 - m_\pi^2)$, which decreases the degree of the divergence down to make it finite. The vanishing of $A(K_1 \to \pi^+\pi^-)$ in the SU(3) limit proved for a non-leptonic hamiltonian transforming as an octet [10], holds also for the 27 representation: in fact Cabibbo's proof can be generalized, since the completely symmetric part of the tensor product of three octets contains only one 8 and one 27, both with the wrong C to contribute to A$(K_1 \to \pi\pi)$. We introduce CP violation in the $|\Delta S| = 1$ effective lagrangian adding to (3.1) and (3.2) the term

$$\frac{f^2}{4} h_8' tr\lambda_7 D_\mu \Sigma D^\mu \Sigma^\dagger \qquad (3.6)$$

The contribution of the intermediate state K^+K^- state to $A(K_2 \to 2\gamma_{||})$ comes out proportional to $m_{K^+}^2 - m_{K^0}^2$ and can be neglected; the dominant $\pi^+\pi^-$ contribution, performed as in ref. [2], gives

$$\eta_{||} = \frac{A(K_L \to 2\gamma_{||})}{A(K_S \to 2\gamma_{||})} = \tilde{\epsilon} + \frac{< \pi^+\pi^-|H_W|K_2 >}{< \pi^+\pi^-|H_W|K_1 >} = \epsilon + \epsilon' e^{-i(\delta_2 - \delta_0)} \qquad (3.7)$$

which is different from the ratio quoted by Chau and Cheng[8]: $\epsilon + \epsilon'$. The difference, however has a small practical consequence since $\frac{\epsilon'}{\epsilon}$ is small.

4. DECAY OF THE S=0 PSEUDOSCALAR MESONS INTO TWO PHOTONS.

The short range contributions implied by the diagram in Fig. 1 are of little relevance also in the case where the final photons have perpendicular polarizations. In fact the loop integral[4] is a function F$(\frac{m_i^2}{m_W^2})$, where m_i is the mass of the intermediate quark. The contributions for m_i=0 (anomaly contribution) cancel when we sum over all the u-like quarks (GIM mechanism). The function F has the peculiar property to go quickly to zero for $\frac{m_i^2}{m_W^2} \to \infty$ as a consequence of the fact that m_i behaves like the Pauli-Villars cut-off of the integral appearing in the anomaly. So we expect the graph appearing in Fig. 1 to be less relevant for the CP

violating amplitude to which only the intermediate t-quark contributes. The main part [4,5] of the amplitude is expected to come from the intermediate pseudoscalar mesons according to the expression†:

$$A(K^0 \to 2\gamma_\perp) = \sum_{P=\pi^0,\eta,\eta'} \frac{< P|H_W|K^0 >}{m_K^2 - m_P^2} A(P \to 2\gamma_\perp) \qquad (4.1)$$

The contributions of π^0 and η_8, assuming SU(3) symmetry for the amplitudes and Gell-Mann Okubo formula for the square masses of the pseudoscalar mesons, would just cancel; in fact only the U-spin singlet $1/2(\sqrt{3}\pi^0 + \eta_8)$ is concerned in both the amplitudes in the numerator of the r.h.s. of (4.1) and GMO formula implies:

$$m_K^2 - m_\pi^2 = 3(m_{\eta_8}^2 - m_K^2) \qquad (4.2)$$

Also the component along the 27 representation of the weak non-leptonic hamiltonian, which also has U=1, couples K^0 to the U spin singlet $1/2(\sqrt{3}\pi^0 + \eta_8)$. Therefore to get a reliable value from (4.1) one has to keep into account the $\eta - \eta\prime$ mixing and the other SU(3) breaking effects; also the contribution of $\eta\prime$ cannot be neglected due to the tendency of the nearer poles π^0 and η, to cancel each other. In the quark language it is the combination $4\bar{u}u + \bar{d}d + \bar{s}s$, which couples to two photons; this implies, by assuming SU(3) and nonet symmetry

$$A(\eta_8 \to 2\gamma) = \frac{1}{\sqrt{3}} A(\pi^0 \to 2\gamma) \qquad (4.3)$$

$$A(\eta_0 \to 2\gamma) = 2\sqrt{\frac{2}{3}} A(\pi^0 \to 2\gamma) \qquad (4.4)$$

One has the theoretically well established prediction [11] for π^0 decay:

$$\Gamma(\pi^0 \to \gamma\gamma) = \frac{\alpha^2 m_\pi^3}{64\pi^3 f^2} \qquad (4.5)$$

which gives 7.6 eV for the l.h.s. of (4.5) in fair agreement with the experimental value 7.3 $\pm$ .3 eV. The amplitudes for the decays of η and η' into two photons depend also on the mixing angle θ which diagonalizes the 2×2 square mass matrix of the I=0 pseudoscalar mesons:

$$\eta = \eta_8 \cos\theta - \eta_0 \sin\theta \quad \eta' = \eta_8 \sin\theta + \eta_0 \cos\theta \qquad (4.6)$$

$$\tan^2\theta = \frac{(m_{\eta_8}^2 - m_\eta^2)}{(m_{\eta'}^2 - m_{\eta_8}^2)} \qquad (4.7)$$

The sign of θ is the same of $< \eta_0|M^2|\eta_8 >$, which we expect to be negative for physical reasons (the s-quark is heavier than u and d). Chiral perturbation theory modifies (4.2)[12] and (4.3)[13], one has

$$m^2_{\eta_8} = \frac{4}{3}m^2_K - \frac{1}{3}m^2_\pi + \frac{4}{9}(m^2_K - m^2_\pi)\xi$$

$$A(\eta_8 \to 2\gamma) = \frac{1}{\sqrt{3}}\frac{A(\pi^0 \to 2\gamma)}{1+\xi} \tag{4.8}$$

where ξ is the cut-off dependent parameter appearing also [12] in:

$$\frac{f_K}{f_\pi} = 1 + \frac{3}{4}\xi \tag{4.9}$$

The modifications induced by (4.8) have little effect on:

$$\frac{A(\eta \to 2\gamma)}{A(\pi^0 \to 2\gamma)} = \frac{1}{\sqrt{3}}[\frac{\cos\theta}{1+\xi} - 2\sqrt{2}\sin\theta] \tag{4.10}$$

In fact the increase of the r.h.s. of (4.10) due to the larger mixing is almost exactly compensated by the decrease of the octet contribution. The amplitude $A(\eta' \to 2\gamma)$ is a slowly decreasing function of ξ:

$$\frac{A(\eta' \to 2\gamma)}{A(\pi^0 \to 2\gamma)} = 2\sqrt{\frac{2}{3}}[\cos\theta + \frac{\sin\theta}{2\sqrt{2}(1+\xi)}] \tag{4.11}$$

The value $\frac{f_K}{f_\pi}$ has been deduced from experiment by various authors [14] with a result in the range (1.15, 1.225) corresponding (according to (4.9)), to the range (.2, .3) for ξ: the prediction for $\Gamma(\eta' \to \gamma\gamma)$ from (4.7) and (4.11) comes out larger than the experimental value (4.6 $\pm$ .6) KeV; to reach the agreement between theory and experiment we modify (4.4) into [13]:

$$A(\eta_0 \to 2\gamma) = \frac{F_\pi}{F_0}2\sqrt{\frac{2}{3}}A(\pi^0 \to 2\gamma) \tag{4.12}$$

and get $\frac{F_\pi}{F_0}$=.89. From (4.8) and (4.12) we then get $\Gamma(\eta \to \gamma\gamma)$ as a function of ξ; as it can be seen in Table I the dependence on ξ is very small and the values found lie in the range (356, 372)eV slightly smaller than the experimental value (420 $\pm$ 70)eV. It is worth stressing however that the quoted value for $\Gamma(\eta \to \gamma\gamma)$[15] is obtained as a compromise between the result found with η produced by two virtual photons coming from e^+e^-[16], and the previous ones based on Primakoff effect[17]. To find agreement with the more recent measurements the authors of

ref. [13] take θ larger than the value obtained from the diagonalization of the mass-squared matrix.

5. EVALUATION OF A($K^0 \to 2\gamma_\perp$).

For the matrix elements of the weak hamiltonian we get:

$$< \pi_0|H_W|K^0 >= if_\pi \frac{m_K^2}{m_K^2 - m_\pi^2} < \pi_0\pi_0|H_W|K^0 > \tag{5.1}$$

The factor $\frac{m_K^2}{m_K^2-m_\pi^2}$, which corrects the PCAC result, is a consequence of the vanishing of $< \pi_0\pi_0|H_W|K^0 >$ in the SU(3) limit.

Chiral perturbation theory modifies the SU(3) prediction, which is a consequence of the U=1 property of the $\Delta S = 1$ weak hamiltonian into[6]:

$$< \eta_8|H_W|K^0 >= \frac{(1 + \frac{2}{3}\xi)}{\sqrt{3}} < \pi_0|H_W|K^0 > \tag{5.2}$$

To get information on the matrix element $< \eta_0|H_W|K^0 >$ it is appropriate to consider the effective $|\Delta S| = 1$ weak hamiltonian, which is reasonably described by the following combination of four-quarks operators[18]:

$$\begin{aligned} H_{|\Delta S|=1} = 2\sqrt{2}G_F \sin\theta\cos\theta[c_1(\bar{u}_L\gamma_\mu s_L \bar{d}_L\gamma^\mu u_L - \bar{u}_L\gamma_\mu u_L \bar{d}_L\gamma^\mu s_L)+ \\ c_S(\bar{u}_L\gamma_\mu s_L \bar{d}_L\gamma^\mu u_L + \bar{u}_L\gamma_\mu u_L \bar{d}_L\gamma^\mu s_L)+ \\ c_5\bar{d}_L\gamma_\mu\lambda^a s_L(\bar{u}_R\gamma^\mu\lambda^a u_R + \bar{d}_R\gamma^\mu\lambda^a d_R + \bar{s}_R\gamma^\mu\lambda^a s_R)+ \\ c_6\bar{d}_L\gamma_\mu s_L(\bar{u}_R\gamma^\mu u_R + \bar{d}_R\gamma^\mu d_R + \bar{s}_R\gamma^\mu s_R)] + h.c. \end{aligned} \tag{5.3}$$

where λ^a are the eight Gell-Mann matrices for $SU(3)_{colour}$. The coefficients c_1 and c_S are modified with respect to the bare values $\frac{1}{2}$ by the short-range QCD corrections and the terms proportioned to c_5 and c_6 arise in the GRE regime between m_c and m_s and are related to the penguin diagram in Fig. 3.

Within the factorization approximation the first (last) two operators in (5.3) connect the neutral kaons to the quark pair $u\bar{u}$ (to the combination $d\bar{d} + s\bar{s}$); so one has[19]:

$$< \eta_0|c_1O_1 + c_SO_S|K^0 >= \sqrt{\frac{2}{3}} < \pi_0|c_1O_1 + c_SO_S|K^0 >$$

$$< \eta_0|c_5O_5 + c_6O_6|K^0 >= -2\sqrt{\frac{2}{3}} < \pi_0|c_5O_5 + c_6O_6|K^0 > \tag{5.4}$$

where we call O_i the operator multiplying c_i in (5.3).

In the standard model the CP violation in the $\Delta S = 1$ weak amplitudes come from the penguin diagram, which gives the right order of magnitude for ϵ'. Therefore one expects for the CP violating amplitudes $< \eta_0|H_W|K_1 >$:

$$< \eta_0|H_W|K_1 >= -2\sqrt{\frac{2}{3}} < \pi_0|H_W|K_1 > \tag{5.5}$$

From (5.2) and (5.5), the mixing angle θ and the values obtained for $A(P \to 2\gamma)$ one is able to get the ratio $\frac{A(K_1 \to 2\gamma_\perp)}{A(K_1 \to 2\gamma_\perp)_{\pi_0}}$ as a function of ξ, which is reported in Table I. Here we write this ratio as equal to $1+b_{\eta_8} + b_{\eta_0} = 1 + b_\eta + b_{\eta'}$ where $b_{\eta_8}(b_{\eta_0})$ is the contribution proportional to $< \eta_8|H_W|K_1 > (< \eta_0|H_W|K_1 >)$, b_η and $b_{\eta'}$ are instead the contributions from the η and η' pole. The contributions of the η and η' intermediate states almost cancel each other. The result depends rather strongly on the values given for $< \eta_0|H_W|K_1 >$ and $< \eta_8|H_W|K_1 >$, as it can be seen from the fact that b_{η_8} and b_{η_0} are large and opposite. The CP conserving amplitudes $< P|H_W|K_2 >$ receive contributions from all the operators introduced in (5.3); in particular the ratio $\frac{<\eta_0|H_W|K_2>}{<\pi_0|H_W|K_2>}$ depends, according to (5.4), on the relative contribution to $< \pi_0|H_W|K_2 >$ of the terms appearing in (5.3). In fact, from (5.1) and (5.4) one gets:

$$\frac{< \eta_0|H_W|K_2 >}{< \pi_0|H_W|K_2 >} = \frac{3f-1}{2} \tag{5.6}$$

where f is the fraction of the amplitude $< \pi_0\pi_0|H_W|K_1 >$ due to the last two terms in (5.3).

From (4.1), (4.5), (5.1) and the experimental values:

$$\Gamma(K_L \to \gamma\gamma) = (7.7 \pm .2)10^{-12} \quad eV$$

$$\Gamma(K_S \to \pi_0\pi_0) = (2.32 \pm .02)10^{-7} \quad eV$$

one gets for C$\equiv \frac{A(K_1 \to 2\gamma_\perp)}{A(K_1 \to 2\gamma_\perp)_{\pi_0}}$:

$$|C| = \frac{\pi}{\alpha}\left|\frac{1+\frac{\omega}{\sqrt{2}}}{e^{i\delta_0}+\frac{e^{i\delta_2}\omega}{\sqrt{2}}}\right|\left(\frac{m_K^2-m_\pi^2}{m_K^2}\right)^2\sqrt{1-\frac{4m_\pi^2}{m_K^2}}\sqrt{\frac{2\Gamma(K_L \to \gamma\gamma)}{\Gamma(K_S \to \pi_0\pi_0)}} = .88 \tag{5.7}$$

Since the contribution proportional to $< \eta_0|H_W|K_1 >$ in $\frac{A(K_1 \to 2\gamma_\perp)}{A(K_1 \to 2\gamma_\perp)_{\pi_0}}$ is positive and f is commonly believed to be less than 1 from (5.6) one expects

$$\frac{A(K_2 \to 2\gamma_\perp)}{A(K_2 \to 2\gamma_\perp)_{\pi_0}} < \frac{A(K_1 \to 2\gamma_\perp)}{A(K_1 \to 2\gamma_\perp)_{\pi_0}} \tag{5.8}$$

Since the ratio in the r.h.s. of (5.8) is slightly larger than 1 and $\frac{\partial C}{\partial f} \sim 3$ we are able to find, for each value of ξ, two values of f in agreement with (5.7) with opposite values of C: f_- and f_+.

One finds in the literature different predictions for the value of f. We relate it to a combination of S-wave amplitudes for hyperon non-leptonic decays[20,21] which does not receive contributions from the first two terms in (5.3).

$$f = \frac{2Gm_K^2 m_\pi^2[\sqrt{3}A(\Lambda \to p\pi^-) - A(\Sigma^+ \to p\pi^0) + \sqrt{3}A(\Xi \to \Lambda\pi^-)]}{(m_{\Xi^-} - m_{\Sigma^-})|A_{exp}(K_1 \to \pi_0\pi_0)|} \cdot$$

$$\cdot \frac{2(\frac{f_K}{f_\pi} - 1)}{1 - 2(\frac{f_K}{f_\pi} - 1)} = (1.12 \pm .11)\frac{\frac{3}{2}\xi}{1 - \frac{3}{2}\xi} \tag{5.9}$$

where the 10 % error arises from the uncertainty on $A(\Sigma^+ \to p\pi^0)$: f depends strongly on ξ and crosses f_- (f_+) at the lower (upper) boundary of the range of ξ considered. The values of f corresponding to the crossing points $f(\xi = .19) = .45$ and $f(\xi = .3) = .92$ are near the numbers proposed in ref. [22] and [20] respectively. Then we get two almost opposite possibilities for the ratio:

$$\frac{A(K_1 \to 2\gamma_\perp)}{A(K_2 \to 2\gamma_\perp)} = \begin{pmatrix} -1.15 \\ or \\ 1.21 \end{pmatrix} \frac{< \pi_0\pi_0|H_W|K_2 >}{< \pi_0\pi_0|H_W|K_1 >} = \begin{pmatrix} -1.15 \\ or \\ 1.21 \end{pmatrix} i\frac{ImA_0}{ReA_0}\frac{1}{1 - \sqrt{2}\omega} \tag{5.10}$$

where the upper (lower) value is obtained with f_- (f_+) From the expression for ϵ'

$$\epsilon' = -ie^{i(\delta_2 - \delta_0)}\frac{\omega}{\sqrt{2}}\frac{ImA_0}{ReA_0} \tag{5.11}$$

From (2.10) and the fact that $\delta_2 - \delta_0 + \frac{\pi}{2} = 48^o \pm 8^o$ is very near to the phase predicted for $\epsilon, 43.67^o \pm .14^o$, we get:

$$\frac{ImA_0}{ReA_0} = -\frac{\sqrt{2}|\epsilon'|}{\omega} = -|\epsilon|(.097 \pm 0.035) \tag{5.12}$$

From (5.10) and (5.12) we get

$$\eta_\perp = \frac{A(K_S \to 2\gamma_\perp)}{A(K_L \to 2\gamma_\perp)} = \epsilon - \frac{\sqrt{2}|\epsilon'|}{\omega}i\begin{pmatrix} -1 + \nearrow & -1.23 \\ & \\ & \searrow\ 1.29 \end{pmatrix} \tag{5.13}$$

In conclusion we find:

$$R\eta_{||}^* + \eta_\perp = (R+1)Re(\epsilon) + iIm(\epsilon)(1-R) + i|\epsilon|(0.097 \pm 0.035)\begin{pmatrix} R\omega + \nearrow & -2.23 \\ & \\ & \searrow\ 0.29 \end{pmatrix} \tag{5.14}$$

To decrease the error in R we use the experimental value of $\Gamma(K_L \to \gamma\gamma)$ and the theoretical value for $\Gamma(K_S \to \gamma\gamma)$ (as we can see from (5.14) the asymmetry is very sensitive to the value of R). The difference between the superweak and the standard model results to be very tiny in the case of a large f, while gives a change in the imaginary part for the case of small f:

$$Im(R\eta_{||}^{*} + \eta_{\perp}) = \begin{pmatrix} -1.52 \\ -1.05 \pm .17 \\ -1.6 \pm .024 \end{pmatrix} \cdot 10^{-3} \quad \begin{matrix} superweak \\ f = f_{-} \\ f = f_{+} \end{matrix} \tag{5.15}$$

The value of the asymmetry $\Delta(t)$ defined in (2.1) is reported in Fig. 4 for the superweak theory and for the standard model with the two possible values for f. In Table II we reported the integrated asymmetries $\Delta_{int}(T)$ for three values of T (0.6, 1.2, 1.8 τ_S) and in correspondence of a range of values of R consistent with our present knowledge in the case of the superweak theory and in our approach with the choice f=f$_-$. As it can be seen in Table II the distinction between the two theories requires a better precision on the value of R, since an increase of .2 for this quantity has almost the same effect of the direct CP violating predicted. This precise measurement of R can be obtained in the same experiment by separating in $A_+(t)$ the term proportional to $e^{-\Gamma_S t}$ and $e^{-\Gamma_L t}$ respectively.

6.CONCLUSIONS.

We find, in agreement with previous authors [8], that the main difference for the CP violating effects in the $K^0(\bar{K}^0) \to 2\gamma$ decays between the standard and the superweak models is expected in the final state with perpendicular polarizations. The amplitude $A(K^0 \to 2\gamma_\perp)$, which we assume to be dominated by the intermediate pseudoscalar mesons, depends crucially on SU(3) violation and $\eta - \eta'$ mixing angle. Neverthless we are able to evaluate the CP violating amplitude $A(K_1 \to 2\gamma_\perp)$ with a result very smoothly dependent upon the chiral symmetry breaking parameter $\xi = \frac{4}{3}(\frac{f_K}{f_\pi} - 1)$. The CP conserving amplitude $A(K_2 \to 2\gamma_\perp)$ depends strongly on the parameter $f = \frac{A(K_S \to 2\pi^0)_{peng}}{A(K_S \to 2\pi^0)}$ and takes the two opposite values consistent with $\Gamma(K_L \to \gamma\gamma)$ in correspondence of the values .45 and .92 for f. These two possibilities imply:

$$\frac{A(K_S \to 2\gamma_\perp)}{A(K_L \to 2\gamma_\perp)} = \epsilon - \frac{\sqrt{2}|\epsilon'|}{\omega} i \begin{pmatrix} -1.23 \\ -1 + \nearrow\searrow \\ 1.29 \end{pmatrix}$$

The main difference with respect to the previous evaluation arises from our choice for the $\eta - \eta'$ mixing of the value deduced by the square mass matrix, which

is smaller than the value taken to fit the rate $\Gamma(\eta \to \gamma\gamma)$ to the result found in the crystal ball experiment. In favor of our choice we remark that, once modified the result of chiral lagrangians for $\eta - \eta'$ mixing, there is no reason to believe in their predictions for $\frac{<\eta_8|H_W|K^0>}{<\pi_0|H_W|K^0>}$ and $\frac{A(\eta_8 \to 2\gamma)}{A(\pi^0 \to 2\gamma)}$ which play an important role in the evaluation of $\frac{A(K_S \to 2\gamma)}{A(K_L \to 2\gamma)}$.

FOOTNOTES

† -In φ Factories one may get tagged K_S, which by regeneration would give rise to combinations with $|z| < 1$.

‡ -We have also evaluated the absorbtive contribution of 3π's intermediate state to $A(K^0 \to 2\gamma_\perp)$. The vertices are given by chiral lagrangian when we include the Wess-Zumino term. We find negligible contributions for the CP violating and the CP conserving part. Indeed for the CP conserving part:

$$\frac{A(K_2 \to 3\pi \to 2\gamma_\perp)}{A(K_2 \to \pi^0 \to 2\gamma_\perp)} \sim .03$$

References

[1] P. Pavlopoulos, in: Flavour Mixing in Weak Interactions, edited by L. L. Chau. Series editor: A. Zichichi, (1984)

[2] G. D'Ambrosio and D. Espriu, Phys. Lett. B 175 (1986) 237; J. I. Goity, Z. Phys. C 34 (1987) 341.

[3] H. Brukhardt, P. Clarke, D. Cundy, N. Doble, L. Gatignon, R. Hagelberg, G. Kesseler, J. van der Lans, I. Mannelli, T. Miczaika, H. G. Sander, A. C. Schaffer, P.Steffen, J. Steinberger, H. Taureg , H. Wahl, C. Youngman, G. Dietrich, W. Heinen, R. Black, D. J. Candlin, J. Muir,K. J. Peach, B. Pijlgroms, I. P. Shipsey, W. Stephenson, H. Blumer, M. Kasemann, K. Kleinknecht, B. Panzer, B. Renk, E. Auge', R. L. Chase, M. Corti, D. Fournier, M. Hassan, P. Heusse, A. M. Lutz, L. Bertanza, A. Bigi, M. Calvetti, R. Carosi, R. Casali, C. Cerri, E. Massa, A. Nappi, G.M. Pierazzini, C. Becker, D. Heyland, M. Holder, G. Quast, M. Rost, W. Weihs and G. Zech, (NA 31 collaboration), Phys. Lett. B 199 (1987) 139.

[4] M. K. Gaillard and B. W. Lee, Phys. Rev. D 10 (1974) 897.

[5] E. Ma and A. Pramudita, Phys. Rev. D 24 (1984) 2476.

[6] J. F. Donoghue, B. R. Holstein and Y-C. R. Lin, Nucl. Phys. B 277 (1986) 651

[7] R. Decker, P. Pavlopoulos and G. Zoupanos, Z. Phys. C 28 (1985) 117.

[8] L. L. Chau and H. Y. Cheng, Phys. Rev. Lett. 54 (1985) 1768; Phys. Lett. B 195 (1987) 275

[9] H. Brukhardt , P. Clarke, D. Cundy, N. Doble, L. Gatignon, V. Gibson, R. Hagelberg, G. Kesseler, J. van der Lans, I. Mannelli, T. Miczaika, A. C. Schaffer, P.Steffen, J. Steinberger, H. Taureg , H. Wahl, C. Youngman, G. Dietrich, W. Heinen, R. Black, D. J. Candlin, J. Muir,K. J. Peach, B. Pijlgroms, I. P. Shipsey, W. Stephenson, H. Blumer, M. Kasemann, K. Kleinknecht, B. Panzer, B. Renk, E. Auge', R. L. Chase, M. Corti, D. Fournier, P. Heusse, L. Iconomidou-Fayard, A. M. Lutz, H. G. Sander, A. Bigi,M. Calvetti, R. Carosi, R. Casali, C. Cerri, G. Gargani, E. Massa, A. Nappi, G.M. Pierazzini, C. Becker, D. Heyland, M. Holder, G. Quast, M. Rost, W. Weihs and G. Zech, (NA 31 collaboration), Phys. Lett. B 206 (1988) 163.

[10] N. Cabibbo, Phys. Rev. Lett. 12 (1964) 62; M. Gell-Mann, Phys. Rev. Lett. 12 (1964) 155.

[11] J. Wess and B. Zumino, Phys. Lett. B 37 (1971) 95.

[12] P. Langacker and H. Pagels, Phys. Rev. D 10 (1974) 2904.
[13] J. F. Donoghue, B. R. Holstein, and Y-C. R. Lin, Phys. Rev. Lett. 55 (1985) 2766.
[14] M.M. Nagels, Th. Rijken, J.J. De Swart, G.C. Oades, J.L. Petersen, A.C. Irving, C. Jarlskog, W. Pfeil, H. Pilkuhn and H.P.Jacob, Nucl. Phys. B 147 (1979) 189 E. A. Paschos and U. Turke, Phys. Lett. 116 B (1982) 360; E. P. Shabalin, Sov. J. Nucl. Phys. 42 (1985) 164; A. Pich, B. Guberina and E. de Rafael, Nucl. Phys. B 277 (1986) 197.
[15] Particle Data Tables: Phys. Lett. B 204 (1988).
[16] S. Cooper, in: Proceedings of the 1985 Europhysics Conference on High Energy Physics, Bari, Italy, edited by L. Nitti and G. Preparata, (1985) 945.
[17] A. Browman, J. DeWire, B. Gittelman, K. M. Hauson, E. Loh, and R. Lewis, Phys. Rev. Lett. 32 (1974) 1067.
[18] L. B. Okun: Leptons and Quarks, North-Holland (1980).
[19] J. Donoghue and B. Holstein, Phys. Rev. D 29 (1984) 2088.
[20] A. I. Vainshtein, V. I. Zakharov, and M. A. Shifman, Sov. Phys. JETP 45 (1977) 670.
[21] E. P. Shabalin, Sov. J. Nucl. Phys. 48 (1988) 172.
[22] W. A. Bardeen, A. Buras and J.-M. Gerard, Phys. Lett. 192B (1987) 138.

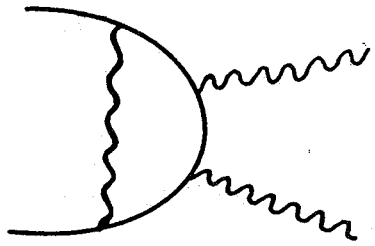

FIG. 1

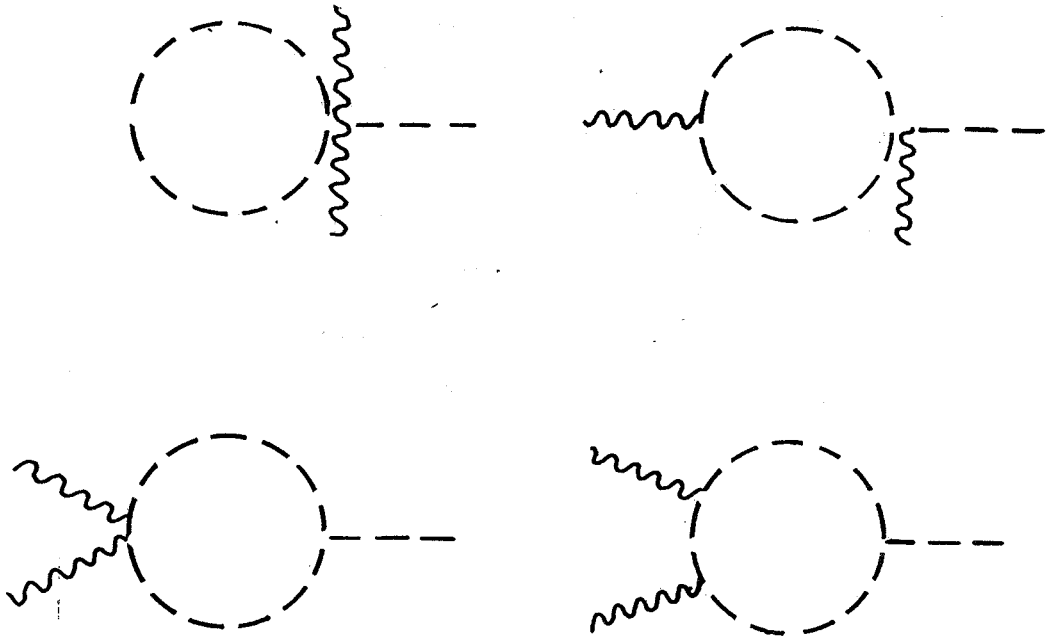

FIG. 2

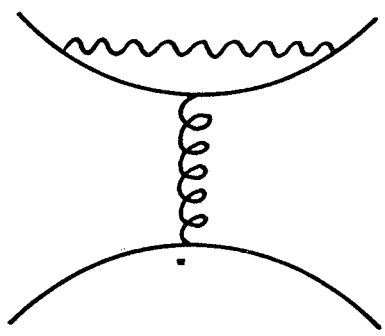

FIG. 3

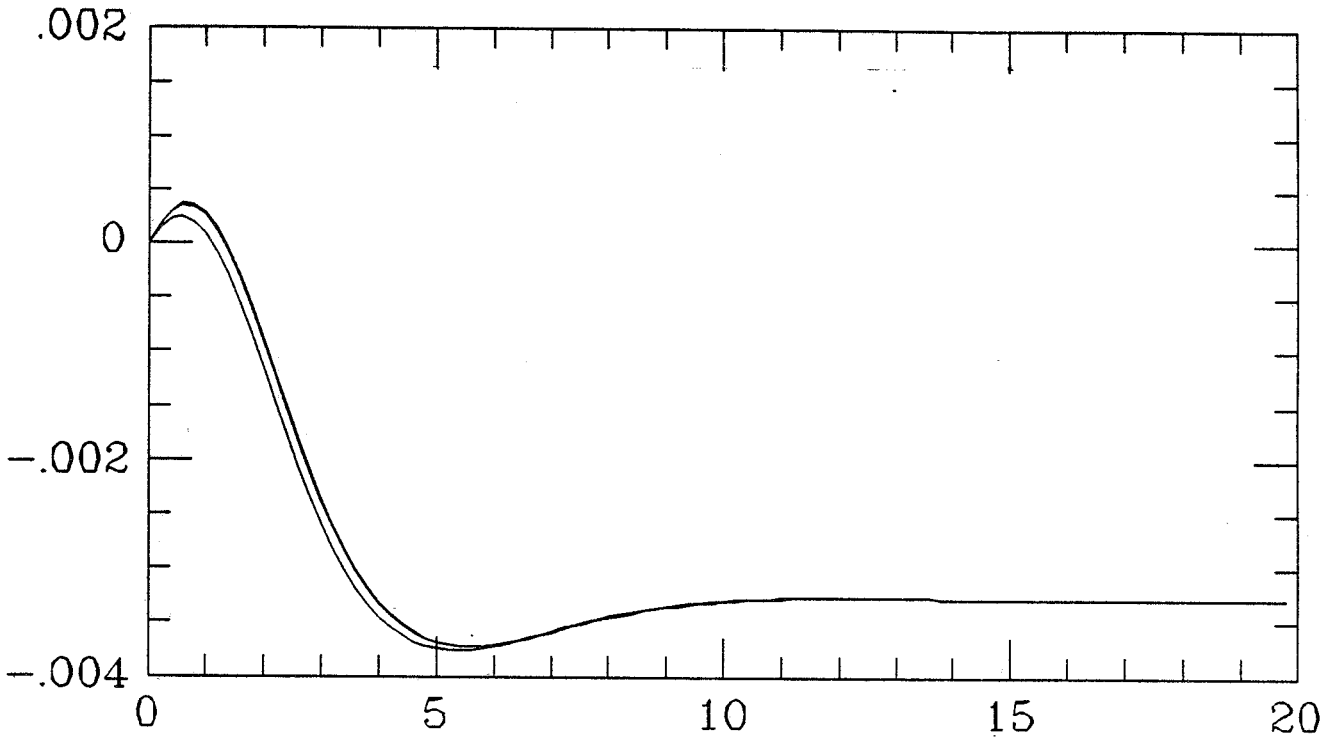

TABLE I

ξ	θ	Γ_η (eV)	b_{η_8}	b_{η_0}	b_η	$b_{\eta'}$	$\frac{A(K_2 \to 2\gamma_\perp)}{A(K_2 \to 2\gamma_\perp)_{\pi^0}}$	$\frac{A(K_1 \to 2\gamma_\perp)}{A(K_1 \to 2\gamma_\perp)_{\pi^0}}$
.18	$-14.8°$	367	-2.21	2.23	$-.73$	.75	$-.94$	1.01
.20	$-15.2°$	364	-2.22	2.23	$-.72$	.73	$-.7$	1.02
.22	$-15.6°$	364	-2.23	2.27	$-.70$	.74	$-.5$	1.03
.24	$-15.9°$	364	-2.26	2.31	$-.69$	.74	$-.2$	1.05
.26	$-16.3°$	367	-2.27	2.32	$-.69$	.74	$+.1$	1.05
.28	$-16.6°$	367	-2.32	2.39	$-.68$	.75	$+.3$	1.06
.30	$-17.0°$	367	-2.33	2.40	$-.69$	.76	$+.76$	1.07
.32	$-17.3°$	367	-2.32	2.45	$-.63$	.77	$+1.24$	1.13

TABLE II

R	$\Delta_{int}(T)10^4$ *superweak* $T = .6, 1.2, 1.8\tau_S$			$\Delta_{int}(T)10^4$ $f = f_-$ $T = .6, 1.2, 1.8\tau_S$		
1.37	.4	$-.8$	-2.9	$-.2$	$-2.$	-4.3
1.57	.9	.3	-1.5	.4	$-.6$	-2.8
1.77	1.4	1.2	-0.2	0.9	0.3	-1.4
1.97	1.9	2.1	0.8	1.4	1.2	-0.2
2.17	2.2	3.	1.9	1.8	2.	0.9
2.37	2.6	3.5	2.8	2.2	2.8	1.9
2.57	3.	4.1	3.7	2.6	3.4	2.8

A ϕ factory to understand light and narrow mesons

D. Cocolicchio

CERN,CH-1211 Geneve 23, Switzerland

ABSTRACT

In this letter it is proposed an investigation to understand the mixing properties and the quark structure of the light meson resonance $S^*/f_0(976)$

The understanding of meson spettroscopy is of fundamental importance in the search for gluonium or hybrid states [1]. The search for narrow scalar mesons below 1 GeV has been carried out in the radiative decay of the J/ψ to $\pi\pi$ and $K\overline{K}$, with negative results [2]. The hadronic decay of the J/ψ, on the other hand, shows good evidence for $S^*/f_0(976)$ production in the $\pi^+\pi^-$ spectrum recoiling against $\phi(1020)$ resonance. A still unexplained structure is also visible in the 1.4 GeV region of the $\pi^+\pi^-$ spectrum opposite the $\phi(1020)$ for which a scalar contribution seems to be present [3]. Due to the narrow widths and substantial low masses, the two 0^{++} states: the $S^*/f_0(976)$ and the $\delta/a_0(983)$, do not seem to fit into the same nonet as the broader and heavier states, the $f_0(1300)$ and the $k_0(1430)$.

The higher statistics studies with incident pions leads to the conclusion that a broad $\epsilon/f_0(1400)$ and a narrow S^*/f_0 exist. The possible production of the S^*/f_0 in $\gamma\gamma$ collisions has been reported [4]. The ϕ particles were recently seen in heavy ions collisions [5]. Evidence for the S^*/f_0 has also been found in the decay [6]

$$D_s \rightarrow S^*/f_0\pi \rightarrow \pi\pi\pi \tag{1}$$

Furthermore, the two-photon decays of the scalar mesons $\delta_0(983)$ and the S^*/f_0 have finally been determined [7]:

$$\begin{aligned} \Gamma(S^* \rightarrow \gamma\gamma) &= (0.27 \pm 0.12)\ KeV \\ \Gamma(\delta \rightarrow \gamma\gamma) &= (0.23 \pm 0.09)\ KeV \end{aligned} \tag{2}$$

The above results appear to suggest a substantial $s\bar{s}$ component in the S^*/f_0 wave function [8]. A particular property of the S^*/f_0 is that it often appears as sharp drop in the $\pi^+\pi^-$ mass spectrum and only in a few cases as a narrow peak.

A recent analysis of central dipion production [9] indicates a different scenario: the S^*/f_0 is a gluonium state while an $s\bar{s}$ scalar resonance may be present in the threshold region of the $K\overline{K}$ spectrum. Besides all that, there are also suggestions that the S^*/f_0 could be a 4-quark state [10] or a $K\overline{K}$ molecule [11].

One can attempt to understand the mixing properties and the quark structure of the S^*/f_0 by investigating the $\pi\pi$ and the $K\overline{K}$ systems produced by the radiative decay of the $J^{PC} = 1^{--}$ ϕ resonance:

$$\phi \rightarrow S^*\gamma \rightarrow \begin{cases} \pi\pi \\ \\ K\overline{K} \end{cases} \gamma \quad . \tag{3}$$

The ϕ mesons being copiously produced in high-luminosity electron-positron collider operating near the ϕ resonance at 1020 MeV (ϕ factory) have recently excited much interest [12]. Active programs are in progress mainly at Frascati, at Vancouver (TRIUMF), at the Soviet Novosibirsk Laboratory, where a collider is already operational at that energy range, at NIKHEF. New ideas are also being explored in connection with the planned Elettra synchroton light source at Trieste [13], and detector designs covering a nearly complete solid angle were under investigations [14] for the measurement of CP violating parameters in the coherent decay in $K^\circ\overline{K}^\circ$.

As stressed by many people [15] the ϕ meson decays in an antisymmetric K_SK_L state, and from the study of the 4π final states (time asymmetry in $\pi^+\pi^-$, $\pi^0\pi^0$ [16] or different branching ratios in different charge configurations [17]) one can hope to get a clean determination of the ratio ϵ'/ϵ.

Very recently Nussinov and Truong [18] remarked the presence of a background deriving from the following chain of decays:

$$\phi \rightarrow \gamma + S^*/f_0(976) \rightarrow \gamma + \left(K^\circ\overline{K}^\circ\right)_{C=+} \rightarrow \gamma + \frac{1}{\sqrt{2}}\left(K_SK_S - K_LK_L\right) \qquad (4)$$

In principle, the mass spectrum of the kaon pairs cannot distinguish the direct ϕ decay from that derived by an intermediate S^*/f_0 state. Since the ϕ is produced at rest the maximum energy of the photon is 24 MeV. Due to the small boost and the width of the S^*/f_0, this will not be a perfectly monochromatic distribution but seemingly the design feasibilities cannot detect this radiation efficiently. Only the mass spectrum of the kaon pairs peaked around the ϕ meson mass can manifest the presence of this resonance.

The K_SK_S component of the $\phi \rightarrow S^*/f_0\gamma$ decay, anyway dominates at very short flight-times (a few τ_S) near the collision point. It is evident that ($K^\circ\overline{K}^\circ$, $C = -$) decays are largest compared to the ($K^\circ\overline{K}^\circ$, $C = +$) ones coming from the S^*/f_0 only in a suitable intermediate time-flight region in which the C-even events are suppressed almost completely [19]. On the other hand, very far from the vertex, the ϕ radiative decays in six pions can easily be reconstructed since it is also dominant due to the K_LK_L component of the decay [19].

The branching ratio of the process $\phi \rightarrow S^*/f_0\gamma$, anyway, is strongly model dependent.

Nussinov and Truong obtained a partial width $\Gamma(\phi \rightarrow \gamma + K^\circ\overline{K^\circ}) = 1.5 \cdot 10^{-7}$ MeV, which corresponds to $\Gamma(\phi \rightarrow \gamma + S^*/f_0) = 6 \cdot 10^{-6}$ MeV.

An eventual small contamination of non strange quarks in the S^*/f_0 can be put in evidence by assuming that the mixing relative to the quark basis of the physical

isoscalar S^*/f_0 state is in the form

$$|S^* >= \frac{\sin\varphi_s}{\sqrt{2}}|u\bar{u} + d\bar{d} > + \cos\varphi_s|s\bar{s} > \tag{5}$$

Assuming a quark triangle picture, the decay rate ratio gives

$$\frac{\Gamma(S^* \to \gamma\gamma)}{\Gamma(S^* \to \gamma\gamma)} = \frac{1}{9}\left(5\sin\varphi_S + \sqrt{2}\cos\varphi_S\left(\frac{m}{m_s}\right)\right)^2 = 1.17 \pm 0.70 \tag{6}$$

where $m/m_s \sim 0.7$ weights the strange relative to the nonstrange mass transversing the quark triangle. In addition using the previous result for the $S^* \to \pi\pi$ decay rate, we get the ratio

$$\frac{\Gamma(S^* \to \pi\pi)}{\Gamma(\delta \to \eta\pi)} = \left(\frac{\sin\varphi_S}{\cos\varphi_P}\right)^2 \cdot \frac{3}{2} \cdot \frac{p_{S^*}}{p_\delta}\left(\frac{m_\delta}{m_{S^*}}\right)^2 \tag{7}$$

where the value of the pseudoscalar mixing φ_P was computed in [20] and in this quark basis is $\sim 40°$. Besides many uncertainties, this analisys suggests $\varphi_s \sim 20°$. So that the $S^*/f_0(976)$ appears presently mostly due to two strange quarks, as the nearby $\phi(1020)$ vector meson.

In this approach, the magnetic dipole ϕ radiative transition could be eventually foreseen once a calibration process $\Gamma(1^- \to 0^+\gamma)$ would be detected and no deviation from a single quark content of the S^* is present with the following prescription

$$\Gamma(\phi \to S^*\gamma) = \Gamma(1^- \to 0^+\gamma) \cdot \cos^2\varphi_S \cdot \frac{4}{9}\left(\frac{p_{S^*}}{p_\pi}\right)^3\left(\frac{m}{m_{S^*}}\right)^2 \tag{8}$$

The same conclusion for the ϕ decay can be derived using a non relativistic potential model as done for radiative decays of the radial excitation $c\bar{c}$ vector meson ψ'. In this case one has for a confining linear potential $\Gamma(\phi \to \gamma + S^*/f_0) \simeq 6 \cdot 10^{-5}$. Whereas if the confining potential is quadratic, the decay width reaches nearly 10^{-4} MeV [19].

The above $s\bar{s}$ assignment for the S^*, which appear favoured by the $S^* \to \gamma\gamma$ measurement, must face out with some properties of these mesons which disagree with the expectations of the naive $q\bar{q}$ SU(3) model: they are nearly degenerate in mass and very light relative to the other scalars to fit into the expected pattern of weak spin-orbit splittings. If $q\bar{q}$, the near degeneracy of the S^* and δ^0 constrains the S^* to have almost no $s\bar{s}$ content. With $1/\sqrt{2}(u\bar{u} + d\bar{d})$ states one can predict $\Gamma(S^* \to \pi\pi)/\Gamma(\delta \to \eta\pi) \approx 4$ in disagreement with the observed value of 0.6 ± 0.2. Another SU(3) $q\bar{q}$ prediction is that $\Gamma(S^* \to KK)/\Gamma(S^* \to \pi\pi) \approx p_K/3p_\pi$ with $p_K(p_\pi)$ the kaon (pion) kinetic

energy. The data do not support this expectation. Furthermore the latest experimental measurements

$$\Gamma(S^* \to \gamma\gamma)\mathrm{BR}(\pi\pi) = 0.19 \pm 0.05 \pm 0.12 \text{ KeV} \quad \text{Mark II Collab.}$$

$$\Gamma(\delta^0 \to \gamma\gamma)\mathrm{BR}(\eta\pi) = \begin{cases} 0.19 \pm 0.07 \pm 0.09 \text{ KeV} & \text{Crystall Ball Collab.} \\ 0.29 \pm 0.05 \pm 0.04 \text{ KeV} & \text{JADE Collab.} \end{cases} \tag{9}$$

appear consistent with the coupled channel $K\bar{K}$ molecule picture but not with $1/\sqrt{2}$ $(u\bar{u} + d\bar{d})$ content, although a definite measurement would be of great interest.

None of these models is very compelling, therefore one should not trust too much the smallness of the values obtained and expect a clear S^*/f_0 signal.

Thus the detection of suitable kaon pairs close or far the colliding e^+e^- beams can easily increase our knowledge of the resonance.

For completeness, the partial widths to $\pi\pi$ and $K\overline{K}$ from the S^*/f_0 can be given

$$\begin{aligned} \Gamma_\pi &= g_\pi \left(\frac{m^2}{4} - m_\pi^2 \right)^{\frac{1}{2}} \\ \Gamma_K &= g_K \left[\left(\frac{m^2}{4} - m_{K^+}^2 \right)^{\frac{1}{2}} + \left(\frac{m^2}{4} - m_{K^0}^2 \right)^{\frac{1}{2}} \right], \end{aligned} \tag{10}$$

where g_π^2 and the g_K^2 are the squares of the couplings of the S^*/f_0 to $\pi\pi$ and $K\overline{K}$. A recent preliminary analysis of CERN-WA76 experiment [21] gives

$$\begin{aligned} g_\pi &= 0.25 \pm 0.02 \quad , \\ g_K &= 0.20 \pm 0.04 \quad . \end{aligned} \tag{11}$$

A high luminosity ϕ factory can support this prediction and definitively solve the problem if

$$S^*/f_0 \quad \text{is} \quad \begin{cases} s\bar{s} \text{ state} \\ s\bar{s} \cdot (d\bar{d} + u\bar{u}) \quad \text{state} \\ \text{glueball} \\ K\overline{K} \quad \text{molecule} \end{cases} \tag{12}$$

References

[1] S. Sharpe, Proc. of BNL Workshop, 1988.

[2] J.Adler et al.,XXI Int. Conf. on HEP, Aug. 1988, Munich.

[3] A. Falvard et al., Phys. Rev. **D38** (1988) 2706.

[4] J. K. Bienlein, preprint DESY 88-165, (1988).

[5] M. C. Abeau et al., CERN-NA38 Collab., preprint LAPP-EXP 89-15 (1989).

[6] J. C. Anjos et al., Phys. Rev. Lett. **62** (1989) 125.

[7] Crystall Ball Collab., R. Clare et al., XXI Int. Conf. on HEP, Aug. 1988, Munich; W.S. Lockman, MARK III Collab., preprint SLAC-PUB 5139 (1989).

[8] A. Bramon and M. D. Scadron, preprint UAB-FT-222 (1989).

[9] T. Akesson et al., Nucl. Phys. **B264** (1986) 154;
K. L. Au, D. Morgan and M. Pennington, Phys. Rev. **D35** (1987) 1633.

[10] R. Jaffe, Phys. Rev. **D15** (1977) 267;
N.N. Achasov et al., Phys. Lett. **96B** (1980) 168, Z. Phys. **C16** (1982) 52.

[11] J. Weinstein and N. Isgur, Phys. Rev. Lett. **48** (1982) 659; Phys. Rev. **D27** (1983) 588; R. Kokoski and N. Isgur, Phys. Rev. **D35** (1987) 907;
T. Barnes, Phys. Lett. **165B** (1985) 434,preprint UTPT-87-20 (1987).

[12] U. Amaldi and G. Coignet, *Proceedings of the Workshop on Heavy Quark Factory and Nuclear Physics Facility with Superconducting Linacs*, E. De Sanctis, M. Greco, M. Piccolo and S. Tazzari eds. (Courmayeur, 1987) p. 59.

[13] C. Rubbia, "*A $\phi \rightarrow K_L K_S$ factory using the Trieste synchroton light source*", CERN UA1 Internal Note (1988).

[14] G. Barbiellini and C. Santoni, CERN preprint CERN-EP/89-88 (1989).

[15] T. Kamae, T. Kifune and T. Tsumemoto, Prog. Theor. Phys. **41** (1967) 1267;
H. J. Lipkin, Phys. Rev. **176** (1968) 1715.

[16] I. Dunietz, J. Hauser and J. L. Rosner, Phys. Rev. **D35** (1987) 2166.

[17] J. Bernabeu, F. J. Botella and J. Roldan, Phys. Lett. **B211** (1988) 226; University of Valencia preprint, FTUV/89-35 (1989).

[18] S. Nussinov and T. N. Truong, Phys. Rev. Lett. **63** (1989) 2003.

[19] D. Cocolicchio, G. L. Fogli, M. Lusignoli and A. Pugliese, CERN preprint CERN–TH. 5610/89 (1989).

[20] N. Paver, preprint "$\eta - \eta'$ mixing from ϕ radiative decays".

[21] I am obliged with A. Palano for this communication.

A Φ-factory to investigate the foundations of Quantum Mechanics

Decio Cocolicchio
Dipartimento di Fisica, Università di Bari, Bari, Italy
Istituto Nazionale di Fisica Nucleare, Sezione di Bari, Italy

ABSTRACT

A bound on the $K\overline{K}$ oscillating parameter has been obtained by some models of non locality. In this paper we stressed the fact that a Φ-factory to test the CP-violating parameters in the K-system can also probe, through correlated observations of two $\bar{K}^0$, the incompatibility between the Quantum Mechanics and these formulations of the local realism.

Recently a lot of attention has been devoted to the incompatibility between the quantum mechanics and the local realism approach in elementary particle physics. Some tests of the quantum mechanical correlation in the decays of $J^P = 0^-$ mesons $\eta_c(2980)$ and J/ψ into a Λ-hyperon plus $\bar{\Lambda}$-antihyperon pair (with the subsequent decays $\Lambda \to p + \pi^-$ and $\bar{\Lambda} \to \bar{p} + \pi^+$) was recently analyzed [1].

The well confirmed quantum mechanical prediction of the Λ-decay asymmetry appears to disagree up to the 10% from several particular approaches to non-classical effects. It is a hard task to adfirm the universality of this result for any model, locally realist.

Some recent results from Argus and Cleo Collaborations [2] appear to give a final answer as for the incompatibility between quantum mechanics and local realism in the formulation of Furry [3].

A more convenient place to verify the incompatibily between quantum mechanics and local realism in elementary particle physics can be found in the decay of a $J^{PC} = 1^{--}$ vector meson into a pair of neutral pseudoscalar mesons. For the $K^0\bar{K}^0$ system obtained from the decay of the spin-1 $\phi(1020)$ resonance, Six [4] suggested that the joint probability $\omega_{--}(t_a, t_b)$ of a double $\bar{K}^0$ observation on the left and right hemisphere at the time t_a and t_b represents an experimental test of Einstein-Podolski-Rosen [5] paradox.

K^0 and $\bar{K}^0$ mesons are charge coniugate of one another and are states of definite

strangeness $+1$ and -1 respectively (conserved in strong productions $\Delta S = 0$, violated in weak decays $\Delta S = 1$). However, they do not have definite lifetimes for weak decay nor do they have any definite mass, this means that they are not eigenstates. The mass eigenstates are linear combinations of the states $|K^0>$ and $|\bar{K}^0>$ namely $|K_S^0>$ and $|K_L^0>$, which have definite masses and lifetimes. The short lived $|K_S^0>$ meson decays into the two predominant modes $\pi^+\pi^-$ and $\pi^0\pi^0$ each with the CP eigenvalue $+1$, whereas the long lived $|K_L^0>$ mesons has among its decay modes $\pi^+\pi^-\pi^0$ and $\pi^0\pi^0\pi^0$, which are eigenstates of CP with eigenvalue -1.

With the conventional choice of phase we can write

$$\begin{aligned} CP|K^0> &= -|\bar{K}^0> \\ CP|\bar{K}^0> &= -|K^0> \end{aligned} \tag{1}$$

therefore, we have

$$\begin{aligned} |K_1^0> &= \frac{1}{\sqrt{2}}(|K^0> + |\bar{K}^0>) \qquad & CP|K_1^0> &= -|K_1^0> \\ |K_2^0> &= \frac{1}{\sqrt{2}}(|K^0> - |\bar{K}^0>) \qquad & CP|K_2^0> &= +|K_2^0> \end{aligned} \tag{2}$$

However, in 1964 it was observed [6] that there is a small but finite probability for the decay $K_L^0 \to \pi^+\pi^-$, in which the final state has the CP eigenvalue $+1$. Thus we cannot identify K_L^0 with K_1^0 and K_S^0 with K_2^0.

If we asumme the CP invariance for the mass eigenstates, there are two complemetary ways to describe neutral kaons:

1) In terms of the mass eigenstates $K_{L,S}$, which do not posses definite strangeness

$$
\begin{aligned}
|K_S(t)> &= |K_S(0)> e^{-\alpha_S t} \qquad \alpha_S = im_S + \frac{\gamma_S}{2} \\
|K_L(t)> &= |K_L(0)> e^{-\alpha_L t} \qquad \alpha_L = im_L + \frac{\gamma_L}{2}
\end{aligned}
\tag{3}
$$

where now

$$
\begin{aligned}
|K_S(0)> &= \frac{1}{\sqrt{2}}(|K^0(0)> - |\bar{K}^0(0)>) \\
|K_L(0)> &= \frac{1}{\sqrt{2}}(|K^0(0)> + |\bar{K}^0(0)>)
\end{aligned}
\tag{4}
$$

2) In terms of the flavour eigenstates, whose time evolution is more complex

$$
\begin{aligned}
|K^0(t)> &= f_+(t)|K^0(0)> + f_-(t)|\bar{K}^0(0)> \\
|\bar{K}^0(t)> &= f_-(t)|K^0(0)> + f_+(t)|\bar{K}^0(0)>
\end{aligned}
\tag{5}
$$

with

$$
\begin{aligned}
f_+(t) &= \frac{1}{2}(e^{-\alpha_S t} + e^{-\alpha_L t}) = \frac{1}{2}e^{-\alpha_S t}\left[1 + e^{-(\alpha_L - \alpha_S)t}\right] \\
f_-(t) &= \frac{1}{2}(e^{-\alpha_S t} - e^{-\alpha_L t}) = \frac{1}{2}e^{-\alpha_S t}\left[1 - e^{-(\alpha_L - \alpha_S)t}\right]
\end{aligned}
\tag{6}
$$

The two bases $\{K_S, K_L\}$ and $\{K^0, \bar{K}^0\}$ are completely equivalent.

We consider ϕ in the K^0 $\bar{K}^0$ channel decay. The temporal evolution of the two particles can be obtained by associating each of the particles to different times $t_a = t_L$, $t_b = t_R$, one for each emisphere left and right. The ϕ system in terms of CP-invariant states and in terms of weak eigenstates is given by

$$
\begin{aligned}
|\psi_\phi(0,0)> &= \frac{1}{\sqrt{2}}(|K^0(0)>_a |\bar{K}^0(0)>_b - |\bar{K}^0(0)>_a |K^0(0)>_b) \\
&= \frac{1}{\sqrt{2}}(|K_S(0)>_a |K_L(0)>_b - |K_L(0)>_a |K_S(0)>_b) \quad .
\end{aligned}
\tag{7}
$$

The time evolution of this state is

$$|\psi_\phi(t_a,t_b)>=\frac{1}{\sqrt{2}}\frac{1}{[f_+^2(t_a)-f_-^2(t_a)][f_+^2(t_b)-f_-^2(t_b)]}\cdot$$
$$\{[f_+(t_a)f_+(t_b)-f_-(t_a)f_-(t_b)]\,|K^0(t_a)>|\bar{K}^0(t_b)>+$$
$$[f_-(t_a)f_+(t_b)-f_+(t_a)f_-(t_b)]\,|K^0(t_a)>|K^0(t_b)>+ \qquad (8)$$
$$[f_+(t_a)f_-(t_b)-f_-(t_a)f_+(t_b)]\,|\bar{K}^0(t_a)>|\bar{K}^0(t_b)>+$$
$$[f_-(t_a)f_-(t_b)-f_+(t_a)f_+(t_b)]\,|\bar{K}^0(t_a)>|K^0(t_b)>\}\quad .$$

The probability $\omega_{--}(t_a,t_b)$ to find a $\bar{K}^0(t_a)\bar{K}^0(t_b)$ state is

$$|<\bar{K}^0(t_a)\bar{K}^0(t_b)|\psi_\phi(t_a,t_b)>|^2 =$$
$$\frac{e^{-(\gamma_L t_a+\gamma_S t_b)}+e^{-(\gamma_S t_a+\gamma_L t_b)}-2e^{-\frac{1}{2}(\gamma_L+\gamma_S)(t_a+t_b)}\cos[(m_L-m_S)(t_a-t_b)]}{e^{-(\gamma_L+\gamma_S)(t_a+t_b)}} \qquad (9)$$

Since $\tau_L >> \tau_S$ the amplitude $\gamma_L << \gamma_S$, then for a range t_a, $t_b \simeq (4-5)\frac{1}{\gamma_S}$ we have $e^{-\gamma_L} \simeq 1$ and

$$\omega_{--}(t_a,t_b) \simeq e^{-\gamma_S t_a} y(\Delta t) \qquad (10)$$

In an old paper, Selleri [7], using a more general notion of local realism based on Einstein interpretation, derived an upper bound for $y(\Delta t)$:

$$y(\Delta t) \leq y_E(\Delta t) = 1 + e^{-\gamma_S \Delta t} \qquad (11)$$

This upper bound differs from quantum mechanical prescription by the manifest absence of a dumped oscillation term deriving from interference. The discrepancy is at most of 12% for $\gamma_S(t_b - t_a) \simeq 5$ (Fig. 1). This approach however suffers the need to consider time interval t_a, t_b shorter than K_L, K_S lifetimes.

The possibility to overcome this difficulty can be a ϕ mesons factory as a source of kaons.

Recently it was proposed to measure the CP-violating parameters ϵ and ϵ' in the decay $\phi \to K_S K_L$ [8] with a high accuracy by realizing or a high luminosity machine [9] sending an electon beam from a superconducting LINAC against the positron stored in a circular ring or by building a ϕ-factory using the Syncroton Light Source [10].

We wish to stress that with a luminosity of the order of $10^{32} \quad cm^{-2}sec^{-1}$ it appears feasible to performe also a careful analysis of the quantum non separability and local realism in particle physics.

The ϕ can be produced very clearly in e^+e^- annihilation with a cross section of $\sigma_\phi \simeq 4\mu b$ and with a large branching ratio to $K_S K_L$: BR($\phi \to K_S K_L$)=(34.4±0.9)% [11].

The time-dependent correlations in the final two pions states from the kaon decays are an interesting $\frac{\epsilon'}{\epsilon}$ probe. Here, however, we are mainly interested in showing that such experiment is particularly suited to test the foundations of quantum mechanics. Such test requires to be sure to detect a $\bar{K}^0$ both at the left-emisphere time t_a and at the right emisphere time t_b. The practical realization of this aim requires the knowledge of the branching ratio of a peculiar decay channel of $\bar{K}^0$. We propose the clear semileptonic signature of the $K \to \pi(e,\mu)\nu$ decays with a total branching fraction of nearly 65%. Folding these previsions with the joint probability required for a double $\bar{K}^0$ observation on the left and right emisphere respectively at the times t_a and t_b such that $\Delta t \sim 5\tau_S$, we need a luminosity of $6 \cdot 10^{32} cm^{-2} sec^{-1}$ to produce 10^8 ϕ-mesons that is of the same order of the numbers of mesons that we need to perform the measurements of the phase difference to test the parameters of the kaon system associated with the CP violation.

In conclusion the building of a ϕ-factory to measure the CP-violating parameters can be easily adapted to realize a powerful test of the incompatibility between the quantum mechanics and local realism.

ACKNOWLEDGEMENTS

I would like to thank P. Bloch, A. Garuccio, L. Maiani, M. Quattromini and F. Selleri for some helpful and clarifying discussions.

Helpful suggestions of G. Barbiellini and J.S. Bell and their careful reading of the manuscript are gratefully acknowledged.

References

[1] N. A. Törnqvist, *Found. Phys.* **11** (1981) 171;
N. A. Törnqvist, *Phys. Lett.* **117A** (1986) 1.

[2] ARGUS Colaboration, H. Albrecht et al., *Phys. Lett.* **192B** (1987) 245;
CLEO Collaboration, A. Jawahery et al., talk at the XXIV International Conference on High Energy Physics, Munich, August 1988, ed. by R. Kotthaus and J. H. Kuhn (Springer 1989), p. 545.

[3] A. Datta and D. Home, *Phys. Lett.* **119A** (1986) 3.

[4] J. Six, *Phys. Lett.* **114B** (1982) 200.

[5] A. Einstein, B. Podolski and N. Rosen, *Phys. Rev.* **47** (1935) 777.

[6] J. H. Christenson, J. W. Cronin, V. L. Fitch and R. Turlay, *Phys. Rev. Lett.* **13** (1964) 138.

[7] F. Selleri, Lett. Nuovo Cimento, **36** (1983) 521.

[8] I. Dunietz, J. Hauser and J. L. Rosner, *Phys. Rev.* **D35** (1987) 2166.

[9] G. Barbiellini and C. Santoni, in the *Proceedings of the Workshop on Heavy Quark Factory and Nuclear Physics Facility with Superconducting Linacs*, E. De Sanctis, M. Greco, M. Piccolo and S. Tazzari eds. (Courmayeur, 1987) p. 441.

[10] C. Rubbia, A $\phi \rightarrow K_L K_S$ Factory using the Trieste Syncroton Light Source, Trieste preprint (1988).

[11] Particle Data Group, G. P. Yost et al., *Phys. Lett.* **204B** (1988) 1.

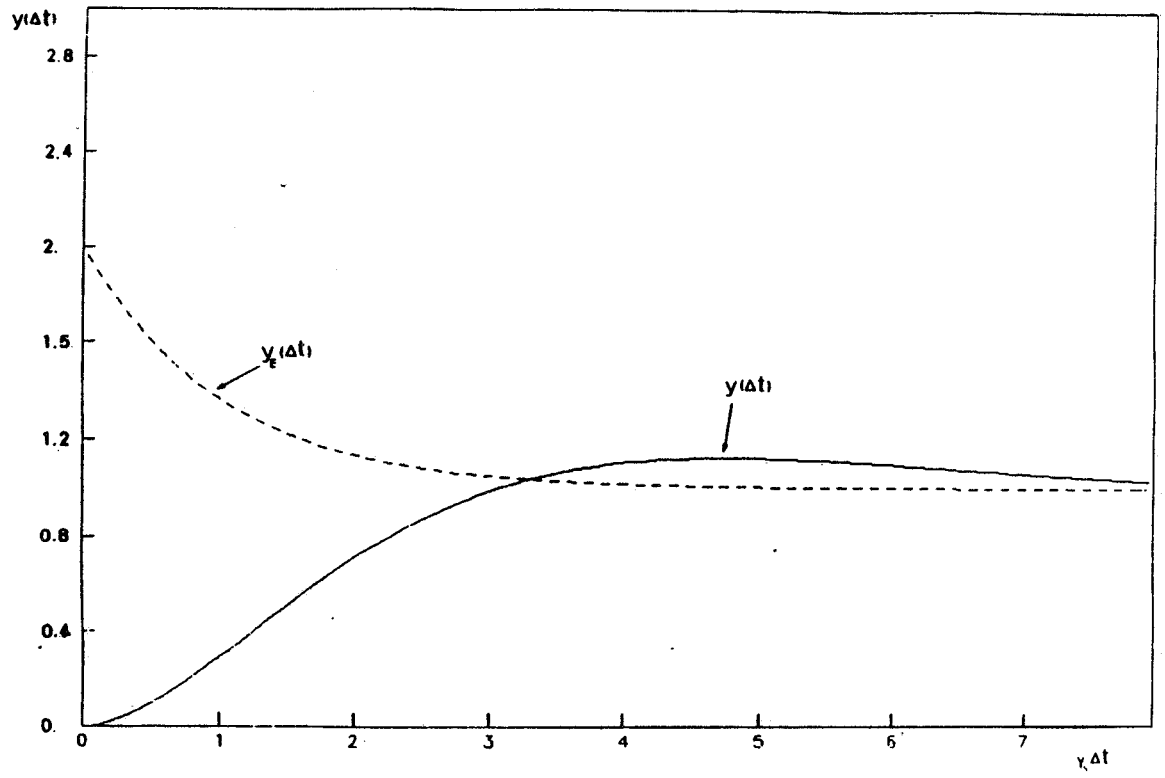

Fig. 1 - The forecasting upper bound for the correlated observations of two $\bar{K}^0$ deriving from a ϕ decay in the case of local realism with respect to quantum mechanics.

A MEASUREMENT OF ϵ'/ϵ IN A ϕ FACTORY

G. Barbiellini [1] and C. Santoni [2]

Abstract

This paper reports the results of a study of the feasibility of a measurement of the CP violation parameters in an e^+e^- ϕ factory.

---

[1] CERN, Geneva, Switzerland, and Dip. di Fisica, Univ. di Trieste and INFN Sez. di Trieste, Trieste, Italy.
[2] CERN, Geneva, Switzerland, and Physics Department, Univ. of Basle, Basle, Switzerland.

Until now, CP violation effects have been observed in the $K^0 - \bar{K}^0$ system only. In the Standard Model they are described by the parameter ϵ appearing in the mass matrix element responsible for the $\Delta S = 2$ transition ($K^0 \leftrightarrow \bar{K}^0$) and the parameter ϵ' appearing in the decay matrix element ($\Delta S = 1$ transition). A determination that gives a ratio ϵ'/ϵ different from zero [$\epsilon'/\epsilon = (3.1 \pm 1.1) \times 10^{-3}$] has been obtained from the measurement of the decay rates of K^0_L (K^0 long) and K^0_S (K^0 short) into two pions, which was done by the NA31 Collaboration at CERN [1]. Experiment E731 at Fermilab indicates a null value of ϵ'/ϵ, and the quoted result lies between -1.0×10^{-3} and $+1.0 \times 10^{-3}$, with an error in the range $\pm 1.3 \times 10^{-3} < \sigma(\epsilon'/\epsilon) < \pm 1.6 \times 10^{-3}$, but the authors do not commit themselves [2] to reporting a more precise value.

In the e^+e^- annihilation, the ϕ resonance is produced with a cross-section of 4 μb and high-luminosity machines (ϕ factories [3 – 7]) are necessary in order to improve the quoted results statistically. The branching ratio of the decay of the ϕ into two neutral kaons is 34%, and since the ϕ has the strong-interaction-conserved quantum number $C = -1$, a K^0_L and a K^0_S are produced in the final state.

Studying the events induced by the chain

$$e^+e^- \rightarrow \phi \rightarrow K^0_L K^0_S \rightarrow \pi^+\pi^-\pi^0\pi^0 , \tag{1}$$

a measurement of the ratio ϵ'/ϵ can be obtained from the determination of the asymmetry [8]

$$A = \frac{N(\Delta d > 0) - N(\Delta d < 0)}{N(\Delta d > 0) + N(\Delta d < 0)} , \tag{2}$$

where $\Delta d = d_1 - d_2$; d_1 and d_2 are the paths of the K^0's decaying into $\pi^+\pi^-$ and $\pi^0\pi^0$, respectively, and $N(\Delta d > 0)$ [$N(\Delta d < 0)$] is the number of events in which the path of the K^0 decaying into $\pi^+\pi^-$ is longer [shorter] than that of the other K^0 decaying into $\pi^0\pi^0$. Assuming that ϵ and ϵ' are real and that there is an equal fiducial volume FV of the charged and neutral decays ($d_1^{FV} = d_2^{FV}$), Eq. (2) is related to the CP violation parameters according to

$$A \approx 3 \times \epsilon'/\epsilon .$$

To understand this relation, note that for the events in the non-interference region ($\Delta d \gg d_S$, where d_S is the K^0_S mean decay path)

$$A = \frac{P(K^0_S \to \pi^0\pi^0)P(K^0_L \to \pi^+\pi^-) - P(K^0_S \to \pi^+\pi^-)P(K^0_L \to \pi^0\pi^0)}{P(K^0_S \to \pi^0\pi^0)P(K^0_L \to \pi^+\pi^-) + P(K^0_S \to \pi^+\pi^-)P(K^0_L \to \pi^0\pi^0)} \tag{4a}$$

$$= \frac{P(K^0_L \to \pi^+\pi^-)/P(K^0_S \to \pi^+\pi^-) - P(K^0_L \to \pi^0\pi^0)/P(K^0_S \to \pi^0\pi^0)}{P(K^0_L \to \pi^+\pi^-)/P(K^0_S \to \pi^+\pi^-) + P(K^0_L \to \pi^0\pi^0)/P(K^0_S \to \pi^0\pi^0)}, \tag{4b}$$

and, since $P(K^0_L \to \pi^+\pi^-)/P(K^0_S \to \pi^+\pi^-) = (\epsilon' + \epsilon)^2$ and $P(K^0_L \to \pi^0\pi^0)/P(K^0_S \to \pi^0\pi^0) = (\epsilon - 2\epsilon')^2$, we obtain

$$A = [3\epsilon'/\epsilon]/[1 - \epsilon'/\epsilon], \tag{5}$$

where terms $O[(\epsilon'/\epsilon)^2]$ have been neglected.

The study of the events induced by the reaction chain (1) as a function of Δd in the region $\Delta d < 2.5 d_S$ would allow also the difference between the phases of ϵ and ϵ' to be determined.

Experimental measurement of the asymmetry A requires identification of the decays $K^0 \to \pi^+\pi^-$ and $K^0 \to \pi^0\pi^0$, and also measurement of the decay paths d_1 and d_2 with a good control of the efficiency as a function of these paths. The CP violation parameters can also be obtained by measuring the relative rates of decay chains such as $\phi \to K^0_L K^0_S \to \pi^+\pi^-\pi^+\pi^-$ and $\phi \to K^0_L K^0_S \to \pi^0\pi^0\pi^0\pi^0$ [9], but in this case a knowledge of the absolute values of the reconstruction efficiencies is required.

The statistical error in A is related to the total number of events N induced by the reaction chain (1) according to

$$(\Delta A_{stat})^2 = [(1 + A) \times (1 - A)]/[N \times (1 - e^{d^{FV}/d_L})], \tag{6}$$

where d^{FV} is the maximum decay path for the accepted events and d_L is the mean decay path of K^0_L's. In the case of ϕ's produced at rest ($E_{e^+} = E_{e^-}$), the K^0's are monochromatic with a momentum $p_{K^0} = 110$ MeV/c and $d_L = 342$ cm. The mean decay path of the K^0_S's is $d_S = 0.6$ cm. To combine the need for a large event acceptance and reasonable detector dimensions, a spherical decay fiducial volume of radius $d_1^{FV} = d_2^{FV} = d^{FV} = 100$ cm was assumed. Table 1 shows the number

of the events expected in the fiducial volume in one year of running time (10^7 s) for machine luminosities $L = 2.5 \times 10^{32}$ cm^{-2} s^{-1} and $L = 1.0 \times 10^{33}$ cm^{-2} s^{-1}. The latter value is the expected luminosity at the Novosibirsk machine, now under construction [7]. The statistical errors in A and ε'/ε, calculated assuming that $\varepsilon'/\varepsilon = 0$, are also reported in the table.

In the study of the backgrounds, events induced by the reactions

$$K^0_L \to \pi^0\pi^0\pi^0 , \qquad K^0_S \to \pi^+\pi^- \qquad \text{(Back. 1)} \tag{7}$$

$$K^0_L \to \pi^+\pi^-\pi^0 , \qquad K^0_S \to \pi^0\pi^0 \qquad \text{(Back. 2)} \tag{8}$$

$$K^0_L \to \pi\mu\nu , \qquad K^0_S \to \pi^0\pi^0 \qquad \text{(Back. 3)} \tag{9}$$

$$K^0_L \to \pi e\nu , \qquad K^0_S \to \pi^0\pi^0 \qquad \text{(Back. 4)} \tag{10}$$

have been considered. The event rates relative to the signal are shown in Table 2. Reactions (7) and (8) will simulate the events induced by the reaction chain (1) if two gammas coming from neutral pion decays are not identified.

Figure 1a shows the distribution of the events induced by process (1) as a function of Δd for a value of $\varepsilon'/\varepsilon = 3 \times 10^{-3}$ [1]. The corresponding asymmetry A is of the order of 10^{-2}. For the backgrounds (8) to (10), since the K^0_L decays into two charged particles, almost all the events have $\Delta d > 0$ (see Fig. 1b) and the asymmetry is $\approx +1$. For the background induced by reactions (7), $A \approx -1$. In the case of high background rejection, obtainable with high-precision measurements of the particle energies and with very good particle identification, the residual events induced by reactions (7) to (10) are negligible compared with the events induced by process (1), and the measured asymmetry is given by

$$A_{meas} \approx A + \Sigma_i \, b_i \times s_i , \tag{11}$$

where b_i is the relative rate of the background i (i = 1, ..., 4) with respect to the signal (see Table 2) multiplied by a rejection factor r_i, and $s_i = -1$ for i = 1 and +1 for i = 2, 3, and 4. The experimental study of the backgrounds would allow a determination of b_i to few per cent, and in order to make the systematic error due to the background subtraction negligible compared with the statistical one, a reduction such that $b_i \approx 10^{-3}$ is required. The rejection factors r_i for obtaining $b_i = 10^{-3}$ are given in Table 2.

In the design of the detector, the energy of the particles involved in the reaction chain (1) is one of the main criteria for choosing the detector parameters. The momentum distribution of the charged pions, with a mean value of 212 MeV/c, is shown in Fig. 2. The energy distribution of the gammas produced in the π^0 decays is shown in Fig. 3; the mean value is 127 MeV and the lowest photon energy is 15 MeV. The schematic of the detector is shown in Fig. 4. It is a 4π detector with a central tracking region for reconstructing the momentum of the charged particles and their point of origin, a liquid Cherenkov detector for identifying muons, pions, and electrons, and an electromagnetic (e.m.) calorimeter for measuring the energy and the impact point of the converted photons used to reconstruct the path of K^0's decaying into $\pi^0\pi^0$.

The tracking region is a cylinder of 2 m radius and 4 m height. Since the fiducial volume is represented by a sphere of 1 m radius, all the the charged-particle tracks will be reconstructed over a path of 1 m. The momentum measurement is given by the sagitta of the circle made by the particles in a magnetic field B = 0.2 T. The resolution is dominated by the multiple scattering, and to reduce such an effect, low-Z gas mixtures such as He (95%) + dimethylether (5%), having a radiation length $X_0 >$ 2000 m [10], must be used. In the Monte Carlo program the charged tracks were assumed to be reconstructed making use of a Time Projection Chamber (TPC) having a spatial resolution, for a single point, of 700 μm along the z-axis parallel to the e^+e^- beams, and 200 μm in the perpendicular plane. Measuring 64 points per track it is expected to obtain the resolutions $\sigma_\theta = \sigma_\phi = 1$ mrad and $\sigma_{p_T}/p_T = 6 \times 10^{-3}$, where θ and ϕ are the particle angles at the point of origin with respect to the z-axis and in the perpendicular plane, respectively, and p_T is the transverse momentum. The resolutions are still dominated by multiple scattering but, as we will see, they make it possible to obtain the necessary background rejections and a very good reconstruction of the path of the K^0's decaying into $\pi^+\pi^-$. Owing to the interactions in the beryllium walls of the vacuum chamber and of the TPC, which are assumed to have a total thickness of 1 mm, the angle of the particles generated inside the beam pipe is measured with a resolution $\sigma_\theta = \sigma_\phi = 2$ mrad. For a beam pipe with a radius of 2 cm, about 50% of the charged pions are generated inside the pipe. In the Monte Carlo simulation, the angles of all the particles were smeared according to Gaussian distributions having $\sigma_\theta = \sigma_\phi = 2$ mrad independently of their origin.

A liquid Cherenkov counter having C_6F_{14} as the radiator with a refraction index n = 1.278 is adequate for identifying π, μ, and e in the momentum range 150 − 270 MeV/c. Figure 5 shows the expected Cherenkov angle θ_{Ch}, defined by $\cos\theta_{Ch} = 1/(\beta n)$, where β is the particle velocity in units of c, the velocity of light, for π, μ, and e. The error in the measurement of θ_{Ch} is dominated by the multiple scattering of the particles on the radiator and on the quartz windows of the detector [11, 12]. In the simulation, a conservative value of $\sigma(\theta_{Ch}) = 8$ mrad has been used.

The e.m. calorimeter under consideration is an homogeneous device containing liquid xenon [12] or liquid krypton [13], having a thickness of $13X_0$. This device allows the detection of gammas that have an energy down to 10 MeV, and a measurement of the energy with a resolution $\sigma(E_\gamma)/E_\gamma = 0.01/\sqrt{E_\gamma}$ (GeV). The impact point of the converted photons is reconstructed with a precision of 3 mm along the calorimeter axis and $\sqrt{2}$ mm in the perpendicular plane.

The background rejections have been studied, simulating the reconstruction of the events induced in the detector by reactions (8) to (11) and (1). For the Back. 1 induced by reactions (7), the required rejection factor is $r_1 = 8.4 \times 10^{-6}$. With an efficiency of 98% for detecting a single gamma, a first rejection factor $r_1' = 5 \times 10^{-3}$ is obtained, corresponding to the fraction of events having four detected photons. As shown in Fig. 6, the total energy distributions of the four detected gammas for the events induced by reactions (1) and (7) are quite different. In the case of the background events, the two lost gammas were assumed to be those with the lowest energies. By selecting events that have a total gamma energy larger than 470 MeV, a second rejection factor $r_1'' < 10^{-4}$ was found.

For the Back. 2 induced by reactions (8), a rejection factor $r_2 = 2.9 \times 10^{-5}$ is required. The good coverage of the e.m. calorimeter makes it possible to have a first rejection factor $r_2' = 3.6 \times 10^{-4}$. The measurement of the invariant mass of the two charged particles clearly allows the necessary rejection factor to be reached, as shown in Fig. 7.

The semileptonic decays of reactions (9) and (10) were simulated using the form-factor parameters $\zeta(t = 0) = -0.11$, with $t = (p_K - p_\pi)^2$, and $\lambda = 0.034$ [14]. The following cuts reduced the events induced by Back. 3 by $r_3' = 1.9 \times 10^{-3}$:

$$\theta_c > 2.6 \text{ rad},$$

$$105 < p < 116 \text{ MeV/c},$$

$$503 < E < 516 \text{ MeV},$$

where θ_c is the angle between the two charged particles, and p and E are the reconstructed momentum and energy of the K^0. The missing rejection factor $r_3'' = 7.5 \times 10^{-3}$, which is necessary in order to reach the desired rejection of 1.4×10^{-5} (see Table 2), can be obtained using the Cherenkov measurements, as shown in Fig. 8.

For the background induced by reactions (10), a rejection factor of $r_4 = 1.0 \times 10^{-5}$ is required. Applying the cuts (12), a first rejection $r_4' = 2.8 \times 10^{-3}$ was found. Because of the very different θ_{Ch} yields for electrons and pions (Fig. 5), the missing rejection factor can easily be obtained using the Cherenkov measurements. For the events induced by the signal reaction chain (1), the efficiency of the above-mentioned selection criteria is $\approx 90\%$.

Other possible sources of systematic errors are briefly discussed below. The determination of the quantity Δd requires the measurement of the decay paths of K^0's into $\pi^+\pi^-$ and into $\pi^0\pi^0$. Scaling the resolutions of the CP−LEAR experiment [15], we expect $\sigma(\Delta d) < 0.5$ cm. This uncertainty is dominated by the error in the path of the K^0 decaying into two neutral pions $\sigma(d_2)$, i.e. $\sigma(d_1) \approx 0.5$ mm. The error in ε'/ε induced by $\Delta\sigma(\Delta d)$ was studied, making use of a simple Monte Carlo simulation. It was observed that an error equal to $d_S/2$ (3 mm) resulted in a value of ε'/ε that differs from the true value by $\Delta(\varepsilon'/\varepsilon) = +1.5 \times 10^{-5}$.

Another possible source of systematic error is represented by the uncertainty in the definition of the fiducial volume. The effects on the measurement of ε'/ε that are caused by an error in d_2^{FV} are more important; if $\Delta d_2^{FV} = +d_S/5$, the experimental value of ε'/ε differs from the true one by $+1.7 \times 10^{-4}$.

A systematic error in the determination of ε'/ε can also be due to any possible dependence of the detection efficiency η on the decay paths d_1 and d_2 of the K^0's. The quantity $|[\eta(\Delta d > 0)] - [\eta(\Delta d < 0)]|$ must be known with a precision of $\approx 10^{-4}$. The dependence of η on d_1 and d_2 is expected to be small owing to the large dimensions of the detector and to the broad angular distribution of the gammas with respect to the K^0 direction.

The systematic errors discussed above can be studied experimentally using the events induced by the reactions with four neutral (charged) pions in the final state and replacing two $\pi^0\pi^0$ ($\pi^+\pi^-$) coming from a K^0 by two $\pi^+\pi^-$ ($\pi^0\pi^0$). A control of these systematic errors can also be made by studying the event distribution as a function of Δd (see Fig. 1a).

About 16% of the charged pions decay before reaching the Cherenkov detector. The efficiency of detecting such events can depend on the decay position, and can introduce a systematic error in the determination of ε'/ε. Figure 9, with a binning of 5 mrad, shows the angular distribution of the muons with respect to the direction of the charged pions. Since the θ_μ resolution is 2 mrad, a large fraction of the decay events can be measured and a small systematic error due to the π decay correction is expected.

The different angular resolutions for the pions generated inside and outside the beam pipe would introduce a small systematic error because -- also in the case of the worse resolution -- the efficiency of the signal events with respect to the selection criteria (12) is 100%, and because the decay-point reconstruction is so good that it is possible to know whether the decay took place inside or outside the beam pipe.

The trigger system will depend on the detailed realization of the detector and on the strategy used for collecting the data. If the storage of $\approx 10^{10}$ events -- which corresponds to the statistics necessary to obtain the required precision when determining ε'/ε -- is not a major problem, the trigger would be very inclusive. If event selection is necessary at the trigger level, a faster tracking detector must be used and the events can be identified on the basis of the neutral- and charged-particle multiplicities, the origin of the particles, and the invariant mass of the particle pairs [15].

The regeneration effects are not expected to affect the determination of A, because they are independent of the decay mode of the K^0 and because of the small amount of material in the decay region.

In conclusion, the determination of ε'/ε using K^0's produced in the decay of ϕ's at rest requires high-luminosity e^+e^- rings ($L = 10^{32} - 10^{33}$ cm^{-2} s^{-1}) and a large and sophisticated 4π detector. Assuming that the fiducial volume is 1 m and taking into account the efficiency of the selection criteria, the expected statistical error in one year of running is $\sigma(\varepsilon'/\varepsilon) = 3.3 \times 10^{-4}$ and $\sigma(\varepsilon'/\varepsilon) = 1.6 \times 10^{-4}$ for luminosities $L = 2.5 \times 10^{32}$ and 1.0×10^{33} cm^{-2} s^{-1}, respectively. Using the detector described here, the systematic error due to the background subtraction is expected to be smaller than the statistical one. Other sources of systematic errors have been discussed. Their contribution to the total error is expected to be negligible, but a more detailed simulation of the detector response is necessary for a better understanding of such errors.

REFERENCES

[1] H. Burkhardt et al., Phys. Lett. 199B (1987) 139.

[2] B. Winstein, to appear in Proc. Conf. on CP Violation in Particle Physics and Astrophysics, Blois, 1989.

[3] C. Rubbia, A $\phi \rightarrow K_L K_S$ factory using the Trieste Synchrotron light source, UA1 report, CERN (1988).

[4] U. Amaldi and G. Coignet, Proc. Workshop on Heavy-Quark Factory and Nuclear-Physics Facility with Superconducting Linacs, Courmayeur, 1987, eds E. De Sanctis, M. Greco, M. Piccolo and S. Tazzari (Editrice Compositori, Bologna, 1988), p. 59.

[5] J.I.M. Botman et al., Initial design of a ϕ factory, NIKHEF note, Amsterdam (1988).

[6] W.A. Barletta et al., A linear collider ϕ factory and beam dynamics test machine, Center for Advanced Accelerators, UCLA (1989).

[7] L.M. Barkov et al., ϕ-factory project in Novosibirsk, Novosibirsk note (1989).

[8] H.J. Lipkin, Phys. Rev. 176 (1968) 1715.
I. Dunietz, J. Hauser and J.L. Rosner, Phys. Rev. D35 (1987) 2166.
G. Barbiellini and C. Santoni, same Proceedings as Ref. [4], p. 441.

[9] J. Bernabeu, F.J. Botella and J. Roldan, Phys. Lett. 211B (1988) 226.

[10] See, for example, F. Grancagnolo, same Proceedings as Ref. [4], p. 599.

[11] R. Arnold et al., Nucl. Instrum. and Methods A270 (1988) 255.

[12] A. Brandt et al., Proposal CERN SPSC/88−13, SPSC/P238 (1988).

[13] A. Onuchin, private comunication.

[14] Particle Data Group, Review of Particle Properties, Phys. Lett. 204B (1988) 193.

[15] L. Adiels et al., Proposals CERN PSCC/85−6 P82 (1985); PSCC/85−30 P82 (1985); PSCC/86−34 M234 (1986); PSCC/87−14 M272 (1987).

Table 1

Statistical errors

Luminosity	Signal events	ΔA_{stat}	$\Delta(\varepsilon'/\varepsilon)$
2.5×10^{32}	1.12×10^{6}	9.4×10^{-4}	$3.1 \times 10^{-}4$
1.0×10^{33}	4.48×10^{6}	4.7×10^{-4}	1.5×10^{-4}

Table 2

Background rates and necessary rejections

Background		Rate relative to the signal	Rejection factor r_i
$K^0_L \to \pi^0\pi^0\pi^0$,	$K^0_S \to \pi^+\pi^-$	119	8.4×10^{-6}
$K^0_L \to \pi^+\pi^-\pi^0$,	$K^0_S \to \pi^0\pi^0$	34	2.9×10^{-5}
$K^0_L \to \pi\mu\nu$,	$K^0_S \to \pi^0\pi^0$	70	1.4×10^{-5}
$K^0_L \to \pi e\nu$,	$K^0_S \to \pi^0\pi^0$	100	1.0×10^{-5}

Figure captions

Fig. 1 Distributions, as a function of $\Delta d = d_1 - d_2$, of the events induced (a) by the signal reaction chain (1), and (b) by the background reactions (8) to (10).

Fig. 2 Momentum distribution of the charged pions produced in the signal reaction chain (1).

Fig. 3 Energy distribution of the gammas from the neutral pions produced in the signal reaction chain (1).

Fig. 4 Schematic of the detector used in the simulation.

Fig. 5 Cherenkov angle yield for π, μ, and e, in the momentum range $150-270$ MeV/c.

Fig. 6 Total energy distribution of the four detected gammas in the events induced by the signal reaction chain (1) and the background reactions (7) (see text).

Fig. 7 Distribution of the measured invariant mass of the two charged pions produced in the signal reaction chain (1) and in the background reactions (8).

Fig. 8 Smeared Cherenkov angle yield for pions produced in the signal reaction chain (1) and muons produced in the background reactions (9). The expected experimental resolution is shown.

Fig. 9 Distribution of the angle of the muons produced in the decay of the charged pions with respect to the parent's direction.

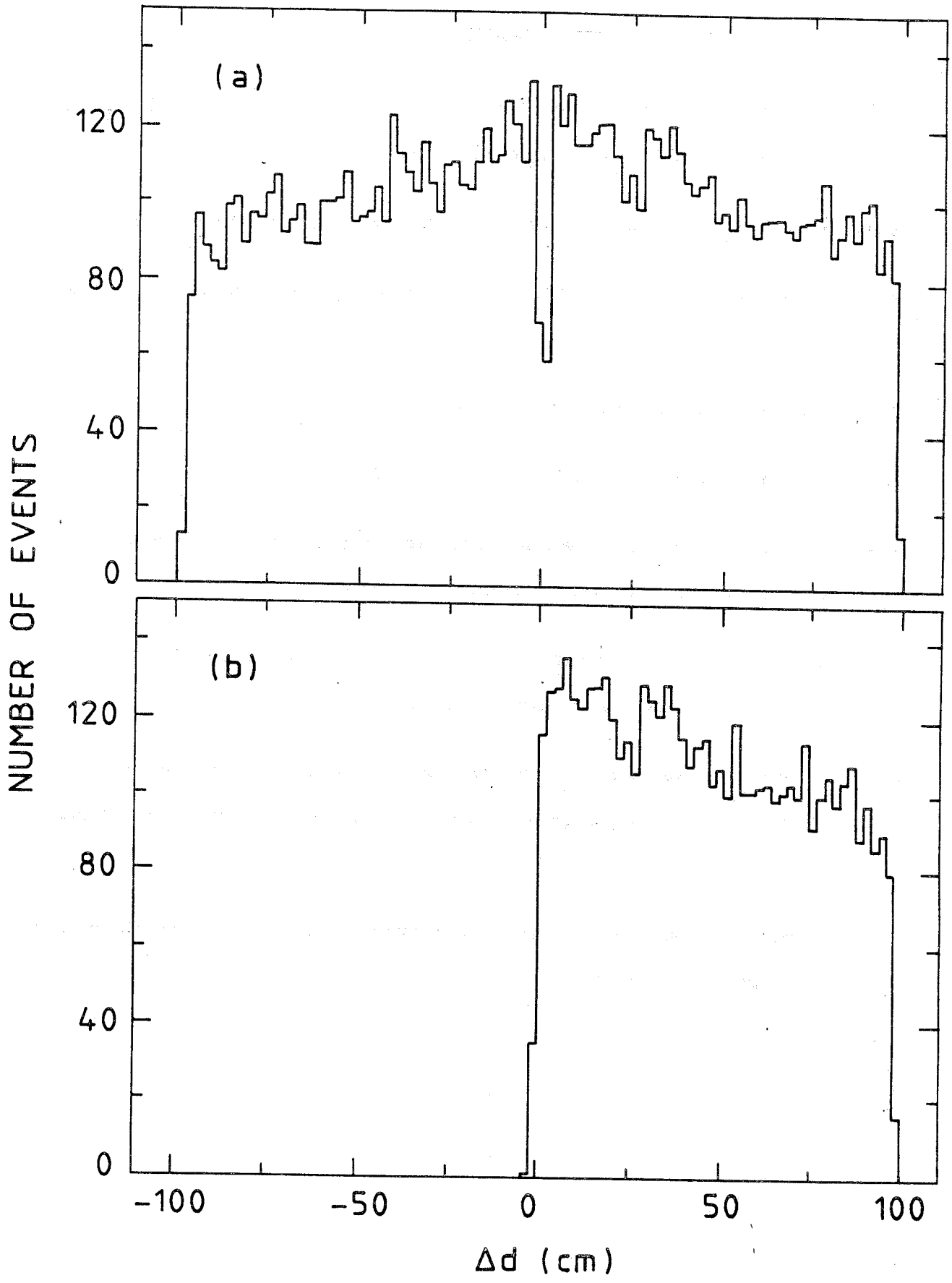

Fig. 1

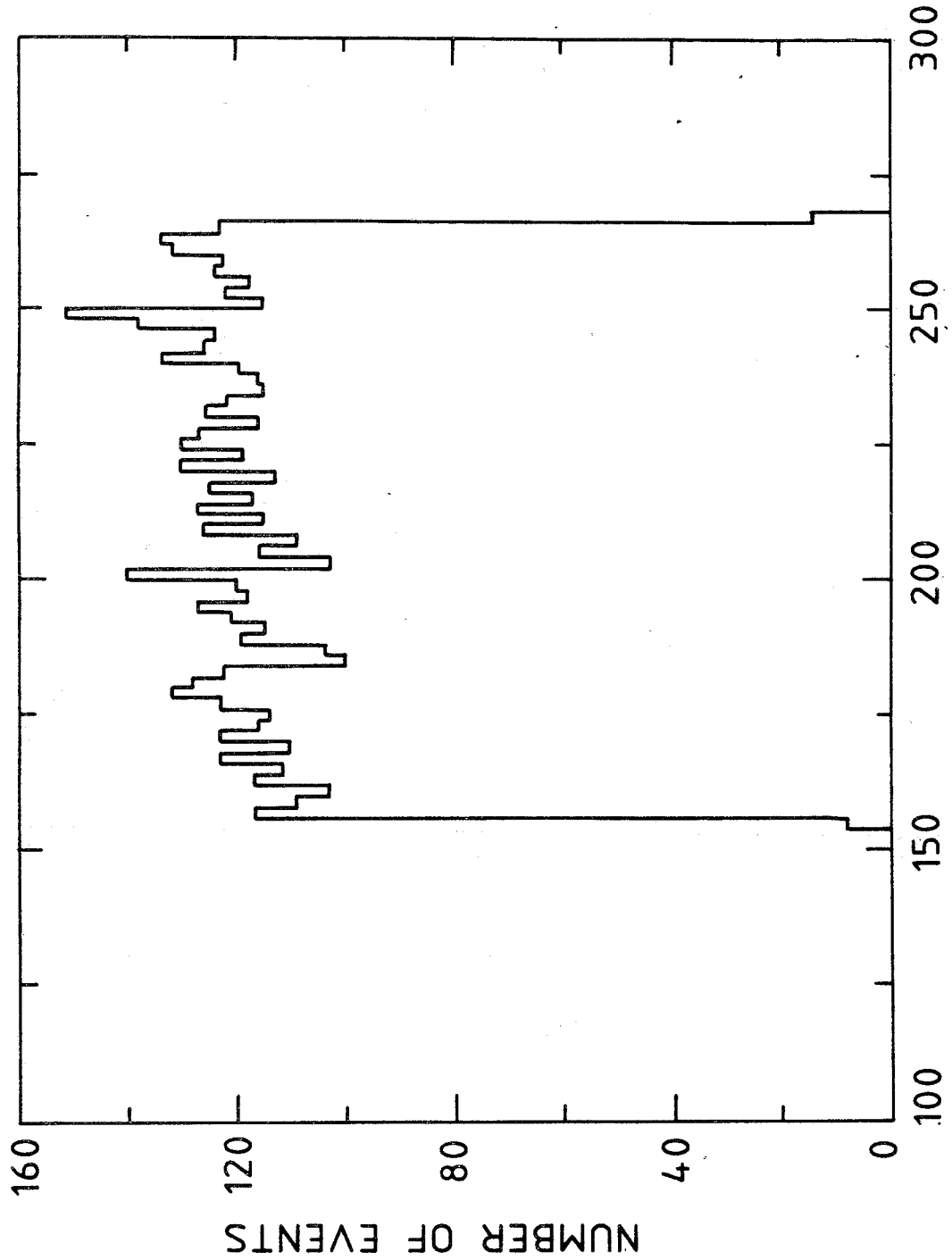

Fig. 2

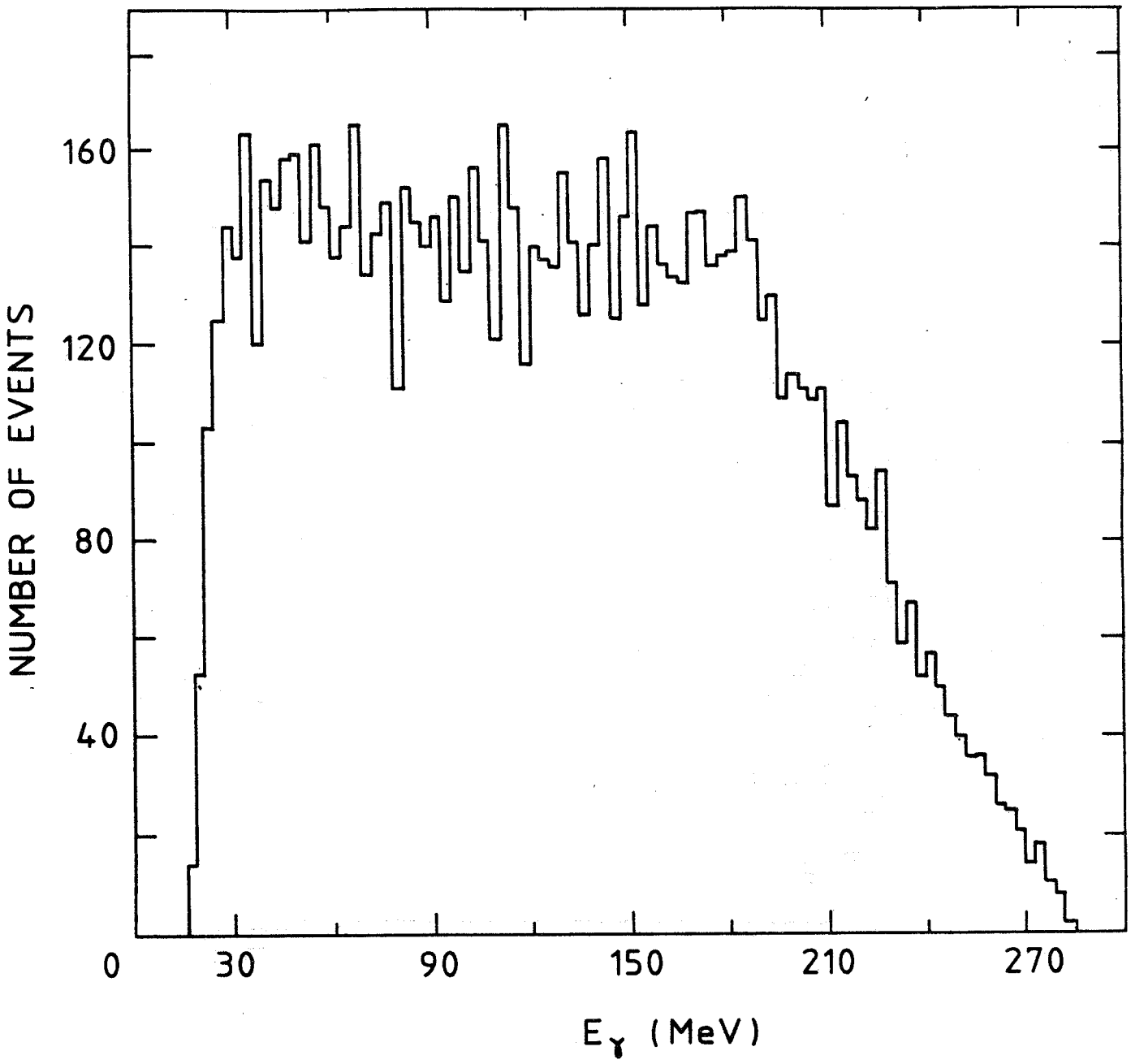

Fig. 3

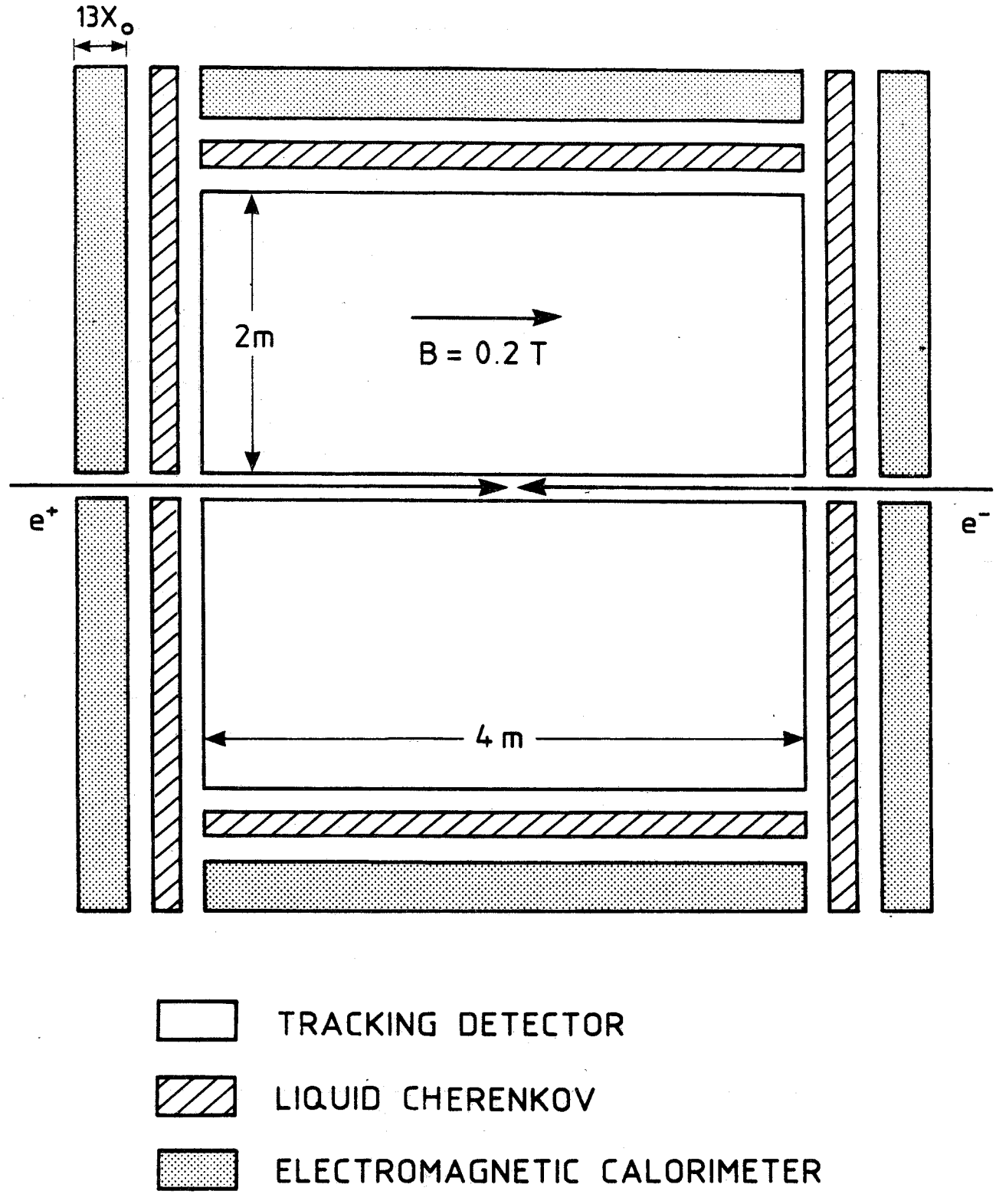
13X$_o$
2m
B = 0.2 T
e$^+$
e$^-$
4 m
TRACKING DETECTOR
LIQUID CHERENKOV
ELECTROMAGNETIC CALORIMETER

Fig. 4

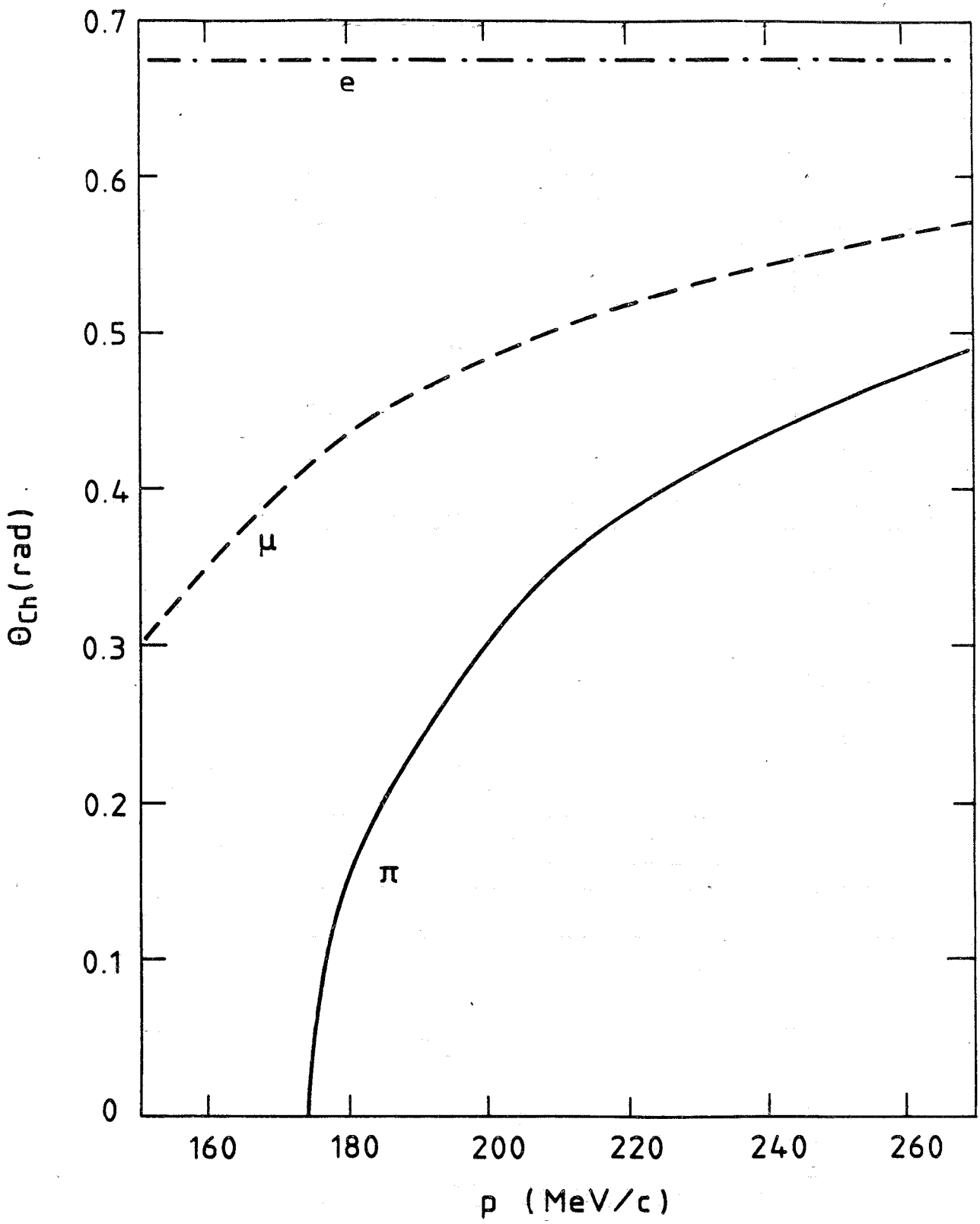

Fig. 5

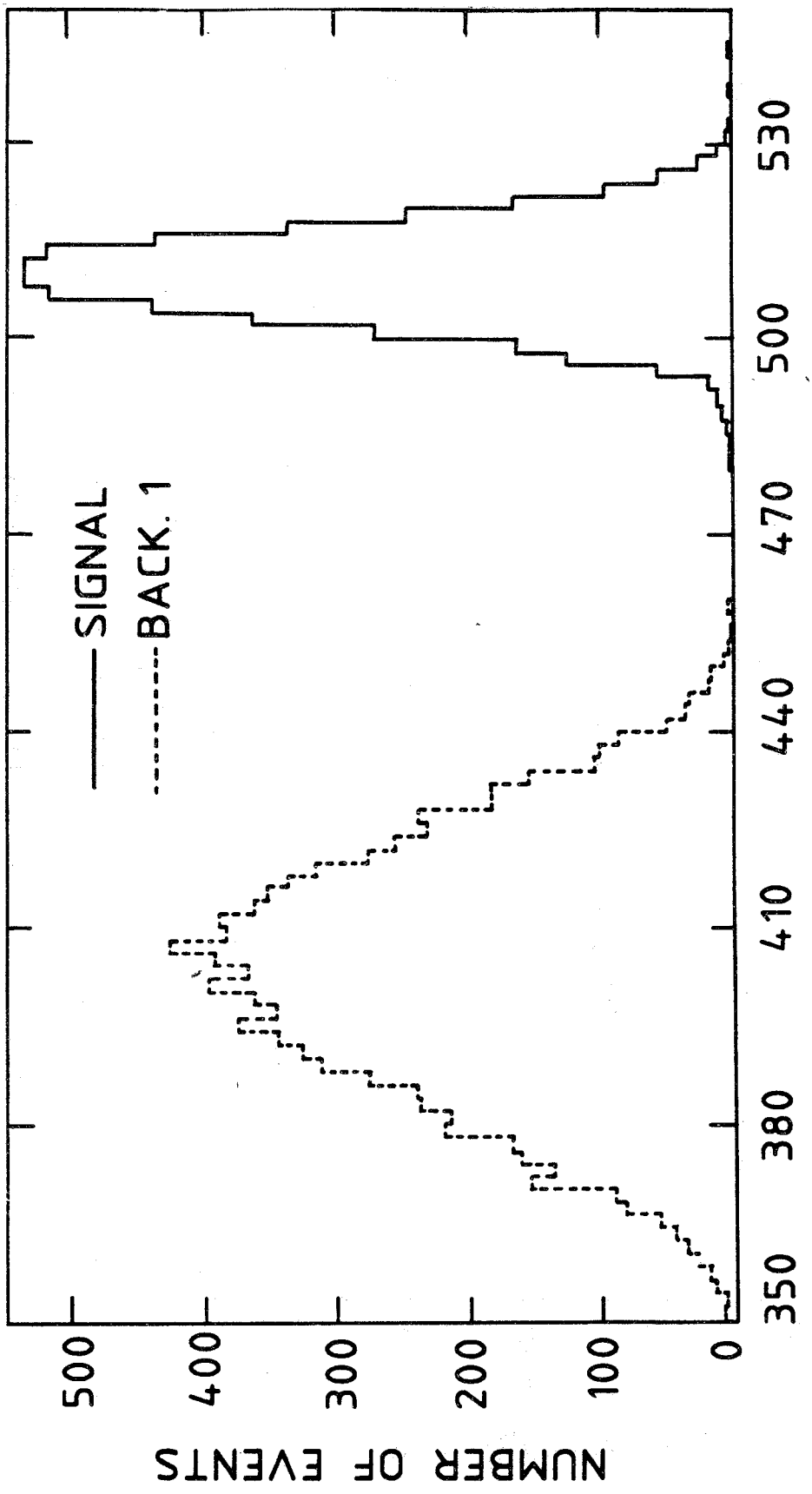
SIGNAL
BACK. 1
NUMBER OF EVENTS
0
100
200
300
400
500
350
380
410
440
470
500
530
Σ Eγ (MeV)

Fig. 6

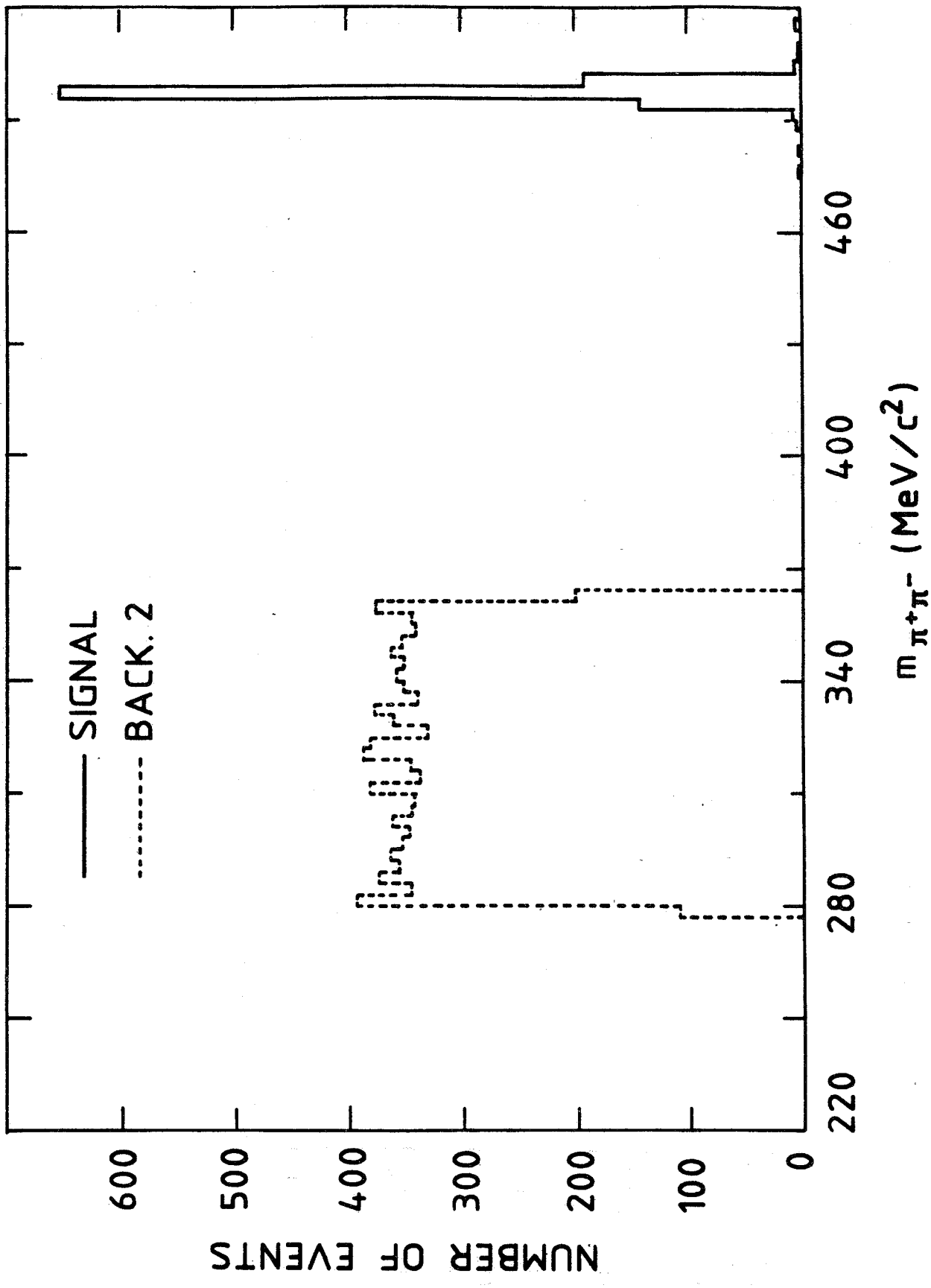
SIGNAL
BACK. 2
NUMBER OF EVENTS
0
100
200
300
400
500
600
220
280
340
400
460
$m_{\pi^+\pi^-}$ (MeV/c^2)

Fig. 7

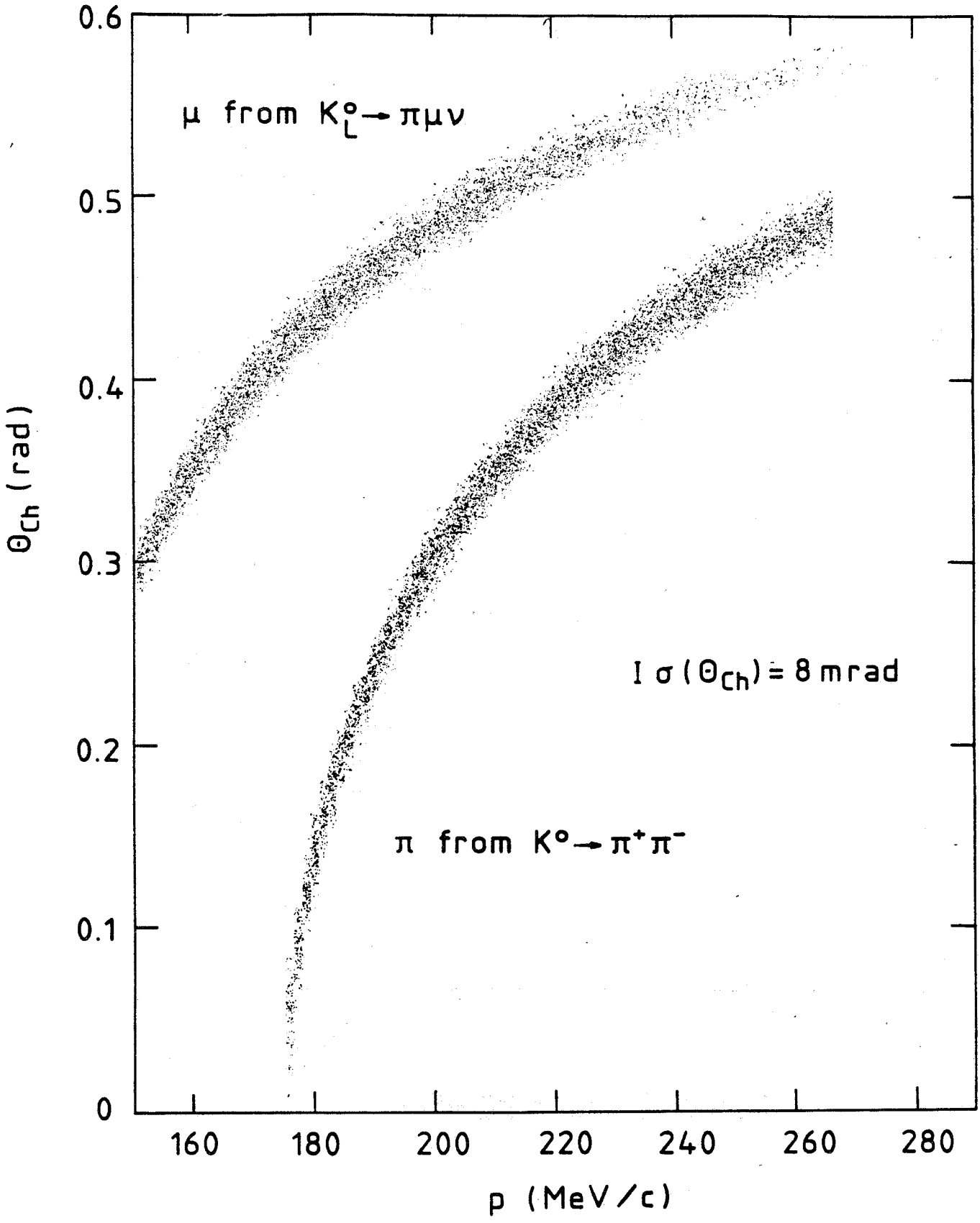
μ from $K^0_L \to \pi\mu\nu$
$1\,\sigma(\theta_{Ch}) = 8$ mrad
π from $K^0 \to \pi^+\pi^-$
θ_{Ch} (rad)
p (MeV/c)
0.6
0.5
0.4
0.3
0.2
0.1
0
160
180
200
220
240
260
280

Fig. 8

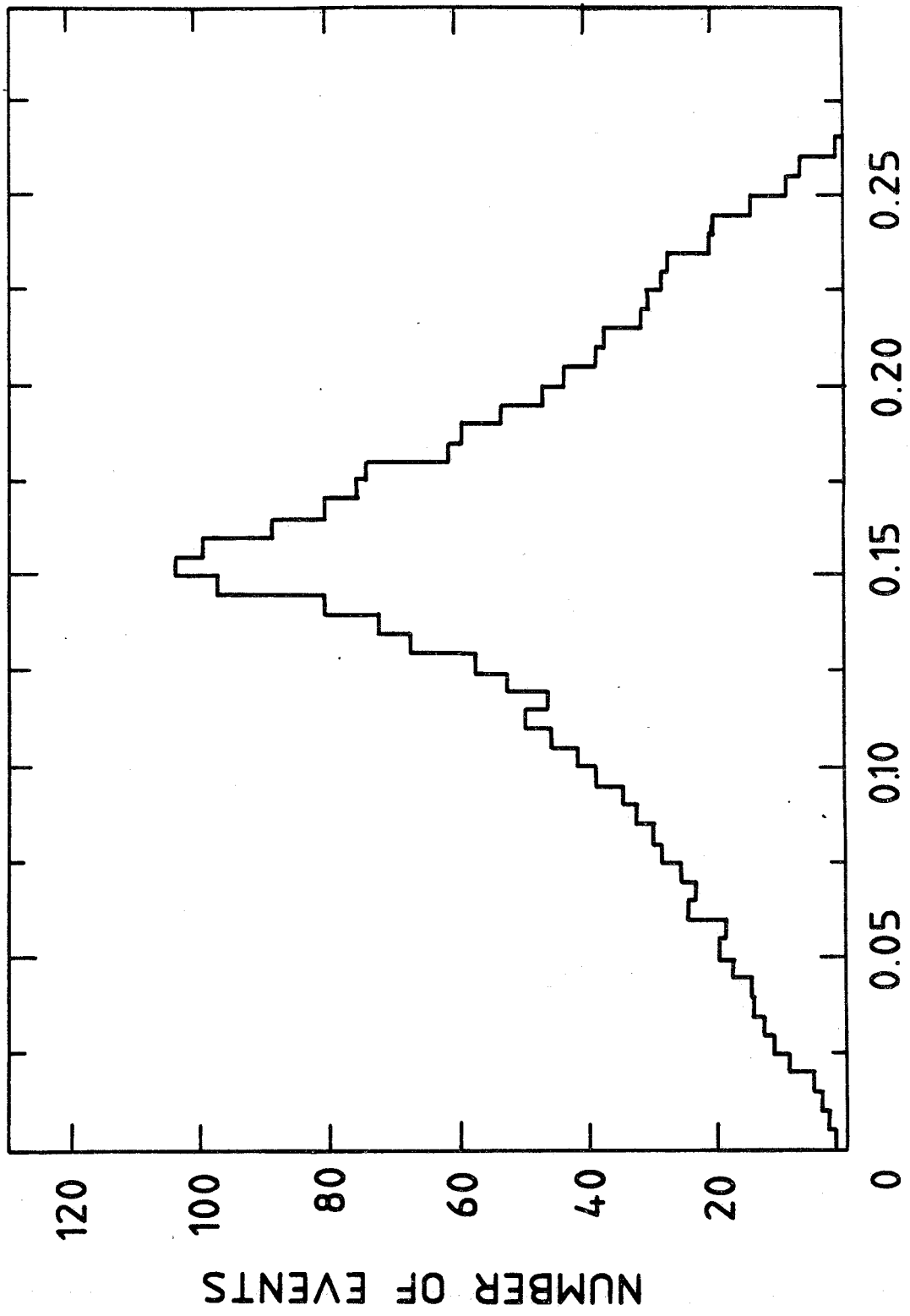

Fig. 9

REFERENCES

[1] H. Burkhardt et al., Phys. Lett. 199B (1987) 139.

[2] B. Winstein, to appear in Proc. Conf. on CP Violation in Particle Physics and Astrophysics, Blois, 1989.

[3] C. Rubbia, A $\phi \rightarrow K_L K_S$ factory using the Trieste Synchrotron light source, UA1 report, CERN (1988).

[4] U. Amaldi and G. Coignet, Proc. Workshop on Heavy-Quark Factory and Nuclear-Physics Facility with Superconducting Linacs, Courmayeur, 1987, eds E. De Sanctis, M. Greco, M. Piccolo and S. Tazzari (Editrice Compositori, Bologna, 1988), p. 59.

[5] J.I.M. Botman et al., Initial design of a ϕ factory, NIKHEF note, Amsterdam (1988).

[6] W.A. Barletta et al., A linear collider ϕ factory and beam dynamics test machine, Center for Advanced Accelerators, UCLA (1989).

[7] L.M. Barkov et al., ϕ-factory project in Novosibirsk, Novosibirsk note (1989).

[8] H.J. Lipkin, Phys. Rev. 176 (1968) 1715.
I. Dunietz, J. Hauser and J.L. Rosner, Phys. Rev. D35 (1987) 2166.
G. Barbiellini and C. Santoni, same Proceedings as Ref. [4], p. 441.

[9] J. Bernabeu, F.J. Botella and J. Roldan, Phys. Lett. 211B (1988) 226.

[10] See, for example, F. Grancagnolo, same Proceedings as Ref. [4], p. 599.

[11] R. Arnold et al., Nucl. Instrum. and Methods A270 (1988) 255.

[12] A. Brandt et al., Proposal CERN SPSC/88−13, SPSC/P238 (1988).

[13] A. Onuchin, private comunication.

[14] Particle Data Group, Review of Particle Properties, Phys. Lett. 204B (1988) 193.

[15] L. Adiels et al., Proposals CERN PSCC/85−6 P82 (1985); PSCC/85−30 P82 (1985); PSCC/86−34 M234 (1986); PSCC/87−14 M272 (1987).

KAON PHYSICS AT A Φ FACTORY

R. Baldini-Celio, M.E. Biagini, S. Bianco, F. Bossi, M. Spinetti, A. Zallo
INFN - Laboratori Nazionali di Frascati, P.O.Box 13, I-00044-Frascati, Italy

S. Dubnička
Joint Institute for Nuclear Research, JINR, Dubna, USSR

ABSTRACT

Various items are reviewed concerning kaon physics at a powerful Φ factory, namely: Quantum Mechanics tests on a large scale, statistical accuracy on the measurement of $(\frac{\epsilon'}{\epsilon})$ *and detection of CP violation in* 3π *decay,* $K\bar{K}$ *molecules production and the kaon form factor.*

Quantum Mechanics tests on a large scale

The Φ decay into a neutral kaon pair is a very suitable process to test Quantum Mechanics (QM) on a large scale. Many authors have emphasized paradoxes related to this process [1], which are a good illustration of the celebrated Einstein, Podolsky, Rosen arguments [2].

In the following two particularly non intuitive QM expectations are pointed out, which may be exploited at a powerful Φ factory.

Actually paradoxes arise because the Φ and the neutral kaons are both superposition of states. Namely the Φ is

$$|\Phi >= \frac{1}{\sqrt{2}}[|K^0(p) > |\bar{K}^0(-p) - |\bar{K}^0(p) > |K^0(-p) >]$$

to achieve a $C = -1$ eigenstate, and the strongly interacting neutral kaons are superposition of the short-living and long-living mass eigenstates

$$|K_S >= a|K^0 > +b|\bar{K}_0 >$$

$$|K_L >= c|K^0 > +d|\bar{K}_0 > .$$

If CPT is conserved: $a = c$, $b = -d$. If CP is also conserved: $a = c = b = -d = \frac{1}{\sqrt{2}}$. Therefore, if neutral kaons decay without interacting, it is also

$$|\Phi >= \frac{1}{\sqrt{2}}[|K_S(p) > |K_L(-p) > -|K_L(p) > |K_S(-p) >]$$

and only events $K_S(p), K_L(-p)$ will be detected.

If a thin regenerator is introduced on one side coherent regeneration takes place and a fraction of the events, decaying downstream the regenerator, will be either $K_S(p)K_S(-p)$ or $K_L(p)K_L(-p)$.

Yet coherent regeneration cannot arise for a spherical regenerator (Fig. 1). Things are as if a neutral kaon, crossing a regenerator, knows what is occurring simultaneously to the other neutral kaon, no matter how far one kaon is from the other. This paradox is predicted by QM because the Φ decomposition is invariant under the simultaneous trasformations

$$|K^0(\pm p) >= |K^0(\pm p) > +\alpha\,|\bar{K}^0(\pm p) >$$

$$|\bar{K}^0(\pm p) >= |\bar{K}^0(\pm p) > +\beta\,|K^0(\pm p) >$$

where α and β are the coherent regeneration amplitudes.

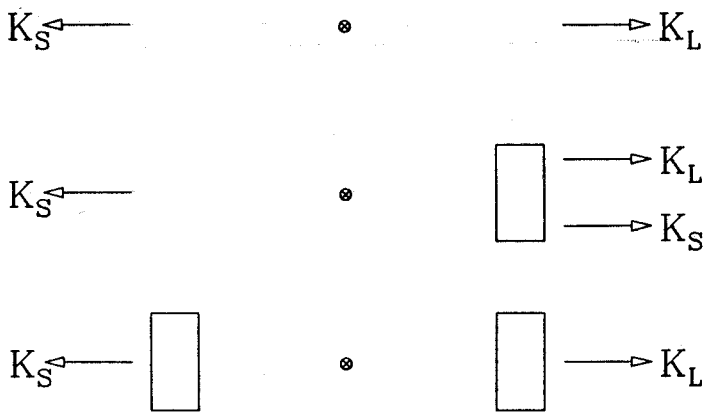

Fig. 1 Illustration of the regenerator Q.M. paradox.

The doughnut of the storage ring is an appropriate regenerator to verify this prediction. By the way this argument supports the suitability of a Φ factory to study CP violation in neutral kaon decay. In fact this effect reduces in practice K_S regeneration in the apparatus, which may simulate a CP violating decay.

Detection of CP violation in neutral kaon decay provides another striking QM paradox. Namely if the two final states are available to both K_S and K_L decays, the time evolution is:

$$< f_1 f_2|\Phi > \propto \eta_2 e^{i(\Gamma_S t_1 + \Gamma_L t_2)} - \eta_1 e^{i(\Gamma_S t_2 + \Gamma_L t_1)}$$

where

$$\eta_i = \frac{< f_i|K_L >}{< f_i|K_S >}, \qquad \Gamma = m + \frac{i}{2\tau}.$$

If CPT holds, it is expected:

$$Rate \propto \eta_2^2 e^{-\frac{t_1}{\tau_S} - \frac{t_2}{\tau_L}} + \eta_1^2 e^{-\frac{t_1}{\tau_L} - \frac{t_2}{\tau_S}} - 2\eta_1\eta_2 cos(\Delta m \Delta t) e^{-(\frac{1}{\tau_S} + \frac{1}{\tau_L})\frac{t_1+t_2}{2}}$$

The interference term introduces a correlation between the two decay times, again no matter how far one kaon is from the other. In particular if the final states are the same

or with the same number of pions the two kaons cannot decay at the same time, as shown by the dip at the origin in Fig. 2. Detection of such a dip is well within the capabilities of the suggested detector and storage ring.

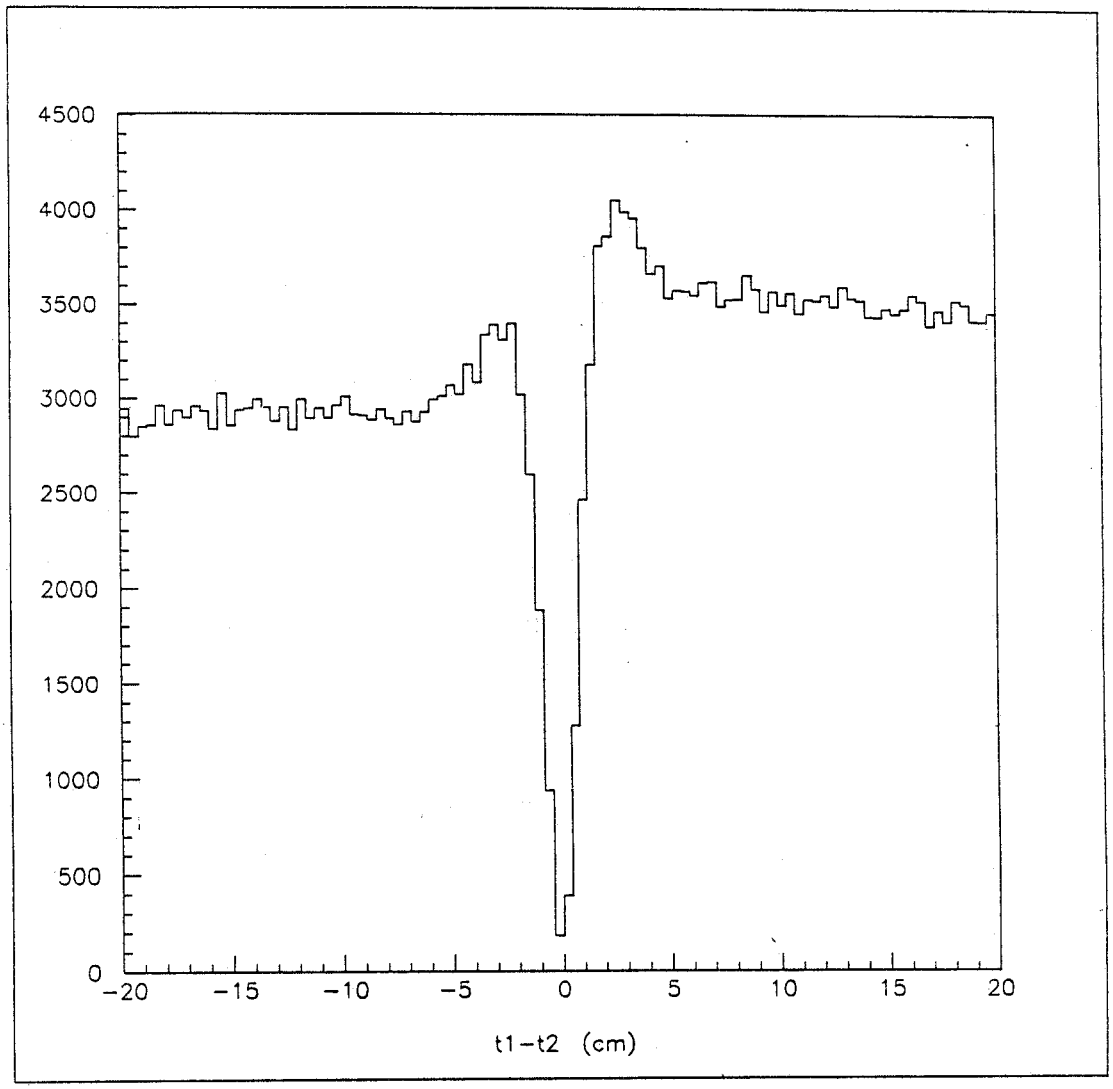

Fig. 2 Correlation between the two decay times t_1, t_2, as caused by the interference term; one kaon decays to $\pi^+\pi^-$ and the other to $\pi^0\pi^0$ $(\frac{\epsilon'}{\epsilon} \sim 3 \cdot 10^{-2})$.

Statistical accuracy in a measurement of $Re(\frac{\epsilon'}{\epsilon})$ and detection of CP violation in 3π decay

A new measurement of $(\frac{\epsilon'}{\epsilon})$ is the most important result to be achieved at a Φ factory. It is relevant to do a correct evaluation of statistical and systematical errors in such a measurement.

Proposals have been done for suitable variables and number of Φ to be produced, to reach a given statistical error [3,4]. In the following different proposals are reviewed emphasizing the possibility, available at a Φ factory, to perform internal checks and to reduce systematical errors.

The exemplifying case of a $(\frac{\epsilon'}{\epsilon})$ vanishing phase is considered, as required if CPT invariance holds. Concerning time integrated rates N_i, the interference term between K_S and K_L amplitudes may be neglected in evaluating $(\frac{\epsilon'}{\epsilon})$, as far as higher order terms in $\frac{\tau_S}{\tau_L} = 1.72 \cdot 10^{-3}$ are negligible. Therefore, in this approximation, the first decaying particle is identified as K_S and the time integrated rates are:

$$\frac{N(K_S \to \pi^+\pi^-)\, N(K_L \to \pi^0\pi^0)}{N(\Phi \to K_S K_L)} \sim \frac{\epsilon^2}{2}(1 - 4\frac{\epsilon'}{\epsilon})$$

$$\frac{N(K_S \to \pi^0\pi^0)\, N(K_L \to \pi^+\pi^-)}{N(\Phi \to K_S K_L)} \sim \frac{\epsilon^2}{2}(1 + 2\frac{\epsilon'}{\epsilon})$$

$$\frac{N(K_S \to \pi^+\pi^-)\, N(K_L \to \pi^+\pi^-)}{N(\Phi \to K_S K_L)} \sim \epsilon^2(1 + 2\frac{\epsilon'}{\epsilon})$$

$$\frac{N(K_S \to \pi^0\pi^0)\, N(K_L \to \pi^0\pi^0)}{N(\Phi \to K_S K_L)} \sim \frac{\epsilon^2}{4}(1 - 4\frac{\epsilon'}{\epsilon})$$

Any of these rates is suitable to evaluate $(\frac{\epsilon'}{\epsilon})$, the latter may be too difficult to handle from an experimental point of view. Contributions proportional to $(\frac{\epsilon'}{\epsilon})$ have different signs in different rates, and overall coherence reduces statistical and systematical errors.

A weighted mean has a statistical error

$$\sigma_N(\frac{\epsilon'}{\epsilon}) = \frac{1}{6\sqrt{N_1}},$$

where $N_1 = N(K_S \to \pi^+\pi^-)N(K_L \to \pi^0\pi^0)$. Therefore to achieve $\sigma(\frac{\epsilon'}{\epsilon}) \sim 2 \cdot 10^{-4}$, with an ideal fully efficient apparatus, in 100 typical running days, a mean luminosity $\bar{L} = 0.8 \cdot 10^{32} cm^{-2} sec^{-1}$ is required.

The asymmetry

$$A = \frac{N_2 - N_1}{N_2 + N_1} \sim 3\frac{\epsilon'}{\epsilon}$$

is a suitable quantity to evaluate $(\frac{\epsilon'}{\epsilon})$; only CP violating events are selected and systematical errors would be reduced.

The corresponding statistical error is

$$\sigma_A(\frac{\epsilon'}{\epsilon}) = \frac{1}{3\sqrt{2}\sqrt{N_1}}.$$

Therefore to achieve $\sigma(\frac{\epsilon'}{\epsilon}) \sim 2 \cdot 10^{-4}$ in 100 days from the asymmetry measurement, a mean luminosity $\bar{L} = 1.5 \cdot 10^{32} cm^{-2} sec^{-1}$ is required.

Of course finite dimensions of the experimental apparatus must also be taken into account. On the other hand non integrated rates carry more informations. Hence a simulation has been done for a spherical fiducial volume with a radius $R = 1.5\,m$, taking into account a finite resolution $\sigma = \pm 3\,mm$ in the vertex reconstruction. No background has been simulated. The t_1, t_2 distribution has been fitted with the expected distribution. To achieve $\sigma(\frac{\epsilon'}{\epsilon}) = 2 \cdot 10^{-4}$ in 100 running days the required mean luminosity is $\bar{L} = 2.5 \cdot 10^{32} cm^{-2} sec^{-1}$.

The observation of the decay $K_S \to 3\pi$ (up to now undetected) is also in the capabilities of an experiment at a powerful Φ factory. In particular $K_S \to 3\pi^0$ and isotropic $K_S \to \pi^+\pi^-\pi^0$ are CP violating decays. The decay $K_S \to \pi^+\pi^-\pi^0$ is allowed, but strongly reduced, if orbital angular momenta are involved. Concerning the CP violating amplitude it is predicted

$$B_{CPviol}(K_S \to 3\pi) \sim B(K_L \to 2\pi) \cdot B(K_L \to 3\pi) \cdot (\frac{\tau_S}{\tau_L})^2 \sim 3 \cdot 10^{-9}$$

if CP violation is mainly due to the mass mixing. The CP allowed decay is predicted [5], yet never detected:

$$B_{CPcons}(K_S \to \pi^+\pi^-\pi^0) \sim (2 \pm 1) \cdot 10^{-7}.$$

In the $\pi^+\pi^-\pi^0$ final state the two amplitudes may interfere, increasing the possibility to detect CP violation in this K_S decay. The $\pi^+\pi^-\pi^0$ Dalitz plot must be uniform for the CP

violating decay. On the contrary the CP allowed decay must have a strong radial dependence: the simplest distribution [6],taking into account the spherical harmonics involved, is like $[(T_1 - T_2)(T_2 - T_3)(T_3 - T_1)]^2$. CP violation manifests itself as an interference with alternate signs in the six sectors of the Dalitz plot. A factor 2 is gained in sensitivity by looking at the interference in the $\pi^+\pi^-\pi^0$ final state, with respect to the $3\pi^0$ final state, taking into account the different branching ratios [7].

CP violation in the decay $K_L \to \pi^+\pi^-\pi^0$, with non zero orbital angular momenta, might be detected as well. The relative width is related to the above mentioned widths, if CP violation is mainly due to the mass mixing. Namely:

$$B_{CPviol}(K_L \to \pi^+\pi^-\pi^0) \sim B_{CPviol}(K_S \to \pi^+\pi^-\pi^0)\,\frac{\tau_L}{\tau_S} \sim 0.6 \cdot 10^{-9}.$$

Yet this amplitude must interfere with the large, CP allowed, K_L decay amplitude. Finally, K_L regeneration could be implemented in principle, to add informations on the phases of these amplitudes.

Other physics in Φ decays into kaon pairs.

There are interesting features also in other Φ decays into kaon pairs, for instance in the radiative Φ decay into kaon and pion pairs. By the way the decay $\Phi \to K^0\bar{K}^0\gamma$ as been considered [8] as a possible source of background in the measurements of $(\frac{\epsilon'}{\epsilon})$. However it has been demonstrated [9] that such a background may be eliminated on the basis of relative decay times distributions. This radiative decay must occur via the production of the rather narrow resonances $S^*(970)$ and $\delta(980)$ [now called $f_0(975)$ and $a_0(980)$], whose widths are 34 and 57 Mev.

Therefore it is very likely that the energy-momentum resolution of the proposed detector will isolate almost all these events (even if the radiative photon is not detected) and a measurement of the radiative Φ decay into neutral and charged kaons and pions is interesting per se. In fact the nature of these resonances is far from being established. There is now a considerable body of evidence that the S^* and δ are not simple $q\bar{q}$ $^3P_0$ mesons and the fascinating hypothesis has been put forward that they are $K\bar{K}$ molecules [10], roughly analogous to the deuteron.

An anomalous feature of these resonances is their width, much narrower than expected. The close values of masses and widths between S^* and δ strongly suggests an ideally mixed pair of mesons, like ρ and ω, hence the 2π decay width should be much larger than observed. On the contrary, in the $K\bar{K}$ molecule interpretation masses, widths and decay modes are naturally explained.

The radiative Φ decay width into these resonances is relevant because of the controlled environment, especially if compared to the $\Phi \to \eta'\gamma$ width. In particular

$$\Gamma(\Phi \to S^*\gamma) \sim 10^{-3} MeV$$

is expected [8] if the S^* is also a $s\bar{s}$ state, yet a very different width is expected if a molecular state must be produced in the radiative decay.

A similar discrepancy has been already observed [11] in another e.m. process, namely the S^* and δ widths into $\gamma\gamma$ much narrower then expected [12] (Tab.I).

meson	$\Gamma_{\gamma\gamma}$ (KeV)	$\Gamma^{q\bar{q}}_{\gamma\gamma}$ (KeV)
S^*	0.27 ± 0.12	4.5
δ	0.23 ± 0.09	1.5

Finally a more accurate determination of the kaon form factor is also an interesting byproduct at a Φ factory. An accurate Φ excitation curve measurement would allow to disentangle the ρ and ω contributions [13], by means of their interference with the Φ.

A measurement at somewhat higher energies than the Φ peak would allow the detection of predicted, yet still undetected, spectacular interference patterns in the neutral kaon form factor (Fig. 3).

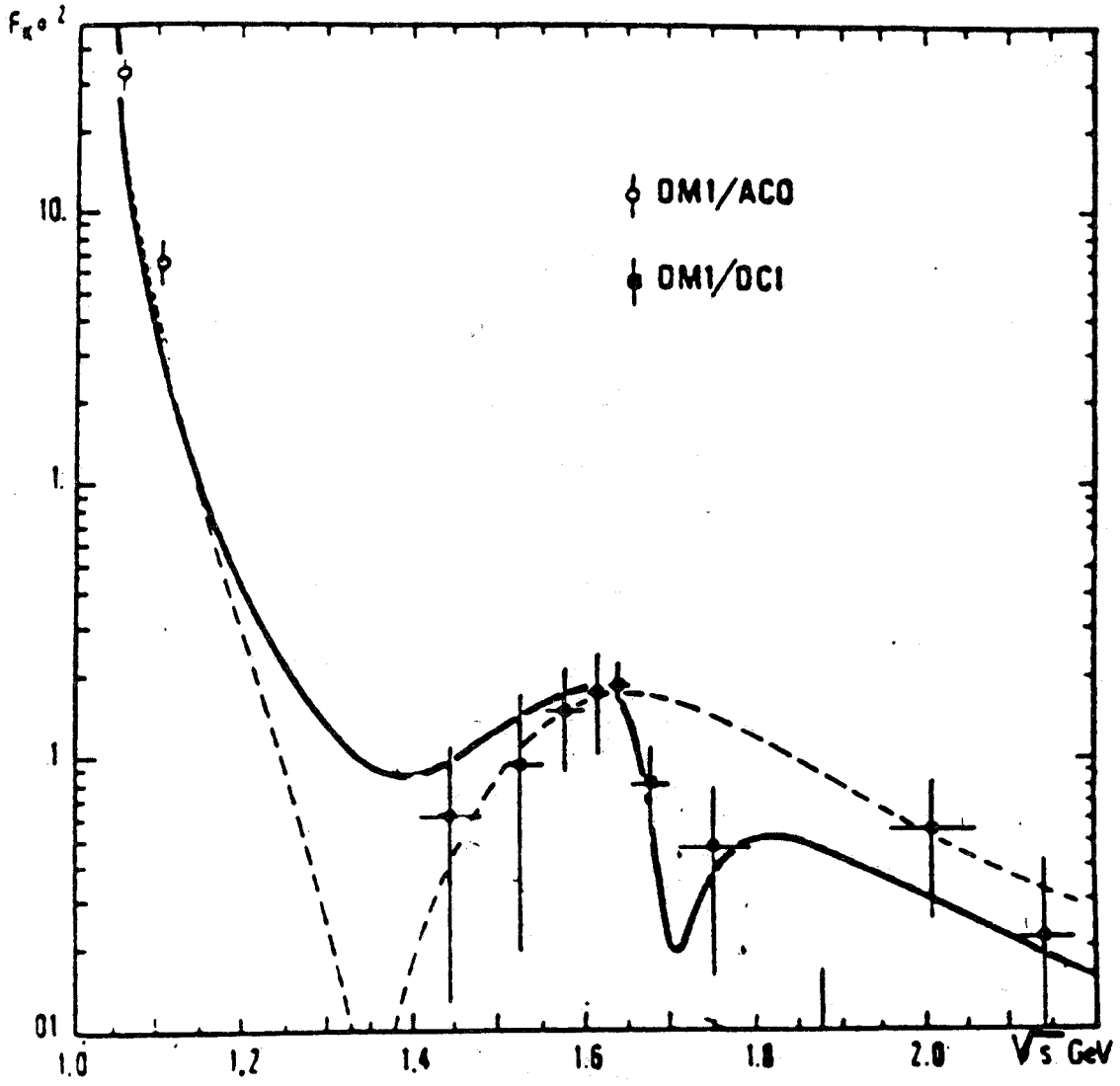

Fig. 3 K^0 squared form factor [dashed curve = $\rho\omega\Phi$ tail + $\rho'(1600)$, solid curve = $\rho\omega\Phi$ tail + many ρ', Φ' states].

REFERENCES

[1] H.J.Lipkin, Phis.Rev. **176**,1715(1968).

C.Bernardini, Fisica e strumenti matematici, Ed. Riuniti (1979).

F.Selleri, Lett.Nuovo Cimento **36**,521(1983).

D.Cocolicchio, Internal Report Universitá Bari TH/88-35.

[2] A.Einstein, B.Podolski, N.Rosen, Phis.Rev. **47**,777(1935).

[3] I.Dunietz, J.Hanser, J.Rosner, Phis.Rev. **D35**,2166(1987).

[4] J.Bernabeu, F.J.Botella, J.Roldan, Phis.Lett. **B211**,226(1988).

[6] C.Bouchiat, P. Meyer, Phis.Lett. **B25**,282(1967).

[6] D.H.Perkins, Introduction to High Energy physics, Add. Wesley (1982).

[7] N.W.Tanner, R. H. Dalitz, Rev.Mod. Phys. **53**,373(1981).

[8] S.Nussinov, T.N.Truong, Rev. Mod. Phys. **63**,1349(1989).

[9] D.Cocolicchio, *et al., These proceedings.*

[10] J.Weinstein, N. Isgur, Phis.Rev. **D27**,588(1983).

[11] A.Nilsson, Proc. XXIV Int. Conf. on High Energy Physics, Munich (1988).

[12] T.Barnes, Phis.Let. **B165**,434(1985).

[13] M.E.Biagini, S.Dubnicka, E.Etim, LNF 90-002.

STATISTICAL ACCURACY ON THE MEASUREMENT OF ϵ'/ϵ AT A Φ -FACTORY

M.P. BUSSA[1] , G. CARBONI[2]

(1) INFN, Sezione di Torino

(2) INFN, Sezione di Pisa

The availability of high-luminosity ϕ - factories will allow a completely new experimental approach to the problem of the study of CP violation on the Kaon system. It would by no means be premature (and perhaps incorrect) to say that systematic errors are less important in the case of a measurement made at a ϕ -factory than for high-energy Kaon beam experiments. However, they will certainly be of a different nature, and this should help in assessing the significance of the results. Also, we would like to mention that present CP violation experiments performed on high-energy Kaon beams are mostly sensitive to the value of the real part of ϵ'/ϵ , their precision on the imaginary part being about one order of magnitude worse than those on the real part. On the other hand, CP violation experiments at high-luminosity ϕ -factories allow to measure both the real and the imaginary parts at the same time, thus offering the possibility of reducing significantly the error on $\mathrm{Im}(\epsilon'/\epsilon)$.

We have used a MC to compute the statistical accuracy on the measurement of $\mathrm{Re}(\epsilon'/\epsilon)$ and $\mathrm{Im}(\epsilon'/\epsilon)$ at a ϕ -factory . In this simulation we considered the decays $\phi \longrightarrow K_l K_s \longrightarrow \pi^+\pi^-\pi^0\pi^0$, the CP violation showing up as an asymmetry of the decay rate between negative and positive time differencies:

$$\tau = t_{+-} - t_{00}$$

(Times are always measured in units of K_s lifetimes). The differential decay probability for the coherent $K^0\overline{K^0}$ $C = -1$ state [1] [2] was integrated first over $t_{+-} + t_{00}$ to get, apart from a multiplicative factor:

$\tau > 0$

$$I(\tau) = |\eta_{+-}|^2\, e^{-\gamma_L|\tau|} + |\eta_{00}|^2\, e^{-\gamma_S|\tau|} - 2Re(\eta_{+-}\eta_{00}^*\, e^{i\Delta m|\tau|}) \cdot e^{-\frac{1}{2}(\gamma_L+\gamma_S)|\tau|} \quad (1a)$$

$\tau < 0$

$$I(\tau) = |\eta_{+-}|^2\, e^{-\gamma_S|\tau|} + |\eta_{00}|^2\, e^{-\gamma_L|\tau|} - 2Re(\eta_{+-}\eta_{00}^*\, e^{-i\Delta m|\tau|}) \cdot e^{-\frac{1}{2}(\gamma_L+\gamma_S)|\tau|} \quad (1b)$$

where $\eta_{+-} = \epsilon + \epsilon'$, $\eta_{00} = \epsilon - 2 \cdot \epsilon'$, $\Delta m = m(K_l) - m(K_s)$, $\gamma_L = 1/\tau(K_l)$, $\gamma_S = 1/\tau(K_s)$.

The asymmetry was defined as

$$A(\tau) = \frac{I(\tau) - I(-\tau)}{I(\tau) + I(-\tau)}$$

For large $|\tau|$, neglecting terms $O(\mathrm{Im}^2)$, the asymmetry approaches:

$$A \longrightarrow \frac{|\eta_{+-}|^2 - |\eta_{00}|^2}{|\eta_{+-}|^2 + |\eta_{00}|^2} = 3Re(\epsilon'/\epsilon)$$

so at large $|\tau|$ the asymmetry is **insensitive to** $\mathrm{Im}(\epsilon'/\epsilon)$.

The asymmetry for small $|\tau|$ is shown in Fig. 1 for the two cases: a) purely real ϵ'/ϵ and b) purely imaginary ϵ'/ϵ . These "near" asymmetries become relatively large for $|\tau| < 5$, however one should keep in mind that in this region the number of useful events drops quickly for a fixed luminosity because

i) the acceptance decreases like $|\tau|$

ii) $I(\tau) \longrightarrow 0$ for $|\tau| \longrightarrow 0$.

Also, from Fig.1 we see that the asymmetry in the purely real case peaks at much smaller $|\tau|$ values than for the purely imaginary case. So the peak would be easily washed out by resolution effects (we point out that $\sigma(\tau) = 1$ corresponds to a vertex separation of 0.6 cm). Our conclusion is that from the standpoint of statistical power the "near" region is not competitive with the "far" one for the measurement of $\mathrm{Re}(\epsilon'/\epsilon)$. Measurements in the "far" region are also relatively insensitive to the resolution since $I(\tau)$ decreases slowly, going like $e^{-\tau/\tau(K_l)}$. In order to get the best accuracy, the τ acceptance should be as large as possible. In that case, the accuracy on $\mathrm{Re}(\epsilon'/\epsilon)$ is simply $1/(3\sqrt{N})$ where N is the number of observed decays.

As far as $\mathrm{Im}(\epsilon'/\epsilon)$ is concerned, it can only be measured in the "near" region, provided of course sufficient vertex resolution is obtained, in order not to wash out the asymmetry. The accuracy achievable will be however less than for the real part for a fixed number of decays.

In the MC we have generated events according to distributions (1a) and (1b). From those events we have constructed an "experimental" asymmetry distribution (Fig. 2). Then we first fitted the asymmetry over the region $0 < |\tau| < 200$, with $\mathrm{Re}(\epsilon'/\epsilon)$ as a free parameter. Next we fitted the asymmetry over the regions $0 < |\tau| < 10$ and $0 < |\tau| < 20$, $\mathrm{Im}(\epsilon'/\epsilon)$ being the free parameter. For $\mathrm{Re}(\epsilon'/\epsilon)$ we used the value from the previous fit. The results of the MC simulation are given in Table I as a function of the number of events and for the two different "near" time intervals.

In the present study we did not include the effects of finite vertex resolution. From inspection of Fig. 1, we can only conclude that results should not be affected dramatically provided the resolution is not worse than 5 τ , corresponding to 3 cm on vertex separation.

TABLE I

N events $0 < \|\tau\| < 200$	Error on $\mathrm{Re}(\epsilon'/\epsilon)$ $0 < \|\tau\| < 200$	Error on $\mathrm{Im}(\epsilon'/\epsilon)$ $0 < \|\tau\| < 10$	Error on $\mathrm{Im}(\epsilon'/\epsilon)$ $0 < \|\tau\| < 20$
500,000	$4.7 \cdot 10^{-4}$	$6.3 \cdot 10^{-3}$	$5.6 \cdot 10^{-3}$
1,000,000	$3.3 \cdot 10^{-4}$	$4.5 \cdot 10^{-3}$	$4.0 \cdot 10^{-3}$

Note: 10^6 events corresponds approximately to $10^{10}\phi$' s assuming a detector fiducial radius of 120 cm (200 $\tau(K_s)$).

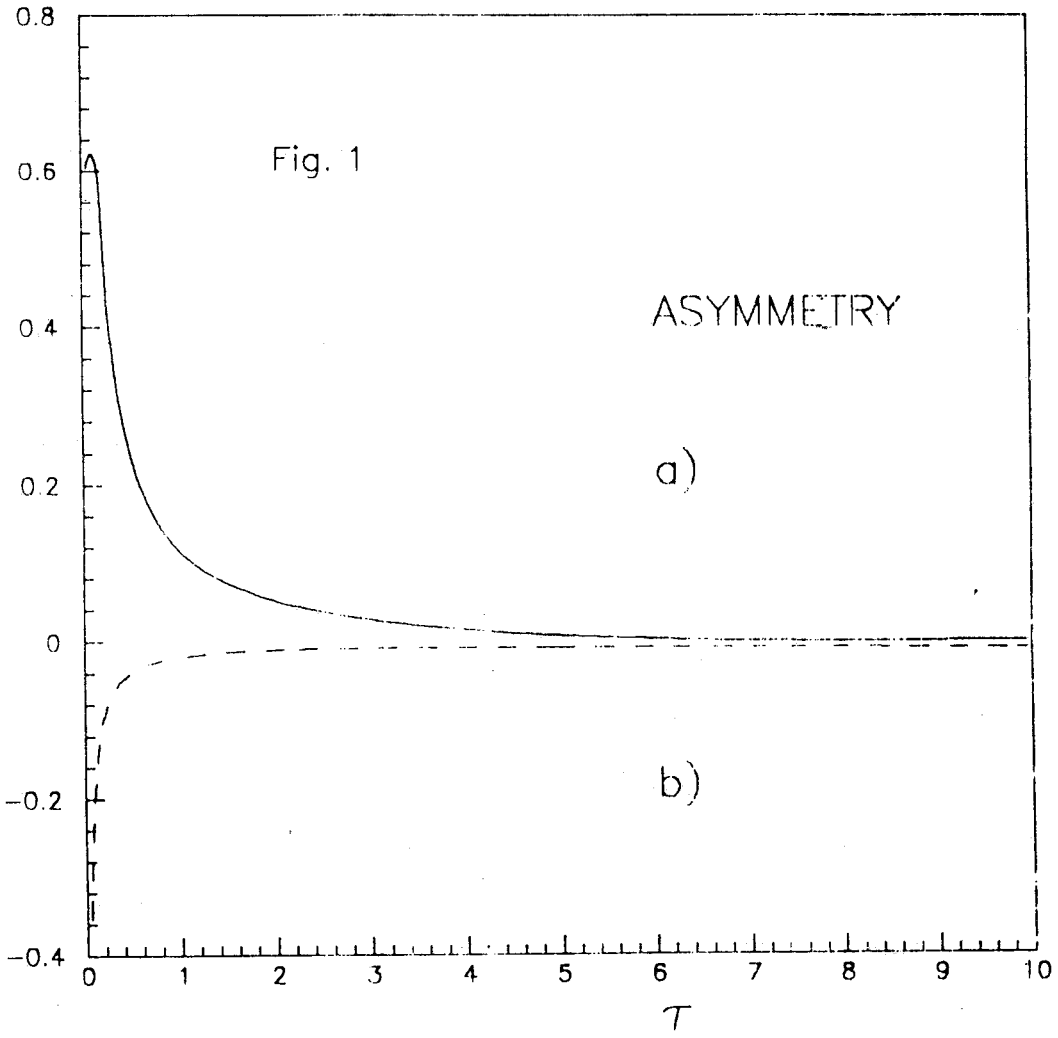

1. Computed asymmetries vs. $|\tau|$ for two choices of ϵ'/ϵ : a) Real part = 0.0, Imaginary part = 0.02; b) Real part = 0.003, Imaginary part = 0.0.

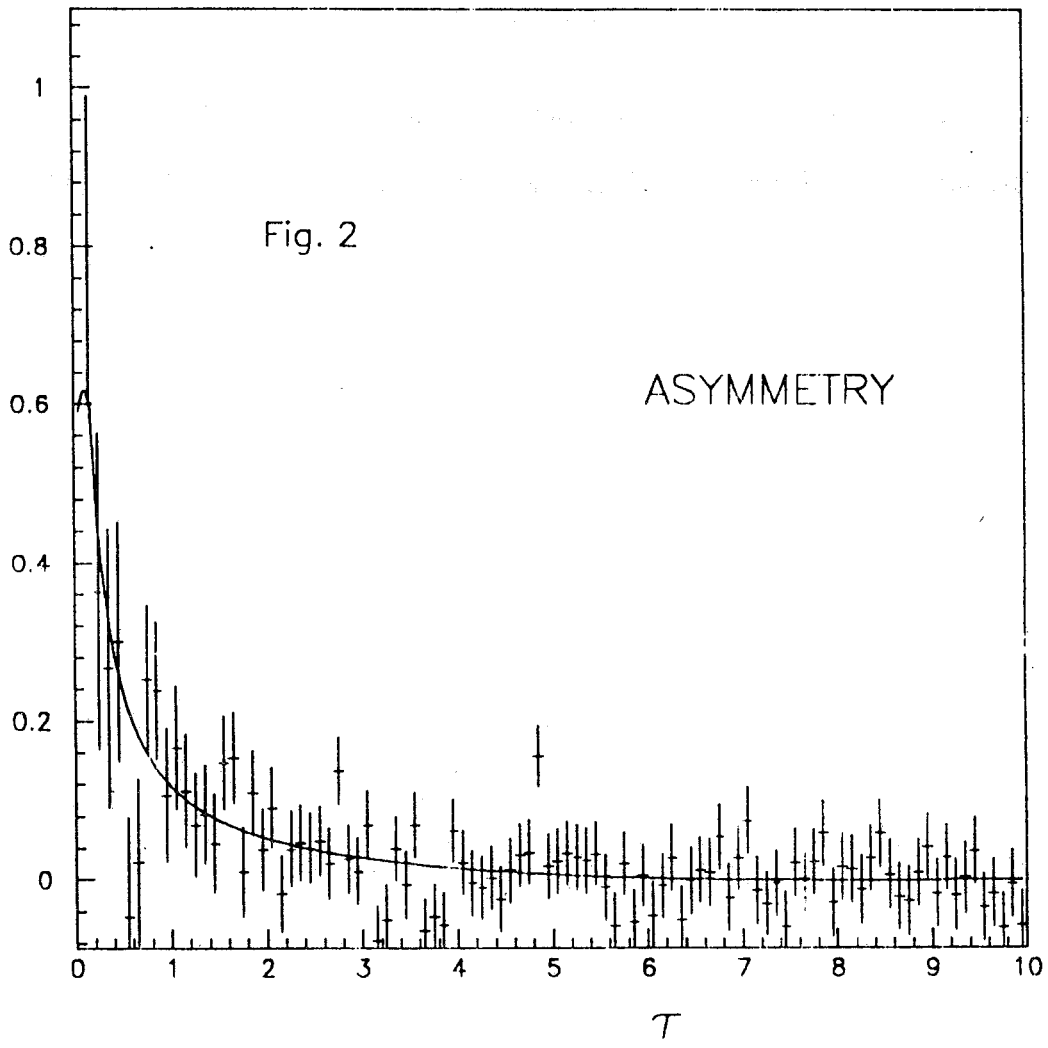

2. Asymmetry vs. $|\tau|$ generated by MC, assuming a purely imaginary ϵ'/ϵ, $\mathrm{Im}(\epsilon'/\epsilon) = 0.02$. The curve represents the result of the fit.

REFERENCES

1. I. Dunietz, J. Hauser and J.L. Rosner, Phys. Rev. D 35, p. 2166 (1987).

2. J. Bernabeu, F.J. Botella and J. Roldan, Phys. Lett. B 211, p. 226 (1988).

Measurement of K_L^o decay point and mass via kinematic fits.

A. CALCATERRA, R. DE SANGRO, P. DE SIMONE

Laboratori Nazionali di Frascati dell' I.N.F.N, Frascati, Italy

Frascati, April 1990

1. Introduction

The purpose of this work is to test the performance of kinematic fit techniques in the analysis of one of the signals of interest at a ϕ–factory, namely the CP–violating decay $K_L^o \rightarrow \pi^o\pi^o$, as a function of the calorimeter's response. The two issues of reconstructing the K_L^o decay point and invariant mass are both addressed.

The first method tested does not make use of energy measurements in the calorimeter, but relies only on its fine grained segmentation, to determine a pair of (ϕ, θ) angles and a conversion point for each photon shower. First, the angle information is used to fit the event geometry (independently of energy distribution between photons) and find the K_L^o vertex. Then the energy–conservation constraints and the π^o masses are imposed, and the K_L^o mass is calculated. It is found that the method is viable, and its performance is well understood; the K_L^o mass resolution is good, but the vertex determination is rather poor, due to the intrinsic difficulty of measuring the direction of low energy photon showers.

The second method is based on measuring energies and conversion points of the photons, and forcing all constraints in a single–pass fit. The K_L^o mass and vertex are both good, and the final vertex resolution seems to be limited (for a realistic detector) more by the errors on the apices than by the energy resolution or absolute scale. The fit presents the remarkable feature that the vertex resolution does not depend on the K_L^o flight distance (or, equivalently, on the distance between the decay point and the conversion apices), an explaination of which will be given below.

Both methods require the K_L^o line of flight to be reconstructed, using the K_S^o decay, in order to eliminate two of the three degrees of freedom in the definition of the K_L^o vertex.

2. Event simulation and parameter smearing

The simulation starts by creating the main event vertex ($e^+e^- \rightarrow K^o_S\ K^o_L$) and giving to the kaons the $sin^2(\theta)$ distribution expected for a pair of scalar mesons. The total energy equals exactly the ϕ mass: radiative and finite width effects have not been considered. The vertex position is the geometric center of the detector: the effect of non–negligible beam spots is unimportant at this level of precision.

The K^o_L is allowed to decay into either $\pi^o\pi^o$ or $\pi^o\pi^o\pi^o$, or a mixture of these two modes with a ratio of 1:240 (ratio of the B.R.s of the two channels). The angular distribution of the π^o in the K^o_L center of mass is isotropic, as also is the γ direction in the π^o c.m.s. The photon spectra for the two decay modes are shown in fig. 1 .

The events analyzed are those for which the K^o_L decay length is smaller than 150 cm, to insure that the 4 needed photons do not hit at grazing incidence the calorimeter, which is very schematically reduced to its inner detection layer: a cylinder with a radius of 200 cm and a halflength of 500 cm, closed by two discs of outer radius 200 cm and inner radius 30 cm.

A photon is considered inside detector acceptance if its trajectory intersects the first detection layer. In other words, all photons which cross the first layer are assumed *a*) to leave a detectable energy deposition in it, and *b*) to develop a shower whose axis will be reconstructed (this information will not be used in the second fit). Only events with exactly 4 detected photons are kept. A very mild lower cut on photon energy (20 MeV) is used, to avoid occasional fit misbehaving.

To postulate γ interaction in the first layer is of course not justifiable, even though the cryostat should increase the probability of early photon conversion; the effect is to underestimate photon flight paths, leading to a slight deterioration of vertex resolution for the first fit only.

The requirement that the K_L^o decay inside the said fiducial volume implies an acceptance factor of $\sim 35\%$ (at this energy the decay length of the K_L^o is 348 cm). The additional request of exactly 4 detected photons does not change much the efficiency for the $\pi^o\pi^o$ channel, but yields a drastic rejection factor of $5 \cdot 10^{-5}$ for the $\pi^o\pi^o\pi^o$ mode.

The four impact points are then calculated and gauss–smeared in three dimensions, with a typical σ of 1 cm. The geometric response of the calorimeter is simulated by gaussian smearing of the (ϕ, θ) angles of each photon, with

$$\sigma_\phi = \sigma_\theta = 26.5mr/[E(GeV)]^{\,0.7}$$

for both angles, based on a detailed *GEANT* computation, and giving a standard deviation of 100 mr at 150 MeV . The difference between the original angles and the smeared ones can be seen in fig. 2 : the convolution of the σ given above with the photon spectrum gives for both angles a broad distribution, with a standard deviation of ~ 140 mr.

Energies are smeared according to a general type of resolution like:

$$\sigma_E = K \cdot \sqrt{E(GeV)}$$

where the typical value used for K is 5%.

3. Fitting with photon axes.

The resolution simulated above comes from *independent* shower reconstruction, via "local" fit of charge centroids in successive detector layers. The shower axes should be much better defined by the lines joining the photon conversion points to a common point somewhere inside the detector volume, chosen in such a way as to minimize the angular difference between the said lines and the "measured" (*i.e.* smeared) shower angles.

The χ^2 to be minimized is given by:

$$\chi^2 = \sum_n \sum_{i,j} [Q_n^{exp} - Q_n^{th}(\vec{v})]_i \; (W_n^{-1})_{ij} \; [Q_n^{exp} - Q_n^{th}(\vec{v})]_j$$

in which Q^{exp} are the measured quantities, Q^{th} their expected values for a given choice of the vertex $\vec{v}$, W_n^{-1} is the inverse covariance matrix and the first sum runs over the four detected photons. More precisely:

- Q^{exp} are $tan(\phi)$ when $|tan(\phi)| < 1.$ and $1./tan(\phi)$ when $|tan(\phi)| > 1.$, and similarly for θ.
- $\vec{v}$ is actually function of only one parameter: the (positive definite) distance from the event vertex to the K_L^o decay point along the K_L^o direction
- the covariance matrix is diagonal (no correlation imposed between the ϕ and θ measurements) and the errors are propagated to $tan(\phi)$, $tan(\theta)$ from $\Delta\phi, \Delta\theta$ errors of 140 mr, independently of photon energy.

The fit is initialized with a decay path of 75 cm, corresponding to the middle of the defined fiducial volume, and the minimization procedure is iterated until the path difference between iterations becomes negligible.

The effect of this fit on the photon directions can be seen from the comparison of fig. 3 with fig. 2: the distributions are somewhat non–gaussian (due to the

superposition of different gaussians: see below) but the raw standard deviations have gone down by more than a factor 2 in ϕ and a factor 4 in θ.

The difference between the generated K_L^o path length and the fitted one is shown in fig. 4 , which actually is the superposition of normal curves with σ depending on the path length: according to fig. 5 the resolution is better for long K_L^o decay lengths, corresponding to smaller distances between photon conversion points and fitted vertex. Fitting to a single gaussian the central part of fig. 4 one obtains $\sigma = (11.4 \pm 0.2)$ cm.

With the simultaneous measure of a pair of (ϕ, θ) angles for each photon, the following system:

$$\begin{cases} E_1 + E_2 + E_3 + E_4 = E_0 \\ E_1\vec{n}_1 + E_2\vec{n}_2 + E_3\vec{n}_3 + E_4\vec{n}_4 = P_0\vec{n}_0 \\ 2E_1E_2(1 - \vec{n}_1 \cdot \vec{n}_2) = M_{\pi^o}^2 \\ 2E_3E_4(1 - \vec{n}_3 \cdot \vec{n}_4) = M_{\pi^o}^2 \end{cases}$$

of 6 equations in the 6 unknowns E_i, E_0, P_0 is exactly solvable, up to one ambiguity. If only the solution which gives the best K_L^o mass is kept, one obtains the plot of fig. 6 . The comparable plot for the $K_L^o \rightarrow \pi^o\pi^o\pi^o$ case would contain a completely negligible background of 2–3 events in the K_L^o mass window. The product of the bigger B.R. times the solid angle suppression factor is indeed additionally lowered by the fact that many solutions correspond to unphysical cases of negative E_0, P_0 or square K_L^o mass.

These results relate to the case in which only $K_L^o \rightarrow \pi^o\pi^o$ events are generated. For $\pi^o\pi^o\pi^o$ events all resolutions are slightly worse, because of the softer photon spectrum, but the same phenomenology applies.

4. Fitting with photon energies.

The fitting procedure for this case is different from before: the χ^2 is computed using energies and photon apices, and the 6 equations of the above system are imposed as constraints during the minimization procedure. Moreover, the K^o_L mass is forced as a seventh costraint between E_0 and P_0. The vertex coordinate is initialized as before with a length of 75 cm. The procedure changes, according to their relative weights, photon energies and impact points, satisfying at each step the 6 constraints, and gives, after a number of iterations, the correct value for the decay length.

As shown in fig. 7 , the resolution obtained in his case is better than the previous one by an order of magnitude: the fit shown yields a σ of (1.02 ± 0.02) cm. Moreover, it does not depend on the K^o_L flight length, as can be seen in fig. 8 .

This feature can be understood as follows: since the smearing of the apices is constant, as one gets nearer to the calorimeter, the "extrapolation distance" becomes smaller, but the angle resolution of the line vertex–apex, *being determined by only one "real" measured point,* becomes worse, and the two effects cancel each other when calculating the vertex position. This effect is masked in the previous fit procedure by the fact that shower axes are so poorly measured that a resolution of 1 cm on photon apices yields in that case essentially the same result as perfect resolution.

Also, using realistic assumptions on resolutions ($\sigma_E = 5\% \cdot \sqrt{E(GeV)}$ and $\sigma_{xyz} = 1$ cm for apices) variation around the "right" energy perturbs the constraint equations much more than a corresponding variation of the apices around their "true" position. As a result, the fit reconstructs the correct energies much

better than the photon apices, giving the energy resolution of fig. 9 , with an overall standard deviation of less than 2 MeV, and the ultimate vertex resolution appears to depend more on the detector's spatial accuracy than on its energy resolution.

5. Conclusions

It has been shown that reasonable calorimeter parameters, and a combination of kinematic fit techniques, allow complete reconstruction, with good accuracy, of the decay $K_L^o \rightarrow \pi^o \pi^o$.

But, as is generally the case in constrained fits, the price to pay consists in the (implicit!) loss of degrees of freedom: having imposed an exact K_L^o mass, for example, no cut can be used on this quantity. To suppress background via a χ^2 cut, one has to rely on an exact and thoroughly understood simulation of the detector.

FIGURE CAPTIONS

1. Photon spectra in the Laboratory; *a*) photons from $K_L^o \rightarrow \pi^o\pi^o$; *b*) photons from $K_L^o \rightarrow \pi^o\pi^o\pi^o$
2. Smearing of photon angles; *a*) ϕ angle; *b*) θ angle.
3. Resolution on photon angles after type-I fit.
4. Error on K_L^o path length (type–I fit).
5. Error on path length vs. path length (type–I fit).
6. Reconstructed K_L^o mass for $\pi^o\pi^o$ events (type–I fit).
7. Error on K_L^o path length (type–II fit).
8. Error on path length vs. path length (type–II fit).
9. Energy resolution of type–II fit.

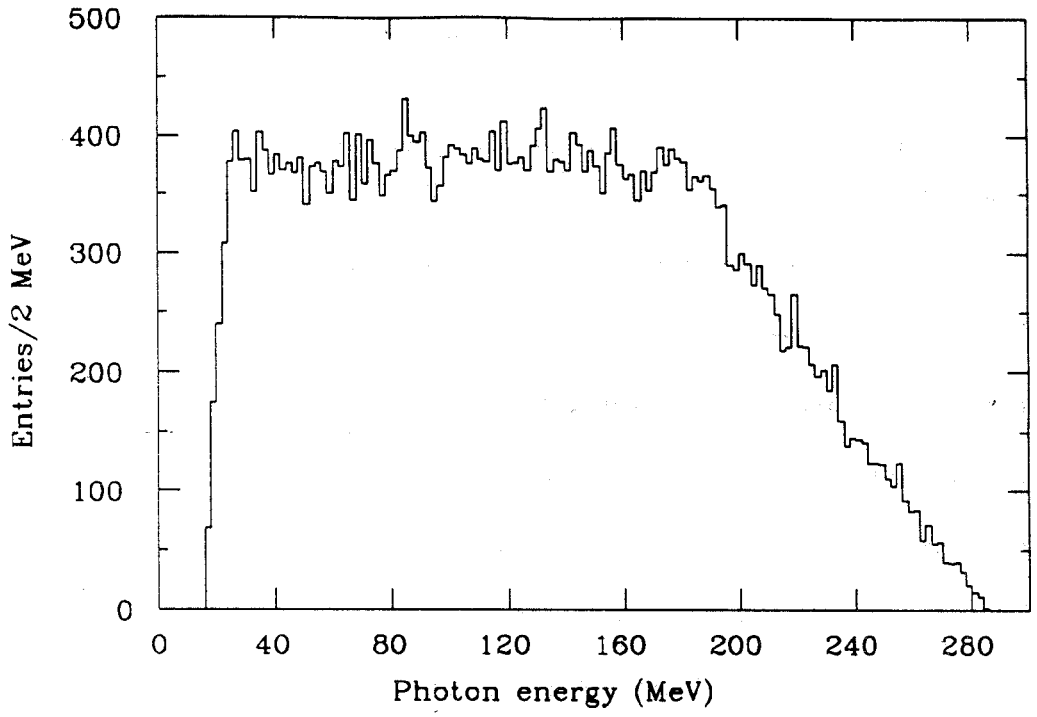
500
400
300
200
100
0
Entries/2 MeV
0
40
80
120
160
200
240
280
Photon energy (MeV)

FIG. 1a

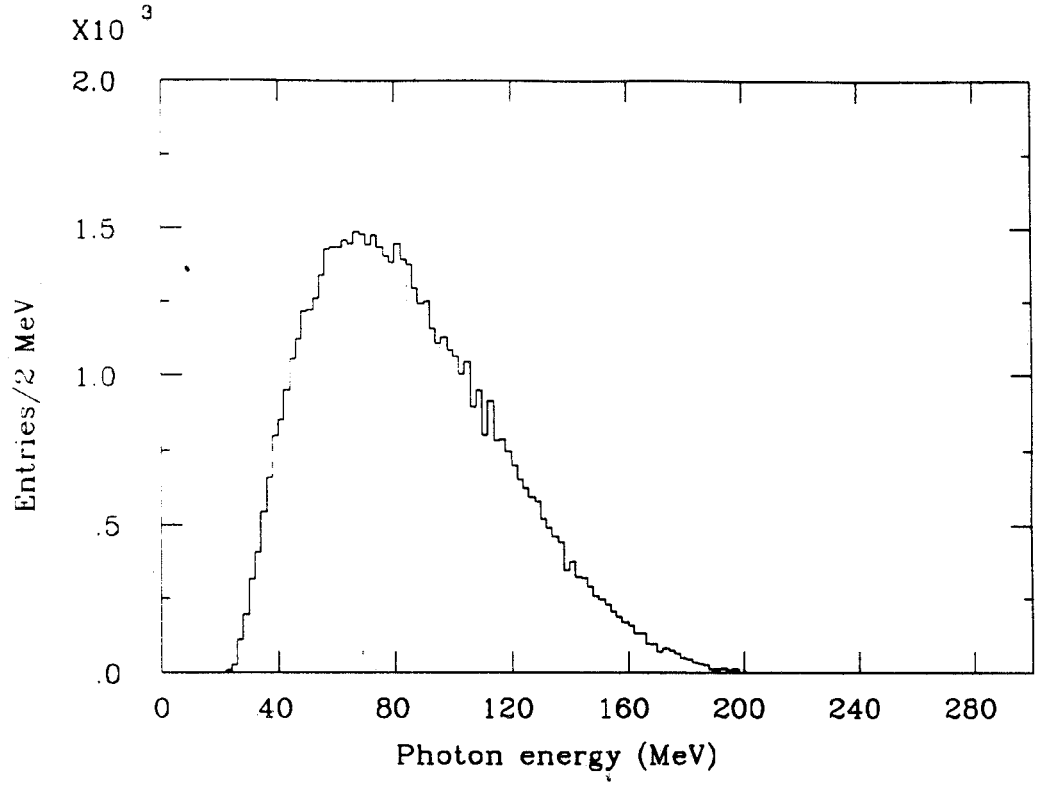
X10 3
2.0
1.5
1.0
.5
.0
Entries/2 MeV
0
40
80
120
160
200
240
280
Photon energy (MeV)

FIG. 1b

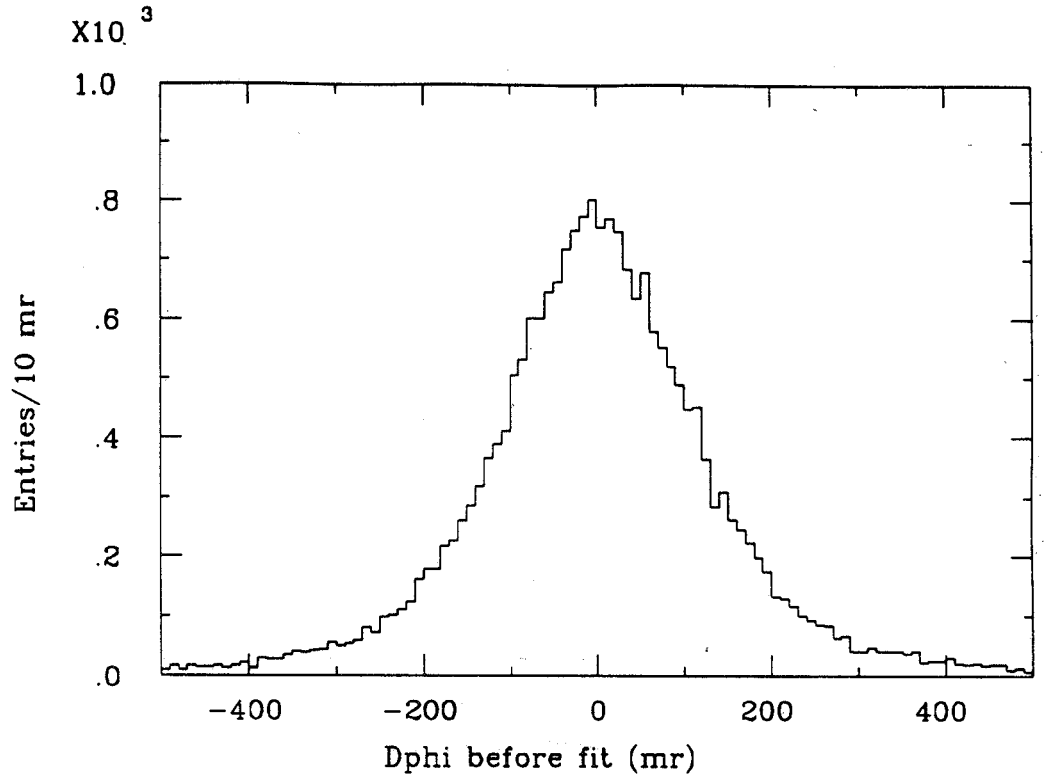
X10 3
1.0
.8
.6
.4
.2
.0
Entries/10 mr
-400
-200
0
200
400
Dphi before fit (mr)

FIG. 2a

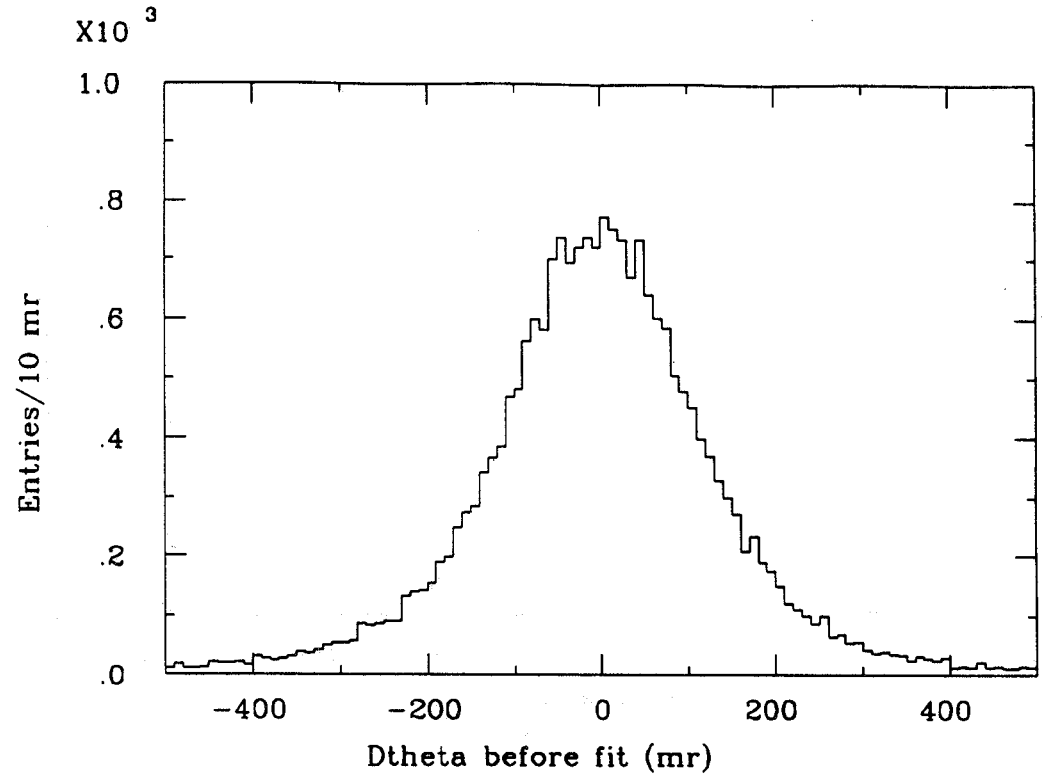
X10 3
1.0
.8
.6
.4
.2
.0
Entries/10 mr
-400
-200
0
200
400
Dtheta before fit (mr)

FIG. 2b

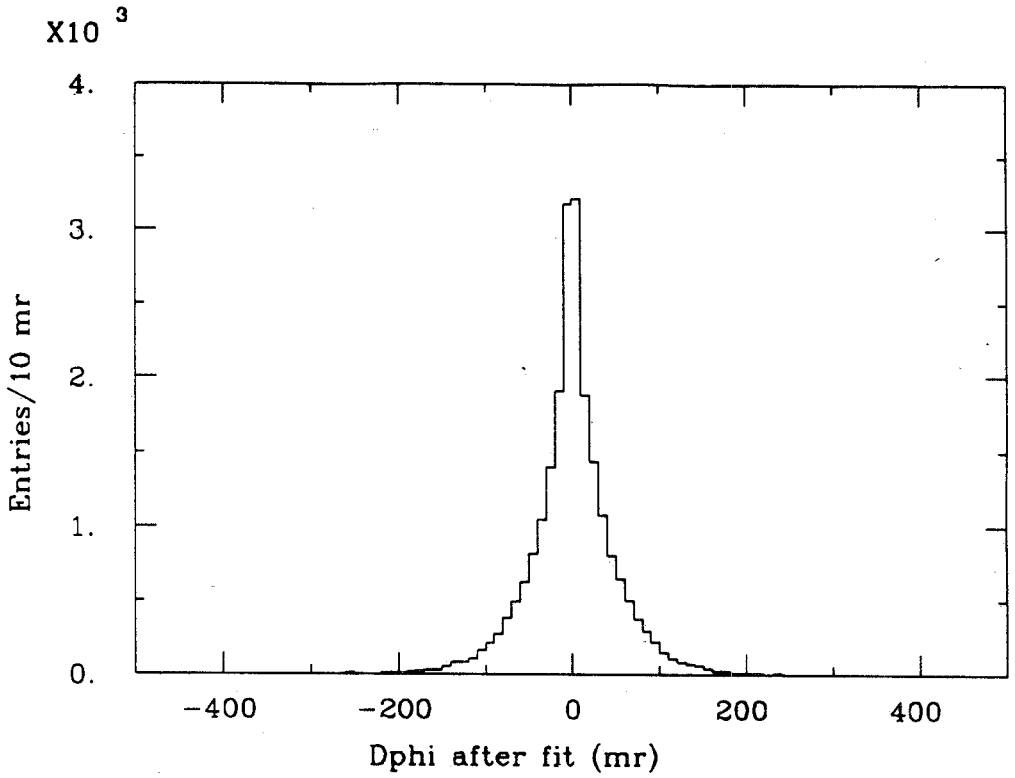
X10 3
4.
3.
2.
1.
0.
Entries/10 mr
-400
-200
0
200
400
Dphi after fit (mr)

FIG.3a

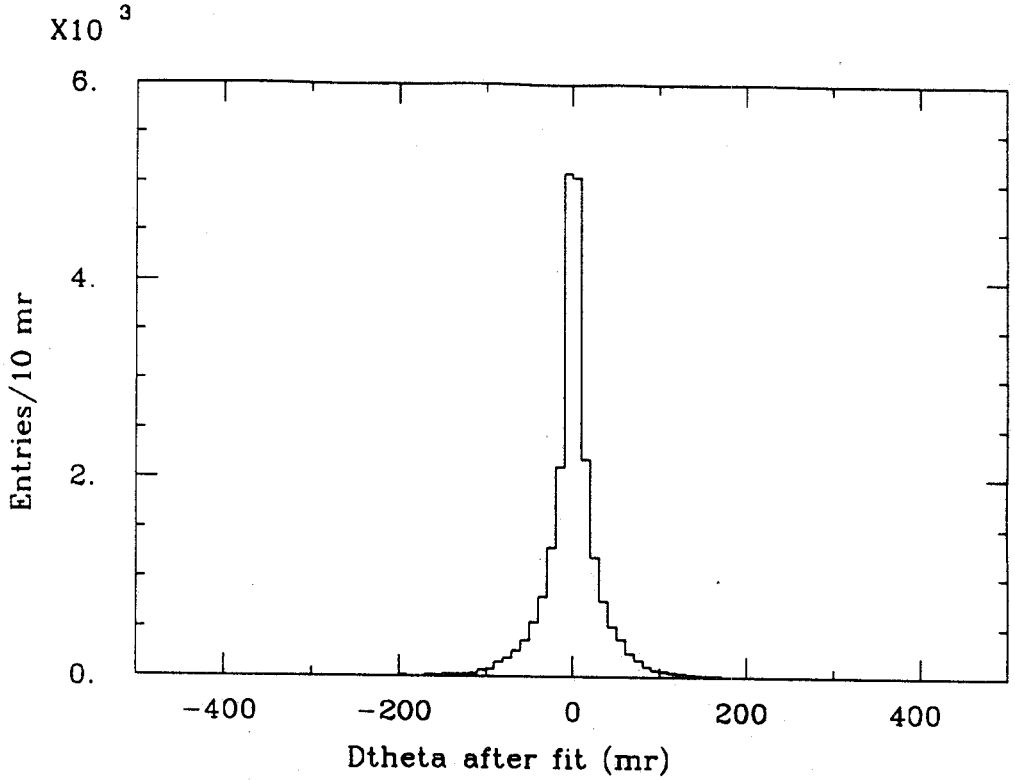
X10 3
6.
4.
2.
0.
Entries/10 mr
-400
-200
0
200
400
Dtheta after fit (mr)

FIG.3b

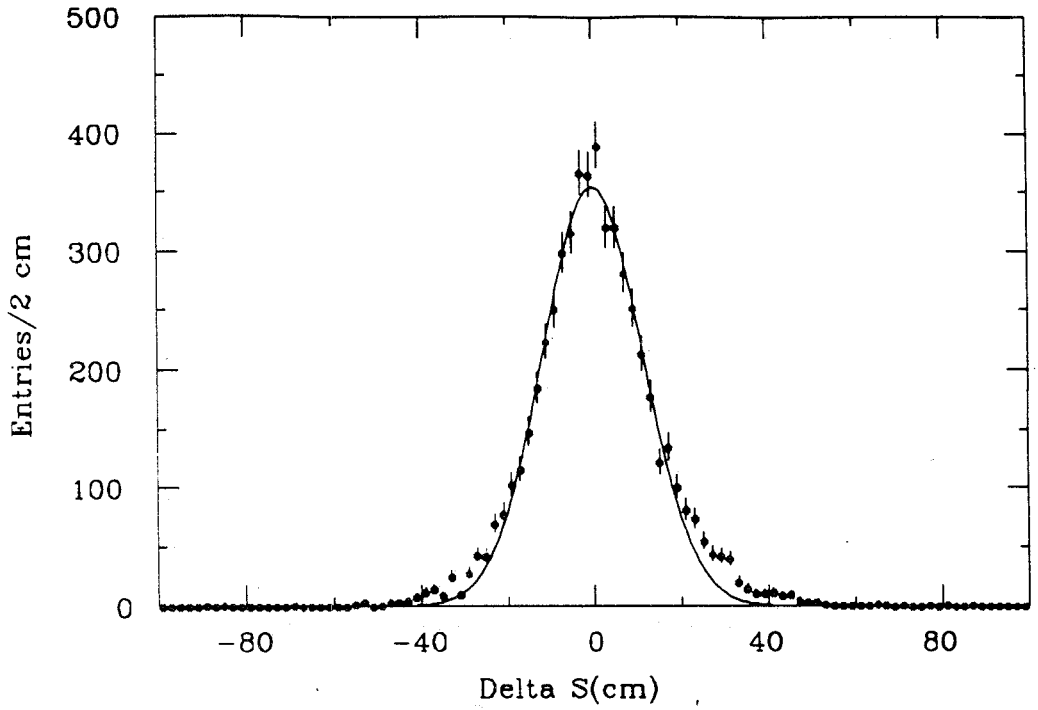
500
400
300
200
100
0
Entries/2 cm
-80
-40
0
40
80
Delta S(cm)

FIG. 4

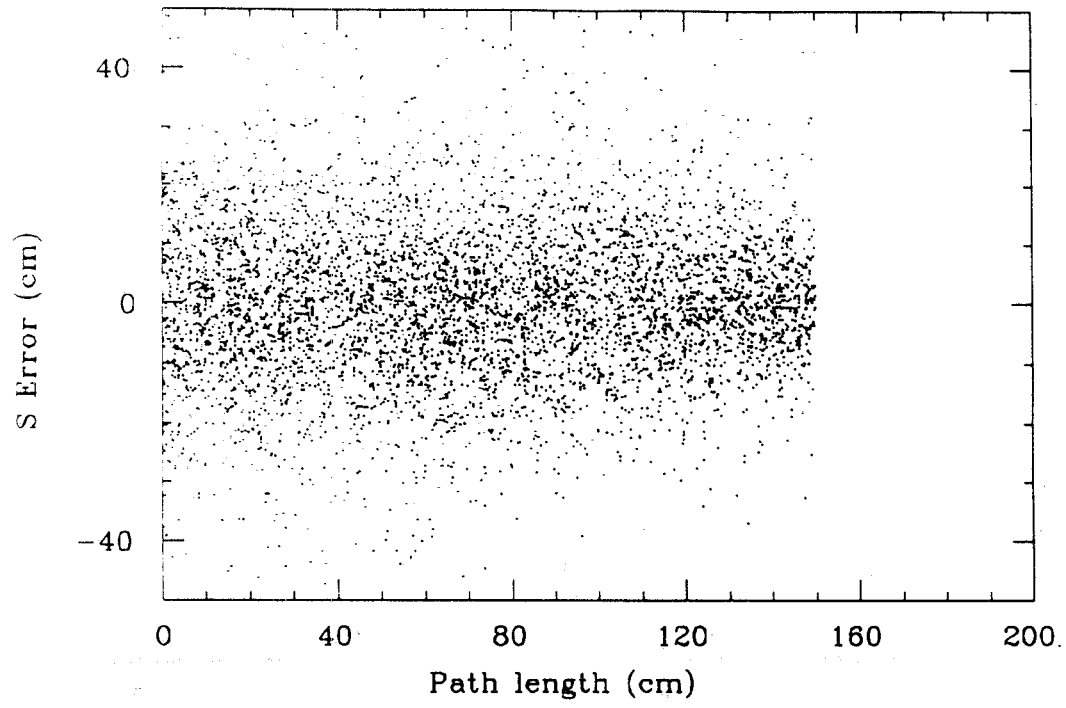
40
0
-40
S Error (cm)
0
40
80
120
160
200
Path length (cm)

FIG. 5

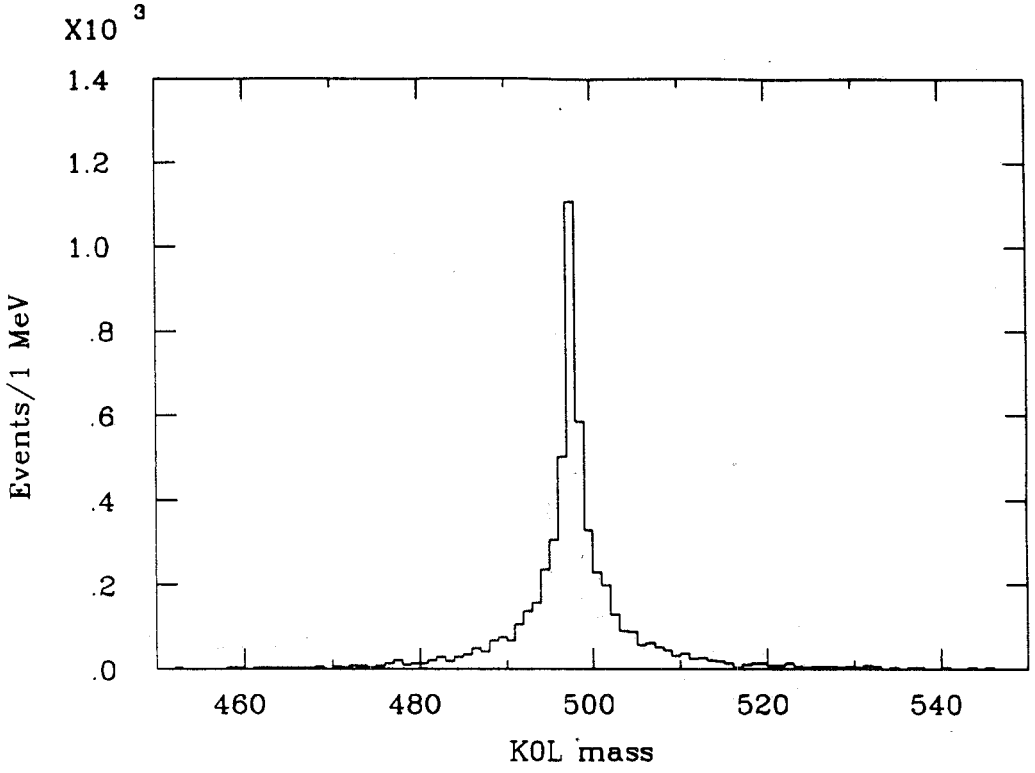
X10 3
1.4
1.2
1.0
.8
.6
.4
.2
.0
Events/1 MeV
460
480
500
520
540
K0L mass

FIG. 6

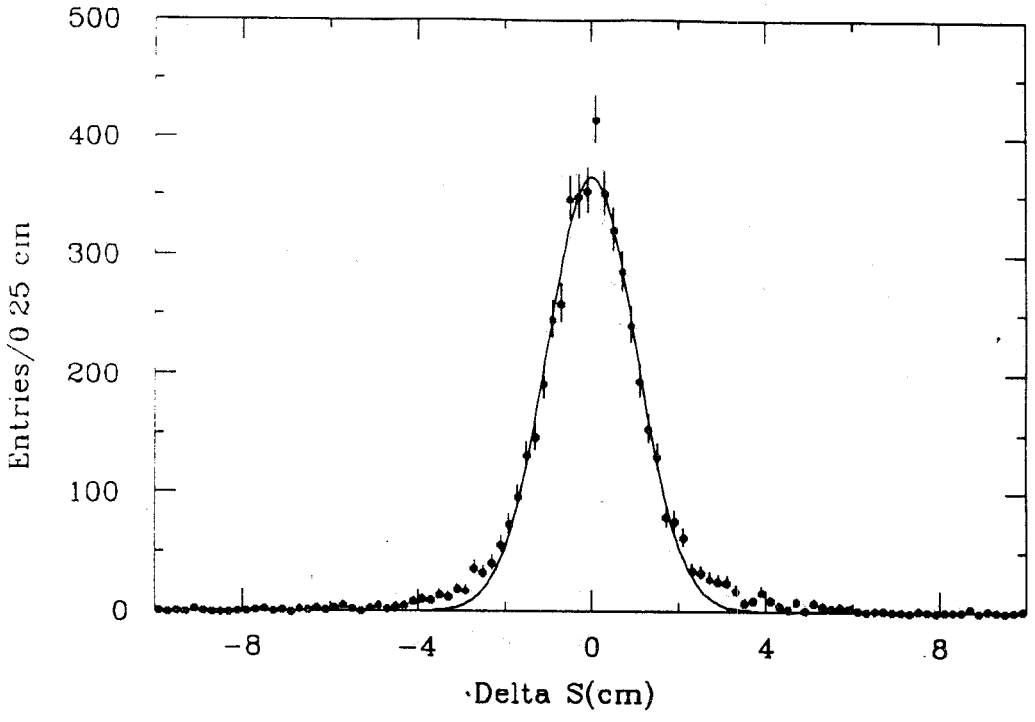
500
400
300
200
100
0
Entries/0 25 cm
-8
-4
0
4
8
Delta S(cm)

FIG. 7

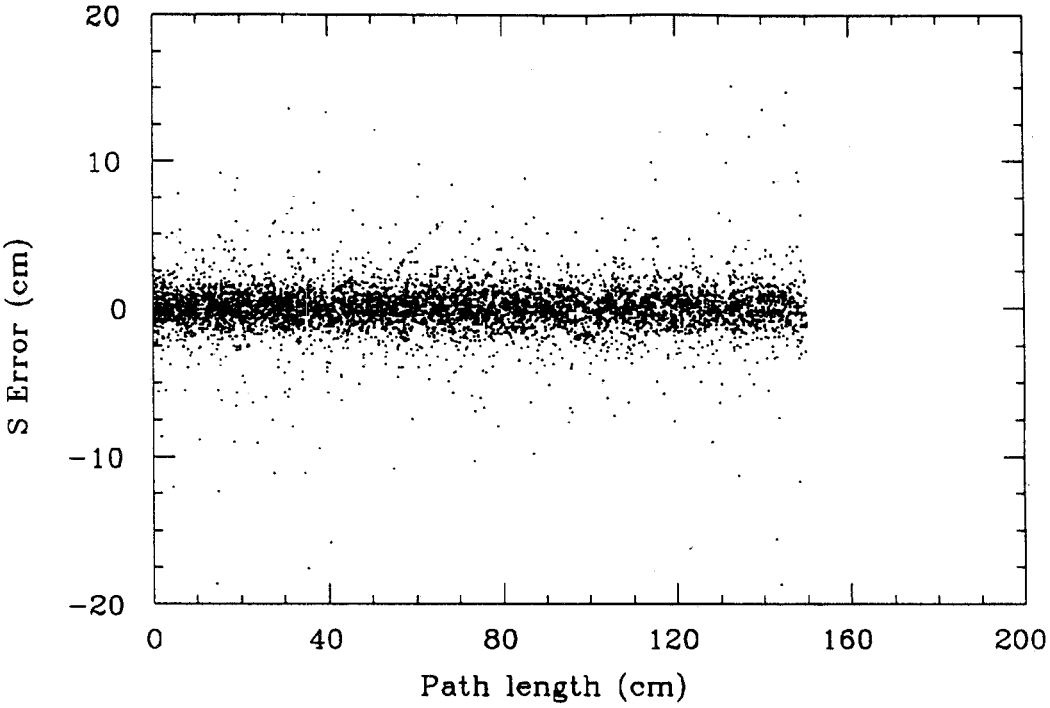
20
10
0
-10
-20
S Error (cm)
0
40
80
120
160
200
Path length (cm)

FIG. 8

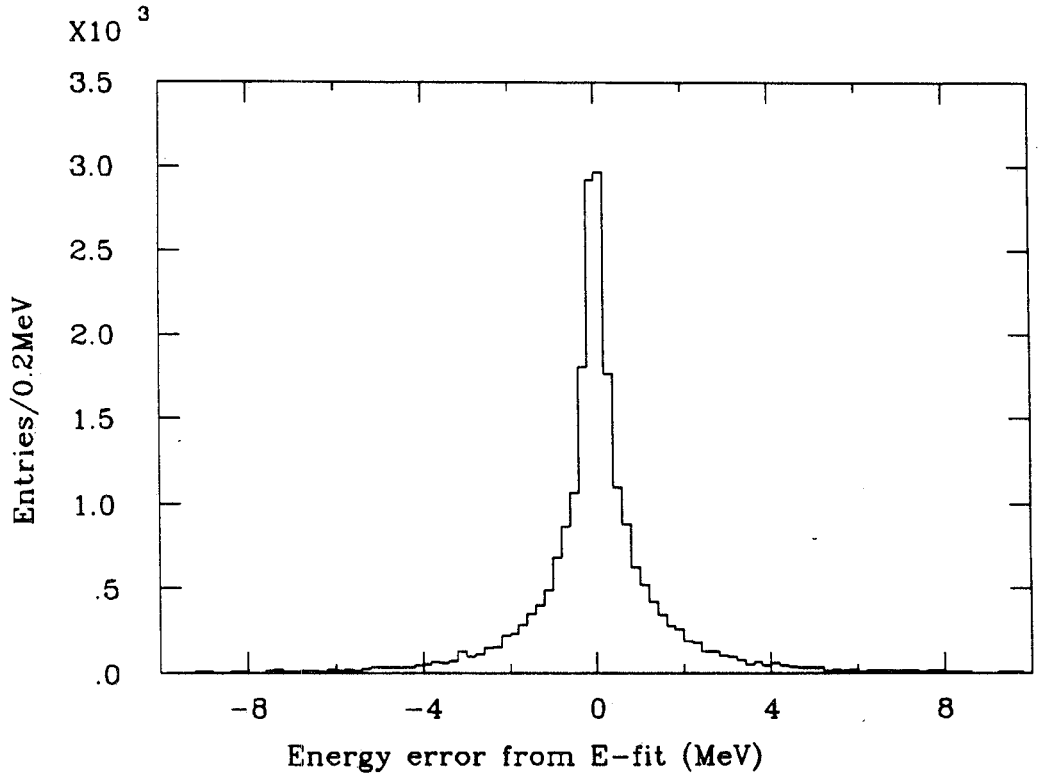
X10 3
3.5
3.0
2.5
2.0
1.5
1.0
.5
.0
Entries/0.2MeV
-8
-4
0
4
8
Energy error from E-fit (MeV)

FIG. 9

A modern apparatus for the study of the $K^0\overline{K}^0$ system from the $\phi(1020)$ produced in e^+e^-

G.Batignani [1] F.Forti [1] M.A.Giorgi [2] G.Triggiani [1]

Abstract

The $K^0\overline{K}^0$ system is the only one in which a violation of the CP symmetry has been observed. The measurement of the parameters of this violation is not satisfactory yet, and in some case (Re ε'/ε) present experimental situation is not very clear.
In this paper we present a study of the possibilities opened in this field by a modern dedicated apparatus observing the $K^0\overline{K}^0$ decay of the $\phi(1020)$ meson produced in a tuned, high luminosity e^+e^- collider.

(lecture given by M.A.Giorgi at the winter school held in Folgaria(TN), 4th course, february, 6-11, 1989)

1) INFN sezione di Pisa
2) INFN sezione di Pisa and University of Napoli

1. INTRODUCTION

CP violation has been so far observed only in the $K^0 \overline{K}^0$ system and can be described in terms of a parameter ε measuring the CP violating part of the mass matrix mixing, and ε' measuring the CP violating amplitude in the decay matrix. There is no evidence for a non zero ε'/ε ratio, although regions with a sizeable (CPT violating) Im ε'/ε are still experimentally unprobed.
In present experiments, whether they make use of kaon beams[1,2] or tagged kaons from pp reaction[3], only one K decay is observed in every event. It is possible, however, to produce at the same time a K_S and a K_L in a given initial state through the decay $\phi \rightarrow K_S K_L$ ($J^{PC} = 1^{--}$) and to observe the two decays in the same event. This will allow [4] the detection of interference phenomena through correlations between the two decay times, besides a virtually systematics-free rate measurement.
As a matter of fact, the possibility of building a high luminosity e^+e^- machine tuned on the $\phi(1020)$ mass (a so called ϕ factory) is being intensly investigated by several physicists [5].
In this paper we will concentrate on the feasibility of such an experiment and on the general features of the apparatus. In 2. we will briefly present the notation commonly used to describe the $K^0\overline{K}^0$ system. In 3. the main experimental issues at a ϕ factory are investigated, exploring the possibility of measuring all the CP violation parameters and not only the real parts. In 4. we focus on a possible apparatus for the ϕ factory and present the results of a simulation we have performed to evaluate the number of events needed to measure the different parameters.

2. NOTATIONS

2.1 Neutral Kaon States

The weak interactions are both responsable of the decay and mixing of the K^0 and $\overline{K}^0$ mesons. The effective, free Hamiltonian is written

1) $H = M - i\Gamma/2$

Where M and Γ are the hermitian mass and decay matrices. H eigenvalues are: $\lambda_{L,S} = m_{L,S} - i/2\ \gamma_{L,S}$ corresponding to the eigenstates K_L, K_S that can be written as linear combinations of the K^0, $\overline{K}^0$ mesons

2) $$|K_L\rangle = \frac{1}{\sqrt{2}} \frac{1}{\sqrt{1+|\varepsilon|^2}} ((1+\varepsilon)\ |K_0\rangle + (1-\varepsilon)\ |\overline{K}_0\rangle)$$

3) $$|K_S\rangle = \frac{1}{\sqrt{2}} \frac{1}{\sqrt{1+|\varepsilon|^2}} ((1+\varepsilon)\ |K_0\rangle - (1-\varepsilon)\ |\overline{K}_0\rangle)$$

With this definition $|K_L\rangle$ and $|K_S\rangle$ are not orthogonal and ε is the CP violation parameter since

4) $$\langle K_L | K_S \rangle = \frac{2\ Re(\varepsilon)}{1+|\varepsilon|^2}$$

And $K_L\rangle$ and $|K_S\rangle$ are CP eigenstates only if $\varepsilon=0$.

Let now $|K_{L,S}\rangle$ be a pure neutral kaon (long or short) state defined at t=0, and let $|f_{L,S}(t)\rangle$ be any permitted final state coming from the K decay. The time evolution of our state can be written as

5) $$|\Psi_{L,S}(t)\rangle = |K_{L,S}\rangle\ e^{-im_{L,S}t}\ e^{-\gamma_{L,S}t} + |f_{L,S}(t)\rangle$$

And there is a finite probability to find, for $t\neq0$, a $\overline{K}^0$ in a beam that was defined as pure K^0 for t=0. With small effort one can calculate the probabilities for changing (or not) state as functions of time:

6) $$P(K^0 \to \overline{K}^0) = \frac{1}{4} \left| \frac{1-\varepsilon}{1+\varepsilon} \right|^2 \left(e^{-\gamma_L t} + e^{-\gamma_S t} - 2e^{-\gamma t} \cos(\Delta m)t \right)$$

$$7)\quad P(\bar{K}^0 \to \bar{K}^0) = \frac{1}{4}\left(e^{-\gamma_L t} + e^{-\gamma_S t} + 2e^{-\gamma t}\cos(\Delta m)t\right)$$

The K_L decay is expected to show a charge asymmetry in presence of CP violation[13]. It can be expressed saying that $\delta \neq 0$, where δ is defined as:

$$8)\quad \delta = \frac{\Gamma(K_L \to l^+ \pi^- \nu) - \Gamma(K_L \to l^- \pi^+ \nu)}{\Gamma(K_L \to l^+ \pi^- \nu) + \Gamma(K_L \to l^- \pi^+ \nu)}$$

2.2 Two Pion Decay

The two pion decay of neutral Kaons is the most studied channel up to now (NA 31, E 773 FNAL(1989), CERN PS 195). It is possible to define important CP violation parameters from the ratios of K_L and K_S decay amplitudes:

$$9)\quad \eta_{+-} = \frac{A(K_L \to \pi^+ \pi^-)}{A(K_S \to \pi^+ \pi^-)} \approx \varepsilon + \varepsilon'$$

$$10)\quad \eta_{00} = \frac{A(K_L \to \pi^0 \pi^0)}{A(K_S \to \pi^0 \pi^0)} \approx \varepsilon - 2\varepsilon'$$

where:

$$11)\quad \varepsilon' = \frac{e^{i(\delta_2 - \delta_0)}}{\sqrt{2}}\, Im\frac{A_2}{A_0}$$

$$12)\quad A_0 e^{i\delta_0} = <\pi\pi(I=0)|T|K^0>$$

$$13)\quad A_2 e^{i\delta_2} = <\pi\pi(I=2)|T|K^0>$$

If $\varepsilon' \neq 0$ then one gets a direct CP violation effect, within the predictions of the model based on the Cabibbo - Kobayashi - Maskawa matrix. The measure of ε' is often related to the measure of the four two pion amplitudes by the following expression (measured by the CERN experiment NA31 [6]) :

$$14) \quad \frac{|\eta_{00}|^2}{|\eta_{+-}|^2} = \frac{\Gamma(K_L \to \pi^0\pi^0)\,\Gamma(K_S \to \pi^+\pi^-)}{\Gamma(K_L \to \pi^+\pi^-)\,\Gamma(K_S \to \pi^0\pi^0)} \approx 1 - 6\,\mathrm{Re}\left(\frac{\varepsilon'}{\varepsilon}\right)$$

Or to the equivalent form based on K^0, $\overline{K}^0$ decay amplitudes (CERN PS 195 [3])

$$15) \quad \frac{I_{00}}{I_{+-}} = 1 - 6\,\mathrm{Re}\left(\frac{\varepsilon'}{\varepsilon}\right)$$

where:

$$16) \quad I_{+-} = \frac{\Gamma(K^0 \to \pi^+\pi^-) - \Gamma(\overline{K}^0 \to \pi^+\pi^-)}{\Gamma(K^0 \to \pi^+\pi^-) + \Gamma(\overline{K}^0 \to \pi^+\pi^-)}$$

$$17) \quad I_{00} = \frac{\Gamma(K^0 \to \pi^0\pi^0) - \Gamma(\overline{K}^0 \to \pi^0\pi^0)}{\Gamma(K^0 \to \pi^0\pi^0) + \Gamma(\overline{K}^0 \to \pi^0\pi^0)}$$

2.3 Three Pion Decay

If now we focus our attention on the 3π decay of the K, we see that while $K_S \to 3\pi^0$ is a CP violating decay, $K_S \to \pi^+\pi^-\pi^0$ is not CP violating, even if suppressed because it may only proceed through the partial wave with l=1, I=2. This suppression is of the order $(kr)^4$, and since $k \approx 100$ MeV and $r \approx 1/m_K$, then $(kr)^4 \approx 10^{-3}$.
Because of this non-violating contribution, it is essential to study in

detail the temporal dependence of the interference between K_L and K_S in the decays of a pure K^0 (or $\overline{K}^0$) beam (E 621 FNAL, CERN PS 195). This interference is written:

$$18)\quad I_{+-0} \alpha \left\{ e^{-i\gamma_L t} + |\eta_{+-0}|^2 e^{-\gamma_S t} + 2|\eta_{+-0}| e^{-\gamma t} \cos\left((\Delta m)t + \phi_S - \phi_L\right) \right\}$$

where:

$$19)\quad \eta_{+-0} = \frac{<\pi^+ \pi^- \pi^0 \ (CP=-)\ |T|\ K_S>}{<\pi^+ \pi^- \pi^0 \ (CP=-)\ |T|\ K_L>}$$

$$20)\quad \eta_{000} = \frac{<\pi^0 \pi^0 \pi^0\ |T|\ K_S>}{<\pi^0 \pi^0 \pi^0\ |T|\ K_L>}$$

3. THE ϕ FACTORY

3.1 Current Experiments Vs. a ϕ Factory

The present experiments studying CP violation make use of high energy K_L and K_S beams (Brookhaven [7], Fermilab [2] and CERN [1]). Due to the different decay length of K_L and K_S these experiments perform the measurement with different (beam, target position, rigenerators) setups. However even if both kaons are studied in the same apparatus, their decays are uncorrelated. Tagged K^0 ($\overline{K}^0$) can be obtained in low energy experiments, as in LEAR [3] by the use of the reaction $\overline{p}p \rightarrow K^-\pi^+K^0$ ($K^+\pi^-\overline{K}^0$). If we now think to an e^+e^- collider tuned to a center of mass energy corresponding to the ϕ (1020 MeV), we see that one can get correlated pairs of neutral or charged Kaons through the reactions:

$$21) \quad e^+e^- \to \phi(1020) \begin{matrix} \to K^0\bar{K}^0 \\ \to K^+K^- \end{matrix}$$

The initial state being a pure $J^{PC}=1^{--}$ state [9,12]. Moreover the ϕ decays into these channels with a B.R. $\approx 84\%$, giving clean events containing only the kaons and their decay products. Using the C invariance of the strong and electromagnetic interactions we know that the initial state of the $K^0\bar{K}^0$ system is written as:

$$22) \quad |i\rangle = \frac{1}{\sqrt{2}} \left(|K^0(+)\rangle |\bar{K}^0(-)\rangle - |\bar{K}^0(+)\rangle |K^0(-)\rangle \right)$$

Where the (+) and (-) indices refer to the direction with respect to an arbitrarily defined K flight axis. If we invert eqs. 2) and 3) and substitute into 22) we find a completely similar relation (forgetting $O(\varepsilon^2)$):

$$23) \quad |i\rangle = \frac{1}{\sqrt{2}} \left(|K_L(+)\rangle |K_S(-)\rangle - |K_S(+)\rangle |K_L(-)\rangle \right)$$

Now we choose any two final states f_1 and f_2 (e.g. $\pi^+\pi^-$, $\pi^0\pi^0$, $\pi\mu\nu$, $\pi^0\pi^0\pi^0$...) coming from the (-) or (+) direction at time t_1 or t_2 and observe the decay amplitude $\langle f|i\rangle$. We define $\Delta\lambda = \Delta m - i\Delta\gamma/2$, $\Delta t = t_2 - t_1$ and (by generalizing 9), 10), 19) and 20)) $\eta_i = \langle f_i|K_L\rangle / \langle f_i|K_S\rangle$, we make use of the 5) and obtain:

$$24) \quad \langle f_1(t_1)(+), f_2(t_2)(-) | i \rangle =$$

$$= \frac{1}{\sqrt{2}} \langle f_1|K_S\rangle \langle f_2|K_S\rangle e^{-imt} e^{-\gamma t/2} \left[(\eta_2 - \eta_1) \cos\left(\frac{\Delta\lambda\Delta t}{2}\right) + i(\eta_2 + \eta_1) \sin\left(\frac{\Delta\lambda\Delta t}{2}\right) \right]$$

This formula is of primary importance in understanding the ϕ factory possibilities. First notice that for $f_1=f_2$ we get $\eta_1=\eta_2$ and the amplitude 24) vanishes for $\Delta t=0$ (see fig. 1). The ϕ factory can unveal this interference that is a macroscopic consequence of the quantum properties of K pair creation [8,10] (Einstein-Podolsky-Rosen

paradox). Moreover, one can sense directly the CP violation parameters by choosing different final states, e.g. let $f_1 = \pi^+\pi^-$, $f_2 = \pi^0\pi^0$, the amplitude 24) is now proportional to $\eta_{+-} - \eta_{00} = 3\varepsilon'$ and a measurement of the direct CP violation parameter is possible. to be compared with present experiments that are sensitive only to Re ε'/ε. What's more the cleanliness of reaction 21) allows for very low background rates to any decay channel one wants to observe, and measuring K_L and K_S decays in the same apparatus at the same time greatly reduces systematic errors. A ϕ factory would allow for:

a) a detailed study of <u>all</u> the CP violation parameters in K^0 decays
b) a study of the rare kaon decays, such as $K_S \rightarrow 3\pi$, $K^0 \rightarrow \gamma\gamma$

3.2 Different Solutions to a ϕ Factory

If one needs a statistic sample of $\approx 10^{10}$ $K^0\overline{K}^0$ events, $\approx$1800 hours of data taking are needed, if the luminosity of the machine is $\approx 10^{33} cm^{-2}\ s^{-1}$ and the time efficiency is 100%. Current machines cannot achieve such a luminosity, thus forcing to the construction of a new collider, to have reasonable data taking periods.
Two alternatives are possible in conceiving such an e^+e^- collider:

a) a symmetric machine with $E^+ = E^- = 510$ MeV
   (4π apparatus)
b) an asymmetric machine with E^+ ($\approx$100 MeV) $\neq$ E^- ($\approx$5 GeV)
   (fixed target like apparatus)

The first solution implies $\beta_L = \beta_S$ and one gets $\gamma\beta c\tau_S \approx 0.5$ cm, $\gamma\beta c\tau_L \approx 3.5$ m. The typical momentum of the particles in the final state is 100÷300 MeV/c. Almost all K_L decays are contained in a sphere of radius r$\approx$5 m around the interaction point, that is a reasonable tracking volume. Neutral Kaons are very slow in the lab, thus allowing for good TOF measurements. A possible longitudinal polarization of the beams would enhance the large angle (to the beam axis) decay of the ϕ, thus favouring the measure of the position of the K decay vertices (in charged channels). The events

are highly symmetrical, and kinematical constraints make the reconstruction and analysis easier. The small momentum of the decay products forces the tracking system of an experiment to be very transparent, as the multiple scattering and K regeneration may lead to relevant errors.
The second solution gives an higher mean momentum for the charged tracks, but still the angles can be rather large (the exit angle of the pions in K -> $\pi\pi$, $<\theta>\approx 30°$), and $\gamma\beta c\tau_L$ may be as long as 35 m. This forces an experiment to the use of a non symmetrical, very big (and costly) apparatus.
For this reasons we choose the symmetrical option as an hypothesys and see its implication on an experiment to study CP violation.

4. AN APPARATUS FOR THE ϕ FACTORY

4.1 Considerations on the Apparatus

We know that each event at the ϕ factory could contain in the final state up to 4 charged particles or 10 γ, depending on the decay channel of the Kaons. In figs. 2÷7 we report the momentum spectra for the decay products in different channels. In view of this, let's try now to outline the main features of the experimental set up needed to perform such an experiment.

- As we have seen the mean decay length for the K_L is 3.5 m. Obviously not all the K_L decays will be observed in a finite size experiment, and this loss has to be taken into account during the analysis. To keep the corrections as low as possible the experiment fiducial volume should be the largest we can afford reasonably, say it should contain a 5 m radius sphere.

- The whole apparatus must ensure a good discrimination between π, μ, e, γ by means of tracking, TOF and calorimetric measurements.

- The natural scale length to be resolved is given by the mean

decay path of the K_S , in this case 5 mm. Our requirement is that the apparatus can measure the position of the decay vertices (in charged particles) of the kaons with an accuracy ≈1 mm (1/5 $\gamma\beta c\tau_S$).

- The tracking system must be as transparent as possible in terms of radiation length, and must have enough points on each track to identify the kinks due to the decay $\pi \rightarrow \mu\nu$, since most pions decay within our fiducial volume. This seems to be the most critical part of the apparatus, as particles produced in K decay have a very low momentum (100 to 300 MeV) and are therefore extremely sensitive to multiple scattering. For instance a 100 MeV π crossing 10^{-4} radiation lengths undergoes an mean angular deviation due to multiple scattering of about 2 mrad.

- The time of flight for charged particles should be measured at least in two points: in the inner region (K_S region) and the external layer, out of the fiducial volume, where the TOF for photons must be measured too. This measurement should be as accurate as possible, that is ≈200 ps with current techniques.

- The sign and momentum measurement for charged particles force to the presence of a magnetic field within the fiducial volume, however it may be rather weak (300÷500 Gauss), but well known. The required precision for momentum measurement is below 1% in the 100÷300 MeV range.

4.2 Feasible Results

As we pointed out in sec. 3.1 the main goal for an experiment at the ϕ factory is the measurement of the time and the channel for each K decay. The decay channel reconstruction is made harder by the fact that we make comparisons between common decay rates and rare or CP violating ones, whose B.R. is 3÷4 orders of magnitude smaller. This requires high rejection factors when we select rare decay channels. In this sub-section we will list interesting channels together with the contamination one gets to these selections from

common decay modes. We can concentrate on the example given in sec. 3.1, with $f_1 = \pi^+\pi^-$, $f_2 = \pi^0\pi^0$. Let the K_S undergo f_1 (or f_2) decay with B.R. = 68.61% (and 31.39%), and look for $K_L \rightarrow f_2$ (or f_1) decays.

4.2.1 $K_L \rightarrow \pi^0\pi^0$

We wrote a montecarlo program in the Geant framework[11] to simulate the events one could have at the ϕ factory, as depicted in sec. 3.2. In this montecarlo the ϕ is produced at rest at (0.,0.,0.) in the lab, and forced to decay in a K_S K_L pair. The K_S is traced until its decay, that may proceed through the $\pi^+\pi^-$ or the $\pi^0\pi^0$ channel, and is confined in a sphere of few cm from the interaction point. The apparatus is inspired by the requirements of sec. 4.1 and it's simulated by:

- A vertex detector, constituted by two thin barrels at r = 10, 20 cm. This detector provides a clean, unambiguous and accurate measurement in time and space of the two pions from $K_S \rightarrow \pi^+\pi^-$.

- A tracking system extending from r = 40 cm to 4 m capable of measuring charged tracks with an accuracy $\sigma(\theta) = \sigma(\phi) = 2$ mrad and $\sigma(P_T)/P_T = 0.5\%$ in a magnetic field of 300 Gauss. Our specifications for the tracking system are well within reach with current techniques, but the realization of such a detector would require outstanding capabilities in designing a very light structure, as angular errors are dominated by multiple scattering.

- A closed calorimeter, cylindrical in shape, with radius = 5 m, half length = 5 m. This detector measures TOF (σ(TOF) $\approx$200 ps), incident point ($\sigma(x) \approx 2$ mm), and energy ($\sigma(E)/E \approx 1\%/\sqrt{E(GeV)}$ for the e.m. component down to 10 MeV) of charged particles and photons with high efficiency. These specifications would require a careful detector developement to be met.

The pions from K_S, and the K_L are propagated within the apparatus until they decay or interact with the experiment material. The K_L

decay channel(s) can be selected by the program's steering cards, allowing for separate study of each background. After tracking the event undergoes a simulated reconstruction and a flexible user analysis, dedicated to the optimization of our kinematical cuts.
Let' s concentrate on the process we' re interested in:

25) $e^+e^- \to \phi(1020) \to K_S K_L \to \pi^0\pi^0$
$\qquad\qquad\qquad\qquad\qquad\qquad\qquad\qquad\qquad\qquad\quad \hookrightarrow \pi^+\pi^-$

First we trigger with full efficiency on events having two charged tracks pointing to the K_S decay region and no γ in the calorimeter within a time (corrected for the dip angle) t_0= 17.6 ns [figs. 8÷9]. Good events clearly show 4 photon hits in the calorimeter in 92% of the triggered events, corresponding to a detection efficiency of 98% for $E(\gamma) \geq 15$ MeV/c [fig. 2].
Background events are mainly due to the decay $K_L \to \pi^0\pi^0\pi^0$, in which the two less energetic photons are not seen. Assuming a photon detection efficiency of 90% for these low energy photons we are left with 1% of the $3\pi^0$ events. If we sum the 4 remaining γ energies and compare with the same plot for the good events [figs. 10÷11] we can see that a 4σ cut from the K^0 mass retains less than 10^{-4} of the $3\pi^0$ events thus leading to a total rejection factor of 10^{-6}.

4.2.2 $K_L \to \pi^+\pi^-$

First we trigger on events with at least two γ's arriving on the calorimeter within the (corrected) time t_0. Background events are due to:

a) $K_L \to \pi^+\pi^-\pi^0$
b) $K_L \to \pi\mu\nu$

In the first case the usual rejection factor of 10^{-2} accounts for the loss of two photons. Then the invariant mass plots of two charged prongs [fig. 12÷13] shows that a 4σ cut from the K^0 mass rejects all

our montecarlo $\pi^+\pi^-\pi^0$ events. In this case we estimate a rejection factor $< 5\ 10^{-7}$, but its exect determination would require the use of non gaussian error tails.
In the second case we hypotize that the apparatus is not able to discriminate the μ from the π. Once given the μ track a dummy π mass, the same invariant mass cut as in a) is applied [fig. 14] for a rejection factor of 2%. For the events left we sum the reconstructed momenta of the two charged prongs and plot its projections P_T and P_{Long} (with respect to the flight line of the K_L from the origin to its decay vertex) one against the other. Good ($K_L \rightarrow \pi^+\pi^-$) events accumulate on $P_{Long} = E(K)-2m_\pi$ while three body decays spread in this plane [figs 15÷16]. This selection retains .2% of the events left for a total rejection factor of $4\ 10^{-5}$. This number indicates us that this channel dominates the background with kinematical cuts only.
In [4] one can find detailed calculations on number of ϕ's needed in order to get a given precision on ε' having accounted for all other parameters involved in this experiment.

4.3 Possible Solution for the Apparatus

What we describe in this section

- For the vertex detector one might use silicon pixel detectors. In this application 100μm x 100μm pixels on 1 cm^2 elements would be suited. A very simple electronics (2 transistors/pixel) is integrated on chip. If the detector is 200 μm thick each of these pixels would have a capacitance C= 8pF, a minimum ionizing particle would release a charge ≈16000 electrons thus giving rise to a voltage signal ≈250 mV, suited for driving the circuit logic. The layout arrangement is similar to a memory chip, or a computer keyboard, and the signal can be read out by scanning serially the lines corresponding to the orthogonal cohordinates.

- The central tracking detector has to be a gaseous detector, very transparent in terms of radiation length. Various solutions are possible, amongst which a TPC is preferable for easyness of

reconstruction and uniformity of resolution. The field used, the event rate, and the light weight required have to be carefully studied to choose between a single, big TPC or various layers of smaller drift space ones, like the VTPC's of the CDF experiment.

- A very interesting detector (RPC) is being developed by INFN-Roma and could be adopted for our calorimeter. This detector is an evolution of the parallel plate condenser detectors, and its working principle is based on the use of conductive plastic materials (phenolic polymers). Each ionizing particles crossing this detector produces a streamer, which is then stopped by the local discharge of the condenser plates, whose resistivity is $10^{10\div12}\ \Omega$ cm. The gas used is an argon - butane - freon mixture. Butane stops UV rays produced in the avalanche, which can propagate the discharge to the whole chamber, while freon captures peripheral electrons for its stong electronic affinity. Prototypes of the RPC detector have been measured, giving $\leq$1 ns resolution time and $\geq$95% efficiency on low momentum tracks. An RPC counter - lead multilayer sandwich of several X_0 would constitute a simple and cheap calorimeter for our apparatus.

5. REFERENCES

1) Burkhardt H. et al., Nucl. Instr. Meth. A268 (1988) 116
2) Bernstein R.H. et al., Phys. Rev. Lett. 54 (1985) 1631
3) Adiels L. et al., CERN/PSCC/85-6
4) Dunietz I., Hauser J. and Rosner J.L., Phys. Rev. D35 (1987) 2166
5) Barletta W.A. et al., Center for Advanced Accelerators, UCLA, May 1989
6) Burkhardt H. et al., Phys. Lett. 206B (1988) 169
7) Black, J.K. et al., Phys. Rev. Lett. 54 (1985) 1628
8) Datta A., Home D. and Raychadhuri A., Phys. Lett. 123 (1987) 4
9) Lipkin H.J., Phys. Rev. 176 (1968) 1715
10) Day T.B., Phys. Rev. 121 (1961) 1204
11) CERN report, DD/EE/84-1
12) Bernabeu J. et al., Phys. Lett. 211B (1988) 226
13) Steinberger J., CERN report 70-1 (1970)

6. FIGURE CAPTION

1) Probability of finding a $\pi^+\pi^-\pi^+\pi^-$ final state as a function of the decay time difference (see eq. 24).
2) Energy spectrum of γ from $K_L \rightarrow \pi^0\pi^0$.
3) Energy spectrum of γ from $K_L \rightarrow \pi^0\pi^0\pi^0$.
4) Momentum spectrum of charged π from $K_L \rightarrow \pi^+\pi^-$.
5) Momentum spectrum of charged π from $K_L \rightarrow \pi^+\pi^-\pi^0$.
6) Momentum spectrum of charged π from $K_L \rightarrow \pi\,\mu\,\nu$.
7) Momentum spectrum of μ from $K_L \rightarrow \pi\,\mu\,\nu$.
8) Arrival time of photons from $K_S \rightarrow \pi^0\pi^0$.
9) Arrival time of photons from $K_L \rightarrow \pi^0\pi^0$.
10) Sum of the 4 most energetic γ energies from $K_L \rightarrow \pi^0\pi^0$.
11) Sum of the 4 most energetic γ energies from $K_L \rightarrow \pi^0\pi^0\pi^0$.
12) Invariant mass distribution of $\pi^+\pi^-$ from $K_L \rightarrow \pi^+\pi^-$.
13) Invariant mass distribution of $\pi^+\pi^-$ from $K_L \rightarrow \pi^+\pi^-\pi^0$.
14) Invariant mass distribution of $\pi\,\mu$ for $K_L \rightarrow \pi\,\mu\,\nu$ giving the μ a fake π mass.
15) Longitudinal vs. transverse momentum distribution of the two charged prongs system from $K_L \rightarrow \pi^+\pi^-$ (possibly followed by $\pi \rightarrow \mu\,\nu$ decay).
16) Longitudinal vs. transverse momentum distribution of the two charged prongs system from $K_L \rightarrow \pi\,\mu\,\nu$.

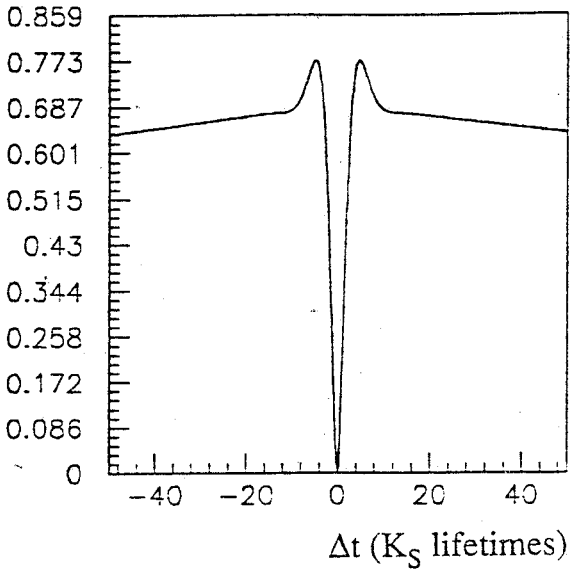

Fig. 1)

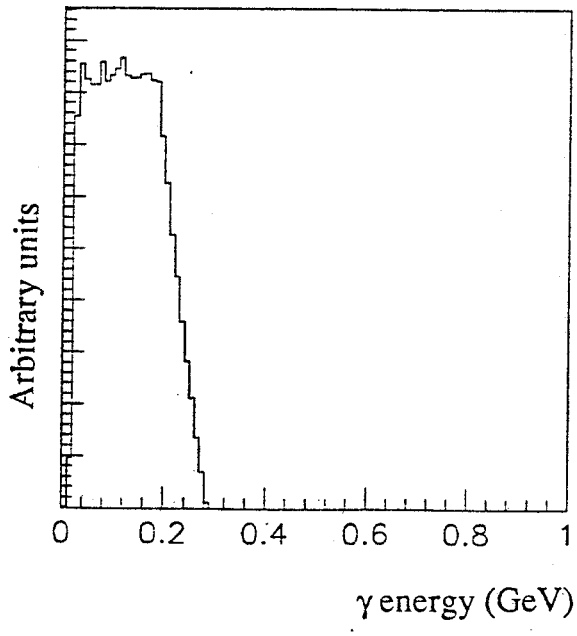

Fig. 2)

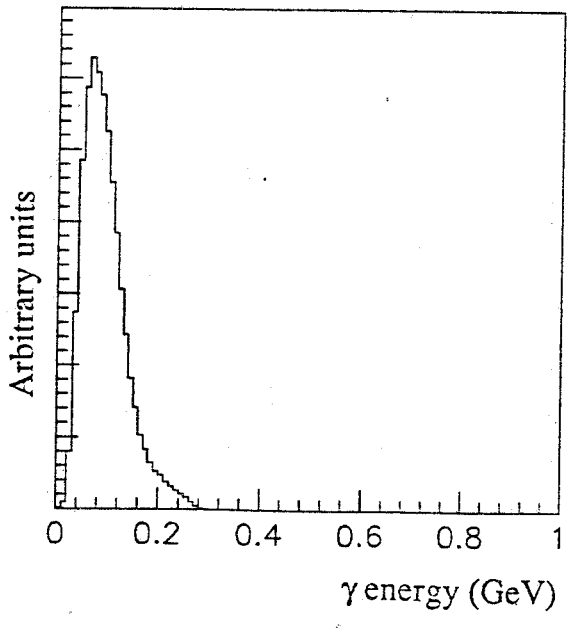

Fig. 3).

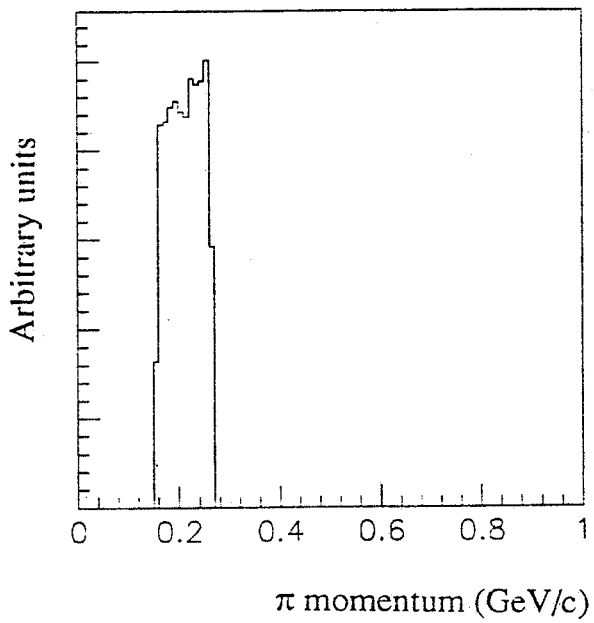

Fig. 4)

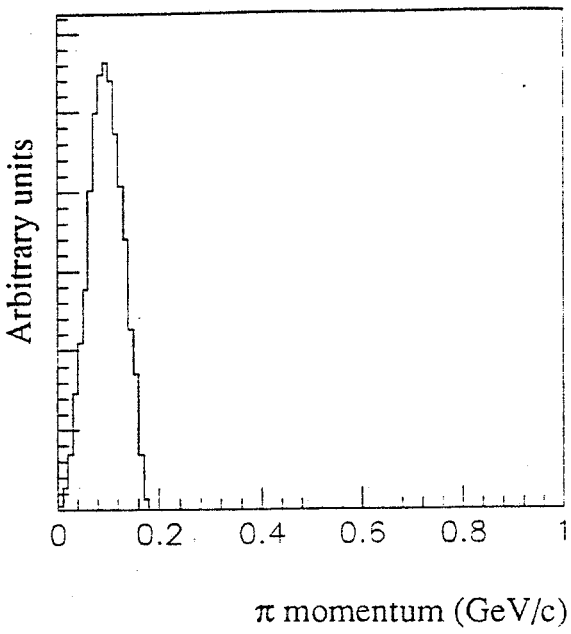

Fig. 5)

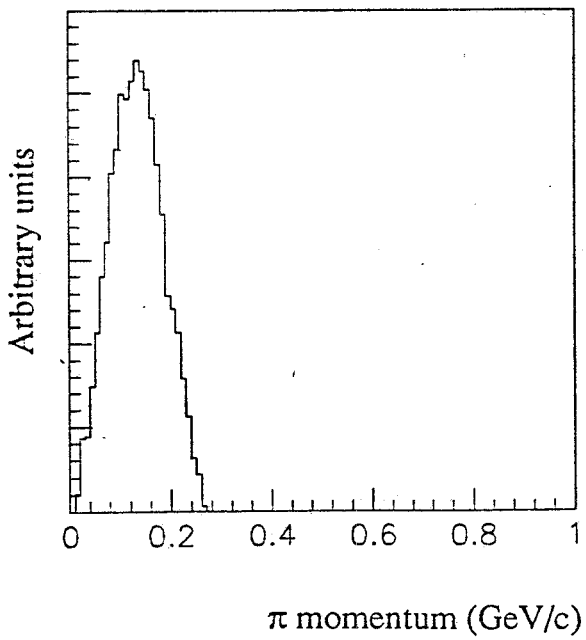

Fig. 6)

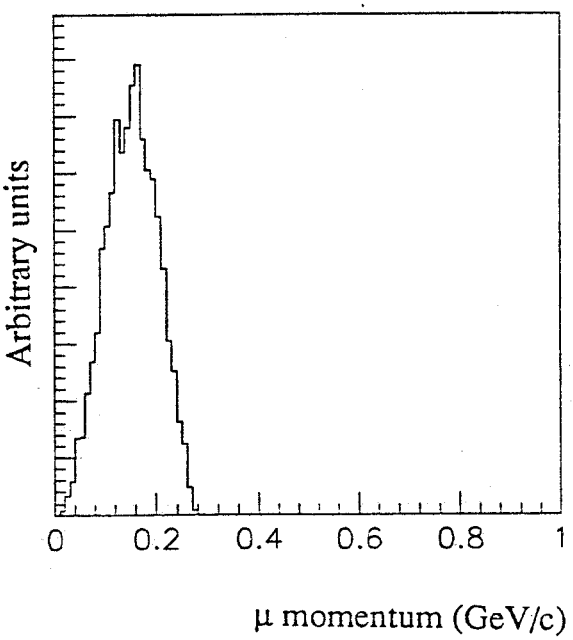

Fig. 7)

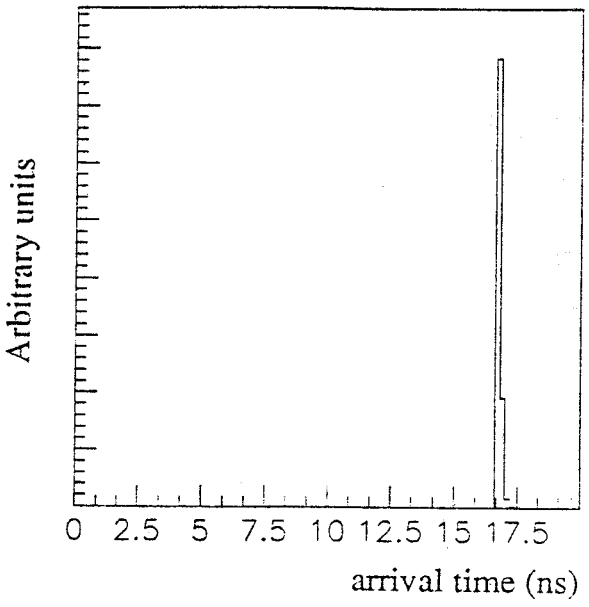

Fig. 8)

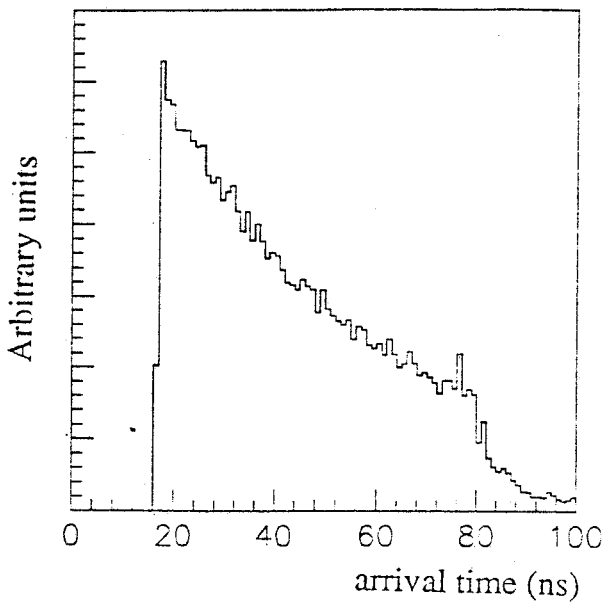

Fig. 9)

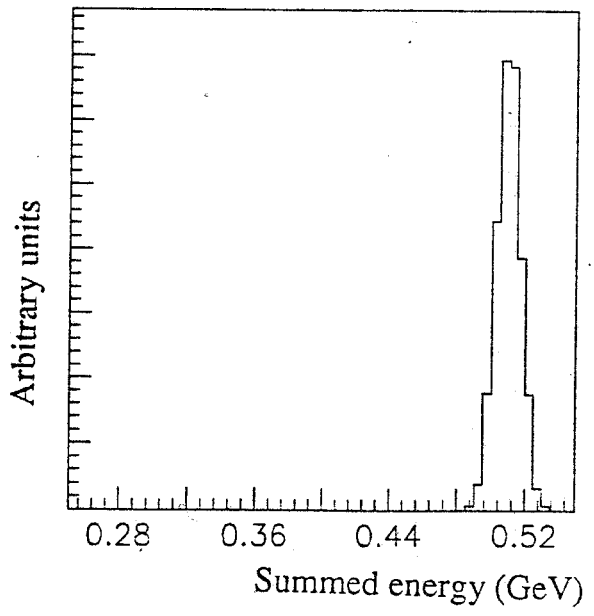

Fig. 10)

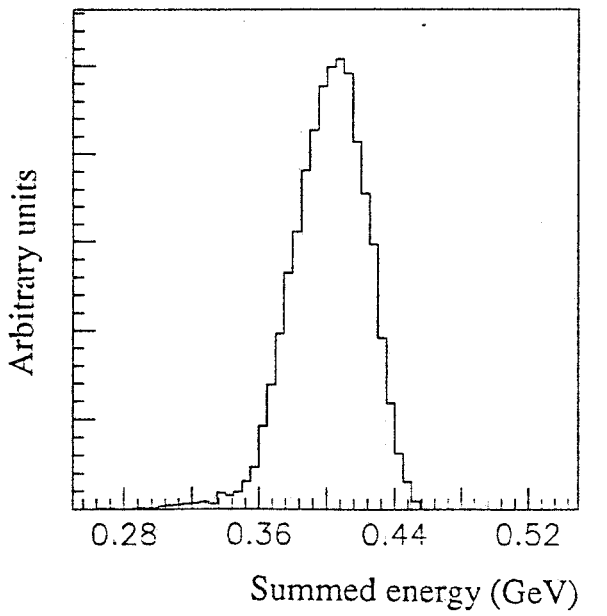

Fig. 11)

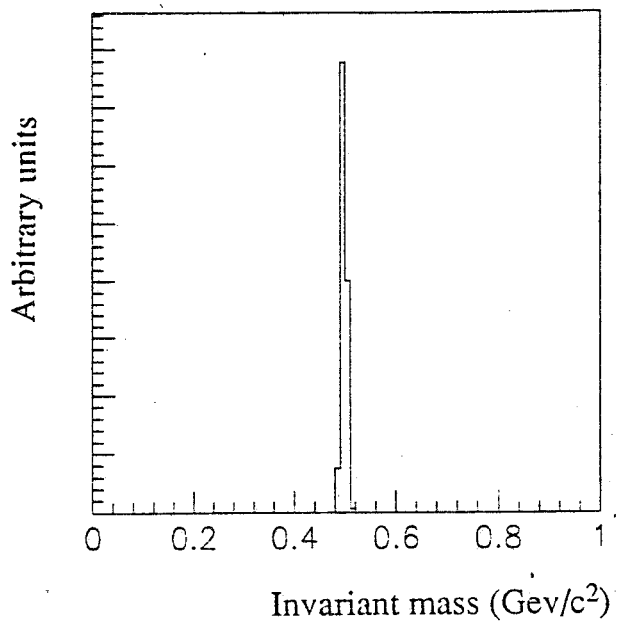

Fig. 12)

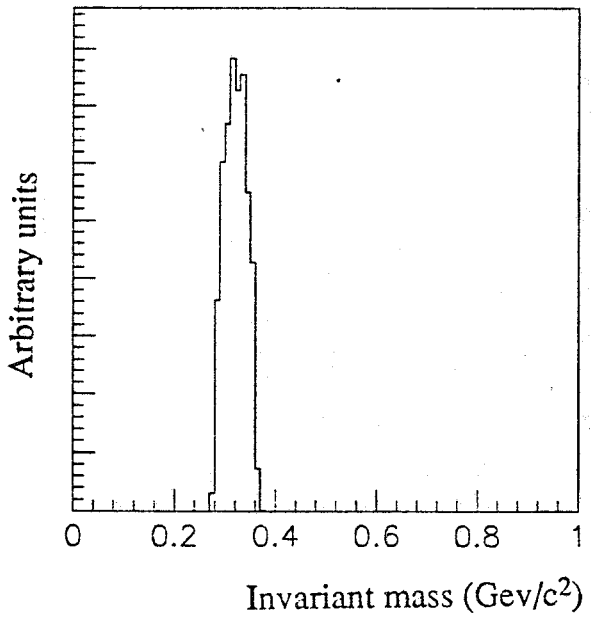

Fig. 13)

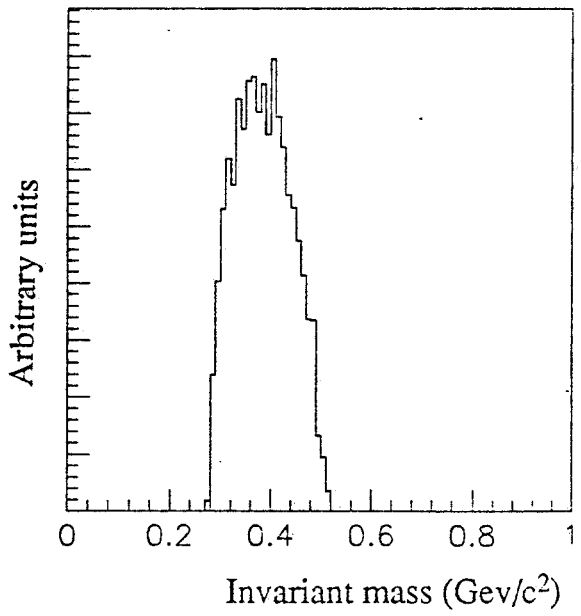

Fig. 14)

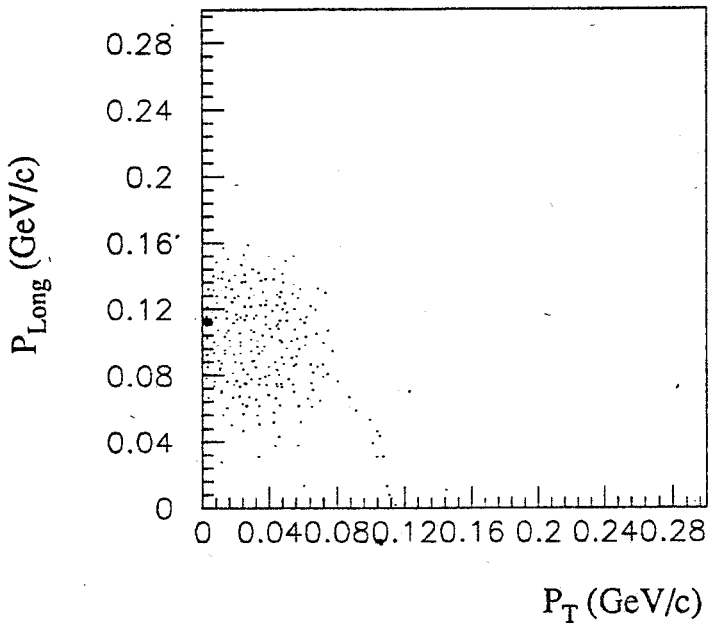
0.28
0.24
0.2
0.16
0.12
0.08
0.04
0
0 0.040.080.120.16 0.2 0.240.28
P_{Long} (GeV/c)
P_T (GeV/c)

Fig. 15)

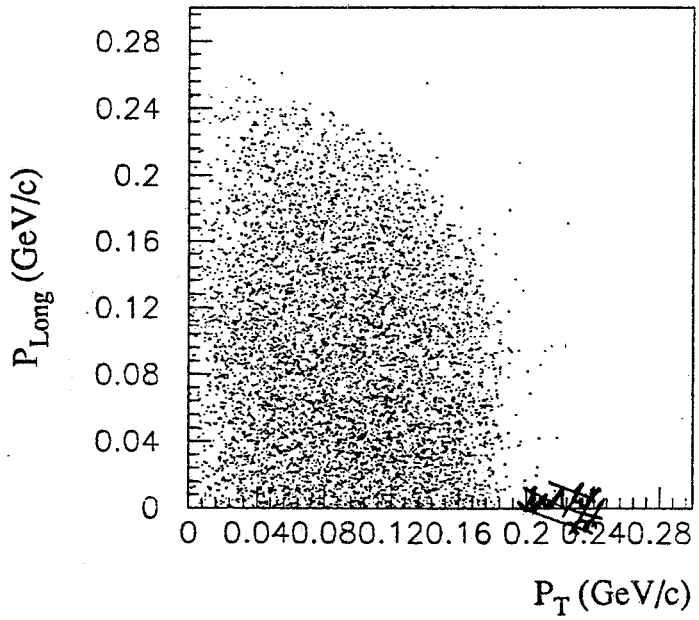
0.28
0.24
0.2
0.16
0.12
0.08
0.04
0
0 0.040.080.120.16 0.2 0.240.28
P_{Long} (GeV/c)
P_T (GeV/c)

Fig. 16)

Monte Carlo study of the development of a low energy electromagnetic shower: preliminary results

A.Del Guerra(1), W.R. Nelson(2), C.Rizzo(3), P.Russo(1)

(1) Universita' di Napoli, Dipartimento di Scienze Fisiche and INFN,Sezione di Napoli, Pad.20, Mostra d'Oltremare, I-80125 Napoli
(2) Stanford Linear Accelerator Center, Stanford 94309,CA,USA
(3) INFN,Sezione di Trieste,Trieste

Abstract

The general purpose Monte Carlo code EGS4 has been implemented to study the development of a low energy (20-300 MeV) electromagnetic shower. A conventional lead/gas sampling calorimeter has been simulated. The results show that the combined single-particle/ multi-particle behavior of a γ ray in this energy range can impose severe limits to the angular and energy resolution of the reconstructed photon.

1. INTRODUCTION

The knowledge of the shower development of a low energy (20-300 MeV) photon is extremely important for the design of a 2π apparatus for "photon tracking and calorimetry" at a ϕ-factory. The physics requirements for the detector are a high tracking resolution, so as to localise the γ vertex to $\leq$ 1mm with a "modest" energy resolution. The use of a high Z scintillator (such as BGO) with a tremendous granularity would be much too expensive and does not always ensure the required tracking resolution. On the other hand, a sampling calorimeter could be an affordable solution, once the absorber/active region and their geometry have been accurately chosen. A sampling calorimeter made of a series of absorbing lead slabs with MultiWire Proportional Chambers (MWPC) was used in the axion search E-137 experiment at SLAC for the detection of GeV photons [1].

The general purpose EGS4 [2] code is widely used for electron and photon transport studies, expecially in high energy physics [3]. We have implemented the EGS4 code to simulate the shower of 20-300 MeV photons entering a sampling calorimeter. Preliminary results for the tracking and the energy resolution capability of such a detector are presented.

2. THE MONTE CARLO SIMULATION

We have chosen a simple lead/gas configuration for the e.m calorimeter made of ten modules (for a total length of 12 cm), each consisting of:

- 2 mm pure lead
- 10 mm active gas region (Ar-Methane, 70-30, at 1 atm) to simulate a typical gas multiwire proportional chamber.

The total thickness (~3.6 r.l) should be enough for the tracking of the photon, while the energy could also be measured by a total absorber scintillator downstream of the sampling calorimeter.

For a realistic simulation of the response of an e.m. calorimeter with the EGS code it is extremely important [4] to choose the correct ESTEPE (kinetic energy loss per electron step) and to use the proper ECUT (the lower energy cut-off for the electron transport). As cut-offs we have chosen 10 keV both for electrons (ECUT) and photons (PCUT),since below that value the results may be not realistic.Instead of the ESTEPE parameter we have used the PRESTA algorihtm [5], which may be more CPU time consuming, but avoids any step-size dependence in the results of the calculation. The simulations have been done with photons always entering the calorimeter orthogonally in its center (i.e. x=y=z=0.0).

3. MONTE CARLO RESULTS

A random selection of "showers" of a single photon in the sampling calorimeter is shown in figures 1a,1b and 1c for 20 , 100 and 300 MeV, respectively; the longitudinal "particle leakage" is also illustrated by the figures. The shift from single-particle to shower behavior is clearly evident with increasing energy.

Figures 2a and 2b are the 2-D plots of the shower development for one thousand photons with an energy of 20 and 100 MeV, respectively. The abscissa of the plot is along the photon direction (z-axis). Only the electrons and positrons in the gas regions are plotted: each dot corresponds to one interaction. Figure 3 shows the corresponding lateral profiles of the shower in the gas region 7, after ~2.5 r.l, i.e. near the expected maximum of the shower for 100 MeV photons.

In order to reconstruct the photon direction it is important to know the number of "active" regions which are hit by each photon shower. Figures 4a and 4b show the multiplicity distributions as obtained for one hundred incident photons of 20 and 100 MeV, respectively: 55% of the 20 MeV photons do not produce a sufficient number of interactions (a signal in $\geq$ 2 regions); 14% in the 100 MeV case. For the events with $\geq$2 "active" regions an averaging is performed for each module both in x and z; a linear fit [$x=\alpha z+\beta$] gives the projection of the reconstructed photon

trajectory onto the x-z plane. The intersection of the fitted line with the z=0 plane represents the distance from the entrance x-coordinate, of the simulated photon. A similar procedure is applied to the projection onto the y-z plane. The results are presented in fig. 5a and 5b. The statistics is poor: only 100 photons have been considered, which have produced 45 and 86 reconstructable events for the 20 and the 100 MeV case, respectively.However, the distributions are clearly very broad: a FWHM of 5 cm is a reasonable estimate for the 100 MeV case (see fig.6).

If one assumes that the two recostructed lines are the projections of the photon trajectory, the angular error on the photon tracking can be evaluated in the following way: the two reconstructed projections are given as

1) $x = \alpha z + \beta$

$y = \gamma z + \delta$,

and their intercepts onto the z=0 plane are

2) $x_0 = \beta$

$y_0 = \delta$,

and

3) $\rho_0^2 = \beta^2 + \delta^2$,

where ρ_0 is the distance of the origin from the intercept of the reconstructed photon trajectory with the z=0 plane and represents the spatial displacement in the reconstruction. In a translated polar coordinate system with the new origin in $(x_0,y_0,0)$, every point of the photon trajectory will be given as

4) $x = r \operatorname{sen}\theta \operatorname{sen}\phi$

$y = r \operatorname{sen}\theta \cos\phi$

$z = r \cos\theta$,

where θ represents the angular displacement in the reconstruction. By using 1) and 4) θ can be simply written as:

5) $\theta = \arccos \{ z/ (x^2+y^2+z^2)^{1/2} \} = \arccos\{ (\alpha^2+\gamma^2+1)^{-1/2} \}$.

The angular error can be extremely large, with a median value of the ditribution around 15 degrees for the 100 MeV case. Figures 7a and 7b show the 2-D plot distributions in ρ_0 and θ for the 20 and the 100 MeV case, respectively.

Finally, figures 8 shows the distribution of the energy deposition in the active regions of the sampling calorimeter for one thousand 100 MeV photons; of course the longitudinal energy leakage is very high (see fig.1b), but it can be measured by positioning a total absorption active detector, downstream of the sampling calorimeter.

The simulation is still very preliminary. However, the results obtained so far clearly show that tracking and calorimetry of a low energy (20-300 MeV) photon is rather difficult because of the combined single-particle/multi-particle behavior of the photon in this energy range.

The possibility of using a sampling lead/gas calorimeter has been investigated. The necessity of a lateral confinement to interrupt the electron tracks so as to achieve a much better photon tracking is evident from the simulation. We are currently evaluating the possible use of matrices of small tubes of high lead content (density = 5-6 g/cm^3)as a sampling calorimeter. In this case the tube walls (100-200 μm) will be the passive absorber and the hole within the tubes (0.5 -1.0 mm)the active gas region. We have already used this technology both for very low energy (511 keV) and high energy (2-5 GeV) photons[6]. The Monte Carlo simulation for this particular application is now under development.

References

[1] A. Abashian, J. Bjorken, C. Church, S. Ecklund, L. Mo, W. R. Nelson, T. Nunamaker, P. Rassman, and D. Scherer, "Search for Neutral, Penetrating, Metastable Particles Produced in the SLAC Beam Dump", presented at the Fourth Moriond Workshop on Massive Neutrinos in Particles and Astrophysics, La Plague,France (15-21 Jan 1984).

[2] W.R.Nelson, H.Hirayama, D.W.O.Rogers, "The EGS4 Code System", SLAC Report 265 (1985).

[3] A.Del Guerra, W.R. Nelson,"High Energy Physics Applications of EGS", in Monte Carlo Transport of Electrons and Photons, Ed. by T.M.Jenkins, W.R.Nelson, and A.Rindi, Plenum Press,(1988) 599.

[4] G.Lindstrom, M. Eberle, I. Fedder, E. Fretwurst, V. Riech, M. Siedel, "MC-Simulations with EGS4 for Calorimeters with thin Silicon Detector, DESY Report, Desy 89-104 (August 1989).

[5] A.F.Bielajev, D.W.O.Rogers, "PRESTA: the Parameter Reduced Electron Step Transport Algorithm for Electron Monte Carlo Transport", Nucl.Instr.Meth., B18 (1987) 165.

[6] A. Del Guerra, M. Conti, P. Maiano, V. Perez-Mendez, C. Rizzo, "The macrochannel plate: a suitable detector for low energy γ-rays and high energy e.m. showers', Nucl.Instr. Meth., A273 (1988) 500.

Figure Captions

Fig.1 - Random selection of "showers" of a single photon in the sampling calorimeter. Charged particle are shown as solid lines; photons as dotted lines: a) 20 MeV; b) 100 MeV; c) 300 MeV.

Fig.2 - 2-D plot of the shower development in the gas region of the sampling calorimeter for one thousand incident photons: a)20 MeV; b)100 MeV.

Fig.3 - Lateral profile of the shower development in the gas region #7 (~after 2.5 r.l) for one thousand incident photons.

Fig.4 - Multeplicity distribution of hit gas regions for each "shower", as obtained with one hundred incident photons: a) 20 Mev; b) 100 MeV.

Fig.5 - Scattered plot showing the x and y intercepts of the reconstructed photon trajectory with the z=0 plane, as obtained with one hundred incident photons: a) 20 MeV; b) 100 MeV.

Fig.6 - Distribution of the χ intercept of the reconstructed photon trajectory with the z=0 plane, as obtained with one hundred incident photons of 100 MeV.

Fig.7 - Scattered plot showing the spatial (ρ_0) and the angular (θ) displacement of the reconstructed photon trajectory, as obtained with one hundred incident photons: a) 20 MeV; b) 100 MeV.

Fig.8 - Distribution of the energy deposition in the gas regions of the sampling calorimeter for one thousand 100 MeV photons.

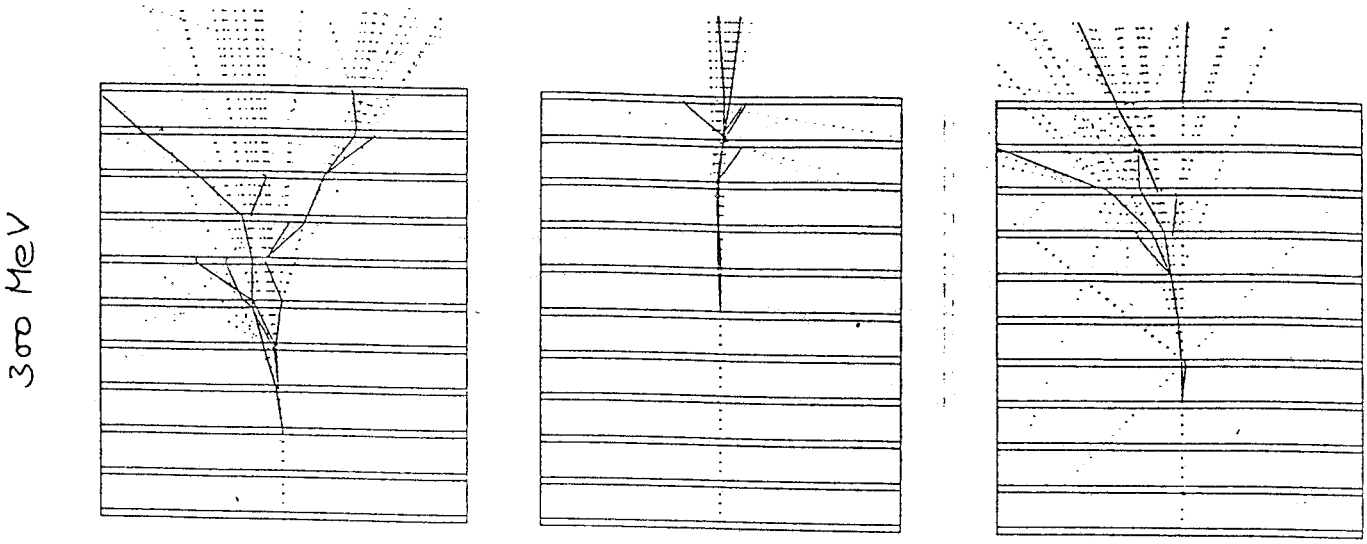

FIG. 1a

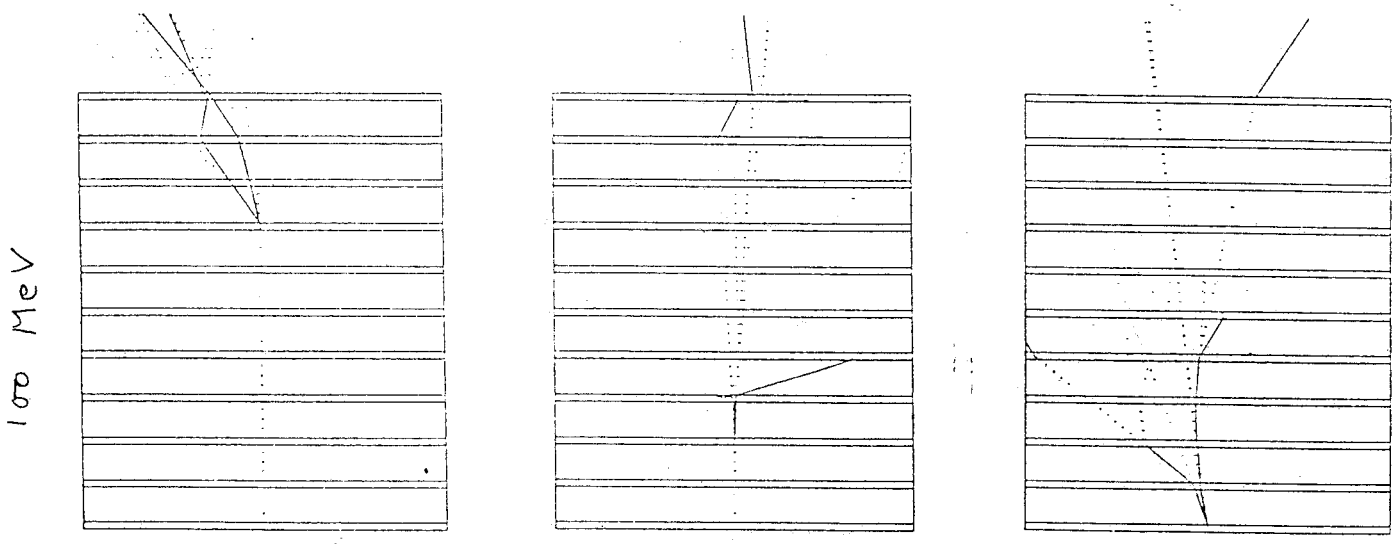

FIG. 1b

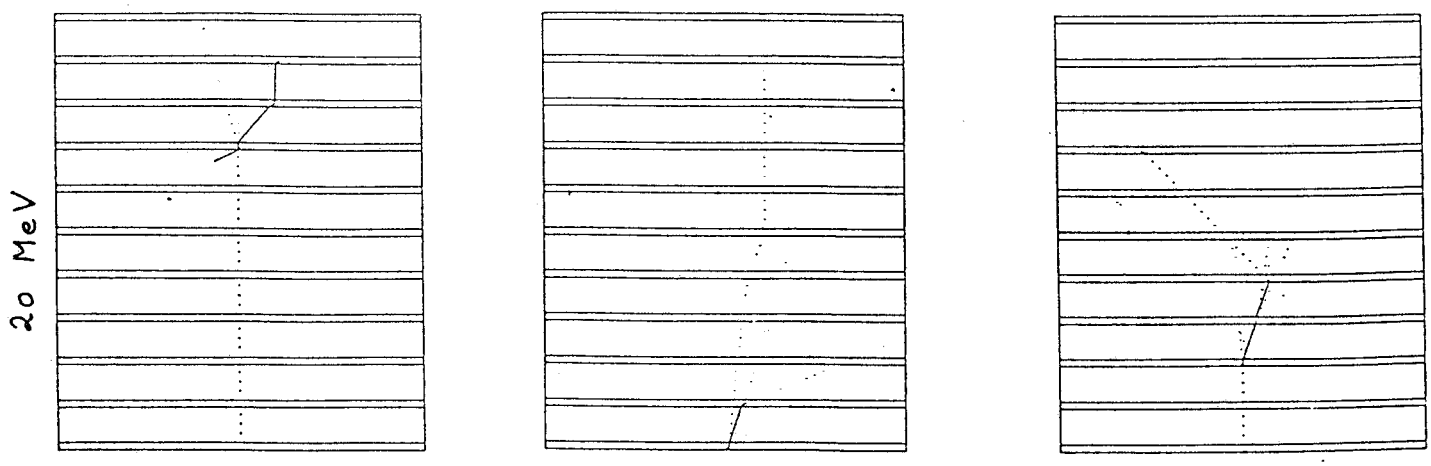

FIG. 1c

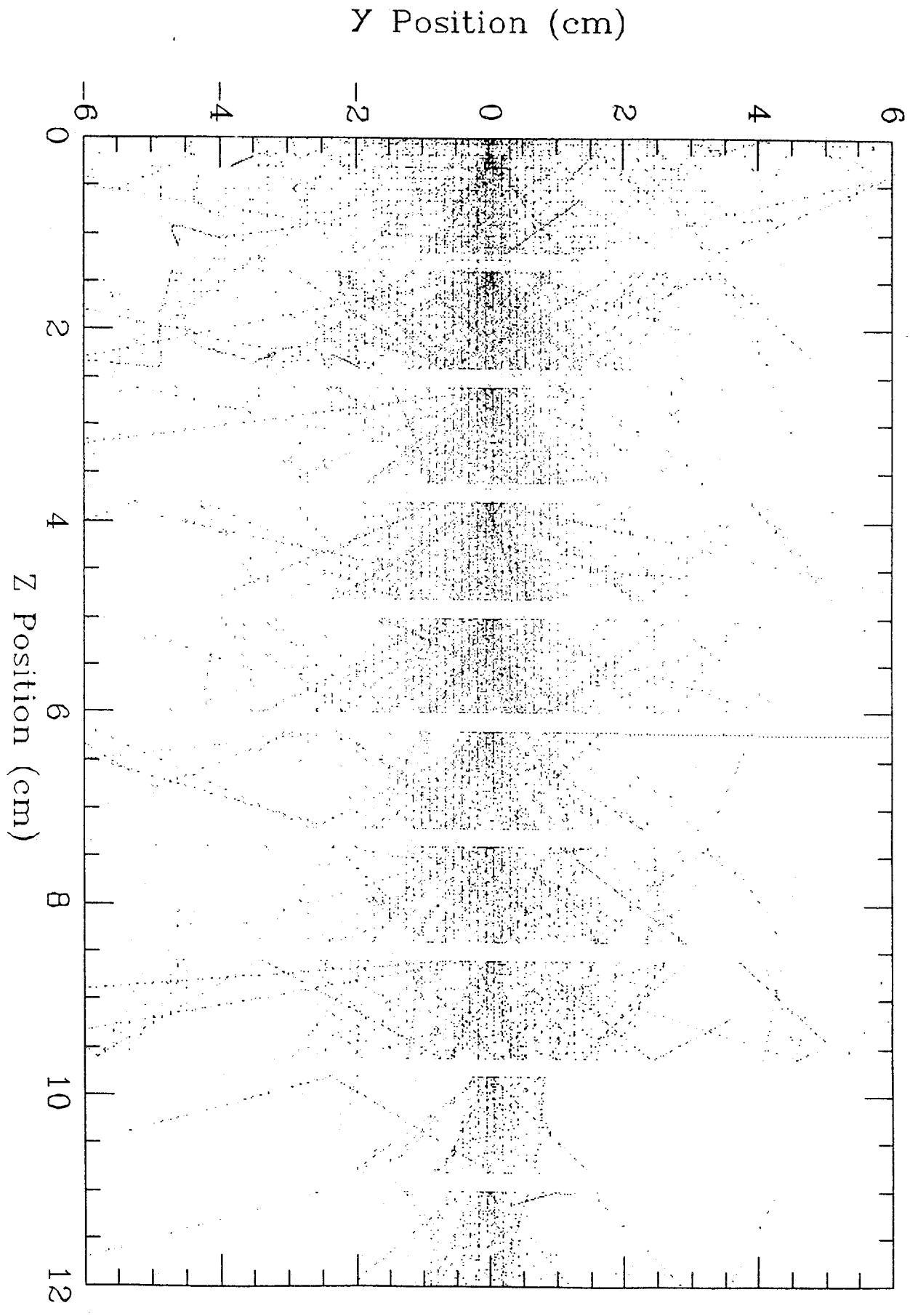

FIG. 2a

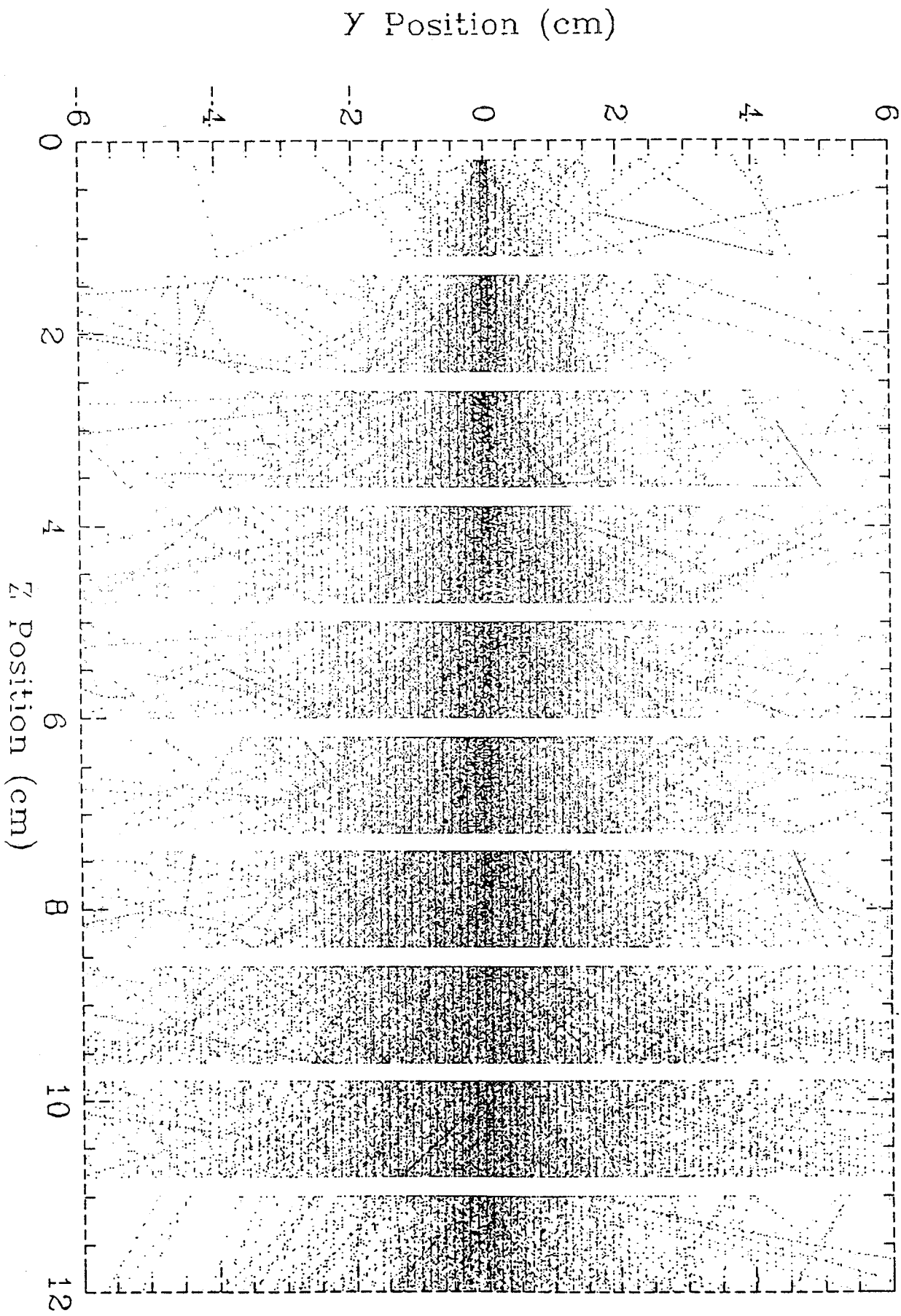

FIG. 2b

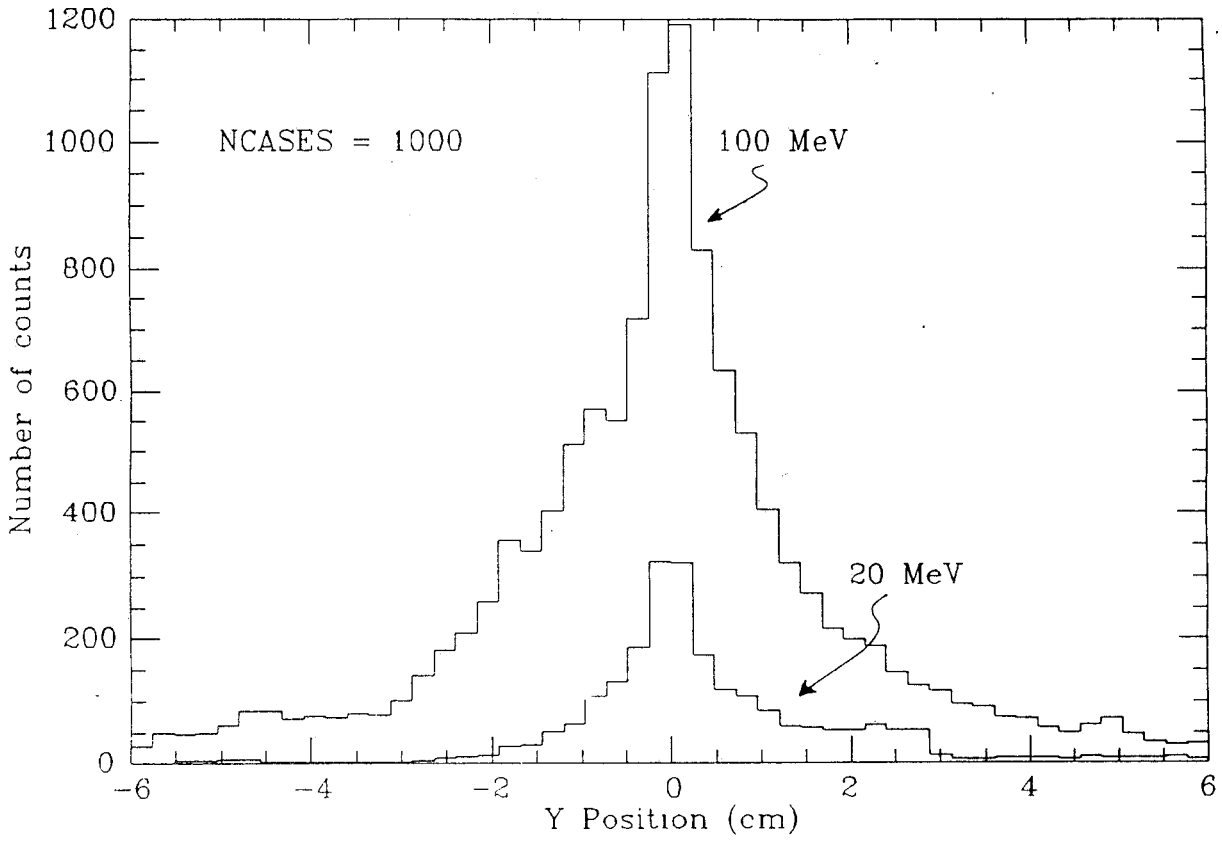
1200
1000
800
600
400
200
0
Number of counts
NCASES = 1000
100 MeV
20 MeV
−6
−4
−2
0
2
4
6
Y Position (cm)

FIG. 3

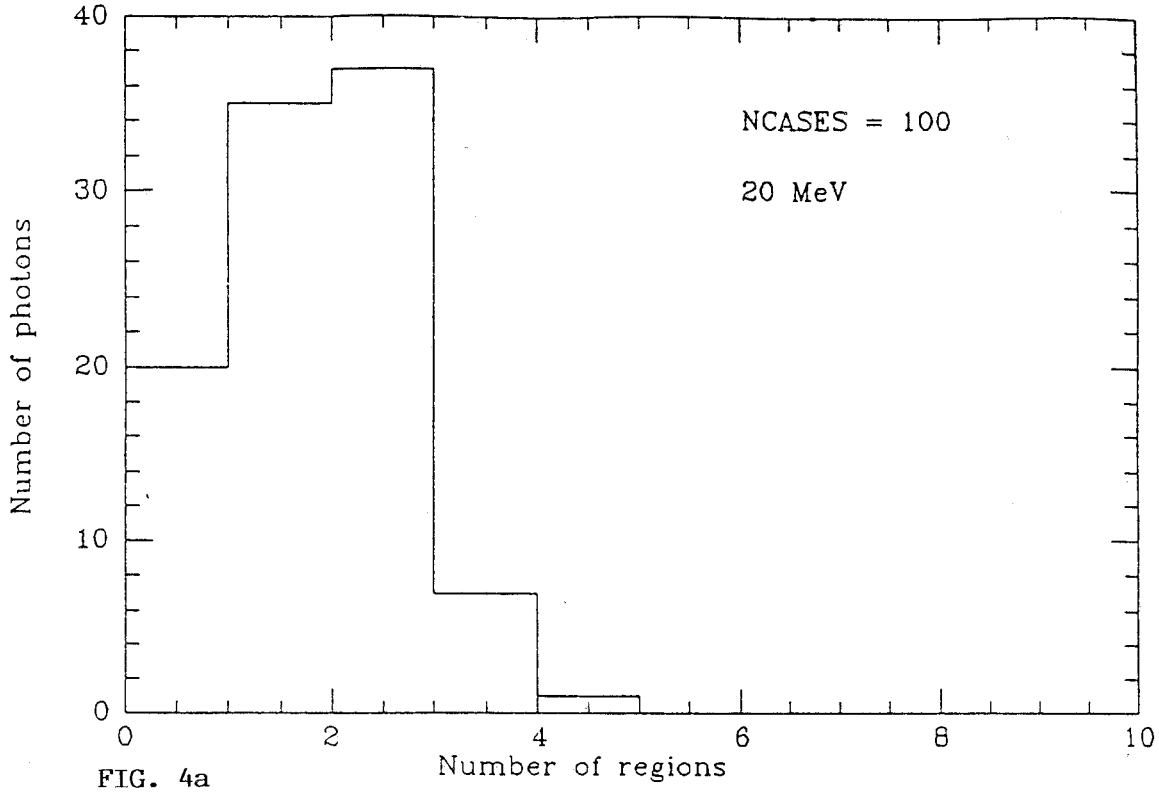
NCASES = 100
20 MeV
Number of photons
Number of regions
0
10
20
30
40
0
2
4
6
8
10

FIG. 4a

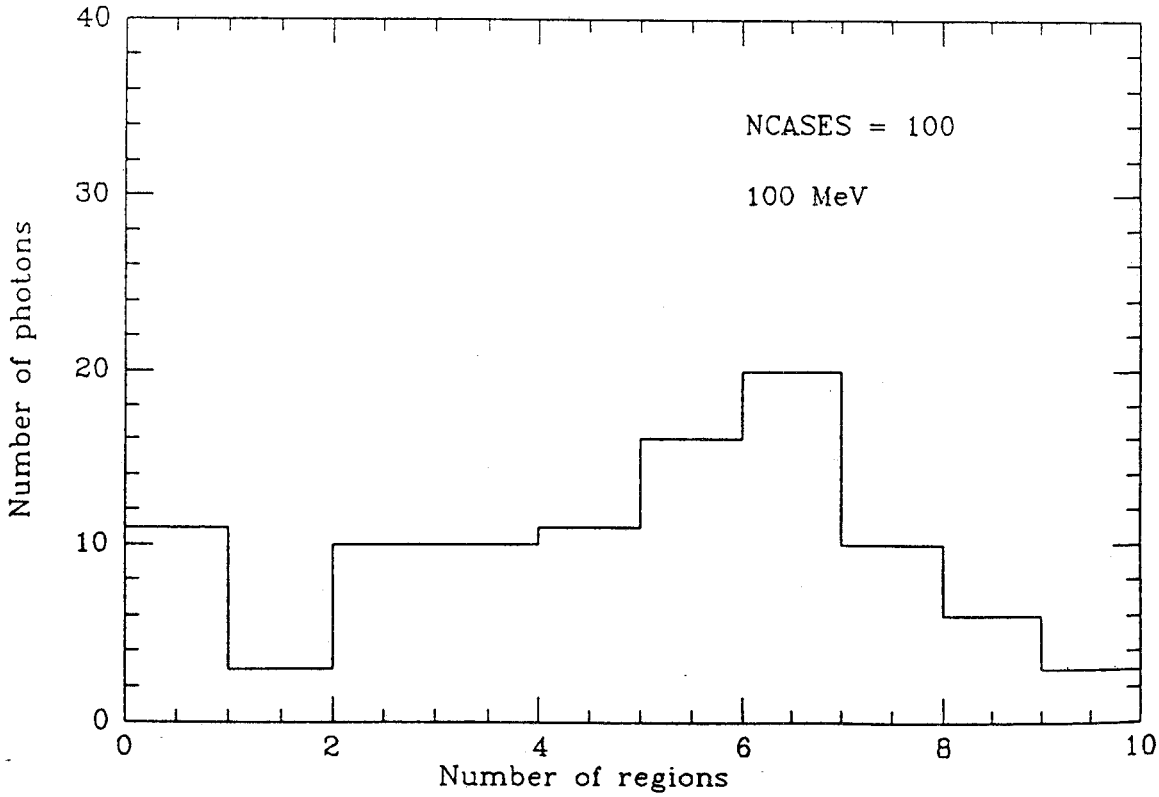
NCASES = 100
100 MeV
Number of photons
Number of regions
0
10
20
30
40
0
2
4
6
8
10

FIG. 4b

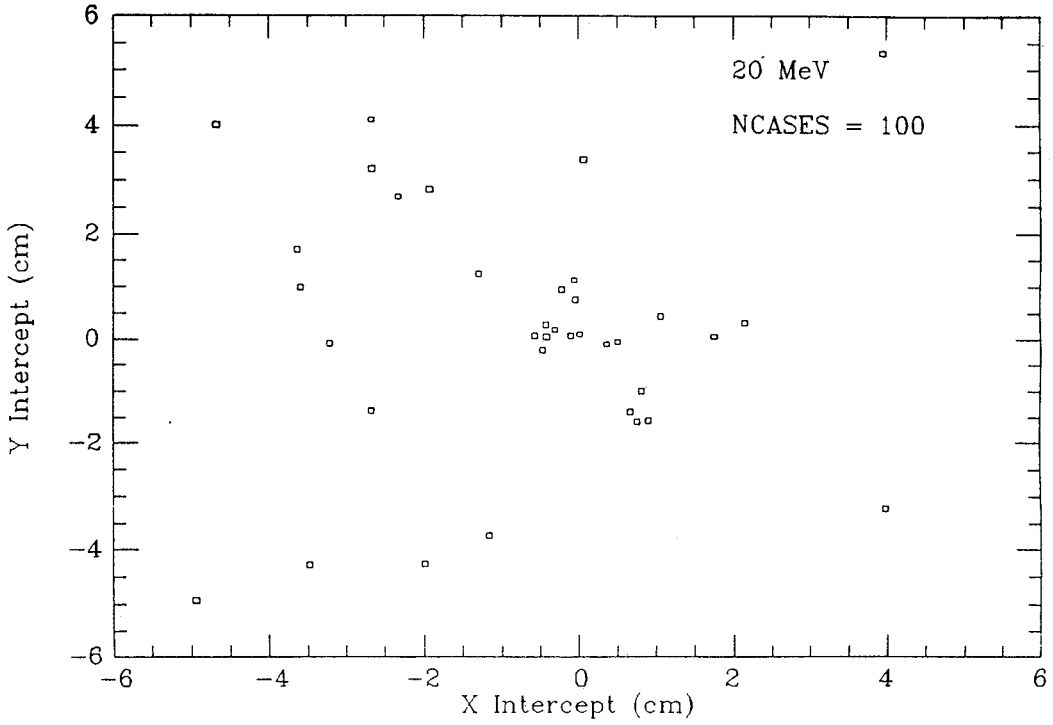
20 MeV
NCASES = 100
Y Intercept (cm)
X Intercept (cm)
6
4
2
0
-2
-4
-6
-6
-4
-2
0
2
4
6

FIG. 5

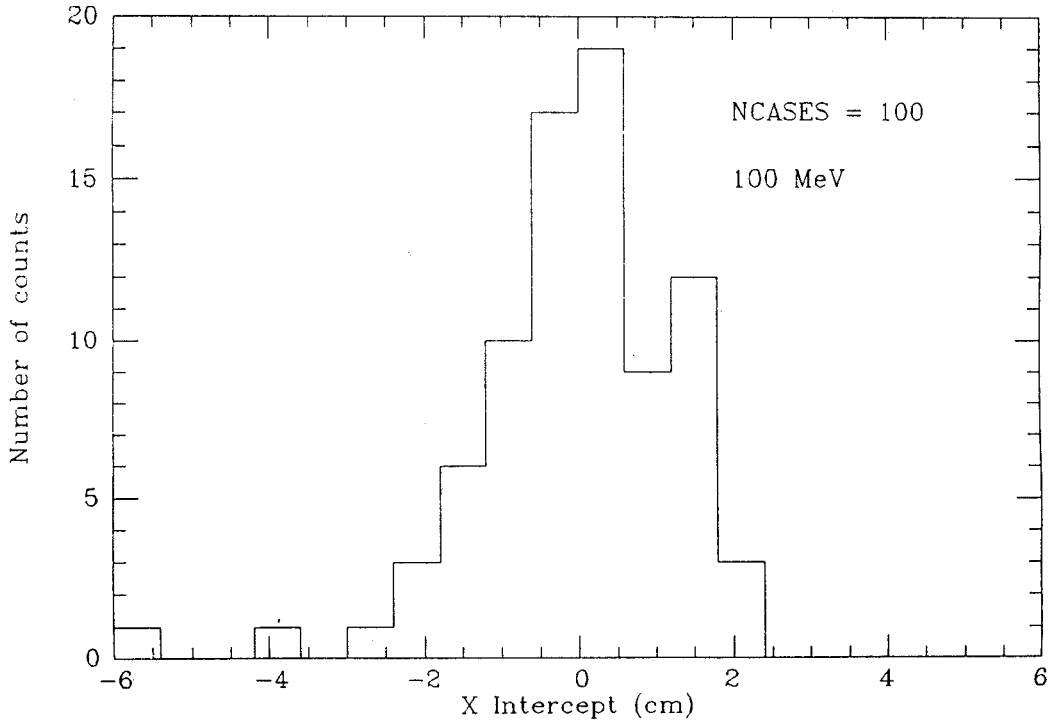
NCASES = 100
100 MeV
Number of counts
X Intercept (cm)
20
15
10
5
0
-6
-4
-2
0
2
4
6

FIG. 6

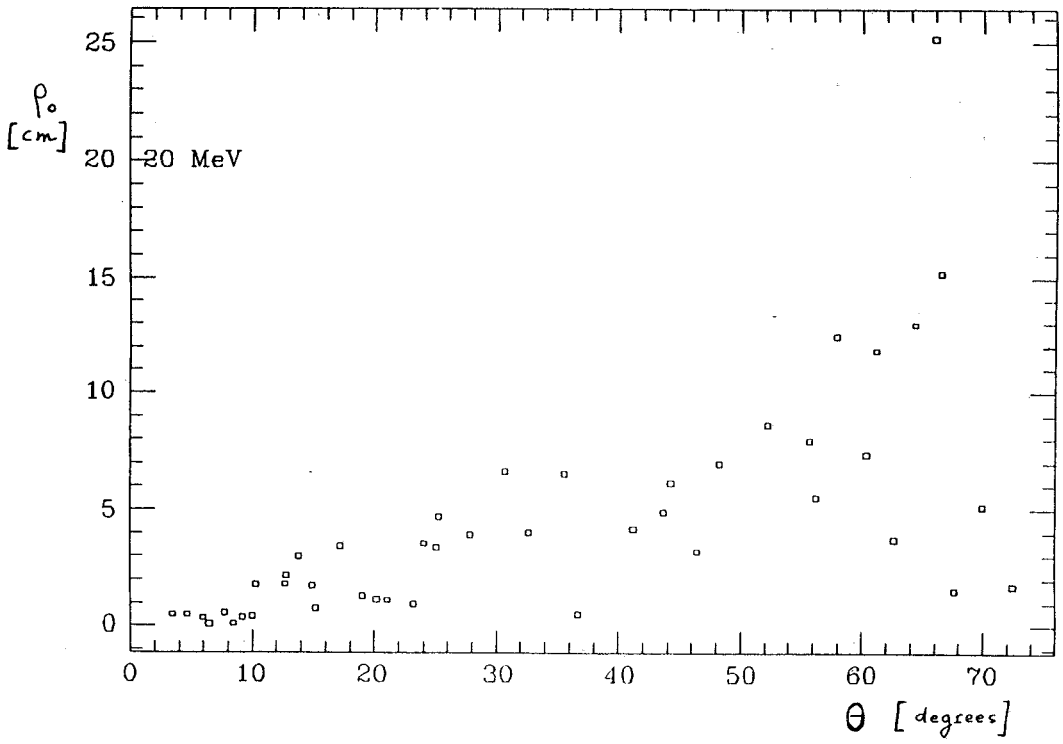
ρ₀ [cm]
20 MeV
25
20
15
10
5
0
0
10
20
30
40
50
60
70
θ [degrees]

FIG. 7a

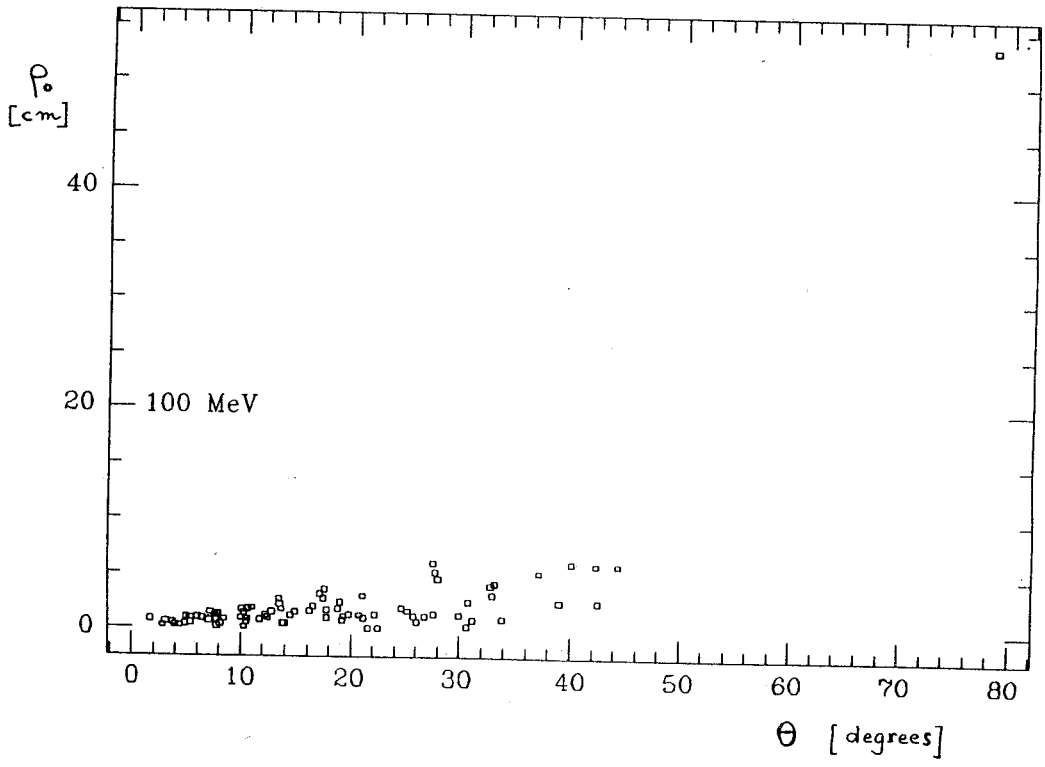
ρ₀ [cm]
100 MeV
40
20
0
0
10
20
30
40
50
60
70
80
θ [degrees]

FIG. 7b

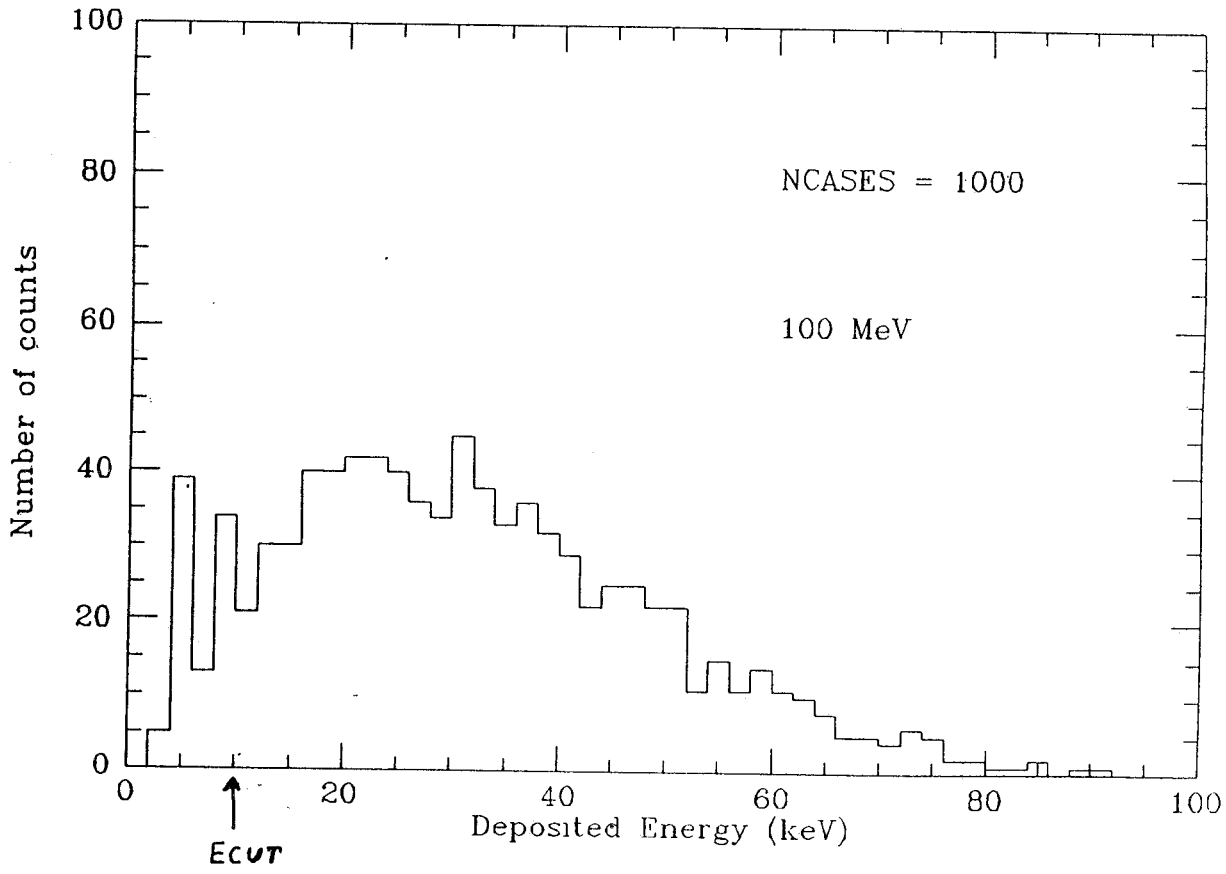
100
80
60
40
20
0
Number of counts
NCASES = 1000
100 MeV
0
20
40
60
80
100
Deposited Energy (keV)
ECUT

FIG. 8

SOLENOIDAL MAGNET DESIGN OF THE PHI-FACTORY DETECTOR

C.Sanelli
INFN - Laboratori Nazionali di Frascati P.O. Box 13, 00044 Frascati (Italy)

The main features of the Phi-Factory detector has been drawn up by M. Piccolo and G. Vignola[1] and are listed below :

-	Axial length	10	m
-	Radius	5	m
-	Axial magnetic field	≤ 1	kGauss
-	Field at the beam location	≈ 0	

Our goal is to carry out the main engineering specifications for the experimental solenoidal magnet and to study an efficient field shielding on the beam trajectory without compromising the field uniformity.

We can divide the all detector in two regions bounded by a conical surface with half aperture angle of 8.5° on each side of the Interaction Point (I.P.).

The requirement is to cancel the field inside this region and to keep good field uniformity outside.

Physically no shield can be placed in a region of $\pm$ 22 cm around the IP where the experiment requires very thin wall.

A first design has been carried out complying with the above requests. The solenoid producing the magnetic field and the iron yoke that conveys the flux outside the solenoid, with its iron plate on the terminal part of the magnet, have been designed.

The solenoid main coil studied has the following geometrical characteristics :

-	average radius	437.5	cm
-	thickness	25	cm
-	total length	9	m

Perhaps the thickness of the solenoid can be reduced increasing the field homogeneity and the free space for the detector.

The iron yoke has the following characteristics :

-	maximum external radius	5	m
-	thickness	25	cm
-	thickness of the holed iron plate	25	cm
-	iron plate hole radius	75	cm

A first design estimate of the main solenoid current can be made in current sheet approximation. The current per meter of solenoid, k, is given by :

$$k=B_o*(h^2+d^2)^{1/2}/(h*\mu_o) \ [Amp/m]$$

where : Bo = Central field = 0.1 T d = solenoid diameter = 8.75 m
h = solenoid length = 9 m μ_o =vacuum permeability=$4\pi 10^{-7}$

The value obtained is ≈ 111000 A/m, but it doesn't take into account the reluctance reduction due to the iron back-leg.

The correct value has been determined by means of POISSON runs.

POISSON indicates that a field greater than 0.1 T can be obtained with about 88900 A/m.

1. Passive shielding

As first approach, iron has been added and shaped near the solenoid axis to cancel the magnetic field in the central region.

Figs. 1 and 2 show the magnetic field on the axis and the iron geometry respectively .

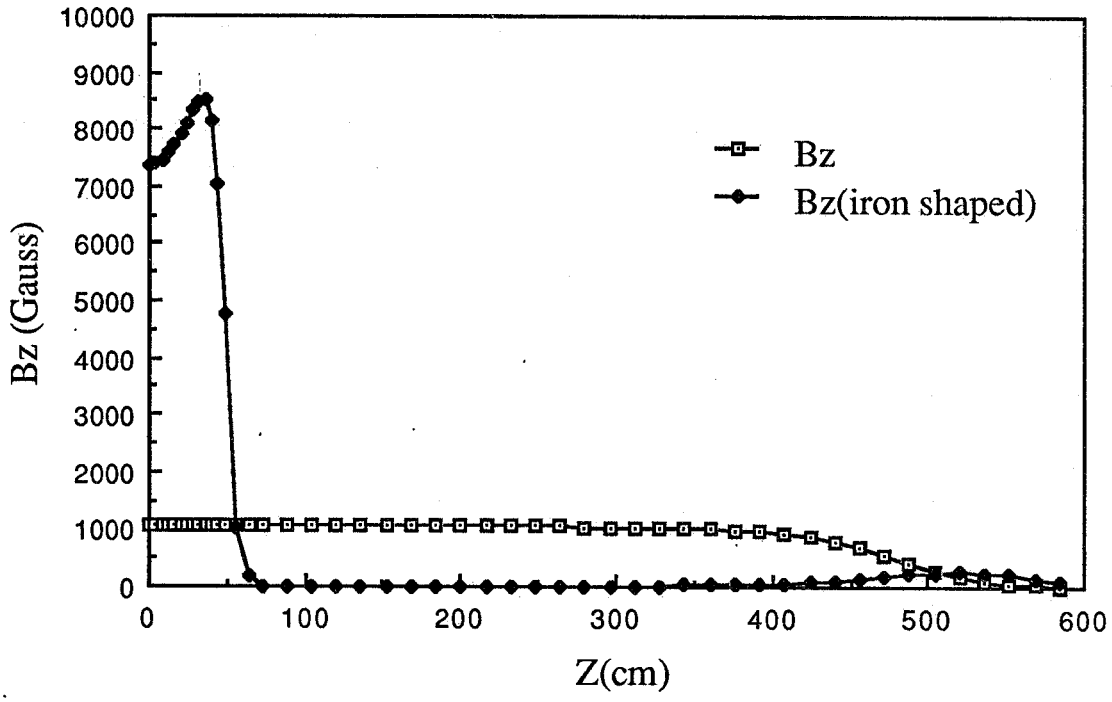

FIG. 1 - Field along the axis with and without iron shield.

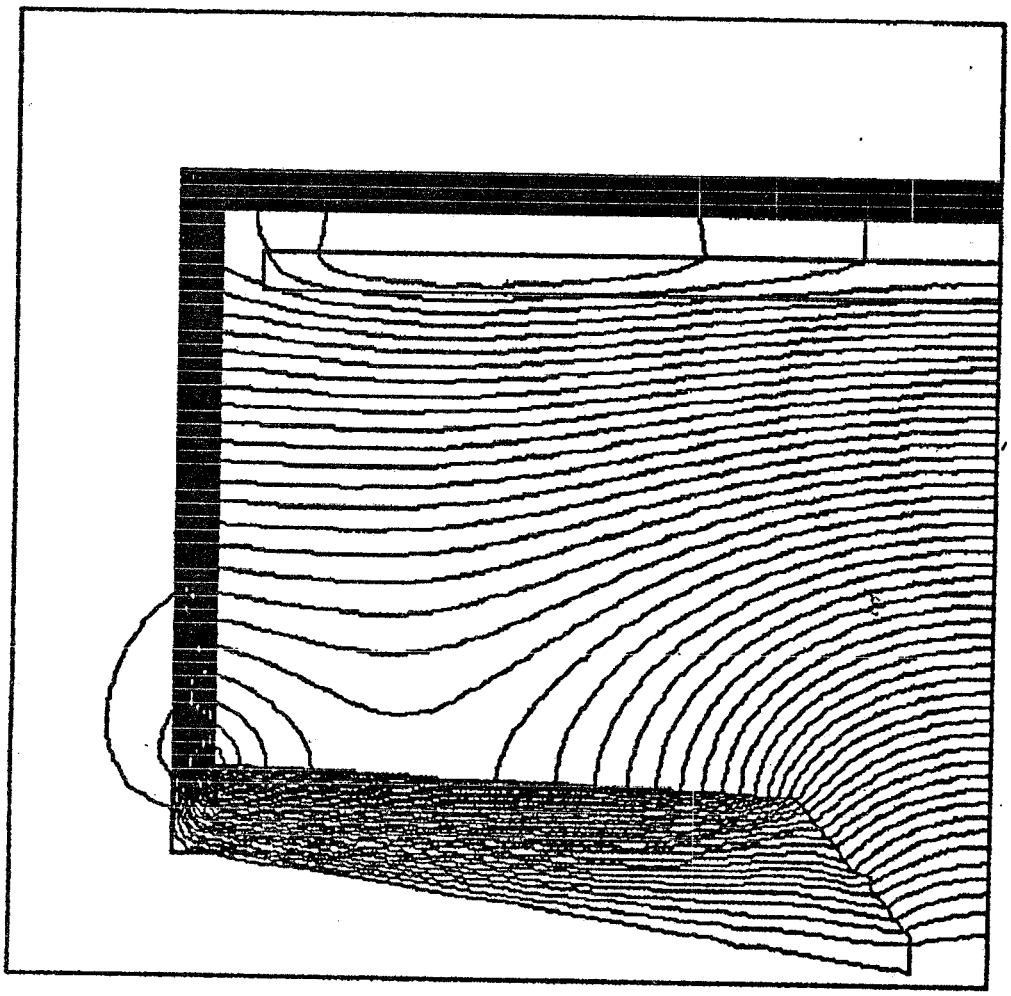

FIG. 2 - Iron geometry and flux lines for the field slope shown in Fig.1.

Because the iron acts as flux concentrator, there is a very strong peak field near the center of the apparatus (about 0.9 T).

The field bump at the end of the curve is due to saturation effects of the iron that is not optimized in these calculations.

The main disadvantage of this type of shielding is the substantial reduction of the free solid angle of the detector.

2. Active shielding

A second shielding system by current sheets has been investigated.

A conical solenoid has been inserted starting at 24 cm from the IP with an inclination of 8.5°, up to 200 cm from the IP. At this distance the radius of the solenoid is 30 cm and, being this radius large enough to install quadrupoles and so on, another solenoid, this time parallel to the axis, has been placed up to 500 cm.

The new geometry is shown in Fig. 3.

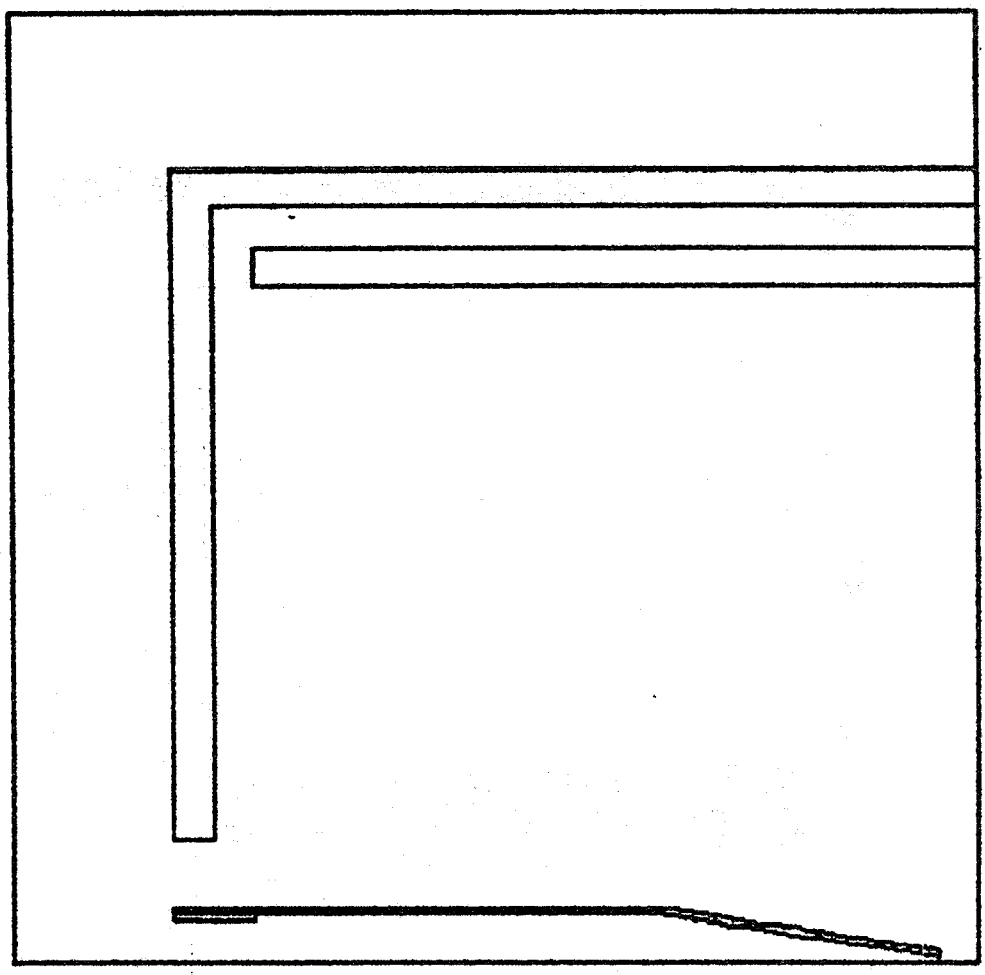

FIG. 3 - Geometry with secondary compensator windings.

To obtain better results the solenoid has been divided in 4 parts, everyone with its proper current, and an additional solenoid has been added at the end of the system to compensate the fringe field effects mainly due to the iron plate.

Fig. 4 shows the magnetic field along the axis of the apparatus in three cases :

1) solution with only two solenoids, one of which is conical and the other is parallel to the axis;
2) solution with 4 windings, as in Figure 3 but without the terminal one;
3) solution with 5 windings, as shown in Figure 3.

The field peak has been reduced to about 1000 Gauss and good results have been obtained in the central region of the magnet. The oscillations of the field around zero are ±10 Gauss.

Let us point out that the peak field is due for lack of shield around the IP, so we find there the magnetic field produced by the main solenoid.

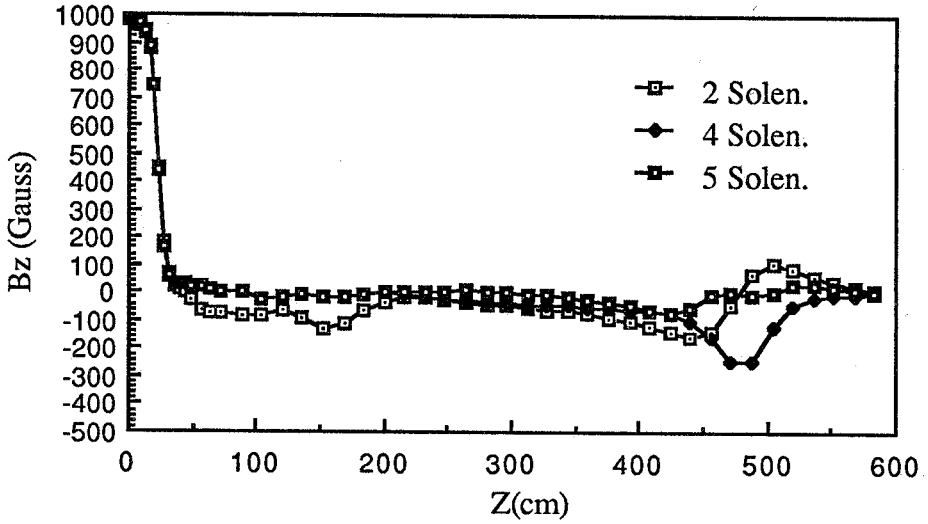

FIG. 4 - Field along the axis with secondary compensator windings.

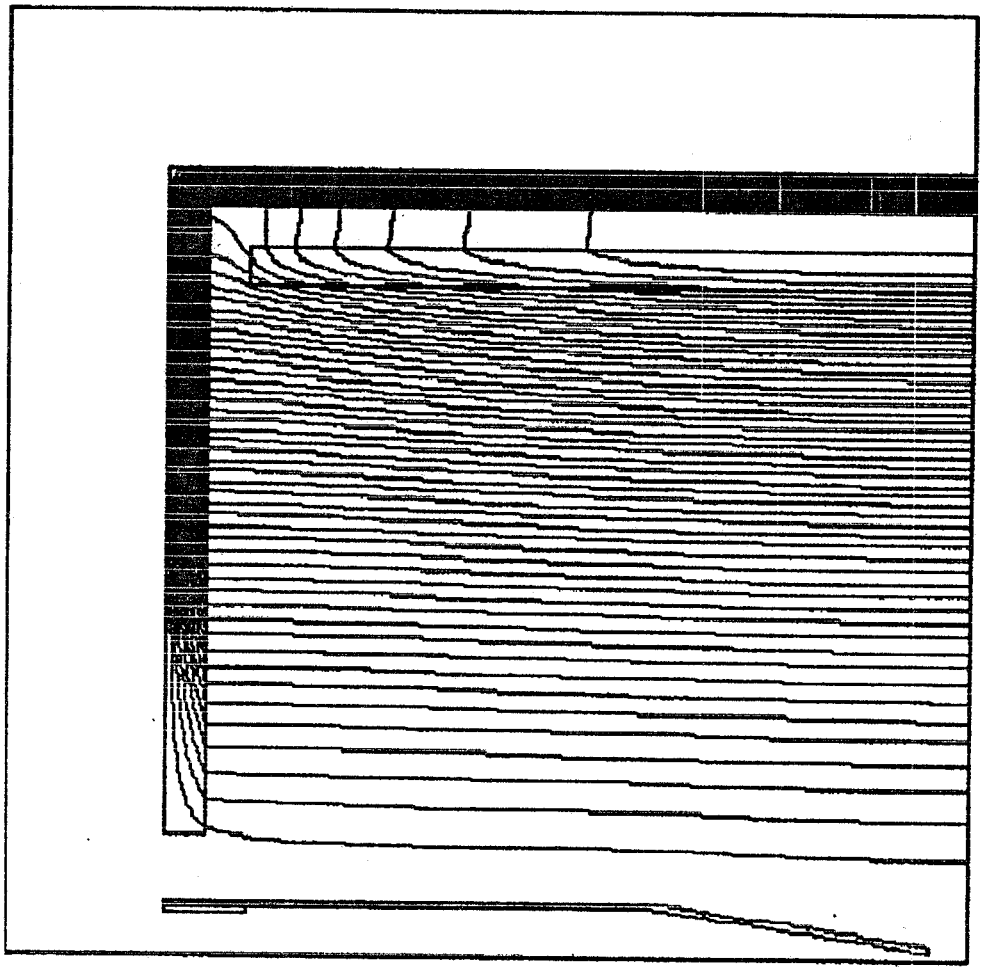

FIG. 5 - Flux lines in the final configuration.

No particular attention has been spent in the ending region where the fringe field must be optimized. The third solution indicates that it is possible to reduce the field variations compensating them with additional coils, but also another way must be studied : to shape the ending part of the iron plate.

Fig. 5 shows the magnetic flux lines in the last solution studied.

The axial field homogeneity in the radial direction is shown in fig. 6 for z = 0, z = 1 m, 2 m, 3 m and z = 4 m as function of the radial coordinate.

Fig. 7 shows the radial field component along the radius for z=1 m, 2 m, 3 m and 4 m. The values for z=0 are not shown because they are, for symmetry reason, always zero.

The number of Amper-turns needed by each solenoid is listed below :

Type	Amp-turns	Length (m)
Main solenoid (full winding)	800,000	9
1° conical solenoid	-62,200	2 * 0.77
2° conical solenoid	-56,000	2 * 0.66
"Elbow" solenoid	-63,000	2 * 0.70
Straight solenoid	-220,000	2 * 2.65
Ending solenoid	-18.700	2 * 0.5

The "elbow" winding needs the maximum value of Amper-turns per meter of solenoid, 90,000 A/m. This value is compatible with a conventional design of the windings; in fact if, for example,we choose a 12 * 12 Ø 7 copper conductor, having 105 mm^2 of useful surface, we can put 77 turns per meter, this means a current of about 1,700 A with a current density of 11.1 A/mm^2. This current density can be easily reached without any cooling problem.

The main advantages are the thinness of the windings, that means a better field homogeneity and then consequently a greater free volume for the detector. Moreover a very standard technology can be used.The main disadvantage is the electrical power necessary, in fact the main solenoid will dissipate ≈ 5 MW. This power must be taken away through forced water cooling that will require a very efficient hydraulic system. The power supply specifications and coil parameters are :

-	Voltage	4.2	kV
-	Current	1.16	kA
-	Main coil resistance	≈ 3.64	Ω
-	Main coil inductance	≈ 3.6	H
-	Total stored energy	≈ 2.5	MJoules

The power, for the field compensator windings, is only ≈ 400 kW in total.

What we suggest is to design a superconducting main solenoid, helium cooled, and to use conventional technique for the compensator solenoids.

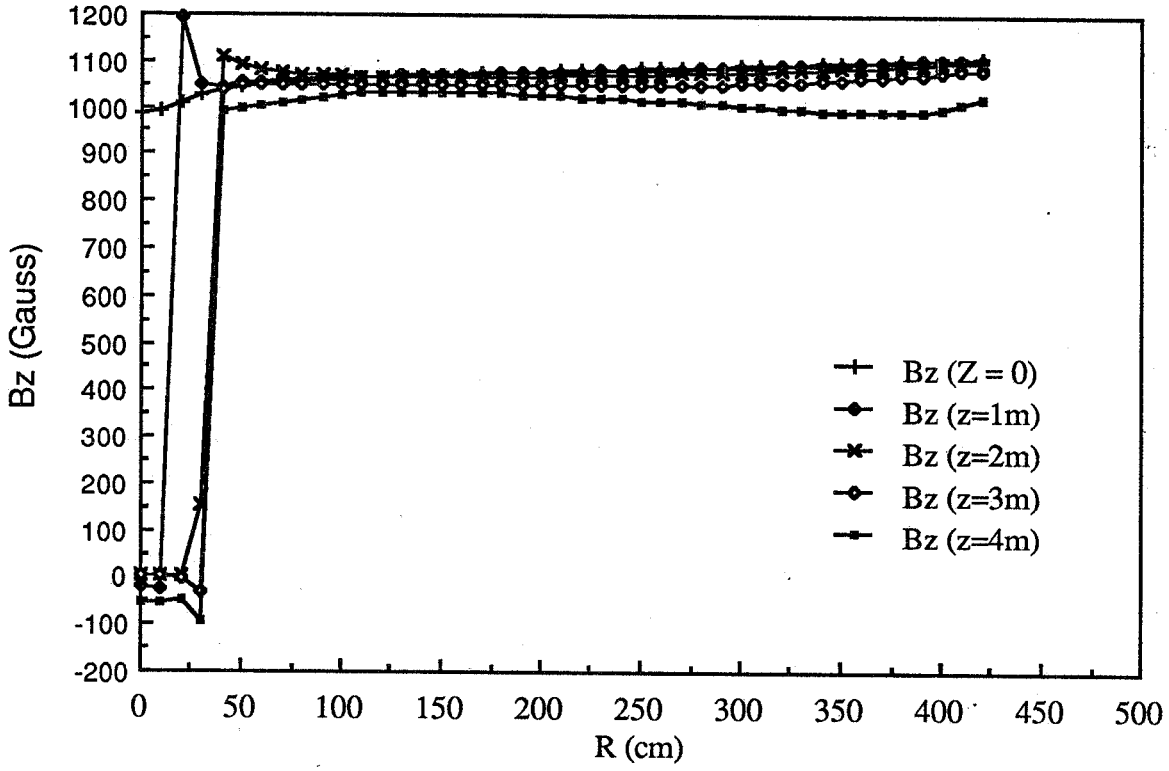

FIG. 6 - Axial field component along the radius.

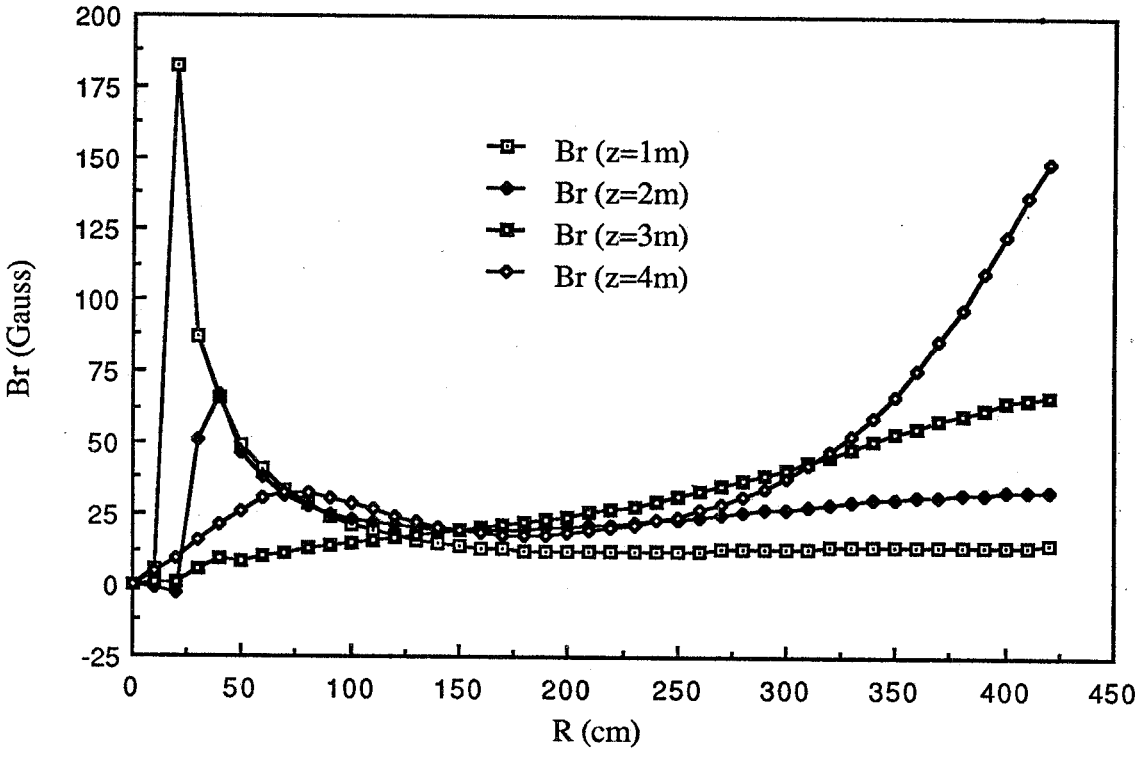

FIG. 7 - Radial field component along the radius.

But, if the axial magnetic field is reduced, for example, to 500 Gauss, the power decreases to 1.25 MW and this value becomes competitive with the power necessary to the cryogenics. This means that the solution whith a conventional main solenoid must be seriously investigated from the economic point of view.

Fig. 8 shows a mechanical lay-out of the proposed solution

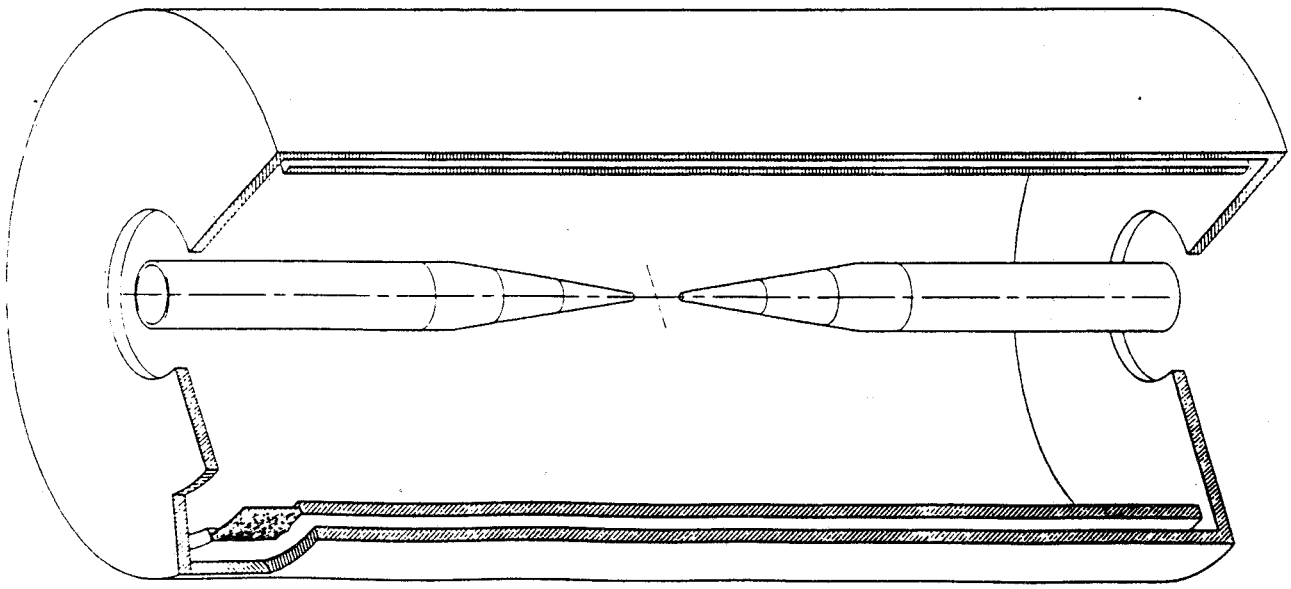

FIG. 8 - Mechanichal lay-out of the proposed active shielding.

REFERENCE

(1) M.Piccolo, G.Vignola - Private communication.

ϵ'/ϵ MEASUREMENTS AT HADRON MACHINES

A. NAPPI

University of Pisa and INFN , Sezione di Pisa

Introduction

Recent measurements of the ϵ'/ϵ parameter have reached a sensitivity in the range of 10^{-3} . However the experimental situation is somewhat inconclusive. The CERN NA31 experiment [1] has measured a non zero value

$$Re(\frac{\epsilon'}{\epsilon}) = (3.3 \pm 0.7(stat) \pm 0.8(syst)) \times 10^{-3}$$

showing the first evidence of an effect of direct CP violation with a significance of three times the error. A recent result presented by the Fermilab E731 experiment [2] to the Stanford Lepton and Photon Interactions conference, while not in significant disagreement with the previous result, is compatible with zero:

$$Re(\frac{\epsilon'}{\epsilon}) = (-0.5 \pm 1.4(stat) \pm 0.6(syst)) \times 10^{-3}$$

A reduction of the error and/or additional measurements with different systematics are called for, in order to confirm (or disprove) the effect found by NA31.

This paper will try to review the present limitations to the statistical and systematic errors and possibilities of improvement. The plan is as follows. Section 1 will present a summary of the errors on the latest measurements; systematic errors will be divided in categories and each of them will be discussed in detail in section 2, in an attempt to identify general limitations of the different kinds of techniques and possible ways to overcome them. Section 3 will give some information on the expectations for forthcoming measurements. Finally section 4 will introduce some ideas for improved measurements which are being investigated.

The level of the discussion will be mainly qualitative and the information on the experiments will be sparse and incomplete. For a more complete treatment I refer to the original papers and to the review contributed by M.Calvetti to this volume.

1. Errors on ϵ'/ϵ measurements: present status

The measurement of the ϵ'/ϵ parameter is obtained, through the relation

$$1 - 6Re(\frac{\epsilon'}{\epsilon}) = \frac{|\eta_{00}|^2}{|\eta_{+-}|^2} = \frac{\Gamma(K_L^0 \to \pi^0\pi^0) \cdot \Gamma(K_S^0 \to \pi^+\pi^-)}{\Gamma(K_S^0 \to \pi^0\pi^0) \cdot \Gamma(K_L^0 \to \pi^+\pi^-)} \qquad (1)$$

from the measurement of the double ratio (R) of decay rates of K_L^0 and K_S^0 defined in (1). In the following I will always refer to this quantity, rather than to ϵ'/ϵ . It will be understood that the error on ϵ'/ϵ is 1/6 of the error on R.

The statistical error is limited by the rarer decay channel $K_L^0 \to \pi^0\pi^0$. The published NA31 result is based on 109000 events in this channel. The corresponding number for the E731 result is 52000. Both experiments are analyzing additional data (more than 2 times the previous sample for NA31, $\approx$ 4 times for E731). This leads to errors on the double ratio in the order of 0.5 % or better.

Some informations on the conditions in which the statistics for the existing results was collected will be useful to show that rates are not yet a problem

per se. For NA31, the published data correspond to a period of ≈3 months of data taking in a beam operated at a flux of $1.8 \times 10^6 K^0$'s per SPS pulse (which required $\approx 10^{11}$ protons on target per pulse). The decays were accepted on a fiducial decay length of $\approx 40m$ and the acceptance of the apparatus for neutral events, including all cuts used in the analysis, was $\approx 15\%$. Typical single counting rates during data taking were $\approx 10^5 Hz$. For E731 the events were collected in ≈20 days in a more intense beam ($1.4 \times 10^7 K^0$'s , corresponding to $\approx 3 \times 10^{12}$ protons on target per pulse) and with the more favorable duty cycle of the Fermilab Tevatron. The fiducial decay length for E731 was only $17m$.

With the advent of these high statistics experiments, systematic errors are more and more a reason of concern. They arise from uncertainties in the knowledge of factors needed to evaluate the decay rates in formula (1) from measured event numbers. The search of measurement techniques allowing total or partial cancellations of these factors is an important element for the reduction of the errors.

Cancellation of the flux normalization is considered a necessary requirement in the latest generation of experiments. This is achieved by the simultaneous detection of two (or more) of the decay channels appearing in the double ratio R. Three classes of techniques have been considered:

a) K_L^0 and K_S^0 beams are alternated, charged and neutral decay modes are detected simultaneously (BNL E749[3] , CERN NA31[1]) ;

b) K_L^0 and K_S^0 beams are simultaneous, charged and neutral decay modes are detected alternately* (FNAL E617[4] , E731 test[5] and E731, for part of the run);

---

* flux cancellation is achieved, statistically, by an experimental arrangement that makes the ratio of fluxes in the two beams equal, in average, when detecting the charged and the neutral decay modes (for E617 and E731 this is obtained by alternating a regenerator between the two sides of a double K_L^0 beam)

c) K_L^0 and K_S^0 beams are simultaneous, charged and neutral decay modes are detected simultaneously (FNAL E731[2] ; also, broadly speaking, a Φ - factory experiment is an example of this type of technique).

The situation can be summarized by saying that flux normalization is no longer an issue. Correction factors related to the detection of the events are now the limiting factor. Many different aspects enter to determine the systematic errors: one is cancellation, that leads to small corrections, but, on one side, cancellation is often approximate and, on the other, the presence of internal checks to constrain the corrections is also important.

For the purpose of the following discussion it may be useful to group the effects that can lead to an experimental correction in the following classes:

- acceptance and detection efficiencies independent of time ;
- time stability of detector response and efficiency;
- rate effects;
- effects of resolution and biases in the measurements;
- background subtraction.

A qualitative discussion of each of these classes will be given in the next section. Here I will try to give an idea of the state of the art by summarizing the performances of NA31 and E731 on each of these points. This summary is shown in Table I, which tries to give not only an indication of the quoted systematic error associated with each correction, but also of the amount of cancellation present in the experiment. This is done in two ways: first with a subjective assessment, in the style of the Michelin guide, and then by giving a figure for the correction (or limit on the correction) associated with each item. It is to be noted that each point usually contains several contributions that are estimated separately and sometimes have opposite signs: a better idea of the amount of cancellation is then given not by the overall correction, but by the largest of the individual contributions.

TABLE I

Contributions to the systematic errors for NA31 and E731

		NA31			E731	
Effect	Cancell.	Correction to R	Systematic error	Cancell.	Correction to R	Systematic error
Acceptance	***	0.70%	0.17%	*	4.4%	0.25%
Time stability		< 0.10%	0.10%	***	—	—
Rate effects	*	0.35%	0.20%	**	< 0.1%	0.10%
Resolution and biases	**	0.70%	0.30%	**	< 0.15%	0.20%
Background subtraction		4.0%	0.28%		4.7%	0.18%

2. Discussion of the sources of systematic errors

2.1 ACCEPTANCE

Cancellation is obtained if the acceptances are the same for K_L^0 and K_S^0 decays to the same channel. If the beam spots at the detector are equal in the two beams, and the limiting apertures are all in one plane, this could be achieved by evaluating the double ratio in small bins of momentum and decay vertex position. However, to avoid effects of event migration through bins due to measurement errors, one would like not to bin variables for which the distributions in K_L^0 and K_S^0 are very different. This is indeed the case for the longitudinal position (z) of the decay vertices, due to the different life times. Thus it appears that the requirement to have negligible acceptance corrections conflicts with the one to have negligible resolution effects.

On the basis of these considerations, E731 prefers not to bin in z. This leads to a relatively large acceptance correction, in spite of the fact that some cancellation exists, because the z ranges for K_L^0 and K_S^0 overlap. The correction, evaluated by a Monte-Carlo simulation of the detector, is the main source of systematic uncertainty in that experiment. It must be said that the quoted error is surprisingly small. To reach this result, the Monte Carlo simulation is subject to many checks, the most sensitive of which are based on its ability to reproduce the distributions observed for K_L^0 decays, for which very high statistics ($\approx 10^7$ events) have been collected.

NA31, instead, tries to accommodate the two conflicting requirements by an arrangement whereby the K_S^0 beam can be "massaged" to reproduce the z distribution typical of the K_L^0 beam (the target is mounted on a moveable train that scans the 50m long K_L^0 decay region). One has to note that the NA31 trick (or any other similar trick) implies that the conditions of the K_S^0 beam have to change with time. This point will be of some importance for the discussion of section 4 , concerning ideas for future measurements..

2.2 TIME STABILITY

The double ratio (1) is insensitive to variations in time of response and efficiency of the detectors, if K_L^0 and K_S^0 data are collected in the same detector, at the same time. This is an advantage of techniques b) and c), which have both been used by E731, in different phases of their data taking. In experiments performed with technique a) , instead, this point requires great attention because a change with time of the detection efficiency will reflect into a change of efficiency between K_L^0 and K_S^0 and a bias on the double ratio.

However the NA31 experience shows that these effects can be kept under control. Long term time drifts can be calibrated off and possible remaining effects can be minimized alternating the two beams at short time periods (in NA31 about one day) and computing the double ratio for data taken in contiguous

periods. Possible short term instabilities, instead, cannot be calibrated and, if present, they would add a source of fluctuations. The monitoring of these possible effects requires a painstaking labour which has two important aspects. The first is a regular control of the quality of the data, provided, for example by checks of the consistency of the rates measured in different components of the detector or by comparing K^0_S data (for which a high statistics is easily obtained) against themselves. The second involves direct measurements of efficiencies, when possible, or determination of limits on possible drifts and of the sensitivity of the double ratio to drifts within these limits. A more detailed discussion would be beyond the scope of this paper, but the NA31 conclusion is that random time instabilities are not a major limitation of the technique. More important are systematic differences between K^0_L and K^0_S , of which the most important are those discussed in the next paragraph.

2.3 RATE EFFECTS

This is the main example of an effect that affects the response of the detector in a way which depends on the type of beam particle (K^0_L or K^0_S). Such effects are present in technique a) , but also in techniques b) and c) to the extent that the decay products of the two beams illuminate different parts of the detector in a different way (this is indeed the case for E731, where the spatial separation of the beams in the detector is relied upon to identify the parent particle of each decay) . In all techniques some degree of cancellation is possible* , but it seems unavoidable that a correction has to be applied.

In both experiments the effect of accidental events is estimated by a simulation based on the software superposition of events collected with a random trigger to real (NA31) or Monte-Carlo (E731) events. The correction and the

---

* in techniques b) and c) this is automatic, since the parts of the detector that see K^0_L and K^0_S decays are not disjoint. In technique a) the effects on K^0_L and K^0_S events can be made similar by adjusting the rates in the two beams, but the choice of the rates to be equalized is not well defined, since the composition of the events from the two beams is totally different.

systematic errors quoted by E731 are smaller, which probably reflects a better level of cancellation of these effects in that experiment. NA31 quotes a relatively large systematic error. The additional data, which are being analyzed now, contain additional timing information which will probably allow to reduce the error; however it is believed that eventually this will be one of the most important limitations of the technique.

2.4 RESOLUTION AND BIASES

Measurement errors on a variable that is binned or restricted to a limited range, imply a bias on the double ratio if the distribution of this variable is different in K_L^0 and K_S^0 . The most important example is the measurement of the kaon energy (E) and of the longitudinal decay vertex position (z) . There are effects of scale as well as of resolution. For a given uncertainty on these quantities, the effect on the double ratio can be made small, by making the E and z distribution as similar as possible in K_L^0 and K_S^0 .

As already discussed, in the approach of NA31, this is possible for the z distribution, by a careful subdivision of the running time among the different K_L^0 and K_S^0 target stations and application of station dependent weights to correct for deviations from the ideal subdivision. For the energy it is not possible to make the K_L^0 and K_S^0 distributions absolutely identical, but a compromise can be found by a careful choice of the parent proton energies and targeting angles. In the published measurement the beam conditions were not optimized for the energy distributions (parent energy and production angle were equal in K_L^0 and K_S^0), and the optimization for the z distributions was not perfect (the subdivision of running time among target stations was not controlled tightly) . This explains why the correction, determined by resolution, and the systematic error, determined by scale, are not negligible, in spite of the good cancellation capabilities of the technique. On this, the data being analyzed now, will do better.

The approach of E731 to this problem is totally different. As already mentioned, in order to avoid large resolution corrections, they do not bin the z distribution, and, to minimize the sensitivity of the result to scale errors they try to optimize the cuts in such a way that there is compensation between events gained and lost through different edges of the accepted regions for E and z.

2.5 BACKGROUND SUBTRACTION

This is an intrinsically asymmetric correction for which no cancellation can be conceived. Thus it has to be made small and its estimate (which usually relies on extrapolation in the distribution of some discriminating variable) has to be reliable. The problem is specially severe for K_L^0 decays, where the dominating CP conserving three body decays have to be rejected at a level of $\approx 10^5$. The suppression has to be particularly effective in the charged channel, where the presence of semileptonic and non leptonic decays with different kinematics characteristics (and therefore different distributions of the kinematical discriminating variables) is an additional source of uncertainty. For example NA31 quotes the same uncertainty (0.2 % of the 2π events) on the subtraction of the charged and of the neutral background, in spite of the fact that the estimated subtraction is 0.65 % for the charged and 4 % for the neutral channel.

The background for the Fermilab experiment has a different composition. Here the three body K_L^0 decays have a better suppression than in NA31: in the charged channel this is explained by the presence of magnetic analysis, in the neutral channel mainly by the shorter decay path (17m instead of 50m) that they use* . However the use of a regenerator to produce K_S^0 introduces the need of corrections, that are peculiar to this technique, for the effects of incoherent regeneration. Incoherent regeneration has to be subtracted not only from K_S^0 data, but also from K_L^0 data, because it causes a large fraction (4.7 %

* the reconstruction technique based on the measurements of the energies and transverse coordinates of the photons implies that events with missing photons are reconstructed with a decay vertex shifted downstream

in the neutral channel) of "cross-overs", i.e. incoherently produced K_S^0 events erroneously attributed to the K_L^0 beam. This last problem is a direct consequence of a change in the trigger policy of the experiment dictated by the need for high statistics. In fact it was absent in previous data (ref. 5) collected by the same collaboration, where the conversion of one of the photons was required, in order to allow a direct measurement of the line of flight of the K.

3. Forthcoming measurements

As mentioned previously, both NA31 and E731 are analyzing additional data, for which results could be expected in one year. For NA31 the main purpose of these data is a reduction of the systematic errors. To this end, some changes to the beam and the apparatus have been made. A description of these changes would require to go into details about the apparatus that have not been given in this paper[6] . So I will limit myself to summarize the results of these changes: the optimization of the beam will reduce, probably by a factor three, the systematic errors due to uncertainties in the energy scale; the improved rejection of the background from K_{e3}, should allow a reduction in the systematic error due to the charged background subtraction; improvements to the K_L^0 beam will allow the use of a fiducial region for the decay vertex, where the neutral background is smaller, without reducing the statistics appreciably; finally, additional timing information from the shower detector will allow more consistency checks on the correction for accidental effects. It is not possible to quantify the improvement to the systematic errors that will be obtained, because this will be a result of the analysis, which is under way now.

For E731 the additional data should yield a factor five in statistics, which would bring their statistical error to the level of their presently quoted systematic errors. However the data have been collected in experimental conditions which are different from those used for their recent result : charged and neutral events have been collected at different times, and, for the neutral data, in presence

of a thin photon converter. Thus one cannot automatically assume that the systematic error will be the same, but this is what they expect.

In conclusion the situation on the ϵ'/ϵ measurement should be clarified within the next year. At least it should become clear whether the 2 sigma discrepancy between NA31 and E731 is significant or not, since both experiments are aiming at errors on Re ϵ'/ϵ smaller than 1×10^{-3} .

4. Long term projects

It is possible to imagine a scenario in which the existence of direct CP violation will not be settled by the forthcoming measurements from E731 and NA31. This will make a new measurement, with improved precision, necessary. A minimal goal for the next generation of experiments is a reduction of a factor 3 in the error. This will be by no means a trivial task. Statistics in the order of 10^6 $K_L^0 \rightarrow \pi^0\pi^0$ events would be needed. The necessary rates would not pose problems by themselves, but the point is being able to control the detection efficiencies at the level of one or two permill in presence of the higher rates. An experimental approach based on simultaneous detection of K_L^0 and K_S^0 decays (techniques b or c of section 1) seems indicated. Type c) technique seems particularly attractive, because it would appear that, within that technique, one could devise experiments that allow the maximum number of cancellations of correction factors. In particular one could hope to combine the favorable features of NA31 (acceptance cancellation) with those of E731 (cancellation of time dependencies and rate effects) . Some components of the NA31 collaboration have investigated possible approaches in this direction. Two ideas have emerged[7] .

One is based on the use of two beams that cross at the detector plane at an angle large enough that, also for the neutral channel, the parent beam can be identified from a measurement of the directions of the showers. This scheme would have the advantage that the beams are separated in the decay region, so that it would allow the use of a moving target station for the K_S^0 beam, as in

the present experiment. On the other side the cancellation of time dependencies and rate effects would not be complete, because not all the K_L^0 decays originate from the same fiducial region as the K_S^0 taken at the same time. Other difficult problems in this technique would be how to symmetrize the detector at different planes (the beam images coincide only in one plane) and the design of a detector that allows the assignment of a decay to the correct beam with a negligible fraction of mistakes.

These difficulties have led to consider a second scheme, in which one would have two nearly collinear beams, the K_S^0 produced on a target close to the decay region, the K_L^0 on a far target . In this scheme the identification of the parent beam will rely on a tagging technique, based on a coincidence with a proton in the beam hitting the K_S^0 target. The advantages of this scheme would be that the two beams would be practically coincident not only at one plane. This eases the constraints on the detector and makes the cancellation of time dependence and rate effects very effective. However, in this technique, the small separation of the beams no longer allows the use of a moveable K_S^0 target station and thus the acceptance correction would not cancel. The situation then would become similar to the E731 one, but some distinct improvements with respect to that situation can be identified. The first is the absence of a regenerator, which is a source of high rates due to neutron interactions and introduces, as explained in section 2.5 , some peculiar problems of background subtraction. The second is the fact that the beam spots at the detector could be made practically coincident, which would make many cancellations, like, e.g., for rate effects, even more effective than in E731.

More daring ideas have been put forward [8] by members of the E731 collaboration . The use of the new Main Injector at Fermilab is envisaged as a means to produce beams that should allow measurements of rare K_L^0 decays of interest within the problematics of direct CP violation (in particular $K_L^0 \rightarrow \pi^0 e^+ e^-$) and measurements of ϵ'/ϵ with statistical precision better than 10^{-4}.

None of these ideas has evolved yet into a design of an actual experiment. The key point will be to prove that the systematic errors can be kept at the level which is aimed for. Even allowing for some correlation between statistical and systematic errors, due to the possibility of more precise consistency checks, the problems are arduous and the measurements will not be a trivial extrapolation of the present ones.

Since this is a paper contributed to a Φ - factory study, I wish to conclude by saying that similar considerations could be made for a possible experiment at a Φ - factory . Setting considerations of statistics aside, it seems to me that the effects discussed in section 2.1 , 2.4 , 2.5 can be limiting factors also in a Φ - factory experiment and will have to be addressed in the design of the experiment. I hope that the considerations of this paper can be of some use for the interesting work that will go in this direction.

REFERENCES

1. H.Burkhardt et al., Phys. Lett. B206 (1988) 169.
2. B.Winstein, A measurement of ϵ'/ϵ by E731, EFI 89-60, to appear in the Proceedings of the XIV International Symposium on Lepton and Photon Interactions (Stanford 1989) .
3. J.K.Black et al., Phys. Rev. Letters 54 (1984) 1628 .
4. R.H.Bernstein et al., Phys. Rev. Letters 54 (1984) 1631 .
5. M.Woods et al., Phys. Rev. Letters 60 (1988) 1695 .
6. More detailed information on this subject can be found in:

   D. Fournier, NA31 results on CP violation in K decays, and a test of CPT, CERN-EP/90-01, to appear in the Proceedings of the XIV International Symposium on Lepton and Photon Interactions (Stanford 1989) ;

   A. Nappi, The NA31 ϵ'/ϵ measurement, to appear in the Proceedings of the EPS Conference on High Energy and Particle Physics (Madrid 1989).

7. G.D.Barr et al., Feasibility study for precision CP-violation and rare decay experiments in a high intensity neutral kaon beam at the SPS, CERN/ SPSC/ 89-39, SPSC/I 175 (1989).
8. B.Winstein et al., CP violation in the kaon system with the Fermilab upgrade, in Proc. of the Rare Decay Symposium (Vancouver 1988) ed. by D.Bryman et al., Singapore: World Sci., 1989.

RELAZIONE SULLA SITUAZIONE SPERIMENTALE DELLA VIOLAZIONE DI CP NEI DECADIMENTI DEI MESONI K NEUTRI

M. Calvetti
Dipartimento di Fisica e INFN dell'Università di Perugia.

I decadimenti dei mesoni K neutri sono l'unico fenomeno fisico in cui sia stata osservata la violazione di CP.

La ricerca di effetti nei decadimenti dei mesoni contenenti quark pesanti (B-mesons) é naturalmente possibile,ma le difficoltà sperimentali incontrate nella ricostruzione di stati finali a molte particelle, tipici dei loro decadimenti, e le difficoltà di produzione sono tali che presumibilmente i mesoni K resteranno l'unico sistema fisico in cui la violazione di CP sarà osservata ancora per molti anni.

In questa relazione si descrive la situazione sperimentale attuale e si discutono le caratteristiche che dovranno avere gli esperimenti della prossima generazione.

FENOMENOLOGIA E DEFINIZIONI DEI PARAMETRI CHE DESCRIVONO LA VIOLAZIONE DI CP

L'unicità dei mesoni K risiede nel fatto che sono le particelle di massa più bassa dotate di stranezza. Una volta che sono stati prodotti in interazioni adroniche o in annichilazioni e^+e^- possono decadere soltanto attraverso le interazioni deboli ,violando la stranezza,in sistemi di particelle di massa più bassa come pioni, elettroni,mesoni μ e neutrini.

La necessità di decadere tramite le interazioni deboli (quelle forti ed elettromagnetiche conservano la stranezza), cioé attraverso l'emissione ed assorbimento di W virtuali,insieme con il limitato numero di canali accessibili, fa si che le vite medie siano molto lunghe,fino a 50 nsec, e ciò rende possibile la realizzazione in laboratorio di fasci di K che rendono la sperimentazione relativamente facile.

Nella descrizione fenomenologica del fenomeno é utile introdurre gli stati K_1 e K_2 (autostati di CP degeneri in massa ma con stranezza opposta) combinazioni lineari degli stati $K0$ -$\overline{K0}$:

$$K_1 = (K0 + \overline{K0})/2 \quad CP = +1$$
$$K_2 = (K0 - \overline{K0})/2 \quad CP = -1$$

Gli stati fisici dei mesoni K neutri a vita media lunga (K-long) e corta (K-short) sono combinazioni lineari di K_1 e K_2:

$$K_S = (K_1 + \varepsilon K_2)/\sqrt{(1 + \varepsilon^2)}$$
$$K_L = (K_2 + \varepsilon K_1)/\sqrt{(1 + \varepsilon^2)}$$

dove ε é il parametro che misura la componente impura di CP negli autostati di massa.

L'evidenza sperimentale della violazione di CP consiste nell'osservazione del cambiamento di segno della figura di interferenza quando si osservano le distribuzioni in tempo proprio dei decadimenti in due pioni da fasci di K0 e $\overline{K0}$.

Ciò é possibile perché il K_L,a causa della sua componete K_1 dovuta al mixing, decade in due pioni nel 2‰ dei casi .

I rapporti tra le ampiezze di decadimento in due pioni del K_Le K_S sono comunemente indicati come:

$$\eta^{+-} = \frac{<\pi + \pi - |K_L>}{< \pi + \pi - |K_S>} \qquad \eta^{oo} = \frac{<\pi^o\pi^o|K_L>}{<\pi^o\pi^o|K_S>}$$

Nel modello superdebole di Wolfenstein (ref6)del 1964 la violazione di CP è generata nella matrice di massa ,cioé esclusivamente nel fenomeno di mixing, mentre l'ampiezza di decadimento $<\pi\pi|K_2> = 0$. In tale scenario si ammette l'esistenza di una interazione superdebole che al primo ordine permette le transizioni K0-$\overline{K0}$ violando CP ($\Delta S = 2$),mentre il decadimento avviene tramite le interazioni deboli con $\Delta S = 1$ che non la violano.

In questo schema si ha:

$$\eta^{+-} = \eta^{oo} = \varepsilon$$

Nel caso generale invece é possibile che la violazione si abbia anche nell'ampiezza di decadimento,cioé che $<\pi\pi|K_2> \neq 0$ che é il caso del modello standard attraverso grafici del tipo Penguin.

Indicando con A_2 ed A_0 le ampiezze di decadimento negli stati finali a due pioni con spin isotopico totale 2 e 0 rispettivamente .

Si ha:

$<\pi\pi|K0> = A0\, e^{i\delta 0}$ variazione di spin isotopico $\Delta I = 1/2$

$<\pi\pi|K0> = A2\, e^{i\delta 2}$ " " " $\Delta I = 3/2$

dove δ_0 e δ_2 sono gli sfasamenti introdotti nelle ampiezze di decadimento dalle interazioni forti dei due pioni nello stato finale in onda S.

Usando le definizioni di η^{oo} e η^{+-} ed esprimendo i due possibili stati di carica in funzione degli autostati di isospin si puo' dimostrare che:

$$\eta^{oo} = \varepsilon - 2\varepsilon' \quad \eta^{+-} = \varepsilon + \varepsilon'$$

dove $\varepsilon' = (i/\sqrt{2})\ \mathrm{Im}(A2/A0)\ \exp(\delta 2 - \delta 0)$

In generale se esistono due ampiezze diverse (A0 ed A2) che conducono allo stesso stato finale (carico o neutro) e che non sono relativamente reali, allora CP é violata nell'ampieza di decadimento.

In questo caso $\eta^{oo} \neq \eta^{+-}$.

I parametri fondamentali che descrivono la violazione di CP sono quindi i due numeri complessi ε ed ε'. Il primo descrive l'intensità della violazione nel processo di mixing mentre il secondo misura il contributo dato dall'ampiezza di decadimento.

La fase di ε' é determinata dalla differenza degli sfasamenti $\delta 2$-$\delta 0$ misurati sperimentalmente

$$\delta 0 - \delta 2 = 45° +\!- 15°$$

da cui risulta

$$\Phi(\varepsilon') = \pi/2 + \delta 2 - \delta 0 = 45° +\!- 15°$$

La fase di ε si ottiene osservando che se si scrive l'hamiltoniana del sistema K0-K0 come

$$\begin{pmatrix} M_{11} & M_{12} \\ M_{12}^* & M_{11} \end{pmatrix} - i/2 \begin{pmatrix} \Gamma_{11} & \Gamma_{12} \\ \Gamma_{12}^* & \Gamma_{11} \end{pmatrix}$$

si ha $$\varepsilon = \frac{(1/2)\mathrm{Im}\,\Gamma_{12} - i\,\mathrm{Im}M_{12}}{\Delta m - i\,\mathrm{Re}\Gamma_{12}}$$

Sapendo che $\Delta m = -2\mathrm{Re}M_{12}$

$$\Gamma_l - \Gamma_s = -2\mathrm{Re}\Gamma_{12}$$

$$\Delta m = (\Gamma_S - \Gamma_l)/2 \ \text{(sperimentale)}$$

si ottiene

$$\phi(\varepsilon) = \tan - 1\ (2(ml - ms)/(\Gamma_S - \Gamma_l) = 43.7° +\!- 0.2°$$

ε ed ε' hanno quindi fasi simili e si possono considerare relativamente reali.

In questa ipotesi supponendo, come si verifica sperimentalmente, che

$$|\varepsilon'/\varepsilon| << 1$$

si ottiene :

$$|\eta^{00}/\eta^{+-}|^2 = 1 - 6\,\varepsilon'/\varepsilon$$

Questa relazione é stata usata nell'ultima generazione di esperimenti per la misura di ε'/ε come sarà descritto in seguito.

La presenza di una componente di opposta CP negli stati Ks e Kl, insieme con la regola $\Delta S = \Delta Q$ per le interazioni deboli, genera anche una asimmetria di carica osservabile nei decadimenti semileptonici

$$\delta = \frac{\langle \pi^- l^+ \nu \mid K_l\rangle - \langle \pi^+ l^- \nu \mid Kl\rangle}{\langle \pi^- l^+ \nu \mid Kl\rangle + \langle \pi^+ l^- \nu \mid Kl\rangle} = 2\mathrm{Re}\varepsilon = (3.3 +- 0.1)^{*}10^{-3}$$

misurato nei decadimenti Ke3 e Kμ3.

I parametri usati per descrivere la violazione di CP nei decadimenti dei K neutri sono quindi:

ε	violazione di CP nel mixing K0-$\overline{K0}$	
ε'	violazione diretta di CP nel decadimento (circa 1/1000 di e)	
$\eta\,00$	$= \varepsilon - 2\varepsilon'$	rapporto delle ampiezze di decadimento Kl -Ks
$\eta +-$	$= \varepsilon + \varepsilon'$	= = = = =
δ	$= 2\mathrm{Re}\,\varepsilon$	asimmetria di carica nei decadimenti semileptonici
Δm	$= M_l - M_S$	differenza di massa
τ_s		vita media Ks
τ_l		= = Kl
$\delta 2 - \delta 0$		phase-shifts in onda S per i pioni nello stato finale.

SITUAZIONE SPERIMENTALE

Una rassegna della situazione sperimentale sulla misura dei vari parametri descritti é stata presentata da H.Wahl al "Rare Decay Symposium" Vancouver 1988 (CERN-EP/89-86).Se ne presenta un estratto con alcuni aggiornamenti:

1) **Phase-shift**

				referenza
$\delta 2 - \delta 0 =$	53°+-5°	1976	Kleinknecht	8
	41°+-8°	1979	Devlin e dickey	9
	29°+-3°	1981	Biswas et all	10
	56°+-3°	1986-7	Kamal-Cheng	11

Si notino le notevoli discrepanze tra i risultati sperimentali specialmente tra le due misure più recenti che quotano l'errore minimo.

Non é chiaro quale sia il valore da usare, tuttavia risulta indubbio che il valore reale non é molto diverso dalla fase di ε e l'approssimazione fatta di considerare ε ed ε' relativamente reali é valida.

2)Asimmetria di carica δ.

Solo i risultati che differiscono meno di tre deviazioni standard dal valore medio sono riportati:

δ =	3.46+-0.33	Ke3	1970 Marx et al.	12
	2.78+-0.61	Kμ3	1972 Piccioni et al.	13
	3.33+-0.50	Ke3+Kμ3	1973 Williams et al.	14
	3.18+-0.38	Ke3	1973 Fitch et al.	15
	3.41+-0.18	Ke3	1974 Geweniger et al.	16
	3.13+-0.29	Kμ3	1974 Geweniger et al.	16

$\delta=(3.30+-0.12)\times10^{-3}$ media

La parte reale di ε risulta quindi essere $Re\varepsilon = (1.65+-0.06)\times10^{-3}$

3)Differenza di massa Kl-Ks

Il valore di Δm é stato misurato in esperimenti che usano il metodo del doppio rigeneratore:

Δm	= 0.542+-0.006		1970 Cullen et al.	28
	= 0.534+-0.0026+-0.0015		1974 Geweniger at al.	9
	= 0.5351+-0.004 +-0.0016		1974 Gjesdal et al.	30

$\Delta m = (0.5351+-0.0024)\times10^{10}\ sec^{-1}$ in media

4) vite medie τ_S, τ_l

Nella tabella seguente sono riportati i risultati degli esperimenti che hanno misurato la vita media del Ks:

$\tau s\ (10^{-10})$ sec	#eventi		
0.8920+-0.0044	214K	Grossman '87	62
0.8810+-0.0094	26K	Aronson '76	63
0.8913+-0.0032		Carithers '75	31
0.8937+-0.0048	6M	Geweniger '74	17
0.8958+-0.0045	50K	Skjeggest '72	61

0.8922+-0.0045 in media

Da notare che in tutti questi esperimenti è stato necessario ricorrere alla simulazione dell'apparato per la valutazione numerica dell'efficienza. I dati di Aronson et al dell'82 non sono

stati inclusi nel calcolo del valore medio perchè mostravano una dipendenza della vita media dall'energia del K.

La vita media del Kl è stata sostanzialmente misurata da un solo esperimento con una statistica di 400K eventi ottenendo il risultato

τ_L = (5.154+-0.044)x10^{-10}sec Vosburgh et al '72 64

5) η+-

Il modulo di η+- é stato misurato in vari esperimenti misurando il rapporto tra il branching-ratio in $\pi^+\pi^-$ ed i branching-ratios nei canali a tre corpi per i decadimenti del Kl:

$\pi^+\pi^-/\pi^+\pi^-\pi^0$	(1.64+-0.04)x10-2	1973 Messner	24
$\pi^+\pi^-$/ke3+kμ3	(3.04+-0.13)x10-3	1977 DeVoe	25
$\pi^+\pi^-$/ke3+kμ3	(3.13+-0.14)x10-3	1985 Coupal	26

dai quali si deduce un Br(Kl $\rightarrow \pi^+\pi^-$) = (2.03+-0.043)x10-3

Usando Br (Ks $\rightarrow \pi^+\pi^-$) = 0.6861+-0.0026
τs = (0.8922+-0.002)x10^{-10}sec
τl = (518+-4)x10^{-10} sec

si ottiene η+- :

$|\eta+-|$ = (2.272+-0.0217)x10^{-3}

Il modulo e la fase di η+- possono essere misurati direttamente osservando la figura di interferenza dei decadimenti Kl e Ks in due pioni:

$$I(t) = N (e^{-\Gamma st} + |\eta^{+-}|^2 e^{-\Gamma lt} + 2D |\eta^{+-}| e^{-(\Gamma l+\Gamma s)t/2} \cos(\Delta mt-\Phi^{+-}))$$

Il fit ai dati della figura di interferenza é a molti parametri, (η+-, ϕ+-, Δm, τs, τl, D, N) e ci sono delle forti correlazioni tra di essi.

Per migliorare la precisione di misura in genere si fissano i valori di alcuni parametri, come Δm e le vite medie, al valore più probabile ottenuto in esperimenti precedenti meno sensibili alla forma della figura di interferenza.

Combinando i vari metodi di misura si ottiene

$|\eta^{+-}|$ = (2.272+-0.021)x10-3

mentre la fase Φ+- é data in termini della differenza di massa Δm essendo con essa direttamente correlata:

arg η^{+-}	= 49.4+-1 + 305 (Δm/0.54 -1)	1974 Geweniger et al.	18
	= 45.5+-2.8 +120(1-0.5348/Δm)	1975 Carithers et al.	31
	= 41.7+-3.3+300(ΔM/0.5351-1)	1979 Christenson et al.	32

arg Φ+- = 45.6+-1.4 valore medio trovato usando il Δm quotato precedentemente.

Il valore di Φ+- comunemente più quotato di 44.6°+-1.2° é stato ottenuto includendo anche i risultati dell'esperimento di Jensen et al.(1970) che tuttavia contiene un bias dovuto alle correlazioni ed ai valori assunti per τs e $|\eta$+-| che non può essere corretto.

6) η^{00}/η^{+-}

Il modulo di η^{00} é stato misurato indirettamente misurando il rapporto η^{00}/η+- in vari esperimenti:

$\lvert\eta^{00}/\eta^{+-}\rvert^2$	= 1.00+- 0.06	1972 Holder et al.	40
	= 1.03+-0.07	1972 Banner et al.	41
	= 1.00+- 0.09	1979 Christenson et al.	19
	= 1.02+-0.09 in media		
ε/ε'	= 0.002+-0.007+-0.004	1985 Black et al.	20
	= -0.005+-0.005+-0.004	1985 Bernstein et al.	21
$R = \lvert\eta^{00}/\eta^{+-}\rvert^2$	= 1.015 +-0.03 in media		
	ε'/ε = 0.0032+-0.0028+-0.0012	1988 Woods et al.	22
$R = \lvert\eta^{00}/\eta$+-$\rvert^2$	= 0.98+-0.004+-0.005	1988 Burkhardt et al.	2
R= $\lvert\eta^{00}/\eta$+-$\rvert^2$	= 0.980+-0.006 in media		
	Re ε'/ε =(3.3+-1.0)x10-3		

Inoltre:

arg η^{00}/η^{+-}	= 7.6°+-18°	1973 Barbiellini et al.	34
arg η^{00}	= 55.7°+-5.8°+215°(Δm/0.535-1)	1979 Christenson et al.	19
arg η^{00}/η^{+-}	= +0.3+-2.6+-1.1	1989 NA31	

MISURA DI ε'/ε

Il modello standard che descrive la violazione di CP come una conseguenza naturale dell'esistenza di tre famiglie di quarks introducendo una fase δ nella matrice di Kobayashi-Maskawa prevede un valore di ε'/ε dell'ordine di 1-3%° per valori della massa del quark-t tra 70-100 Gev.

E' chiaro che la verifica sperimentale dell'esistenza della violazione diretta ($\varepsilon'/\varepsilon \neq 0$) è di primario interesse scientifico.

Il metodo usato per la misura é quello del doppio rapporto:

$\varepsilon'/\varepsilon = 1/6(1- |\eta^{oo}/\eta^{+-}|^2)$

Vengono contati il numero di eventi di decadimento in $\pi^+\pi^-$ e $\pi^o\,\pi^o$ con fasci di Kl e Ks.Col metodo del doppio rapporto le efficienze di rivelazione (10% circa a seconda dell'energia del K e della geometria dell'apparato) ed i flussi integrati si cancellano al primo ordine.

Il fascio Kl viene prodotto ponendo la targhetta lontano dalla zona di fiducia dell'esperimento,mentre i Ks possono essere prodotti sia attraverso la rigenerazione di un fascio Kl (esperimento E731 FNAL), sia ponendo la targhetta vicino all'esperimento (NA31 CERN).

NA31-CERN (Ref.43)

Vengono raccolti dati alternando i fasci di Kl e Ks rivelando contemporaneamente i decadimenti carichi e neutri.La stazione di produzione dei Ks viene spostata lungo la zona di fiducia dell'esperimento (50 metri circa) al fine di generare una distribuzione spaziale dei decadimenti simile per Ks e Kl.

Le principali caratteristiche dell'esperimento sono le seguenti (vedi Fig.1) :

- i fasci Kl e Ks si propagano nel vuoto attraverso tutto l'apparato
- contatori anulari di anticoincidenza esterni all'accettanza geometrica del rivelatore per ridurre il numero di decadimenti a tre corpi rivelati.
- due camere a fili distanti 25m con risoluzione spaziale di +-0.5 mm.
- calorimetro elettromagnetico ad argon liquido che misura la posizione dei fotoni con risoluzione +-0.5 mm e l'energia con risoluzione σ=+-7%/$\sqrt{}$(E).
- calorimetro adronico ferro-scintillatore con risoluzione energetica +-65%/$\sqrt{}$(E).
- contatori e logica di trigger per selezione degli eventi.

Il problema principale è la reiezione del fondo,sia a livello di trigger che di selezione finale degli eventi,nel caso dei decadimenti a due corpi del Kl.

Nella tabella 1 sono riportati i vari canali di decadimento del Kl e la loro intensità relativa rispetto ai due corpi.

TABELLA 1

$K_l \rightarrow 2\pi^o$	(segnale)	0.094 %	x
$\rightarrow 3\pi^o$	fondo	21.5 %	230x
$K_l \rightarrow \pi^+\pi^-$	(segnale)	0.203%	x
$\rightarrow \pi e \nu$	fondo	38.7 %	190x
$\rightarrow \pi \mu \nu$	"	27.1 %	130x
$\rightarrow \pi^+\pi^-\pi^o$	"	12.4 %	60x
$\rightarrow \pi e \nu\, \gamma$	"	1.3 %	6x
$\rightarrow \pi\pi\gamma\gamma$	"	4.4x10 -5	0.02x

$\pi^\circ\pi^\circ$

I decadimenti $\pi^\circ\pi^\circ$ sono ricostruiti selezionando eventi con 4 e solo 4 fotoni.Il vertice di decadimento è calcolato imponendo la massa invariante del K ai 4 fotoni.Indicando con zd-zv la distanza tra il rivelatore e la posizione del vertice di decadimento si ha:

$$z_d - z_v = (1/m_k)\sqrt{(\Sigma_{i>j} E_i E_j[(x_i-x_j)^2 + (y_i-y_j)^2])}$$

dove x, y, E sono le posizioni e le energie dei 4 fotoni.

Una volta trovato il vertice si accoppiano i fotoni due a due calcolandone la massa invariante.Si sceglie la combinazione che genera le masse più vicine alla massa del π°.

In Fig.2 sono mostrati i risultati ottenuti con fascio Kl.Il fondo da sottrarre si ottiene estrapolando la distribuzione ottenuta nella zona del segnale.Il fondo risulta essere circa il 4% (in media) ed é dovuto esclusivamente ad eventi con tre π° nei quali due gamma sono stati persi.La distribuzione spaziale tuttavia non é uniforme.

Nel caso si perdano due gamma la ricostruzione del vertice di decadimento risulta sbagliata. La perdita energetica dovuta alla non rivelazione di due fotoni viene compensata avvicinando il vertice di decadimento all'apparato sperimentale per aumentare gli angoli e recuperare la massa invariante del K che viene imposta.

Il rapporto segnale fondo cambia dall'1% all'15% nella zona di decadimento da 0-50m .

L'energia totale del K é ricostruita sommando le energie dei 4 fotoni.

La tecnologia dell'argon liquido garantisce una grande stabilità di risposta del calorimetro elettromagnetico. La stabilità dell'elettronica é controllata usando un sistema di calibrazione funzionante continuamente durante la presa dati.

$\pi^+\pi^-$

Il vertice viene ricostruito usando l'informazione delle camere proporzionali con una risoluzione di +-1m nella direzione di propagazione del fascio .Si ricostruisce la massa invariante usando le energie delle due tracce misurate nel calorimetro elettromagnetico.

L'energia totale viene calcolata usando l'angolo di apertura Θ tra le due tracce cariche ed il rapporto delle loro energie R=E1/E2

$$E = \frac{(1+R)\sqrt{(Rm_k^2-(1+R)^2m_k^2)}}{R\Theta}$$

ottenendo una risoluzione energetica dell'1% per $0.5<R<2.5$.

Questo metodo rende insensibile la misura dell'energia totale dalla scala assoluta delle energie misurate col calorimetro. La scala assoluta delle energie è quindi data dalla geometria delle camere proporzionali e puo' essere controllata con una precisione dello 0.7 %°.

Le camere proporzionali vengono usate anche per calibrare la geometria del calorimetro elettromagnetico. Si usano a questo scopo elettroni dai decadimenti Ke3.La posizione degli elettroni, definita come il baricentro delle energie depositate nel calorimetro, viene fatta appartenere all'estrapolazione della traccia misurata con le camere. Si determina non solo la posizione x-y nel piano trasversale al fascio ma anche la profondità all'interno del calorimetro.

La scala assoluta delle energie per i decadimenti neutri e' quindi determinata ricostruendo l'inizio della zona di decadimento definito da un contatore di anticoincidenza.

In definitiva le scale di energia, carica e neutra, sono definite dalla geometria dell'esperimento (precisamente dal rapporto tra la scala trasversale e longitudinale) e sono conosciute con precisione di 0.7%°.

Il fondo per i decadimenti carichi viene misurato usando le distribuzioni in d_{tar}, dove d_{tar} é la distanza della targhetta di produzione dal piano definito dalle due tracce cariche.

Per eventi a due corpi d_{tar} é nullo (a parte l'allargamento dovuto agli errori di misura) mentre i decadimenti a tre corpi sviluppano una coda ad alti d_{tar} che viene estrapolata sotto il segnale (vedi Fig.3).

In Tabella sono mostrati i contributi dei vari tipi di fondo.

origine	sottrazione %	errore %	tecnica
$\pi+\pi-\pi^\circ$	0.06	<0.06	eventi con γ addizionali
π e ν	0.5		
π μ ν	0.05	+-0.1	estrapolazione d_{tar}
errori ricostr.	0.05		
altre componenti ad alto d_{tar}	0.1	+-0.3	"
totale 0.76	+-0.35		

Per i carichi ed i neutri sono stati selezionati eventi nell'intervallo 70-170 Gev con vertice di decadimento compreso tra 10-50 m di distanza dall'ultimo collimatore.

Il doppio rapporto è stato calcolato suddividendo i dati in 10 intervalli in energia (10 Gev) ed in 32 intervalli (1.2m) in z. La correzione al risultato dovuta alla non perfetta cancellazione delle efficienze nel rapporto (differenza di distribuzione in energia e divergenza tra i due fasci) viene stimata per mezzo di un Montecarlo.

Nella tabella sono mostrati i contributi dei vari effetti sistematici sul valore del doppio rapporto:

$R = \lvert \eta^{\circ\circ}/\eta^{+-} \rvert^2$	%
sottrazione fondo $2\pi^\circ$	0.2
sottrazione fondo $\pi^+\pi^-$	0.2
$2\pi^\circ/\pi^+\pi^-$ diff. della scala in energia	0.3
rigenerazione in Kl (collim.)	<0.1
scattering in Ks (collim.)	0.1
Ks inefficienza anticontatore	<0.1
Ks/Kl divergenza dei fasci	0.1
stabilita' del calorimetro	<0.1
accettanza del montecarlo	0.1
accidentali (rate)	0.2
efficienza del trigger	0.1
incertezza sistematica totale	+- 0.5%

ESPERIMENTO FNAL E 731(Ref.44)

In questo esperimento si usano due fasci paralleli di KL distanti circa 15 cm.
Un rigeneratore attivo è posto alternativamente sui due fasci per generare KS.
La Fig.4 mostra l'apparato sperimentale.
Le tecniche usate sono le seguenti:

- contatori di anticoincidenza per la reiezione di eventi a tre corpi
- camere proporzionali (150μ di precisione col 98% di efficienza per filo)
- campo magnetico bipolare (1.47m di distanza tra i poli, +-200Mev/c di impulso trasverso trasferito)
- calorimetro elettromagnetico con vetro al piombo (804 elementi di 5.82x5.81x60.96 cm^3, 2x2x20 r.l, risoluzione energetica σ = 1.5%+-5.5%/$\sqrt{E}$, risoluzione sulla posizione dei gamma +- 3mm)
- convertitore di 0.1 rl. per convertire un gamma , ricostruire la posizione del vertice ed associare l'evento al fascio (Ks o Kl).

Il numero dei decadimenti provenienti dal fascio Kl (V) é proporzionale al parametro
$V \propto |\eta|^2$

mentre quelli provenienti dal fascio con rigeneratore (R) é proporzionale a

$$R \propto |\eta + \rho e^{[i\Delta m-(\Gamma_S/2)\,t]}|^2$$

dove ρ é l'ampiezza di rigenerazione coerente.

La misura di R/V, per decadimenti carichi e neutri, permette la misura del doppio rapporto.

L'indeterminazione sulle fasi di ρ, η e l'errore su Δm non contribuiscono significativamente alla precisione di misura di ε'/ε.

Nel caso specifico $|\rho| \sim 10\,|\eta|$ per cui

$$R/V \sim |\rho/\eta|^2$$

$$(R/V)^{+-}/(R/V)^{oo} = |(|\rho|/|\eta|)^{+-}/(|\rho|/|\eta|)^{oo}|^2 = |\eta^{oo}/\eta^{+-}|^2$$

Il vantaggio di questo metodo di misura é che che i due fasci Kl e Ks sono presenti contemporaneamente,per cui il risultato e' insensibile a derive temporali dell'apparato ed a probabili effetti di "rate".

Lo svantaggio stà nella diversa distribuzione spaziale, sia longitudinale che trasversale, dei decadimenti Kl e Ks che rendono necessaria una precisa valutazione numerica dell'accettanza relativa usata per correggere il doppio rapporto ottenuto.

La collaborazione E731 ha raccolto dati in due condizioni diverse:

1) richiedendo la conversione di un gamma e rivelando i 4 modi di decadimento contemporaneamente (75% dei dati)

2) senza richiedere la conversione di un gamma ma rivelando i decadimenti carichi e neutri alternativamente (25% dei dati). In questo caso l'associazione dell'evento al fascio viene fatta usando il centro di massa delle energie depositate nel calorimetro elettromagnetico.

Il risultato presentato recentemente, e discusso in seguito, si riferisce ad una analisi preliminare effettuata sui dati senza conversione di γ, corrispondente al 20% della statistica totale raccolta.

La sottrazione del fondo dà un importante contributo all'errore sistematico.In questo esperimento il fondo è dovuto, oltre ai decadimenti a tre corpi, alle interazioni dei neutroni del fascio con il rigeneratore ed allo scattering incoerente dei K (sempre nel rigeneratore).

La componente incoerente dei K deve essere sottratta se si vuole usare il metodo descritto precedentemente dove solo l'ampiezza di scattering coerente e' presente.Questo tipo di fondo viene misurato estrapolando sotto il segnale le distribuzioni di impulso trasverso ed usando un rigeneratore attivo.

I decadimenti $\pi^+\pi^-$ vengono identificati calcolando la massa invariante del K usando l'impulso dei pioni misurato nel campo magnetico.

In Fig.5 è mostrata la distribuzione ottenuta .

In Fig.6 è mostrata la distribuzione in p-trasverso del K ed il taglio usato per la selezione degli eventi e la sottrazione del fondo.

Per il canale neutro si selezionano eventi con 4 e solo 4 fotoni che abbiano due π° provenienti dallo stesso vertice(si impone la massa del π°) quindi usando quel vertice si ricostruisce la massa del K(questo metodo e' sostanzialmente identico a quello di NA31).La distribuzione di massa invariante ottenuta e' mostrata in Fig.7

In Fig.8 sono mostrate le distribuzione dei vertici ricostruiti Kl e Ks per il caso $\pi^\circ\pi^\circ$.

Nella tabella seguente sono mostrati i vari contributi all'errore sistematico totale per l'esperimento E731.

Contributi in % all'errore sistematico su R di E731:

accidentali	0.10
sottazione del fondo	0.18
scale delle energie e risoluzione	0.20
accettanza	0.25
totale	0.38

Come si vede l'errore sistematico piu' grosso e' quello dovuto alla correzione per l'accettanza.

Nella tabella seguente inoltre vengono mostrati i vari contributi all'errore dovuti alla sottrazione del fondo:

Modo	processo	correzione %	errore%
$KL\to\pi^+\pi^-$	$\pi e\nu$	0.31	0.06
$KL\to 2\pi^\circ$	$3\pi^\circ$	0.37	0.07
$KL\to 2\pi^\circ$	cross over	4.66	0.14
$KS\to\pi^+\pi^-$	incoh.regen.	0.13	0.01
$KS\to 2\pi^\circ$	incoh.regen.	2.58	0.07

Come si puo' notare le correzioni piu' grandi sono fatte per il canale neutro (caso senza conversione di gamma). Nel 4.66% dei casi l'associazione dell'evento al tipo di fascio è sbagliata (cross-over).

Nella Tabella seguente sono confrontati gli esperimenti più recenti:

Esperimento	BNL #749	FNAL E617	FNAL E731	CERN NA31	FNAL E731(20% dei dati)
presa dati	'84	'84	'85	'86	'88
segnale (numero di eventi)					
$KL\rightarrow 2\pi^\circ$	122	3152	6750	109K	52K
$KL\rightarrow \pi+\pi-$	8506	11K	36K	295K	43K
$KS\rightarrow 2\pi^\circ$	3317	5663	22K	932K	201K
$KS\rightarrow \pi+\pi-$	21K	26K	130K	2.3M	179K
fondi%					
$KL\rightarrow 2\pi^\circ$	17.5	11.3	1.6	4.0	5.1
$KL\rightarrow \pi+\pi-$	2.0	3.5	1.2	0.6	0.42
$KS\rightarrow 2\pi^\circ$	2.7	15.5	2.9	0.3	2.57
$KS\rightarrow \pi+\pi-$	0.2	1.9	0.3	0.3	0.12
accidentali %	-	-	10	2.6	3
risultato R	0.990	1.028	0.981	0.980	1.03
err.statist. +-	0.043	0.032	0.017	0.004	0.0084
err.sistem. +-	0.026	0.014	0.007	0.005	0.0038
$(Re\varepsilon'/\varepsilon)\ x10^3$	7	-4.6	3.2	3.3	-0.5
errore +-	8.2	5.8	3.0	1.1	1.5

Si noti che nell'esperimento NA31,il piu' preciso,l'errore statistico e l'errore sistematico sono comparabili.La collaborazione ha raccolto dati nel 1989 registrando un numero di eventi uguale a quello del 1986.

L'analisi sarà completata e probabilmente l'errore statistico diminuirà corrispondentemente mentre ci si aspetta un miglioramento dell'errore sistematico dovuto all'uso di un rivelatore a radiazione di transizione per l'identificazione e la misura del fondo da Ke3.

La collaborazione E731 stà analizzando il resto dei dati (l'80%).

Nel corso del 1990 dovrebbero terminare le due analisi e si dovrebbero avere i risultati con errori statistici su ε'/ε dell'ordine di $0.5x10^{-3}$ corrispondenti ad un campione di 250000 eventi $KL\rightarrow 2\pi^\circ$ (il più raro) per ciascun esperimento. Non è possibile adesso prevedere quale sarà l'errore sistematico finale per i due esperimenti.

CP-LEAR. PS195(Ref.60)

Un altro esperimento è in corso al CERN per la misura di ε'/ε.
Si studiano reazioni di annichilazione P-P del tipo:

$$p\bar{p} \rightarrow \bar{K}^0\pi^-K^+ \qquad p\bar{p} \rightarrow K^0\pi^+K^-$$

che avvengono con una frequenza di $4x10^{-3}$ per annichilazione.

La stranezza del K neutro viene data dal segno della carica del K carico mentre la sua energia viene ricostruita misurando l'impulso dei carichi.

L'esperimento è schematicamente mostrato in Fig.9.

- Campo magnetico solenoidale con raggio interno di 1m.
- Camere proporzionali ed a deriva misurano la traiettoria delle particelle cariche.
- Un calorimetro elettromagnetico a "streamer tubes" (rms=2.2mm nella misura della posizione e rms=30%/√E in energia)
- Contatori Cerenkov per identificare i K carichi(570 Mev/c di impulso medio)
- Contatori per la misura del tempo di volo.(130 ps di risoluzione con base di TOF di 1m)

Il metodo della misura si basa sul fatto che la distribuzione temporale dei decadimenti da K° di stranezza definita è data da:

$$\begin{pmatrix} K^0 \\ \bar{K}^0 \end{pmatrix} \rightarrow f \pm Re\varepsilon \cdot [|a_S|^2 e^{-\Gamma_S t} + |a_L|^2 e^{-\Gamma_L t} \pm 2\,|a_S|\,|a_L|\, e^{-(\Gamma_S/2+\Gamma_L/2)t} \cdot \cos(\Delta m t + \Phi_S - \Phi_L)]$$

dove a_S ed a_L sono le ampiezze di transizione Ks -Kl in uno stato finale f.

L'asimmetria dei decadimenti è data da due contributi, uno legato alla parte reale di ε, indipendente dall'ampiezza di decadimento e dominante per $t \rightarrow \infty$, l'altro dovuto alle ampiezze di decadimento.

L'informazione relativa alla violazione di CP è contenuta nel termine di interferenza che è massimo per $t = 12\tau s$ nel caso dei decadimenti a due pioni(CP +).

Le asimmetrie integrate dei decadimenti sono legate ad ε' ed ε dalle relazioni:

$$I^{+-} = (K^0(\pi^+\pi^-) - \bar{K}^0(\pi^+\pi^-))/(K^0(\pi^+\pi^-) + \bar{K}^0(\pi^+\pi^-)) = 2Re\varepsilon + 4Re\varepsilon'$$

$$I^{00} = (K^0(2\pi^0) - \bar{K}^0(2\pi^0))/(K^0(2\pi^0) + \bar{K}^0(2\pi^0)) = 2Re\varepsilon - 8Re\varepsilon'$$

Si ottiene $Re\varepsilon'/Re\varepsilon = 1/6\ x(1-I^{00}/I^{+-})$

Nella misura delle asimmetrie le efficienze di rivelazione si cancellano con buona approssimazione, tuttavia il metodo usato è meno potente dal punto di vista dell'errore statistico che è dominato dalla misura di $I^{\circ\circ}$. Essendo l'asimmetria aspettata dell'ordine del 3‰ si devono rivelare almeno 10^9 decadimenti $\pi^\circ\pi^\circ$ per avere un errore del $3\cdot10^{-5}$ su $I^{\circ\circ}$.

L'esperimento deve osservare 10^{13} annichilazioni PP al rate di 2.10^6 annichilazioni al secondo.

Attualmente e' in corso di istallazione al CERN.

Nei prossimi anni dovrebbe produrre un risultato su ε'/ε con errore statistico simile a quello attualmente pubblicato.

PREVISIONI PER IL FUTURO.

Il valore previsto dal modello standard per ε'/ε dipende dal valore della massa del quark t.

Attualmente solo limiti inferiori su m_t sono stati dati dagli esperimenti ai collider adronici UA2, UA1, e CDF.La massa del top è maggiore di 78 Gev al 95% di confidence level.

Inoltre la differenza di massa tra la Z° e la W è legata, tramite le correzioni radiative alla massa del top.

In Fig.10 sono mostrati i risultati sperimentali relativi alle masse dei bosoni e le previsioni del modello standard sulla differenza di massa M_{Z°-M_W in funzione di m_t.

Il valore di m_t che meglio si adatta al modello standard è dell'ordine di 120 Gev.

In Fig.11 inoltre è mostrato ε'/ε in funzione di m_t (sempre modello standard) oltre ai risultati di NA31 ed E731.

Il valore teoricamente aspettato è compreso tra 1‰ e 3‰.

La media tra i risultati CERN e FNAL e' ~ 2‰.

Come gia' detto i due esperimenti stanno analizzando altri dati che aumenteranno la statistica più di un fattore due mentre CP-LEAR nel prossimo futuro darà un risultato con errore comparabile a quello attuale.

E' nostra opinione che un nuovo esperimento che produrrà risultati tra vari anni, debba essere progettato per avere un errore di misura dello 0.2-0.3‰ (circa tre volte inferiore a quello attuale), qualunque sia il valore di ε'/ε, se vuol dare un contributo sostanziale alla problematica discussa.

Calcolo della luminosità richiesta per una macchina e+e- $\Phi\rightarrow$K|Ks per misurare ε'/ε con errore statistico dello 0.6‰ in un anno di presa dati.

Il metodo proposto è quello di misurare le asimmetrie dei decadimenti combinati Kl-Ks.

$$e^+e^-\rightarrow\Phi\rightarrow K_l\, K_s\rightarrow\pi^+\pi^-\pi^\circ\pi^\circ$$

Il decadimento da K_l viene identificato richiedendo che il vertice di decadimento abbia una distanza d>>ds, dove ds e' il cammino libero medio dei K_s. Se l'altro decadimento è vicino ai fasci allora viene associato al K_s. Definendo l'asimmetria A come segue si ha:

$$A = \frac{[\ Ks(2\pi^\circ)\ Kl(\pi^+\pi^-)\ -\ Ks(\pi^+\pi^-)\ Kl(2\pi^\circ)\ ]}{\text{"} \qquad + \qquad \text{"}} = 3\ \varepsilon'/\varepsilon$$

Il numero di decadimenti osservati nell'esperimento è dato da :

$$N1 = K_S(2\pi^\circ)K_l(\pi^+\pi^-)= = L\ \sigma\ \Delta t\ Br(K_S\ 2\pi^\circ)Br(K_l\ \pi^+\pi^-)\ eff(\pi^\circ\pi^\circ)eff(\pi^+\pi^-)(1-e^{-dt/dl})$$

$$N2 = K_l(2\pi^\circ)K_S(\pi^+\pi^-)= = L\ \sigma\ \Delta t\ Br(K_l\ 2\pi^\circ)Br(K_S\ \pi^+\pi^-)\ eff(\pi^\circ\pi^\circ)eff(\pi^+\pi^-)(1-e^{-dt/dl})$$

dove

Δt = tempo di misura
L = luminosità media della macchina
σ = sezione d'urto di produzione della Φ in KL KS al picco 1.2 μbarn
dt = 100cm circa, regione di osservazione dei decadimenti Kl
dl = 342cm cammino libero medio di un Kl alla Φ-factory.

$eff(\pi^+\pi^-)$ = efficienza di rivelazione carichi
$eff(\pi^\circ\pi^\circ)$ = " " neutri

$Br(Ks\rightarrow\pi^+\pi^-)= 68.61\%$ Branching-ratios
$Br(Ks\rightarrow\pi^\circ\pi^\circ)= 31.39\%$
$Br(Kl\rightarrow\pi^+\pi^-)= 0.2\%$
$Br(Kl\rightarrow\pi^\circ\pi^\circ)= 0.094\%$

$1-e^{-dt/dl} = 0.25$ circa.

Assumendo che il prodotto delle efficienze di ricostruzione dell'evento completo sia dell'ordine dell'80% (geometrica e di ricostruzione) si ottiene che:

$$N1 \sim N2 = 1.3\ 10^{-4}\ L\ \sigma\ \Delta t$$

L'errore statistico sulla misura dell'asimmetria A = (N1-N2)/(N1+N2) e' dato da:

$\sigma^2_A = 1/2N$ dove N~N1~N2

Essendo A = 3 ε'/ε si ottiene in un anno di presa dati (10^7 sec) con σ = 1.3μbarn:

$$\sigma(\varepsilon'/\varepsilon) = 1/\sqrt{(18\ N)} = 0.6\ 10^{13}\ L^{-1/2} \qquad (L \text{ in } cm^{-2}sec^{-1})$$

Con una luminosita' media di 10^{32} $cm^{-2}sec^{-1}$ in un anno di presa dati si ottiene quindi un errore statistico dello 0.6%°, simile ha quelli attualmente pubblicati.

Commenti sull'errore sistematico sono stati fatti da G. Barbiellini e C.Santoni (ref65).

In questo tipo di approccio, essendo la regione di decadimento dei Ks e KL completamente disgiunte, la valutazione numerica delle efficienze di rivelazione e' di importanza primaria.I prodotti di decadimento, carichi e neutri, attraversano l'apparato in modo diverso per i Ks ed i KL. Le lunghezze delle tracce e gli angoli di incidenza dei fotoni nel calorimetro sono diversi. L'errore sulla valutazione numerica delle efficienze entra al primo ordine nel calcolo dell'asimmetri. E' l'unico esperimento in cui non c'è cancellazione (nemmeno parziale come nel caso di E731).

Un altro punto critico, secondo noi, e' la definizione della zona di decadimento nel caso dei decadimenti da KL.Questa deve essere la stessa per i $\pi^+\pi^-$ ed i $\pi^\circ\pi^\circ$ che sono misurati con due parti diverse dell'apparato. (Il caso dei Ks è meno critico perche' il taglio viene fatto sulla coda della distribuzione). L'errore di scala nella misura del vertice per carchi e neutri entra al primo ordine nella misura dell'asimmetria.

Considerando che l'apparato avra' un raggio dell'ordine di 2.5 m, una lunghezza di 5m e che l'energia totale misurata sarà di 1Gev distribuita tra 6 particelle, ci sembra un problema assai stimolante dal punto di vista strumentale.

REFERENCES

1) The NA31 experiment at CERN is performed by the following collabortion: *CERN*: H. Burkhardt, P. Clarke, D. Coward, D. Cundy, N. Doble, L. Gatignon, V. Gibson, R. Hagelberg, G. Kesseler, J. van der Lans, T. Miczaika, A.C. Schaffer, P. Steffen, J. Steinberg, H. Taureg, H. Wahl, C. Youngman; *Dortmund*: G. Dietrich, F. Eisele, W. Heinen; *Edinburgh*: R. Black, D.J. Candlin, J. Muir, K.J. Peach, B. Pijlgroms, I.P. Shipsey, W. Stephenson; *Mainz*: H. Blumer, M. Kaseman, K. Kleinknecht, B. Panzer, B. Renk, S. Rohn; Orsay: E. Auge, R.L. Chase, M. Corti, L. Iconomidou-Fayard, D. Fournier, P. Heusse, A.M. Lutz, H.G. Sander; *Pisa*: A. Bigi, M. Calvetti, R. Carosi, R. Casali, C. Cerri, G. Gargani, R. Fantechi, S. Galeotti, I. Mannelli, E. Massa, A. Nappi, D. Passuello, G. Pierazzini; *Siegen*: C. Becker, D. Heyland, M. Holder, G. Quast, M. Rost, W. Weihs and G. Zech.
2) H. Bukhardt et al., First evidence for direct CP violation, Phys. Lett. B206, 169 (1988)
3) P. Clarke et al., A measurement of the phase difference of η_{00} and η_{+-} in CP vilating $K^0 \rightarrow 2\pi$ decays, proposal CERN/SPCS/86-6 (1986)
4) D. Cundy et al., Measurement of $|\eta_{00}|^2/|\eta_{+-}|^2$, proposal CERN/SPSC/81-110 (1981), and Measurement of ε'/ε in CP violating K^0 decays, Memorandum CERN/SPCS/87-48 (1987)
5) J.H. Christenson et al., Evidence for the 2π decay of the K_2^0 meson, Phys. Rev. Lett. 13, 138 (1964)
6) L. Wolfenstein, Violation of CP invariance and the possibility of very weak interactions, Phys. Rev. Lettt. 13, 562 (1964)
7) T.T. Wu and C.N. Yang, Phenomenological analysis of violation of CP invariance in decay K^0 of and $\overline{K^0}$, Phys. Rev. Lett, 13, 380 (1964)
8) K. Kleinknecht, CP violation and K^0 decay, Annu. Rev. Nucl. Sci, 26, 1-50 (1976)
9) T.T. Devlin and J.O. Dickey, Weak hadronic decays: $K \rightarrow 2\pi$ and $K \rightarrow 3\pi$, Rev. Mod. Phys. 51, 237-250 (1979)
10) N.N. Biswas et al., Determination of the s-wave $I = 0$ π-π phase shifts from thereshold to 0.96 GeV, Phys. Rev. Lett. 47, 1378 (1981)
11) A.N. Kamal, Amplitude analysis for $D \rightarrow K\pi$ decays, J. Phys. G12, L43 (1986)
12) J. Marx et al. Charge asymmetry in K_{e3} decay and Re ε, Phys. Lett. B32, 219 (1970)
13) R. Piccioni et al., Measurement of the charge aymmetry in the decay $K_L^0 \rightarrow \pi^{\#} \mu^{\#} \nu$, Phys, Rev. Lett. 29, 1412 (1972) and Phys. Rev. D9, 2939 (1974)
14) H.H. Williams et al., Measurement of the lepton charge asymmetry in $K_L^0 \rightarrow \ell^{\#} \mu^{\#} \nu$ decays, Phys. Rev. Lett. 31, 1521 (1973)
15) V.L. Fitch et al., K_{e3}^0 charge asymmetry, Phys. Rev. Lett. 31, 1524 (1973)
16) C. Geweniger et al., Measurement of the charge asymmetry in the decays $K_L^0 \rightarrow \pi\, e\, \nu$ and $K_L^0 \rightarrow \pi\, \mu\, \nu$, Phys. Lett. 48B, 483 (1974)
17) G. Geweniger et al., A new determination of the $K^0 \rightarrow \pi^+ \pi^-$ decay, parameters, Phys. Lett. 48B, 487 (1974)
18) C. Geweniger et al., The phase Φ_{+-} of CP violation in the $K^0 \rightarrow \pi^+ \pi^-$ decay, Phys. Lett. 52B, 119 (1974)
19) J.H. Christenson et al., Measurement of the phase and magnitude of η_{00}, Phys. Rev. Lett. 54, 1628 (1985)
20) J.K. Black et al., Measurement of the CP-nonconservation parameter ε'/ε, Phys. Rev. Lett. 54, 1628 (1985)
21) R.H. Bernstein et al., Measurement of ε'/ε in the neutral kaon system, Phys. rev. Lett. 54, 1631 (1985)

22) M. Woods et al., First result on a new measurement of ε'/ε in the neutral kaon system, Pys. Rev. Lett. 60, 1695 (1988)

23) J. Bricman et al., New of particle properties, Phys. Lett. B75, 1-250 (1978)

24) R. Messner et al., New measurement of the $K_L^0 \to \pi^+ \pi^-$ branching ratio, Phys. rev. Lett. 30, 876 (1973)

25) R. DeVoe et al., Measurement of the branching ratio $\Gamma(K_L \to \pi^+ \pi^-)/\Gamma(K_L \to \text{all})$, Phys. Rev. D16, 565 (1977)

26) D.P. Coupal et al., Measurement of the ratio $\Gamma(K_L \to \pi^+ \pi^-)/\Gamma(K_L \to \pi l \nu)$ for K_L with 65 GeV/c laboratory momentum, Phys. Rev. Lett 55, 566 (1985)

27) G.P. Yost et al., Review of particle properties, Phys. Lett. B204, 1-486 (1988)

28) M. Cullen et al., A precise determination of the K_L - K_S mass difference, Phys. Lett. B32, 523 (1970)

29) C. Geweniger et al., Measurement of the kaon mass difference m_L-m_S by the two-regenerator method, Phys. Lett. B52, 108 (1974)

30) S. Gjesdal et al., Measurement of the K_L - K_S mass difference from the charge asymmetry in semileptonic kaon decays, Phys. Lett. B52, 113 (1974)

31) W.C. Carithers et al., Measurement of the phase of the CP-nonconservation parameter η_{+-} and the K_S total decay rate, Phys. Rev. Lett. 34, 1244 (1975)

32) J.H. Christenson et al., Measurement of the phase and magnitude of η_{+-}, Phys. Rev. Lett. 43, 1212 (1979)

33) D.A. Jensen et al., Measurement of the relative phase of the $K_L \to \pi^+ \pi^-$ and $K_S \to \pi^+ \pi^-$ decay amplitudes by vacuum regeneration, Phys. Rev. Lett. 23, 615 (1969) and Ref. 2 in Phys. Rev. Lett. 25, 1057 (1970)

34) G. Barbillini et al., Determination of the difference of phase between η_{00} and η_{+-}, Phys. Lett. 43B, 529 (1973)

35) V.V. Barmain et al., CPT symmetry and neutral kaons, Nucl. Phys. B247, 293-312 (1984)

36) M. Kobayashi and K. Maskawa, CP violation in the renormalizable theory of wead interaction, Prog. Theor. Phys. 49, 652 (1973)

37) J. Ellis, M.K. Gaillard and D.V. Nanopoulos, Left-handed currents and CP violation, Nucl. Phys. B109, 213 (1976); F.J. Gilman and M.B. Wise, The $\Delta I = 1/2$ rule violation of CP in the six-quark model, Phys. Lett. 83B, 83 (1979) and Effective Hamiltonian for $\Delta S = 1$ weak non-leptonic decays in the six-quark model, Phys. Rev. D20, 2392 (1979); B. Guberina and R. Peccei, Quantum chromodynamic effects and CP violation in the Kobayashi-Maskawa model, Nucl. Phys. B163, 289 (1980); L. Wolfenstein, Present status of CP violationm Annu. Rev. Nucl, Sci. 36, 137-170 (1986)

38) A.J. Buras and J.M. Gerard, ε'/ε in the Standard Model, Phys. Lett. B203, 272 (1988)

39) A.J. Buras, Quark mixing and CP violation, MPI report PAE/PTh 70/88, and The present status of CP violation in the Standard Model, these proceedings

40) M. Holder et al., On the decay $K_L \to \pi^0 \pi^0$, Phys. Lett. 40B, 141 (1972)

41) M. Banner et al., Measurement of $|\eta_{00}/\eta_{+-}|$, Phys. rev. Lett. 28, 1597 (1972)

42) L. Adiels et al. Tests of CP violation with K^0 and $\overline{K}^0$ at LEAR, proposal CERN/PSCC/85-6 (1985)

43) H. Burkhardt et al., The beam and detector for a high-precision measurement of CP violation in neutral kaon decays, Nucl. Instr. Methods A268, 116 (1988)

44) G. Gollin et al., Measurement of the magnitude of ε'/ε in the neutral kaon system to a precision of 0.001, Fermibal proposal No. 731 (1982)

45) Y.B. Hsiung, Measurement of ε'/ε at Fermibal, Fermibal report Conf. 88/164 and to appear in Proc. 9th European Symposium on Antiproton-Proton Interactions and Fundamental Symmetries (mainz 1988); T. Yamanaka, The ε'/ε measurement at Fermibal, these proceedings

46) G. Barr et al., The NA31 transition radiation detector, to appear in Proc. IEEE Nuclear Science Symposiums (Orlando 1988)

47) H. Burkhardt et al., Observation of the decay $K_S \rightarrow 2\gamma$ and measurement of the decay rates $K_L \rightarrow 2\gamma$, and $K_S \rightarrow 2\gamma$, Phys. Lett. B199, 139 (1987)

48) M. Aguilar-Benitez et al., Review of particle properties, Phys. Lett. B170, 1-350 (1986)

49) H.W.M. Norton, A determination of the branching ratio fo K_L to $\gamma\gamma$, PhD thesis (Chicago, 1984); B. Winstein, private communication (1988)

50) V.V. Barmin et al., Search for $K_S^0 \rightarrow 2\gamma$ decay, Nuovo Cimento 96A, 159 (1986)

51) L.L. Chau and H.Y. Cheng, $K^0(\overline{K}^0) \rightarrow 2\gamma$ decays: Phenomenology and CP nonconservation, Phys. rev. Lett. 54, 1768 (1985); G. D'Ambrosio and D. Espriu, Rare decay modes of the K mesons in the chiral Lagrangian, Phys. Lett. B175, 237 (1986); J.L. Goity, The decays $K_S^0 \rightarrow \gamma\gamma$ and $K_L^0 \rightarrow \gamma\gamma$ in the chiral approach, Z. Phys. C34, 341 (1987)

52) L.L. Chau and H.Y. Cheng, Further comments on $K^0(\overline{K}^0) \rightarrow 2\gamma$, Phys. Lett. 195B, 275 (1987)

53) M. Mannelli et al., A search for effective flavour changing neutral currents in K_L^0 decays, Proc. 23rd Rencontre de Moriond (Les Arcs 1988) 373 and paper No. 484 D contributed to the Int. Conf. on High-Energy Physics (Munich 1988)

54) J.F. Donoghue, B.R. Holstein and G. Valencia, $K_L \rightarrow \pi^0 e^+ e^-$ as a probe of CP violation, Phys. Rev. D35, 2769 (1987)

55) A.S. Carroll et al., Observation of the Dalitz decay mode of the K_L^0, Phys. Rev. Lett. 44, 525 (1980)

56) G.D. Barr et al., Search for the decay $K_L \rightarrow \pi^0 e^+ e^-$, Phys. Lett. B214, 303 (1988)

57) L.K. Gibbons et al., New li;its on $K_{L,S} \rightarrow \pi^0 e^+ e^-$,Phys. Rev. Lett. 61, 2661 (1988)

58) E. Jastrzembski et al., Li;its on $K^0_L \rightarrow \pi^0 e^+ e^-$ and $K^0_L \rightarrow \pi^0 e^+ e^-$, Phys. Rev. Lett. 61, 2300 (1988)

59) G.D. Barr et al., Search for a neutral Higgs particle in the decay sequence $K_L \rightarrow \pi^0 H^0$ and $H^0 \rightarrow e^+ e^-$, CERN-EP/89-156.

60) Adiels,l et al 1985 CERN experimental proposal n.PSSC/85-6.

61) Skjegges NP B48-343 (1972).

62) Grossman PRL 59-18 (1987).

63) Aronson NC 32A 236 (1976).

64) Vosburgh PR D6 1834 (1972), PRL26 866 (1971).

65) G. Barbiellini and C. Santoni CERN-EP/89-88.

NA 31

(a)

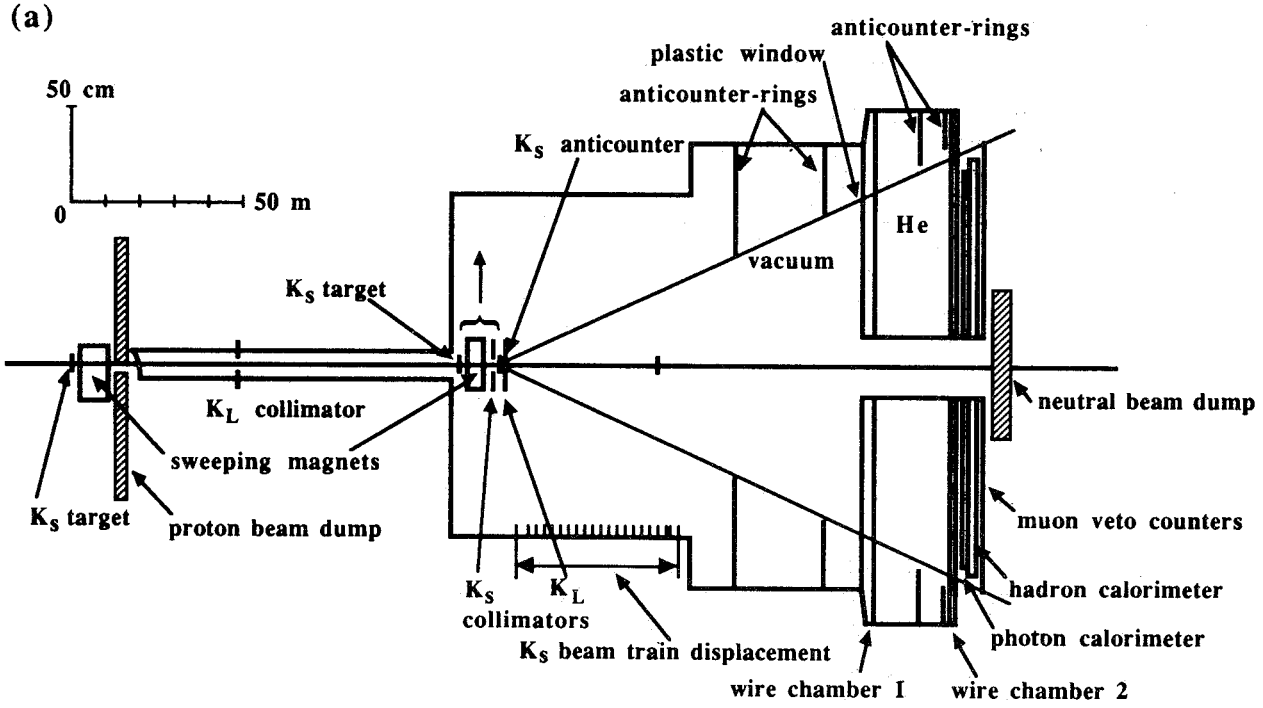

(b)

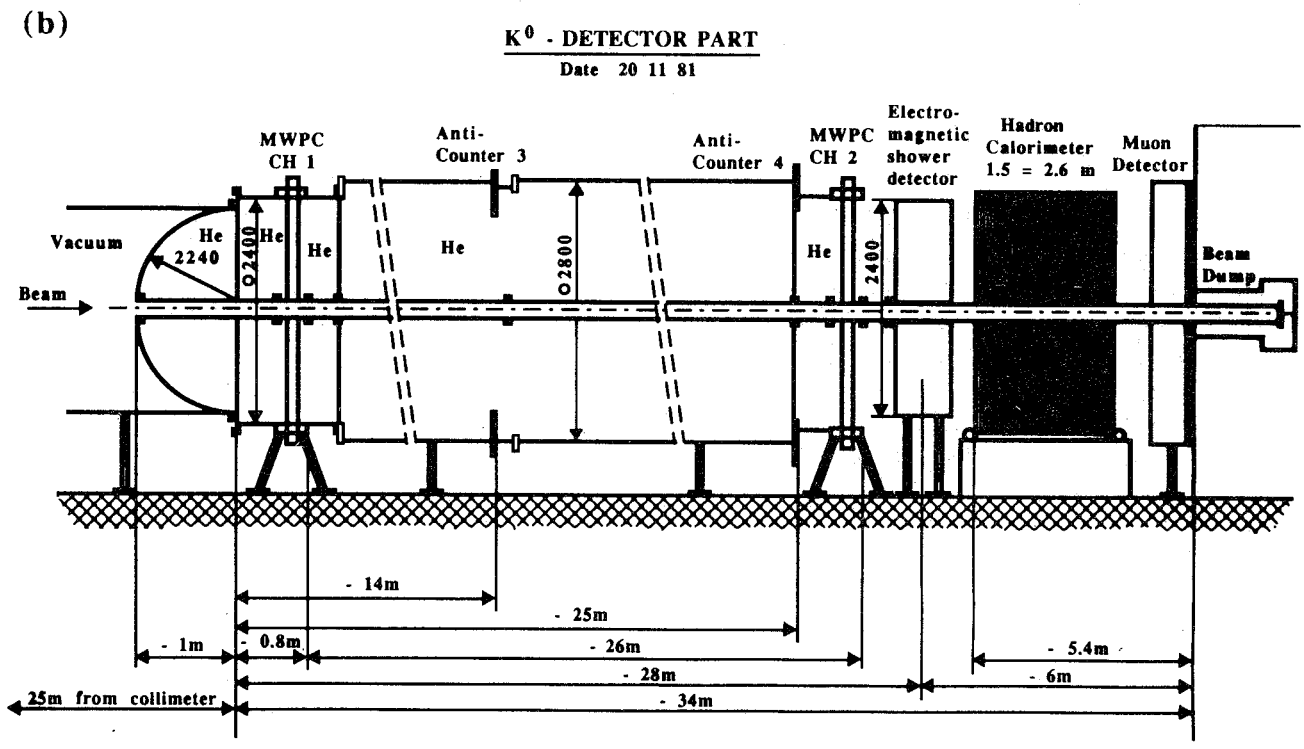

FIG. 1(a) - Schematic layout of apparatus and beams for the experiment.**(b)** Layout of the detector section.

(a)

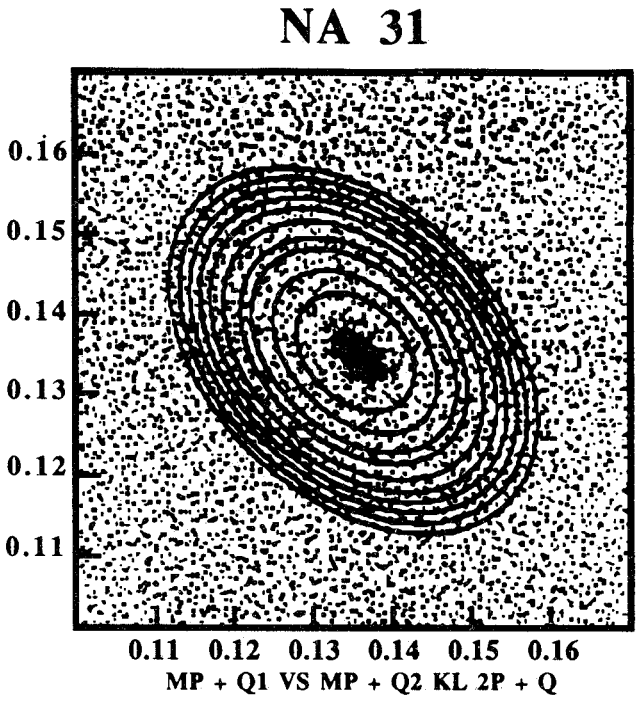

(b)

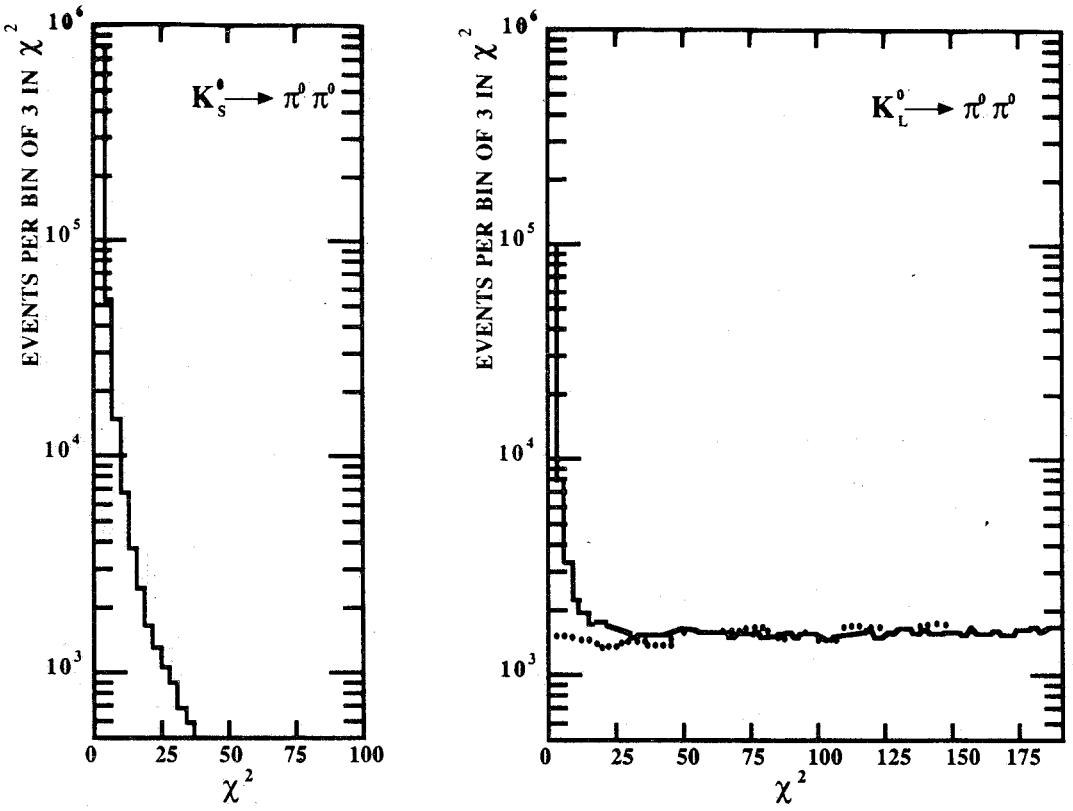

FIG. 2(a) - 2γ mass.combinations of two photon pairs in the K_L beam. **(b)** Number of accepted 4 events as a function of χ^2, for $K_S \rightarrow 2\pi^0$ and $K_L \rightarrow 2\pi^0$ data, and a Monte Carlo calculation for background originating from $K_L \rightarrow 3\pi^0$ decays. The segnal region is taken as $\chi^2 < 9$.

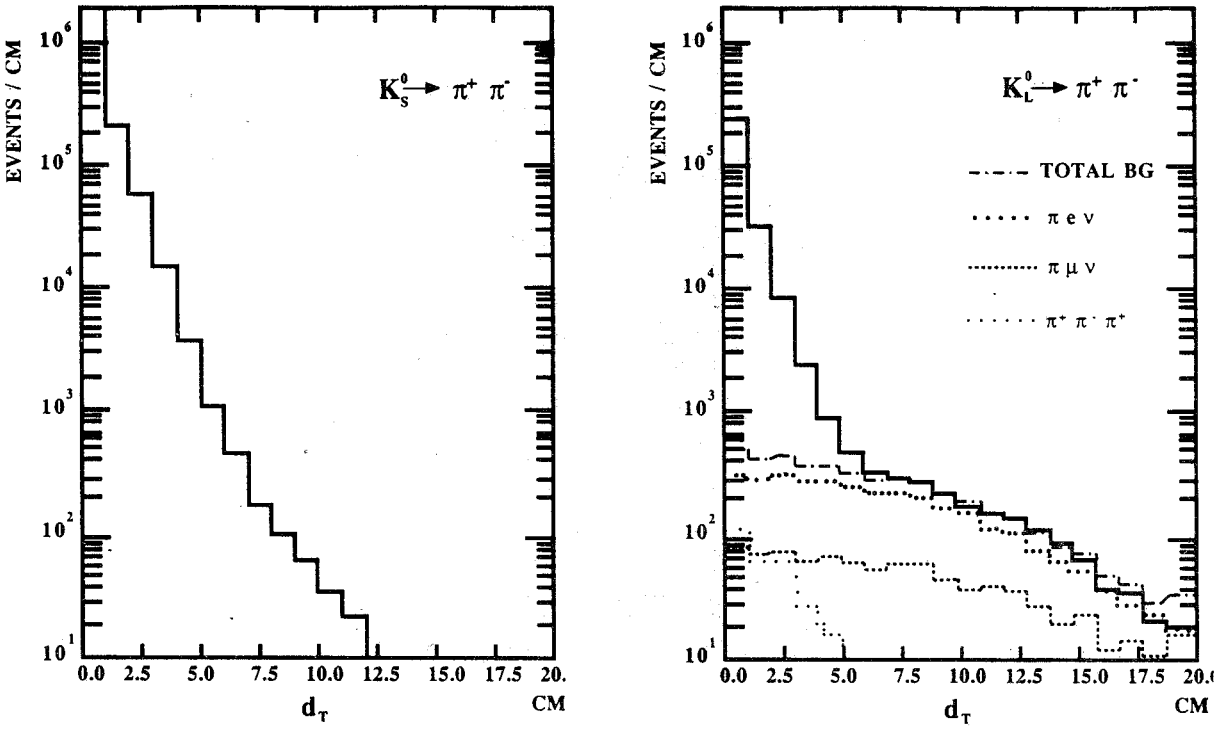

FIG. 3 - Event distribution for charged decays as a function of the distance d_r between the decay plane and the production target, for K_S and K_L decays and for various background components.

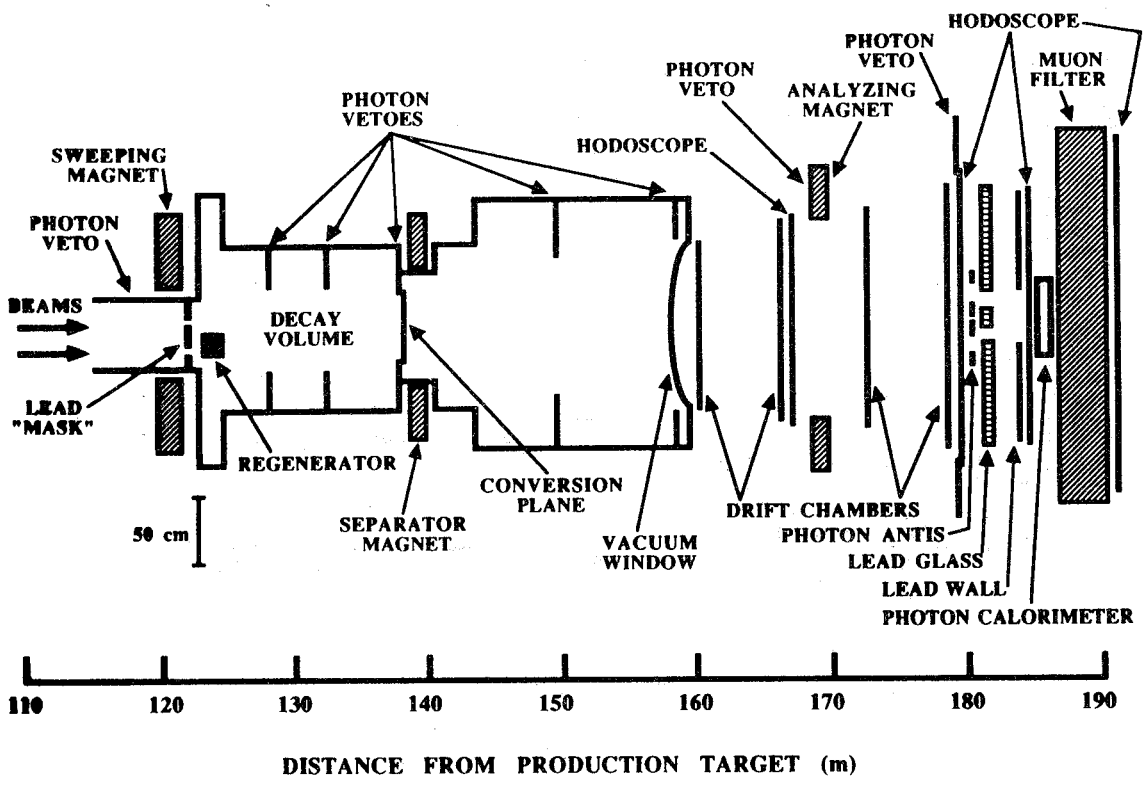

FIG. 4 - Elevation view of the detector for FNAL E731.

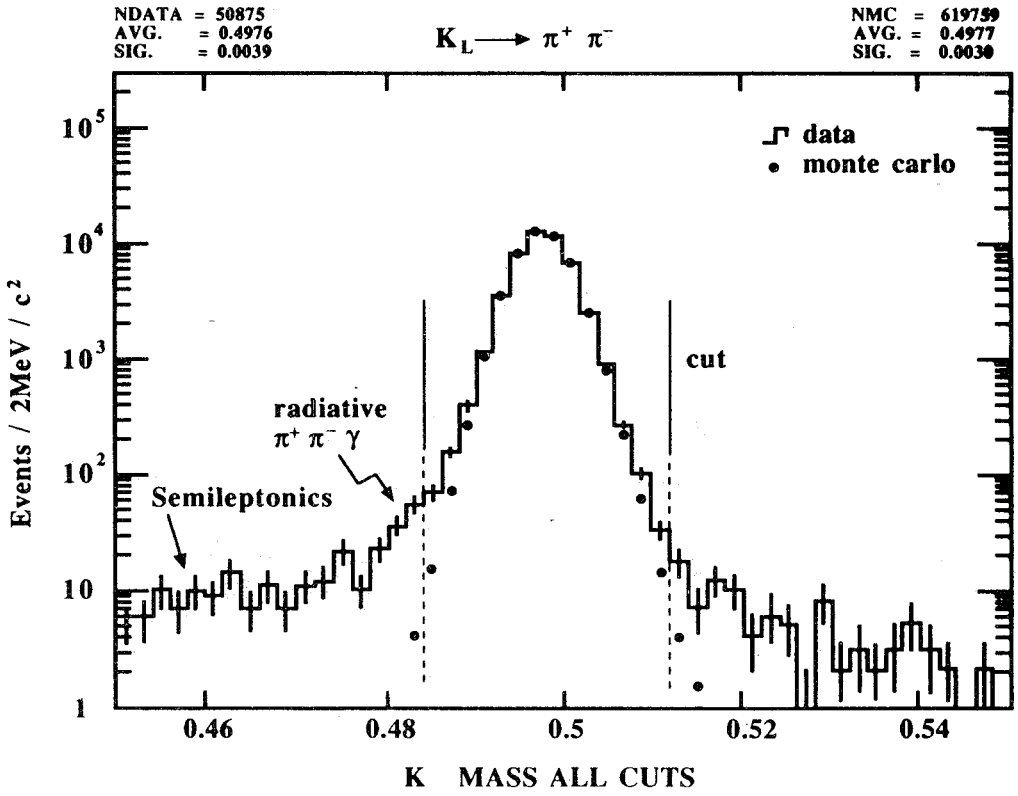

FIG. 5 - Massa invariante K_L π-π+ E731.

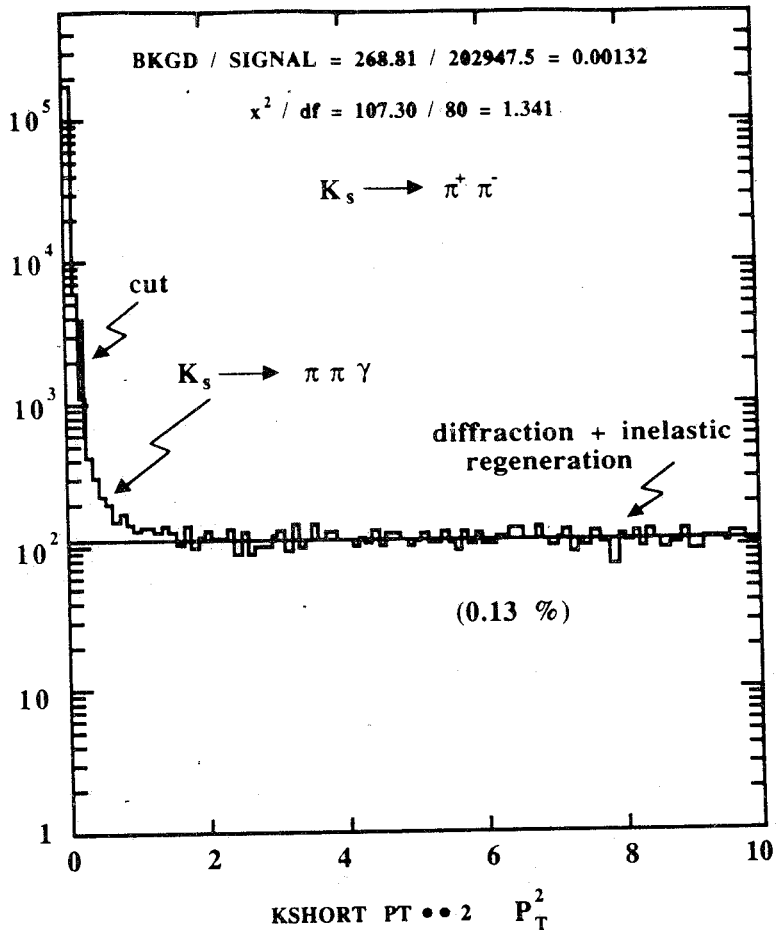

FIG. 6 - Distribuzione di P^2_T E731.

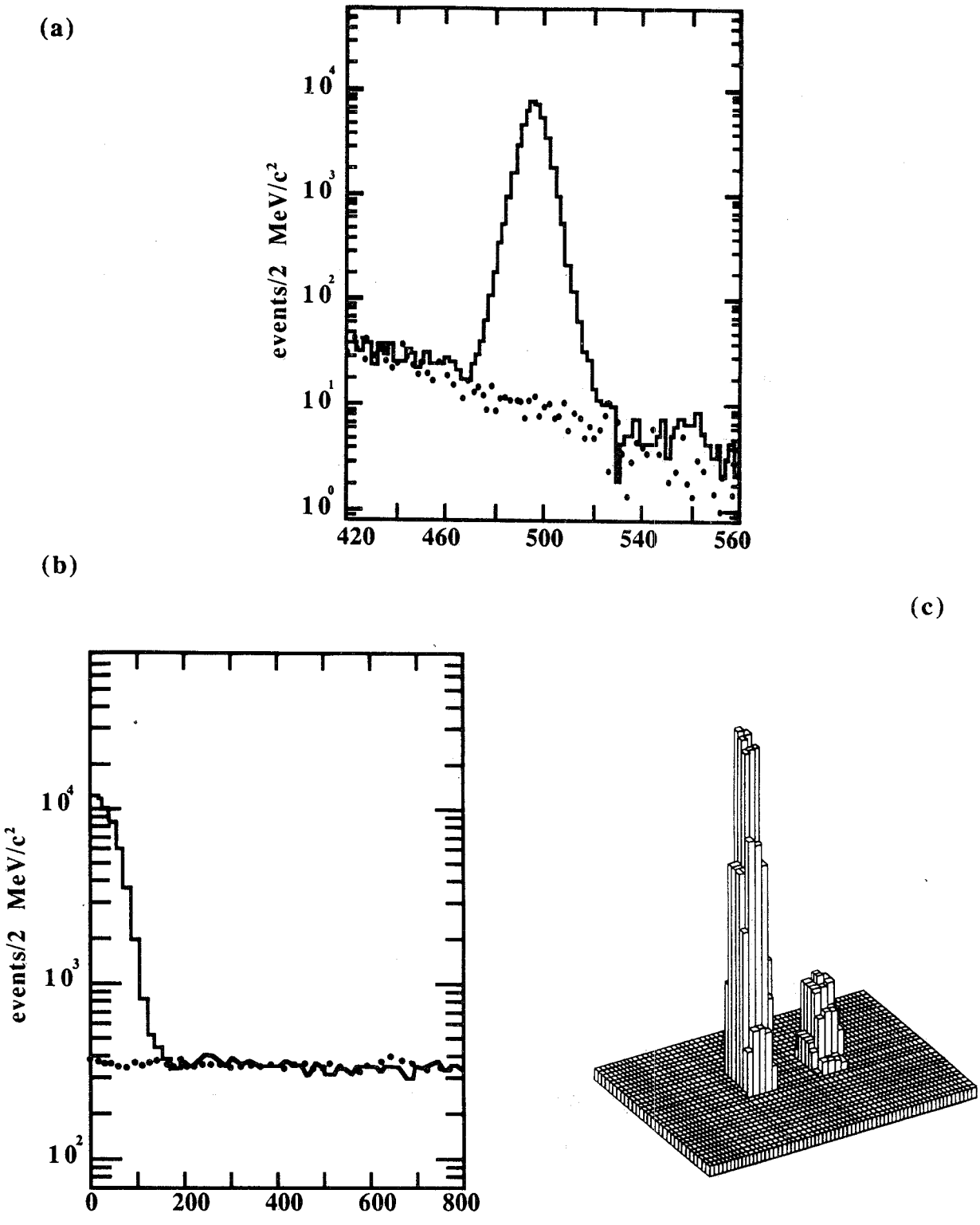

FIG. 7(a) - Invariant $K_L \rightarrow 2\pi^0$ events. The solid dots represent the $K_L \rightarrow 3\pi^0$ background.**(b)** Ring distribution for $K_L \rightarrow 2\pi^0$ events. The solid dots represent the inelastic background.**(c)** The center of energy distribution for $K_{L,S} \rightarrow 2\pi^0$ at the lead glass. the hight (low) peak is $K_S(K_L)$.

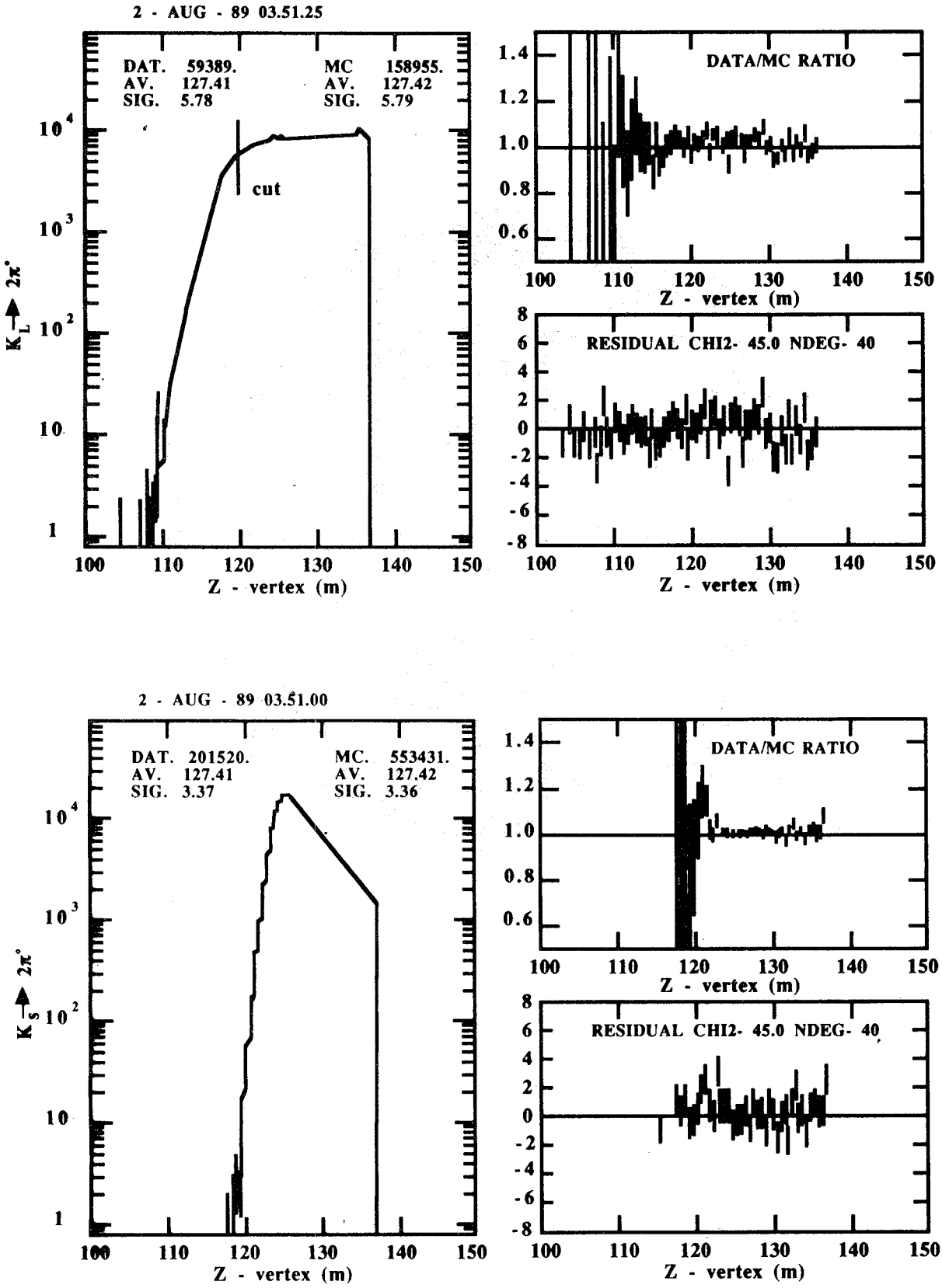
2 - AUG - 89 03.51.25
DAT. 59389.
AV. 127.41
SIG. 5.78
MC 158955.
AV. 127.42
SIG. 5.79
cut
$K_L \rightarrow 2\pi^\circ$
Z - vertex (m)
DATA/MC RATIO
RESIDUAL CHI2- 45.0 NDEG- 40
2 - AUG - 89 03.51.00
DAT. 201520.
AV. 127.41
SIG. 3.37
MC. 553431.
AV. 127.42
SIG. 3.36
$K_S \rightarrow 2\pi^\circ$

FIG. - 8 E731.

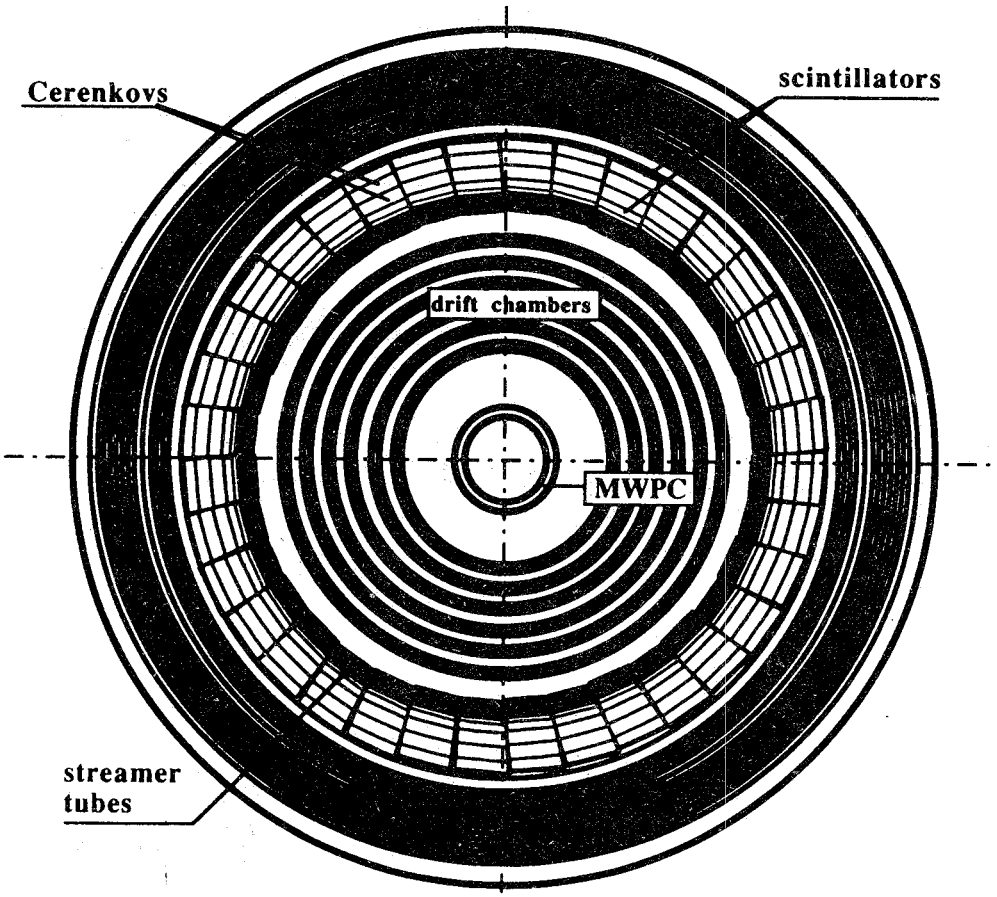

FIG. 9 - Transverse view of the detector for CERN PS195.

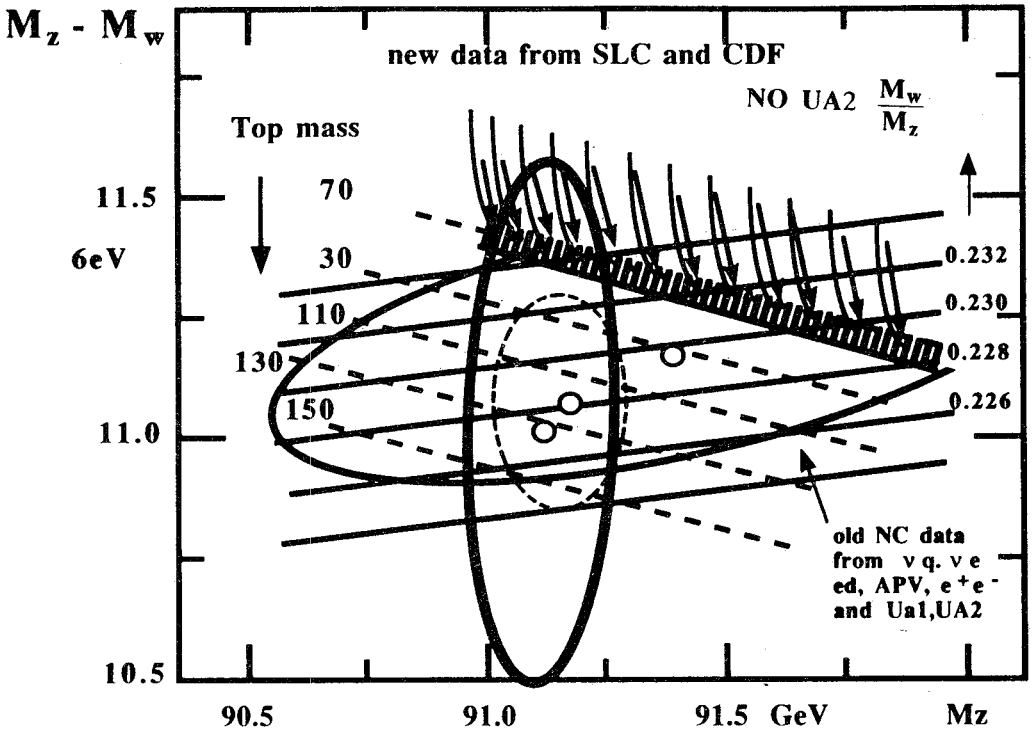
$M_z - M_w$
new data from SLC and CDF
NO UA2 $\frac{M_w}{M_z}$
Top mass
70
30
110
130
150
11.5
6eV
11.0
10.5
0.232
0.230
0.228
0.226
old NC data
from ν q. ν e
ed, APV, e+e-
and Ua1,UA2
90.5
91.0
91.5 GeV
Mz

FIG. 10

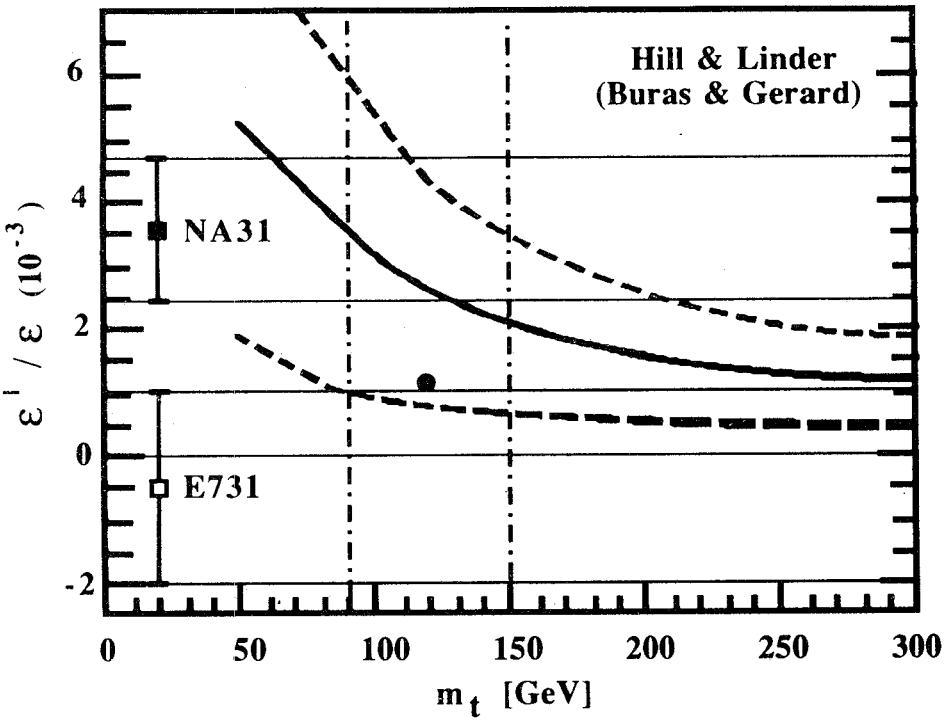
Hill & Linder
(Buras & Gerard)
NA31
E731
$\varepsilon' / \varepsilon\ (10^{-3})$
6
4
2
0
-2
0
50
100
150
200
250
300
m_t [GeV]

FIG. 11

TESTS OF CP VIOLATION WITH K^0 AND $\overline{K}^0$

CP LEAR Collaboration

R. Adler[2], A. Angelopoulos[1], A. Apostolakis[1], E. Aslanides[12], G. Backenstoss[2], C.P. Bee[10], J. Bennet[10], E.V. Beveren[5], P. Bloch[4], Ch. Bula[14], G. Burgun[15], P. Carlson[4], J. Carvalho[5], M. Chardalas[17], S. Charalambous[17], S. Dedoussis[17], M. Dejardin[15], J. Derre[15], M. Dodgson[10], J G. Dousse[8], J. Duclos[15], A. Ealet[4], L. Faravel[8], P. Fassnacht[12], J.L. Faure[15], Ch. Felder[2], R. Ferreira-Marques[5], W. Fetscher[18], M. Fidecaro[4], D. Francis[16], J. Fry[10], C. Fuglesang[4], E. Gabathuler[10], R. Gamet[10], D. Garreta[15], T. Geralis[12], H.J. Gerber[17], A. Go[3], P. Gumplinger[18], C. Guyot[15], P.F. Harrison[10], P.J. Hayman[10], W.G. Heyes[4], R.W. Hollander[6], H.U. Johner[8], K. Jon-And[16], K. Jansson[16], A. Kerek[16], J. Kern[8], P.R. Kettle[14], C. Kochowski[15], P. Kokkas[7,9], E. Kossionides[7], T. Lawry[8], R. Le Gac[13], E. Machado[4], P. Maley[10], G. Marel[15], G. Marel[15], M. Mikuz[11], J. Miller[3], F. Montanet[12], T. Nakada[14], A. Onofre[5], B. Pagels[2], T. Paradelis[7], M. Pavlopoulos[4,7], F. Pelucchi[12], J. Pinto da Cunha[5], A. Policarpo[5], H. Postma[6], R. Rickenbach[2], L. Roberts[3], E. Rozaki[1], L. Scks[10], L. Sakeliou[1], P. Sanders[10], C. Santoni[2], K. Sarigianis[1,7], L. Schaller[8], A. Schopper[4], S. Szilagyi[16], L. Tauscher[2], C. Thibault[13], F. Touchard[13], C. Touramanis[7,17], F. Triantis[9], D.A. Troester[2], M. Van den Putte[6], C.W.E. Van Eijk[6], G. Varner[3], S. Vlachos[7,10], C. Witzing[18] and D. Zavrtanik[11]

Athens[1], Basel[2], Boston[3], CERN[4], Coimbra[5], Delft[6], Democritos INP[7], Fribourg[8], Ioannina[9], Liverpool[10], Ljubljana[11], Mareseille[11], Marseille[12], CSNSM Orsay[13], PSI Villigen[14], Saclay[15], Stockholm MSI[16], Thessaloniki[17], Zurich ETH[18]

TESTS OF CP VIOLATION WITH K^0 AND $\overline{K}^0$

CP LEAR Collaboration

Abstract

The aim of the CP LEAR experiment is to study symmetry-violation effects, making use of tagged K^0's and $\bar{K}^0$'s. The detector, although missing some electronic components, have been operational for a few weeks at the CERN LEAR (Low Energy Antiproton Ring) machine. At the moment the analysis of the data is in progress. In this paper a description is given of the experimental method and of the detector; the sensitivities of some measurements are also discussed.

For any final state f (f = $\pi^+\pi^-$, $\pi^0\pi^0$, $\pi^+\pi^-\pi^0$, $e\nu_e\pi$, ...) the decay rates of K^0 and $\bar{K}^0$ as a function of the proper time t are given by

$$R_{K^0(\bar{K}^0)\to f} = [1/2 -(+)\,\mathrm{Re}\,\varepsilon]\,\{|a_S^f|^2\, e^{-\gamma_S t} + |a_L^f|^2\, e^{-\gamma_L t} + (-)\,2|a_S^f| \times |a_L^f|\, e^{-1/2(\gamma_S+\gamma_L)t}\cos(\Delta m t - \phi_f)\}\,. \quad (1)$$

The quantities $\gamma_{S,L}$ are the decay widths of the K^0 short (S) and of the K^0 long (L), and Δm is the difference of their masses ($\Delta m = m_{K_L} - m_{K_S}$). The parameter ε describes the CP- violation in the mass matrix. The decay amplitudes $a_{S,L}^f = \langle f|H|K_{S,L}\rangle$ are a function of the two CP-violation parameters ε and of ε'. The term ϕ_f is the difference of the phases of a_S^f and a_L^f.

Since $\Delta m \approx \gamma_S$, it is possible to measure the K_S-K_L interferences [the third term in eq. (1)]. The CP LEAR experiment [1] will study these interferences and hence determine both the magnitude and the phase of the CP-violation parameters in 2π decays as well as CP-violation effects in other channels such as 3π, $\gamma\gamma$, ... The measurement of the difference of the phases in $\pi^0\pi^0$ and $\pi^+\pi^-$ decays is a test of the CPT symmetry. The T and CP symmetries and the $\Delta S = \Delta Q$ rule will be tested by studying the semileptonic decays. The quantity ΔS (ΔQ) is the difference between the strange (charge) quantum numbers of the initial and final states.

The K^0's and $\bar{K}^0$'s are produced symmetrically in the annihilation at rest of antiprotons according to the reactions

$$\bar{p}p \rightarrow K^+\pi^-\bar{K}^0 \quad \text{and} \quad \bar{p}p \rightarrow K^-\pi^+K^0 , \tag{2}$$

each having a branching ratio of 0.2%. The particles produced in reactions (2) have a small momentum, the average K^0 momentum is $<p_{K^0}> \approx 550$ MeV/c and, for example, in the case of $K^0 \rightarrow 2\pi^0$ the average energy of the γ's produced in the decay of π^0's is $<E_\gamma> \approx 160$ MeV. The experimental set-up and a typical event are shown in Fig. 1. A field of 0.44 T has the direction of the detector axis, perpendicular to the plane of the figure.

Antiprotons of 200 MeV/c moving along the detector axis are stopped in a spherical target of gaseous hydrogen at 15 atm. The charged kaon produced in reactions (2) is identified by the scintillator-Cherenkov anticoincidence. The pions, having a β above the threshold, will produce a signal in both the scintillators and the Cherenkov. To improve the kaon identification a momentum larger than 300 MeV/c is required for the kaon-track candidate. The inner scintillation counters also provide a time of flight (TOF) measurement. The magnetic field allows identification of the sign of the kaon charge and hence of the strangeness of the neutral kaon, making possible an independent normalization of K^0's and $\bar{K}^0$'s. The neutral kaon is reconstructed from the measurement of the charged-kaon and charged-pion momenta, making use of multiwire proportional chambers, proportional drift chambers, and streamer tubes. The charged particles produced in neutral-kaon decays produce tracks in the chambers. In the case of decays into γ's or π^0's, the γ's will be identified and reconstructed using the electromagnetic calorimeter information. The decay paths of K^0 and $\bar{K}^0$,

which are necessary for the determination of t, will be obtained from the measurement of the decay products.

The antiprotons stopping in the target are triggered using a 1 mm thick scintillator. Figure 2 shows the beam profile measured with a multiwire proportional chamber with cathode-strip readout [2]. For the next runs the profile, with a better beam diagnostic, is expected to be improved. Owing to the high pressure of the hydrogen target, having a radius of 7 cm, the antiprotons will stop in a very small region, the full width at half maximum (FWHM) of the transvere (longitudinal) distribution being 1 cm (5 cm).

The two cylindrical proportional chambers [1], having a radius of 9.5 and 12.7 cm respectively, provide the first two points of the charged-particle trajectories. The chamber efficiency, as measured in an exposure of a prototype to a test beam at the Paul Scherrer Institute (PSI), is larger than 99%.

The six proportional drift chambers [1] occupy a cylindrical annulus, the radius of the inner (outer) chamber being 25.5 cm (50.9 cm). They are equipped with wires and strips to provide the $r\phi$ and z coordinates. A full-scale planar prototype has been tested at the CERN Synchro-cyclotron (SC). The position of the beam particles was defined by a set of silicon strips (60 μm in lateral size). The position resolution obtained with the wires (strips) was 250 μm (150 μm), and the measured efficiency was 97.5% for the wires and 98.7 for the strips. The expected average momentum resolution is 5%.

The two layers of streamer tubes [1], located at radii of 58.2 and 60 cm, will provide the last three-dimensional point of the charged-particle track. Figure 3 shows a preliminary distribution of the events as a function of Δz, the difference between the z coordinates measured in the inner and outer layers corrected for the track slope. The root mean square of the Gaussian curve fit is 2.14 cm.

The particle-identification device consists of 32 trapezoidal sectors of scintillator (S1)/ Cherenkov (C)/ scintillator (S2) sandwich placed around a cylinder of 65 cm radius[3]. Measurements of the impact point (z) dependence of the photoelectron yield have been performed at the PSI, the obtained photoelectron multiplicity is 12 (38) for $z = 0$ cm ($z = \pm 40$ cm).

The scintillation counters S1 allow a determination of the TOF of the particles. A preliminary distribution of the difference of the TOF of charged particles in one event, obtained using the on-line data, is shown in Fig. 4. The FWHM of the distribution is 600 ps.

The electromagnetic calorimeter is a lead sampling calorimeter placed inside the magnet coil with a total thickness of 6.2 radiation lengths. It consists of 18 layers made of a lead converter plate, followed by a plane of streamer tubes placed between two strip planes. The tubes, in the case of single-crossing tracks, have an efficiency of 85% as measured in a test beam at the PSI. The efficiency of the strips is $\approx$ 98% and the average multiplicity $\approx$ 1.3. The energy of the converted photons is measured by counting the number of tubes hit in the shower. The lower limit of the efficiency of photon detection obtained in the PSI test run for a photon energy of 50 MeV (> 100 MeV) is 58% (90%). The hit resolution multiplied by the square root of the photon energy in GeV is 13% for photons of 160 MeV. The strip and the wire information will be used to determine the photon impact point. The expected resolutions are: $\sigma(r\phi)$ = 3 mm and $\sigma(d)$ = 5 mm, where d is the longitudinal coordinate, r is the radial one, and ϕ is the azimuthal angle. Such precisions would allow a determination of the decay path of $K^0 \rightarrow \pi^0\pi^0$ with a resolution of $\approx$ 1.6 cm, corresponding to $\tau_S/2$ (τ_S is the K^0 short lifetime) [4]. The calorimeter will also provide identification of electrons and pions to a level of a few per cent, making use of the different patterns of the electron- and pion-induced showers.

The high rate of the stopping antiprotons (2×10^6 $\bar{p}$/s) and the low branching ratio of the interesting reactions (2) require a filter mechanism to select only those events of potential physics interest. A system of four trigger levels has been designed [5]. The pretrigger, already installed, determines the charged-particle multiplicity and finds the kaon candidates having a transverse momentum p_T larger than 250 MeV/c. The first-level trigger reconstructs the charged tracks and then the kinematics of the event. The second-level trigger improves the kaon identification by using the Cherenkov analog signals and the TOF information. The number of showers in the calorimeter is also determined. The third-level trigger identifies the showers induced by γ's, and, in the case of 4 γ, reconstructs the path of the K^0 decaying into $\pi^0\pi^0$. The expected data reduction is 5×10^{-5}. The acceptance of the events induced by reactions (2) is expected to be $\approx$ 20%. VME microprocessors are used to perform the data acquisition, transport, and monitoring of the data. Central control is maintained by a VAX computer [5].

During the data taking two types of events have been collected: those with at least one hit in the S1 scintillators and those satisfying the pretrigger conditions. To the first class of events belong essentially pionic annihilations. Events with two tracks have been selected. Figure 5 shows the energy distribution of the charged pions for the events having a mass missing from the $\pi^+\pi^-$ system in the region of the π^0 mass (at present the electromagnetic calorimeter is only partially equipped and the π^0's cannot be reconstructed). The distribution shows a peak around 780 MeV corresponding to ρ^0 production. The second class of events contains a large fraction of annihilations with a charged kaon in the final state. In a preliminary analysis we looked for events induced by reactions (2) with the K^0 decaying into $\pi^+\pi^-$. Figure 6 shows the invariant mass square distribution obtained using the on-line information for $\pi^+\pi^-$ having an origin at a distance larger than 2 cm from the annihilation point. The distribution shows a clear peak in the K^0 mass square region.

In the following we discuss the precision that is expected to be obtained in the determination of some CP, T, and CPT parameters in the case of 10^{13} antiprotons stopped in the target.

In Fig. 7 is shown the expected differential asymmetry in the case of $\pi^+\pi^-$ decay

$$A_{+-} = [R[\bar{K}^0 \to \pi^+\pi^-](t) - R[K^0 \to \pi^+\pi^-](t)]/[R[\bar{K}^0 \to \pi^+\pi^-](t) + R[K^0 \to \pi^+\pi^-](t)] \ . \quad (3)$$

The same distribution will also be measured for $\pi^0\pi^0$ decay. From these determinations the values of the phases $\phi_{\pi^+\pi^-}$ and $\phi_{\pi^0\pi^0}$ will be obtained, allowing a test of the CPT symmetry [6]. The statistical and the systematic errors in the difference of the two phases are expected to be $\sigma(\phi_{\pi^+\pi^-} - \phi_{\pi^0\pi^0})_{stat} \approx 0.3°$ and $\sigma(\phi_{\pi^+\pi^-} - \phi_{\pi^0\pi^0})_{syst} \leq 1°$. The systematic error is dominated by the uncertainty in the measurement of the decay path of K^0 ($\bar{K}^0$) into $2\pi^0$, the resolution being $\approx$ 1.6 cm. For $K^0 \to \pi^+\pi^-$ the decay length will be reconstructed with a precision of $\approx$ 2 mm.

The ε'/ε ratio will be determined from the integrated asymmetries

$$I_{\pi^0\pi^0} = [(\bar{N}_{\pi^0\pi^0}/\bar{N} - N_{\pi^0\pi^0}/N)]/[(\bar{N}_{\pi^0\pi^0}/\bar{N} + N_{\pi^0\pi^0}/N)] \quad (4)$$

and

$$I_{\pi^+\pi^-} = [(\bar{N}_{\pi^+\pi^-}/\bar{N} - N_{\pi^+\pi^-}/N)]/[(\bar{N}_{\pi^+\pi^-}/\bar{N} + N_{\pi^+\pi^-}/N)] \ , \quad (5)$$

where N ($\bar{N}$) is the total number of events having a mass missing from the $K^-\pi^+$ ($K^+\pi^-$) system compatible with the K^0 ($\bar{K}^0$) mass, and $N_{\pi^+\pi^-}$ ($\bar{N}_{\pi^+\pi^-}$) and $N_{\pi^0\pi^0}$ ($\bar{N}_{\pi^0\pi^0}$) are the events belonging to the previous classes and decaying into $\pi^+\pi^-$ and $\pi^0\pi^0$ in the fiducial volume corresponding to $\approx 20\tau_S$.

The background due to annihilation channels is expected to be a few per cent. It can be separated from the signal by studying the mass missing from the system of the particles identified as the charged pion and the charged kaon. The expected precision in the reconstruction of the missing mass in the case of processes (2) is $\sigma = \pm 75$ MeV/c^2. The background due to the three-body decay of K^0 is expected to be < 3%.

The $|\varepsilon'/\varepsilon|$ ratio will be obtained from the asymmetries (4) and (5) according to

$$|\varepsilon'/\varepsilon| = 1/6\,(1 - I_{\pi^0\pi^0}/I_{\pi^+\pi^-}) \ . \qquad (6)$$

The expected statistical error is $\sigma(|\varepsilon'/\varepsilon|)_{stat} \approx 1.5 \times 10^{-3}$. The systematic error due to background subtraction, to the variation of $\pi^+\pi^-$ and $\pi^0\pi^0$ reconstruction efficiencies as a function of the proper time, and to the momentum-dependent efficiency in tagging the neutral kaon, is expected to be smaller. This measurement has systematic errors that are completely different from those occurring in the determination of the $|\varepsilon'/\varepsilon|$ ratio performed making use of K_S and K_L [7].

No evidence of CP-violation has so far been detected in the decays of K^0 and $\bar{K}^0$ into 3π. If the value of $\eta_{3\pi} = a(K_S \to 3\pi)/a(K_L \to 3\pi)$ is equal to $\eta_{2\pi}$, the branching ratio of the K_S decay into 3π is expected to be $R(K_S \to 3\pi) \approx 10^{-9}$, and thus very difficult to measure. In the case of $\pi^+\pi^-\pi^0$ decay a Dalitz-plot analysis is required to identify the CP of the three pions. The interference term is expected to be $\approx 10^{-3}$ (see Fig. 8), and a measured value different from zero is clear evidence of CP-violation also for the $\pi^+\pi^-\pi^0$ decay [8]. The expected statistical error in the determination of $\eta_{\pi^+\pi^-\pi^0}$ is $\sigma(\eta_{\pi^+\pi^-\pi^0})_{stat} \approx 6 \times 10^{-4}$. The systematic error will be of the same order.

The measurement of the semileptonic decays, $K^0(\bar{K}^0) \to e\pi\nu$, will allow an improvement of the limit on the $\Delta S = \Delta Q$ violating amplitude. In Figs. 9a and 9b the expected distributions of the quantity

$$A = \{R[\bar{K}^0 \to e\pi\nu](t) - R[K^0 \to e\pi\nu](t)\}/\{R[\bar{K}^0 \to e\pi\nu](t) + R[K^0 \to e\pi\nu](t)\} \qquad (7)$$

are shown as a function of the proper time for Im x = 0 and Im x = 2×10^{-3}, respectively. The quantity x is the amplitude ratio $x = a(\Delta S = -\Delta Q)/a(\Delta S = \Delta Q)$. The value of Im x in Fig. 9b is ten times smaller then the present limit. The quantity δ in the figures is the CPT-violation parameter of the mass matrix. The measurement of the semileptonic decay mode will also allow a determination of Δm with a precision of $\sigma(\Delta m)/\Delta m = 1.2 \times 10^{-3}$. The present precision is 4.1×10^{-3}. A direct determination of the T violation can be obtained from the measurement of the asymmetry A_T [9]

$$A_T = \frac{R[\bar{K}^0 \to e^+\pi^-\nu](t) - R[K^0 \to e^-\pi^+\nu](t)}{R[\bar{K}^0 \to e^+\pi^-\nu](t) + R[K^0 \to e^-\pi^+\nu](t)}. \tag{8}$$

Assuming the rule $\Delta S = \Delta Q$ to be valid, a value of Eq. (8) different from zero corresponds to a difference in the probabilities $P(K^0 \to \bar{K}^0)$ and $P(\bar{K}^0 \to K^0)$, and thus to an evidence of the violation of the T symmetry in the mass matrix. The expected relative precision on A_T is 6%. The determination of the quantities Δm and A_T requires e, π identification.

In Table 1 the expected accuracies (1σ), including systematic errors, assuming 10^{13} stopped antiprotons, are summarized. The present experimental results [7, 10, 11] are also reported.

The experiment is expected to be fully operational by the end of 1990.

REFERENCES

[1] L. Adiels et al., Proposals CERN PSCC/85-6 P82 (1985); PSCC/85-30 P82 (1985); PSCC/86-34 M234 (1986); PSCC/87-14 M272 (1987).

[2] M. van der Putte et al., $\bar{p}$-beam monitor system for CP LEAR, submitted for publication in the Proc. of the IEEE Conference, San Francisco, January 1990.

[3] R. Rieckenbach et al., Nucl. Instrum. Methods A279 (1989) 305.

[4] A. Schopper, Proc. Int. School of Physics with Low Energy Antiprotons – Fundamental Symmetries, Erice, 1986, eds. P. Bloch, R. Klapisch and P. Pavlopoulos (Plenum Press, New York, 1988), p. 211.

[5] C. Bee et al., Proc. Conf. on VME Bus in Research, Zurich, 1988, eds. C. Eck and C. Parkman (Elsevier Science Publishers B. V. and North-Holland, Amsterdam, 1988); p. 170.

[6] V.V. Barmin et al., Nucl. Phys. B274 (1984) 293.

[7] See, for example, H. Burkhardt et al., Phys. Lett. 206 (1988) 169.

[8] L.M. Seghal and L. Wolfenstein, Phys. Rep. 162 (1987) 1362.

[9] P.K. Kabir, Phys. Rev. D2 (1970) 540.

[10] B. Winstein, A measurement of ϵ'/ϵ by E731, Invited presentation at the XIV Int. Symposium on Lepton and Photon Interactions, Stanford, 1989.

[11] Review of Particle Properties, Phys. Lett. 204B (1988).

Table 1

Present experimental results and expected accuracies

Parameters	Present situation	Expected precision
ϵ'/ϵ	$(3.3 \pm 1.1) \times 10^{-3}$ [7]	$< 2 \times 10^{-3}$
"	$(-0.5 \pm 1.5) \times 10^{-3}$ [10]	
$\phi_{\pi^+\pi^-} - \phi_{\pi^0\pi^0}$	$(-9.4 \pm 5.1)°$ [11]	$\leq 1°$
$\eta_{\pi^+\pi^-\pi^0}$	< 0.35 [11]	7×10^{-4}
Re x	< 0.02 [11]	6×10^{-4}
Im x	< 0.026 [11]	7×10^{-4}
$\sigma(A_T)/A_T$	–	6×10^{-2}
$\sigma(\Delta m)/\Delta m$	4.0×10^{-3} [11]	1.2×10^{-3}

Figure captions

Fig. 1 Layout of the CP LEAR detector. From the centre we have the target, the two proportional chambers, the six drift chambers, the two layers of streamer tubes, the scintillators S1 and S2 with the Cherenkov in between, and the calorimeter. A typical event with the reconstructed values of the transvere momentum of the charged particles is shown.

Fig. 2 Antiproton beam profile with the present beam diagnostic, a) vertical projection, b) horizontal projection. The strips have a transvere dimension of 2 mm.

Fig. 3 Preliminary on-line distribution of the difference of the z coordinates of the charged tracks measured in the inner and outer streamer tube layers.

Fig. 4 Preliminary distributions of the time-of-flight difference for charged particles produced in proton-antiproton annihilation.

Fig. 5 Preliminary total energy distribution of the π^+ and π^- produced in the reaction $\bar{p}p \rightarrow \pi^+\pi^-\pi^0$.

Fig. 6 Preliminary invariant mass square distribution of π^+ and π^- coming from K^0 produced in reaction (2). It shows the present quality of the "quasi" on-line data.

Fig. 7 Rate asymmetry for the $\pi^+\pi^-$ decay channel as a function of the proper time t.

Fig. 8 The deviation from unity of the K^0 and $\bar{K}^0$ decay rates into $\pi^+\pi^-$ and $\pi^0\pi^0$ as a function of the proper time t [$u_{+-0} = 1 - R[K^0 \rightarrow \pi^+\pi^-\pi^0](t)/R[\bar{K}^0 \rightarrow \pi^+\pi^-\pi^0](t)$].

Fig. 9 The asymmetry A of semileptonic decays as a function of the proper time t for two values of the quantity Im x [$x = a(\Delta S = -\Delta Q)/a(\Delta S = \Delta Q)$].

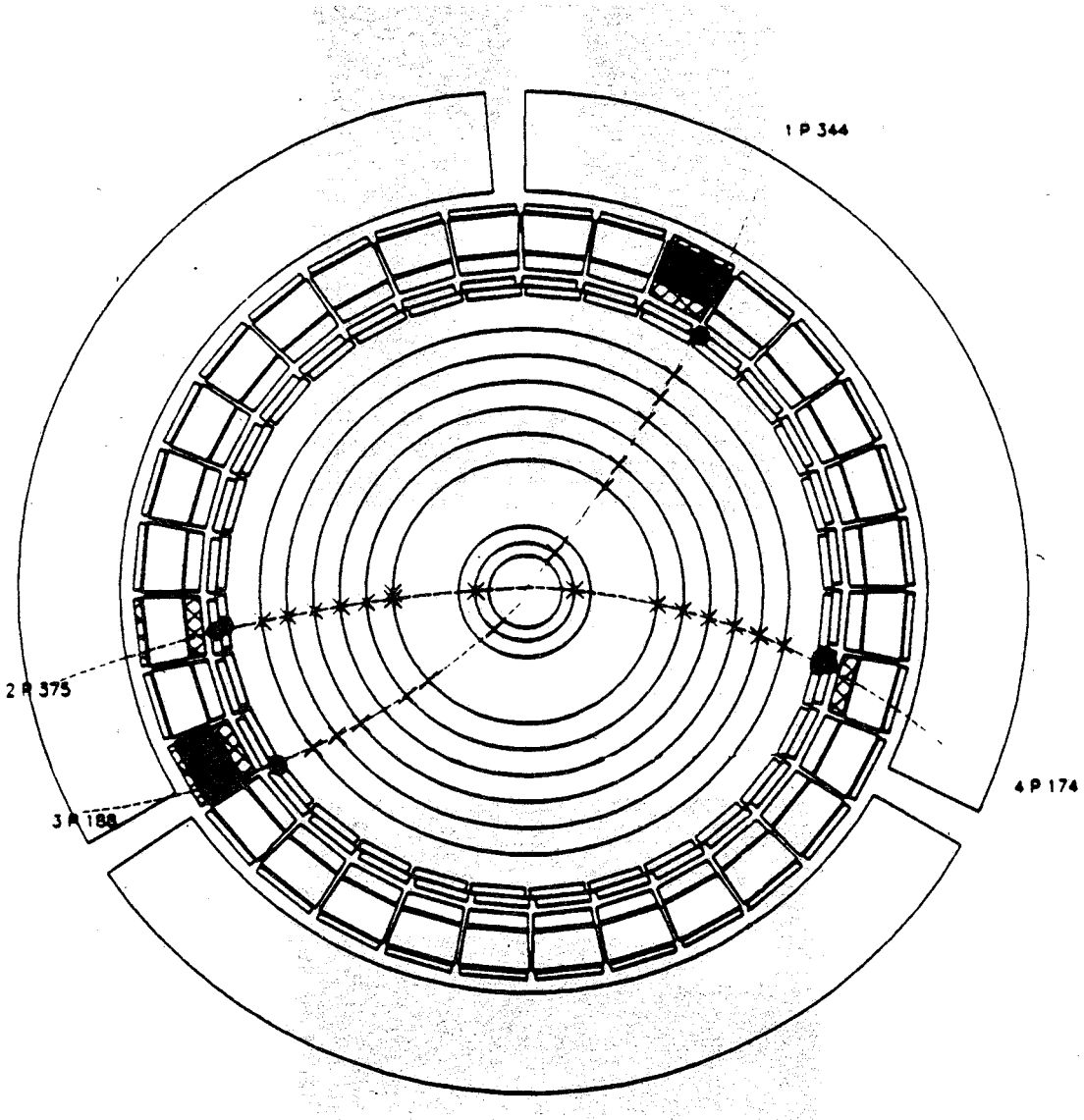

FIG. 1

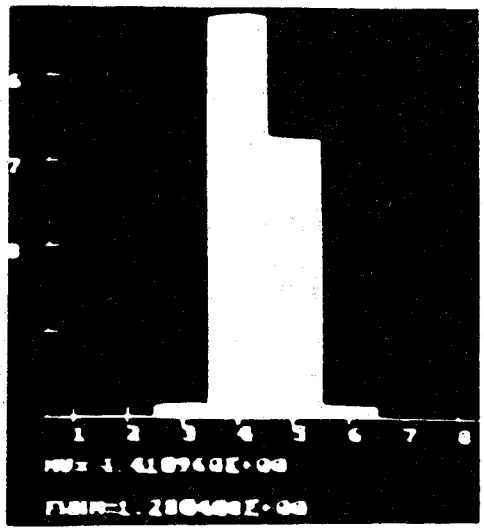

FIG. 2a

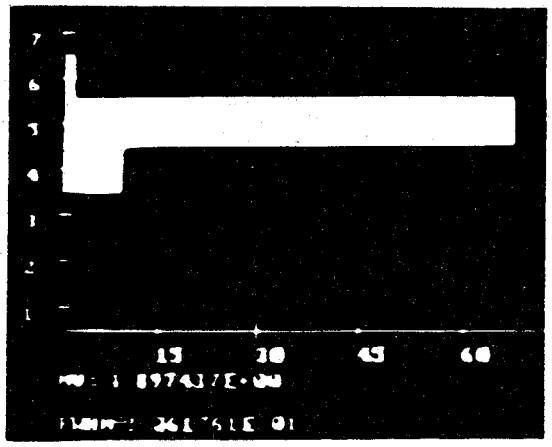

FIG. 2b

PRELIMINARY

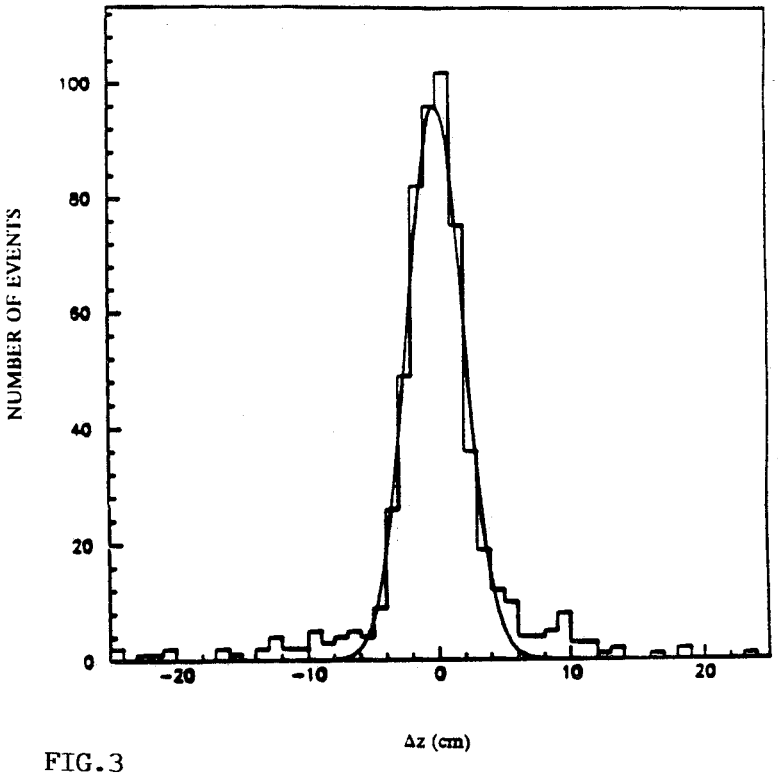

FIG.3

PRELIMINARY

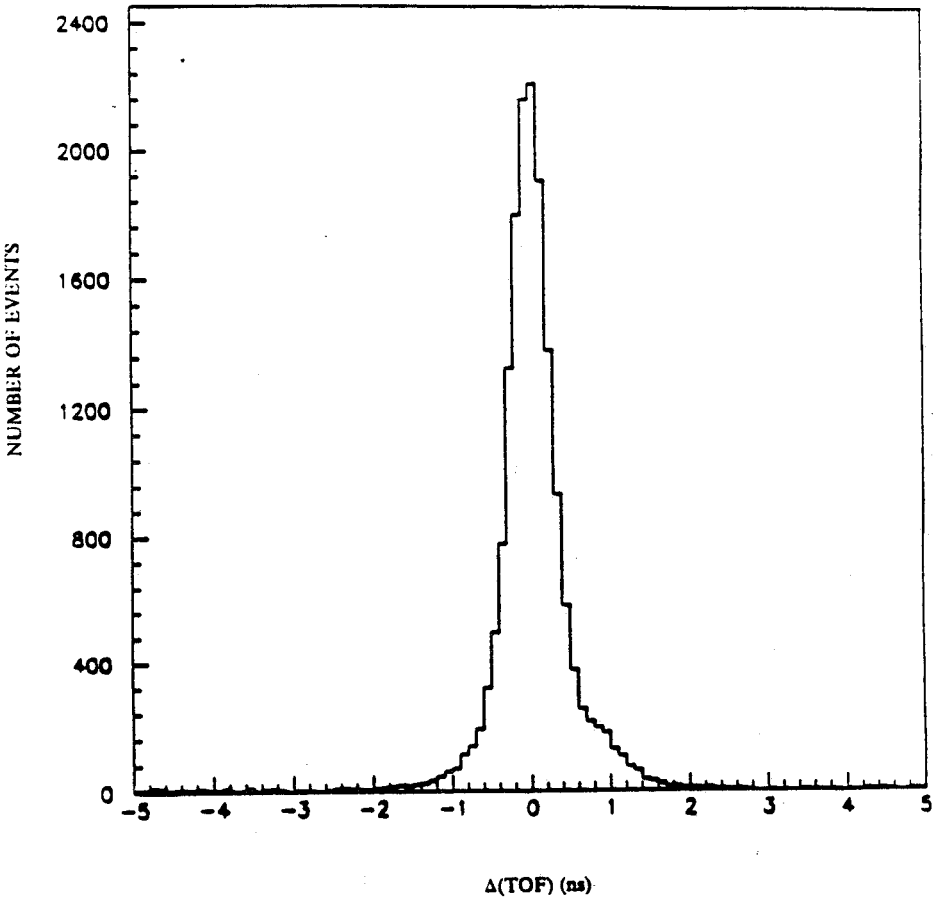

FIG. 4

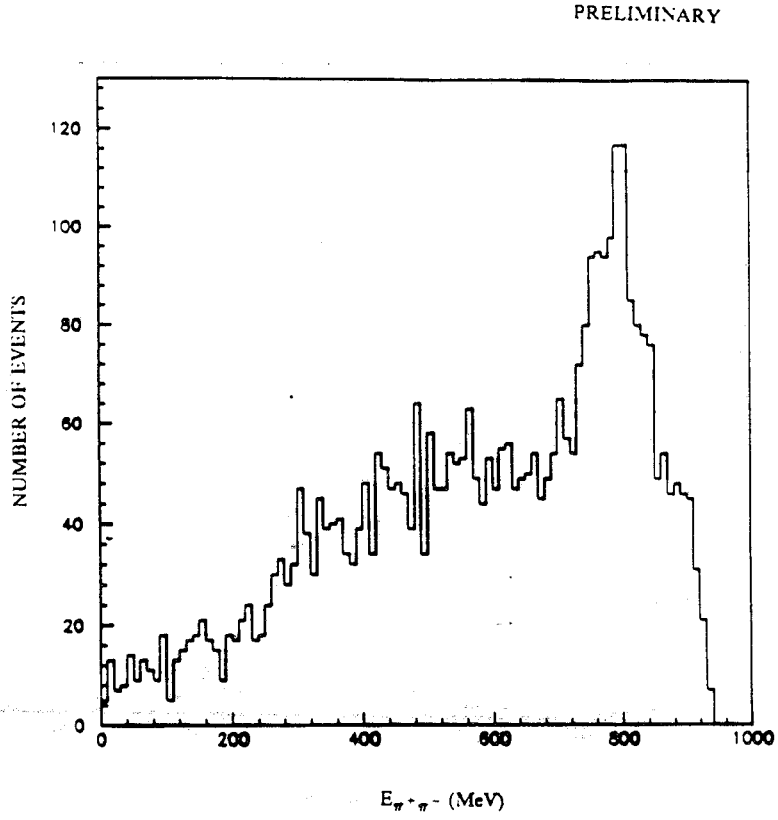
PRELIMINARY
NUMBER OF EVENTS
0
20
40
60
80
100
120
0
200
400
600
800
1000
$E_{\pi^+\pi^-}$ (MeV)

FIG. 5

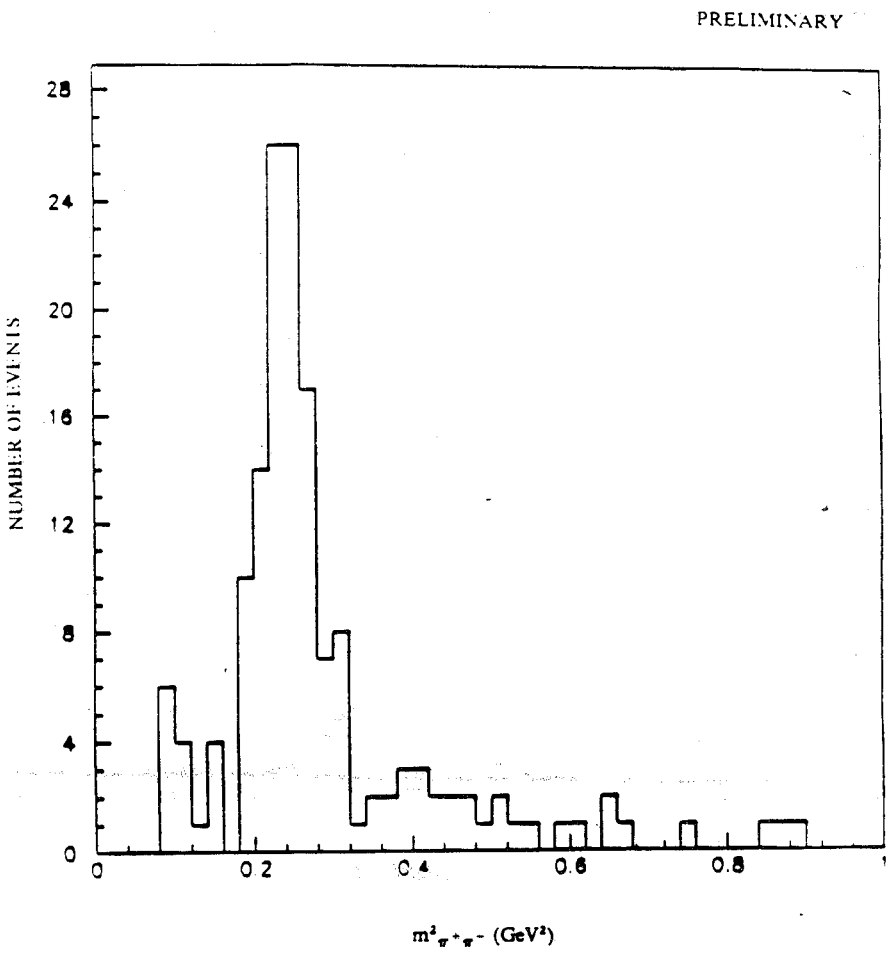
PRELIMINARY
NUMBER OF EVENTS
0
4
8
12
16
20
24
28
0
0.2
0.4
0.6
0.8
$m^2_{\pi^+\pi^-}$ (GeV^2)

FIG. 6

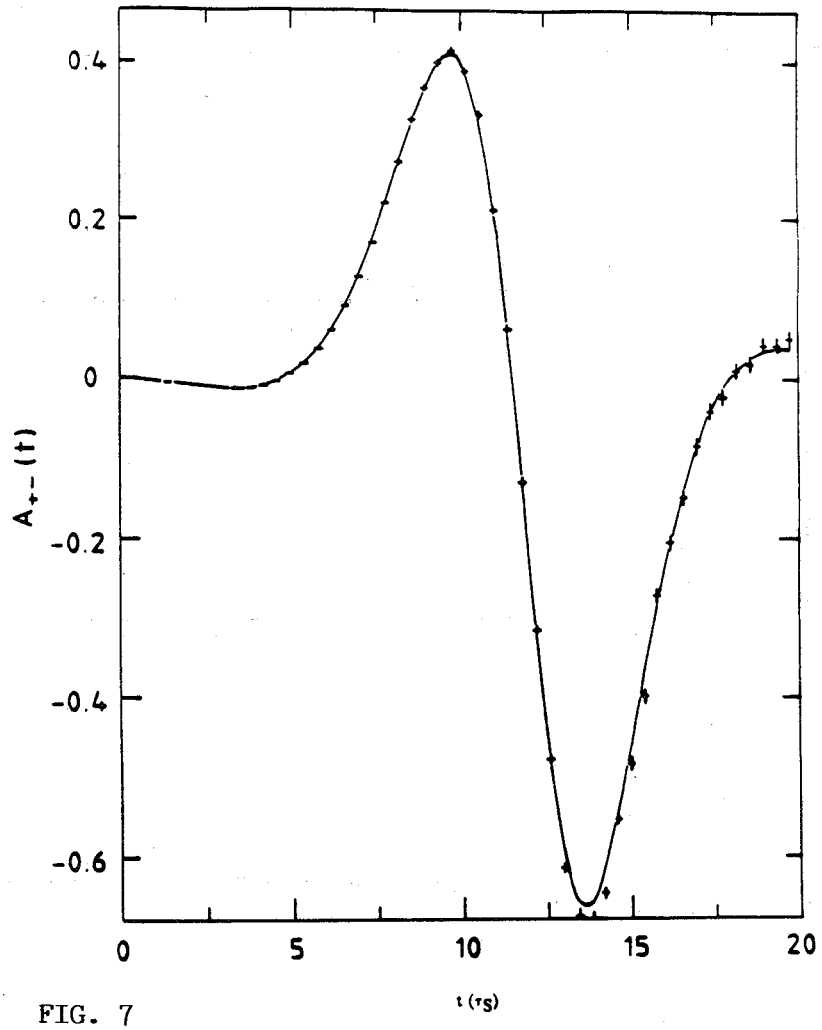
0.4
0.2
0
-0.2
-0.4
-0.6
$A_{+-}(t)$
0
5
10
15
20
t (τS)

FIG. 7

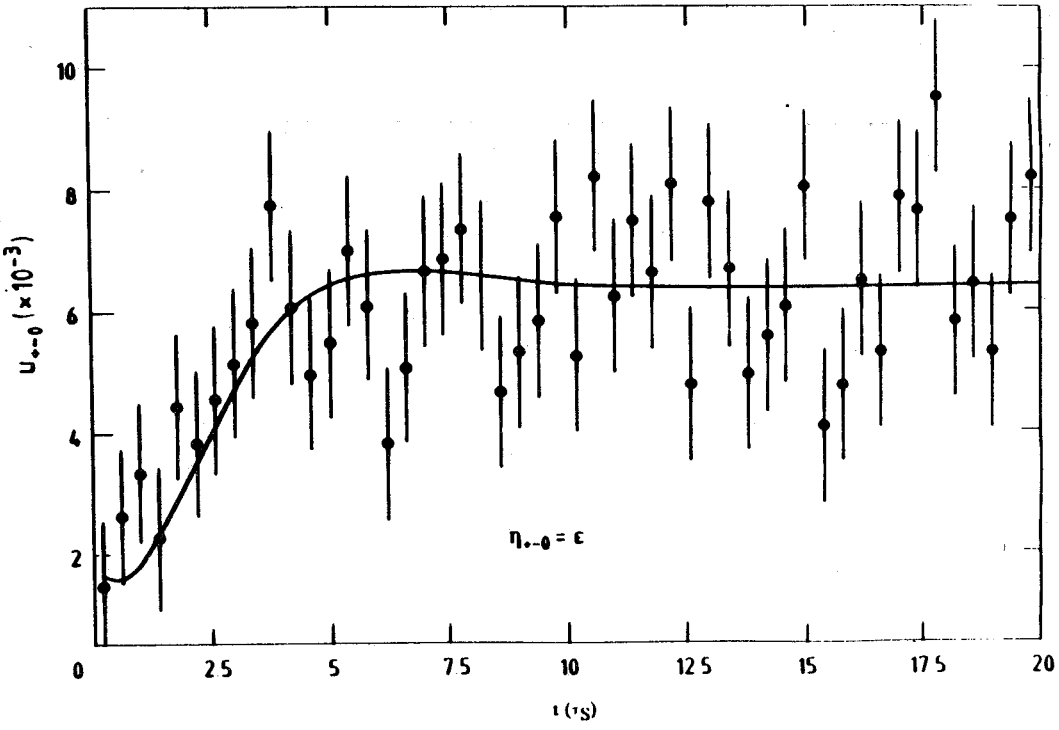
10
8
6
4
2
U_{+-0} (×10⁻³)
$\eta_{+-0} = \epsilon$
0
2.5
5
7.5
10
12.5
15
17.5
20
t (τS)

FIG. 8

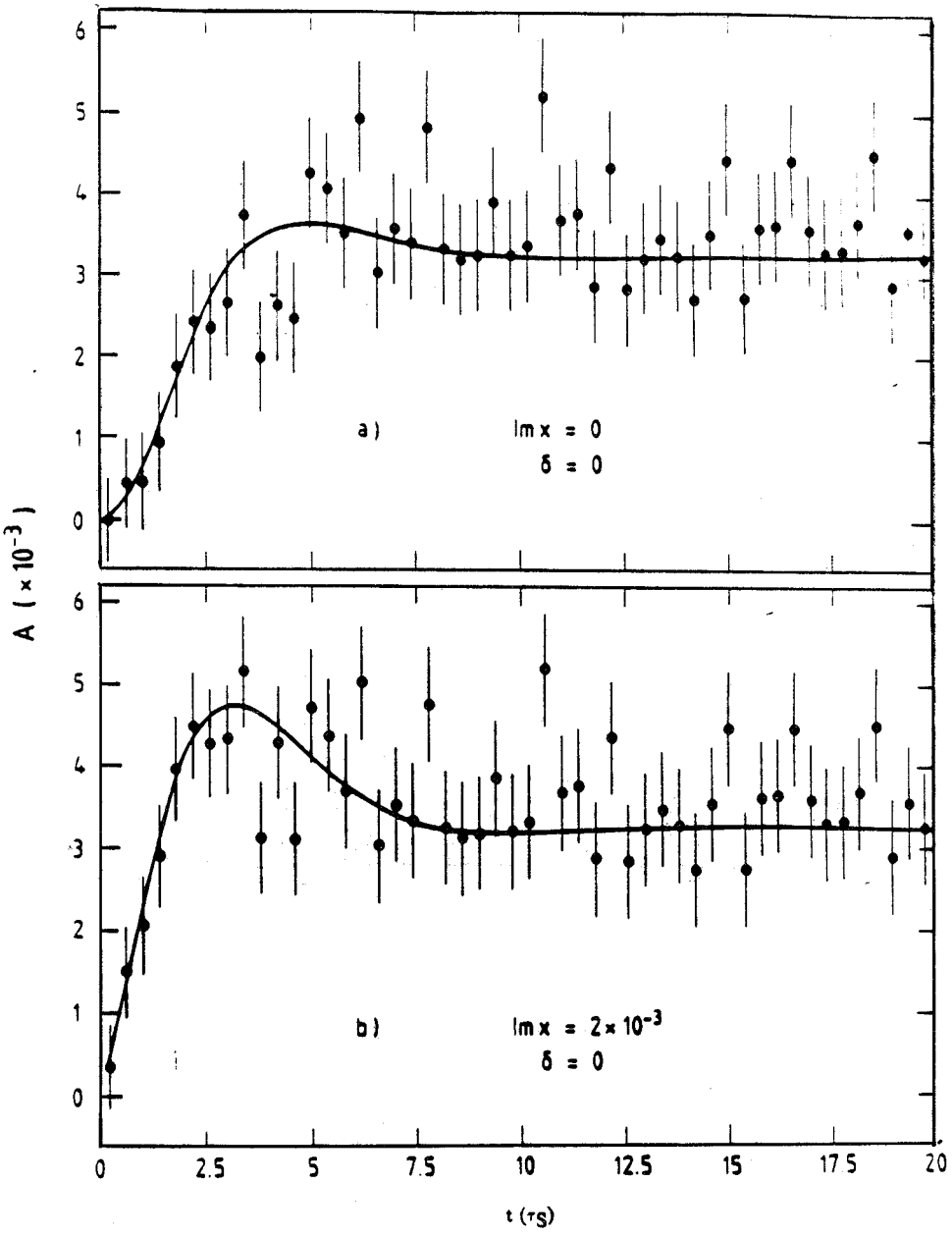

FIG. 9

Measurement of the ν_μ mass at a Φ - factory

P. F. Loverre

Facoltà di Agraria, Università della Basilicata, Potenza, Italy

Istituto Nazionale di Fisica Nucleare , Sezione di Roma, Italy

January 8, 1990

This note investigates the possibility of improving the limits on the muon neutrino mass by studying the 3-body K_L^0 decay at a Φ - factory .

The existing limits on the ν_μ mass are derived from several experiments of increased accuracy, studying the 2-body π decay both in flight and at rest. The best result was obtained by Abela et al.[1] :$m_{\nu_\mu} < 250\ KeV$. It seems very difficult to significantly improve this limit by studying the pion decay.

A less stringent limit ($m_{\nu_\mu} < 650\ KeV$) was obtained in 1974 by an experiment (Clark et al. [2]) studying the $\pi\,\mu\,\nu_\mu$ decay of a K_L^0 beam with momentum range 0.8 - 3.2 GeV/c at the Bevatron. The 3-body decay allows in principle better sensitivity to the neutrino mass because of the possibility of producing the neutrino at rest in the c.m. of the decay (E_ν is then linear in m_{ν_μ}). In fact, Clark et al. studied the end point of the ($\pi\,\mu$) invariant mass spectrum. The spectrum ends at $m(\pi\mu) = m(K_L^0)$ if $m_{\nu_\mu} = 0$. For $m_{\nu_\mu} \neq 0$ it ends at $m(\pi\mu) = (\,m(K_L^0) - m(\nu_\mu)\,)$. The shape of the spectra resulting from 8.9×10^9 K_L^0 decays, are shown in fig.1 for the two cases: $m_{\nu_\mu} = 0$ and $m_{\nu_\mu} = 1MeV$. The limit on m_{ν_μ} is determined by the distortion of the spectrum compared to the shape expected for zero ν_μ mass.

A Φ - factory with high luminosity will allow to study the K_L^0 decay in much cleaner conditions than those obtainable with a separated beam (reconstruction of the charged particles up to the decay vertex, no contamination from neutral particles other than the K_L^0).

To have a first glance at the accuracy obtainable at a Φ - factory , I made some calculations assuming for the machine luminosity $L = 2 \times 10^{33} cm^{-2} sec^{-1}$ and $2 \times 10^7\ sec$ of effective data taking ($\approx 2/3$ of a year). I assumed as a working hypotheses to use a detector with the same performances as the one designed by Barbiellini and Santoni[3] . The relevant figures are the following: sphere of 1m radius as useful volume for the K_L^0 decay vertex; angular resolution on the charged tracks: $\Delta\theta = \Delta\phi = 1mrad$;

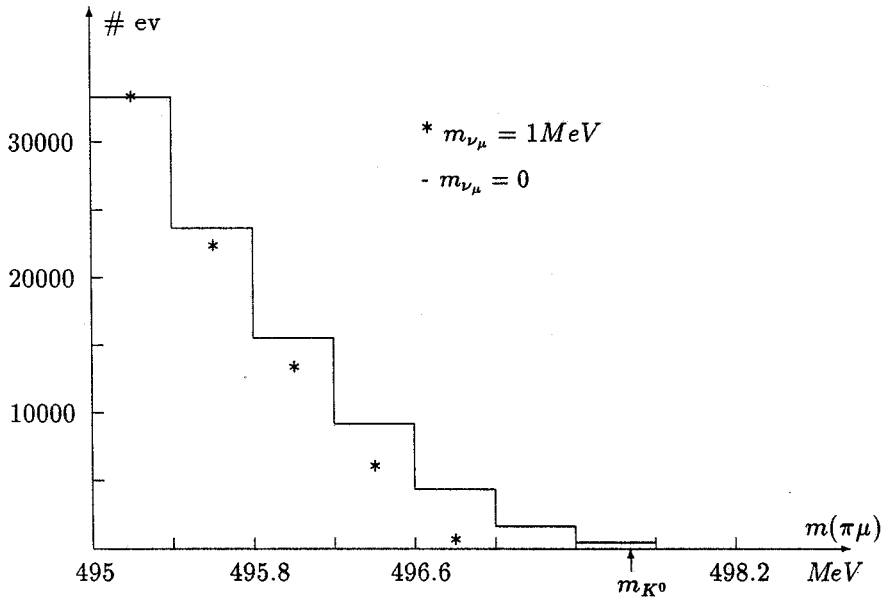

Figure 1: $(\pi\mu)$ mass spectrum

momentum resolution: $\Delta p_t/p_t = 0.006$, where p_t is the momentum component transverse to the beam direction. With these assumptions, taking into account the Φ cross-section ($\sigma = 4.8 \times 10^{-30} cm^2$) , the $\Phi \longrightarrow K_S^0\ K_L^0$ branching ratio (= 34.4 %), the $K_L^0 \rightarrow \pi\mu\nu$ branching ratio (= 27.0%), and the K_L^0 lifetime ($\tau = 5.2 \times 10^{-8} sec$), one gets 4.5×10^9 observed K_L^0 decays. In order to evaluate the experimental possibilities at a Φ - factory events were generated by Monte-Carlo, starting from the simulation of the $\Phi \longrightarrow K_S^0\ K_L^0$ decay, followed by the 3-body decay of the K_L^0 . The momenta of the pion and of the muon were then smeared with gaussian errors of the size given above. The M.C. was run for different values of m_{ν_μ} , so allowing to compare the reconstructed spectra of the $(\mu\pi$) effective mass.

Figure 2 shows the difference between the spectrum corresponding to zero ν_μ mass and the one corresponding to ν_μ = 500 KeV . The error bars correspond to the above quoted number of observed K_L^0 decays: $N_K = 4.5 \times 10^9$. The difference is statistically significant. Computing the same spectrum for different values of m_{ν_μ} , one finds that the minimum detectable value is of the order of 280 KeV .

Perhaps, more than comparing M.C. results for different situations it is interesting to have a formula which shows the dependence of the sensitivity from the two relevant parameters: the statistics and the resolution $\sigma(\pi\mu)$ on the effective $(\pi\mu)$ mass. Since the resolution is anyway of the order of 1 MeV ($\sigma(\pi\mu)$ =1.5 MeV for the above discussed detector) it is not possible to determine directly the end point of the $(\pi\mu)$ spectrum with an accuracy of few hundreds KeV . The upper limit on the ν_μ mass is then basically determined by comparing, in a region of total width of the order of

few $\sigma(\pi\mu)$ centered at $m(\pi\mu) = m_K$, the number of observed events, N_o , with the number of events N_e expected in case of zero ν_μ mass. The size of the effect is then given by $N_s/\sqrt{N_e}$, with $N_s = (N_e - N_o)$, the *signal events*. From the shape of the $(\pi\mu)$ spectrum it turns out that N_s grows as

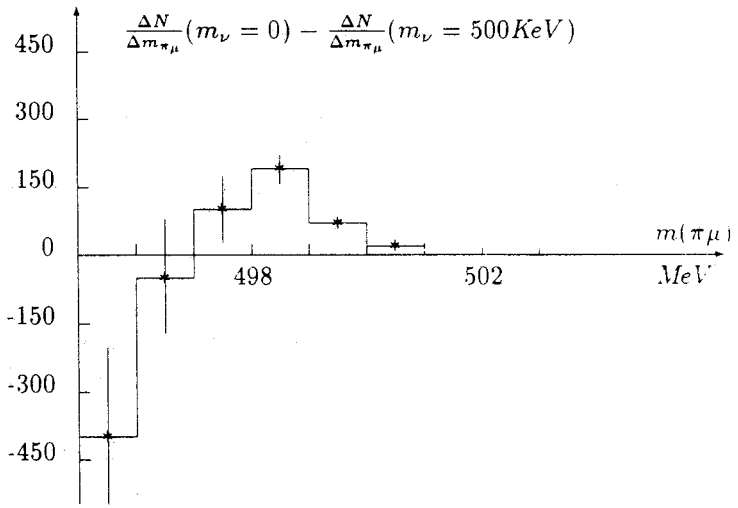

Figure 2:

$m^3_{\nu_\mu}$ A rough numerical esitmate is given by the equation:

$$N_s = (m_{\nu_\mu})^3 \times 1.5 \times 10^{-6} \times N_K \tag{1}$$

where m_{ν_μ} is in MeV and N_K represents the total number of K^0_L decays.

Consider now N_e . The events contributing to the relevant mass interval would be, in the case of zero ν_μ mass, the ones with non-smeared $(\pi\mu)$ mass close to m_K . Assume for instance the condition $m(\pi\mu) > [m_K - \sigma(\pi\mu)]$; N_e is then given by $N_e = \sigma(\pi\mu)^3 \times 0.5 \times 10^{-6} N_K$ $(\sigma(\pi\mu)$ in MeV). Combining the different formulas, one finally gets

$$\frac{N_s}{\sqrt{N_e}} = \frac{(m_{\nu_\mu})^3}{\sqrt{\sigma(\pi\mu)^3}} \times 2.1\ 10^{-3}\sqrt{N_K} \tag{2}$$

Aiming at a 1.64 standard deviations effect (90% C. L.), one has:
$1.64 = (N_s/\sqrt{N_e})$ and hence

$$m_{\nu_\mu} = \frac{\sqrt{\sigma(\pi\mu)}}{N_K{}^{\frac{1}{6}}} \times 9.2 \tag{3}$$

with m_{ν_μ} and $\sigma(\pi\mu)$ in MeV .

The meaning of eq.3 is the following: in a given experiment the 90% C.L. limit obtainable on the ν_μ mass improves with the square root of the resolution on the $(\pi\mu)$ mass and only with the sixth root of the statistics (note that this is only the case if $m_{\nu_\mu} < \sigma(\pi\mu)$) .

Numerically eq.3 was adjusted to match the M.C. results. In fact, by M.C. one finds that in the given experimental configuration the resolution $\sigma(\pi\mu)$ is of the order of 1.5 MeV . With $N_K = 4.5\times10^9$, one gets from eq.3 $m_{\nu_\mu} \leq 277$ KeV . Clark et al. had 75 times smaller statistics and a resolution $\sigma(\pi\mu) =$ 1.3 MeV . Inserting these numbers in Eq.3 one gets $m_{\nu_\mu} = 535$ KeV in agreement with the 90 % C.L. limit $m_{\nu_\mu} = 550$ KeV obtained by Clark without taking into account systematical errors.

In summary, eq.3 shows that big improvements on m_{ν_μ} at a Φ - factory will be very hard to obtain. However, a good $(\pi\mu)$ mass resolution turns out to be important; work on the detector and selections on the geometry of the events could improve the resolution, perhaps by a factor two (note that the detector proposed in [3] was not designed to study this reaction; it gives a resolution of 1.5 MeV on the $(\pi\mu)$ mass . Clark et al. , in a different experimental situation reached a value of 1.3 MeV) . In this case the sensitivity could be pushed to values of the neutrino mass of the order of 150-200 KeV , definitely smaller than the present limits.

Before concluding it is important to mention two other sources of error, which have not been studied in this note.

To make a comparison between the observed $(\pi\mu)$ spectrum and the one expected for zero ν_μ mass, a detailed knowledge of the resolution on $m(\pi\mu)$ is needed. For instance, distortions of the tails of the resolution function by non-gaussian effects could spoil the precision of the measurement. To evaluate the importance of this effect M.C. events should be generated with a complete description of the detector response. The second problem is the correct identification of the $K_L^0 \rightarrow \pi\mu\nu$ events. Contamination from $K_L^0 \rightarrow \pi\pi$ decays (b.r.= 0.20 %), followed by the decay in flight of one of the pions, would distort the $(\pi\mu)$ mass spectrum just in the region of interest ($m(\pi\mu) = m_K$). In this respect however, the Φ - factory would allow a precise evaluation of the effect (and hence of the correction needed) by studying it in the $K_S^0 \rightarrow \pi\pi$ channel.

References

[1] R. Abela et al.,*Phys.Lett. B146 (1984) 431*

[2] A.R.Clark et al., *Phys. Rev. D9 (1974) 533*

[3] G.Barbiellini and C.Santoni, *CERN-EP/89-88 (1989)*

PART II: THE MACHINE

A Φ-FACTORY IN THE ADONE AREA

M. Bassetti and G. Vignola

Introduction

In the ARES Design Study (LNF-90/005) a site-independent accelerator complex was presented, which consists of:
- a two-ring colliding beam Φ-factory
- a 510 MeV Superconducting LINAC injector.

We propose to use a conventional LINAC as an injector. This choice allows to place the Φ-factory complex inside existing LNF buildings: the ADONE hall and the LINAC tunnel.

In the following, we discuss this option, and give the cost estimate and time schedule.

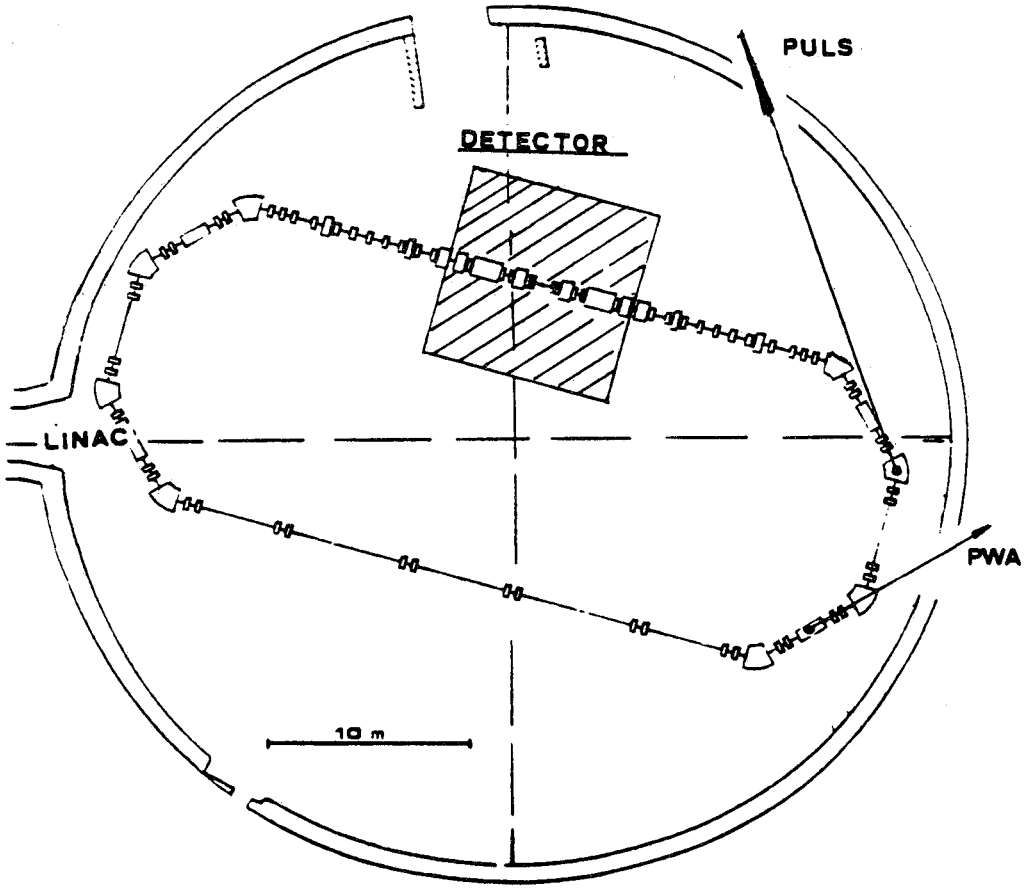

The Φ-factory in the ADONE Hall: the machine is oriented in such a way to illuminate the existing PULS and PWA beamlines.

The Φ-factory storage rings

The Φ-factory storage rings are the same as described in LNF-90 (see Appendix 1). The storage rings are located in the existing ADONE hall and are oriented in such a way to illuminate the existing PWA and PULS beam lines, by a wiggler and a bending magnet respectively. We envisage a two phase project.

PHASE I is supposed to end with the achievement of the design luminosity by optimizing the most conventional parameters. We are quite confident that at this stage a luminosity of 10^{32} cm^{-2} sec^{-1} can be reached.

PHASE II: here machine improvements are scheduled to further upgrade machine performance. They can be divided into two main classes:

1) Increase of damping and fluctuations by additional wigglers
2) Increase of the collision frequency by crab-crossing.

In Appendix 2 a preliminary crab-crossing scheme is presented which should give a luminosity enhancement factor of the order of 5.

In conclusion this design has a final luminosity goal which is near to 10^{33} cm^{-2} sec^{-1}.

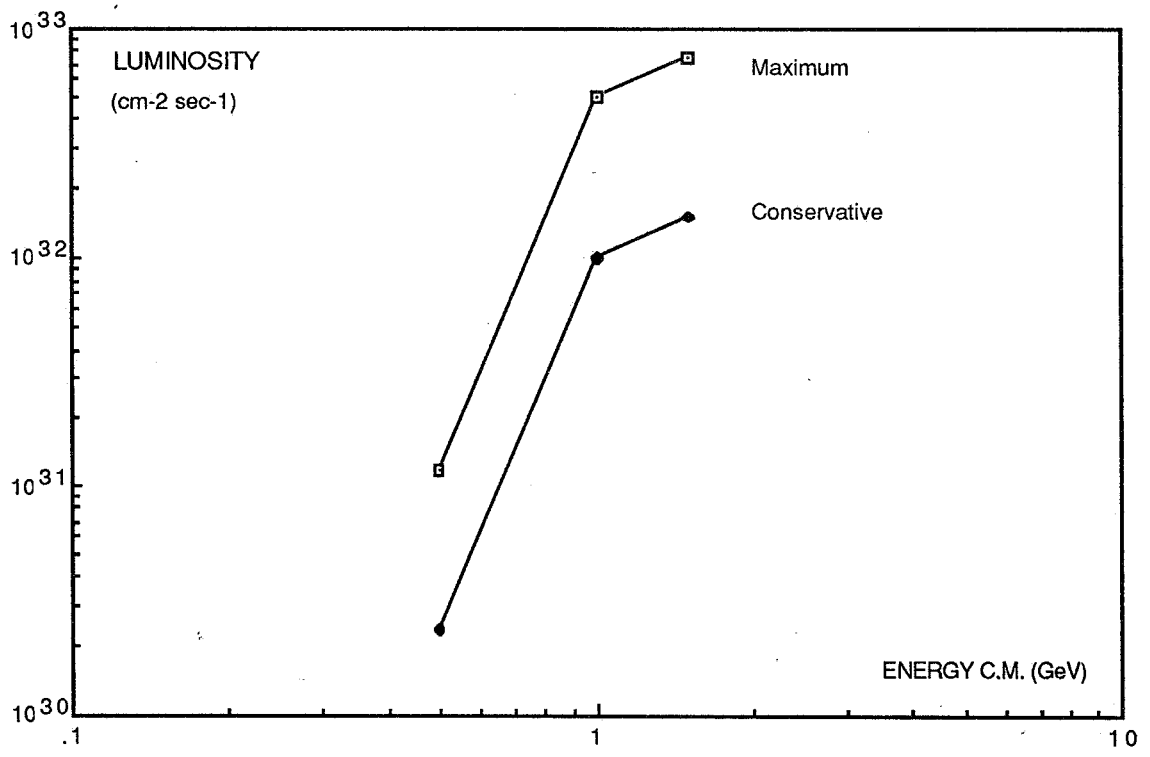

We point out that a crab-crossing scheme implies necessarily two opposite crossings. The second crossing can be made parasitic or perfectly equivalent to an insertion for another experiment.

The Φ-factory Injector

The ADONE-LINAC is so obsolete that we are forced to consider a new one, but the existing tunnel is adequate to accomodate the injection system. The Φ-factory injector is a new warm LINAC, similar to the one used for LEP, made up of:

a) 200-220 MeV high-current conventional LINAC;
b) a positron converter;
c) 550 MeV low-current conventional LINAC.

Such a LINAC fits without any problems in the existing 80 m long tunnel and its cost is estimated to be about 13 GLit.

Φ-Factory tentative summary cost estimate

PHASE I:

1)	**Storage rings:**	
	Components, controls etc.	26.0
	Building(*) and Conv. Plants	4.0
	Contingency (10%)	3.0
	IVA (19%)	6.3
		39.3

(*) Experimental area not included

2)	**Injector:**	
	LINAC (500 MeV e^+)	13.0
	Building and Conv. Plants	3.0
	Transport Line	1.0
	Contingency (10%)	1.7
	IVA (19%)	3.6
		22.3
3)	**R & D**	4.7
	PHASE I Total	**66.0**

PHASE II:

1)	**Crab-crossing**	9.0
2)	**Wigglers**	6.0
	PHASE II Total	**15.0**

PHASE I: Tentative time schedule

YEARS	1991	1992	1993	1994	1995
DESIGN AND PROTOTYPES	xxxxxxxxx				
PROCUREMENT AND TEST		xxxxxxxxxxxxxxxxxx			
BUILDING UPGRADING (*)			xxxxxxxxxx		
INSTALLATION				xxxxxxx	
COMMISSIONING (**)					xxxxxxx

(*) Shutdown of the existing facilities.

(**) PHASE II can be implemented rather continuosly, without major disturbance of experimental activities

APPENDIX 1

THE Φ-FACTORY STORAGE RINGS

P. Amadei, A. Aragona, M. Barone, S. Bartalucci, M. Bassetti, M.E. Biagini, C. Biscari, R. Boni, M. Castellano, A. Cattoni, N. Cavallo, F. Cevenini, V. Chimenti, S. De Simone, D. Di Gioacchino, G. Di Pirro, S. Faini, G. Felici, M. Ferrario, L. Ferrucci, S. Gallo U. Gambardella, A. Ghigo, S. Guiducci, S. Kulinski, M.R. Masullo, P. Michelato, G. Modestino, C. Pagani, L. Palumbo, R. Parodi, P. Patteri, A. Peretti, M. Piccolo, M. Preger, G. Raffone, C. Sanelli, L. Serafini, M. Serio, F. Sgamma, B. Spataro, L. Trasatti, S. Tazzari, F. Tazzioli, C. Vaccarezza, M. Vescovi and G. Vignola

(from LNF-90/005)

3. - THE Φ-FACTORY

3.1. - INTRODUCTION

The main goals of the ARES Φ-Factory are:

- Achievement of 10^{32} $cm^{-2}sec^{-1}$ luminosity at 510 MeV.
- Construction and commissioning in 5-6 years .
- Possibility to investigate the linear-against -circular collision scheme.

The nature of a Φ-Factory in itself dictates a minimum target luminosity of 10^{32} $cm^{-2}sec^{-1}$, and at least a non negligible probability that an improvement factor of the order of 3 can be gradually achieved.

A luminosity of 10^{32} $cm^{-2}sec^{-1}$ has never been reached or even approached in a reliable way on existing machines in the Φ energy range; the system parameters must therefore be carefully researched, chosen and optimized and new solutions must be identified.

On the other hand, the luminosity optimization process itself is uncertain because there is no theory that fully explains the performance limitations of existing storage rings.

Our philosophy has been to make educated guesses on the basis of the available data, models and scaling laws.

Moreover, when one considers the tight time schedule, one concludes that the design should not require more than a limited amount of R&D, and must be flexible enough to allow the key machine parameters to be easily changed to fine-tune the luminosity and to exploit alternative collision schemes.

In agreement with the general criteria described above the design presented here

- is based on conventional technology, and
- has two distinctive features:
  - electrons and positrons circulate in two vertically separated storage rings and collide head-on in a single interaction point ;
  - the ring magnetic lattice is a 4 period modified Chasman-Green type with a 1.9 Tesla conventional wiggler magnet inside the achromat. This last choice allows ample emittance tunability and at the same time gives strong radiation damping, one of the fundamental properties that lead to high luminosity.

In case even more damping should prove to be necessary, it can be produced by inserting additional wiggler magnets.

3.2. - DESIGN CRITERIA

3.2.1 - Basic formulae

The single bunch luminosity for an electron-positron storage ring collider is given by the well known formula :

$$L = \frac{f\, N^2}{4\, \pi\, \sigma_x\, \sigma_y} \qquad (3.1)$$

where f is the revolution or collision frequency, N is the number of electrons and positrons (assumed to be the same) and σ_x and σ_y are the horizontal and vertical r.m.s. beam sizes at the interaction point, IP.

During a collision the two bunches focus each other causing a tune shift ΔQ. An appropriate indicator of the focusing force, in a linear approximation, is the tune shift parameter ξ given by

$$\xi_{x,y} = \frac{r_e\, N\, \beta_{x,y}}{2\, \pi\, \gamma\, \sigma_{x,y}\, (\sigma_x + \sigma_y)} \qquad (3.2)$$

where γ is the electron energy in units of its rest mass, r_e the classical electron radius, $\beta_{x,y}$ the value of the horizontal (vertical) betatron function at the IP. For all practical cases :

$$\xi \sim \Delta Q. \qquad (3.3)$$

For a given beam current, ξ is usually different in the horizontal and vertical planes ($\xi_x << \xi_y$). However, in order to achieve the maximum luminosity, it is convenient to have

$$\xi = \xi_x = \xi_y \qquad (3.4)$$

This condition can be satisfied by choosing

$$\kappa = \frac{\varepsilon_y}{\varepsilon_x} = \frac{\beta_y}{\beta_x} = \frac{\sigma_y}{\sigma_x} \qquad (3.5)$$

where κ is the coupling coefficient [1] that can take on any value between 0 and 1. By putting equations (3.2), (3.4), (3.5) together, luminosity and ξ can be rewritten as:

$$L = \pi \left(\frac{\gamma}{r_e}\right)^2 \frac{\xi^2\, f\, \varepsilon\, (1 + \kappa)}{\beta_y} \qquad (3.6)$$

or equivalently

$$L = \pi \left(\frac{\gamma}{r_e}\right)^2 \frac{\xi^2\, f\, \varepsilon\, (1 + \kappa)}{\kappa \beta_x} \qquad (3.7)$$

and

$$\xi = \frac{r_e}{2\pi\gamma}\frac{N}{\varepsilon} \qquad (3.8)$$

Eqs. (3.6) and (3.7) show the interrelation between the luminosity, κ, β_y and β_x . To gain in luminosity, for example, it is not sufficient to assume a small β_y, but it is also necessary to reduce either β_x or the coupling coefficient according to (3.5).

Equations (3.6) and (3.7) also remark, from the quadratic dependence of luminosity on ξ, the leading parameter role of the linear tune shift in collider design.

ξ is generally assumed to depend quadratically on the number of crossings per turn, n_i, namely :

$$\xi \propto \frac{1}{\sqrt{n_i}} \qquad (3.9)$$

n_i is usually equal to twice the number of bunches in one beam.

If one tries to increase the luminosity by increasing n_i, and therefore the collision frequency f, ξ decreases according to eq. (3.9) and defeats the purpose (insofar as 3.9 is exact), as can be seen from eq. (3.6) or (3.7) . This is the reason why electrostatic separating plates are used to reduce n_i while mantaining the same frequency of crossings (see for example CESR[2] where n_i is reduced from 14 to 2 by an electrostatic separation system producing a pretzel like orbit deformation) .

The maximum attainable ξ value can not be computed from theory. Experimentally, however, the maximum value for ξ (in the case of two interactions per turn), averaged over most of the existing electron colliders, is remarkably constant at :

$$<\xi^{max}> = .038 \pm .013 \qquad (3.10)$$

As shown by eq. (3.8), equation (3.10) sets an empirical limit on the ratio between the number of particles N and the beam emittance ε, i.e. a limit on the transverse beam density. Therefore, as ε and N can not be indefinitely increased because of aperture and instability limits, eq. (3.10) sets a limit on the luminosity.

3.2.2 - Collision frequency

From the luminosity point of view one would like the collision frequency to be as high as possible or, equivalently, the storage ring footprint to be as compact as possible.

Ultra-compact rings on the other hand require the use of superconductive dipoles, a feature we do not deem desirable for the machine under design for reasons we try to explain in the following.

Straight superconducting magnets are used in large high energy proton accelerators, whether existing (Tevatron, HERA, etc) or planned (HLC, SSC, RHIC), with very large bending radius.

For a Φ-Factory however the bending radius would be extremely small ($\rho << 1$ m) and one would have to face the engineering problems connected with the design of such 'curved' dipoles, the strong non linearities coming from the small bending radius and the large synchrotron radiation power in a superconducting environment.

While therefore it is true that small superconducting machines are being developed for industrial applications and have also been proposed [3,4] for Φ-factories, the adoption of such a technology is in our opinion more appropriate for an R&D program than for a time-pressed project.

Moreover, we maintain that the gain in collision frequency is not substantial because the ring size will eventually be dominated by the need for space to accomodate the low-β insertion and the experimental apparatus.

In conclusion the most efficient way of increasing the collision frequency is multibunch operation.

In multibunch operation one has of course, according to eq.(3.9), to avoid parasitic collisions that lower the tolerable tune shift parameter ξ . One has the choice of either design complicated separation schemes or store the beams in two (horizontally or vertically) separated rings and collide them head-on in a single interaction point.

We propose to build two vertically separated rings because, for several practical reasons, the gain in collision frequency is greater for the two-ring scheme; the gain factor is $\sqrt{2}$ on $\sqrt{n_i}$ and, consequently, on ξ . We choose the vertical solution because less expensive than the horizontal one from the conventional constructions point of view.

Experience with DORIS[5] has shown that the crossing angle should be as close to zero as possible, and that any residual error crossing angle has to be canceled by accurately monitoring and correcting the orbits.

On the 'minus' side it should also be mentioned that multibunch operation is prone to multibunch instabilities, that have to be carefully suppressed, and it is at risk of ion trapping unless proper, nontrivial countermeasures are taken.

If L_b is the spatial separation between two consecutive bunches and we assume to fill uniformely all the ring circumference, the collision frequency becomes

$$f = \frac{c}{L_b}$$

Our design choice is :

$$\boxed{f = \frac{500}{7} = 71.4 \text{ MHz}, \quad \text{giving} \quad L_b = 4.2 \text{ m}.}$$

The first unwanted crossing would occur at a distance $L_b/2$ from the IP, and the electrostatic separation system must therefore provide a vertical beam separation [6] $\Delta Y > 2\,\sigma_x$ at a distance of 2.1 m from the IP. This distance is not very large but, in our opinion, due to the relatively low energy, a suitable separation scheme can be designed.

3.2.3 - Vertical β-function at the IP

The luminosity increases linearly with the inverse of β_y at the IP. To take full advantage of this dependence, one has to be ready to pay a price in terms of RF system voltage, ring impedance and, because also the r.m.s longitudinal bunch length must be small, of single bunch instabilities. In fact, an empirical rule states that

$$\sigma_z \leq \sim \frac{\beta_y}{1.5}$$

in order to avoid geometrical luminosity reductions.

In addition, the Liouville theorem prescribes that to a very small β_y at the IP there must correspond a large beam divergence; the latter has to be corrected locally, as close as possible to the IP, or the necessary machine acceptance will become too large.

In practice, one is forced to put a very strong quadrupole close to the interaction point that will necessarily limit the solid angle available for the experiment.

This kind of limitation, common to all the low-β schemes, is particularly severe in the case of a Φ-Factory; it imposes a coordinated design of the low-β insertion and the experimental apparatus.

The beam divergence correcting quadrupole also has the effect of raising the machine chromaticity that has to be corrected by the addition of strong sextupoles; the dynamic aperture is consequently reduced.

In conclusion, the value of β_y can not be arbitrarily small; a reasonable choice for the design value turns out to be :

$$\beta_y = 4.5 \text{ cm} \qquad \text{with} \qquad \sigma_z = 3.0 \text{ cm}.$$

The low-β insertion will be designed with a wide range of tunability around this value. Lower values of β_y, such as those claimed by other designs, could therefore be attempted once the machine behaviour has been fully understood, providing an upgrade potential for luminosity.

3.2.4 - Coupling coefficient

The coupling coefficient design value has been chosen to be :

$$\kappa = .01$$

this choice, apparently in contrast with the main goal of maximizing the luminosity (see Eq. 3.6), will be justified in § 3.2.7. We add here a few practical considerations.

From eq. (3.5) we deduce that, with $\kappa = .01$:

$$\beta_x = 100 \cdot \beta_y = 4.5 \text{ m}$$

To achieve such very low value of the coupling coefficient is however not easy; the orbit has to be measured and corrected very precisely, and the vertical dispersion function has to be carefully minimized, especially because of the vertical beam separation scheme. The Touschek effect, limiting the useful lifetime, also becomes of paramount importance. In our case we compute a Touschek lifetime ~ 4 hrs.

The problems are nevertheless solvable; many storage rings in operation have obtained κ values less than 1%. In particular, the Brookhaven 750 MeV VUV ring has reached $\kappa = 0.0017$, after careful machine alignment and after spending one day to correct the residual closed orbit to the desired precision [7].

Alternative solutions, with lower emittance or smaller β_y (small σ_z), would no doubt require stronger coupling to reach an acceptable lifetime.

A potential advantage of the low coupling is the reduction of ion trapping at least when the design dynamic vacuum of ~ 10^{-9} torr is assumed.

3.2.5 - Design emittance

The emittance ε affects the luminosity linearly but cannot be made arbitrarily large; the limit is given by the machine physical and dynamic apertures necessary for a reasonable beam lifetime. Very large emittance also implies that the number of particles, N, necessary to achieve a large ξ is very large (see 3.8).

All considered, a reasonable choice for ε is :

$$\varepsilon = 10^{-6} \text{ m·rad}$$

but, as for the case of β_y , the storage ring is designed to allow a wide range of tunability and consequently has some potential for improvement. The upper emittance limit is essentially determined by aperture requirements, while the lower one is in the 10^{-9} m·rad range.

3.2.6 - The linear tune shift parameter ξ

The linear tune shift ξ, appearing squared in the luminosity formula, plays the most important role and, because of (3.10), is the fundamental, not yet fully understood limiting factor (see also § 3.2.7).

A sensible choice is to estimate the luminosity value on the basis of the experimental average ξ^{max} given by (3.10), namely :

$$\xi^{max} \approx .04$$

By this choice we also implicitly fix the number of particles per bunch, N : by substituting the values of ε and ξ into (3.8) we obtain:

$$N = 8.9\ 10^{10} \text{ particles/bunch}$$

and the resulting average current in each beam is :

$$< i > = e\, f\, N = 1.02 \text{ A}$$

This is an unusually high current value that will require a careful design of the RF and the vacuum systems. Let us however point out that similar current values have been reached at storage rings now in operation : as an example, a current in excess of 1.3 Amp has been accumulated in the BNL VUV ring [7] that runs routinely with stored currents of .8÷.9 Amp.

3.2.7 - Luminosity scaling laws

As often mentioned above, there is no exhaustive explanation of the luminosity limit.

Among existing phenomenological models we have singled out the work by J.Seeman [8] and by M.Bassetti [9], because the former is in reasonable agreement with the ξ^{max} experimental data from several machines, while the latter introduces something new in the direction of a better understanding the luminosity limits. In the following we briefly summarize their results.

Let us first recall the definition of the synchrotron integrals I_2 an I_3 [10] :

$$\int_{Dip} \frac{ds}{\rho^2} \quad ; \quad \int_{Dip} \frac{ds}{|\rho^3|} \qquad (3.11)$$

For an isomagnetic machine with a bending radius ρ, the integrals over one turn are given by :

$$I_2 = \frac{2\pi}{\rho} \quad ; \quad I_3 = \frac{2\pi}{\rho^2} \qquad (3.12)$$

U_o[10] and σ_R[9], the radiation energy loss per turn and the r.m.s. quantum fluctuation per turn respectively, can be expressed through (3.11) as follows :

$$U_{o\,(KeV)} \sim 14.1\, E^4_{(GeV)}\; I_{2\,(m^{-1})} \qquad (3.13)$$

$$\sigma_{R\,(KeV)} \sim 6.5\;\; E^{3.5}_{(GeV)}\; \sqrt{I_{3\,(m^{-2})}} \qquad (3.14)$$

J.Seeman has reviewed, in a very exhaustive paper [8], the data on beam-beam interaction obtained at most of the existing e+e- storage rings; he shows that by empirically fitting the dependence of the linear tune-shift ξ on the various relevant parameters he can explain them all rather well. His best fit shows that the maximum vertical linear tune shift (at the maximum luminosity) divided by the beam energy, increases with the square root of $1/(n_i\rho)$, where n_i is the number of crossings per turn and ρ is the bending radius. This can be expressed as:

$$\left(\frac{\xi_y}{\gamma}\right)^{max} \sim 1.4\;\; 10^{-5} \sqrt{\frac{I_{2\,(m^{-1})}}{n_i}} = \text{const} \sqrt{\frac{1}{\rho\; n_i}} \qquad (3.15)$$

By substituting eq. (3.15) into (3.6) we have a first luminosity scaling law :

$$L^{max} \propto \gamma^6\, I_2 \qquad \text{(Seeman's law)}$$

The open question is if one is allowed to extrapolate the experimental fit (3.15) to the case of a very small bending radius (large U_0); the Novosibirsk Φ-Factory design by Barkov et al.[3] featuring a very small bending radius (ρ = 28cm with 6 Tesla s.c. dipoles), claims a ξ^{max} of $\approx$ .07 in both planes, not far from the value one would calculate from (3.15).

Using the conservative value ξ^{max} = .04 discussed under § 3.2.6 and considering that we have only one crossing point, we obtain from (3.6) and (3.15) the minimum acceptable value of I_2:

$$I_2^{\,min} \sim 11\ m^{-1} \qquad \text{(Seeman's criterion)}$$

or, equivalently through (3.13), the minimum acceptable value of the radiated energy:

$$U_0^{\,min} \sim 10.5\ KeV.$$

In a recent study [9] M. Bassetti suggests that a <u>further luminosity limitation</u> comes from the perturbation of the radiative damping mechanism by the beam-beam interaction. In fact the maximum energy, ΔE_{bb} , lost or gained by a particle working against the electric field of the opposite beam must - according to his model - be lower than the average quantum fluctuation, σ_R ,of the synchrotron radiation between two interactions, in order for the machine to behave properly. According to his formalism ΔE_{bb} is given by:

$$\Delta E_{bb\ (KeV)} \sim 3.58\ 10^3\ r_e\ F\left(\frac{\sigma_y}{\sigma_x}\right)\frac{N}{\beta_y} \qquad (3.16)$$

where F is a form factor shown in Fig. 3.1 that depends strongly on the ratio $\kappa = \frac{\sigma_y}{\sigma_x}$.

By analising the behaviour of existing storage rings, it is found that at maximum luminosity many storage rings have :

$$\sigma_R \geq 9\ \Delta E_{bb} \qquad (3.17)$$

The coefficient has been derived empirically and will require further studies with numerical simulations and experimental check. Eq. (3.17) implies a limitation on the maximum N, independently from the transverse beam density. By using (3.17), according to Bassetti, we can write a luminosity scaling law :

$$L^{max} \propto \gamma^5 \sqrt{I_3} \qquad \text{(Bassetti's law)}$$

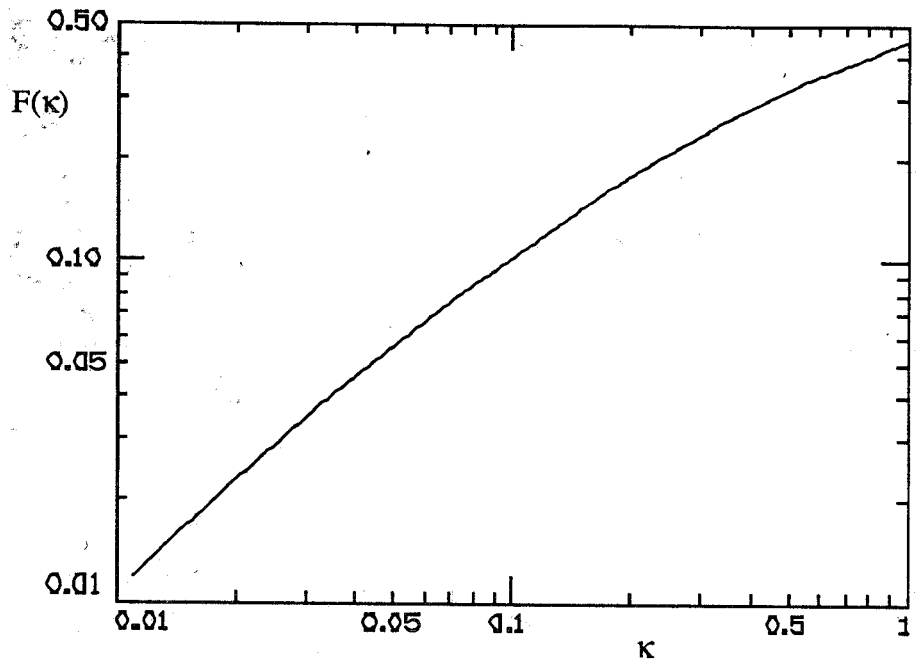

Fig. 3.1 - The form factor F as a function of the ratio $\kappa = \sigma_y/\sigma_x$.

To follow prescription (3.17) while keeping the required value of I_3 manageable, one is forced to choose (see Fig. 3.1) the very small value for the coupling coefficient, $\kappa = .01$, already mentioned in § 3.2.4 . With this value, I_3^{min} computed from eqs. (3.6) and (3.17) is equal to :

$$I_3^{min} = 12.1 \ m^{-2} \qquad \text{(Bassetti's criterion)}$$

(With $\kappa = .10$ the corresponding value for I_3^{min} would have been $\sim 900 \ m^{-2}$!).

Let us point out that, by incorporating the Seeman's and Bassetti's criteria in our design, we are making a conservative luminosity estimate. We also proposed to verify the range of validity of the two models on ADONE [11] before the Φ-Factory parameters are frozen.

3.2.8 - Conclusions

The parameters so far discussed are summarized in Table 3.1. We also summarize, as a conclusion, our basic design philosophy.

TABLE 3.1 - Design Parameters

Luminosity	(cm^{-2} sec^{-1})	10^{32}	Bunch separation	(m)	4.2
Emittance	(m-rad)	10^{-6}	N^{er} of particles/bunch		8.9 10^{10}
κ		.01	Bunch peak current	(Amp)	57
ξ_y		.04	Total average curr.	(Amp)	1.02
ξ_x		.04	I_2^{min}	(m^{-1})	11
β_y	(m)	.045	I_3^{min}	(m^{-2})	12
β_x	(m)	4.5	σ_R	(KeV)	2.0
Bunch length σ_z	(m)	.03	ΔE_{bb}	(KeV)	.22
Collision frequency	(MHz)	71.4	U_o	(KeV)	10.5

For the ARES Φ-Factory we envisage a two stage project : the PHASE I Factory will be entirely based on very conventional technology, and is supposed to reach the specified design luminosity. The design however affords enough flexibility so that any further modification that may prove necessary or desirable to upgrade the machine performance can be incorporated during PHASE II, dedicated to the upgrade of luminosity and to the implementation of alternative collision schemes.

This scheme minimizes the technical risks and we believe that, after a commissioning period of 4÷5 months, the design current can be reached in both rings. At the end of the first year of operation, the luminosity target of 10^{32} $cm^{-2}sec^{-1}$ should have been reached by fine-tuning all other machine parameters (ε, κ, β_y etc.).

3.3. - BEAM OPTICS

3.3.1 - Low-β insertion

The low-β insertion and the vertical separation system are the most crucial parts of the Φ-Factory design, because of the constraints imposed by the experimental apparatus and by the relatively short bunch-to-bunch longitudinal distance L_b.

The experimental apparatus, not yet completely defined, has of course to cover the largest possible solid angle; a solenoidal field of $\approx .5 \div 1.$ kG over a length of approximately 5 meters on each side of the IP is also required. The beam trajectory will be actively shielded from solenoidal field, with the exception of ± 0.5 m around the IP, where the vacuum chamber wall must be very thin and no active or passive shield can be used.

The details of of the residual field compensation and of the resulting shielding arrangement are still under study and only a general feasibility study is therefore presented.

The most serious constraint posed by the experimental apparatus on the design of the low-β insertion is the requirement of a large unencumbered solid angle around the IP. A tentative agreement has been reached with the users on a low-β insertion confined to a cone of half-aperture angle $\theta = 8.5^o$, over a length of ± 5 m from the IP. The distance of the first quadrupole from the IP is ≥ 45 cm and the quadrupole maximum outer diameter $Ø_Q$ is given by:

$$Ø_Q = 2 \cdot \tan(8.5^o) \cdot 45 \text{ cm} = 13.45 \text{ cm}$$

It is important, because of the low κ value chosen, to suppress the vertical dispersion function D_y locally . Moreover the beam separation system has to satisfy the condition:

$$\Delta Y > 2\,\sigma_x$$

at the first unwanted collision point ($L_b/2$) as well as at the second one (L_b).

The relevant lattice design parameters are as follows:

$\beta_y = 4.5$ cm $\beta_x = 4.5$ m $\kappa = .01$ $\varepsilon = 10^{-6}$ m·rad $L_b = 4.2$ m

Starting from the IP, there is a first lattice region, inside the detector, where two electrostatic separators, VS1 and VS2, begin to gradually separate the beams. The separators are schematized as vertical magnets with a bending radius given by

$$\rho_E \text{ (m)} \sim \frac{.511\ \gamma}{E \text{ (MV/m)}}$$

where $E = V / d$ is the electric field value , V the voltage and d the distance between the plates. We assume :

$$\rho_E = 200 \text{ m}, \qquad V = 100 \text{ KV}, \qquad d = 4 \text{ cm}$$

to obtain :

$$E \approx 2.5 \text{ MVolt/m}$$

The β-functions in the region from the IP to the second unwanted crossing are shown in Fig. 3.2; the resulting half-separation Y and the horizontal beam size σ_x are plotted in Fig.3.3

By inspecting Fig. 3.3 we can see that the criterion $\Delta Y > 2\,\sigma_x$ is satisfied.

Let us point out that the first quadrupole, QF1, is rather weak and focussing in the horizontal plane. This provides better control over the β functions along the rest of the insertion.

The mechanical design of the first two quadrupoles, QF1 and QD1, whose maximum allowable outer diameters are

$$\varnothing_{QF1} = 13.45 \text{ cm} \qquad \varnothing_{QD1} = 20.92 \text{ cm}$$

is still under study; at the moment the most likely solution for QF1 foresees the use of permanent magnets.

In the second region, near the edge of the detector, we increase the vertical separation with two thin septum magnets VB1 and VB2 . Two additional vertical magnets VB3 and VB4, of opposite sign, take the beam horizontally to the following dispersion suppressor region. The dispersion suppressor consist of three 120° FODO cells with missing magnets.

The β-functions in the region in between the IP and VB4 are plotted in Fig. 3.4 ; the vertical dispersion D_y is shown in Fig. 3.5 .

Fig.3.6 shows the vertical half separation, Y, along the low-β insertion.

Finally the low-β insertion is connected to the main arcs by a matching section consisting of four quadrupoles.

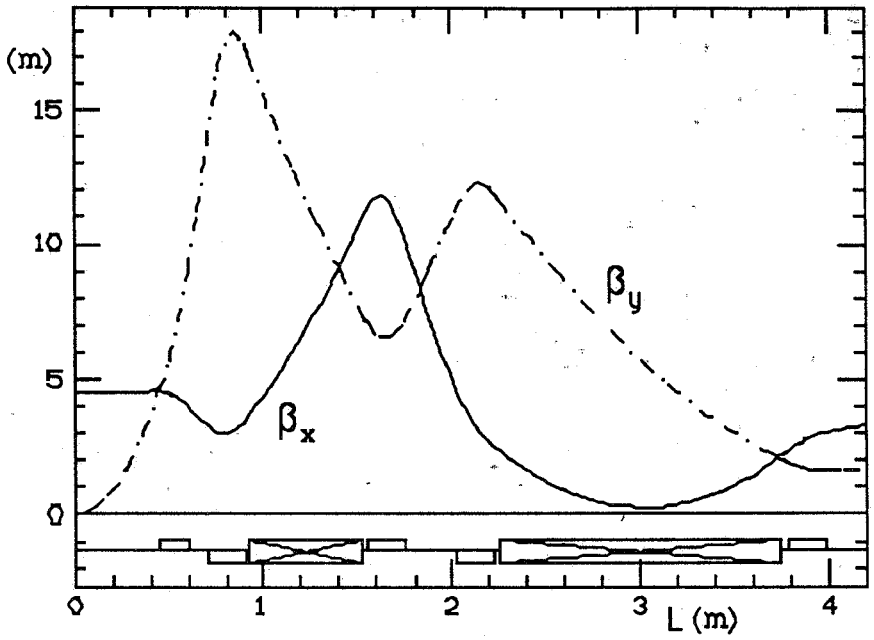

Fig. 3.2 - β-functions from the IP to the 2nd parasitic crossing point.

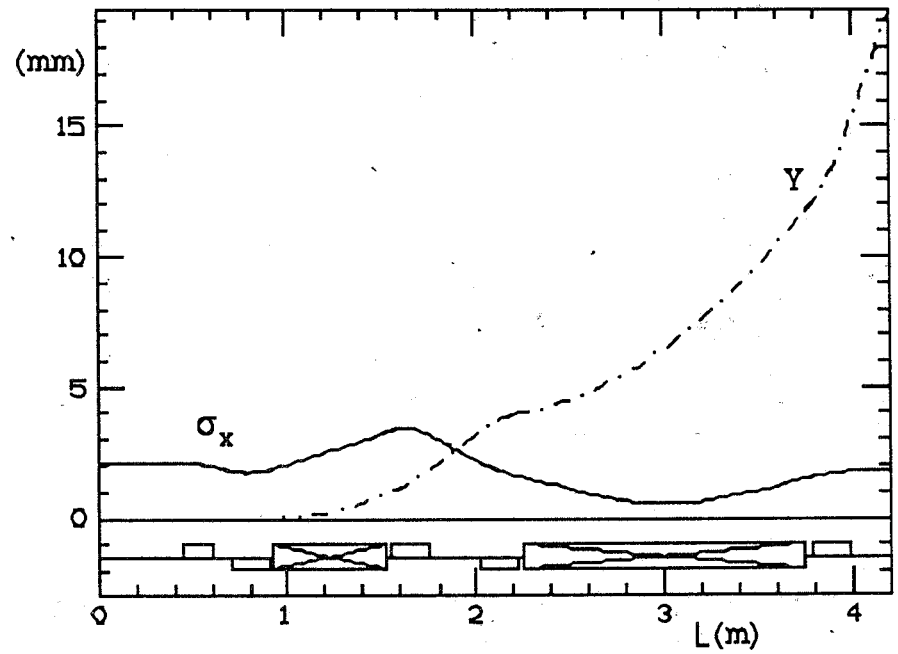

Fig. 3.3 - Half-separation Y and horizontal beam size σ_x from the IP to the 2nd parasitic crossing.

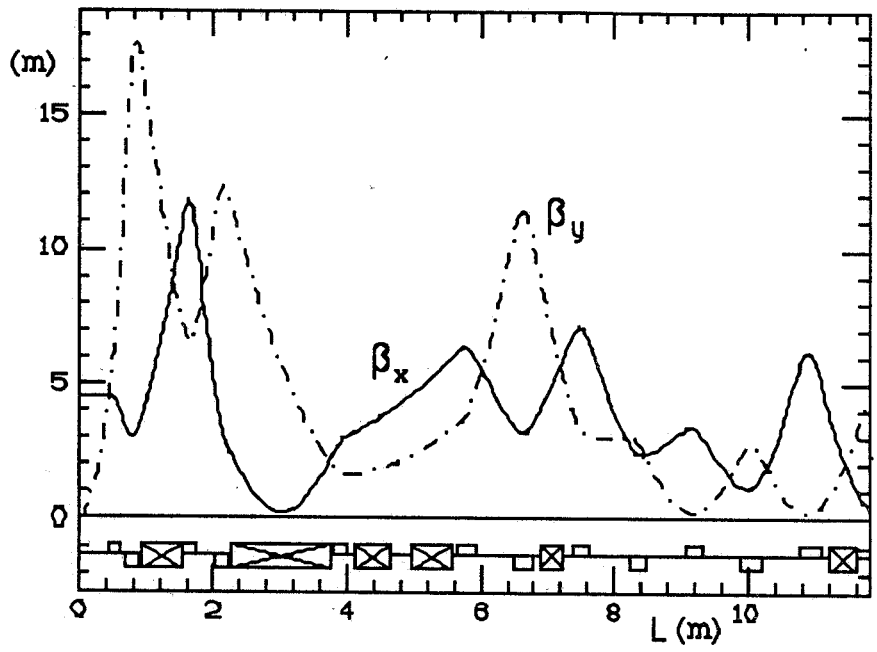

Fig. 3.4 - β-functions in between the IP and the last vertical magnet, VB4.

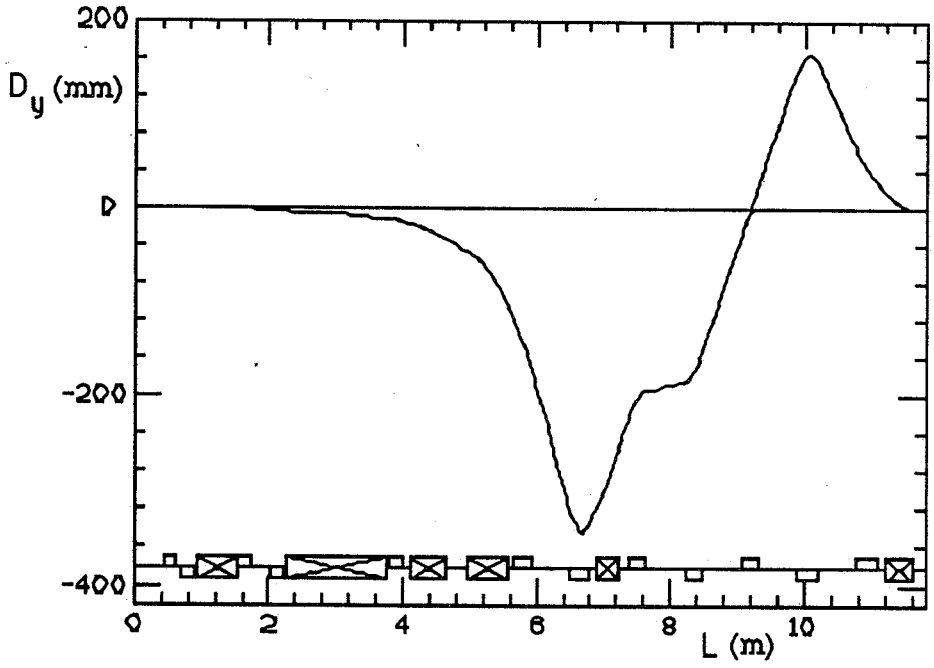

Fig. 3.5 - Vertical dispersion function along the low-β insertion.

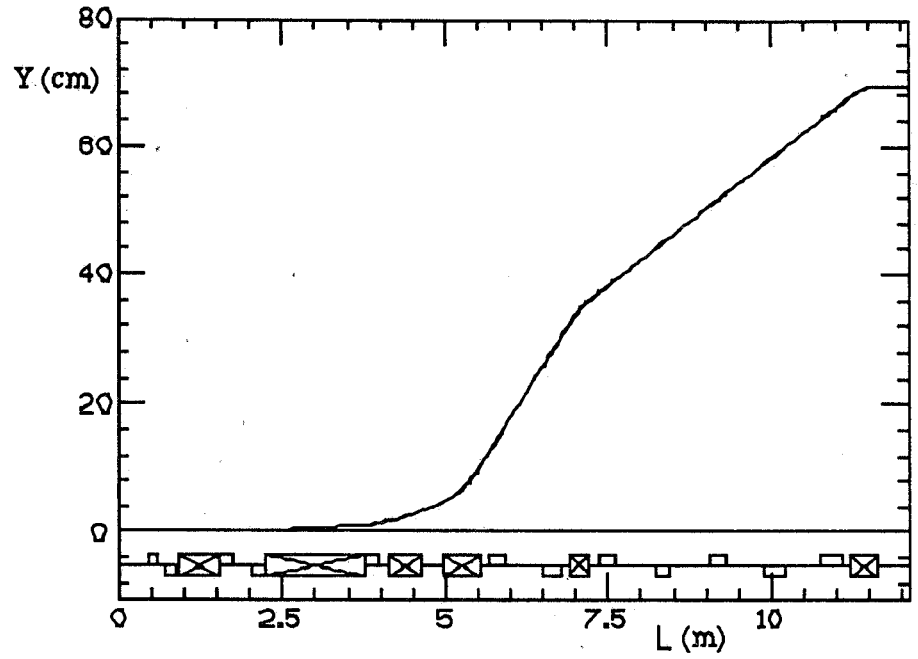

Fig. 3.6 - Half-separation Y along the low-β insertion.

From Fig.3.6 it can be seen that the total vertical separation H between the two storage ring orbits, outside the low-β insertion, cannot be less than

$$H = 1.391 \text{ m}$$

The total length of the insertion is ~ 30 m and it can not be reduced without compromising the lattice flexibility and increasing its chromaticity.

Let us point out that the design leaves room for a raising the collision frequency, and consequently in the luminosity, by $\approx 20\%$ because :

- VS1 and VS2 can probably be operated at higher electric field
- the separation criterion, $\Delta Y > 2\,\sigma_x$ is probably too conservative.

3.3.2 - Storage rings

The storage ring lattice is a four-period modified Chasman-Green[12] type. This kind of lattice is commonly used for low emittance, high periodicity machines and its main limitation then comes from the chromaticity correction wich, because of the small value of the dispersion function, requires strong sextupoles and consequently produces rather small dynamic apertures. In our case this is however not a serious problem because the periodicity is only 4, the lattice is detuned and the dispersion is therefore comparatively high.

To increase the radiated energy per turn, a 1.5 m long, 1.9 T normal-conducting wiggler is incorporated into each achromat. Because the wiggler is in a high dispersion region a rather large emittance of 10^{-6} m-rad is obtained. To emittance value can be adjusted by tuning the dispersion function in the wiggler region by through a D-type Q-pole that is also part of the achromat.

The optical functions , for a four-fold symmetric ring, are shown in Fig. 3.7.

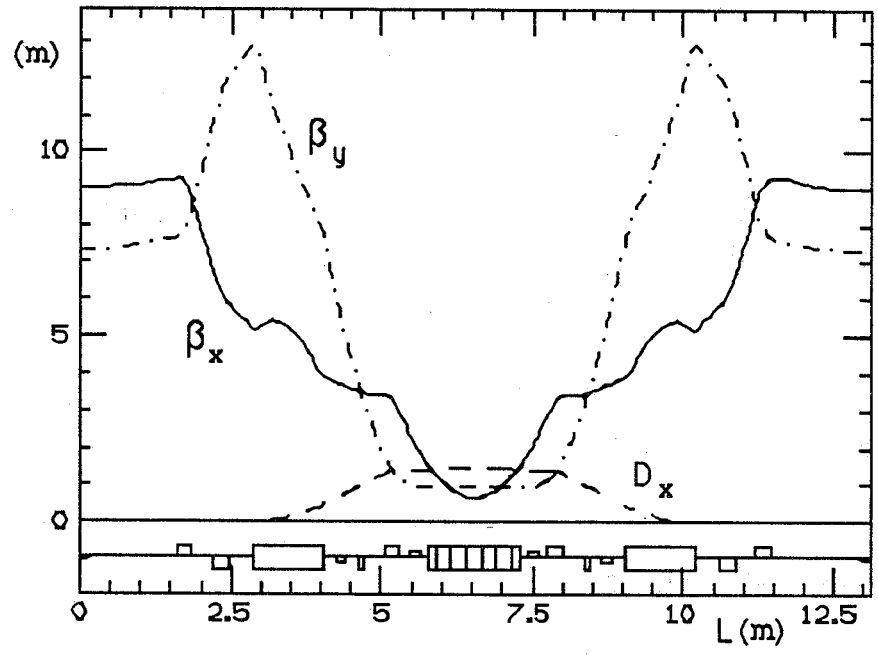

Fig. 3.7 - Main arc optical functions.

Normal conducting wigglers are used to avoid the strong field non linearities created by short bending radius superconducting devices. According to our experience it is instead rather easytask to achieve a very good field quality in a normal wiggler, by making the poles wide enough and by shimming.

In Fig. 3.8 we plot the optical functions over one half the ring, including the low-β insertion; the half-ring layout is shown in Fig. 3.9.

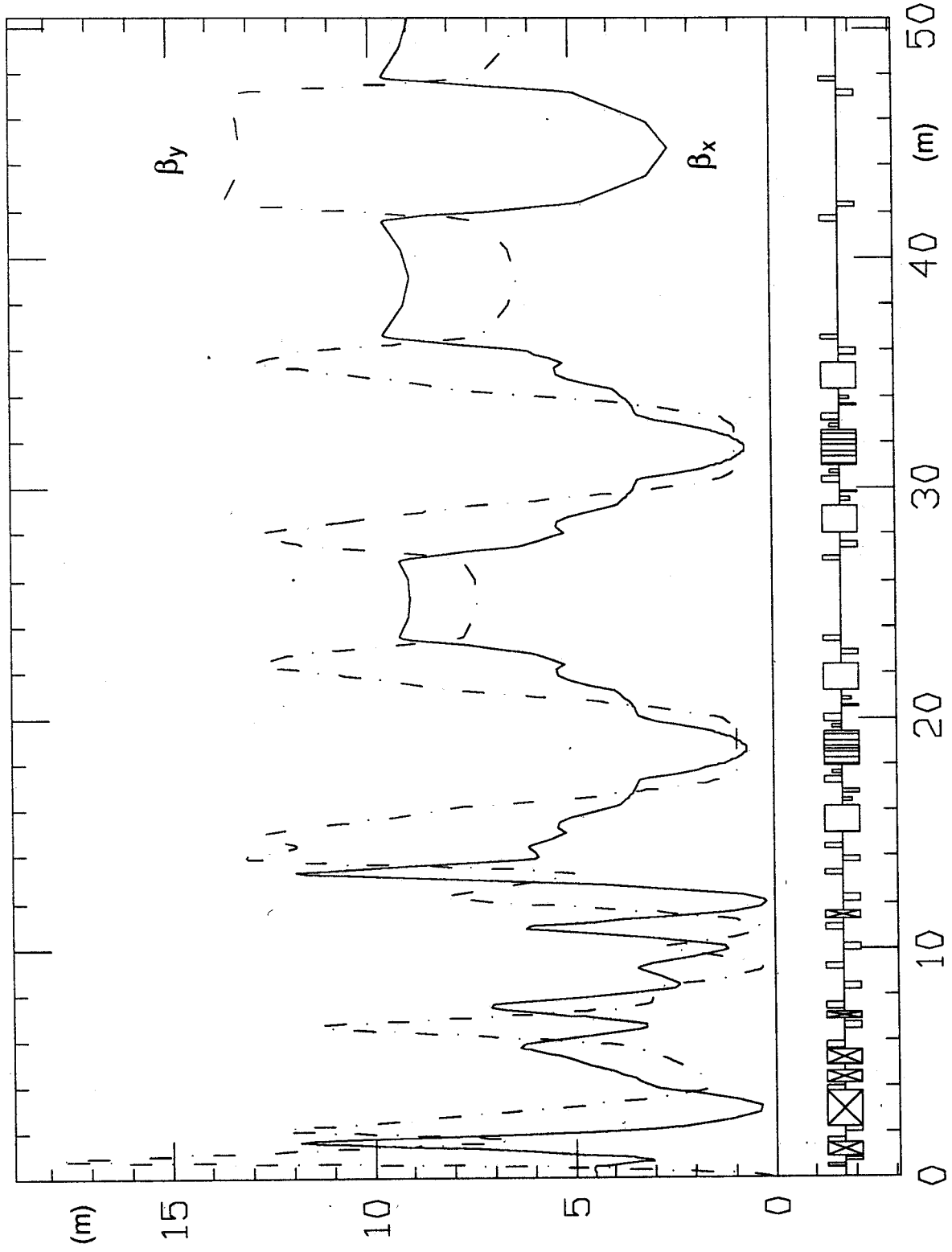

Fig. 3.8 - Optical functions for half ring.

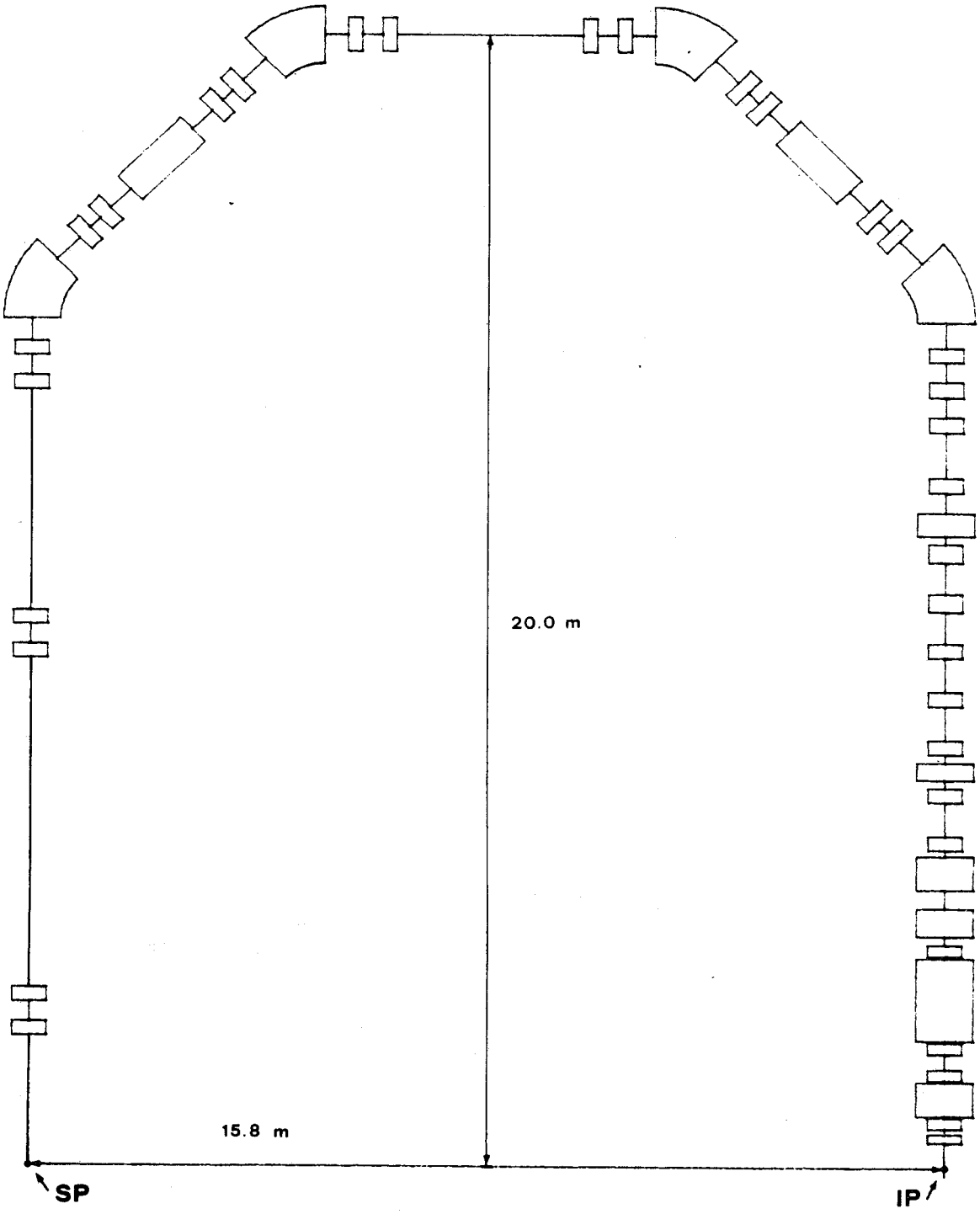

Fig. 3.9 - Layout of one half of the storage ring.

A complete parameter list is given in Table 3.2 , while Tab. 3.3 reproduces the output of the LEDA[13] code, used to design most of the storage ring .

TABLE 3.2 - Parameter List

Energy (MeV)	510.		
Circumference (m)	100.73	Luminosity (cm^{-2} sec^{-1})	10^{32}
Dipole bending radius (m)	1.464		
Wiggler bending radius(m)	0.9	N^{er} of particles/bunch	$8.9\ 10^{10}$
Wiggler length (m)	1.5	N^{er} of bunches	24
Wiggler period (m)	0.5	Collision frequency (MHz)	71.4
Rings separation (m)	1.391	κ	.01
		ξ_y	.04
Horizontal β-tune	5.8	ξ_x	.04
Vertical β-tune	5.85	β_y at I.P. (cm)	4.5
Momentum compaction	.0086	β_x at I.P. (m)	4.5
Energy loss/turn (KeV) :		σ_y at I.P. (μm)	21.1
H. bend. magnets	4.08	σ_x at I.P. (mm)	2.11
V. bend. magnets	0.12	I_2 (m^{-1})	11.7
Wigglers	7.06	I_3 (m^{-2})	11.2
Total	11.26	σ_R (KeV)	2.06
Damping times (msec) :		ΔE_{bb}(KeV)	.20
τ_s	15.2		
τ_x	30.4	RF freq. (MHz)	357.14
τ_y	30.4	Harmonic number	120
Rel. r.m.s. en. spread	$4.25\ 10^{-4}$	RF voltage (MV) at Z/n = 2 Ω	273.
Natural emittances (m-rad) :		at Z/n = 1 Ω	131.
Horizontal	10^{-6}	Parasitic losses (keV Ω)	4.0
Vertical	$1.82\ 10^{-11}$	Bunch length σ_z (cm)	3.0
		Bunch peak current (Amp)	57.
Natural chromaticities :		Total average curr. (Amp)	1.02
Horizontal	-10.3	Synch. Rad. Power/beam (kW)	11.5
Vertical	-16.4		

TABLE 3.3 - LEDA output

ENERGY (MEV) 510.0
B*RO (TESLA*METERS) 1.70
TOTAL BENDING ANGLE (H-V) 0.741971882D+03 0.356509987D+02
NUMBER OF PERIODS 1
PERIOD LENGTH (m) 0.100730266D+03
TOTAL LENGTH (m) 0.100730266D+03

ACHIEVED CONVERGENCE = 0.117552217D-07

HALF-PERIOD LATTICE : REFLECTED SYMMETRY

	NAME	LENGTH (m)	K2(m-2)	RADIUS (m)
1	O	0.450000000D+00	0.000000000D+00	0.000000000D+00
2	QF1	0.150000000D+00	0.600000000D+01	0.000000000D+00
3	O	0.100000000D+00	0.000000000D+00	0.000000000D+00
4	QD1	0.200000000D+00	0.113828586D+02	0.000000000D+00
5	O	0.250000000D-01	0.000000000D+00	0.000000000D+00
6	VS1	0.600000000D+00	0.000000000D+00	-0.200000000D+03
7	O	0.250000000D-01	0.000000000D+00	0.000000000D+00
8	QF2	0.200000000D+00	0.911302561D+01	0.000000000D+00
9	O	0.275000000D+00	0.000000000D+00	0.000000000D+00
10	QD2	0.200000000D+00	0.550094163D+01	0.000000000D+00
11	O	0.300000000D-01	0.000000000D+00	0.000000000D+00
12	VS2	0.150000000D+01	0.000000000D+00	-0.200000000D+03
13	O	0.300000000D-01	0.000000000D+00	0.000000000D+00
14	QF3	0.200000000D+00	0.443788888D+01	0.000000000D+00
15	O	0.150000000D+00	0.000000000D+00	0.000000000D+00
16	VB1	0.500000000D+00	0.000000000D+00	-0.250000000D+02
17	O	0.325000000D+00	0.000000000D+00	0.000000000D+00
18	VB2	0.600000000D+00	0.000000000D+00	-0.500000000D+01
19	O	0.100000000D+00	0.000000000D+00	0.000000000D+00
20	QF4	0.250000000D+00	0.251166800D+01	0.000000000D+00
21	O	0.600000000D+00	0.000000000D+00	0.000000000D+00
22	QD3	0.250000000D+00	0.466394100D+01	0.000000000D+00
23	O	0.150000000D+00	0.000000000D+00	0.000000000D+00
24	VB3	0.300000000D+00	0.000000000D+00	0.370695567D+01
25	O	0.150000000D+00	0.000000000D+00	0.000000000D+00
26	QF5	0.250000000D+00	0.420034400D+01	0.000000000D+00
27	O	0.600000000D+00	0.000000000D+00	0.000000000D+00
28	QD4	0.250000000D+00	0.452639900D+01	0.000000000D+00
29	O	0.600000000D+00	0.000000000D+00	0.000000000D+00
30	QF6	0.250000000D+00	0.384354930D+01	0.000000000D+00
31	O	0.565000000D+00	0.000000000D+00	0.000000000D+00
32	QD5	0.320000000D+00	0.729970000D+01	0.000000000D+00
33	O	0.555000000D+00	0.000000000D+00	0.000000000D+00
34	QF7	0.320000000D+00	0.561495665D+01	0.000000000D+00
35	O	0.150000000D+00	0.000000000D+00	0.000000000D+00
36	VB4	0.410000000D+00	0.000000000D+00	0.514527802D+01
37	O	0.400000000D+00	0.000000000D+00	0.000000000D+00
38	QD6	0.270000000D+00	0.378930439D+01	0.000000000D+00
39	O	0.850000000D+00	0.000000000D+00	0.000000000D+00
40	QF8	0.270000000D+00	0.542510247D+01	0.000000000D+00
41	O	0.300000000D+00	0.000000000D+00	0.000000000D+00
42	QD7	0.270000000D+00	0.334056224D+01	0.000000000D+00
43	O	0.300000000D+00	0.000000000D+00	0.000000000D+00
44	QF9	0.250000000D+00	0.896585488D+00	0.000000000D+00
45	O	0.450000000D+00	0.000000000D+00	0.000000000D+00
46	HB	0.115000000D+01	0.000000000D+00	0.146422540D+01
47	O	0.250000000D+00	0.000000000D+00	0.000000000D+00
48	SD	0.150000000D+00	0.118700000D+02	0.000000000D+00
49	O	0.200000000D+00	0.000000000D+00	0.000000000D+00
50	QD8	0.100000000D+00	0.383721329D+00	0.000000000D+00

TABLE 3.3 - LEDA output - (continue)

	NAME	LENGTH (m)	K2(m-2)	RADIUS (m)
51	O	0.350000000D+00	0.000000000D+00	0.000000000D+00
52	QF10	0.250000000D+00	0.249525412D+01	0.000000000D+00
53	O	0.162500000D+00	0.000000000D+00	0.000000000D+00
54	SF	0.150000000D+00	0.134600000D+02	0.000000000D+00
55	O	0.162500000D+00	0.000000000D+00	0.000000000D+00
56	WIG	0.150000000D+01	0.000000000D+00	0.900000000D+00
57	O	0.162500000D+00	0.000000000D+00	0.000000000D+00
58	SF	0.150000000D+00	0.134600000D+02	0.000000000D+00
59	O	0.162500000D+00	0.000000000D+00	0.000000000D+00
60	QF10	0.250000000D+00	0.249525412D+01	0.000000000D+00
61	O	0.350000000D+00	0.000000000D+00	0.000000000D+00
62	QD8	0.100000000D+00	0.383721329D+00	0.000000000D+00
63	O	0.200000000D+00	0.000000000D+00	0.000000000D+00
64	SD	0.150000000D+00	0.118700000D+02	0.000000000D+00
65	O	0.250000000D+00	0.000000000D+00	0.000000000D+00
66	HB	0.115000000D+01	0.000000000D+00	0.146422540D+01
67	O	0.400000000D+00	0.000000000D+00	0.000000000D+00
68	QD9	0.250000000D+00	0.932084352D+00	0.000000000D+00
69	O	0.350000000D+00	0.000000000D+00	0.000000000D+00
70	QF11	0.250000000D+00	0.140164106D+01	0.000000000D+00
71	O	0.322513294D+01	0.000000000D+00	0.000000000D+00
72	QF11	0.250000000D+00	0.140164106D+01	0.000000000D+00
73	O	0.350000000D+00	0.000000000D+00	0.000000000D+00
74	QD9	0.250000000D+00	0.932084352D+00	0.000000000D+00
75	O	0.400000000D+00	0.000000000D+00	0.000000000D+00
76	HB	0.115000000D+01	0.000000000D+00	0.146422540D+01
77	O	0.250000000D+00	0.000000000D+00	0.000000000D+00
78	SD	0.150000000D+00	0.118700000D+02	0.000000000D+00
79	O	0.200000000D+00	0.000000000D+00	0.000000000D+00
80	QD8	0.100000000D+00	0.383721329D+00	0.000000000D+00
81	O	0.350000000D+00	0.000000000D+00	0.000000000D+00
82	QF10	0.250000000D+00	0.249525412D+01	0.000000000D+00
83	O	0.162500000D+00	0.000000000D+00	0.000000000D+00
84	SF	0.150000000D+00	0.134600000D+02	0.000000000D+00
85	O	0.162500000D+00	0.000000000D+00	0.000000000D+00
86	WIG	0.150000000D+01	0.000000000D+00	0.900000000D+00
87	O	0.162500000D+00	0.000000000D+00	0.000000000D+00
88	SF	0.150000000D+00	0.134600000D+02	0.000000000D+00
89	O	0.162500000D+00	0.000000000D+00	0.000000000D+00
90	QF10	0.250000000D+00	0.249525412D+01	0.000000000D+00
91	O	0.350000000D+00	0.000000000D+00	0.000000000D+00
92	QD8	0.100000000D+00	0.383721329D+00	0.000000000D+00
93	O	0.200000000D+00	0.000000000D+00	0.000000000D+00
94	SD	0.150000000D+00	0.118700000D+02	0.000000000D+00
95	O	0.250000000D+00	0.000000000D+00	0.000000000D+00
96	HB	0.115000000D+01	0.000000000D+00	0.146422540D+01
97	O	0.400000000D+00	0.000000000D+00	0.000000000D+00
98	QD10	0.250000000D+00	0.109236509D+01	0.000000000D+00
99	O	0.350000000D+00	0.000000000D+00	0.000000000D+00
100	QF12	0.250000000D+00	0.154257971D+01	0.000000000D+00
101	O	0.487813862D+01	0.000000000D+00	0.000000000D+00
102	QF13	0.250000000D+00	0.212233908D+01	0.000000000D+00
103	O	0.350000000D+00	0.000000000D+00	0.000000000D+00
104	QD11	0.250000000D+00	0.187078605D+01	0.000000000D+00
105	O	0.465098208D+01	0.000000000D+00	0.000000000D+00
106	QD11	0.250000000D+00	0.187078605D+01	0.000000000D+00
107	O	0.350000000D+00	0.000000000D+00	0.000000000D+00
108	QF13	0.250000000D+00	0.212233908D+01	0.000000000D+00
109	O	0.247087930D+01	0.000000000D+00	0.000000000D+00

TABLE 3.3 - LEDA output - (continue)

```
    PARAMETERS :
    ----------

     QX - QZ                    5.800        5.850
    tunes/period                5.800        5.850
 ETA0  (H/V) - BX0   - BZ0     -.6444E-08  0.6484E-10   4.500       0.4500E-01
ETAMAX (H/V) - BXMAX - BZMAX    1.455       0.1642      11.95        17.94
ETAMIN (H/V) - BXMIN - BZMIN   -.1243E-07  -.3432       0.1734      0.4500E-01
 <ETA> (H/V) - <BX>  - <BZ>     0.2526      -.1236E-01   5.195       6.871

    SYNCHROTRON RADIATION INTEGRALS (R.H.HELM et al.) :

     I1(H-V) (meters)          0.870459662D+00  -0.279060893D-01
     I2(H-V) (1/meters)        0.116985402D+02   0.124342210D+00
     I3(H-V) (1/meters**2)     0.111611031D+02   0.274631442D-01
     I4(H-V) (1/meters)        0.000000000D+00  -0.269400316D-02
     I5(H-V) (1/meters)        0.289805931D+02   0.563461960D-03

    MOM. COMPACTION             0.8641E-02
    U0 (H-V-Tot) (KeV)           11.14       0.1184       11.26
    D (H-V)                     0.0000E+00   -.2279E-03
    JS,JX,JZ                     2.000      1.000        1.000
    DAMPINGS(ms)                 15.22      30.43        30.43
    REL. R.M.S. ENERGY-SPREAD   0.4254E-03
    EMITTANCE(H-V) (m-rad)      0.9876E-06  0.1822E-10


    CHROMATICITIES (M.BASSETTI LEP NOTE 504) :


    TOTAL CROM.      -10.34       -16.44
    COR.TOT.CROM.   0.0000E+00   0.0000E+00
    SEXT (T/M^2)  :    SD =  142.9
                       SF =  182.0
```

TABLE 3.3 - LEDA output - (continue)

BEAM PAR & dN/dt FOR T=293K - P=1nTorr - Z(biatomic)=8 :

REV. FREQUENCY (MHZ)	0.297619048D+01
HARMONIC NUMBER	0.120000000D+03
RF.F.REQUENCY (MHZ)	0.357142857D+03
ENERGY (MEV)	510.0
MOM. COMPACTION	0.8641E-02
U0 (H-V-Tot) (KeV)	11.26
VRF(KV)	131.0
F SYNC.(KHZ)	19.34
RF ACCEPTANCE	0.1170E-01
NAT.BUNCH LENGTH(m)	0.9069E-02
AN. BUNCH LENGTH(m)	0.3036E-01
REL. R.M.S. ENERGY-SPREAD	0.1424E-02
AV.CURRENT/BUNCH(mA)	42.43
# ELECTRONS/BUNCH	0.889917603D+11
PEAK CURRENT/BUNCH(A)	56.16
Nw Th(Z/n=1)/BUNCH(A)	5.012
EMITTANCE(H-V) (m-rad)	0.9876E-06
EMITTANCE COUPL.	0.1000E-01
HOR. APERTURE (m)	0.4000E-01
VER. APERTURE (m)	0.3000E-01
QUANTUM LIFE (hrs)-SANDS	0.2898E+08
LIFETIME GB (min)	2104.
LIFETIME SC (min)	1300.
LIFETIME GBe (min)	0.1295E+05
LIFETIME SCe (min)	0.2144E+05
TOUSCHEK (min)	154.5
LIFETIME TOT.(min)	127.5

Let us conclude with a comment about the emittance: the very low emittance required for linac-storage ring collisions can be obtained by switching off the wigglers inside the achromat (which brings the emittance down to $\approx 10^{-8}$ m-rad) and switching on the wigglers foreseen for PHASE II to finally reach an emittance $\approx 10^{-9}$ m-rad.

3.3.3 - Dynamic aperture

The fully periodic Chasman-Green lattice would have a large dynamic aperture even with only two families of chromaticity correcting sextupoles. When the low-β insertion is included, the dynamic aperture shrinks because of the larger chromaticity and the lower symmetry.

A preliminary on-momentum dynamic aperture at the IP, as evaluated with PATRICIA[14] and with only two sextupole families, is shown in Fig. 3.10.

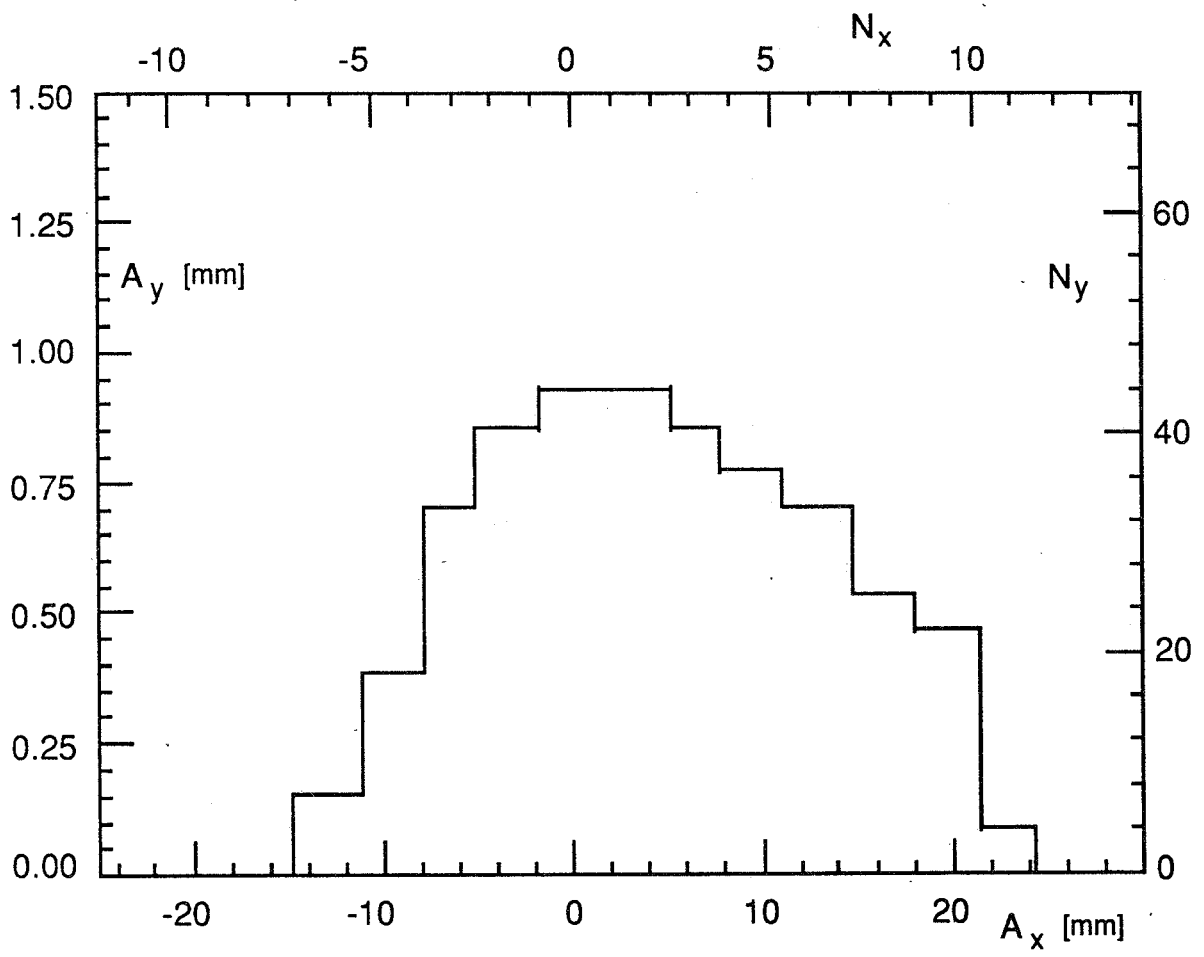

Fig. 3.10 - On energy dynamic aperture at the IP: A_X and A_Y are the horizontal and vertical maximum stable amplitudes, while N_X and N_Y are the same in units of numbers of σ's, for κ=.01.

A more elaborate chromaticity correction scheme and further optimisation of the working point in the tune diagram will allow to achieve a dynamic aperture that matches the lifetime and injection requirements.

3.3.4 - Injection aperture

For injection it is foreseen to implement a conventional full energy scheme based on a thin septum and a fast closed orbit bump produced by four kicker magnets. In order to evaluate the necessary ring aperture, the horizontal and vertical r.m.s. beam size are shown in Fig. 3.11 for the following conservative characteristic parameters of the injected beam :

$$\varepsilon = 2.\,10^{-5} \text{ m rad}$$
$$\kappa = 1.$$
$$\frac{\Delta p}{p} = 1.\,\%$$

The required error closed orbit allowance on the aperture can be of a few millimiters only.

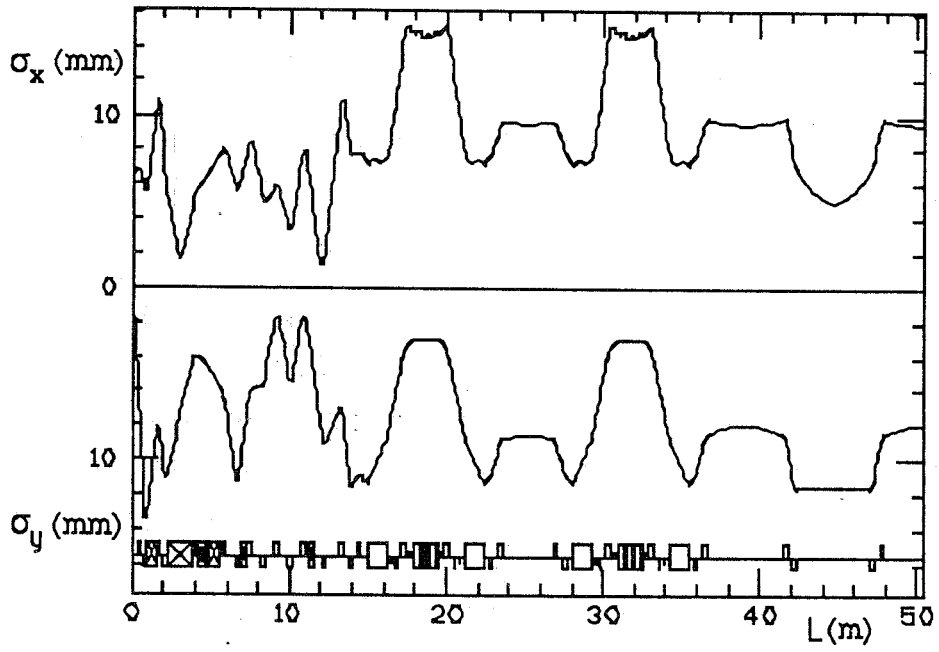

Fig. 3.11 - Horizontal and vertical r.m.s. beam sizes

3.4. - BEAM STABILITY AND LIFETIMES.

High currents in both the single and the multibunch modes of operation, short bunch lengths, long lifetimes and the stablest possible beam conditions are all to be achieved at the same time, thereby putting severe constraints on the design of the overall system.

The above parameters are very much interconnected: single-Tousheck lifetime can be relevant at the energy of 510 MeV and is determined by the bunch density and the momentum acceptance. In turn the bunch density depends on the lattice and RF parameters, and can be affected by intrabeam scattering and by μ-wave instabilities whose current thresholds are related to the vacuum chamber geometry and the RF cavity properties.

A self consistent computation has therefore been carried out to find an optimum. The main phenomena considered in the analysis are : single bunch instabilities including turbulent bunch-lengthening, lifetime limiting effects (such as Tousheck scattering, gas scattering, and beam-beam single bremsstrahlung), coupled bunch instabilities and intrabeam scattering.

3.4.1 - Single bunch dynamics

Instabilities are caused by the electromagnetic fields excited by the interaction of the bunch with the surrounding structure. The effects of these fields on the bunch dynamics are estimated using the concept of "machine impedance".

The single bunch dynamics is affected by those bunch excited fields whose strength is relevant over a distance of the order of the bunch length. The fields are mainly produced in correspondence with vacuum chamber discontinuities (including the cavity irises) and are described in the frequency domain by the so called broadband (BB) impedance. They cause the particles to lose energy depending on their position and therefore induce additional momentum spread and bunch-lengthening.

The threshold peak current of this "turbulent" bunch-lengthening is given by:

$$\hat{I}_l = \frac{2\pi\, \alpha_c\, (E/e)\, \sigma_p^2}{Z/n} \qquad (3.18)$$

With the σ_p and α_c values given in Tab. 3.2, one obtains

$$\hat{I}_l \approx 5\ \text{Amp}\cdot\Omega$$

The 57 A design peak current exceeds the μ-wave threshold for any reasonable choice of RF parameters and BB impedances. In order to keep the bunch length at the design value the values of the RF parameters h (harmonic number) and $\hat{V}$ (Peak voltage) must satisfy the equation:

$$h\hat{V} = \frac{ecN\,R^2}{\sqrt{2\pi}\,\sigma^3}\,\frac{\left(\frac{Z}{n}\right)_{BB}}{\cos(\phi_s)} \qquad (3.19)$$

where

$$\cos(\phi_s) = \sqrt{1 - \left(\frac{U}{e\hat{V}}\right)^2} \qquad (3.20)$$

with $U = U_0 + U_z$, U_0 being the radiation loss and U_z the energy dissipated in the resistive impedance.

Note that U_z depends on the bunch-length (σ_z^{-3}), and therefore for short bunches it may contribute significanlty to the overall losses:

$$U_z\,(\text{keV}) \approx 4\left(\frac{Z}{n}\right)_{BB}(\Omega) \qquad (3.21)$$

Equation 3.19 has been solved for h, as a function of $\hat{V}$ and Z/n. Since the impedance can be only roughly estimated several BB impedance values, chosen in the range

$$\left(\frac{Z}{n}\right)_{BB} = 1 \div 10\,\Omega$$

(a reasonable range covering the measured impedances of almost all existing machines) have been considered.

Fig. 3.12 shows the curves (dashed lines) relating the peak voltage, $\hat{V}$, necessary to obtain the nominal bunch-length of 3 cm, to the harmonic number h. It is apparent that by choosing the RF frequency to be ≈ 350 MHz, the bunch-length can be controlled using reasonable peak voltage values independent of the exact machine impedance value.

On the contrary, the effect of the short-range wakefields on the transverse dynamics is destructive, and most often determines the maximun storable current. By assuming a beam pipe radius b = 3 cm , equal to the bunch-length, and using the relation between the longitudinal and the transverse BB impedance:

$$|Z_\perp| = \frac{2R}{b^2}\cdot\left(\frac{Z}{n}\right)_{BB}$$

one finds that the current stays below the transverse threshold, provided that h and $\hat{V}$ fulfill the condition:

$$h\hat{V}\cos(\phi_s) < 4\,\alpha_c \frac{E}{e} \cdot \left(\frac{R}{<\beta>}\right)^2 \qquad (3.22)$$

where $<\beta>$ is the largest between the horizontal and the vertical β function average. Figure 3.12 shows the limit curve (solid line) below which the eq. 3.22 is satisfied.

Note that, because of the rather weak dependance on impedance through $\cos(\phi_s)$, the four curves corresponding to the four considered impedance values are practically superimposed on each other. The limit is exceeded at the design current if the impedance exceeds $Z/n \approx 5\Omega$. The maximum allowed design impedance is thus defined.

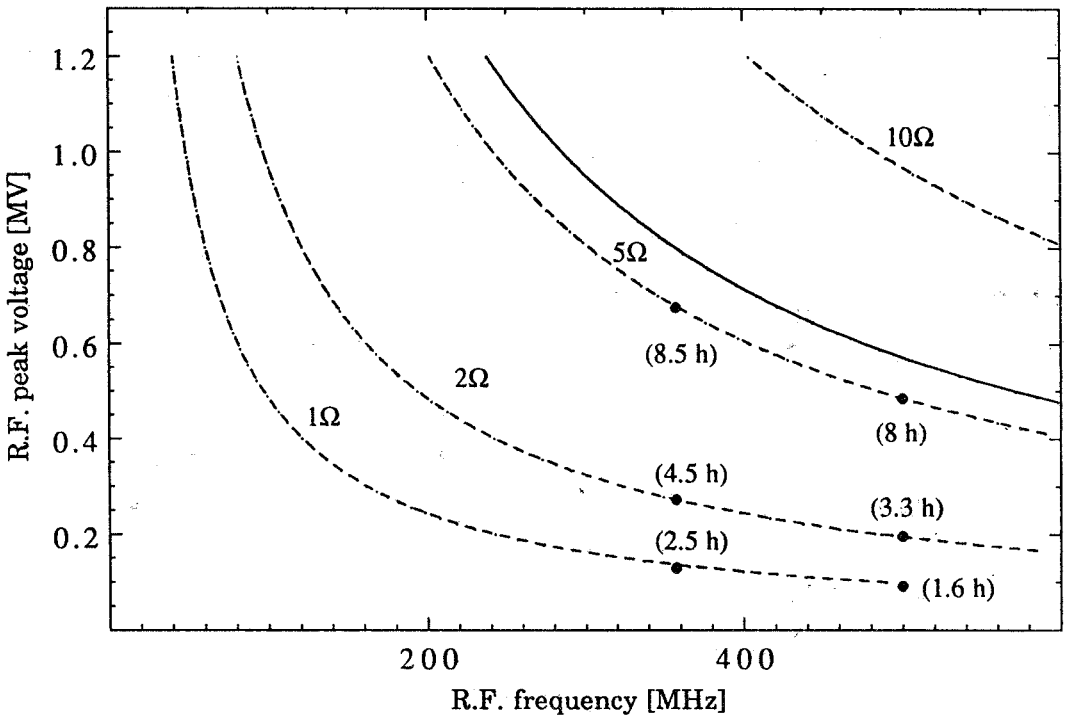

Fig. 3.12 - Peak voltage versus R.F. frequency for different machine impedances (dashed lines). The solid line is the limiting curve for transverse instabilities. The dots are the calculated Toschek life-times for the two different R.F. frequencies: 357 and 500 MHz.

3.4.2 - Beam Lifetime

The single Touschek scattering effect induces a momentum deviation depending on the bunch density and r.m.s. angular divergence $\sigma_{x'}$. The Touschek lifetime τ_T averaged along the machine, has been calculated assuming that the machine acceptance is limited longitudinally by the RF bucket heigth and transversely by the physical aperture. The results of the calculation are shown as dots on the iso-impedance curves in Fig. 3.12 , for the chosen RF parameter values . It is found that, since the bunch volume stays constant along the curves, lifetimes are limited by the physical aperture in the upper-left region while, moving down and to the right, they decrease because the RF momentum acceptance is reduced. Remembering the constraints on the RF parameters deriving from single bunch dynamics, we conclude that an RF frequency around 350 MHz, giving a lifetime of several hours, is the most suitable for our purposes.

At 350 MHz the Touschek lifetime, τ_T, is practically limited only by the RF acceptance, ε_{RF} and by varying the peak voltage in the range 0.1÷ 0.7 MV, ε_{RF} can be changed from 1.2% to 2.8%.

The lifetimes relative to all other mentioned processes are calculated on the basis of this choice.

Radiation in the bending magnets and in the wigglers leads to the loss of those particles with energy deviations larger than the machine energy acceptance. The effect however, even including the momentum spread increase induced by microwave instabilities give a practically infinite quantum life time τ_q provided too high values of the frequency are avoided. As an example, should one choose 500 instead of 350 MHz, for $(Z/n)_{BB} = 1\ \Omega$ one would need only 93 KV peak voltage to keep the bunch length at 3 cm but the R.F. momentum acceptance would be reduced to 0.8% and the quantum lifetime would dramatically drop to 80 minutes.

By choosing a 350 MHz system, the range of R.F. momentum acceptances ($\approx$1.2% ÷ $\approx$ 2.8%) is such that other phenomena causing energy deviations of the particles in the bunch do not affect the overall beam lifetime. Single bremsstrahlung in beam-beam collisions gives a lifetime of 20 hours at least, inelastic scattering on the residual gas a lifetime of 35 hours in the worst case and, elastic scattering on residual gas -causing particles to be lost on the beam pipe - gives a lifetime of 22 hours at the design pressure of $\approx 10^{-9}$ torr.

In conclusion we expect an overall beam lifetime in the range 3÷6 hours limited by Tousheck scattering. Topping-off injection is nevertheless desirable in order to keep the average luminosity high.

3.4.3 - Multibunch instabilities

The impedance of parasitic high order modes (HOM) are characterized by a resonant frequency ω_r, a shunt impedance R_s and a quality factor Q_s:

$$Z_{//}(\omega) = \frac{R_s}{1 + jQ_s\left(\frac{\omega_r}{\omega} - \frac{\omega}{\omega_r}\right)}$$

They are responsible for the multibunch instabilities. Many of such narrow band impedances are originated in the RF cavities or in cavity-like vacuum chamber components coupled to the beams.

The motion of M equidistant bunches is similar to that of M rigid coupled oscillators. The frequency spectrum of the oscillations is given by a set of sidebands at frequencies:

$$f_p = f_o\,(Mp + n + m\nu_s),\ [m = 1,2,...;\ n = 0 \div M-1;\ -\infty < p < +\infty]$$

The amplitude of these sidebands is not constant but depends on the bunch length σ and shape and on the frequency f_p. According to Sacherer's theory [15] a single sideband of the umperturbed distribution will undergo a complex frequency shift $\Delta\omega_m$ because of the coupling. The real part of $\Delta\omega_m$ gives a real frequency shift while its imaginary part causes the oscillation amplitude to grow with a rise time:

$$\tau_m \sim \frac{1}{\Im[\Delta\omega_m]}$$

A simple approximation of the growth rate can be derived [16] under the following assumptions holding in our machine: $M(\sigma/R) << 1$ and a single sideband f_p coupled to the resonator, i.e. $f_r/f_o << Q_s$. In the particular case of full coupling we get:

$$\Im[\Delta\omega_m] \sim \frac{m}{m+1}\,\frac{2^{m-1}}{(2m-1)!!}\,\frac{I\,R_s\,\omega_s}{\omega_{RF}V_{RF}\cos\phi_s}\,\frac{\omega_r^{2m-1}}{\bar{\omega}^{2m-2}}\,\exp\left[-\left(\frac{\omega_r}{\bar{\omega}}\right)^2\right] \qquad \text{with } \bar{\omega} = \frac{c}{\sigma}$$

where I is the total current, and the double factorial applies only to odd terms.

By assuming that this instability is damped by radiation we get the current thresholds for the dipole and quadrupole modes:

$$I_{th}{}^{m=1} = 2\sigma_p \frac{U_o}{R_s} \frac{\exp\left(\frac{\omega_r}{\bar{\omega}}\right)^2}{\left(\frac{\bar{\omega}}{\omega_r}\right)} \qquad I_{th}{}^{m=2} = \frac{9\sigma_p}{4} \frac{U_o}{R_s} \frac{\exp\left(\frac{\omega_r}{\bar{\omega}}\right)^2}{\left(\frac{\bar{\omega}}{\omega_r}\right)^3}$$

Calculations of these thresholds have been done considering as an example the LEP 350 MHz RF cavity whose HOM are listed in Table 3.4 togheter with the corresponding thresholds.

TABLE 3.4 - LEP 350 MHz Cavity Full Coupling Threshold

Parasitic Resonance			Full Coupling Thresholds [mA]		$\frac{\Delta\omega_r}{\omega_r} 10^3$
f_r [MHz]	R_s [MΩ]	Q_r	m=1	m=2	
506	1.3	40600	.02	.24	2.8
920	0.75	40700	.03	.10	2.2
1163	0.33	50400	.06	.13	1.3
1204	0.36	70400	.05	.10	1.0
1745	0.37	66500	.07	.07	0.9
1990	0.20	66700	.16	.12	0.6

It is apparent that coupled bunch coherent instabilities could be harmful under hardly predictable particular conditions; cures to fight them must therefore be envisaged. On the other side for a relatively short machine we expect the instability to be caused by only few offending HOM. We discuss here three main cures and we make an estimate of the required performances:

a) damping of the HOM thereby reducing shunt impedance R_s (HOM damping);
b) shifting of the frequency of the harmful HOM's ;
c) implementing an active feedback system.

In the worst case, corresponding to full coupling, the threshold current is inversely proportional to the shunt impedance of the HOM which therefore should be reduced by a factor quite high and consequently not easily pursuable.

By shifting the HOM frequency there is a strong increase of the current threshold by a factor:

$$\left(2Q_r \frac{\Delta\omega_r}{\omega_r}\right)^2$$

In order to store the design current, a frequency shift of ~ 0.3 % could be required, as shown in the last column of Table 3.4.

Finally the use of a feedback system introduces a damping given by:

$$\frac{1}{\tau_D^{FB}} = \frac{1}{2} \frac{f_o}{E_o} \frac{eV_{FB}}{\Delta p/p}$$

where $\frac{\Delta p}{p}$ is the relative bunch energy deviation.

The feedback signal, in order to damp all possible coupled modes, has to act separately on each bunch. Accordingly the system bandwidth should be at least twice the bunch frequency, therefore the use of broad band longitudinal strip-line kickers is required. The feedback system gain turns out to be very high and most likely limited by the maximum allowed voltage (200÷500 V) on the longitudinal strip-line kickers.

In conclusion, we have given a rather pessimistic estimate of multibunch instabilities, in the worst possible scenario. It is clear however that the problem must be carefully studied foreseeing the combined use of HOM frequencies detuning and of feedback systems, including the one recently developed by Kohaupt [17].

3.5. - GENERAL CONSIDERATIONS ON BEAM DIAGNOSTIC AND INSTRUMENTATION

The beam instrumentation to be implemented in the Φ-Factory storage rings is discussed in the following, with reference to the peculiar features wich influence the design and choice.

The storage rings characteristics, which reflect in particular requirements of the beam instrumentation and of the general hardware, are the following:

- High current (~ 1 A). The longitudinal and transverse parasitic impedance of the vacuum chamber should be the lowest possible to increase the thresholds of collective instabilities.

- Many bunches. The rather large number of circulating bunches calls for a careful design of the RF cavities, where coupled bunch instabilities are most likely to be excited by high order resonating modes. The more seriously offending modes may be identified and damped in the cavities by suitable antennas, but nevertheless a coupled-bunch feedback system must be provided.

- Small bunch dimensions (σ_y <~ 0.02 mm at the IP). Careful closed-loop control of the stability of the IP vs. drifts of the longitudinal and vertical bunch position in the separate rings is required.

- Small coupling factor ($\kappa \sim .01$). To achieve such low value of the coupling factor, a careful control of the closed orbit distorsion at quadrupoles and sextupoles locations is required in order to reduce the strength of the driving term of vertical dispersion. Vertical dispersion is also introduced, and must be suppressed, by the vertical bending of the separator in the Interaction Region and by rotated quadrupoles and vertically misaligned sextupoles. Careful surveying and high absolute accuracy of the beam position monitors is required.

3.6 - RF SYSTEM

With an operating frequency of 357.14 MHz the maximum required RF voltage is ≈ 0.8 MV (see § 3.4).

The energy loss/turn is 11.26 keV and the RF power to the beam is 11.26 kW for a stored current of ≈ 1 A (see Tab. 3.2). The power loss to parasitic HOM's is estimated to be ≈ 4 keV per Ohm of broadband impedance. An 8 kW additional power loss must therefore be taken into account for an overall chamber impedance of 2 Ω. In conclusion, the total required RF power is ≈ 20 kW per beam.

The proposed RF system consists of two normal-conducting single-cell copper cavities in each ring. Each cavity is rated at 400 kV. The main system parameters are summarized in the following Table 3.5 :

Table 3.5 - RF System Parameters

RF Frequency	f_0 =	357.14	MHz
Cavity Q factor	Q_0 =	40.000	
Effective cavity shunt-impedance	ZT^2 =	6	MΩ
RF peak voltage per cavity	V_p =	400	kV
Dissipated power per cavity	P_D =	27	kW
Beam power per cavity	P_B =	10	kW
Cavity to source coupling factor	β =	1.4	
Bandwidth of the System	B_L =	21	kHz
Maximum generator power	P_A =	50	kW
Number of RF chains per ring		2	

Each resonator can be powered by a single 50 kW source; reliable tetrode amplifiers are available on the market in this range of frequency and power.

Standard feedback systems are foreseen to control amplitude, phase and frequency of the resonant cavities.

The cavities will be equipped with HOM couplers to damp the parasitic modes excited by the bunched beam. Some R&D will be necessary to specify and test the performance of the dampers.

3.7 - VACUUM SYSTEM

Ultra high vacuum (UHV) is necessary in an electron storage ring in order to achieve good beam lifetime and to avoid ion trapping.

Good vacuum conditions have to be maintained in the presence of the heavy gas load produced by the radiation induced photo-desorption. Hard radiated photons ($h\nu > 10$ eV) extract photoelectrons from the inside wall of the vacuum chamber; these in turn extract atoms or molecules absorbed on the surface. The process is characterized by the "photodesorption efficiency" parameter, D, wich gives the average number of desorbed molecules per incident photon. Typical values of D are in the range of $10^{-1} \div 10^{-7}$ molecules/photon. The lowest D values are reached with appropriate treatments of the vacuum chamber and after long periods of conditioning with the stored beam ($\approx$ 100 A·h).

From the design parameter values listed in Tab 3.2 we estimate a total gas load, Q, of

$$Q = 8.7\ 10^{-6} \text{ mbar l/s} \quad \text{for} \quad D = 10^{-6} \text{ molecules/photon}$$

The total pumping speed, S, necessary to achieve the design value of 10^{-9} mbar is therefore :

$$S = Q/p = 8700 \text{ l/s.}$$

With 10 identical ion pumps per sector we obtain a required nominal pumping speed of 220 l/s per pump; a rough figure of 400 l/s per pump actual pumping speed is estimated to account for the pumping speed degradation at 10^{-9} mbar and for vacuum chamber conductances. The preferred vacumm chamber material is stainless steel; usual UHV technology precautions such as accurate cleaning procedures, high temperature bake-out, etc., will also have to be taken.

In summary, the main vacuum system components for the two rings are:

- 2 stainless steel vacuum chambers
- bakeout systems
- 80 sputter ion pumps, 400 l/s each.
- 8 cryopumps, 1500 l/s each.
- 8 oil-free roughing pumps.
- 16 U.H.V. gauges.
- 1 mass spectrometer (8 heads).
- interfaces to the central control system.

3.8 - THE DETECTOR SOLENOID

The main specifications for the Detector solenoid are :

- Axial length	≈ 10	m
- Radius	≈ 5	m
- Axial magnetic field	1	kGauss max
- Field on axis	≈ 0	

The main conclusions from of a preliminary feasibilty study of the solenoid are presented here. The details can be found in Reference (18).

The detector and the detector solenoid have to clear the region inside a conical surface, coaxial with the beam, having a half-aperture angle of 8.5° and the vertex on the IP. The beam has to be shielded from the solenoidal field; however, no shield can be foreseen in the ± 22 cm region surrounding the IP because the experiment tolerates only a very thin layer of material in that region.

The solenoid main coil dimensions are:

- average radius	437.5	cm
- thickness	25	cm
- total length	9	m

and the iron yoke ones are :

- maximum external radius	5	m
- thickness	25	cm
- thickness of the terminating iron plates	25	cm
- terminating iron plate hole radius	75	cm

The main solenoid linear current density, determined using POISSON, is ≈ 88900 A/m. An active shielding system using current sheets has also been investigated; a typical layout, including the current sheet profile and the field lines as computed by POISSON, is shown in Figure 3.13.

Finally, the magnetic field on axis is plotted for different shield configurations in Figure 3.14. From these preliminary calculations we do not anticipate any problem in locally compensating the residual solenoidal field even though the correction scheme has not yet been worked out in full detail.

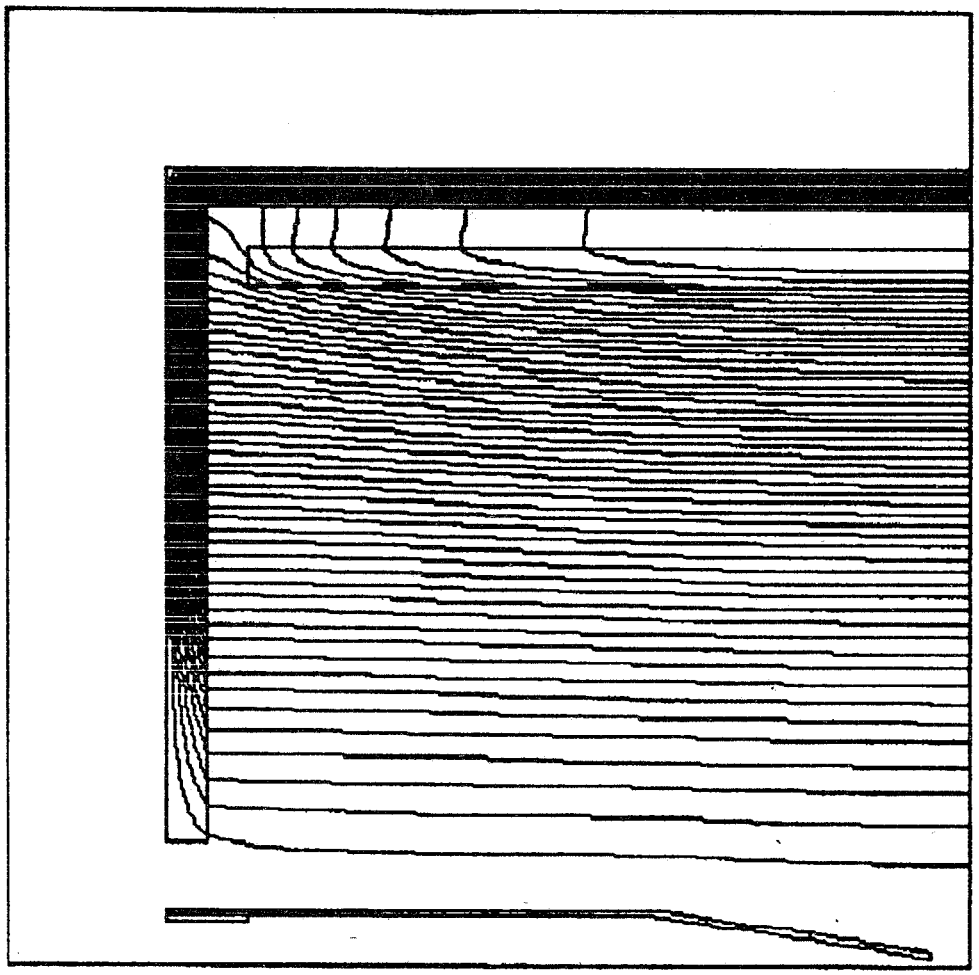

Fig. 3.13 - Magnetic field lines for the shielded solenoid configuration.

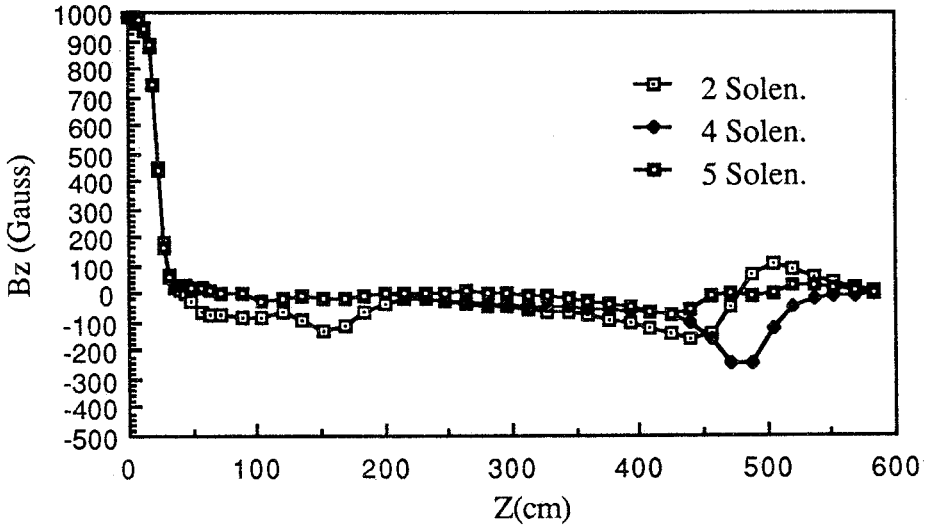

Fig. 3.14 - Magnetic field along the axis with different shield configurations.

References

(1) M.Sands, The physics of electron storage rings. An introduction, SLAC-121,(1970)
(2) R.Littauer et al., XII Intern. Conference on High Energy Accelerators, FNAL (1983)
(3) Barkov et al., The F-Factory project in Novosibirsk, Proc. of 1989 ICFA Meeting on Beam Dynamics, Novosibirsk
(4) W.A.Barletta and C.Pellegrini, A full energy positron source for the UCLA F-Factory CAA 0048,UCLA 10/89
(5) H.Neseman, Proc. UCLA Workshop "Linear Collider, BB Factory, Conceptual design, Jan.1987, Edited by D.H.Stork, World Scientific - Singapore.
(6) S.Myers and J.Jowett, Proceeding of the Tau-Charm Factory Workshop, SLAC-343 (1989)
(7) 1985 NSLS Annual report - BNL 51947
1988 NSLS Annual report - BNL 52167
G.Vignola, private communication
(8) J.Seeman, Lectures Notes in Physics, Vol. 247 (1985) - Springer Verlag Ed.
(9) M.Bassetti, Int. Memo ARES 18 (1989)
(10) R.H.Helm, M.J.Lee, P.L.Morton, M.Sands, IEEE Trans. Nucl. Sci., NS 20 (1973)
(11) M.Bassetti, S.Guiducci, M. Preger, G. Vignola, Int.Memo ARES 26 (1989)
(12) R.Chasman, G.K.Green and M.Rowe, IEEE Trans. Nucl. Sci., NS 22 (1975)
(13) J.B.Murphy and G.Vignola, LEDA : A computer code for linear lattices (Unpublished)
(14) H.Wiedeman, PEP Note 220 (1976)
(15) F.Sacherer, IEEE Trans. Nucl. Sci., NS 24 (1977)
(16) S.Bartalucci and L.Palumbo, Int. Memo T-120 (1985)
(17) R.D. Kohaupt, DESY 86-121 (1986)
(18) C.Sanelli, Int. Memo ARES 32 (1990)

APPENDIX 2

A CRAB-CROSSING OPTION

A CRAB-CROSSING OPTION

S. Bartalucci, M. Bassetti, M.E. Biagini, C. Biscari, S. Guiducci,
M.R. Masullo, L. Palumbo, B. Spataro and G. Vignola

Introduction

The crab-crossing idea was originally proposed by R. Palmer[1] to increase the luminosity in multibunch linear colliders. K. Oide and K. Yokoya[2], by showing that crab-crossing does not induce excitation of synchrobetatron resonances, made this scheme attractive also for circular colliders.

In a crab-crossing the centers of the colliding beams travel along two separate trajectories that form an angle q at the interaction point, IP. A first RF cavity gives an angular kick $\theta/2$ to the front of the bunch and a kick of opposite sign to the back. If the cavity is located $\pi/2$ away from the IP in β-phase angle, the crossing beam geometry is changed into a head-on collision. A second crab cavity, π away from the first one, restores the original bunch orientation.

The crab-crossing geometry, due to the angle between the beam's trajectories, allows a bunch spacing closer than the head-on collision and, consequently, a higher collision frequency f. This increase implies a luminosity enhancement, if one can store large average beam currents and if the experiments can tolerate high collision rate.

The crab crossing requires RF accelerating fields transverse to the beam motion. Recently G.P. Jackson[3] pointed out that the same effect can be obtained with longitudinal RF fields located in a non-zero dispersion region and spaced π away in β-phase angle from the IP.

We are investigating various crab-crossing options[4] that could be easily incorporated in the Frascati Φ-factory design[5] and we present here a first scheme that should give, in principle, a luminosity enhancement factor of the order of 5 .

Basic formulae:

a) Transverse crab

By assuming the bunch length σ_z much smaller than the wavelength λ of the deflecting RF cavity and the crab-crossing angle θ small as well ($\theta/2 \sim \tan(\theta/2)$), the peak voltage required for the crab cavities is

$$V_T = \frac{1}{4\pi} \frac{\theta\lambda(E/e)}{\sqrt{\beta^* \beta_c}}$$

while phase and amplitude stability requirements can be written as[3]

$$\Delta\phi << \frac{4\pi\sigma^*}{\lambda\theta} \qquad \text{and} \qquad \frac{\Delta V}{V} << \frac{1}{\sqrt{N}} \frac{\sigma^*}{\theta_z}$$

where β^*, σ^*, N are the β-function, the beam size and the number of damping turns in the crab plane respectively and β_c is the β-function at the RF cavity position.

b) Longitudinal crab

The voltage required for the crab cavities spaced 2π in β-phase angle can be written as[4]

$$V_L = \frac{1}{4\pi} \frac{\theta\lambda(E/e)}{\sqrt{\beta^*/\beta_c}\, D_c}$$

with the additional constraint

$$\alpha_c + \beta_c \frac{D_c'}{D_c} = 0$$

where D_c, D_c', β_c and α_c are the dispersion function, its derivative and the Twiss coefficients at the RF cavity position respectively. Phase and amplitude tolerances, instead, have the same expression as for the transverse crab.

A low-b insertion for 20 mrad transverse crab

Fig. 1 shows the principle scheme of the Crab-crossing as proposed by R. Palmer[1].

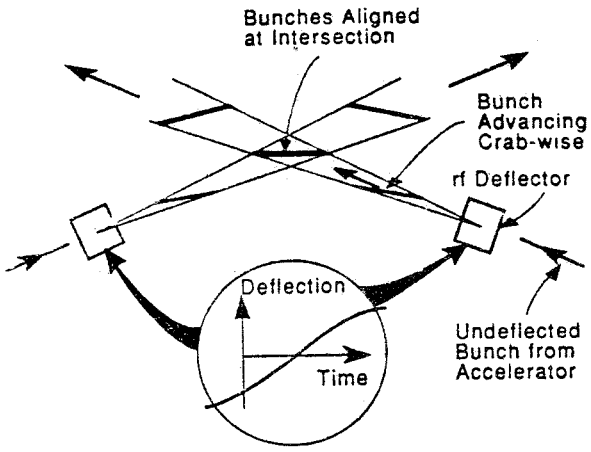

Fig. 1 - Crab-wise crossing

In the following we present a low-β insertion design for a 20 mrad transverse crab-crossing in the vertical plane. This insertion can be easily incorporated as an option in the original design.

Fig. 2 and Fig. 3 show the β-functions, the half-separation and the horizontal beam size σ_x inside the detector region (~ 5 m), while in Fig. 4 and Fig. 5 the same quantities for the whole low-β insertion are plotted.

In this design we use 4 RF crab-cavities, each one located at ~ 9 m from the IP ($3\pi/2$ in β-phase angle).

The peak voltage required for the crab cavities is

$$V_T = 860 \text{ KV}$$

while phase and amplitude stability requirements are

$$\Delta\phi < 0.9^o \qquad \text{and} \qquad \frac{\Delta V}{V} < 2.3\ 10^{-4}$$

The feasebility of the RF cavities as well as the advantages of a longitudinal crab crossing are under study.

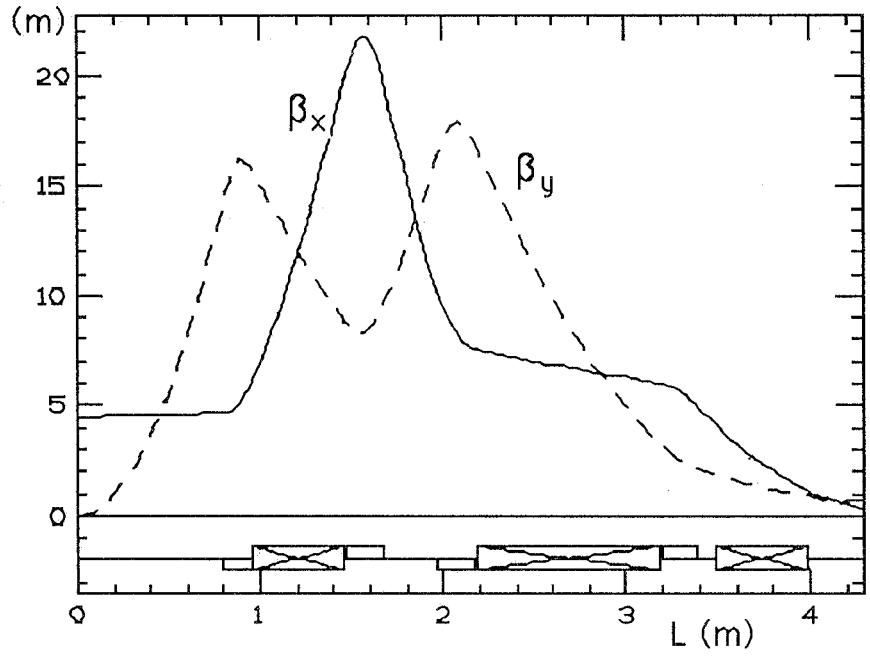

Fig. 2 - β-functions in the detector region

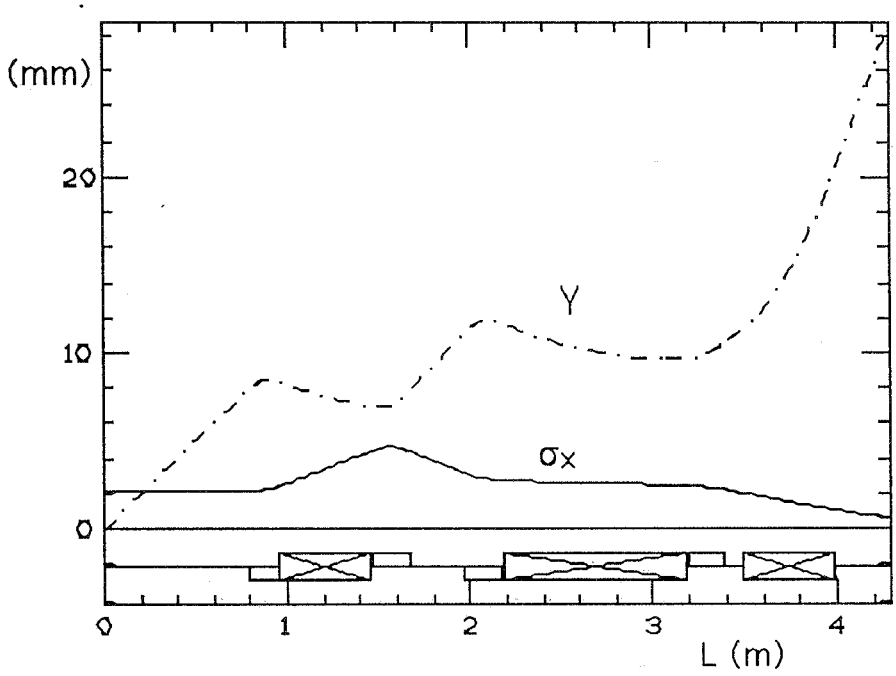

Fig. 3 - Half-separation Y and horizontal beam size σ_x in the detector region

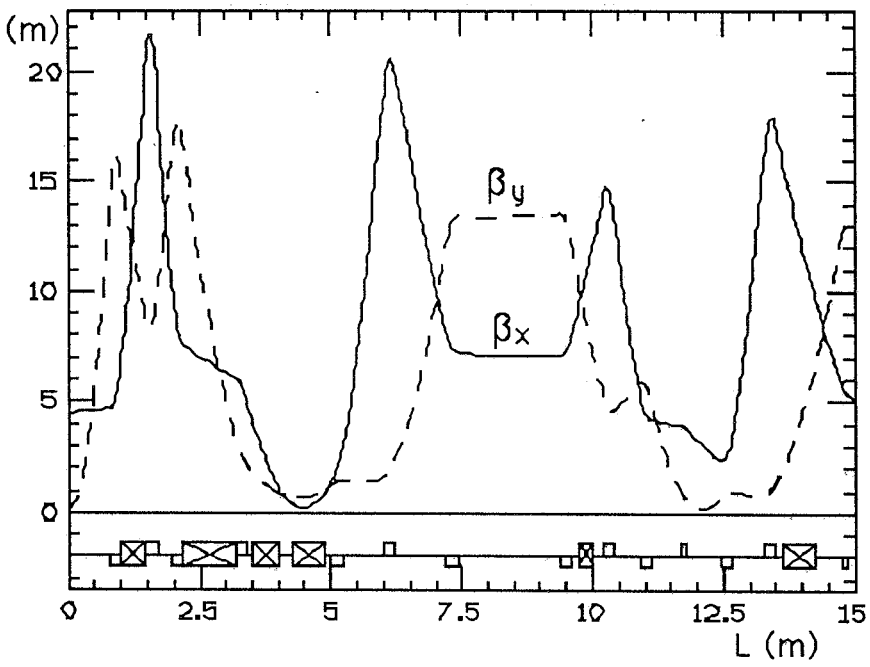

Fig. 4 - β-functions alog the low-β insertion

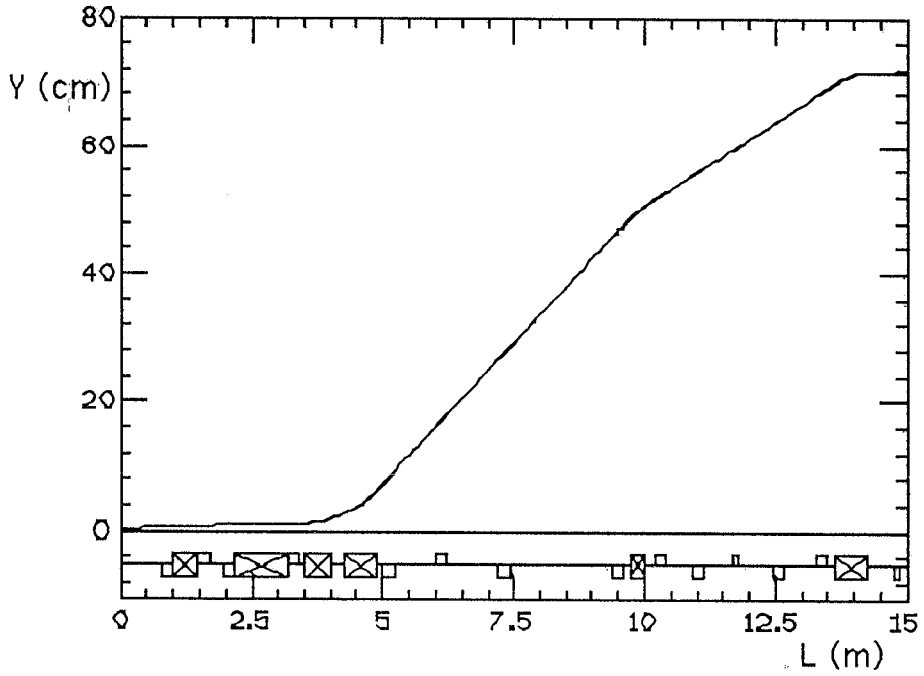

Fig. 5 - Half-separation along the low-β insertion

References

[1] R. Palmer, SLAC-PUB-4707 (1988).

[2] K. Oide, K. Yokoya, SLAC-PUB-4832 (1989).

[3] G. P. Jackson, Workshop on beam dynamics issues of "High Luminosity Asymmetric Colliders Rings", Berkeley (1990).

[4] S. Bartalucci, M. Bassetti, M.E. Biagini, C. Biscari, S. Guiducci, M.R. Masullo, L. Palumbo, B. Spataro and G. Vignola: A crab-crossing option for the Frascati Φ-factory, (to be published).

(5) Ares Design Study: The Machine, LNF-90/005 (1990).